PROBABILISTIC RISK ASSESSMENT
LIMERICK GENERATING STATION
PHILADELPHIA ELECTRIC COMPANY

VOLUME II

March 1981

Docket Nos. 50-352
50-353

LIMERICK GENERATING STATION PROBABILISTIC
RISK ASSESSMENT

Appendix A

INPUT DATA FOR THE PROBABILISTIC
EVALUATION OF ACCIDENT SEQUENCES

APPENDIX A

A.1   ACCIDENT SEQUENCE INITIATORS

The use of event tree/fault tree methodology requires the
definition of the initiating events to be considered in a risk evalua-
tion. Accident initiators that could lead to the release of significant
amounts of radioactivity to the environment must be identified. The
accident sequences discussed here are for core-related events with the
reactor initially at or near full power.

There are a number of approaches to defining the set of accident
initiators to be used in a risk evaluation. These approaches vary in de-
gree from a general initiator category classification (e.g., transients and
LOCAs) to more precise definitions of accident initiators (e.g., rod with-
drawal accident, stuck control rod, loss of main condenser).

In this section, the following methodologies will be discussed:

●   The method used in WASH-1400 to define event tree
    sequence initiators (A.1.1)

●   An alternate general approach (A.1.2)

●   The plant-specific technique used for the Limerick
    analysis (A.1.3).

Figure A.1.1 provides an overview of how the definition of
accident initiators fits into the Limerick risk assessment. Once the
sources of radioactivity to be considered are established, then the
potential modes of failure for release of the radioactivity to the
environment are identified. This process begins with identifying the
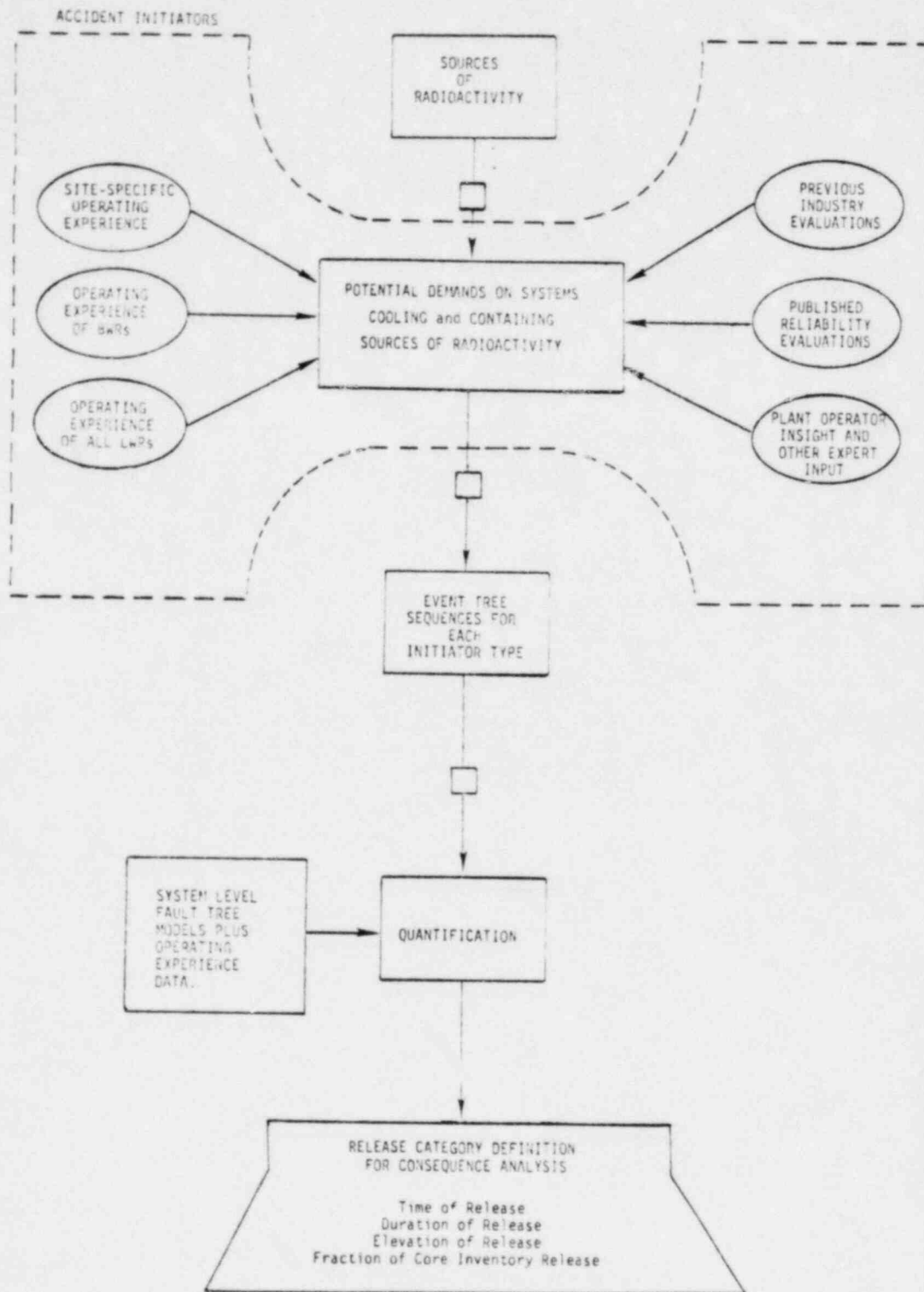
Figure A.1.1   Flow Chart Showing Where Accident Initiators are
            Defined in Risk Evaluations

types of potential demands on the normal and safety systems. These
demands are then propagated through event trees to determine an overall
estimate of unacceptable conditions. Each accident sequence is assigned
to a specific release category that reflects similar parameters defining
the radioactive release. These parameters include:

- Time of radioactive release
- Duration of release
- Fraction of core released
- Elevation of release.

A.1.1   Reactor Safety Study

The Reactor Safety Study (WASH-1400) (A.1-1) divided accident
initiators into two general categories:

1. Loss of coolant accidents (LOCAs)

2. Transients.

Transients were included in WASH-1400 to represent the potential demands
on the reactor shutdown system and the heat removal system, since a failure
of either function following a transient could lead to potential core damage.
WASH-1400 used a simplified approach to the definition of transient sequences
to be considered, as quoted below:

"Transients generally fall into two categories--those that are fairly
likely, or anticipated transients, and those that are unlikely, or
unanticipated transients. In assessing the potential risks due to
these types of transients, the wide variability in frequency of
occurrence of the two categories suggest that only the more likely
ones will be contributors to the overall risk. This is due to the
fact that, except for those that cause LOCAs, all the transients,
where protective systems fail, have essentially the same end point--
a molten core and a ruptured reactor coolant system in an intact
containment. Thus, it should be necessary only to identify the
several most likely ways for core melt to occur and the unlikely
ways that result in the same consequence should not be important
contributors to the risk."

While WASH-1400 identified a list of potential anticipated transients, the analysis assumed that the anticipated transients all had similar effects on the normal and safety systems. Therefore, the method of analysis was to use a single event tree to describe the transient sequences treating all transient initiators as the same.*

In the Limerick risk assessment, various transients are viewed to have a number of peculiar characteristics which makes analysis of a number of transient types and sequences within these transient trees important. The anticipated transients used in WASH-1400 are given in Table A.1.1. The unanticipated transients, while identified, were not explicitly evaluated in WASH-1400 because the associated accident sequences were assumed to result in consequences and system interactions, similar to those identified for anticipated transients, but to be of sufficiently low probability as to not contribute to calculated risk.

A.1.2   Alternate General Approach

An alternate approach to that used in WASH-1400 is to provide general classes of events in which the accident initiators can be placed and then identify the accident sequences which may occur following initiators of these general classes.

The two possible general categories of potential accident initiators which could be considered are:

Category I: Events leading to undercooling of the core

Category II: Events leading to increases in core power beyond the normal cooling capability.

The Category I events may result from two sub-categories of initiator types:

*One exception to this was the separate treatment of loss-of-offsite-power.

A-4

Table A.1.1

BWR TRANSIENT INITIATORS FROM WASH-1400

Likely Initiating Events	Unlikely Initiating Events
1. Rod Withdrawal at Power	1. Rod Ejection Accident[a]
2. Feedwater Controller Failure - Maximum Demand	2. Rod Drop Accident[a]
3. Recirculation Flow Control Failure (Increasing Flow)	3. Compound Initiating Events such as:
4. Startup Of Idle Recirculation Pump	a. Seizure of Two Recirculation Pumps
5. Loss of Feedwater Heating	b. Startup of Idle Recirculation Pump Simultaneously with Turbine Trip
6. Inadvertent HPCI Pump Start	
7. Loss of Auxiliary Power	c. Rod Withdrawal and Simultaneous Startup of Idle Recirculation Loop
8. Loss of Feedwater Flow	
9. Electric Load Rejection (Turbine Valve Closure)	
10. Turbine Trip (Stop Valve Closure)	
11. Main Steam Line Isolation Valve Closure	
12. Recirculation Flow Control Failure (Decreasing Flow)	
13. Recirculation Pump Trip (One Pump)	
14. Recirculation Pump Seizure	
15. T-G Pressure Regulator Failure -- Rapid Opening	

[a] BWR plants have design features provided which make the probabilities for occurrence negligibly small.

1. Loss of Coolant inventory (e.g., LOCA)

2. Reduced heat removal capability.

The Category II events result principally from uncontrolled positive reactivity additions, generally these are a subset of the "transients" category defined in WASH-1400.

However, it is clear that, despite a concerted effort to delineate the categories of event trees and their initiators, there will be an overlap among such general groupings. Figure A.1.2 conceptually displays the difficulty with rigid categorization of events of general categories.
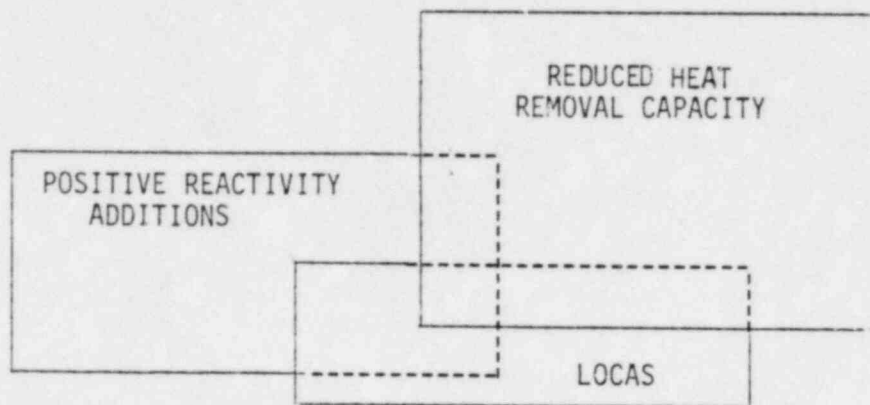
Figure A.1.2 Schematic to Emphasize the Difficulty of Simplistically
Categorizing Accident Sequences.

In spite of this problem of general classification, a clear
definition of specific accident initiators can be made. The extreme case
is that for each type of initiator, an event tree may be required which
will display the functions and/or systems which may interact with the
core and containment during the accident sequence. These event trees
would be developed to include the principal scenarios or sequences which
an accident could take, so that a probabilistic evaluation can be made
of the risk associated with plant operation. However, by the nature of
probabilistic risk assessment, there are sequences which are evaluated
to be so low in probability that they will not affect the calculated
risk. These sequences may be evaluated explicitly or they may be implicitly
neglected. An example of sequences which are implicitly neglected are:

- Two simultaneous LOCAs

- A fire and a LOCA.

A.1.3   Limerick Plant-Specific Analysis

The Limerick analysis includes elements of both the WASH-1400
approach to accident initiator definition and the alternative approach

A-6

previously described. It broadens the scope of accident initiators considered beyond that included in WASH-1400. Specifically, the Limerick analysis includes:

- Event trees for specific transient accident initiators depending upon their effect on the plant

- Inclusion of additional "unantic'pated" transients

- LOCA initiators as a function of size and location.

A.1.3.1   Transient Accident Initiators

The initial screening group of transient accident initiators used in the Limerick analysis come from an EPRI survey of operating experience of nuclear power plants (A.1-2).

selected utilities were requested by EPRI to provide data concerning transients experienced at their plants. Based on the initial response, an expanded, continuing data collection effort was initiated with cooperating utilities. For each transient experienced, the following information was requested:

1.   Date of the scram

2.   A br ef description of the scram sequence including the comp nent failure type and failure mode

3.   The p'ant mode and power level at the time of the scram

4.   The reactor status following the scram

5.   The type of scram.

The data were collected directly from the utilities. Direct communication was established with each plant to clarify the understanding of data items when necessary. These data were used to classify and establish the frequency of broad categories of transients. The results were

compiled to support an EPRI-SAI study on the frequency of anticipated transients in nuclear reactors. They have been described by the NRC in NUREG-0460 (A.1-3) as:

"...the most extensive data on plant transients available to the staff (providing) the best basis for estimating the frequency of anticipated transients in nuclear power plant."

The "anticipated" transient initiator categories used in the EPRI-SAI industry survey for BWRs are shown in Table A.1.2.

In order to emphasize the important accident initiators, the large number and types of potential accident initiators are consolidated into a smaller group which is more easily discussed. This consolidation actually results in some conservatism, but serves the dual purpose of providing an understandable and more realistic assessment of the transients which are encountered, based upon operating experience. These groupings are made based upon the similarity of the accident sequences and their effect on the mitigating systems, not necessarily by the severity of the worst case temperatures and pressure during the postulated transient. The LGS analysis was based on the EPRI evaluation of the frequency of transient initiators.

In summary, the method of analysis used in this report is to categorize initiators together based upon their initial effect on the normal plant systems. The following categories of events are developed:

1. Transients which lead to isolation of the reactor vessel from the main condenser: Referred to as MSIV closure.

2. Transients which result in turbine trip. These transients include turbine trips with bypass capability.

3. Loss of offsite power which leads to the loss of many normal systems at approximately the same time.

Table A.1.2

SUMMARY OF THE CATEGORIES OF BWR TRANSIENTS USED TO CLASSIFY OPERATING EXPERIENCE DATA ON ANTICIPATED TRANSIENTS*

1. Electric Load Rejection
2. Electric Load Rejection with Turbine Bypass Valve Failure
3. Turbine Trip
4. Turbine Trip with Turbine Bypass Valve Failure
5. Main Steam Isolation Valve Closure
6. Inadvertent Closure of One MSIV (Rest Open)
7. Partial MSIV Closure
8. Pressure Regulator Fails Open
9. Pressure Regulator Fails Closed
10. Inadvertent Opening of a Safety/Relief Valve (Stuck)
11. Turbine Bypass Fails Open
12. Turbine Bypass or Control Valves Cause Increase Pressure (Closed)
13. Recirculation Control Failure -- Increasing Flow
14. Recirculation Control Failure -- Decreasing Flow
15. Trip of One Recirculation Pump
16. Trip of All Recirculation Pumps
17. Abnormal Startup of Idle Recirculation Pump
18. Recirculation Pump Seizure
19. Feedwater -- Increasing Flow at Power
20. Loss of Feedwater Heater
21. Loss of All Feedwater Flow
22. Trip of One Feedwater Pump (or Condensate Pump)
23. Feedwater -- Low Flow
24. Low Feedwater Flow During Startup or Shutdown
25. High Feedwater Flow During Startup or Shutdown
26. Rod Withdraw at Power
27. High Flux Due to Rod Withdrawal at Startup
28. Inadvertent Insertion of Rod or Rods
29. Detected Fault in Reactor Protection System
30. Loss of Offsite Power
31. Loss of Auxiliary Power (Loss of Auxiliary Transformer)
32. Inadvertent Startup of HPCI/HPCS
33. Scram due to Plant Occurrences
34. Spurious Trip via Instrumentation, RPS Fault
35. Manual Scram -- No Out-of-Tolerance Condition

*EPRI-SAI Study, (Ref A.1-2)

Table A.1.3
SUMMARY OF THE FREQUENCY OF TRANSIENT INITIATORS AND THE CATEGORIES INTO WHICH THEY HAVE BEEN CONSOLIDATED

ITEM	TRANSIENT	Frequency (Per Reactor Year)			
		EPRI Survey of 12 BWRs			BWR OP. EXP.
		All Years	Exclude Year 1	Exclude Year 1 & <25% Power	GE Assessment
1	MSIV Closure	1.34	.57	.35	1.08
	Closure of all MSIVs (4)**	0.67	0.19	0.13	1.00
	Turbine Trip Without Bypass (5)	0.00	0.00	0.00	0.01
	Loss of Condenser (8)	0.67	0.38	0.22	0.067
2	Turbine Trip	7.62	4.23	2.95	3.98
	Partial Closure of MSIVs (6,7)	0.12	0.14	0.12	0.20
	Turbine Trip with Bypass (3,13,32,33,34,35,36,37)	3.88	1.98	1.21	1.33
	Startup of Idle Recirculation Loop	0.38	0.08	0.09	0.25
	Pressure Regulator Failure (9,10)	0.43	0.35	0.31	0.67
	Inadvertent Opening of Bypass (12)	0.04	0.05	0.00	0.00
	Rod Withdrawal (27,28,29)	0.14	0.14	0.06	0.10
	Disturbance of Feedwater (20,21,23,24,25,26)	1.39	0.65	0.53	0.68
	Electric Load Rejection (1,2)	1.04	0.70	0.63	0.75
3	Loss of Offsite Power (30,31)	.16	.11	.14	.38
4	Inadvertent Open Relief Valve (11)	.20	.08	.03*	.06
5	Loss of Feedwater (2T)	.27	.16	.06	.70
	TOTAL	9.43	5.04	3.51	6.2

* Modifies to 0.07 based upon NUREG-0626.

** Numbers in parentheses refer to transient numbers from Table A.1.2.

4. Inadvertent open relief valve which may lead to an initial heat up or pressurization of containment prior to any attempt to shutdown

5. Loss of Feedwater. The loss of feedwater initiator was separated out, but later combined with MSIV closure.

The consolidation of these transients into groups is defined in Table A.1.3.

Table A.1.4 is a summary of the frequency of transients assumed in four previous risk studies together with an evaluation based on General Electric data. This table provides a range on the past interpretation or estimates of the frequency of "anticipated" transients.

Table A.1.4
SUMMARY OF TRANSIENT INITIATOR FREQUENCIES

Source	Total Transient Initiator Frequency
WASH-1270 (A.1-4)	1
WASH-1400 (A.1-1)	10
NUREG-0460 (A.1-3)	6 to 8
EPRI (A.1-2)	5.04
GE Evaluation (unpublished)	6.2

The results of these data summaries are that there are two principal types of events which require the information on transient initiators:

1. Anticipated transient

2. Anticipated transients without scram (ATWS).

The anticipated transient initiator frequency evaluated by GE (as shown in Table A.1.4) was used to characterize the frequency of all the anticipated transients analyzed in the Limerick PRA. ATWS initiating event frequency was taken from NUREG-0460. (The NUREG-0460 value is felt to be conservative. Recent GE analysis indicates a substantially smaller number may be appropriate.)

In addition to the scram transients, which require immediate response from available systems, there are other conditions which are

more controlled but eventually require the same functions to be performed as noted for scram transients. These other conditions can be generally classed as controlled manual shutdown for maintenance, refueling, test, examinations, or other routine causes.

An analysis for Sandia Laboratory resulted in an estimate of 3.2 manual shutdowns per reactor year based upon a review of data for twelve selected BWRs (A.1-5). Because of the controlled nature of these events, the only significant demand on the system for safe shutdown is the assurance of long term decay heat removal. Therefore, for the purposes of the Limerick risk assessment the manual shutdowns are treated as demands on the heat removal systems. Thus, the TW sequences will have the initiator frequency increased by 3.2 manual shutdowns per reactor year. However, coolant injection functions*, ATWS, and LOCA sequences are not affected by these initiators when they are quantified.

A.1.3.2   LOCA Accident Initiators

Introduction

The data used in WASH-1400 to evaluate pipe failure probability was a compilation from various sources which, in general, were not directly applicable to the nuclear power plant environment. There was an attempt made to identify existing U. S. nuclear experience in order to ensure that the assessed failure data was reasonable in light of the limited experience of that time (approximately 1973).

Since the publication of WASH-1400, SAI has performed a detailed assessment of the failure probability of pipes in nuclear power plants (A.1-6). The purpose of SAI's analysis was to determine a probability of a LOCA occurring based upon actual reactor operating experience. The following areas were addressed:

---

*Loss of coolant injection sequences are considered to be unaffected due to the controlled nature of the shutdown and therefore the increased reliability of feedwater to maintain reactor inventory. In addition, CRD flow is also available under these conditions to maintain coolant inventory.

- Causes of reported pipe failures

- Location of pipe failures within the pipe

- Systems involved in pipe failures

- Failure mode distribution by pipe size

- Distributions of pipe failures by plant age

- Calculating the probability of a LOCA.

Causes of Reported Pipe Failures

Based upon U. S. operating experience, the principal causes of
the reported pipe failures are not the result of inconsistencies or failure
of current design requirements (i.e., ASME Codes). They appear to be the
result of phenomena that are not readily predictable; hence, the methods of
dealing with such phenomena have depended, for the most part, upon engineering
judgment. These causes, ranked by number of reported failures for all sizes
of piping, are:

- High cycle fatigue due to vibration (25.1%)

- Fabrication errors (12.8%)

- Stress corrosion cracking (11.3%)

- Erosion (6.9%)

- Thermal Fatigue (5.4%)

- Corrosion (2.9%).

The observation that high cycle fatigue caused by mechanical vibration or
flow-induced vibration is a major contributor to pipe failures differs
from the observations of earlier pipe failure studies. Earlier studies
concluded that low cycle fatigue was the principal failure mode. Vibra-
tion is the dominant mode in all pipe failures.

The Limerick plant has changed the specified pipe material for
the reactor system from 304 stainless steel to 316L stainless steel which

shows a marked reduction in stress corrosion cracking likelihood. This improvement will tend to reduce the probability of a large LOCA. However, the reduction in probability is difficult to estimate.

Location of Failures Within Pipes

As far as the specific locations of piping failures are concerned, it was observed that:

- 54% of the failures occurred in welds or in the weld heat affected zones (HAZ) of piping.

- 40% of the failures occurred in the pipe wall (base metal).

- 6% of the failures occurred in threaded pipe joints.

Distribution of Pipe Failure by Pipe Size

This section considers the distribution of pipe size versus failure mode and addresses the question of whether certain pipe sizes are more susceptible to certain failure modes than others. The distributions are listed in Table A.1.5 and indicate that vibration is the dominant mode of failure. Fabrication errors are next in line in terms of frequency of failures in one-inch lines. In the BWR plants, stress corrosion cracking accounts for the majority of failures in the one-to-six-inch and in the six-to-ten-inch pipe size category. Due to the small number of failures reported on pipes with a diameter greater than 10 inches, it is perhaps meaningless to consider a dominating failure mechanism for this size category.

LOCA Probability Calculation

The following points must be considered in the assessment of LOCA probabilities:

Table A.1.5

PIPE SIZE VERSUS FAILURE MODE DISTRIBUTION
FOR PIPE FAILURES WITHIN BWR PLANTS*

FAILURE MODE	PIPE SIZE CATEGORY BY DIAMETER				ROW SUM
	(≤1")	(>1",≤6")	(>6",≤10")	(>10")	
Vibration	15(53.6)**	7(17.9)	1(16.7)	0.	23
Thermal & Cyclic Fatigue	4(14.3)	3(7.7)	0	1(50.0)	8
Fabrication	6(21.4)	4(10.3)	1(16.7)	0	11
Corrosion	1(3.6)	3(7.7)	0	1(50.0)	5
Erosion	1(3.6)	7(17.9)	1(16.7)	0	9
Stress Corrosion Cracking	1(3.6)	15(38.5)	3(50.0)	0	19
Column Sums	28	39	6	2	75

*Note: The entries in this table only include the 75 failures out of 121 for which the failure mode and pipe size were both specified.
**Entries in parenthesis represent percentage of column sum.

1. Based on estimates from other sources (e.g., RSS, Bush), a pipe rupture leading to a LOCA is assessed to occur once every 10,000 plant years. With this estimated frequency and the fact that U. S. Cumulative reactor experience is only approximately 260 reactor years, it is difficult to assess the probability of a LOCA accurately by only considering LOCA-sensitive pipes because sufficient operating experience has not accrued;

2. There have been several pipe ruptures reported in high integrity piping in secondary systems of nuclear plants.

   Based upon these rupture failures, a probability of a pipe rupture failure in LOCA-sensitive piping can be estimated using the fact that LOCA-sensitive piping represents approximately 10% of the piping in a reactor plant.

3. For the calculation of small LOCA probability, several incidents of reactor system failures have occurred which can be interpreted as being similar to a small LOCA.

Figures A.1.3 presents comparisons of various estimates of pipe rupture failures from various sources. It is apparent from this figure that there is an appreciable overlap in the error bounds of the estimated pipe failure probabilities.

Based on Figure A.1.4, the probability of a large LOCA may be considered to be slightly higher than that used in WASH-1400 since there is not adequate data to support a lower value. Therefore, the values in Table A.1.6 were used.

A.1.3.3 ATWS Accident Initiators

Since ATWS events are by definition transients, the ATWS initiator frequencies are calculated by using the transient initiator frequencies, as determined in section A.1.3.1, and multiplying them by the scram failure probability. The scram failure probability used in the Limerick analysis is

A-16

the NUREG-0460 value of 3×10^{-5} per demand. This value is felt to be conservative since recent GE analysis indicates that a significantly lower probability may be appropriate.

Limerick ATWS logic will respond to ATWS events for all transient and LOCA initiators throughout the range of initial operating power levels. For the Limerick PRA, ATWS events from all power levels are treated the same, and the ATWS frequency used includes all cases.
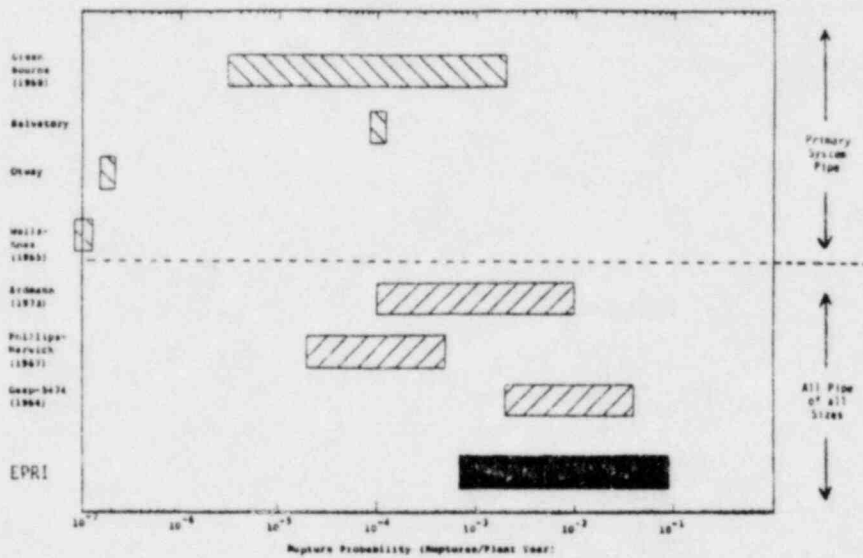
Figure A.1.3 Comparison of Evaluated Rupture Probabilities of Pipe to Estimate Nuclear Power Plant Rupture Probabilities
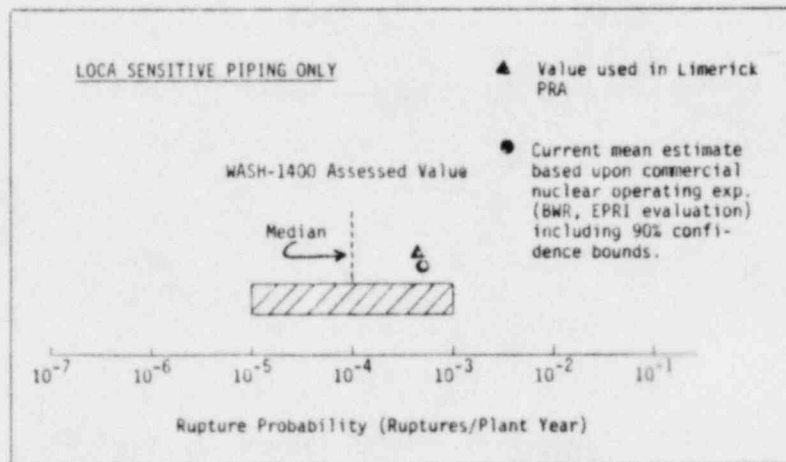
Figure A.1.4 Estimates of LOCA Initiated by A Large Pipe Break

Table A.1.6

PROBABILITY OF A LOCA

PIPE SIZE	BWR* EPRI VALUATION (MEAN)	WASH-1400 (MEDIAN)	VALUE USED IN THE LIMERICK PRA
Large Pipe $\geq 4"\phi$	7.7×10^{-4}	$1.0 \times 10^{-4**}$	4.0×10^{-4}
Medium Pipe $\geq 4"\phi$	3.0×10^{-3}	$1.0 \times 10^{-3**}$	2.0×10^{-3}
Small Pipe $\geq 1"\phi$	8.0×10^{-3}	$1.0 \times 10^{-3**}$	1.0×10^{-2}

* This probability estimate is based upon all high pressure plant piping. Since only the LOCA sensitive pipe is of concern here, the probabilities are reduced by approximately a factor of ten (LOCA sensitive piping is approximately 10% of the plant piping).

** Mean values are approximately three times larger.

REFERENCES

A.1-1   WASH-1400, Reactor Safety Study: An Assessment of Accident
         Risks in U. S. Commercial Nuclear Power Plants, U. S. NRC,
         October 1975

A.1-2   EPRI NP-801, ATWS: A Reappraisal Part III Frequency of
         Anticipated Transients, EPRI, July 1978

A.1-3   NUREG-0460, Anticipated Transients Without Scram for
         Light Water Reactors, U. S. NRC Apr. 1978 (Vol. 1,2),
         Dec. 1978 (Vol. 3)

A.1-4   WASH-1270, Technical Report on Anticipated Transients
         Without Scram for Water-Cooled Power Reactors, U. S.
         NRC, September 1973

A.1-5   ALO-78, SAI-154-79-PA, Component Failures that Lead to
         Reactor Scrams, SAI, April 1980, Also, ALO-79, SAI-180-
         80-PA, Component Failures that Lead to Manual Shutdowns,
         SAI, April 1980

A.1-6   EPRI NP-438, Characteristics of Pipe System Failures
         in Light Water Reactors, EPRI, August 1977

A.2   EQUIPMENT AND COMPONENT FAILURE RATE DATA

Accurate projections of system and plant success probabilities
in the event of an accident initiator require component data which are
directly applicable to the components of each system. The collection
and proper use of component or system failure rate data are subject to
uncertainties because of the quality of the available data. In
this study, several generic data sources plus BWR system operating ex-
perience are provided for comparison. The use of several data sources
provides a basis for the ranges of input variables that were considered
for use in the Limerick assessment.

A.2.1   Summary of Component Data Values

The component failure rate data used as input to the fault tree
model come from three basic sources:

1.   Actual nuclear plant operating experience data as reported
      to the NRC in Licensee Event Reports (LERs) have been reduced
      for the NRC and a demand failure rate evaluated for the fol-
      lowing components:

      •   Pumps (A.2-1)

      •   Diesels (A.2-2)

      •   Valves (A.2-3).

      This is referred to in the text as the NRC data.

2.   General Electric has collected and evaluated BWR operating
      experience data on a wide variety of components to estimate
      their failure rates. Since this data source is from BWRs,
      it lists specific components not readily available elsewhere
      (e.g., SRV valves, level sensors, containment pressure sensors).

3.   The WASH-1400 (A.2-4) assessed median values for failure rates
      which are based upon a combination of experience in the nu-
      clear industry and other industrial applications of compo-
      nents is also used as a source of data.

A-20

A comparison of the key component failure probabilities among WASH-1400, NRC, and GE data sources indicates general agreement; however, there are some differences. The principal differences in data are summarized in Table A.2.1.

Comparing the NRC values to the WASH-1400 base case, the pump failure probabilities are virtually the same while the valve failure rates (MOVs) are approximately three to ten times larger. In addition, the diesel generator failure rate is estimated by the NRC to be larger than that estimated in WASH-1400.

Table A.2.1

COMPARISON OF PRINCIPAL COMPONENT FAILURE
PROBABILITIES FROM THREE DATA SOURCES

Component	WASH-1400	GE	NRC
Pump	2×10^{-3}	2.8×10^{-3}	2×10^{-3}
Valves			
NCFC*	1.25×10^{-3}	0.6×10^{-3}	3×10^{-3}
NCFO*	1.25×10^{-4}	0.6×10^{-4}	$1 \times 10^{-}$
Diesels	3×10^{-2}	--	6×10^{-2}
Relief Valves	1.25×10^{-5}	3×10^{-2}**	5×10^{-3}

*NCFC - Normally Closed Fails Closed
NCFO - Normally Closed Fails Open

**Data Taken in 1968 during a time period in which a generic relief valve problem existed. The problem was subsequently corrected.

The GE estimates of component reliability can be characterized as follows relative to the other two sources:

- Somewhat (40%) higher pump failure rates

- A relatively high SRV failure rate*

- The only failure rate values available for BWR sensors

- Failure rates similar to WASH-1400 for valve failures (MOVs).

Much of the data from the three sources are similar; however, the mean values of failure rates used in WASH-1400 appear lower than mean values reported in the other two data sources mentioned above.

The following is a brief summary of the impact of various types of components on the calculated system failure probability:

Pumps: These components provide the motive force to inject coolant into the core. The pumps possess the following characteristics:

- They are required to change state (i.e., start and run for the course of the accident).

- They require 4160 Volt AC power.

- They also require DC control power.

Based upon the available sources, pumps appear to have a relatively high component failure rate. Therefore, the use of redundant pumps appears to be important.

Valves: Those valves which require a change of state are evaluated to have a relatively high probability of failure (1×10^{-3} to 3×10^{-3}). Because of this relatively high failure probability, those single train systems with the potential for active valve failures can be expected to exhibit a relatively high system unavailability.

---

*Based on data taken during a time period in which a generic relief valve problem was known to exist. The problem was subsequently corrected.

Pipe, Heat Exchangers, Pressure Containing Members: Because of
their relatively low failure rates, the probability of rupture
or flow blockage in these components during an accident sequence
has very little effect on the probabilistic quantification of the
system level fault trees. The system unavailabilities are domi-
nated by active component failures, human errors, and maintenance
outages.

Instrumentation: Instrumentation component failure rates are
relatively low. Also, the components are combined in a logic
which allows proper operation despite some failures. However,
since some instrumentation sensors may be used for actuation
of more than one safety system, a failure of the instrumentation
can lead to a failure to automatically initiate several systems.

A.2.2   Application of the Failure Rate Data

The application of failure rate data to the quantification of
the fault tree model can be done in several ways. WASH-1400 made use of
the concept of demand failure rates for the purpose of quantifying compo-
nent failures in safety systems which were in a standby status and re-
quired to begin operation following an accident initiation. A General
Electric reliability assessment of safety systems used the concept of a
constant hourly failure rate for components in standby. The probability
of failure was calculated as $1-e^{-\lambda\theta/2}$ where λ is the failure rate and θ
is the scheduled time between system tests (e.g., monthly, annually, etc.).

Table A.2.2 gives a comparison of the failure rates from three
available sources. The demand failure rates will be used to describe such
failures as:

- Pump or turbine fails to start

- Valve fails to change state (position)

- Human errors, such as miscalibration of instrumentation

- Relief valve fails to open.

A-23

Table A.2.2

FAILURE RATE DATA COMPARISON

| GENERAL GROUPING | COMPONENT | FAILURE MODE | WASH-1400 | | | GE | | NRC | | |
			MEDIAN	EF	R		R	BWR	PWR	R
VALVES	MOV (Motor operated valve)	NO FO	1×10^{-3}/d	3	A	1.6×10^{-6}/hr	B*	3×10^{-3}/d	2×10^{-3}/d	I
		NC FC	1×10^{-3}/d	3	A	1.5×10^{-6}/hr	B	1×10^{-3}/d	5×10^{-4}/d	I
		NO FC	1×10^{-4}/d	3	A	0.15×10^{-6}/hr	B			
		NC FO	1×10^{-4}/d	3	A	0.16×10^{-6}/hr	B			
	Check Valve	Fails to permit flow	1×10^{-4}/d	3	A	0.15×10^{-6}/hr	B*	1×10^{-4}/d	2×10^{-4}/d	I
		Fails to prevent flow	-	-		1.6×10^{-6}/hr	B	5×10^{-4}/d	2×10^{-4}/d	I
		Rupture, λ_s	1×10^{-8}/hr	10	A					
	Manual Valve	Failure to remain open	1×10^{-4}/d	3	A					
		Rupture, λ_s	1×10^{-8}/hr	10	A					
	Valve, Check Testable	Fails to permit flow				0.22×10^{-6}/hr	B*			
		Fails to prevent flow				2.2×10^{-6}/hr				
	ADS Depressurization Valve	Fails to operate				7×10^{-6}/hr	F			
	Solenoid Operated Valves	Failure to operate	1×10^{-3}/d	3	A					
		Failure to remain open	1×10^{-8}/hr	3	A					
		Rupture, λ_s	1×10^{-7}/hr	10	A					
	Air-Fluid Operated	Failure to operate	3×10^{-4}/d	3	A					
		Failure to remain open	1×10^{-7}/d	3	A					
		λ_s	3×10^{-7}/d	3	A					
		Rupture, λ_s	1×10^{-8}/hr	10	A					
	Relief Valves	Failure to open	1×10^{-5}/d	3	A			5×10^{-3}/d	1×10^{-3}/d	I
		Premature open	1×10^{-5}/d	3	A			4×10^{-3}/d	3×10^{-3}/d	I

Table A.2.2
(Continued)

GENERAL GROUPING	COMPONENT	FAILURE MODE	FAILURE RATES								
			WASH-1400			GE		NRC			
			MEDIAN	EF	R		R	BWR	PWR	R	
BATTERY	Battery Power Systems: (wet cell)	Failure to provide proper output, λ_s	3×10^{-6}/hr	3	C						
CIRCUIT BREAKERS	Fuses	Failure to open	1×10^{-5}/d	3	C						
		Premature open, λ_o	1×10^{-6}/hr	3	C						
	Motors Relays	Failure to energize	1×10^{-4}/d	3	C						
		Failure of NC contacts to close given energizers	3×10^{-7}/hr	3	C						
		Failure of NC contact by opening-not energizing	1×10^{-7}/hr	10	C						
		Short across NC/NC contact, λ_o	1×10^{-8}/hr	10	C						
		Coil open, λ_o	1×10^{-7}/hr	10	C						
		Coil short to power, λ_o	1×10^{-8}/hr	10	C						
	Circuit Breakers	Failure to transfer	1×10^{-3}/d	3	C						
		Premature transfer	1×10^{-6}/hr	3	C						
INSTRUMENTATION AND CONTROL	Switch contacts Relays (HFA)	Coil fails to operate	1×10^{-4}/d	10	C	0.4×10^{-6}/hr	B*				
		Coil fails to open	$3 \times 10^{-}$ /hr	10	C	0.08×10^{-6}/hr	B				
	Temperature Switch	Fails to operate				2.3×10^{-6}/hr	B*				
		Fails closed				0.33×10^{-6}/hr	B				
	Pressure Sensor (Reactor and Containment)	Fails to operate	1×10^{-4}/d	3	C	1.1×10^{-6}/hr	B*				

A-25

Table A.2.2
(Continued)

GENERAL GROUPING	COMPONENT	FAILURE MODE	FAILURE RATES							
			WASH-1400			GE		NRC		
			MEDIAN	EF	R		R	BWR	PWR	R
INSTRUMENTATION AND CONTROL** (cont.)	Flow Controler	Fail to operate				4.2×10^{-6}/hr	B*			
	Manual	Fail to transfer	1×10^{-5}/d	3	C					
	Reactor Water Level Sensor	Fail to operate				3.9×10^{-6}/hr	D			
	Limit Switch		3×10^{-4}/hr	3	C					
	Flow Switch	Failure to operate				0.26×10^{-6}/hr	B*			
	E/S Converter	Fail to operated				4.2×10^{-6}/hr	B*			
	Square Root Converter	Fail to operate				4.2×10^{-6}/hr	B*			
	Power Supply	Fail to operate				4.2×10^{-6}/hr	B*			
	Solid State Dev Hi Power App.	Fails to function, λ_o Fails shorted, λ_o	3×10^{-6}/hr 1×10^{-6}/hr	10 10	C C					
	Solid State Dev Power App.	Fails to function, λ_o Fails shorted, λ_o	1×10^{-6}/hr 1×10^{-7}/hr	10 10	C C					
	Instrumentation General (includes transmitter, amplifier and output devices)	Failure to operate, λ_o Shift in calibration, λ_o	1×10^{-6}/hr 3×10^{-5}/hr		C C					

Table A.2.2
(Continued)

| | | | FAILURE RATES | | | | | | | |
| | | | WASH-1400 | | | GE | | NRC | | |
GENERAL GROUPING	COMPONENT	FAILURE MODE	MEDIAN	EF	R		R	BWR	PWR	R
PUMPS	Pump	Fails to start	1×10^{-3}/d *	3	A	7.9×10^{-6}/hr	B*	2×10^{-3}/d	4×10^{-3}/d	H
		Fails to run (norm)	3×10^{-5}/hr	10	A			4×10^{-6}/hr	8×10^{-6}/hr	H
		Fails to run (standby)	-							
		Fails to run (post	1×10^{-3}/hr	10	A					
		Fails to run (post	3×10^{-4}/hr	10	A					
MOTORS	Motors Electric	Fails to start	3×10^{-4}/d	3	C					
		Fails to run, given start (normal)	1×10^{-5}/hr	3	C	1.0×10^{-6}/hr	B*			
		Fails to run, given start (extreme)	1×10^{-3}/hr	10	C					
PIPE	Pipe Rupture <3"	Rupture (< 3")	1×10^{-9}/hr	30	A					
	Pipe Rupture >3"	Rupture (> 3")	1×10^{-10}/hr	30	A					
HEAT EXCHANGER	Heat Exchanger	Leakage				5.7×10^{-6}/hr	E			
TURBINE/HPCI	Turbine HPCI Assy.	Fail to operate				10×10^{-6}/hr	B*			
DIESELS	Diesels (Complete Plant)	Failure to start	3×10^{-2}/d	3	C			3.2×10^{-2}/d		
		Failure to run	3×10^{-3}/hr	10	C					
		(Emergency conditions given start)	3×10^{-3}/hr	10	C					
	Diesels (Engine only)	Failure to run	3×10^{-4}/hr	10	C					
		(Emergency conditions given start)	3×10^{-4}/hr	10	C					
LUBE OIL COOLER	Lube oil cooler	Fail to operate				1.5×10^{-6}/hr	B*			

GENERAL GROUPING	COMPONENT	FAILURE MODE	FAILURE RATES							
			WASH-1400			GE		NRC		
			MEDIAN	EF	R		R	BWR	PWR	R
TRANSFORMERS	Transformers:	Open circuit, primary or secondary	1×10^{-6}/hr	3	C					
		Short primary to secondary, λ_o	1×10^{-6}/hr	3	C					
ELECTRICAL DISTRIBUTION	Wires (typical Circuits, Several Joints)	Open circuit, λ_o	3×10^{-6}/hr	3	C					
		Short to ground, λ_o	3×10^{-7}/hr	10	C					
		Short to power, λ_o	1×10^{-5}/hr	10	C					
	Terminal Boards	Open connection, λ_o	1×10^{-7}/hr	10	C					
		Short to adjacent circuit, λ_o	1×10^{-8}/hr	10	C					

*This is the "fails to run" failure rate that is used (8.1×10^{-5}/hr-mean) for HPCI.

**General Electric and PECo information on Logic and Sensor Testing indicate six-month test interval for logic and sensor testing, except for ADS which is 18 months. (Therefore, failure probability is a factor of three larger for ADS logic and sensors.)

A-28

Note: Reference Table 4.12 from GE DOCUMENT, NEDE-24809 "Probabilistic Analysis of the Reliability of BWR/4 Systems for Small LOCA Events," April 1980.

Demand failure rates are converted to failure probabilities by multi-plying by the number of demands. This applies to all situations except the HPCI fault tree, where subsequent* automatic starts are possible.

Hourly failure rates are used to describe standby systems that are subject to continuous exposure:

- Instrumentation sensors
- Pipe and pressure containing member failures.

Hourly failure rates are converted to failure probabilities for success-ful initiation of a component using the following failure probability equation. For equipment in a standby condition which can fail, the pro-bability is given by:

$$\text{failure probability} = \text{failure rate (per hour)} \times \frac{\text{exposure time**}}{2} \text{(hours)}^{+.}$$

In addition, there is a probability of failure associated with a component's failure to run for the duration of the accident analysis. For the purposes of failure probability calculations, the exposure/run time for the "accident" is taken to be 20 hours. This time is consistent with the definition of the accident sequence given in Section 1.5.

A.2.3 Comparisons of Data Evaluation Methods

There have been some efforts in recent probabilistic risk analyses to develop a formalized method of calculating the component failure rates on a plant-specific basis. These efforts have focused on the application of a Bayesian statistics approach to the use of available data.

---

*The determination of proper data input for this analysis is complicated by the fact that most applications of data assume a demand failure probability for a single start or demand. In this analysis, the potential unavailability of a system to respond to multiple demands to start is incorporated. The failure pro-bability for these subsequent demands is judged to be less than the demand failure probability for the initial start.
** Interval between tests verifying operation.
+ When failure probability is less than .1.

Probabilistic risk assessment methods allow not only determination of a best estimate frequency for various events, but also the "probability" of this frequency; that is, the frequency results can be expressed not only as an expected value, but also as a probability distribution about this expected value. Determination of the probability distribution for the failure rate parameters which describe the component behavior can be accomplished by utilizing component histories on a plant-specific basis.

The expected value of specific component failure rates as a function of various methods of data assessment were compared. Basically, two methods were investigated: Bayesian and classical statistics. The example chosen for comparison is pump failure to start on demand. Data for this event is taken from the EG&G data summary on pumps (A.2.1). This comparison used the pump experience from BWR's as given in Table A.2.3.

The methodology utilized can be found in several sources. Reference A.2.5 contains information on Bayesian methods and Reference A.2.6, classical statistics.

It is assumed for the following that all the plants in the EG&G study have an underlying pump failure probability in common. (If not, then the data of plants believed to be outliers could be discarded.) By means of some preliminary analysis, a common probability distribution model is fit to the reported pump failure data of each plant in the EG&G study. An adequate prior distribution on the parameter (s) of the model can then be chosen based on the distribution model above. As the Bayesian inference has an ingerent sequen... nature, it can be used to analyze the data of the plants successively to derive a posterior distribution representative of the current "state of knowledge" regarding pump failure probability. The model set-up required for the Bayesian inference includes:

- A prior distribution representative of our previous knowledge.

- A likelihood based on consideration of all the data

A-30

Table A.2.3

PUMP DATA FROM REFERENCE A.2-1

STANDBY PUMPS - MOTOR DRIVEN - DOES NOT OPERATE - 1/72 THRU 4/78 - WITHOUT COMMAND FAULTS

GENERAL ELECTRIC PLANTS

PLANT	CRIT.HRS.	POPULATION	DEMANDS	FAILURES	POP.HOURS	POP.DEMANDS	STANDBY HOUR RATE	DEMAND RATE
BF1	15553.0	10	57	1	155530.0	570	6.4E-06	1.8E-03
BF2	12320.0	10	45	0	123260.0	450	2.4E-05*	6.7E-03*
BF3	11545.0	10	21	0	115450.0	210	2.0E-05*	1.4E-02*
3P1	38622.0	5	76	0	193110.0	380	1.6E-05*	7.9E-03*
BR1	7544.0	8	19	1	60352.0	152	1.7E-05	6.6E-03
BR2	14576.0	8	36	0	116608.0	288	2.6E-05*	1.0E-02*
CO1	27641.0	8	49	2	221128.0	392	9.0E-06	5.1E-03
DA1	22487.0	8	48	0	179896.0	384	1.7E-05*	7.8E-03*
DR1	35600.0	8	76	3	284800.0	608	1.1E-05	4.9E-03
DR2	39390.0	11	76	0	433290.0	836	6.9E-06*	3.6E-03*
DR3	41057.0	11	76	0	451627.0	836	6.6E-06*	3.6E-03*
EN1	23634.0	6	44	0	141804.0	264	2.1E-05*	1.1E-02*
FP1	18189.0	8	41	1	145512.0	328	6.9E-06	3.0E-03
M11	39560.0	13	76	3	514280.0	988	5.8E-06	3.0E-03
HO1	44190.0	8	76	1	353520.0	608	2.8E-06	1.6E-03
NM1	41084.0	19	76	3	780996.0	1444	3.8E-06	2.1E-03
JC1	42170.0	20	76	2	843400.0	1520	2.4E-06	1.3E-03
PB2	24563.0	10	56	0	245630.0	560	1.2E-05*	5.3E-03*
PB3	22737.0	10	45	2	227370.0	450	8.8E-06	4.4E-03
PI1	31756.0	8	76	1	048.0	608	3.9E-06	1.6E-03
QC3	37446.0	8	76	1	29..8.0	608	3.3E-06	1.6E-03
QC2	39780.0	8	72	0	318240.0	576	9.4E-06*	5.2E-03*
VY1	39826.0	8	73	0	318608.0	584	9.4E-06*	5.1E-03*
TOTALS				21	6777627.0	13614		

* DENOTES UPPER 95 PERCENT CONFIDENCE BOUND WHEN NO FAILURES RECORDED

A-31

To assess the sensitivity to various priors and distribution models, the Bayesian methods were applied to the data in the following four combinations of the above two items:

1. A uniform prior* distribution: plant-specific data modeled as a binomial distribution**

2. The Reactor Safety Study log-normal distribution for pumps to fail on demand as the prior and the plant-specific data as binomial distributions

3. A "flat" prior distribution: the plant-specific data being modeled as log-normal distributions with mean and variance the same as the equivalent binomial distribution

4. Chi-square distribution (upper bound).

The results of these various assessments are given in Table A.2.4. As shown, the mean value is relatively insensitive to the method of data assessment. Moreover, those two cases which have the more consistent assumptions, Case 1 and Case 4, agree to three significant figures.

Table A.2.4

	CASE 1		CASE 2		CASE 3		CASE 4
	Prior	Data	Prior	Data	Prior	Data	Frequentist
	Flat	Binomial	RSS	Binomial	Flat	Log-Normal	
EXPECTED VALUE	1.61×10^{-3}		1.48×10^{-3}		2.01×10^{-3}		1.61×10^{-3}

* A uniform or "flat" prior distribution indicates that each failure probability value is equally likely. This generally indicates a lack of prior knowledge of the "real" distribution.

**The binomial distribution is constructed based upon the number of demands at each plant.

As shown above, the failure probability to be used in the
assessment of risk at Limerick can be estimated by a number of methods.
The above example demonstrates that data from individual plants can be
characterized by a common distribution model, and the total population
of plants combined in a Bayesian fashion, to determine a posterior dis-
tribution representing the current state of knowledge. However, it appears
from the results that this method, which may be rather time consuming,
produces point value results which are similar to the a classical statistical
approach. While the establishment of a specific method of combining com-
ponent data from various sources is desirable, there are a number of varia-
tions in the currently available basic data used in the quantification of
the accident sequences. These variations may tend to obscure any usefulness
which could be gained by establishing a rigorous method of combining existing
data. These potential variations in the data are due to such items as:

1. Lack of specificity as to the function/type of component
   (e.g., main circulating water pump or RHR pump). All
   types of pumps are treated together because of the very
   small population available.

2. Age of the components is generally not considered.

3. Variations which occur among different manufacturers
   are not included in the LER reporting scheme.

4. Local plant test and maintenance procedures, training
   programs, and management/personnel factors may vary.

Compared with variations arising from the above listed items which may
be encountered at a specific plant, the calculated "expected values" from
Table A.2.4 show very small differences which do not warrant an extensive
Bayesian analysis. See Appendix F for further discussion of the statisti-
cal treatment used in the analysis.

References

A.2.1   W. H. Sullivan and J.P. Poloski, <u>Data Summaries of Licensee Event Reports of Pumps at U.S. Commercial Nuclear Power Plants January 1972 to April 1978,</u> prepared for U.S. Nuclear Regulatory Commission by EG&G. NUREG/CR-1205, January 1980.

A.2.2   J.P. Poloski and W.H. Sullivan, <u>Data Summaries of Licensee Event Reports of Diesel Generators at U.S. Commercial Nuclear Power Plants - January, 1976 to December 31, 1978,</u> prepared for U.S. Nuclear Regulatory Commission by EG&G. NUREG/CR-1362 March 1980.

A.2.3   Warren H. Hubble and Charles F. Miller, <u>Data Summaries of Licensee Event Reports of Valves at U.S. Commercial Nuclear Power Plants - January 1, 1976 - December 31, 1978,</u> prepared for U.S. Nuclear Regulatory Commission by EG&G. NUREG/CR-1362 June 1980.

A.2.4   Reactor Safety Study: <u>An Assessment of Accident Risks in U.S. Commercial Nuclear Power Plants,</u> U.S. NRC. WASH-1400.

A.2.5   <u>IEEE Transactions on Reliability</u>, Vol. R-21, No.3, August 1972. (The whole issue deals with Bayesian Questions.)

A.2.6   A. Hald, <u>Statistical Theory With Engineering Applications</u>, John Wiley and Sons, Inc., 1952.

A.3   HUMAN FAILURE RATE DATA

        The safety systems provided in boiling water reactors to
prevent and mitigate accidents are generally designed to operate auto-
matically during the initial states of accident sequences. Information
on the conditions in the reactor and on the operation of the safety
systems during an accident would be displayed in the control room so
that the operator would be able to follow the sequence of events, but
no direct human action would usually be required until the accident were
brought automatically under control. However, human intervention would
be required in case of malfunctions in the automatic systems, and human
interaction with the system exists in routine plant operation, testing,
and maintenance. Therefore, human reliability plays a very large role
in safety system reliability.

        Although data on human reliability are sparse and difficult to
apply to specific situations, many attempts along these lines have been
published, usually using subjective estimates by experts in related fields.
Section A.3.1 discusses some of the factors that effect human failure rates.
A brief summary of several data sources, in particular the Handbook of Human
Reliability by Swain and Guttman, is given in Section A.3.2. Finally, data
and evaluations used for the Limerick analysis appear in Section A.3.3.

A.3.1   General Discussion of Causes of Human Error

        Many causes and preventions of human errors must be considered
in order to obtain a reasonable estimate of human failure rates. Some
of the major considerations are:

        •   Plant design

        •   Training and experience

        •   Procedures

        •   Stress.

The following discussion of these items outlines the consid-
erations which have been incorporated in the Limerick assessment to
determine the effect of human error on each accident sequence.

Plant Design: Some reactor control rooms may have potentially
confusing arrangements and labeling of controls. In particular, many
labels are very long and differ in only a few letters or digits. This may
leads to fairly high error rates for manipulating the wrong switch when
controls and displays are close together without separation by functional
flow lines on the panels, especially in emergency conditions. WASH-1400
found that the control arrangements in the plants it studied deviated from
human engineering standards such as those used in the military. Errors
can also be increased due to multiple alarms (several alarms due to one
cause) that confuse the true cause. Human error rates for Limerick are
not subject to high failure rates due to this cause because of improved
plant design such as functional flow lines, annunciators for locked valves,
and improved testing options.

Training and Experience: WASH-1400 stated that the training
of nuclear plant personnel was outstanding, thereby assuming high re-
liability for routine maintenance, calibration, and control room opera-
tion. However, WASH-1400 found that operators were not able to "talk
through" appropriate emergency procedures without hesitation or inde-
cision. This led to the assumption of less reliability in major emer-
gencies. An additional point concerns experience. Although experience
leads to improvement, it can also increase error. For example, a tech-
nician or operator may become so used to seeing a correct instrument
reading that when an out-of-tolerance condition occurs, he may still
"see" the correct reading.

Procedures: Written procedures such as check lists are a
definite aid in human reliability. However, WASH-1400 found that the
written instructions do not conform to established principles of good

writing; they are more typical of military maintenance procedures of approximately 20 years ago. WASH-1400 also found poor printing quality, inappropriate indexing, and poor format which could contribute to potential human error. Check lists are also not always used correctly; some operators or technicians will perform several tasks and then check them all off instead of checking each task as performed. This may be partially prevented and the reliability improved by using checklists that require information (such as a meter reading) to be written down. Additional reliability may be obtained through   verification (a second person verifying that the performance of the first person is correct).

Stress: Reported data on stress and human behavior indicate that the error rate for a task has a relationship to the stress level perceived by the operator. A hypothetical relationship is shown in Figure A.3.1.
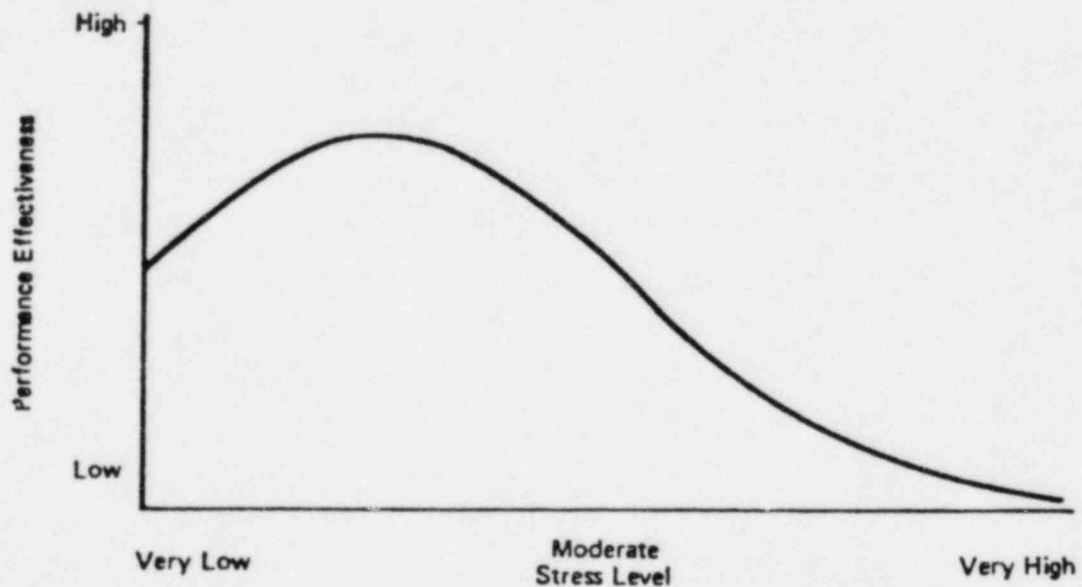

Figure A.3.1. Hypothetical Relationship Between Performance and Stress

A-37

As shown, when stress is low, a task is so dull and unchallenging that most operators would not perform at their optimal level. Passive-type inspection tasks are often of this type and can be associated with error rates of .5 or higher. When the stress level of a job is somewhat higher (high enough to keep the operator alert), optimum performance levels are reached. WASH-1400 determined that control room, maintenance, and calibration jobs were sufficiently challenging to maintain moderate stress and therefore maximum performance. When stress levels are still higher, performance begins to decline again, this time due to the effects of worry, fear, or other psychological responses to stress. At the highest level of stress, human reliability would be at its lowest level. WASH-1400 obtained a value of .2 to .3 as the average error rate for nuclear power plant personnel in a (continuing) high-stress situation such as the time following a large LOCA. This was considered to be conservative and variable for different situations.

Following a major accident, human error would be even higher than the high-stress value due to a probable incredulity response. Since the probability of a major accident is so small, for some moments a potential response would be to disbelieve panel indicators. Under such conditions, especially if false alarms had occurred frequently in the past, no action might be taken at all for at least one minute, and if any action were taken it would likely be inappropriate. WASH-1400 assessed that the error rate is .9 five minutes after an accident, .1 after thirty minutes, and .01 after several hours (Figure A.3.2). It was estimated that by 7 days after an accident there would be a complete recovery to normal, steady-state error rates. These values are based on the assumption that the nuclear plant is appropriately brought under control. For those cases where the situation persists or becomes worse, Swain (A.3-2) suggests that the error rate levels off at .25 after the initial peak.

A.3.2   Sources of Data

There are many sources of estimated human failure rates, but most are too specific or too general to allow easy comparison or averaging of values. Some of these data sources are presented here:

WASH-1400: The WASH-1400 Human Error Rate estimates were obtained from a variety of data sources, mostly non-nuclear, but in fields with similar tasks. Table A.3.1 was then derived by the independent judgments of two human reliability analysts* based on knowledge of various factors such as plant design, training, procedures, and stress. The two specialists attempted to avoid underestimating or overestimating the error rates.
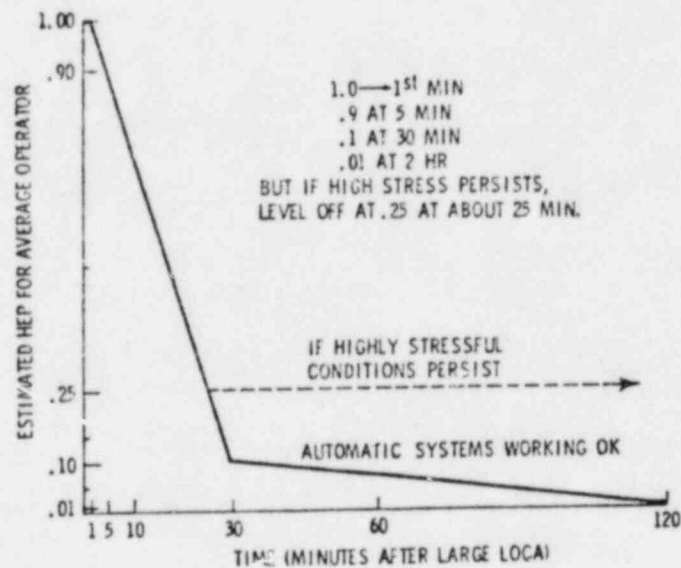

Figure A.3.2   Estimated Human Performance After a Large LOCA

---

*Alan D. Swain and Henry E. Guttmann

Table A.3.1

GENERAL ERROR RATE ESTIMATES[a,b]*

Estimated Rates	Activity
10^{-4}	Selection of a key-operated switch rather than a non-key switch (this value does not include the error of decision where the operator misinterprets a situation and believes key switch is correct choice).
10^{-3}	Selection of a switch (or pair of switches) dissimilar in shape or location to the desired switch (or pair of switches), assuming no decision error. For example, operator actuates large handled switch rather than small switch.
3×10^{-3}	General human error of commission, e.g., misreading label and therefore selecting wrong switch.
10^{-2}	General human error of omission where there is no display in the control room of the status of the item omitted, e.g., failure to return manually operated test valve to proper configuration after maintenance.
3×10^{-3}	Errors of omission, where the items being omitted are embedded in a procedure rather than at the end as above.
3×10^{-2}	Simple arithmetic errors with self-checking but without repeating the calculation by redoing it on another piece of paper.
$1/x$	Given that an operator is reaching for an incorrect switch (or pair of switches), he selects a particular similar appearing switch (or pair of switches), where x = the number of incorrect switches (or pair of switches) adjacent to the desired switch (or pair of switches). The 1/x applies up to 5 or 6 items. After that point, the error rate would be lower because the operator would take more time to search. With up to 5 or 6 items, he doesn't expect to be wrong and therefore is more likely to do less deliberate searching.
10^{-1}	Given that an operator is reaching for a wrong motor operated valve MOV switch (or pair of switches), he fails to note from the indicator lamps that the MOV(s) is (are) already in the desired state and merely changes the status of the MOV(s) without recognizing he had selected the wrong switch(es).
~1.0	Same as above, except that the state(s) of the incorrect switch(es) is (are) not the desired state.
~1.0	If an operator fails to operate correctly one of two closely coupled valves or switches in a procedural step, he also fails to correctly operate the other valve.
10^{-1}	Monitor or inspector fails to recognize initial error by operator. Note: With continuing feedback of the error on the annunciator panel, this high error rate would not apply.
10^{-1}	Personnel on different work shift fail to check condition of hardware unless required by checklist or written directive.
5×10^{-1}	Monitor fails to detect undesired position of valves, etc., during general walk-around inspections, assuming no checklist is used.
.2 - .3	General error rate given very high stress levels where dangerous activities are occurring rapidly.
$2^{(n-1)}x$	Given severe time stress, as in trying to compensate for an error made in an emergency situation, the initial error rate x, for an activity doubles for each attempt, n, after a previous incorrect attempt, until the limiting condition of an error rate of 1.0 is reached or until time runs out. This limiting condition corresponds to an individual's becoming completely disorganized or ineffective.
~1.0	Operator fails to act correctly in the first 60 seconds after the onset of an extremely high stress condition, e.g., a large LOCA
9×10^{-1}	Operator fails to act correctly after the first 5 minutes after the onset of an extremely high stress condition.
10^{-1}	Operator fails to act correctly after the first 30 minutes in an extreme stress condition.
10^{-2}	Operator fails to act correctly after the first several hours in a high stress condition.
x	After 7 days after a large LOCA, there is a complete recovery to the normal error rate, x, for any task.

[a] Modification of these underlying (basic) probabilities were made on the basis of individual factors pertaining to the tasks evaluated.

[b] Unless otherwise indicated, estimates of error rates assume no undue time pressures or stresses related to accidents.

* Taken from WASH-1400

Nuclear Experience Data: Fullwood and Gilbert (A.3-3, A.3-4) used data reported to the NRC under the requirements of Regulatory Guide 1.16 in the form of all BWR and PWR citations in the Nuclear Safety Information Center (Oak Ridge, TN) up to the time of the search. There were 7,038 citations for LWRs, which were individually read to avoid misclassifications, and 1,490 or 21% contained identifiable human errors. Of this number, only 28 or 1.9% of the human factors citations were for compound human error. These events were grouped as appeared natural to the event descriptions.

The accumulated experience represented in the reports for 61 plants was 260 plant-years. The unprocessed categorization of data is presented in Table A.3.2. By using data on the number of people involved in various operational phases and making estimates as to task frequency, the data of Table A.3.2 were normalized and are presented in Table A.3.3.

Human Reliability Handbook: Swain and Guttmann have prepared a handbook to aid in analyzing the reliability of human actions in a power plant. This handbook explains the basic terms, performance-changing factors, and human performance models. It also provides numerous examples of the application of analysis methods. Table A.3.4 summarizes some of the derived Human Error Probabilities (HEPs) for tasks in a nuclear plant. It should be pointed out that these data are not from objective observations, but instead are estimated from related (sometimes only marginally so) measurements of human performance. In general, Swain's handbook contains such a large amount of information on human failures that there may be several interpretations of the data or methods used to apply the data. Each interpretation may result in a different failure probability.

Table A.3.2

UNITED STATES NUCLEAR POWER PLANT EXPERIENCE CATEGORIZED BY TYPE OF HUMAN ERROR*

	Maintenance error	Failure to comply/complete procedure	Incorrect Instrument settings	Incorrect procedural sequence	Incorrect instrument used	Judgmental error	Misunderstanding of task	Communications failure	Failure to respond to alarm	Unidentified operator error	Clerical error	Administrative error	Procedural Deficiency	Analysis error	Design error	Fabrication error	Installation error	TOTALS
Reactor Type	340	277	137	40	29	43	26	9	28	27	15	48	53	27	193	77	121	
PWR	172	150	69	22	14	24	10	5	20	10	4	35	32	17	130	53	70	837
BWR	168	127	68	18	15	19	16	4	8	17	11	13	21	10	63	24	51	653
Reactor Mfg																		
AC	9	4	5	3	3	2	–	–	–	3	–	–	1	–	4	2	–	36
B&W	42	36	20	11	5	10	3	–	5	3	1	14	12	5	34	14	16	231
CE	20	19	9	4	2	5	2	–	2	–	1	8	4	1	32	9	18*	136
GE	159	123	63	15	12	17	16	4	8	14	11	13	20	10	59	22	51	617
WEST	110	95	40	7	7	9	5	5	13	7	2	13	16	11	64	30	36	470
Reactor Function Mode																		
Unknown or N/A	133	115	40	13	18	22	11	5	11	24	12	33	29	22	76	30	48	642
Preoperational	3	5	1	1	1	1	–	–	1	–	–	6	2	–	26	22	21	90
Operating unknown level	7	20	13	5	3	7	–	3	6	1	1	–	3	6	6	–	2	77
Startup	11	25	9	7	2	3	3	–	4	–	–	1	2	1	6	3	7	84
Run	112	72	48	7	2	7	10	2	5	1	3	6	12	4	49	10	26	376
Standby	3	2	–	–	1	–	–	–	1	–	–	–	–	–	–	–	1	8
Shutdown	46	27	20	4	2	6	2	2	1	–	–	3	6	–	24	7	14	164
Refueling	27	11	7	3	1	1	–	1	1	1	–	–	3	–	8	5	8	77
Totals	342	277	138	40	30	47	26	13	30	27	16	49	57	27	195	77	127	
Ranking	1	2	4	10	11	9	15	17	12	13	16	8	7	14	3	6	5	

A-42

*Reference A.3.2

Table A.3.3

ASSESSMENT OF HUMAN FAILURE RATES FROM
UNITED STATES POWER REACTOR EXPERIENCE*

Item No.	Error Type	Events	Personnel/ Reactor-Year	Error Rate Per Man-Year	Error Rate Per Task
1	Maintenance	342	1368	2.5×10^{-1}	1.4×10^{-3}
2	Failure to Comply/ Complete	277	6156	4.5×10^{-2}	1.8×10^{-4}
3	Design	195	8291	2.4×10^{-2}	1.2×10^{-4}
4	Incorrect Settings	138	1368	1.0×10^{-1}	6.2×10^{-4}
5	Installation	127	1.9×10^{4}	6.7×10^{-3}	1.3×10^{-4}
6	Fabrication	77	1.9×10^{4}	4.1×10^{-3}	7.9×10^{-5}
7	Procedural Deficiency	57	6156	9.3×10^{-3}	3.8×10^{-5}
8	Administrative	49	6156	8.0×10^{-3}	3.2×10^{-5}
9	Judgmental	47	6156	7.6×10^{-3}	3.0×10^{-5}
10	Incorrect Sequence	40	6156	6.5×10^{-3}	2.6×10^{-5}
11	Wrong Instrument	30	1368	2.2×10^{-3}	1.4×10^{-5}
12	Failure to Respond	30	6156	4.9×10^{-3}	2.0×10^{-5}
13	Unspecified Operator Error	27	6156	4.4×10^{-3}	1.8×10^{-5}
14	Analysis	27	6156	4.4×10^{-3}	1.8×10^{-5}
15	Misunderstanding	26	6156	4.2×10^{-3}	1.7×10^{-5}
16	Clerical	16	6156	2.6×10^{-3}	1.1×10^{-5}
17	Communications	3	6156	4.9×10^{-4}	2.0×10^{-6}
18	Compound Personnel Errors	28	6156	4.5×10^{-3}	1.8×10^{-5}

*Reference A.2

Table A.3.4

HEPS FOR SELECTED TASKS ABOUT A NUCLEAR POWER PLANT*

Task	HEP
Walkaround inspections. Failure to recognize an incorrect status, using checklist correctly.	.01 (.003 - .03)
Walkaround inspections. Failure to recognize an incorrect status, using checklist incorrectly.	.1 (.05 - .5)
Walkaround inspections. Failure to recognize an incorrect status, no checklist. First walkaround.	.9 (.5 - .99)
Failure to use checklist correctly.	.5 (.1 - .8)
Failure to follow established policies or procedures.	.01 (.003 - .03)
Passive inspection.	.1 (.02 - .2)
Failure to respond to an annunciator (1 of 1).	.0001 (.00005 - .001)
Read annunciated lamp.	.001 (.0003 - .003)
Read digital display	.001 (.0003 - .003)
Read analog meter	.003 (.001 - .01)
Read analog chart recorder	.006 (.002 - .02)
Read a graph	.01 (.003 - .03)
Read printing recorder (cluttered)	.05 (.01 - .2)
Record more than 3 digits	.004 (.001 - .01)
Arithmetic errors	.03 (.01 - .1)
Failure to detect a deviant analog display during initial audit (with limit marks)	.001 (.003 - .003)
Check-read specific meters with limit marks	.001 (.0003 - .003)
Check-read specific meters without limit marks.	.001 (.0003 - .003)
Check wrong indicator lamp in a group of similar lamps.	.003 (.001 - .01)
Failure to note incorrect status of an indicator lamp (in a group)	.99 (.97 - .997)
Failure to note incorrect status of a legend lamp (in a group)	.98 (.94 - .994)
Failure to remember oral instructions, 1 of 1	.001 (.0003 - .03)
Select wrong panel control:	
a. Among a group of similar controls	.003 (.001 - .03)
b. If functionally grouped	.001 (.0003 - .03)
c. If part of a mimic type panel	.0005 (.00005 - .005)
Set a multiposition switch	.001 (.0001 - .1)
Mate a connector	.01 (.001 - .05)

*Reference A.3.2

A-44

Table A.3.4 (continued)

Task	HEP
Failure to initiate task	.001 (.0005 - .005)
Turn control in wrong direction:	
a. If no violation of population sterotype	.0005 (.0005 - .005)
b. If populational sterotype is violated	.01 (.005 - .1)
Select manual valve from a group of similar valves	.005 (.002 .02)
Omission errors*	
Each item on a short list**, using checkoff	.001 (.0001 - .05)
Each item on a long list, using checkoff	.003 (.0008 - .01)
Each item on a short list, not using checkoff	.003 (.0008 - .01)
Each item on a long list, not using checkoff	.01 (.003 - .03)
Read value from indicator lamps used as quantitative display	.001 (.0005 - .01)

*Omission errors include steps in any kind of procedure, valve operations, switching operations, locking of valves, etc.

**Short list - 10 items or less; long list - more than 10 items.

Other Data Sources: There are many other sources of data for specific activities, such as the human reliability assessments from work related to the aerospace industry given in Table A.3.5 (A.3-5).

Some experimental data has also been taken from controlled situations. Green (A.3-6) used a device to measure the time taken to respond to a simulated alarm signal superimposed over normal control room tasks. This device required a well-specified response to a clearly defined but random occurring stimulus. These experiments showed a log-normal cumulative distribution with a 0.5 probability of success occurring at 0.9 sec., and a standard deviation of 0.3 sec. when the stimulus rate was 1.5/hour (a lower activity rate gave a longer time for the same response correctness). An example of the data obtained is shown in Figure A.3.3.

A.3.3   Evaluations Prepared for Limerick

The Limerick analysis used the WASH-1400 stress situation error
probabilities for most of the human failure rates relating to actions
required during the course of an accident. These are repeated here (see
also Figure A.3.2):

Action required within:	Probability of error
1 minute	1.0
5 minutes	.9
30 minutes	.1
Several hours	.01
7 days	Normal error probability

Most of the other human failure probabilities were based on
evaluations similar to those found in Swain's Handbook of Human Reliabi-
lity. Some examples of these evaluations are given in the following
subsections.

A.3.3.1   Miscalibration of Four Level Sensors During Regularly
           Scheduled Maintenance for Which a Procedure Exists

This example is an extension of an example evaluated explicitly
in Swain's Handbook*. The probability that the technician would miscali-
brate all four sensors independently is negligible, so an estimate of
the common-mode failure is needed. The dominant common-mode failures are
judged by Swain to be due to a faulty setup, such as using the wrong
scale or connecting at an incorrect point. An estimate of this probability

*Pages 7-22.

Table A.3.5

SELECTED ITEM FROM HUMAN RELIABILITY
ASSESSMENTS IN AEROSPACE ACTIVITIES*

Task or Task Element	Failure Probability/Task (10^{-3})
Remove 40 nuts and bolts from perimeter using ratchet wrench.	2.5
Raise missile container cover by means of handling equipment.	2.1
Pull out two splines.	1.0
Remove semicircular metal ring.	0.7
Connect 4 electrical connectors between aircraft and launcher	2.9
Connect 6 quick-disconnect hydraulic connections between aircraft and launcher.	2.8
Connect 2 Marmon clamps on two air hoses between aircraft and launcher.	1.4
Operatore selector valve controls on trailer to lower adapter.	3.0
Hoist: Operate hand pump to raise missile-nylon until forward alignment pins engage holes (release brakes) and aft attach fitting is seated in link. Permit only tapered portion of pins to engage	4.2
Torque bolts, left forward attach, _____ to _____ inch-pounds.	3.3
Torque bolts, right forward attach, _____ to _____ inch-pounds.	3.3
Connect APU power cables to trailer using power cable adapter.	1.3
Operate 5 levers, to raise missile within 6" of position	7.2
Actuate power toggle switch (1 of 1).	0.2
Monitor power-on indicator (1 of 1).	0.3
Push lamp test button (1 of 1).	0.2
Monitor 4 indicator lights: "PDU Ready," "Load Oper Tape," "Start", and "Self Test" (4 of 10).	1.7
Turn rotary switch on panel to "AV" position	0.4
Observe 5 indicator lights, illuminate followed by extinguishing on warmup.	1.1
Crank tilt lift control, using ratchet wrench, until pins are completely seated.	4.9
Position 5 levers, 2 simultaneously, to lower trailer and cradle/missile approximately 12"	6.8
Monitor multimeter indicator needle for lack of movement.	0.6
Turn hydraulic selector valve to wheel cylinder position.	0.7
Operate hand pump carefully, until end of trailer rails are just above level of mated rail joint.	8.3

*Reference A.3.5

Task or Task Element	Failure Probability/Task (10^{-3})
Slip protective cover (round, aluminum, with handle; silicon rubber seal) over missile body.	1.1
Tighten Marmon clamp on cover, using standard socket drive.	0.7
Install magnetic tape.	2.1
Remove magnetic tape.	0.8
Connect oscilloscope to test adapter group	2.5
Turn on oscilloscope, observe waveform and compare with T.O. value	17.2
Disassemble 2 electrical connectors (1 at each end of harness) and remove insert.	4.3
Remove insullation from wire (each end), to prepare wire for crimping.	1.2
Disassemble electrical connector and remove insert.	2.9
Loosen "starboard" coolant line hose clamps (2) and remove "starboard" coolant line hose to the umbilical.	1.3
Tighten coolant hose clamps (2).	0.6
Unsolder and replace small electronic part.	9.2
Resolder loose electrical connections.	8.3
Find test point (unlabeled) by referring to schematic diagram.	50.4
Determine defective circuit card by reading schematic diagram (all relevant symptoms known)	70.4
Remove and replace faulty circuit cards (2 cards united by a sealed electrical connector).	4.5
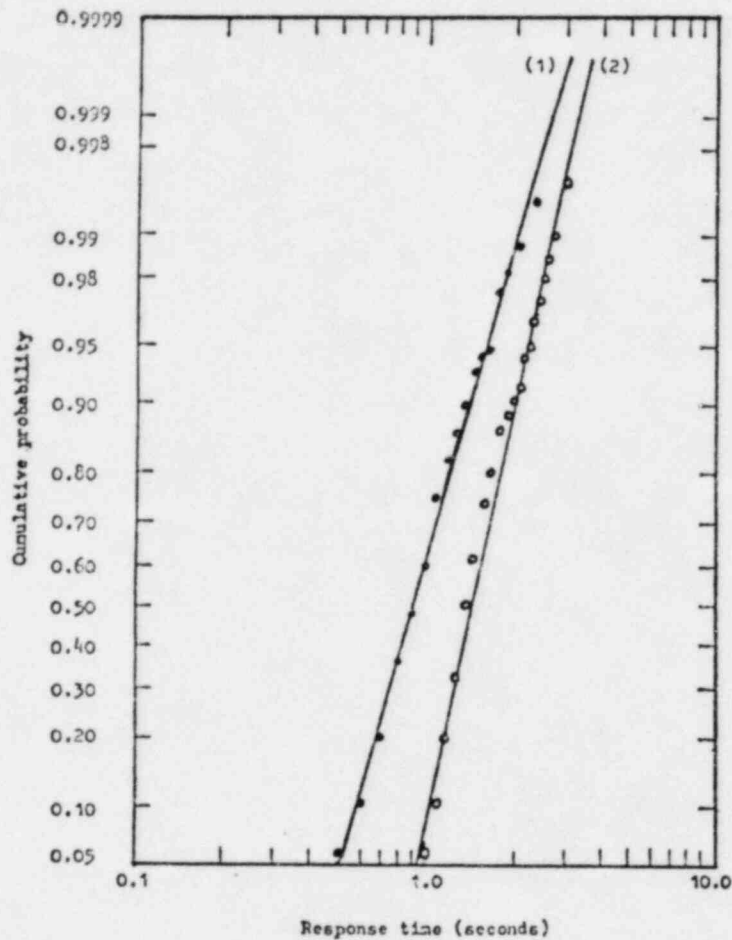
Figure A.3.3. Operator Response Tests in Reactor Control Room

is 10^{-2}. It is further assumed that half of the time this error leads to small (not unusual) miscalibrations on all future measurements, and half of the time it leads to large (very unusual) miscalibrations. Recovery of the setup error is entered into the estimate as follows: it was reasoned that when the technician discovered a small miscalibration of the first sensor, he would change the calibration. It was further reasoned that when the second sensor was also incorrect by a small amount, 30% of the time he would be suspicious and would recheck the setup. If the technician was not suspicious and the third sensor also had a small miscalibration, then 50% of the time he would become suspicious and recheck the setup. Finally, it is assumed that if the technician had not yet discovered the error, then he would not become suspicious after the fourth sensor. Similarly, if the test setup led to a large miscalibration error, the technician would recheck the setup 90% of the time after the second, and 99.9% of the time after the thrid. Again, if the technician did not discover the error after the first three sensors, he would also err on the fourth. The final assumption is that if the technician rechecked the setup, he would find the error and make the appropriate correction.

Using the probability tree in Figure A.3.4, the probability of miscalibrating all four sensors is approximately 2×10^{-3}.

S = success*
F = failure
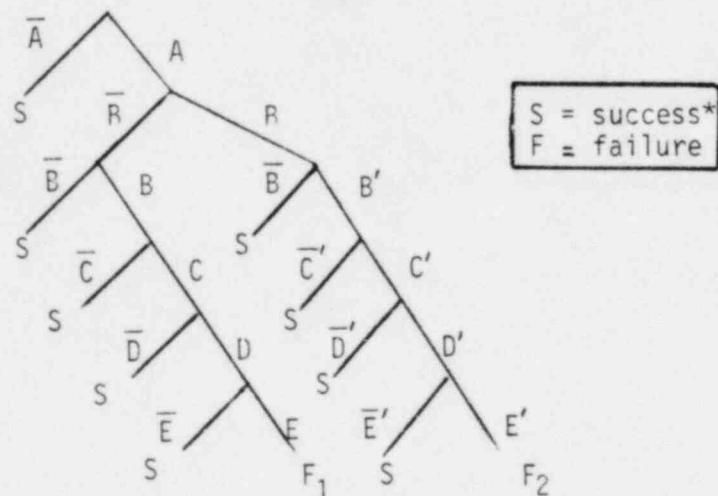
*Key is on next page.

Figure A.3.4 Human Error Probability Tree
Describing Sensor Miscalibration

A-50

(Key to Figure A.3.4)

A: Probability that equipment is set up incorrectly = .01

R: Probability that error is large   = .5

B: Probability of not being suspicious after 1st small msicalibration = 1.0

C: Probability of not being suspicious after 2nd small miscalibration = 0.7

D: Probability of not being suspicious after 3rd small miscalibration = 0.5

E: Probability of not being suspicious after 4th small miscalibration = 1.0

B′: Probability of not being suspicious after 1st large miscalibration = 0.1

C′: Probability of not being suspicious after 2nd large miscalibration = 0.01

D′: Probability of not being suspicious after 3rd large miscalibration = 0.001

E′: Probability of not being suspicious after 4th large miscalibration = 1.0.

The probability of failure (miscalibrating all four sensors due to
incorrect setup) is:

$$P(F_1)+P(F_2)=[A x \bar{R} x B x C x D x E]+[A x R x B' x C' x D' x E']$$

$$=[.01x.5x1.0x.7x.5x1.0]+[.01x.5x.1x.01x.001x1.0]$$

$$= .0018 + 5x10^{-9}$$

$$\approx 2x10^{-3}$$

A-51

A.3.3.2 Operator Fails to Manually Initiate One Automatic Safety
System Under Scram Conditions (Within 30 Minutes)

Swain's handbook includes an example of manual switching from
normal feedwater to auxiliary feedwater on a reactor trip signal. In
Table 21-1 of Swain's handbook, he obtained a probability of 10^{-3} for
failure to make the change within 30 minutes when no operator is dedi-
cated to that job. This probability value takes into account the arrival
of the shift supervisor, and assumes special orders for initiation. For
more general cases, the operator may choose the incorrect safety system
with probability 10^{-3}. Using Figure A.3.5, the probability of failure to
initiate a safety system is assessed to be 2×10^{-3}.
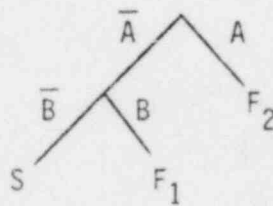
A: Probability of not responding   = 10^{-3}

B: Probability of not incorrect response = 10^{-3}

Figure A.3.5 Human Error Probability Tree Describing
Failure to Initiate One Safety System

Probability of failure (failing to initiate a safety system):

$$= F_1 + F_2 = \overline{A} \times B + A$$
$$= (1-10^{-3}) \times 10^{-3} + 10^{-3}$$
$$\approx 2 \times 10^{-3}$$

This evaluation is used for Limerick analyses for cases of normal transients and small LOCAs   where it is presumed that minimal stress exists on the operator. For other, more stressful situations, the WASH-1400/Swain stress curve is used to establish the time-dependent operator behavior.

A.3.3.3   Operator Fails to Manually Initiate the Second Safety
           System Under Scram Conditions (Within 30 Minutes)

The handbook assumes that initiation of the first and second safety system is cued by the same or similar indications. The conservative assumption is made that failure to initiate the first system implies that the operator will not respond to the second, either. Similarly, it is assumed that if the operator initiates the first safety system, he will respond to the indication for the second with certainty. Thus, the probability of not responding to the indications of the second safety system is 10^{-3}.

Similarly, the probability for the operator to make an incorrect response is 10^{-3} and we can compute the probability of failure to initiate the second safety system can be computed as follows:

$$10^{-3}+(1-10^{-3})\times10^{-3}\approx2\times10^{-3}$$

A.3.3.4   Initiate a Normal Plant Function Following a Reactor Scram

The annunciator response model of Table 20-4 in Swain is used. It is assumed that the operator may tend to focus on other displays, so the failure probability of initiating a normal plant function within a certain length of time is higher than that for initiating the safety systems. The probabilities are:

Failure to Initiate Within:	Human Error Probabilities
20 min.	.25
2 hrs.	.025
20 hrs.	.025

A.3.3.5   Turn Off Emergency System

An error-of-commision involving emergency systems cannot be
assigned a probability using the techniques of the Swain handbook. As a
gross estimated, the basic error-of-commission probability of 0.001 can
be used. This number should be doubled for stressful situations. The
Limerick analysis does not explicitly valuate accident scenarios involving
errors-of-commission by the operator.

A.3.3.6   Open a Single Manual Valve Within 30 Minutes

The failure probability of not properly opening a single manual
valve is 0.02 under stressful conditions such as a 30 minute time limit.
The probability of selecting the wrong manual valve from a group of similar
valves is 0.01 under stress, and the probability of the valve failing is 0.001.
In addition, the operator may fail to notice that the valve failed (probability
0.02, again under stress). Using the probability tree given in Figure A.3.6,
the probability of failing to open the manual valve is determined to be 0.03.
However, in reality, the manual valve may be some distance from the control room.
Because of this, plus the time required to reach the decision that the valve
must be open (especially if the operator does not have clear indication
that the valve needs to be opened), the error probability is often taken
to be approximately .9 to 1.0.

A Ā A

B̄ B F₁

C̄ C F₂

S D̄ D

S F₃
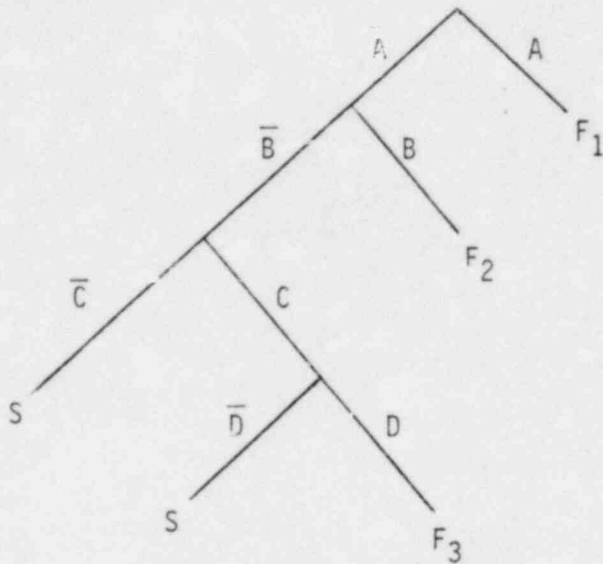
A: Probability that the operator does not follow procedure (stress) = .02

B: Probability that the operator selects incorrect valve from group (stress) = .01

C: Probability that the valve fails = .001

D: Probability that the operator fails to notice and to correct the failed valve (stress) = .02

Probability of failure (valve is not opened) =

$$F_1 + F_2 + F_3 = A + (\bar{A} \times B) + (\bar{A} \times \bar{B} \times C \times D)$$

$$= .02 + (.98 \times .01) + (.98 \times .99 \times .001 \times .02)$$

$$\approx .03$$

Figure A.3.6   Human Error Probability Tree Describing Failure
to Open Single Manual Valve

A.3.3.7 Ensure Valves Are in Correct Line-up

The failure of an operator to return both of two manual valves to the correct position is discussed as example 1.5 in Chapter 21 of Swain's handbook. Two major types of error are possible: (1) neglecting to reposition a valve following a TCIT; and (2) not opening a valve completely.

The handbook assumes that the line-up is scheduled using tags and checked by a second operator. The scheduled activity is regarded as an oral instruction, with a probability of .001 for failure of an operator to initiate the task. With only two valves, the probability of failure to restore the second valve is .003.

The probability of a valve failing is assumed to be .001, and the probability that an operator corrects for the failure is .01. According to Swain, the probability of a checking operator to make the same mistakes as the first operator is 10 times larger.

Using the probability tree given in Figure A.3.7, the probability of not ensuring the correct line-up is approximately .0001.

Given the events shown in Figure A.3.7, the probability of failure (both valves not lined-up) is:

$$= F_1 + F_2 + F_3$$

$$= (A \times A) + (\bar{A} \times B \times B^1) + (\bar{A} \times \bar{B} \times C \times D \times D^1)$$

$$= (.001 \times .01) + (.999 \times .003 \times .03) + (.999 \times .997 \times .001 \times .01 \times .1)$$

$$\approx .0001$$

S = success
F = failure
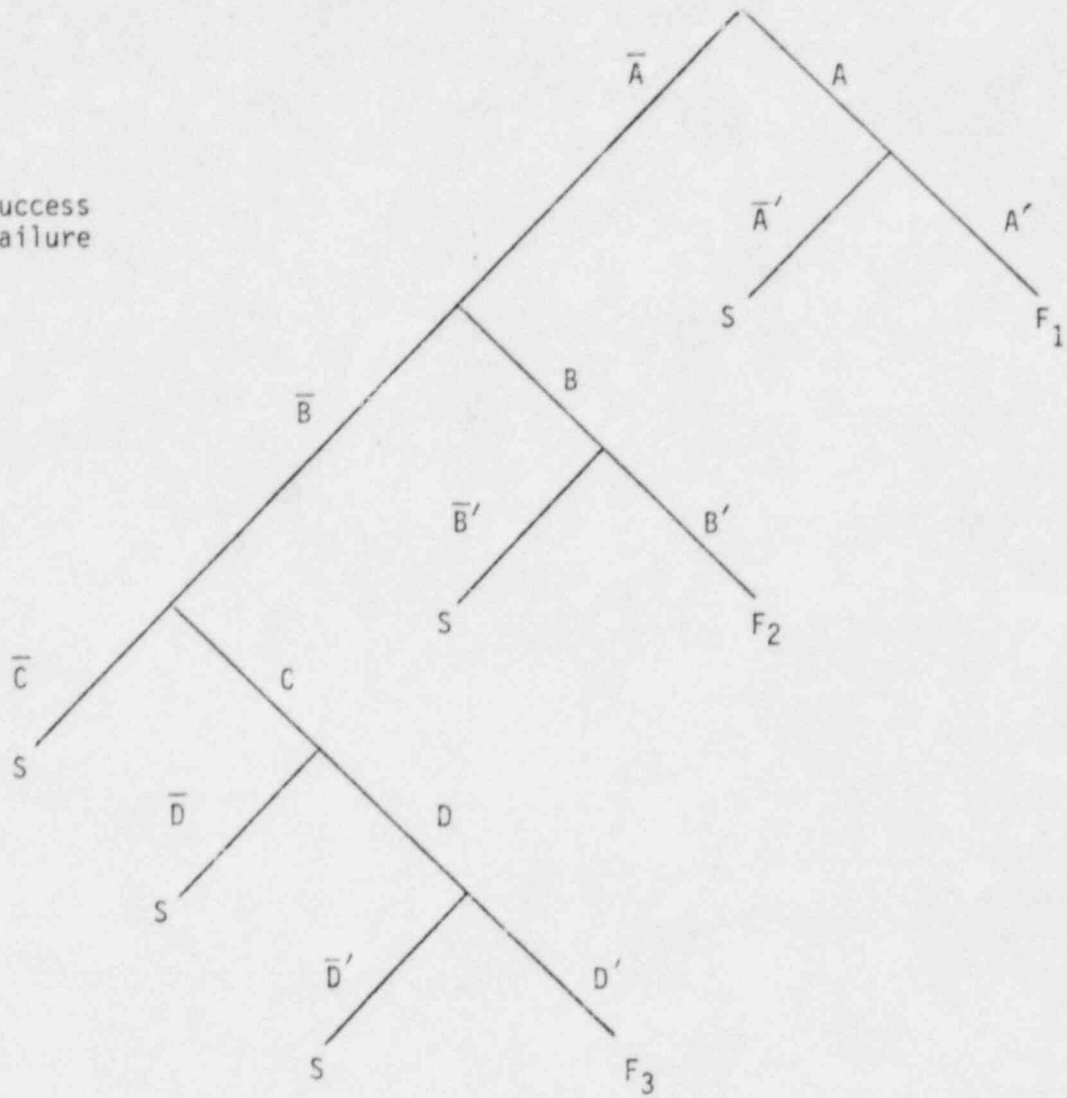
A = Failure to initiate task   = .001

A' = Failure of checker to initiate task   = .01

B = Failure to restore second valve   = .003

B' = Failure of checker to restore second valve   = .03

C = Valve sticks   = .001

D = Failure to restore a sticking valve completely   = .01

D' = Failure of checker to restore a sticking valve completely = .1

Figure A.3.7 Human Error Probability Tree Describing Failure
to Line up Valves Correctly

REFERENCES

A.3-1   M. H. Appley and R. Trumbull, (ed) Psychological Stress
         Appletons-Century-Crofts, New York, 1967.

A.3-2   A. D. Swain and H. E. Guttmann, Handbook of Human Reliability
         Analysis with Emphasis on Nuclear Power Plant Applications,
         NUREG/CR-1278, April 1980.

A.3-3   R. R. Fullwood and K. J. Gilbert, "An Assessment of the Impact
         of Human Factors on the Operation of the CRBR SCRS", SAI-010-
         76-PA, August 1976.

A.3-4   R. R. Fullwood and K. J. Gilbert, "Data and Assessment of Human
         Factor Impact on Nuclear Reactors", Transactions of American
         Nuclear Society, Vol. 26, p. 385, dated June 1977.

A.3-5   C. W. Gend, C. S. Parker, and A. B. Pontecorvo, "Human Performance
         Reliability Estimates and Application", Boeing Report D8AGH20328-1,
         June 3, 1968.

A.3-6   A.E. Green, Safety Assessment of Automatic and Manual Protective
         Systems, AHSB(S)R-172, Authority Health and Safety Branch,
         United Kingdom Atomic Energy Authority. Risley, England, 1969.

A.4   SYSTEM UNAVAILABILITY DUE TO MAINTENANCE DURING REACTOR OPERATION

One of the principal contributors to safety system unavailability
may be the outage time associated with maintenance operations.* The reason
for this unavailability is that while maintenance is occurring on one
component in a system (or one leg of a two-leg system) that system may be
incapacitated.** One available source of maintenance frequencies and dura-
tions based upon operating experience at nuclear power plants is WASH-1400.
However, WASH-1400 does not state whether or not simultaneous maintenance
activities are included and does not differentiate between on-line and off-
line maintenance. The WASH-1400 data also include several startup problems
in early BWRs which have been subsequently corrected. General Electric
does not believe the data to be representative of present-day conditions.
General Electric has performed a search of their Component Information
Retrieval system and completed an analysis of the data. In addition,
Philadelphia Electric has provided detailed maintenance information on
each of the Peach Bottom 2 and 3 safety systems, based upon operating ex-
perience. Both of these sources confirm that maintenance unavailabilities
are substantially less than assumed in WASH-1400. In addition, Philadelphia
Electric Nuclear Plant operating philosophy dictates that all normal main-
tenance of safety systems be performed during outages when there will be
no demand for the safety system. General Electric maintenance availability
values were used in this analysis.

A.4.1   Calculated Maintenance Unavailabilities

For comparison purposes, maintenance information from WASH-1400
is provided. WASH-1400 assessed the mean time between component failures
to be 4.55 months (.22 failures/month), while the mean time to repair (MTTR)
is a function of both:

---

*WASH-1400 found on-line maintenance to be a major contributor to individual
system unavailability; however, operating experience and maintenance philosophy
of the operating PECo BWRs at the Peach Bottom Atomic Power Station support
a significantly lower estimate.
**Note that there may be some maintenance acts from which the operator can
recover the system for use as a safety system; however, this is not considered
in this model.

1. The component, and

2. The upper bound on the allowed system outage time (e.g., for HPCI it is 7 days with RCIC operational). The technical specifications define these combinations of system unavailabilities. The Limiting Conditions of Operation from the technical specifications for Peach Bottom* are reproduced in Table A.4.1.

The WASH-1400 evaluation of MTTR for components which are anticipated to lead to maintenance outages is summarized in Table A.4.2.

Table A.4.2

SUMMARY OF MEAN TIME TO REPAIR (HOURS) BY COMPONENT
TYPE ASSUMING A LOG NORMAL DISTRIBUTION OF REPAIR TIMES AND
A MAXIMUM ALLOWED OUTAGE TIME OF 7 DAYS (WASH-1400 ANALYSES)

Component Type	MTTR (hours)
Pumps	19
Valves	19
Diesels	21
Instrumentation (I&C)	7

The following brief summaries of each system provide the number of components by type, the evaluated mean time to repair (MTTR) for each component, and the calculated unavailability of safety systems due to maintenance while the plant is operating.

---

*As noted in the groundrules for this study, the Limerick technical specifications are not written or approved and therefore Peach Bottom technical specifications are used as typical.

Table A.4.1

LIMITING CONDITIONS OF OPERATION FOR THE PLANT USED IN THIS ANALYSIS

SYSTEMS REQUIRED TO BE OPERATIONAL

System/Component Out of Service	Redundant Core Spray Subsystems	LPCI	Both Core Spray Subsystems	Remaining LPCI Subsystems	Remaining Containment Cooling Subsystem Components	Diesel for Operable Loop	RCIC	ADS	HPCI	Remaining Diesel Generators	Containment Cooling Subsystems	Remaining Relief Valves	Remaining Recirc. Loop	Allowable Out of Service Time (days)	Shutdown
One Core Spray Subsystem	X	X												7	
Both Core Spray Subsystems		X												2	X
One LPCI Pump			X	X										7	
One LPCI Subsystem			X	X										7	
Both LPCI Subsystems			X											2	X
Two RHRSW Pumps					X									30	
Three RHRSW Pumps					X									15	
Three Containment Cooling Subsystem Loops					X	X								7	
All Containment Cooling Subsystem Loops														1	X
HPCI							X	X						7	
RCIC									X					7	
One ADS Valve									X					7	
More Than One ADS Valve														1	X
One Diesel Generator		X	X							X	X			7	
More Than One Diesel															X
Safety Valve Function of One Relief Valve												X		30	
Safety Valve Function of Two Relief Valves												X		7	
Safety Valve Function of More Than Two Relief Valves														1	X
One Recirculation Loop													X	1	
More Than One Inoperable Control Rod in a 5x5 Array														1	X
Withdrawn Control Rod Which Can't be Moved Because of Possible Collet Housing Failure														2	X

NOTES

1. With irradiated fuel in reactor vessel and reactor in cold shutdown condition, both core spray subsystems, the LPCI and containment cooling subsystems may be inoperable, provided no work is being done which has the potential for draining the reactor vessel.

2. During a refueling outage, refueling operation may continue with one core spray system or the LPCI system inoperable for a period of thirty days.

In the determination of the maintenance unavailabilities for HPCI, RCIC, and RHR, the number of components used in assessing the maintenance outages are for the specific system. Components involved in the room cooling and ventilation are not included in this estimate of maintenance unavailability.

HPCI: HPCI is a single leg series system as described in Appendix B. The following evaluation of HPCI unavailability due to maintenance is based upon the data and assumptions used in WASH-1400; a General Electric assessed value for HPCI maintenance unavailability (from BWR operating data available to General Electric); and Peach Bottom-specific data (see Table A.4.3).

Table A.4.3

SUMMARY OF MAINTENANCE ASSUMPTIONS USED IN EVALUATING HPCI UNAVAILABILITY

Component	Number	MTTR (Hours)	Unavailability*
Turbine	1	19	5.80×10^{-3}
Pump	1	19	5.80×10^{-3}
Valves			
MOV	8	19	4.64×10^{-2}
AOV	1	19	5.80×10^{-3}
Turbine	2	19	1.16×10^{-2}
C&I	1 set	7	2.10×10^{-3}
TOTAL (WASH-1400 Assumptions)			7.75×10^{-2}
GENERAL ELECTRIC ASSESSED VALUE			1.0×10^{-2}

* Based on 22 failures per month

RCIC: RCIC is similar in design and function to HPCI. Table A.4.4 summarizes the unavailability analysis for RCIC using the same techniques as described for HPCI.

Table A.4.4

SUMMARY OF ASSUMPTIONS USED IN EVALUATING RCIC UNAVAILABILITY DUE TO MAINTENANCE

Component	Number	MTTR (Hours)	Unavailability*
Turbine	1	19	5.80×10^{-3}
Pump	1	19	5.80×10^{-3}
Valves			
MOV	7	19	4.06×10^{-2}
AOV	1	19	5.80×10^{-3}
Turbine	2	19	1.16×10^{-2}
I&C	1 set	7	2.10×10^{-3}
TOTAL (WASH-1400 ASSUMPTIONS)			7.17×10^{-2}
GENERAL ELECTRIC ASSESSED VALUE			1.10×10^{-2}

* Based on .22 failures/month

LPCI: Each of the four LPCI legs in conjunction with ADS, can perform successful coolant injection for most accident scenarios. The limiting conditions of operation are based upon allowing one entire leg to be out for maintenance. Using the assumptions and data from WASH-1400, the unavailability of each leg due to maintenance can be calculated as shown in Table A.4.5.

Table A.4.5

CALCULATED UNAVAILABILITY OF ONE LPCI/RHR LEG
DUE TO MAINTENANCE

Component	Number	MTTR (Hours)	Unavailability*
Pump	1	19	5.80×10^{-3}
Valves			
MOV	3	19	1.74×10^{-2}
Heat Exchanger	1	19	5.80×10^{-3}
I&C	1 set	7	2.10×10^{-3}
TOTAL (WASH-1400 Assumptions)			3.11×10^{-2}
General Electric Assessed Value (LPCI Loop)			4.0×10^{-3}

* Based on .22 failures/month

Core Spray (CS): Table A.4.1 of the Limiting Conditions of Operation indicates that one core spray subsystem can be out for mainte-nance if LPCI and the remaining core spray subsystem are available. For this analysis, a core spray subsystem is treated as two core spray legs in one loop (i.e., A and C are loop 1; B and D are loop 2). Therefore, the calculation of the maintenance unavailability is based upon all the components in one loop (see Table A.4.6).

Diesels: Diesel generator unavailability calculated from the data in WASH-1400 yields a value of 6.4×10^{-3} using a mean time to repair of 21 hours and a frequency of .22 maintenance acts per month. However, the Peach Bottom data, as analyzed by General Electric, are found to yield an on-line maintenance unavailability of 1×10^{-3} per diesel. See Section A.5.1 for a discussion of the applicability of Peach Bottom diesel data for Limerick.

Table A.4.6

CALCULATED UNAVAILABILITY OF ONE CS LOOP (TWO PUMP LEGS) DUE TO MAINTENANCE

Components	Number	MTTR (Hours)	Unavailability*
Pump	2	19	1.16×10^{-2}
Valves			
MOV	4	19	2.32×10^{-2}
AOV	0		
I&C	1 set	7	0.21×10^{-2}
TOTAL (WASH-1400 Assumptions)			3.69×10^{-2}
General Electric Assessed Value			2.0×10^{-3}

*Based on .22 failures/month

RHR Service Water (Containment Cooling): The four RHRSW pumps are divided into two loops, each with two pump legs. The limiting condition of operation for RHRSW allows three of the four pumps to be unavailable due to maintenance for up to 15 days. The unavailability per leg is assessed to be attributed primarily to the pump and therefore is approximately 5.8×10^{-3}. The Peach Bottom data, as assessed by General Electric, yields a value of 2×10^{-3} per RHRSW loop.

The unavailabilities for each system are summarized in Table A.4.7 for the calculated component values, the WASH-1400 system data, and for the General Electric assessed values. The values assessed by General Electric were used in the LGS analysis as they are more representative of present-day conditions and of the Limerick plant-specific situation.

Table A.4.7

SUMMARY OF THE CALCULATED SYSTEM OR PARTIAL SYSTEM UNAVAILABILITIES DUE TO MAINTENANCE

FAULT TREE IDENTIFIER	SYSTEM	CALCULATED UNAVAILABILITY	WASH-1400	GENERAL** ELECTRIC
HTM	HPCI	7.75×10^{-2}	7.5×10^{-2}	1.0×10^{-2}
RCICTM	RCIC	7.17×10^{-2}	6.9×10^{-2}	1.10×10^{-2}
D1T, D2T	LPCI	3.11×10^{-2}	2.3×10^{-2}	4.0×10^{-3}
L1T, L2T	CS (1Loop*)	3.69×10^{-2}	4.1×10^{-2}	2.0×10^{-3}
	Cont. Cooling (RHRSW)	5.8×10^{-3}	--	2.0×10^{-3}
E1M, E2M, E3M, E4M	Diesel	6.4×10^{-3}	--	1.0×10^{-3}
	CRD	5.8×10^{-3}	--	--
ATMC1,2,3,4,5	ADS	5.8×10^{-3}	--	--
STMA, STMB	SLC	2.32×10^{-2}	--	2×10^{-3}

*A loop is considered the two pump legs which discharge to the same header (Loop 1 is A and C, Loop 2 is B and D)

** These values were used in the Limerick Analysis

A.4.2 Derivation of Maintenance Unavailabilities as Implemented in the Fault Tree Model

The best determination of the unavailability of a system due to on-line maintenance is a plant-specific estimate based upon plant-specific data. However, due to the limited data available for the study, the approach used in this analysis is similar to that originally presented in WASH-1400. WASH-1400 made use of a limited sample of operating experience maintenance data (approximately 2 years) to estimate the unavailability of a system based upon the number of active components in the system. The limiting conditions of operation (LCOs) identified in the plant technical specifications are factored into the Limerick fault tree logic models.

The maintenance unavailabilities for each system are combined in the fault tree logic model through the use of NOT gates. The "NOT" gate maintenance logic implements the requirements of the limiting conditions of operation (LCOs) which specify the maximum number of systems which can be unavailable due to maintenance while the plant is operating at power.

Table A.4.8 gives a summary of safety-related systems required for normal operation. The operating experience data assembled to represent the maintenance on systems is compiled from data which results from normal plant operation where the maintenance represents operations carried out in accordance with the LCOs. For example, the maintenance unavailability for RCIC from operating experience data represents the unavailability associated with RCIC when HPCI is operating. Therefore, there is a condition on the RCIC operation requiring HPCI to be available which must be reflected in the fault tree model.
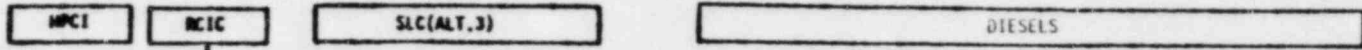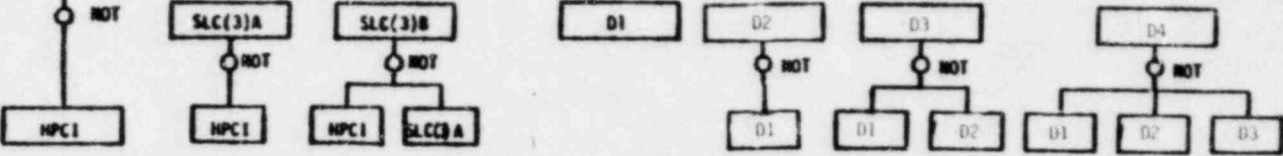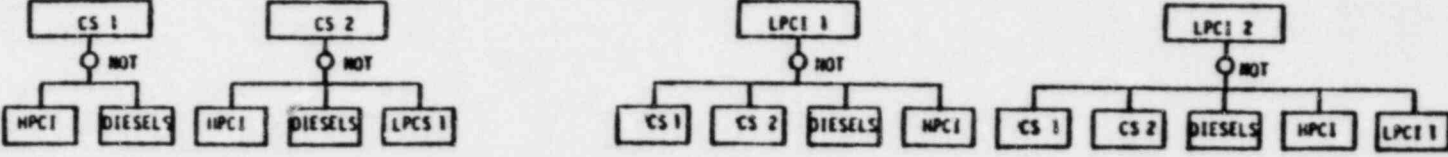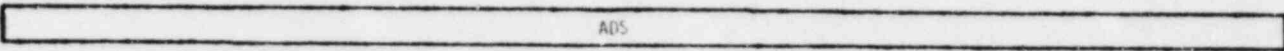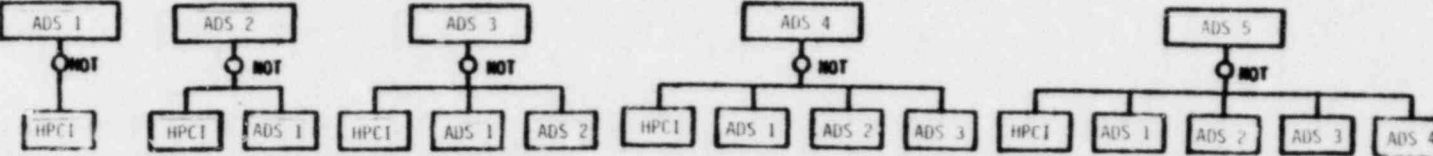
This section summarizes the relationship of the fault tree model logic to the probability that a system is in maintenance. Because of the dependencies among systems (summarized in the Limiting Conditions of Operation) and the "NOT" gate formalism used in this analysis, the input probabilities to the fault tree are not immediately obvious. Therefore, this section presents the Boolean algebra used to derive these input probabilities in terms of the known probabilities.

The maintenance evaluation included in this analysis includes two contributions to system unavailability. These two contributions are:

1. The dependent portion of systems unavailable due to maintenance, which provides that a portion of the safety systems may be unavailable if the remainder of the safety systems are operational.

2. An independent portion of system unavailability which can be attributed to those cases in which both legs of a system are found to require maintenance. In general, the allowed outage time associated with these conditions is 24 to 48 hours. For this analysis, this condition is assumed to occur once every ten years, which corresponds to an unavailability of 2.74×10^{-4} to 5.48×10^{-4}.

A-67

Table A.4.8

SUMMARY OF THE MAINTENANCE LIMITING CONDITIONS OF OPERATION*
FROM THE PLANT TECHNICAL SPECIFICATION

SYSTEM: HPCI | RCIC | SLC(ALT.3) | DIESELS

System Which Cannot Be in Maintenance Simultaneously:

- RCIC — NOT → HPCI
- SLC(3)A — NOT → HPCI
- SLC(3)B — NOT → HPCI, SLC(3)A
- D1
- D2 — NOT → D1
- D3 — NOT → D1, D2
- D4 — NOT → D1, D2, D3

SYSTEM: CS | LPCI

System Which Cannot Be in Maintenance Simultaneously:

- CS 1 — NOT → HPCI, DIESELS
- CS 2 — NOT → HPCI, DIESELS, LPCS 1
- LPCI 1 — NOT → CS 1, CS 2, DIESELS, HPCI
- LPCI 2 — NOT → CS 1, CS 2, DIESELS, HPCI, LPCI 1

SYSTEM: ADS

System Which Cannot Be in Maintenance Simultaneously:

- ADS 1 — NOT → HPCI
- ADS 2 — NOT → HPCI, ADS 1
- ADS 3 — NOT → HPCI, ADS 1, ADS 2
- ADS 4 — NOT → HPCI, ADS 1, ADS 2, ADS 3
- ADS 5 — NOT → HPCI, ADS 1, ADS 2, ADS 3, ADS 4

*Safety Related Systems which are required to be Operational for Power Operation.

The following discussion summarizes the derivation of the dependent fault tree input parameter values for each system.

RCIC: The RCIC unavailability due to maintenance (Figure A.4.1) is combined with no HPCI maintenance. The assessed General Electric data, as shown in Table A.4.7, yields an estimation of the probability associated with the top event "RCIC in maintenance" (RCICTM). In order to determine RTM (Figure A.4.1), the following relationship is used:

$$RTM = \frac{RCICTM}{(1 - HTM)} = \frac{1.10 \times 10^{-2}}{1 - 1.0 \times 10^{-2}} = 1.1 \times 10^{-2}$$

The above is a simple example of a two-tiered relationship; however, as can be seen from the LCOs or the fault tree model, other systems have more complex relationships in defining the allowable maintenance which can be performed with the plant remaining operational. The remainder of this section is devoted to defining the input probabilities required for the fault tree model in terms of the known values from Table A.4.7.
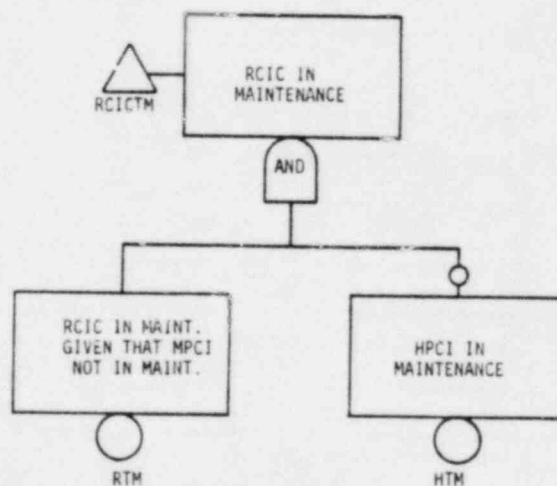
Figure A.4.1 The Structure of the RCIC Maintenance
Unavailability in the RCIC Fault Tree

<u>Diesels</u>: The maintenance representation used for the Diesels is given in Figure A.4.2

Assuming the diesels are statistically symmetrical, each has an equal probability of being in maintenance as defined in Table A.4.7.

$$E1M \equiv E2M \equiv E3M \equiv E4M = 1.0 \times 10^{-3} \qquad (A-1)$$

From the fault tree (see Figure A.4.2)

$$E4M = E4MM \star \overline{ECUM3} \qquad (A-2)$$

$$E3M = E3MM \star \overline{ECUM2} \qquad (A-3)$$

$$E2M = E2MM \star \overline{E1M} \qquad (A-4)$$

Where

$$\boxed{E1M = E1MM = 1.0 \times 10^{-3}} \qquad (A-5)$$

$$ECUM2 = E2MM + E1M - (E2MM)(E1M) \qquad (A-6)$$

$$\overline{ECUM2} = \overline{E2MM} \star \overline{E1M} \qquad (A-7)$$

Similarly,

$$\overline{ECUM3} = \overline{E3MM} \star \overline{ECUM2} \qquad (A-8)$$

$$\overline{ECUM4} = \overline{E4MM} \star \overline{ECUM3} \qquad (A-9)$$

Using (A-4):

$$E2M = E2MM \star \overline{E1M}$$

$$\boxed{E2MM = \frac{E2M}{\overline{E1M}} = 1.0 \times 10^{-3}} \qquad (A-10)$$

Thus, by (A-7):

$$\overline{ECUM2} = .9980$$

And, from (A-3):

$$E3MM = \frac{E3M}{\overline{ECUM2}} = 1.0 \times 10^{-3} \qquad (A-11)$$

By (A-8):

$$\overline{ECUM3} = .9970$$

From (A-2):

$$E4MM = \frac{E4M}{\overline{ECUM3}} = 1.0 \times 10^{-3} \qquad (A-12)$$

(A-9) gives:

$$\overline{ECUM4} = .9960$$

Core Spray (CS): The CS system maintenance is defined in terms of two loops, each with equal probability of a maintenance outage. From Table A.4.7:

$$L1T \equiv L2T = 2.0 \times 10^{-3} \qquad (A-13)$$

where these quantities are defined in terms of (see Figure A.4.3):

$$L1T = LTM1 * \overline{LCUMT} \qquad (A-14)$$

and $LCUMT = ECUM4 + HTM - (ECUM4)(HTM)$

$$\overline{LCUMT} = \overline{ECUM4} * \overline{HTM} = .9860 \qquad (A-15)$$

A-71
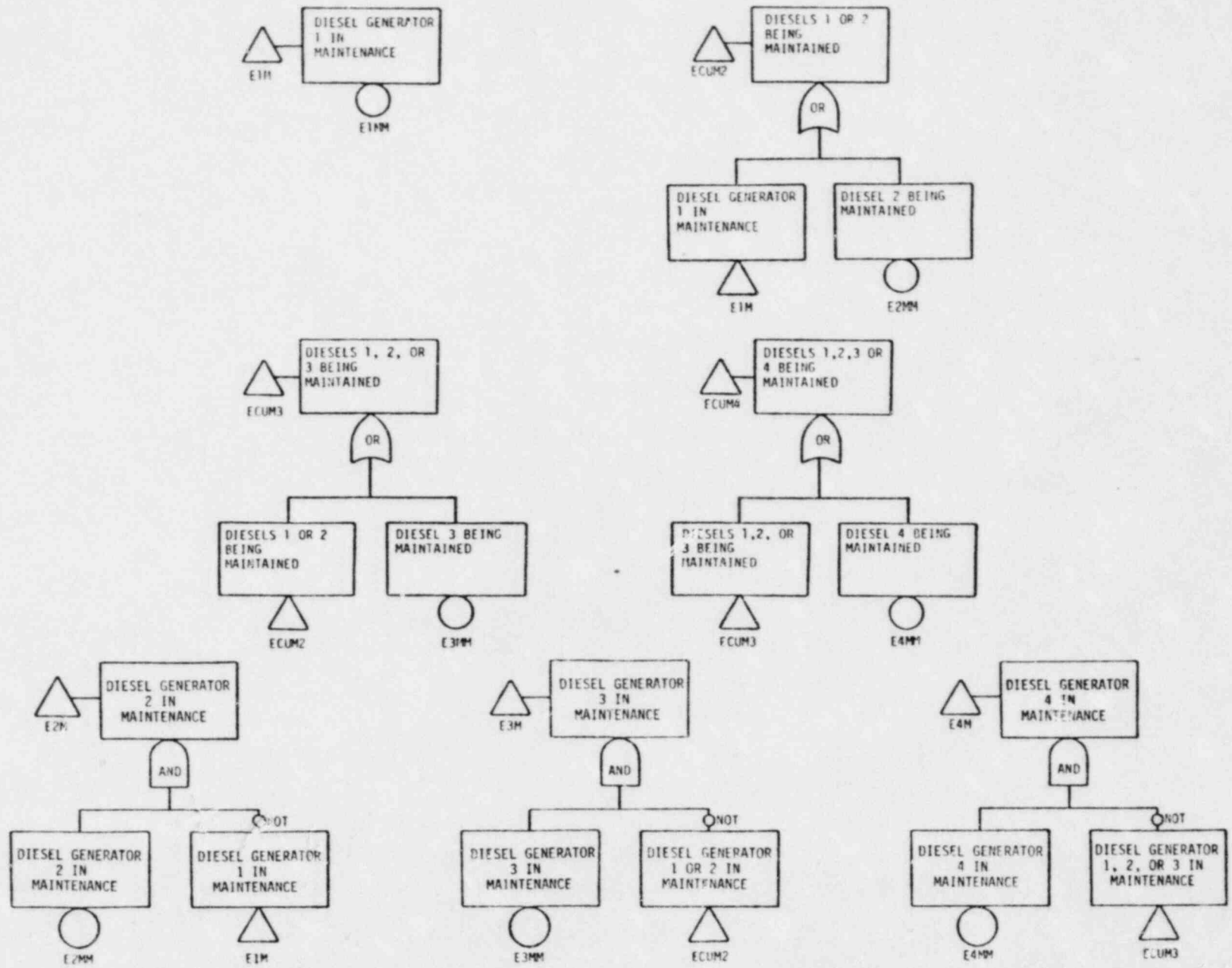
Figure A.4.2   Maintenance Representation Used for the Diesels in the Fault Tree Model

Therefore,

$$\boxed{LTM1 = \dfrac{L1T}{\overline{LCUMT}} = 2.03 \times 10^{-3}}$$ (A-16)

Also, $LCUM1 = LCUMT + LTM1 - (LCUMT)(LTM1)$

$$\overline{LCUM1} = \overline{LCUMT} \star \overline{LTM1} = .9840$$ (A-17)

Now, $L2T = LTM2 \star \overline{LCUM1}$

Hence, $$\boxed{LTM2 = \dfrac{L2T}{\overline{LCUM1}} = 2.03 \times 10^{-3}}$$ (A-18)

LPCI: The derivat   put maintenance probabilities for LPCI follows the discussion c   ... a parallel fashion. The LPCI is defined as a four-leg system for maintenance purposes. From Table A.4.7 :

$$D1T \equiv D2T \equiv D3T \equiv D4T = 4.0 \times 10^{-3}$$ (A-19)

where these quantities are defined in the fault tree (Figure A.4.4).

$$D1T = DMAINT1 \star \overline{DCUM1}$$ (A-20)

and $DCUM1 = LCUM1 + LTM2 - (LCUM1)(LTM2)$

$$\overline{DCUM1} = \overline{LCUM1} \star \overline{LTM2} = .9820$$ (A-21)

Therefore,

$$\boxed{DMAINT1 = \dfrac{D1T}{\overline{DCUM1}} = 4.07 \times 10^{-3}}$$ (A-22)

A-74

CS LOOP 1 UNAVAILABLE DUE TO MAINTENANCE

L1T

AND

CS LOOP 1 IN MAINTENANCE

LTM1

NOT

HPCI OR ANY DIESEL IN MAINTENANCE

LCUMT

CS LOOP 2 UNAVAILABLE DUE TO MAINTENANCE

L2T

AND

CS LOOP 2 IN MAINTENANCE

LTM2

NOT

CS LOOP 1 OR HPCI OR ANY DIESEL IN MAINTENANCE

LCUM1

HPCI OR ANY DIESEL IN MAINTENANCE

LCUMT

OR

DIESELS 1, 2, 3 OR 4 BEING MAINTAINED

ECUM4*

HPCI IN MAINTENANCE

HIM

CS LOOP 1 OR HPCI OR ANY DIESEL IN MAINTENANCE

LCUM1

OR

CS LOOP 1 IN MAINTENANCE

L1M1

HPCI OR ANY DIESEL IN MAINTENANCE

LCUMT

*Defined in the Electric Power Fault Tree

Note that the maintenance contributions may appear unsymmetrical in their contributions to system unavailability. However, the representation is consistent with Bayes equation in Boolean algebra which requires the dependency of events be represented only once.

Figure A.4.3   CS Maintenance Representation Used in the Fault Tree Model

Figure A.4.4 LPCI Maintenance Representation Used in the Fault Tree Model
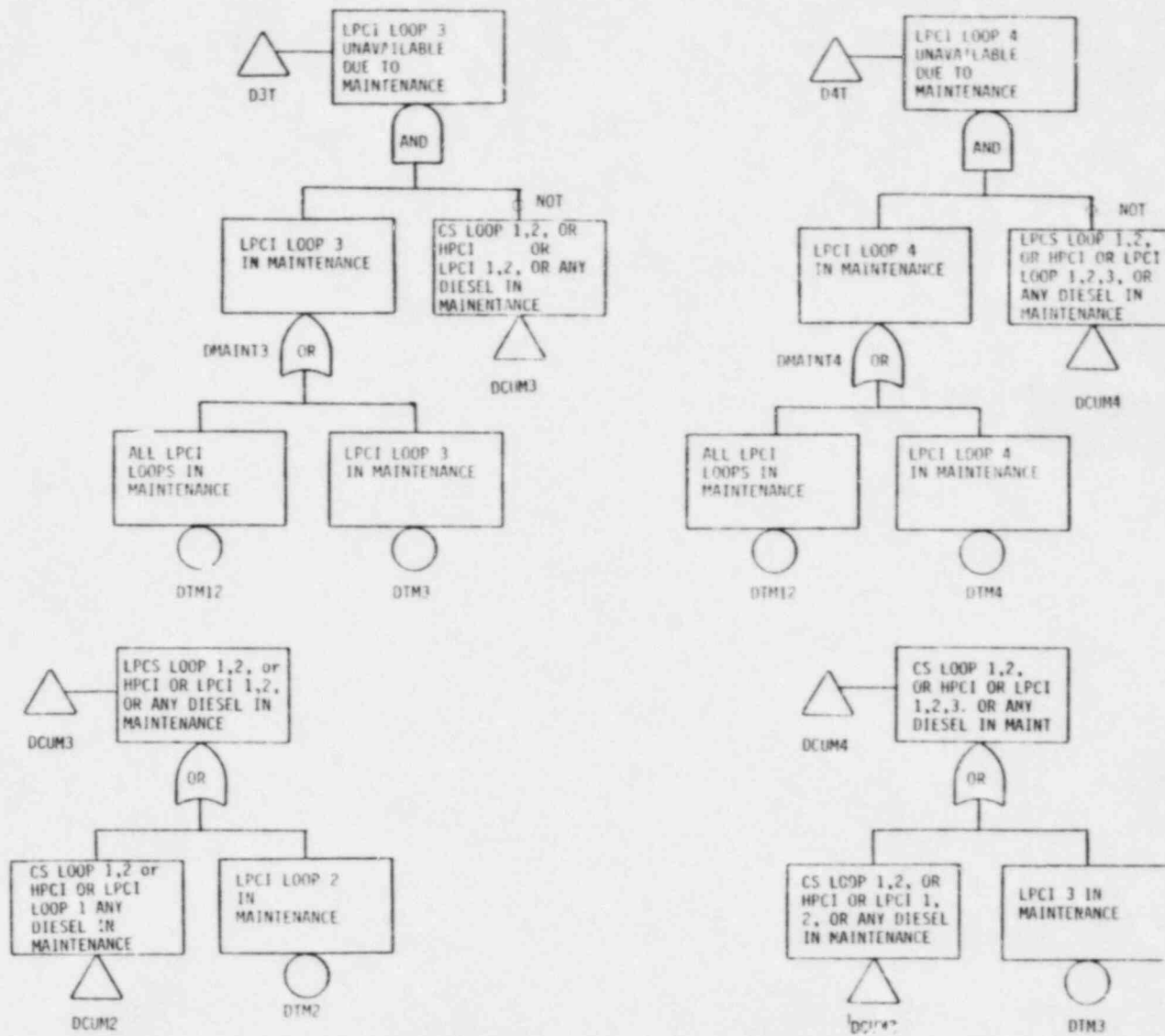
Figure A.4.4 LPCI Maintenance Representation Used in the Fault Tree Model
(continued)

Also,   DCUM2 = DCUM1 + DMAINT1 - (DCUM1)(DMAINT1)

$$\overline{DCUM2} = \overline{DCUM1} \quad \overline{DMAINT1} = .9780 \tag{A-23}$$

Now   D2T = DMAINT2 * $\overline{DCUM2}$

Hence $$\boxed{DMAINT2 = \frac{D2T}{DCUM2} = 4.09 \times 10^{-3}} \tag{A-24}$$

DCUM3 = DCUM2 + DMAINT2 - (DCUM2)(DMAINT2)

$\overline{DCUM3} = \overline{DCUM2} * \overline{DMAINT2} = .9740$

D3T = DMAINT3 * $\overline{DCUM3}$

$$\boxed{DMAINT3 = \frac{D3T}{DCUM3} = 4.11 \times 10^{-3}}$$

DCUM4 = DCUM3 + DMAINT3 - (DCUM3)(DMAINT3)

$\overline{DCUM4} = \overline{DCUM3} * \overline{DMAINT3} = .9700$

D4T = DMAINT4 + $\overline{DCUM4}$

$$\boxed{DMAINT4 = \frac{D4T}{DCUM4} = 4.12 \times 10^{-3}}$$

ADS: The ADS maintenance representation used in the fault tree model of ADS is shown in Figure A.4.5. From the Limiting Conditions of Operation, only one ADS valve can be in maintenance at any one time if the plant is operating. However, if one ADS valve is in maintenance, HPCI cannot also be unavailable. From Table A.4.7:

A-77
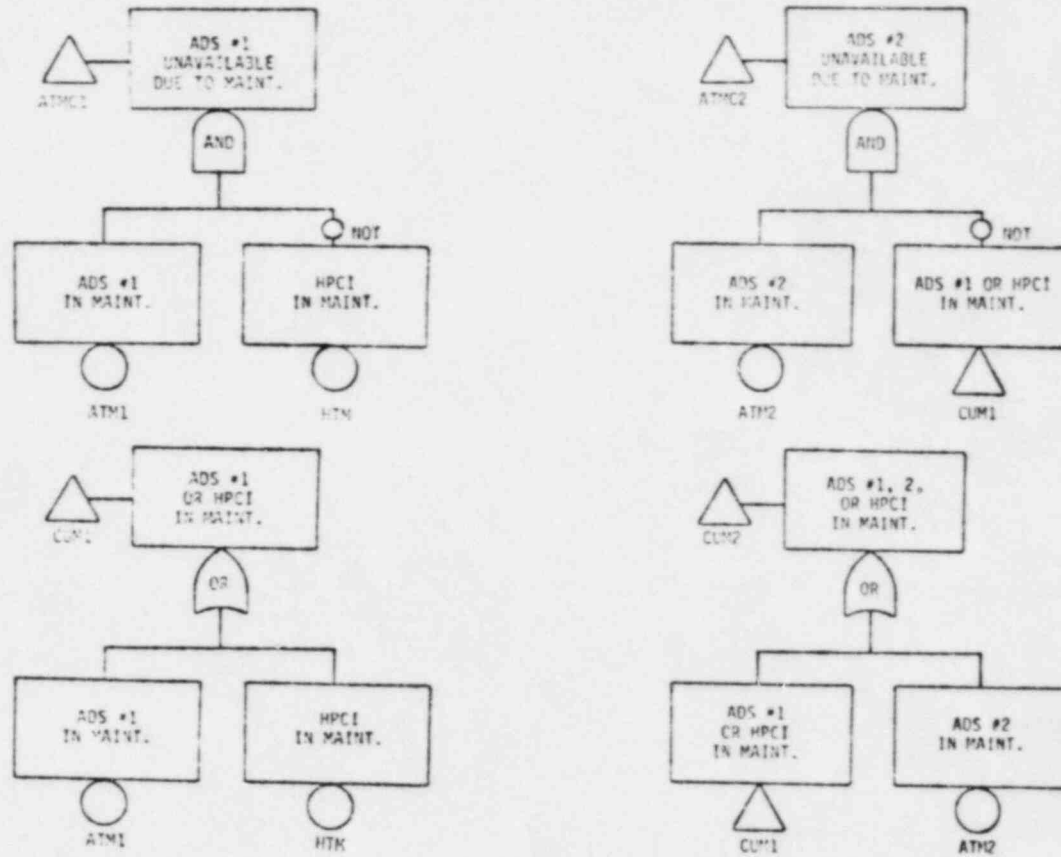
REFERENCE: NEDO 24708 AND PEACH BOTTOM 2 TEHCNICAL SPECIFICATIONS

Figure A.4.5 ADS Maintenance Representation Used in Fault Tree Model

ATMC3 — ADS #3 UNAVAILABLE DUE TO MAINT.
AND
ADS #3 IN MAINT. — ATM3
ADS #1, 2, OR HPCI IN MAINT. — NOT — CUM2

ATMC4 — ADS #4 UNAVAILABLE DUE TO MAINT.
AND
ADS #4 IN MAINT. — ATM4
ADS #1, 2, 3 OR HPCI IN MAINT. — NOT — CUM3

ATMC5 — ADS #5 UNAVAILABLE DUE TO MAINT.
AND
ADS #5 IN MAINT. — ATM5
ADS #1, 2, 3, 4 OR HPCI IN MAINT. — NOT — CUM4

CUM3 — ADS #1, 2, 3, OR HPCI IN MAINT.
OR
ADS #1, 2, OR HPCI IN MAINT. — CUM2
ADS #3 IN MAINT. — ATM3

CUM4 — ADS #1, 2, 3, 4, OR HPCI IN MAINT.
OR
ADS #1, 2, 3 OR HPCI IN MAINT. — CUM3
ADS #4 IN MAINT. — ATM4

Figure A.4.5 (Continued)

$$\text{ATMC1} \equiv \text{ATMC2} \equiv \text{ATMC3} \equiv \text{ATMC4} \equiv \text{ATMC5} = 5.8 \times 10^{-3} \qquad \text{(A-25)}$$

The input quantities for the fault tree can be found as follows:

$$\text{ATMC1} = \text{ATM1} * \overline{\text{HTM}}$$

therefore,

$$\boxed{\text{ATM1} = \frac{\text{ATMC1}}{\overline{\text{HTM}}} = 5.86 \times 10^{-3}} \qquad \text{(A-26)}$$

$$\overline{\text{CUM1}} = \overline{\text{ATM1}} * \overline{\text{HTM}} = .9842 \qquad \text{(A-27)}$$

$$\text{ATMC2} = \text{ATM2} * \overline{\text{CUM1}}$$

$$\boxed{\text{ATM2} = \frac{\text{ATMC2}}{\overline{\text{CUM1}}} = 5.89 \times 10^{-3}} \qquad \text{(A-28)}$$

$$\overline{\text{CUM2}} = \overline{\text{CUM1}} * \overline{\text{ATM2}} = .9784 \qquad \text{(A-29)}$$

Therefore,

$$\text{ATMC3} = \text{ATM3} * \overline{\text{CUM2}}$$

$$\boxed{\text{ATM3} = \frac{\text{ATMC3}}{\overline{\text{CUM2}}} = 5.93 \times 10^{-3}} \qquad \text{(A-30)}$$

$$\overline{\text{CUM3}} = \overline{\text{CUM2}} * \overline{\text{ATM3}} = .9726 \qquad \text{(A-31)}$$

$$ATMC4 = ATM4 * \overline{CUM3}$$

$$\boxed{ATM4 = \frac{ATMC4}{\overline{CUM3}} = 5.96 \times 10^{-3}} \qquad (A-32)$$

$$\overline{CUM4} = \overline{CUM3} * \overline{ATM4} = .9668 \qquad (A-33)$$

$$ATMC5 = ATM5 * \overline{CUM4}$$

$$\boxed{ATM5 = \frac{ATMC5}{\overline{CUM4}} = 6.00 \times 10^{-3}} \qquad (A-34)$$

A-81

A.5   DATA ASSESSMENT FOR DIESEL AVAILABILITY MODELING

Emergency electric power buses (4160 AC) are a vital and necessary function for successful long term core cooling and containment heat removal. Power to these buses can be supplied via any of the offsite power sources (see Section A.6) or the emergency diesels. The emergency diesels can be treated in at least two ways for the quantification of accident sequences. These methods are:

1. Draw a fault tree for the entire diesel generator system, including the auxiliaries. All common links between the diesels, including operator interaction, would need to be modeled.

2. Use operating experience field data on diesel generator performance to characterize the diesels.

Past analyses and data evaluations of diesels have concluded that the diesel failure rate can be relatively high and that potential common-cause events could be the most significant contributor to multiple diesel failures. These conclusions, plus the availability of recent diesel performance data, including PECo-specific data, has led to the choice of method (2) above. In addition to the use of data to characterize individual diesel failures, the model used in the Limerick quantification makes use of the available data on single and multiple diesels plus a Boolean model* for relating the probability of multiple diesel failures.

This section includes the following specific data   as   used in the quantification of the probability of diesel availability:

1. Characterization of the probability of a single diesel failing to start and run using Philadelphia Electric Company nuclear plant experience (Section A.5.1)

---

*This dependency model (see Appendix B) is quite general, but the data used to quantify it must be assumed to come from a population of diesels similar to those at Limerick.

2. Compilations of other sources of data to estimate the proba-
    bility of a single diesel failure, plus the conditional proba-
    bility of multiple diesel failures (Section A.5.2 and A.5.3).

3. Data on the length of time required to restore a diesel to
    operation is also important in the Limerick analysis, since
    the Limerick plant is designed to maintain a safe configura-
    tion even during the loss of all emergency AC power for a
    certain amount of time, i.e., at least two hours (Section
    A.5.4).

4. Summary of data used to characterize the LGS DGs (see A.5.5).

A.5.1   Diesel Performance Data from Philadelphia Electric Company Experience

An analysis of data on diesels from Peach Bottom 2 and 3 has been
performed. This analysis is an attempt to provide a PECo-specific estimate
of the failure probability of a single diesel and additional confirmation of
other estimates of the probability of multiple diesel failure. Table A.5.1
summarizes Philadelphia Electric's experience with the Peach Bottom Units
2 and 3 diesels as reported in Licensee Event Reports (LERs). This in-
cludes the test experience and gives point failure estimates of 0.0078/
demand for failure to start and 0.0099/demand for failure to sustain opera-
tions (or other failures not associated with starting), or a total of 1.8 x
10^{-2}/demand. The test experience used here is based on single unit testing;
however, there have been at least 9 integrated tests (LOCA signal and loss
of two off-site power sources to test the automatic startup of all four
diesels at the same time). Two failures occurred which may be interpreted
as common-mode: the presence of weld beads in the blower drive gears
(6/15/74) and the loss of starting air (6/13/77). Accepting these as
common-mode failures, the point estimate for their occurrence is 2/1409 =
0.0014/D. This may be conservative because the situations that resulted in
the failures have changed.

In addition to the failure probability of a single diesel, the
Peach Bottom data can be used to estimate the probability of restoring
one diesel generator (DG). Table A.5.2 provides the Peach Bottom restora-
tion times.

A-83

Table A.5.1

PEACH BOTTOM ATOMIC POWER STATION - DIESEL TEST DATA 1973-1980

Year	Tests by Diesel Number				Total Tests(a)	Failures to Start(b)	Failures to Sustain(c)	Failure to Start Frequency b/a	Failure to Sustain Frequency - c/a
	1	2	3	4					
1973	7	9	6	9	31	2	0	.064	0
1974	30	30	30	41	131	1	2	.0078	.015
1975	54	55	53	53	215	1	2	.0047	.0093
1976	52	54	52	53	211	3	1	.014	.0047
1977	54	53	53	53	213	3	6	.014	.028
1978	55	55	55	53	218	1	2	.0046	.0092
1979	67	68	72	65	272	0	1	0	.0037
1980*	30	31	29	28	118	0	0	0	0
TOTAL					1409	11	14	.0078	.0099

*Through 9/15/80

Table A.5.2

HISTOGRAM DATA OF DIFFERENTIAL AND CUMULATIVE DG RESTORATION TIMES

Restoration Time (Hrs.)*	Number of Events in the Interval	Cumulative Events to Upper Time
0.0 - 0.5	1	1
0.5 - 1.0	5	6
1.0 - 2.0	3	9
2.0 - 4.0	2	11
4.0 - 10.0	8	19
10.0 - 50.0	6	25
50.0 - 100.0	2	27

*Events specified as exactly the upper limit are taken in that interval.

The probability of restoration of one DG before four hours is $11 \div 27 = 0.41$ based on the Peach Bottom data or 0.5 if the smooth (eye-fit) curve is used for statistical inference. These data do not vary significantly compared with the statistical uncertainties.

The inferred probability of restoration before thirty minutes is more uncertain. Directly from the data, the probability is 0.04; however, there are two problems. One is that there must be a minimum restoration time for personnel to arrive at the DG if the DG cannot be started from the control room. Thus, the probability should decrease at short times as suggested by the curve. The second problem is that the recording of short restoration times tends to be inaccurate because of a tendency to round off to larger values (less than one hour). This is suspected to be a reason for the small amount of data below 0.5 hours. However, because of the large uncertainty and small benefit perceived, no credit is taken for diesel restoration within thirty minutes.

These data were collected under fairly routine plant conditions, i.e., in no case was there an accident that could lead to hazardous conditions. The question arises as to how much faster could a DG be restored under "heroic" action. Based on human factor studies in the literature, it appears that the probability of restoration may increase greatly under accident conditions. People would move faster, but there are certain minimum transit times. There is also a negative effect; the increased stress could accentuate the error rate, causing more mistakes.

The emergency diesel data from Peach Bottom has been included in this analysis as the most appropriate to determine the basic diesel failure rate because of the following items:

1. The diesels are the same size (2.6MW) and by the same manufacturer as those to be used at Limerick; (however, the details of design and auxiliaries are different).

2. Since Peach Bottom is also owned and operated by PECO, it has been subject to the same maintenance practices anticipated at Limerick.

3. Environmental conditions (seasonal variation in humidity and external temperatures) are approximately the same.

4. The data is based upon a detailed search of both tests (demands) and failures by the utility staff who have direct access to the plant logs.

Diesel data from several sources were obtained and analyzed to provide conditional failure rates for characterizing possible multiple diesel failures. These sources are discussed in the remaining sections of this appendix.

A.5.2   Plant X Data Assessment

In general, most sources of data do not provide detailed information as to the exact number of demands of diesels (success plus failures). One source does, however, provide detailed demand data on single, double, triple, and quadruple combinations of diesel demands and failures. In this assessment, these data will be referenced as Plant X.

Data were obtained from Plant X for its four-diesel population. These data yielded:

Diesels Involved	Number of Demands	Number of Failures
1	133	25
2	23	2
3	71	1
4	67	0

These data can then be expanded to count trials and failure combinations. That is, there are two single trials in every double demand. Therefore, the following table can be formed:

	Number of Trials	Number of Failure Combinations
Singles	660	32
Doubles	638	5
Triples	339	1
Quadruples	67	0

Using this information, upper bound estimates can be obtained. These upper bound estimates assume a failure occurs on the next trial. Therefore, the probability of failure on demand becomes:

$$P(s) = P(\text{Single}) = \frac{33}{661} = 4.99 \times 10^{-2}$$

$$P(d) = P(\text{Double}) = \frac{6}{639} = 9.39 \times 10^{-3}$$

$$P(t) = P(\text{Triple}) = \frac{2}{340} = 5.88 \times 10^{-3}$$

$$P(q) = P(\text{Quadruple}) = \frac{1}{68} = 1.47 \times 10^{-2}$$

Note that these assumptions have resulted in an impossible result for quadruple failures. That is, quadruple failures cannot be more likely than lesser combinations. Therefore, another estimate must be obtained. This other estimate can be obtained by recognizing that there was one triple failure where a quadruple failure did not occur. Thus, there was one chance for a fourth failure given three failures. Again, using an upper bound approximation, gives:

$$P(\text{fourth given three failures}) = \frac{1}{2} = .5$$

Other conditional failures can be found as

$$P(\text{second given one failure}) = \frac{P(d)}{P(s)} = .188$$

$$P(\text{third given two failures}) = \frac{P(t)}{P(d)} = .626$$

P(fourth given three failures)=.5 (from above)

A-87

These results are summarized under Plant X in the results tabu-
lated in Sections A.5.3.

A 5.3   Diesel Data Assessment From LERs and Direct Utility Response

A.5.3.1   Assessment of Utility Responses to EPRI Diesel Evaluation

Utility data were used directly to assess Zion and Cook diesels.
A β factor approach was used as these plant data did not allow distinguish-
ing multiple demands. Data were also studied for Zion and Cook from LERs
to determine more precisely the course of failure. A rigorous statistical
data analysis is not likely here due to the nature of the data base available.

Data were then collated to distinguish between independent and
common-cause diesel failures. Three primary contributors to potential
common-mode failures were identified:

- Human error (H)
- Design, fabrication, and installation errors (D)
- Procedural deficiencies (P).

Factors were therefore defined to account for the fraction of
failures which were due to the common-cause contributors;

$$\beta_i \overset{\Delta}{=} \frac{\text{the number of common diesel failure causes of the } i^{th} \text{ type}}{\text{the total number of diesel failure causes}}$$

where:

β_H = Human contribution

β_D = Design, fabrication, and installation contribution

β_P = Procedural contribution.

Three β factors were defined because the plant-specific data
showed that principal common-cause contributions varied among the facili-
ties. In this manner, each plant could be assigned its own relative β
factors.

A-88

Conditional probabilities for multiple diesel failures according to the common-cause contributors were then determined through data review (i.e., the probability of n common-cause diesel failures given that n-1 have failed from the same cause). Results of the β factors and conditional probabilities identified are shown in Table A.5.3. When combined with specific diesel demand data, this table can be used to determine the

Table A.5.3

ZION AND COOK FRACTION β-FACTORS AND CONDITIONAL PROBABILITIES

Facility	β_H	β_D	β_P	$P_H(2/1)$	$P_D(2/1)$	$P_P(2/1)$	$P_H(3/2)$	$P_D(3/2)$	$P_P(3/2)$	β_{TOTAL}
Cook - 1	0/6	4/6	0/6	---	2/4	---				4/6
Cook - 2	1/5	1/5	0/5	1/1	0/1	---				2/5
Zion - 1	3/25	2/25	0/25	0/3	0/2	---	---	---	---	5/25
Zion - 2	4/21	0/21	0/21	0/4	---	---	---	---	---	4/21
Avg. Plant	38/240	31/240	11/240	5/38	6/31	2/11	---	1/1	0/1	80/240

probability of multiple diesel generator failure. These calculations are given in Tables A.5.4 and A.5.5 for Zion and Cook. As shown, if plant-specific conditional probabilities were unavailable, then plant averages were used from Table A.5.3.

A.5.3.2   Evaluation of Diesels Using Licensee Event Reports (LERs)

The final method of diesel assessment was made using LERs. Diesel generator failure data for 36 LWRs (23 LWRs from Reference A.5-1 plus 13 additional LWRs) were collected from LERs and the EG&G diesel report (NUREG/CR-1362). Tables A.5.6 and A.5.7 summarize the failure data which were collected. It is apparent that no additional multiple failures were recognized in the 13 plants reviewed from the EG&G source. The total number of diesel failures from the 36 plants is 432 in 330.9 diesel years of operation.

Table A.5.4

DIESEL FAILURE RATES FOR ZION

	Zion-1	Zion-2
Total Failures[a]	12	12
Total Demands[a]	635	635
Failure/Demand (θ)	$1.89(10^{-2})$	$1.89(10^{-2})$
$\beta_H P_H(2/1)$	$(3/25)(5/38) = 1.58(10^{-2})$	$(4/21)(5/38) = 2.51(10^{-2})$
$\beta_D P_D(2/1)$	$(2/25)(6/31) = 1.55(10^{-2})$	$(0/21)(6/31) = 0$
$\beta_p P_p(2/1)$	$(0/25)(2/11) = 0$	$(0/21)(2/11) = 0$
β_{TOTAL}	5/25	4/21
$P_{CM}(2)$/Demand[b]	$8.96(10^{-4})$	$1.42(10^{-3})$
$P_{CM}(3)$/Demand[c]	$8.79(10^{-4})$	$8.79(10^{-4})$[h]
$P(2)$/Demand[d]	$1.58(10^{-3})$	$2.11(10^{-3})$
$P(3)$/Demand[e]	$9.2(10^{-4})$	$9.43(10^{-4})$
$P(2/1)$/Demand[f]	$8.36(10^{-2})$	$1.12(10^{-1})$
$P(3/2)$/Demand[g]	$5.82(10^{-1})$	$4.47(10^{-1})$

[a] Average for 46 month period as reported from facility

[b] $P_{CM}(2)$ = Probability of 2 diesels failing out of 3 diesels from common mode

$$= \beta_H P_H(2/1) \cdot \theta \cdot 3 \cdot (1-P_H(3/2)_{avg}) + \beta_D P_D(2/1) \cdot \theta \cdot 3 \cdot (1-P_D(3/2)_{avg})$$
$$+ \beta_p P_p(2/1) \cdot \theta \cdot 3 \cdot (1-P_p(3/2)_{avg})$$

[c] $$P_{CM}(3) = \beta_H P_H(2/1) \cdot \theta \cdot 3 \cdot P_H(3/2)_{avg} + \beta_D P_D(2/1) \cdot \theta \cdot 3 \cdot P_D(3/2)_{avg}$$
$$+ \beta_p P_p(2/1) \cdot \theta \cdot 3 \cdot P_p(3/2)_{avg}$$

[d] $P(2)$ = Probability of 2 diesels failing out of 3 diesels

$$= P_{CM}(2) + 3 P_I(1)^2 = P_{CM}(2) + 3 ((1-\beta_T) \theta)^2$$

where I = independent failure

[e] $$P(3) = P_{CM}(3) + P_I(1)^3 + 3P_{CM}(2) \cdot ((1-\beta_T) \theta)$$

[f] $P(2/1)$ = conditional probability of two diesels failing given that 1 diesel fails

$$= P(2)/\theta$$

[g] $$P(3/2) = P(3)/P(2)$$

[h] From data $P_{CM}(3) = 0$, therefore, assume $P_{CM}(3) = 8.79(10^{-4}) = P_{CM}(3)$ for Zion-1

Table A.5.5
DIESEL FAILURE RATES FOR COOK

	Cook-1	Cook-2
Total Failures [a]	14	6
Total Demands [a]	687	211
Failure/Demand (θ)	$2.04(10^{-2})$	$2.84(10^{-2})$
$\beta_H P_H(2/1)$	$(0/6)(5/38) = 0$	$(1/5)(1) = 2.0(10^{-1})$
$\beta_D P_D(2/1)$	$(4/6)(2/4) = 3.33(10^{-1})$	$(1/5)\ 6/31 = 3.87(10^{-2})$
$\beta_p P_p(2/1)$	0	0
TOTAL	4/6	2/5
$P_{CM}(2)$/Demand [b]	$6.79(10^{-3})$	$6.78(10^{-3})$
$P(2)$/Demand [c]	$6.84(10^{-3})$	$7.07(10^{-3})$
$P(2/1)$/Demand [d]	$3.35(10^{-1})$	$2.49(10^{-1})$

[a] As reported from facility

[b] $P_{CM}(2) = \beta_H P_H(2/1) \cdot \theta + \beta_D P_D(2/1) \cdot \theta + \beta_p P_p(2/1) \cdot \theta$

[c] $P(2) = P_{CM}(2) + P_I(1)^2 = P_{CM}(2) + \{(1-\beta_T) \cdot \theta\}^2$

[d] $P(2/1) = P(2)/\theta$

Utility-supplied diesel demand data was available for Zion and Cook stations (discussed above). On an average basis, the number of demands per diesel year are as follows:

- Zion 1 and 2 - 82.1 demands/diesel year
- Cook 1 - 90.4 demands/diesel year
- Cook 2 - 65.9 demands/diesel year.

Based on these four plants, plus data from Plant X (previous section), an average-per-diesel yearly demand was determined to be 65.4 demands/diesel year.

To estimate the number of multiple demands, data available from Plant X was utilized:

Number of single demands   = 133

Number of double demands   =   23

Number of triple demands   =   71

Number of quadruple demands=   67

Total indiv. diesel demands= 660

Table A.5.6

DIESEL FAILURES IDENTIFIED FROM REVIEW OF LERs FOR 23 LWRs

FACILITY	VENDOR	NUMBER DIESELS	PLANT YEARS	DIESEL YEARS	SINGLE FAILURES	DOUBLE FAILURES	TRIPLE FAILURES
Brunswick 1	GE	[a] 4	3.2	18.8	5	1	
Brunswick 2	GE		4.7		18	2	1
Calvert Cliffs 2	CE	[b] 1+1	3.1	6.2	19		
Cook 1	W	2	4.9	9.8	9	2	
Cook 2	W	2	1.8	3.6	4	1	
Crystal River 3	B&W	2	2.9	5.8	5		
Davis Besse	B&W	2	2.3	4.6	6		
Dresden 1	GE	1	20.2	20.2	9		
Dresden 2	GE	1+1	9.9	19.8	55	1	
Palisades	CE	2	8.6	17.2	10		
Peach Bottom 2	GE	4	6.4	25.6	17		
Peach Bottom 3	GE		5.3		1	1	
Pilgrim	GE	2	7.5	15.0	11		
Prairie Island 1	W	2	6.1	12.2	5	2	
Prairie Island 2	W	2	5.1	10.2	2	1	
Salem	W	3	3.1	9.3	7	1	1
St. Lucie	CE	2	3.1	6.2	10	1	
Surry 1	W	1+1	7.5	21.7	15		
Surry 2	W	1+1	6.7		1		
TMI 1	B&W	2	5.5	11.0	10	1	
TMI 2	B&W	2	1.8	3.6	3		
Zion 1	W	2+1	6.4	31.2	34	2	
Zion 2	W	2+1	6.0		27	1	
TOTAL		46	132.1	252.0	283	17	2

[a] } implies all diesels are shared between the plants

[b] + implies dedicated + shared diesel

A-93

Table A.5.7

DIESEL FAILURES IDENTIFIED FROM EG&G DATA FOR 13 LWRs

FACILITY	VENDOR	NUMBER DIESELS	PLANT YEARS	DIESEL YEARS	SINGLE FAILURES	DOUBLE FAILURES	TRIPLE FAILURES
Browns Ferry 1	GE	]ᵃ	3.0		4		
Browns Ferry 2	GE	} 4	3.0	}12.0	0		
Browns Ferry 3	GE		2.3		3		
Calvert Cliffs 1	CE	ᵇ1+1	3.0	3.0	15		
Farley	W	5	1.3	6.5	15		
Fitzpatrick	GE	4	3.0	12.0	9		
Hatch 1	GE	2+1	3.0	}10.0	23		
Hatch 2	GE	2+1	0.5		5		
Indian Point 2	W	3	3.0	9.0	6		
Indian Point 3	W	3	2.8	8.4	5		
Quad Cities 1	GE	1+1	3.0	}9.0	9		
Quad Cities 2	GE	1+1	3.0		2		
Yankee Rowe	W	3	3.0	9.0	10		
TOTAL		31	33.9	78.9	106	0	0

ᵃ] implies all diesels are shared between the plants

ᵇ+ implies dedicated + shared diesel

Table A.5.8

MULTIPLE FAILURES FOR 36 LWRs POPULATION

# DIESELS CONSIDERED	DERIVATION JK MULTIPLE FAILURE NO.
2	# failures of 2 DG's for 2 DG pop. plants: 9 Total operating years = 85.8 $Q(2\|2) = \frac{9}{85.8} = .10/yr = .009/mo. = 12.1 \times 10^{-6}/hr.$
3	# failures of 2 DG's for 3 DG pop. plants: 4 Total operating years = 27.8 $Q(2\|3) = \frac{4}{27.8} = .14/yr = .0../mo. = 1.7 \times 10^{-5}/hr.$
4	# failures of 2 DG's for 4 DG pop. plants: 4 Total operating years = 14.5 + 17.7 = 30.9 $Q(2\|4) = \frac{4}{30.9} = .13/yr = .01/mo. = 1.5 \times 10^{-5}/hr.$
4	# failures of 3 DG's for 3 DG pop. plants: 1 Total operating years = 27.8 $Q(3\|3) = \frac{1}{27.8} = .04/yr = .003/mo. = 4.1 \times 10^{-6}/hr.$
4	# failures of 3 DG's for 4 DG pop. plants: 1 Total operating years = 30.9 $Q(3\|4) \frac{1}{30.9} = .03/yr = .003/mo. = 3.7 \times 10^{-6}/hr.$
4	# failures of 4 DG's for 4 DG pop. plants = 0 = 1 See (3|4) above

A-94

In addition, the following general assumptions were made for multiple diesel plants of population N:

- Single unit demands are primarily due to tests.
- N unit demands are primarily due to non-test actuation signals.
- For N > 2; N-1 unit demands are actually N unit demands when 1 diesel is already unavailable.
- For N > 2; N-2 unit demands are primarily due to testing.

Therefore, based on the ratio of multiple to single demands from Plant X (given below), the average number of demands/diesel year (65.4), and the above assumptions, the following number of general multiple diesel demands were estimated:

Ratio of Multiple Diesel Demands

$$1:Total = .20$$
$$2:Total = .03$$
$$3:Total = .11$$
$$4:Total = .10$$
$$4+3+2:Total = .24$$

Estimation of Diesel Demands/Year

N=2

$$D(total) \simeq (65.4 \times N) \simeq 130$$
$$D(double) \simeq .24 \times D(total) \simeq 31$$

N=3

$$D(total) \simeq (65.4 \times N) \simeq 196$$
$$D(double) \simeq .12 \times D(total) \simeq 24$$
$$D(triple) \simeq .12 \times D(total) \simeq 24$$
$$D(double+triple) = .24 \times D(total)$$

<u>N=4</u>

$$D(total) = (65.4 \times N) = 262$$
$$D(double) = .03 \times D(total) = 8$$
$$D(triple) = .11 \times D(total) = 29$$
$$D(quad.) = .10 \times D(total) = 26$$
$$D(double+triple+quad.) = .24 \times D(total)$$

Using unavailabilities (based on multiple diesel failures) the following failure rate analysis can be made: (See Table A.5.6)

$$Q(2|2) = .10/year$$

$$\lambda_{31}(2|2) = \frac{.10}{31} = .0032 /demand$$

$$Q(2|3) = .14/year$$

$$\lambda_{24}(2|3) = .0058/demand$$

$$Q(2|4) = .13/year$$

$$\lambda_{8}(2|4) = .016/demand$$

$$Q(3|3) = .04/year$$

$$\lambda_{24}(3|3) = .0017/demand$$

$$Q(3|4) = .03/year$$

$$\lambda_{29}(3|4) = .001/demand$$

$$Q(4|4) = .03/year$$

$$\lambda_{26}(4|4) = .0012/demand$$

Probabilities for multiple diesel failures were then taken as the averages of the $\lambda(i|.)$ calculations for $i = 2$, 3, and 4. Results are given below:

$$P(1)_{avg} \approx \frac{432 \text{ Failures}}{(330.9 \text{ diesel years})(65.4 \text{ demands/diesel year})}$$

$$P(1)_{avg} \approx 2.0 \times 10^{-2} \text{ failure/demand}$$

$$P(2)_{avg} \approx .0083 \text{ /demand}$$

$$P(3)_{avg} \approx .0014 \text{ /demand}$$

$$P(4) \approx .0012 \text{ /demand}$$

This evaluation of multiple diesel failures is conservative in nature; however, the lack of data precludes a more realistic calculation.

A.5.3.3   Composite Diesel Assessment

Table A.5.9 presents a summary of the diesel data presented above. The observations which can be made from this data are the following:

1. The failure rate of a single diesel as determined from the various sources is quite similarly varying from 1.89×10^{-2} to 3×10^{-2}.

2. The cumulative effect of the conditional failure probabilities is that the probability of the three remaining diesels failing given that one diesel has failed, varies from .03 to .06.

Table A.5.9

COMPARISON OF DIESEL GENERATOR FAILURE RATE DATA (PER DEMAND)

	PLANT X	ZION/COOK	WASH-1400	3f LWR's	Average Value [c]	Trimmed Value [d]
P(1)	4.99×10^{-2}	$(1.89-2.84) \times 10^{-2}$	3×10^{-2}	$(2.0) \times 10^{-2}$	2.94×10^{-2}	2.61×10^{-2}
P(2)	9.39×10^{-3}	$(1.58-7.07) \times 10^{-3}$	$10^{-3}-10^{-2}$ [b]	$(8.3)10^{-3}$	6.22×10^{-3}	6.55×10^{-3}
P(3)	5.88×10^{-3}	$(9.2-9.43) \times 10^{-4}$	10^{-2}	$(1.4)10^{-3}$	3.8×10^{-3}	3.37×10^{-3}
P(4)	2.94×10^{-3} [a]		10^{-2}	$(1.2)10^{-3}$	3.00×10^{-3}	2.89×10^{-3}
P(2/1)	1.88×10^{-1}	$(.84-3.35) \times 10^{-1}$	$(.33-3.3)10^{-1}$	$(4.2)10^{-1}$	2.32×10^{-1}	2.34×10^{-1}
P(3/2)	6.26×10^{-1}	$(4.47-5.82) \times 10^{-1}$	1.0	$(1.7)10^{-1}$	5.6×10^{-1}	5.52×10^{-1}
P(4/3)	5×10^{-1} [a]		1.0	$(8.6)10^{-1}$	7.86×10^{-1}	8.60×10^{-1}

[a] Estimate

[b] 10^{-3} is the probability for 2 independent failures; 10^{-2} is the probability for common mode

[c] Average of all values - NOTE: P(2), P(3), P(4) averages were calculated from the average conditionals

[d] Mean value after deletion of largest and smallest values

A.5.4   Diesel Repair Rate

In the LGS analysis it is important to know the availability of onsite 4160V AC power during the course of an accident. If AC power is unavailable at the beginning of an accident sequence, it may be restored at a later time. Therefore, it was necessary to determine the diesel repair time (Table A.5.10). Specifically of interest in the LGS evaluation is the probability of recovering the diesels after two hours and four hours following the loss of AC emergency power buses:

Probability Description	Probability Value Estimate
1 diesel recovered within 2 hours	.33
1 diesel recovered within 4 hours	.53

Table A.5.10
SUMMARY OF DIESEL REPAIR TIME FOLLOWING
FAILURES OF INDIVIDUAL DIESELS

From EG&G (normalizing to 100%)

25% of time 1 diesel is repaired within 0-1 hr
28% of time 1 diesel is repaired within 1-4 hr
24% of time 1 diesel is repaired within 4-8 hr
11% of time 1 diesel is repaired within 8-24 hr
12% of time 1 diesel is repaired within >24 hr

Cumulative percentages become:

25% of time 1 diesel is available by 1 hr
53% of time 1 diesel is available by 4 hr
77% of time 1 diesel is available by 8 hr
88% of time 1 diesel is available by 24 hr
12% of time 1 diesel is unavailable after 24 hr

Estimation between 1-8 hr is:
75% of time 1 diesel is unavailable after 1 hr
66% of time 1 diesel is unavailable after 2 hr
57% of time 1 diesel is unavailable after 3 hr
47% of time 1 diesel is unavailable after 4 hr
41% of time 1 diesel is unavailable after 5 hr
35% of time 1 diesel is unavailable after 6 hr
29% of time 1 diesel is unavailable after 7 hr
23% of time 1 diesel is unavailable after 8 hr

A.5.5   Summary of Data Used in the LGS Evaluation

Combining the information from the various sources discussed in this section, the following data are used to characterize the unavailability of tne diesel units for the LGS analysis:

1. The failure to "start and run" probability for a single diesel is taken from the Philadelphia Electric Company experience at the Peach Bottom Station. This is 1.7×10^{-2}/demand.

2. The conditional probability that multiple diesels may fail given that a single diesel fails is taken from the data source with the most information, the evaluated data from 36 LWRs. The values arrived at for the conditional failure probability are:

   - P(2/1) - Conditional Probability of a second diesel failing given that one has failed $\equiv 4.2 \times 10^{-1}$

   - P(3/2) - Conditional Probability of a third diesel failing given that two diesels have failed $\equiv 1.7 \times 10^{-1}$.

   - P(4/3) - Conditional Probability of a fourth diesel failing given that three diesels have failed $\equiv 8.6 \times 10^{-1}$

3. The probability of recovery of a oiesel can be very important in many accident scenarios where the plant can be maintained in a safe condition for two to four hours without 4160V AC emergency power. The available data from Peach Bottom and the NRC evaluated diesel data both agree quite well as to the conditional probability of recovering diesel within 2 hours and within 4 hours. The data used in the Limerick evaluation is the NRC data, which is:

   Probability of Recovering
   1 diesel within 2 hours = .33

   Probability of Recovering
   1 diesel within 4 hours = .53

REFERENCES

A.5.1   McLagan, G. P., Azarm, M. A., Metwally, M. A., Leverenz, F. L.,
        "Preliminary Assessment of Diesel Generator Reliability at
        Light Water Reactors", SAI/Ames, March 30, 1980

A.6   COMPLETE LOSS OF OFFSITE POWER

Complete loss of offsite power to a generating station is an
event which is influenced by local factors such as type of weather ex-
posure, transmission system design, and operating procedures. Therefore,
a local or regional data base is more suitable than a national data base
for predicting the frequency and duration of such events at a specific
plant.

Limerick Generating Station is connected to the Pennsylvania-
New Jersey-Maryland Interconnection (PJM) System and the remainder of
the PECo System via five transmission lines. Section A.6.1 reviews the
PJM/PECo data base and analytical techniques used in this study to
determine (1) the frequency of complete loss of offsite power and (2)
the probability of recovery of offsite power as a function of time
from interruption.

The analyses show a relatively high reliability for the PJM/
PECo plants. Even so, the use of these levels of reliability in this
study is probably conservative since the five transmission line design
at Limerick exceeds the average level of redundancy for the plants in-
cluded in the data base. As a comparison, Section A.6.2 reviews the
data and analyses used in WASH-1400.

Section A.6.3 discusses the specific case of Loss of Offsite
Power caused by trip of the Limerick turbine-generator.

A.6.1   PJM/PECo Experience

Complete loss of offsite power experience for PJM nuclear plants
and PECo fossil plants with three or more transmission lines are summarized
in Tables A.6.1a and A.6.1b, respectively. In total, these plants have an
experience of four occurrences in 94.7 plant years.

Table A.6.1a
COMPLETE LOSS OF OFFSITE POWER

Pennsylvania-New Jersey-Maryland Interconnection (PJM) Nuclear Plant Experience from Initial Criticality through July 1980			
Plant	Exposure (Plant-Years)	Occurrences	Average Duration (Minutes)
Calvert Cliffs	5.8	1	350
Oyster Creek	11.3	1	90
Peach Bottom	6.9	0	-
Salem	3.7	0	-
Three Mile Island	6.2	0	-
	33.9	2	220

Table A.6.1b
COMPLETE LOSS OF OFFSITE POWER

Philadelphia Electric Company Fossil Plant (with Three or More Transmission Lines) Experience from January 1973 through July 1980			
Plant	Exposure (Plant-years)	Occurrences	Average Duration (Minutes)
Chester	7.6	0	-
Cromby	7.6	0	-
Croydon	7.6	1	2
Delaware	7.6	0	-
Eddystone	7.6	0	-
Schuylkill	7.6	0	-
Southwark	7.6	1	48
Richmond	7.6	0	-
	60.8	2	25

The frequency of complete loss of offsite power was modeled as
a Poisson process. Using the PJM/PECo data base and assuming a uniform
prior, a Bayesian analysis found the posterior distribution function. The
frequency of loss of offsite power is shown in Table A.6.2. The mean
value of this posterior distribution, .0528, was used as the frequency
of loss of offsite power in this study.

TABLE A.6.2

POSTERIOR DISTRIBUTION OF FREQUENCY
OF LOSS OF OFFSITE POWER

λ	Density Function	Cumulative Distribution Function
1.00000E-08	3.16847E-24	6.33655E-33
7.74629E-03	5.56689E-01	1.00000E-03
1.12900E-02	1.791755+00	5.00000E-03
1.35003E-02	2.93520E+00	1.00000E-02
2.08106E-02	8.39643E+00	5.30080E-02
2.56884E-02	1.21175E+01	1.00000E-01
3.26343E-02	1.63596E+01	2.00000E-01
3.83799E-02	1.81561E+01	3.00000E-01
4.38134E-02	1.94362E+01	4.00000E-01
4.93407E-02	1.75779E+01	5.00000E-01
5.53192E-02	1.57708E+01	6.00000E-01
6.22238E-02	1.31329E+01	7.00000E-01
7.10016E-02	9.70008E+00	8.00000E-01
8.44432E-02	5.43702E+00	9.00000E-01
9.66942E-02	2.53098E+00	9.50000E-01
1.225950-01	6.52640E-01	9.90000E-01
1.33046E-01	3.36592E-01	9.95000F-01
1.56287E-01	7.10137E-02	9.99000E-01
2.89011E-01	2.89679E-00	1.00000E+00

Means= 5.28150E-2
STD.DEV.= 2.36196E-02
BETA1= 7.95937E-01
BETA2= 4.19959E+00

Another important factor is the probability of recovery of offsite power
within specific times. The PJM/PECo data base was again used in this
assessment. The recovery times for the four occurrences actually ex-
perienced were used to determine the mean recovery time and the variance
of recovery time. A gamma distribution was then constructed to fit the
mean and variance. This distribution is as shown in Table A.6.3.

TABLE A.6.3

PROBABILITY DISTRIBUTION OF RECOVERY TIME

Recovery Time (Min.)	Density Function	Cumulative Density Function
1.00000E-08	3.67898E-01	3.88717E-09
8.46307E-02	3.63946E-01	1.00000E-03
4.23155E-01	3.48140E-01	5.00000E-03
8.46310E-01	3.28381E-01	1.00000E-02
4.23155E+00	1.70311E-01	5.00000E-02
8.76388E+00	9.25098E-03	1.00000E-01
2.11376E+01	7.25624E-03	2.00000E-01
3.64134E+01	5.93326E-03	3.00000E-01
5.50613E+01	4.86381E-03	4.00000E-01
7.79330E+01	3.92027E-03	5.00000E-01
1.06789E+02	3.05372E-03	6.00000E-01
1.44929E+02	2.23894E-03	7.00000E-01
1.99896E+02	1.46223E-03	8.00000E-01
2.95783E+02	7.16099E-04	9.00000E-01
3.93181E+02	3.53724E-04	9.50000E-01
6.22557E+02	6.97990E-05	9.90000E-01
7.21951E+02	3.48574E-05	9.95000E-01
9.51645E+02	7.04579E-06	9.99000E-01
1.47234E+03	1.97949E-07	1.00000E-00

Means= 1.22457E+02
STD.DEV.= 1.34743E+02
BETA1= 4.73406E+00
Beta2= 9.89231E+00

The probability that recovery takes more than a given number of hours can be found from this distribution. Specifically,

P(Recovery of offsite power > 2 hours) = 0.365

P(Recovery of offsite power > 4 hours) = 0.158

P(Recovery of offsite power > 15 hours) = 9×10^{-4}

P(Recovery of offsite power > 24 hours) = 1×10^{-8}

Figure A.6.1 displays graphically the cumulative frequency of the loss of offsite power versus the duration of the loss.
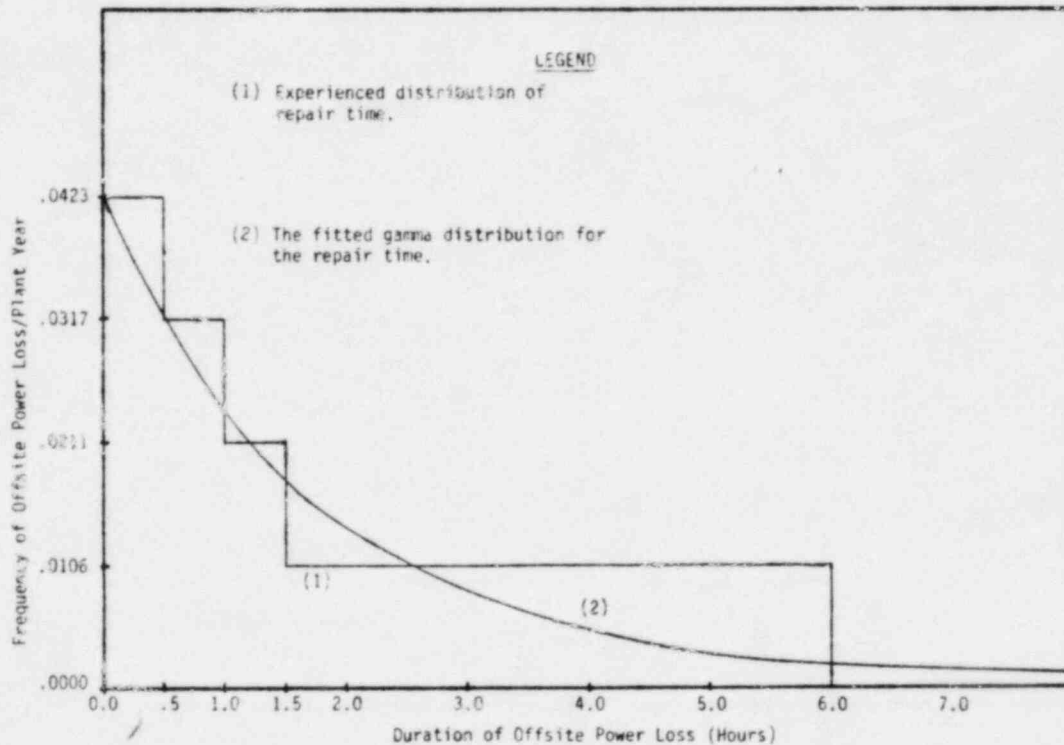
Figure A.6.1   Cumulative Frequency of Offsite Power Loss Vs. Duration

A.6.2   WASH-1400 Assessment of Complete Loss of Offsite Power

The WASH-1400 estimate for loss of offsite power was larger than the estimate for the PJM interconnection, as shown below:

SOURCE	COMPLETE LOSS OF OFFSITE POWER INITIATOR
WASH-1400	0.18 per plant year
PJM Grid (see Section A.6.1)	0.053 per plant year

The PJM value (0.053) was used in this study.

WASH-1400 estimated the frequency of offsite power loss at 2×10^{-5}/hr. based on three occurrences in 1972 for 150,000 hours of operation. If it is assumed that plants are 100% available, this is equivalent to 17.1 plant-years of experience giving an estimated 0.18 offsite power loss/plant year. The estimate becomes 0.12 offsite power loss/plant year if the plants are assumed to be 70% available. Figure A.6.2 can then be utilized to predict frequency/duration characteristics of the offsite power outages. Results are as follows (assuming 70% average availability):

Frequency of offsite power loss (P_0) which is restored in less than 0.01 hour = 0.0001

P_0 restored in 0.01 - 0.032 hours = 0.007

P_0 restored in 0.032 - 0.1 hour = 0.023

P_0 restored in 0.1 - .32 hour = 0.046

P_0 restored in 0.32 - 1.0 hour = 0.015

P_0 restored in 1.0 - 3.2 hour = 0.014

P_0 restored in 3.2 - 10.0 hour = 0.01

P_0 restored in greater than 10 hours = 0.004.

A-107

Percent of Outages Restored to Service by Time (T)

40.0

30.0

20.0

10.0

0.0

Number of Outages

640
480
320
160

1.1% Outages Restored in Less Than 0.01 Hour.

Major Contributor: Switching

6.1% Outages Restored in 0.010 to 0.032 Hour.

Major Contributors: Lightning and Malicious Damage

18.7% Outages Restored in 0.032 to 0.100 Hour.

Major Contributors: Lightning and Accidental Tripping

37.9% Outages Restored in 0.1 to 0.32 Hour.

Major Contributor: Lightning

12.6% Outages Restored in 0.32 to 1.0 Hour.

Major Contributors: Malicious Damage, Lightning, and Terminal Equipment Failures

11.7% Outages Restored in 1.0 to 3.2 Hours.

Major Contributors: Lightning, Storms, and Snow, Frost, or Ice

8.4% Outages Restored in 3.2 to 10.0 Hours.

Major Contributors: Tree in line, Snow, Frost, or Ice, and Malicious Damage

0.001   0.01   0.1   1.0   10.0

Outage Duration Time (Hours)

Figure A.6.2 Histogram -- Restoration of Transmission Line Outages

A.6.3   Loss of Offsite Power Resulting from Turbine/Generator Trip

In-plant transient events causing a turbine or generator trip result in a sudden loss of grid generating capacity. If the sudden loss of generator exceeds the transient stability limit of the local or regional grid system, then all offsite power to the plant could be lost. Based upon information developed for WASH-1400, the probability for complete loss of offsite power following a turbine or generator trip is assumed to be 1×10^{-3}. The probability for any particular plant could be lower depending on the transmission systems, the transient stability limit resulting from high installed capacity, extensive grid connections with other large utilities, and the number of 500 and 230 kV transmission lines connecting the plant to the grid. The probability of 1×10^{-3} is conservative for LGS because of the PJM Interconnection system and the use of five plant transmission lines and is included in the analysis.

A-108

Appendix B

SYSTEM DESCRIPTIONS AND FAULT TREE
LOGIC MODELS

APPENDIX B

The purpose of this appendix is to present, in a consolidated form, the following:

● A system description of the key systems which contribute to plant safety

● A schematic of the system arrangements

● The system level fault tree logic models and top level functional fault trees used in the evaluation of system and plant reliability

● The top level sequence fault trees which combine systems to calculate individual accident sequences.

Included in this appendix are the following systems, as identified by section:

B.1 High Pressure Coolant Systems

    B.1.1 HPCI
    B.1.2 RCIC
    B.1.3 CRD
    B.1.4 Condensate and Feedwater

B.2 Low Pressure Coolant Systems and Pressure Reduction System

    B.2.1 ADS
    B.2.2 LPCI
    B.2.3 CS

B.3 Decay Heat Removal Systems

    B.3.1 RHRSW
    B.3.2 Condenser
    B.3.3 Ultimate Heat Sink

B.4 Containment Systems

    B.4.1 Containment Over-Pressure Relief
    B.4.2 Containment Inerting

B.5 Electric Power System and Instrumentation

B.6   Emergency Service Water System -- HVAC Pump Room Cooling

B.7   Reactor Protection System

B.8   Standby Liquid Control System

In addition, there are two summary sections which organize the individual system trees into the following:

- B.9: Functional level fault trees which combine system trees together to reflect the success criteria for various accident sequences

- B.10: Sequence fault trees which display how each sequence is combined in a Boolean fashion.

B.1   HIGH PRESSURE COOLANT SYSTEMS

B.1.1   High Pressure Coolant Injection System (HPCI)

Purpose

The primary purpose of the high pressure coolant injection (HPCI) is to maintain the reactor vessel water inventory under conditions which do not depressurize the reactor vessel.

Hardware Description

The HPCI system consists of a steam turbine-driven, constant-flow pump assembly and associated system piping, valves, controls, and instrumentation (see schematic in Figure B.1.1). Suction piping comes from both the condensate storage tank (CST) and the suppression pool (SP). Initially, water from the CST is used. Injected water is piped to the reactor vessel by way of the core spray loop B pipe. The steam supply for the turbine is piped from the main steam line in the primary containment. The steam piping has an isolation valve on each side of the primary containment. Remote controls for valve and turbine operation are provided in the main control room.

The pump assembly is located below the water levels of the CST and the SP, to ensure positive suction to the pumps. The steam for the pump turbine is extracted upstream of the main steam isolation valves (MSIVs). Exhaust steam from the HPCI turbine is discharged to the suppression pool.

Automatic and Manual Control

Startup of the HPCI system is completely independent of AC power. Only DC power from the station battery and steam extracted from the nuclear system are necessary. The HPCI controls automatically start the system and bring it to design flow rate with 25 seconds from receipt of a reactor pressure vessel (RPV) low water level signal, or a primary containment (drywell) high pressure signal.
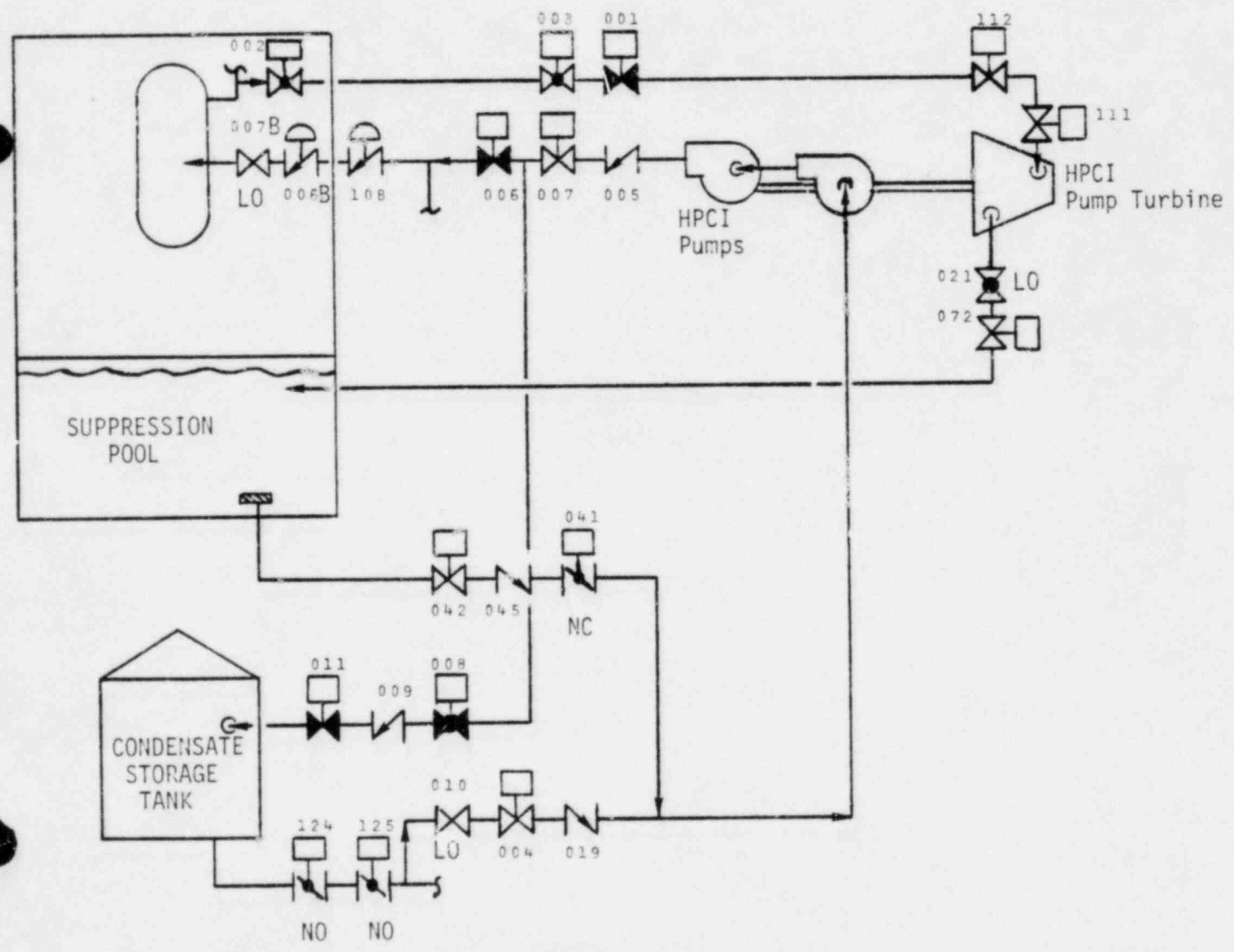
Figure B.1.1   High Pressure Coolant Injection System Schematic

After startup, the controls function to provide design makeup water flow to the reactor vessel until the amount of water delivered to the reactor vessel is adequate (high reactor water level), at which time the HPCI system automatically trips. The controls are arranged to allow remote-manual startup, operation, and shutdown.

The HPCI turbine is shut down automatically by any of the following signals:

- Turbine Overspeed: This prevents damage to the turbine.

- RPV High Water Level: This indicates that core cooling requirements are satisfied. (HPCI will shut off on high level during most transients unless the operator takes control to throttle HPCI).

- HPCI Pump Low Suction Pressure: This prevents damage to the pump due to loss of flow.

- HPCI Turbine Exhaust High Pressure: This indicates a defect in the turbine exhaust line check valve: restriction in HPCI turbine exhaust line due to failure of either vacuum-breaking system or turbine exhaust drain line system caused by water hammering or defective pressure switches.

- High steam flow in steam supply line to the HPCI turbine

- Low steam supply pressure.

If a low-level initiation signal is received after the turbine is shut down, the system restarts automatically if no shutdown signal exists.

In addition to the automatic operational features of the system, provisions are included for remote manual startup, operation, and shutdown (provided automatic initiation or shutdown signals do not exist).

HPCI operation automatically actuates the following valves:

- HPCI pump discharge shutoff valves

- HPCI steam supply shutoff valve

- HPCI turbine stop valve

- HPCI turbine control valves

- HPCI steam line drain isolation valve

- HPCI test valve, if open

- Minimum flow bypass valve.

As mentioned earlier, suction is normally taken from the CST. If the level in the CST falls to a low level, or a high level in the suppression pool occurs, a level sensor initiates an automatic realignment of pump suction to the suppression pool.

Instrumentation and Control

The HPCI-actuated devices are automatically controlled by logic or manually controlled by switches in the control room. Motor-operated valves are provided with appropriate limit or torque switches to turn off the motors when the fully-open or fully-closed positions are reached. Valves that are automatically closed on isolation or turbine trip signals are equipped with manual reset devices so that they cannot be reopened without operator action.

Electric Power Requirements

Only DC electrical power is required for the HPCI system startup. As shown in the electrical power system description, DC divisions B and D supply two separate redundant sources of power. For long-term HPCI operation, room cooling must be available to maintain acceptable temperatures in the HPCI compartment. Automatic room cooling requires 440V AC power from emergency buses B or D for ESW operation.

B.1.2   Reactor Core Isolation Cooling (RCIC) System (See Figure B.1.2)

Purpose

The purpose of the RCIC system is to assure that sufficient water inventory is maintained in the reactor vessel to permit adequate core cooling during the following conditions:

- Transients that include the loss of normal feedwater

- LOCAs with break sizes that do not depressurize the reactor

- Hot shutdown conditions.

Hardware Description

The RCIC system consists of the following components:

- One 100% capacity turbine and accessories

- One 100% capacity pump assembly and accessories

- Piping, Valves, and Instrumentation for the following:

  - Steam supply to turbine

  - Turbine exhaust to suppression pool

  - Makeup supply from the condensate storage tank (CST) to pump suction

  - Makeup supply from the suppression pool to the pump suction

  - Makeup supply from the RHR steam condensing heat exchangers

  - Pump discharge to the feedwater line, spray nozzle, including a test line to the CST, a minimum flow bypass line suppression pool, and a coolant water supply to accessory equipment.
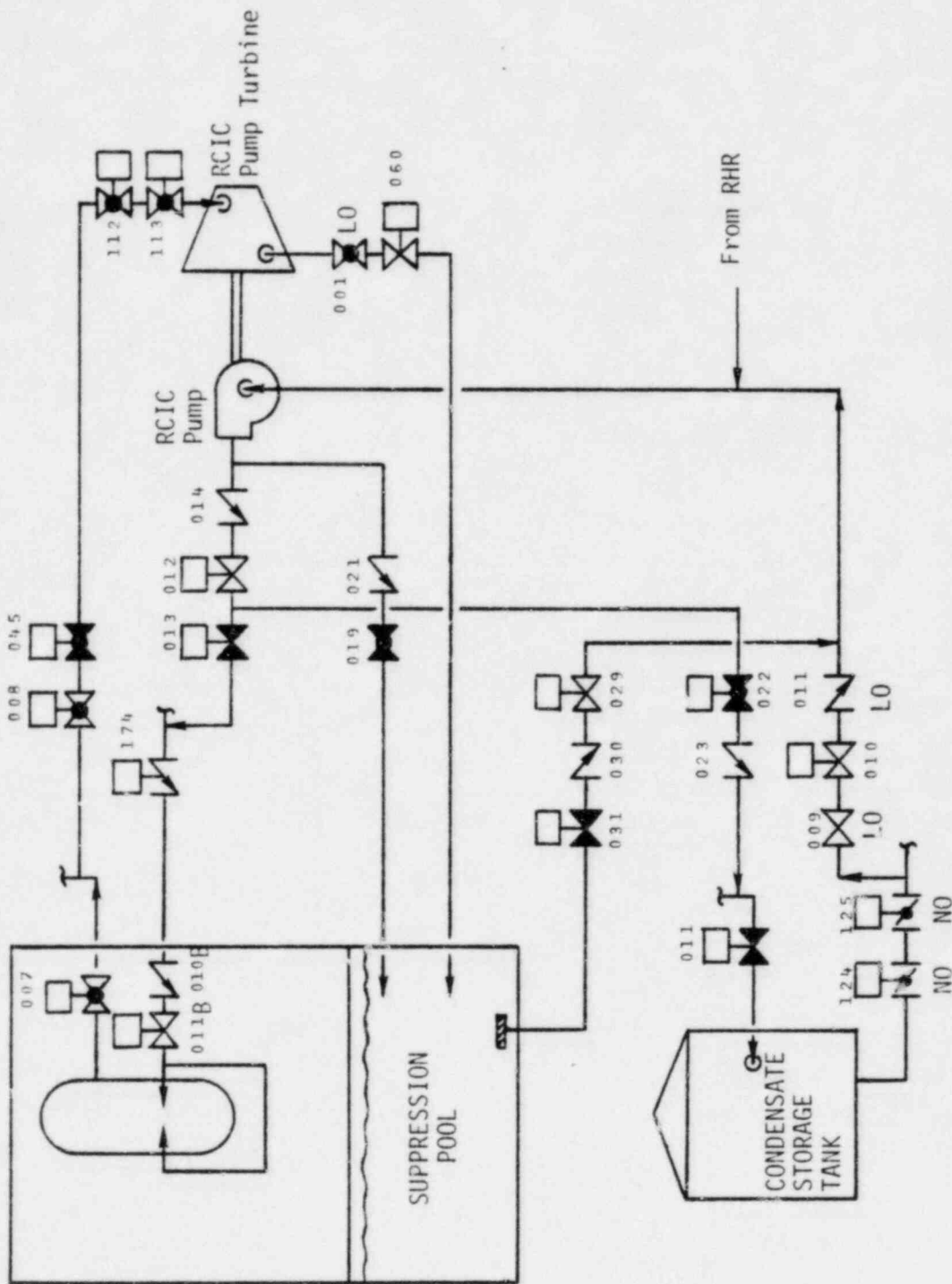
Figure B.1.2 Reactor Core Isolation Cooling System Schematic

Automatic Control

The RCIC is initiated automatically upon a reactor vessel low water level signal. Steam supply to the RCIC turbine is automatically cut off by any of the following signals:

1. High differential pressure across the main steam line

2. High area temperature

3. Low reactor pressure

4. High turbine exhaust pressure

5. Turbine overspeed (mechanical overspeed trip must be reset locally)

6. High reactor water level.

Manual Operation

Provisions are included for remote manual startup, operation, and shutdown of the RCIC system, provided automatic initiation or shutdown signals do not exist. After the RHR system is placed in the steam condensing mode, the operator can select makeup supply from the RHR steam condensing heat exchangers.

Electric Power Requirements

The RCIC system power for startup is obtained from a DC safeguard battery bus. Long term RCIC operation requires room cooling to maintain adequate temperature control. Automatic room cooling requires 440V AC power from either of the emergency buses A or C for ESW operation.

B.1.3   Control Rod Drive Hydraulic System (CRD)

Purpose

The CRD hydraulic system is also a source of high pressure makeup water to the reactor vessel.

Hardware Description

The CRD system consists of drive water pumps, filters, flow control valves, hydraulic control units (HCUs, one per CRD), scram discharge volume, and the associated system piping, valves, controls, and instrumentation (see Schematic in Figure B.1.3). The water source for the CRD system is the condensate treatment system.

Automatic and Manual Control

The CRD pump is in continuous operation and water is continuously pumped into the reactor vessel through one of three flow paths (driving, charging, or cooling water header). The second pump is provided as a backup should the first pump need to be taken out of service. The flow path chosen is determined automatically with provisions for operator intervention.

Instrumentation

Local and remote indicators and alarms are provided to monitor and protect the system.

Electric Power Requirements

The CRD system is normally run off the nonemergency class buses. The operator can manually switch over to emergency class 1E buses at the motor control center.

B.1.4 Condensate and Feedwater System

Purpose

The primary purpose of the condensate and feedwater system is to remove condensed (main) steam from the condenser hotwells, heat it, and return it to the reactor to be converted into steam.
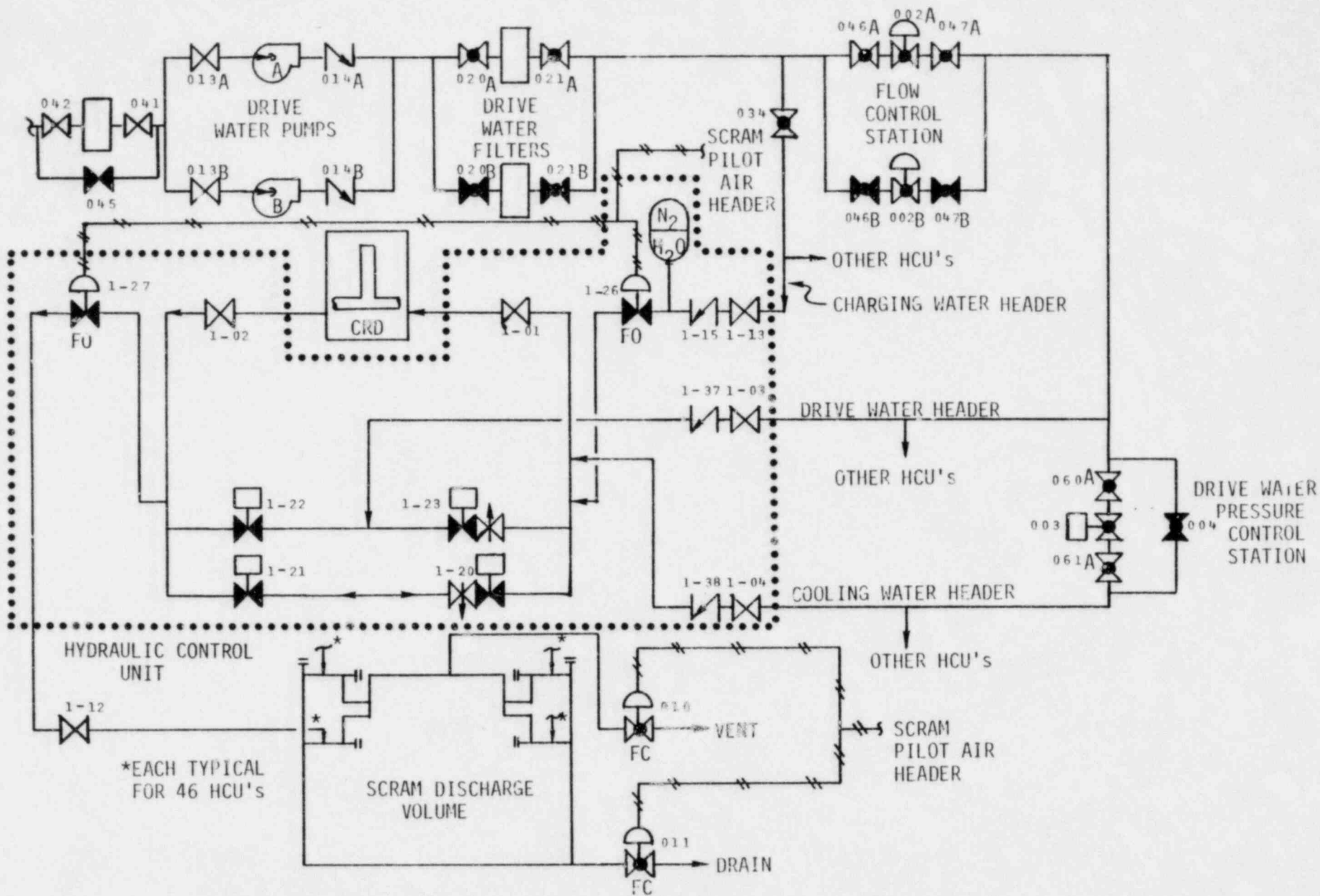
Figure B.1.3   Control Rod Drive Injection Schematic

Hardware Description

The condensate and feedwater (FW) system consists of condensate pumps, steam jet air ejectors, steam packing exhausters, a condensate demineralizer system, low- and high-pressure FW heaters, turbine-driven FW pumps, and associated system piping, valves, controls, and instrumentation (see schematics in Figures B.1.4a and B.1.4b). The steam supply for the FW turbines is piped from the main steam line downstream of the MSIVs for the required high-pressure steam and from the low-pressure steam line downstream of the moisture separators for the required low-pressure steam.

Automatic and Manual Control

The condensate and FW system is not initiated automatically, but it is a normally operating system which automatically controls reactor vessel level within a predetermined range. Manual/automatic startup, operation, and shutdown are provided in the control room. Shutdown of the system, however, can be initiated automatically by isolation of the MSIVs, FW turbine trip, reactor pressure vessel high water level, loss of condenser vacuum or low suction pressure trip. If the condensate or FW system is tripped, operator interaction is required.

Instrumentation

Local and remote indicators, alarms, and pressure relief valves are provided to monitor and protect the condensate and FW system.

Electric Power Requirements

The condensate and FW system is a nonsafety system and failure of the system does not prevent a safe shutdown of the plant. The system is, therefore, run off a nonsafeguard bus.

Figure B.1.4a   Condensate and Feedwater System Schematic
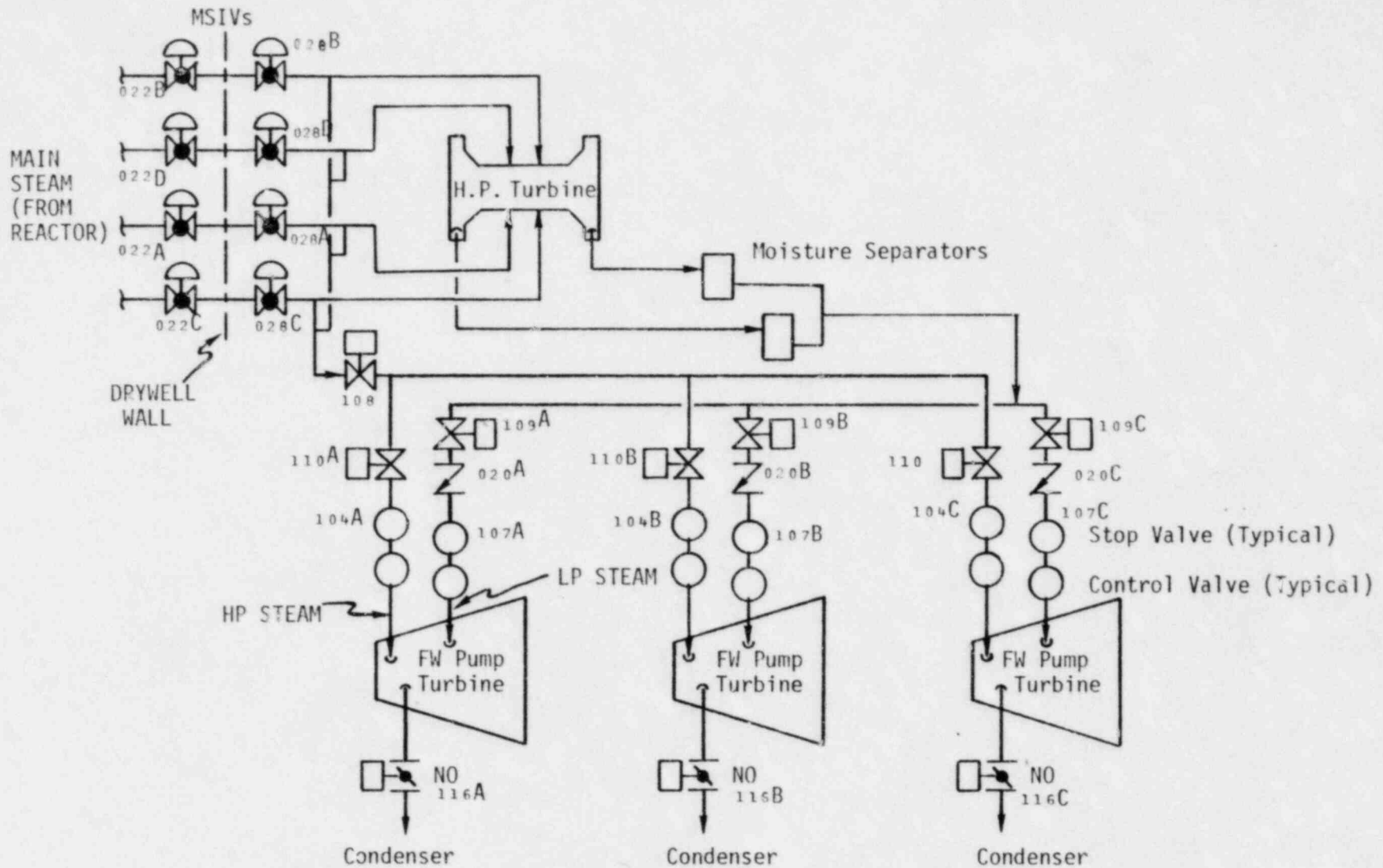
Figure B.1.4b   FW Pump Turbines (Condensate and Feedwater System) Schematic

B.2   LOW PRESSURE COOLANT SYSTEMS AND PRESSURE REDUCTION SYSTEM

B.2.1   Automatic Depressurization System (ADS)

Purpose

The purpose of the automatic depressurization system (ADS)
is to reduce the reactor pressure so that flow from the LPCI and/or
the core spray (CS) systems can enter the reactor vessel in time to
cool the core and limit fuel cladding temperatures in the event that
the RCIC or the HPCI system cannot maintain the reactor water level.

Hardware Description

The ADS employs nuclear steam system safety/relief valves to
relieve high pressure steam to the suppression pool. The safety/relief
valves are installed on the main steam lines inside primary containment.
Five of them are automatically controlled by the ADS. The valves are
dual-purpose, in that they relieve pressure by normal mechanical action
or by automatic action of an electric-pneumatic control system.

The dual-solenoid-operated valves control the pneumatic pressure
applied to an actuator that controls the safety/relief valve directly. An
accumulator is included with the control equipment to store pneumatic energy
for short-term safety/relief valve operation. There are two independent
and redundant solenoid valves associated with each ADS valve; therefore,
each relief valve can be actuated by either of two solenoid-operated valves
supplying air to the relief valve air piston operators.

The operation of the ADS safety/relief valves as a method of
depressurizing the primary system to very low pressures (i.e. approximately
100 psi) requires an air supply. The Limerick ADS has two methods of en-
suring adequate air supply:

1. The plant high-pressure air supply (this is located outside containment and may be isolated under some plant conditions).

2. The accumulators which are located inside containment are the safety grade sources of air for the ADS valves.

Automatic and Manual Control

Automatic Control: Three signals are used for automatic initiation of the ADS:

1. Reactor vessel low water level

2. Drywell high pressure

3. RHR and/or CS pumps running.

All signals must be present to cause the ADS valves to open. Discharge pressure on any one of the LPCI pumps or either pair of the CS pumps is sufficient for condition (3) above to give the permissive signal.

After receipt of the initiation signals and after a delay provided by timers, each of the solenoid-operated valves is energized. This allows pneumatic pressure from the accumulator to act on the air cylinder operator. The air cylinder operator holds the relief valve open.

The dual solenoids in the pilot valve for each ADS valve are individually controlled by ADS Logic A (Division 1) and by ADS Logic C (Division 3).

Manual Control: The operator can use the reset push buttons to delay or prevent the automatic opening of the relief valves if such delay in prevention is prudent. The operator can also manually initiate each safety/relief valve associated with the ADS. The manual initiation signal is sealed-in until reset by the operator.

Interlocks

An interlock prevents both automatic and manual ADS initiation, unless at least one RHR pump or either pair of the CS pumps is capable of delivering water into the vessel.

Instrumentation and Alarms

Instrumentation sensors are used to monitor reactor vessel low water level and high drywell pressure. In addition, there are pressure sensors to monitor the discharge pressure on the CS and RHR pumps.

The primary containment high-pressure signals are arranged to seal-in the control circuitry; they must be manually reset to clear. The level sensing logic and the pumps discharge pressure signals do not seal-in.

A timer is used in each ADS logic. An alarm in the control room is annunciated when either of the timers is timing. Lights in the control room indicate when the solenoid operated valves are energized to open a safety/relief valve.

Electric Power Requirements

The ADS electric control circuitry is powered by DC from plant safeguard batteries.

B.2.2   Low Pressure Coolant Injection (LPCI)

Purpose

The primary purpose of the LPCI system is to provide vessel inventory makeup following large pipe breaks. The LPCI system provides inventory makeup following a small break or other demand for coolant inventory makeup. In both cases the LPCI is only designed to provide cooling water to the reactor core when the reactor vessel pressure is low.

Hardware Description

The LPCI system is an operating mode of the RHR system. It uses four RHR motor-driven pumps to draw suction from the suppression pool and inject cooling water flow into the reactor core via separate vessel nozzles and core shroud penetrations. The LPCI system includes associated valves, control instrumentation, and pump accessories. A schematic of the RHR-LPCI system is shown in Figure B.2.2.

The LPCI system contains four loops (A, B, C, D). Two loops (D and C) are solely injection loops. Loops A and B have several functions since they can pass flow through the RHR heat exchangers (HXs). In the RHR-LPCI mode, the flow in loops A and B is through or bypasses the HXs. In addition, there is a cross-connection between RHR loops A and C and B and D. Water can enter the reactor vessel either directly or via the recirculation loop. In loop A there is an additional path to enter the core via a spray nozzle on top of the reactor vessel.

Automatic and Manual Control

Automatic Control: The LPCI mode of operation of the RHR system is initiated automatically when the following events occur:

- Low water level in the reactor vessel and/or
- High pressure in drywell concurrent with low reactor pressure.

The same sensors and trip units used for initiation of the CS system are used to initiate LPCI (each LPCI pump A, B, C, D is initiated by the same sensors used for the initiation of the corresponding CS pumps A, B, C, D).
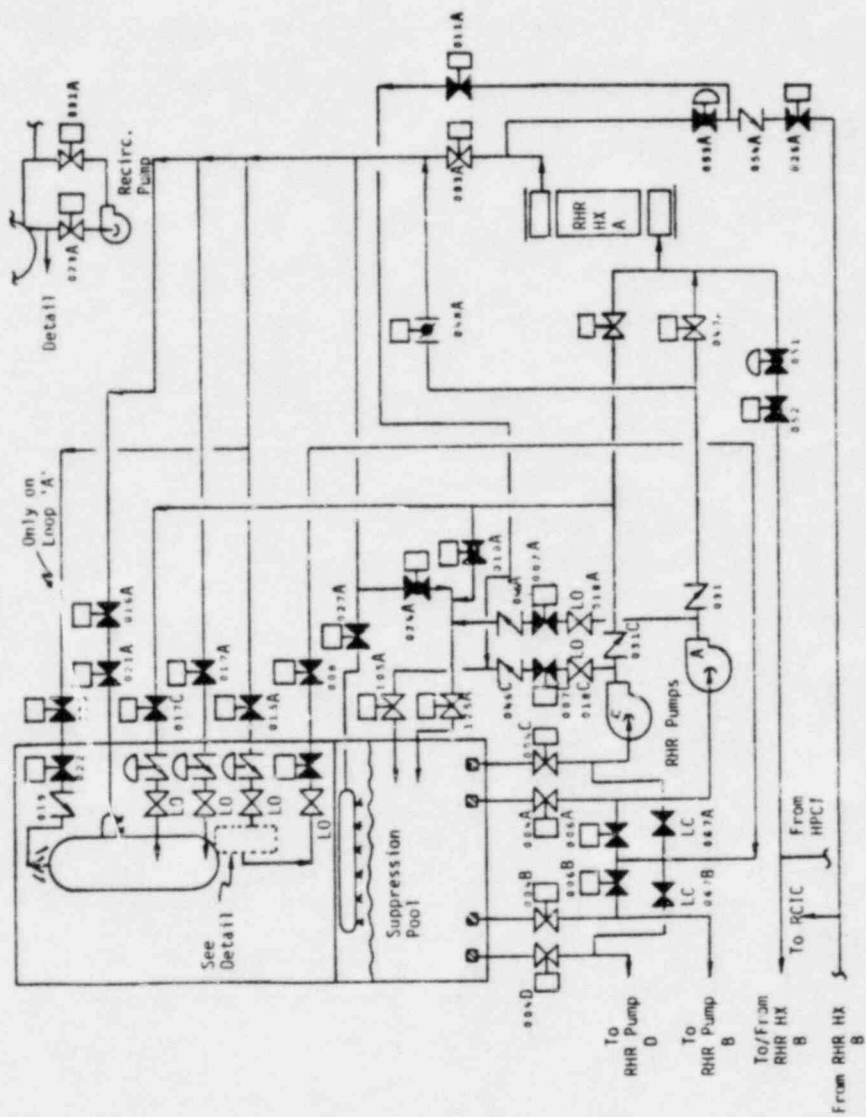
Figure B.2.2 Residual Heat Removal System (Loop A shown, Loop B is identical)

The LPCI initiation signal is generated when:

- Both level sensors are tripped, <u>or</u>

- Four pressure sensors are tripped (two high drywell pressure and two low reactor vessel pressure), <u>or</u>

- Either of two combinations of one level sensor and two pressure sensors (one high drywell and one low reactor pressure) are tripped.

Once the initiation signal is received by the RHR control circuitry, the signal is sealed-in until manually reset.

Four pressure sensors are used to monitor valve differential pressure to provide the pressure permissive signal for opening the injection valves.

Manual Control: LPCI operation can be manually initiated remotely from the control room.

Bypass and Interlocks

The RHR pump motors and injection valves are provided with manual override controls that allow the operator to control the system following automatic initiation.

The valves that allow the diversion of water for suppression pool spray are automatically closed upon receipt of an LPCI initiation signal. The manual controls for these valves are interlocked so that opening the valves by manual action is not possible unless the reactor vessel injection valve, in its respective RHR loop, is closed. The valves that allow diversion of water for containment spray are normally closed. The manual controls for these valves are interlocked so that opening both valves in one drywell spray loop by manual action is not possible unless an LPCI initiation signal is present, the reactor vessel injection valve in its respective RHR loop is closed, and drywell pressure is high.

B-19

Instrument and Alarms

A detection system continuously confirms the integrity of the injection line piping to the reactor vessel. Sensors measure the pressure differential between injection lines of RHR A and C loops and between the B and D loops. If the piping is sound, the pressure differential is very small between these lines. If integrity is lost, an increase in differential pressure initiates an alarm in the control room. Valves have indications of fully-open, intermediate, and fully-closed positions. Pumps have indications for pump running and pump stopped.

Electric Power Requirements

Four separate logic circuits located in separate panels and powered by four independent 125v DC buses are used. Control power for pumps A through D is from corresponding 125v DC buses A through D. AC power for A through D RHR and corresponding ESW* pump motors is supplied from the corresponding A through D 4160v buses. The power for the 4160v buses is normally from the preferred AC power source, and from the stand-' AC power source upon a loss of the preferred source.

B.2.3   Core Spray (CS) System

Purpose

The primary purpose of the core spray (CS) system is to provide inventory makeup and cooling during large LOCA breaks or other conditions requiring low-pressure makeup. Also, following ADS blowdown, CS provides reactor vessel water makeup following a small break.

---

*ESW room cooling required for long-term RHR pump operation.

Hardware Description

The CS system consists of two independent spray loops as shown in Figure B.2.3. Each of the two redundant CS system loops consists of: two 50% capacity centrifugal pumps, a spray sparger in the reactor vessel above the core (a separate sparger for each CS loop), piping and valves to convey water from the suppression pool to the sparger, and associated controls and instrumentation. The controls and instrumentation for the CS system include: the sensors, relays, wiring, and valve operation mechanisms used to start, operate, and test the systems.

Automatic and Manual Control

The CS system is started automatically when the following events occur:

- Low water level in the reactor vessel <u>and/or</u>

- High pressure in the drywell, <u>and if</u>

- Reactor vessel pressure is low enough (when reactor vessel pressure drops to a preselected value, valves open in the pump discharge lines, allowing water to be sprayed over the core).

It should be noted that each of the four CS pumps has its own independent logic and control power source. The sensors used to initiate one CS pump are separated from those used to initiate the other CS pumps. Once the initiation signal is received by the CS control circuitry, the signal is sealed in until manually reset.

Manual Control: The CS pump and all motor-operated valves can be operated individually by manual override control switches located in the control room.
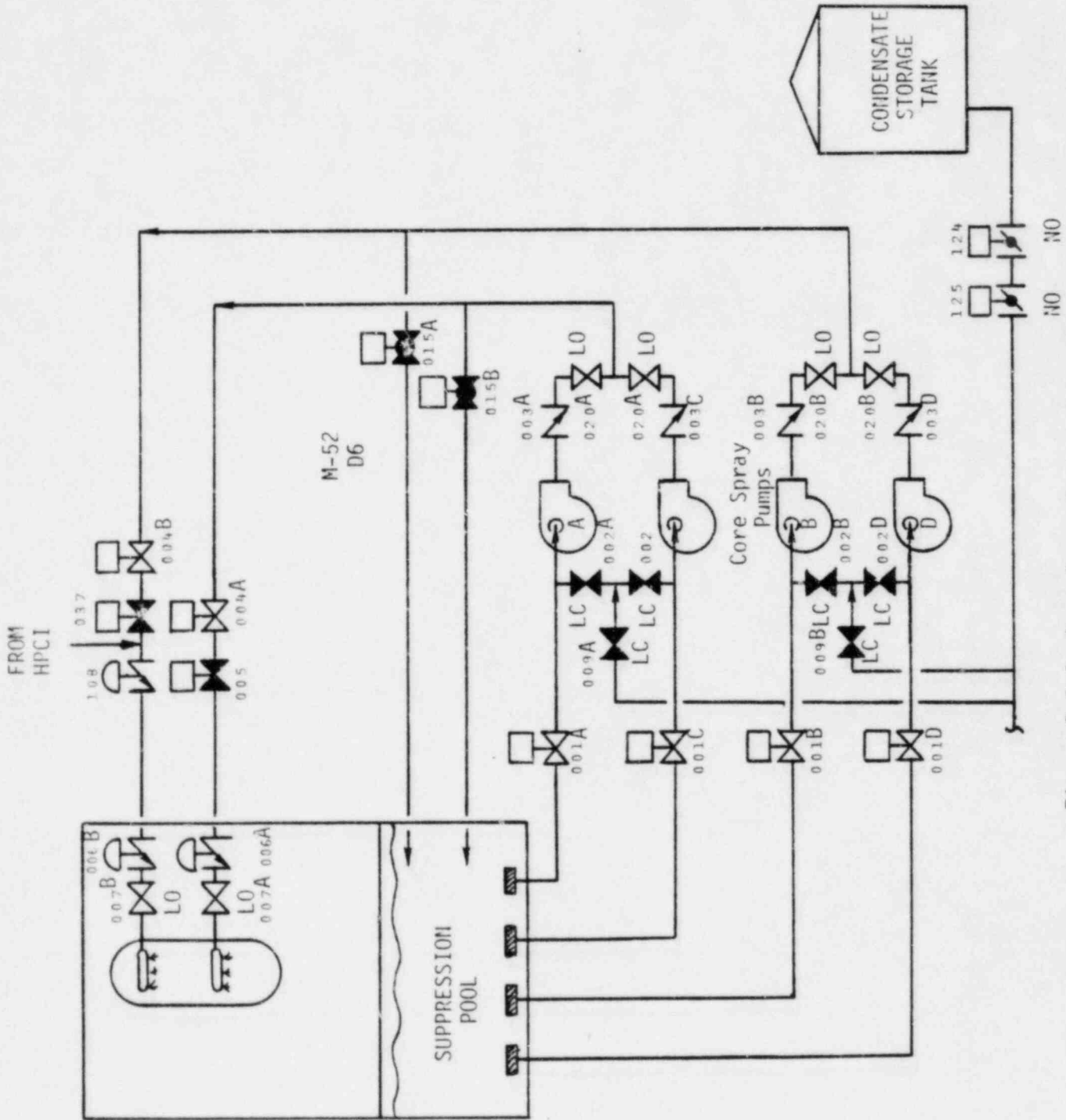
Figure B.2.3 Core Spray System Schematic

Instrumentation and Alarms (Reactor Operator Information)

Sufficient temperature, flow, pressure, and valve position indications are available in the control room for the operator to accurately assess CS system operation. Valves have indications of fully-open and fully-closed positions. The pump has indications for pump running and pump stopped. During manual operation a detection system continuously confirms the integrity of the CS A and B injection line piping to the reactor vessel. A sensor measures the pressure difference between the two injection lines. If the CS A and B piping is sound, the pressure difference will be very small between these lines. If integrity is lost, an increase in differential pressure initiates an alarm in the control room. Pressure in each CS pump suction line is monitored by a local pressure indicator to determine suction head and pump performance. Pressure in the discharge line of each CS loop is monitored by a pressure indicator in the control room to determine pump performance.

Electric Power Requirements

Each CS pump is powered from an independent AC bus that is capable of receiving standby power.* Control power and the power supply for valves in each loop is from one of the same two divisions used for the CS pumps in that loop. Control power for each of the CS pumps comes from separate DC buses. The electric equipment in the control room for one CS loop is separated from that used for the other loop. The CS initiation signal also initiates the corresponding diesel generator. Logic for the A and B loop valves is powered by 125v DC buses A and B, respectively.

B.3   DECAY HEAT REMOVAL

B.3.1   Residual Heat Removal Service Water (RHRSW) System

---

*ESW is required for long term CS pump operation

Purpose

The purpose of the RHRSW system is to provide a reliable source of cooling water for all operating modes of the RHR system including heat removal under post-accident conditions, and also to provide water to flood the reactor core or to spray the primary containment after an accident.

Hardware Description

The RHRSW system is composed of two loops. Each loop services one RHR heat exchanger. Each loop has two pumps located in the spray pond structure.

Manual Control

The RHRSW system is a manually initiated system. However, the common ESW and RHRSW supply and return valves and the spray pond sluice gates are automatically oriented to the spray pond on a start signal from the ESW system.

Manual controls for the RHRSW pumps, cooling water loop valves, and the spray pond sluice gate are available in the control room. Also, manual control of the A and C RHRSW pumps (see Figure B.3.1) and the cooling water loop A valves and associated sluice gates is available in the remote shutdown room.

Once an RHRSW pump is started, it operates until one of the following conditions occur:

- Stopped manually by operator
- Bus lockout
- Phase over current
- Ground fault
- Bus under voltage

RHR SW PUMPS

FROM
COOLING
TOWER

SPRAY
POND

001A 002A 002C 001C

A C

TO UNIT 2

014A

2A205 A

068A

RHR HX

TO
COOLING
TOWER

FROM UNIT 2

032A
NO

032C
NO

001B 002B 002D 001D

B D

SPRAY
POND

014B

1B205 B

068B

TO UNIT 2 RHR HX

TO
COOLING
TOWER

FROM
UNIT 2

SPRAY
POND

032B
NO

032D
NO
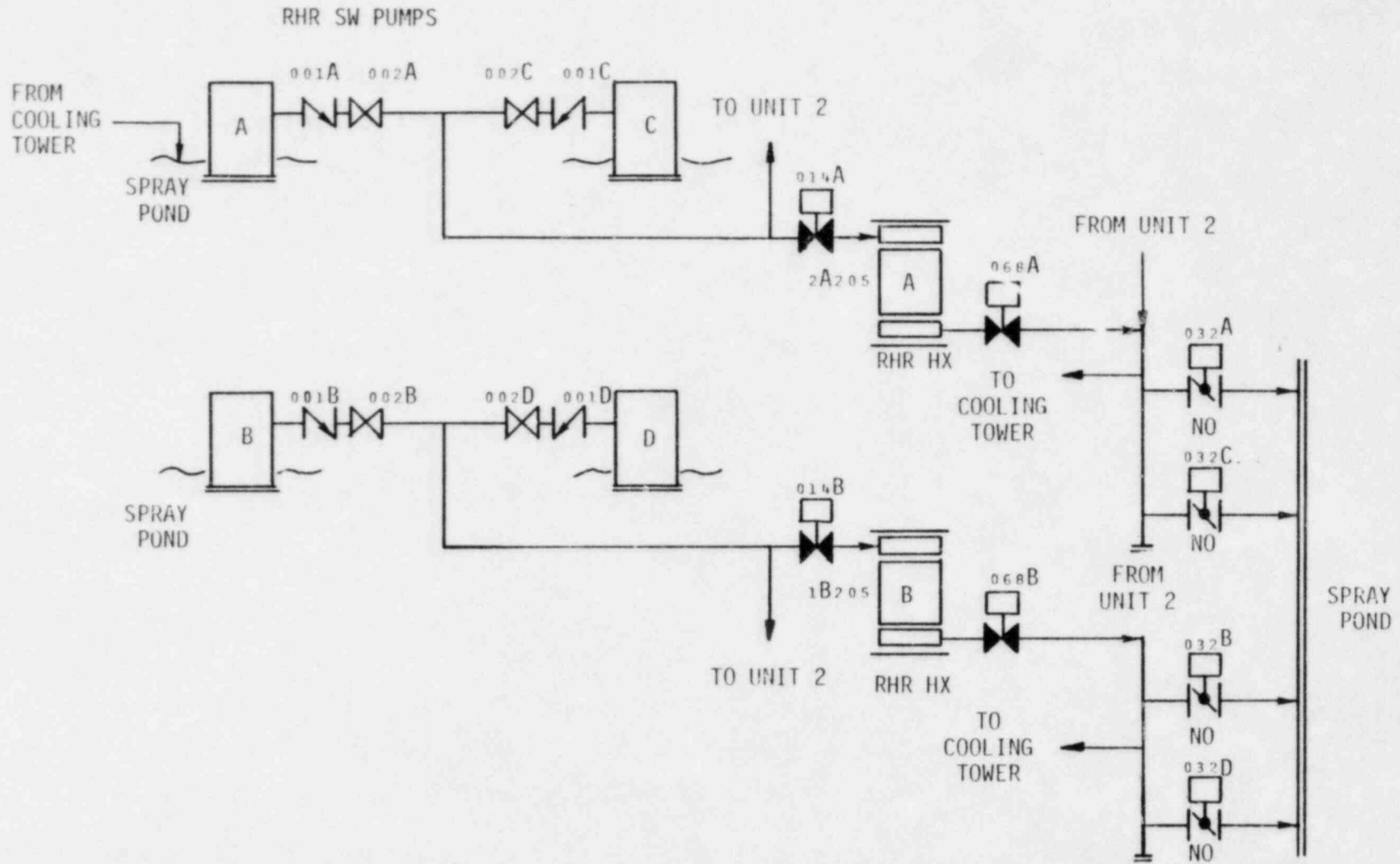
Figure B.3.1   Residual Heat Removal Service Water System Schematic

- Associated cooling water loop heat exchanger return line high radiation signal

- High pump discharge pressure.

The RHRSW system can be aligned to either the spray pond or the cooling tower for cooling water source and loop return. Upon starting of the ESW system, the cooling water source, and return for the ESW and RHRSW system automatically align to the spray pond, if the systems are not already in that mode.

Bypasses and Interlocks

A keylocked manual switch bypass is provided to inhibit the ESW signal that automatically aligns the ESW and RHRSW system from the cooling-tower mode to the spray pond mode. This bypass is provided to permit alignment to the cooling tower if available.

A keylocked manual bypass switch is provided to inhibit the high-radiation signal of the monitor in the associated cooling water loop return to provide the capability to restart the pumps. A control room alarm indicates that the high-radiation trip is bypassed.

Electric Power Requirements

The power for the RHRSW pump motors and cooling water loop motor operated valves is supplied from Class 1E AC buses. Control power for the RHRSW pump motors is supplied from Class 1E DC buses. Instrumentation power is supplied from Class 1E AC buses.

The RHRSW pump motors obtain their power from separate safeguard buses: the A and B pumps from Unit 1 Division I and II, respectively, and the C and D pumps from the Unit 2 Divisions I and II, respectively. The RHRSW valves in loop A receive power from Division I and III and loop B valves from Division II and IV.

B.3.2   Condenser

Purpose

The main condenser system is designed to condense and deaerate
the exhaust steam from the main turbine and provide a heat sink for the
turbine bypass system. The main condenser system is not safety related.

The design bases of the main condenser system are as follows:

1.   To condense and deaerate the exhaust steam from the main
      turbine and reactor feed pump turbines

2.   To accept and deaerate the drains from the feedwater heaters
      and other components in the heat cycle

3.   To serve as a heat sink for the turbine bypass steam, extrac-
      tion steam line dump drains, and heat cycle relief valve dis-
      charge.

4.   To retain for a minimum of 2 minutes the condensate formed
      during full load operation, to allow radioactive decay to occur
      before returning the condensate to the cycle.

Hardware Description

The main condenser is a triple-pressure deaerating type, com-
prising three separate shells, one low-pressure (LP), one intermediate-
pressure (IP), and one high-pressure (HP). The condensers are supported
on the turbine foundation mat, with each of the shells connected to the
exhaust of one of the three LP turbines by a rubber expansion joint, which
is secured between two steel frames, one welded to the turbine exhaust
and the other to the condenser.

During normal operation, steam from each LP turbine is exhausted
directly downward into its condenser shell through exhaust openings in the
bottom of the turbine casings. The condenser also serves as a heat sink
for several other flows, such as exhaust steam from the reactor feed pump

turbines, cascading heater drains, air ejector condenser drain, condensate and reactor feed pump recirculation lines, feedwater heater shell operating vents, crossaround piping relief valves, and condensate pump suction vents. The steam exhausted to the condenser is condensed by water circulated through the condenser tubes by the circulating water system.

The condensers are provided with reheating-deaerating hotwells that remove inleakage of air, plus hydrogen and oxygen formed in the turbine steam due to the dissociation of water in the reactor. These noncondensible gases are cascaded from the HP shell, through the IP shell, to the LP shell, terminating at the cold water inlet end of the LP shell. They concentrate in the air cooling section of the condenser, from which they are removed by the mechanical vacuum pump at startup and by the SJAEs during normal operation.

The condenser design air inleakage rate is 75 cfm. The circulating water is quality-controlled through chemical treatment and blowdown. The oxygen content of the condensate does not exceed 0.0035 cm^3/l through all load ranges, as measured at the discharge of the condensate pumps, with an air inleakage of up to 75 cfm.

The condenser hotwells have sufficient storage capacity together with internal baffling to ensure a minimum retention of 2 minutes for condensate from the time it enters the hotwell until it is removed by the condensate pumps.

The inlet water boxes of the LP condenser shell and the outlet water boxes of the HP condenser shell are each provided with butterfly valves, permitting any of the condenser's four separate circulating water flow paths to be removed from service.

A loss of condenser vacuum trips the turbine and isolates the steam source. However, should the turbine fail to isolate on loss of condenser vacuum, two rupture diaphragms on each turbine exhaust to the condenser protect the condenser and turbine exhaust hoods against overpressure.

The condenser is designed to withstand the blowdown effects of steam from the turbine bypass system with no deleterious effects.

The condenser is fitted with 18 BWG Admiralty tubes, except in high-velocity areas, where 20 BWG stainless steel tubes are used. Direct high-velocity impingement of steam or water on the tubes and structural members inside the condenser is avoided by the use of baffles.

B.3.3   Ultimate Heat Sink (UHS)

Purpose

The purpose of the ultimate heat sink (UHS) is to provide cooling water and act as a heat sink for the emergency service water (ESW) and residual heat removal service water (RHRSW) systems during normal and accident conditions.

Hardware Description

The UHS is a highly reliable, Seismic Category I spray pond which is sized for a water volume adequate for thirty days of cooling under design basis conditions.

The RHRSW and ESW systems receive cooling water via the spray pond pump structure located on the pond perimeter and return the water to the spray pond via the spray networks. Figure B.3.2 shows the arrangement of the spray pond, spray networks, and spray pond pump structure.

The pond is provided with an overflow weir to accommodate normal water level fluctuations and an emergency spillway to limit the maximum water level in the pond during maximum precipitation conditions.

The spray pond pump structure houses the RHRSW and ESW pumps and associated piping and valves. The pump structure is located on the edge of the spray pond. Openings are provided in front of the structure

From Unit 1
Cooling Tower

Butterfly valves

Sluice gate
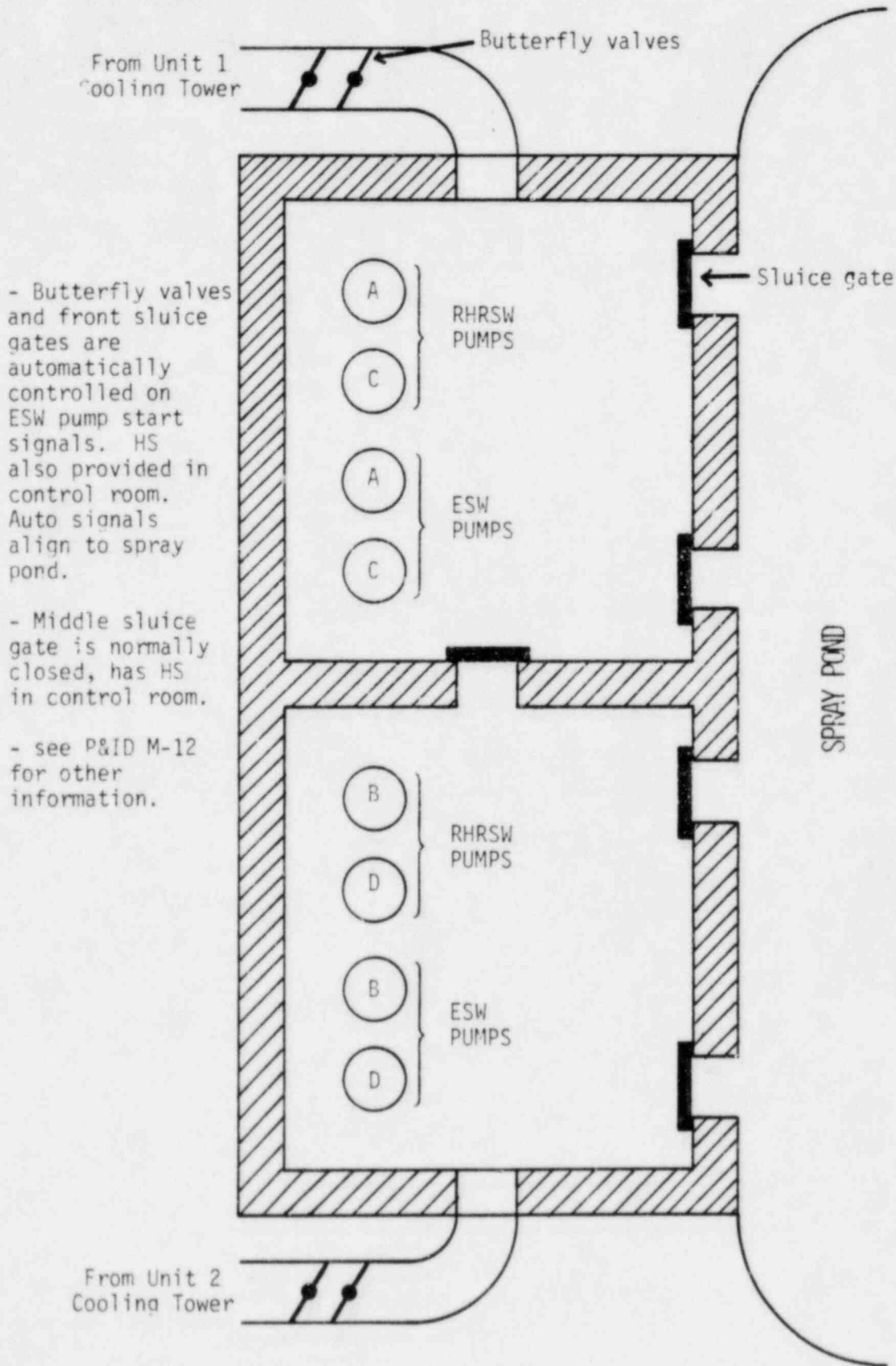
- Butterfly valves
and front sluice
gates are
automatically
controlled on
ESW pump start
signals. HS
also provided in
control room.
Auto signals
align to spray
pond.

- Middle sluice
gate is normally
closed, has HS
in control room.

- see P&ID M-12
for other
information.

A
C
} RHRSW
PUMPS

A
C
} ESW
PUMPS

B
D
} RHRSW
PUMPS

B
D
} ESW
PUMPS

SPRAY POND

From Unit 2
Cooling Tower

Figure B.3.2 Ultimate Heat Sink Schematic

to allow pond water to flow into the wet pits where the pump suctions are located. Closure of the sluice gates on these openings and realignment of system valves allows the ESW and RHRSW systems to shift from the spray pond mode to the cooling tower mode.

The wet pit area is divided into two sections corresponding to the A and B loops of the RHRSW and ESW systems. The two areas are separated by a wall with a sluice gate which can be closed to isolate the two trains. Each pump is installed in its own bay. A removable screen is placed at the entrance of each of the bays.

A winter bypass line is provided for each ESW/RHRSW combined return line to allow bypassing the spray networks and returning the heated water directly to the pond volume.

Makeup water to the pond is supplied via a six-inch branch line from the Schuylkill River makeup line to the cooling towers. The line enters the pond below normal pond water level. Two check valves in the line prevent siphoning from the pond in the event of loss of pressure in the makeup line. The makeup valve is controlled by a level detector in the pond to maintain proper water level.

An 8-inch blowdown line and associated weir are provided on the eastern pond perimeter. The line is used for overflowing excess water during rain conditions and for water quality control.

Two drain sumps are provided in the bottom of the pump structure. The sump pumps discharge to the pond above the water surface to avoid siphoning of the pond to the pump structure.

System Operation

The spray pond is designed to automatically supply cooling water to the ESW and RHRSW systems when required and to continue this function with a minimum of operator attention.

Normal Operation

The spray pond is normally in a standby mode and, except for periodic testing, is used only during emergency or accident situations. Start of the ESW pumps causes sluice gates and system valves to automatically align for spray pond operation, if not already in that position. The operator may subsequently stop and start pumps and remove or add spray networks from service as necessary to maintain proper flows and diesel loadings. The pond is not normally used for cooldown and shutdown operations.

During standby, pond level is automatically maintained at the operating level of 250 feet MSL (9-foot pond depth) by the makeup and blowdown lines. During long-term operation, without makeup and blowdown, the concentration of scale-forming constituents, which can impair heat exchanger performance, increases due to evaporation. Provision will be available for the manual addition of acid to inhibit scale formation from calcium carbonate. Sufficient spray pond inventory is provided such that other scale-producing agents, such as calcium sulfate, will not reach concentrations that might cause scaling during the 30-day post accident period when no makeup or blowdown is assumed.

Winter Operation

The spray pond is designed to perform its safety functions with an initial ice layer on the pond surface.

During icing conditions, return flow to the pond is initially directed to the winter bypasses which inject the warm return water directly to the pond volume. The bypasses are directed toward the ends of the pond to allow the return water to circulate and mix with the pond volume and avoid hydraulic short-circuiting. The increasingly warmer pond water will cause any ice layer present on the pond surface to melt. Once hole formation in the ice layer has occurred, a return path for spray water is available and the spray networks may be used as water temperature dictates.

Cooling Tower Operation

During normal shutdown and cooldown operations, the RHRSW
system uses the cooling tower basins as the source of cooling water
and the cooling towers as the heat sink. The system is aligned for
this mode by shutting the spray pond sluice gates and diverting the
return flow to the towers. Cooled water from the cooling tower basins
flows back to the wet pits.

Should an emergency or accident condition arise while the pond
is in this mode, ESW pump start signals will cause the system to auto-
matically realign to the spray pond mode. Subsequently, and after
assessment of the cooling tower's availability, the system may be placed
in the cooling tower mode if so desired.

B.4   CONTAINMENT SYSTEMS

B.4.1   Containment Overpressure Relief (COR)

One of the features of the Limerick Mark II containment which
can be used to advantage in a number of postulated accident sequences,
is the ability to relieve pressure in the primary containment and possibly
prevent structural failure of the containment. The analysis carried out
for Limerick includes the ability to relieve pressure under the following
circumstances:

●   Pressure in the primary containment exceeds design
      pressure (50 psig)

●   No high radiation exists in containment.

The system design is modeled as follows:

1.   A line leading from the drywell to the reactor building stack

2. Two motor-operated isolation valves in series, capable of opening on a signal from the operator in the control room

3. A logic interlock which prevents pressure relief if there is high radiation in containment.

Figure B.4.1 is a schematic of the arrangement as it is presently modeled in the Limerick PRA analysis. Since the COR design has not been finalized, the schematic is preliminary; however, since the assigned success probability for COR is dominated by operator action, it is judged that the specific design details will not affect the quantification of the CCDF curves.

B.4.2   Containment Inerting

The Limerick BWR4 Mark II containment is inerted with nitrogen during normal power operation, except for short periods of time during startup and shutdown when routine drywell maintenance is performed. During this deinerted period at power there is a probability of hydrogen combustion following a postulated core melt. This hydrogen combustion and potential subsequent containment failure has been included in the Limerick PRA (see Section 3.5.4).

B.4.3   Containment Fan Coolers

BWR Mark II containments have a system, in addition to RHR, which can remove some relatively small amount of heat from containment. This system includes the containment fan coolers. For the Limerick Risk Assessment, the identified accident sequences for which the fan coolers could be used effectively are those for which steam, high temperatures, and high pressure may exist inside containment. However, the fan cooler system is not qualified for operation under these extreme environmental conditions. In addition, the fan cooler system isolates on such signals as low reactor water level and high drywell pressure. Therefore, the fan coolers are not assumed to be available to remove heat from containment.

PRIMARY
CONTAINMENT

REACTOR BLDG.

Initiation of
overpressure relief
is a manual key-
locked switch in
the control room

High Radiation
Monitors Inter-
Lock the Controls
to the MOVs

M

M

NO

NC

STACK

DRYWELL
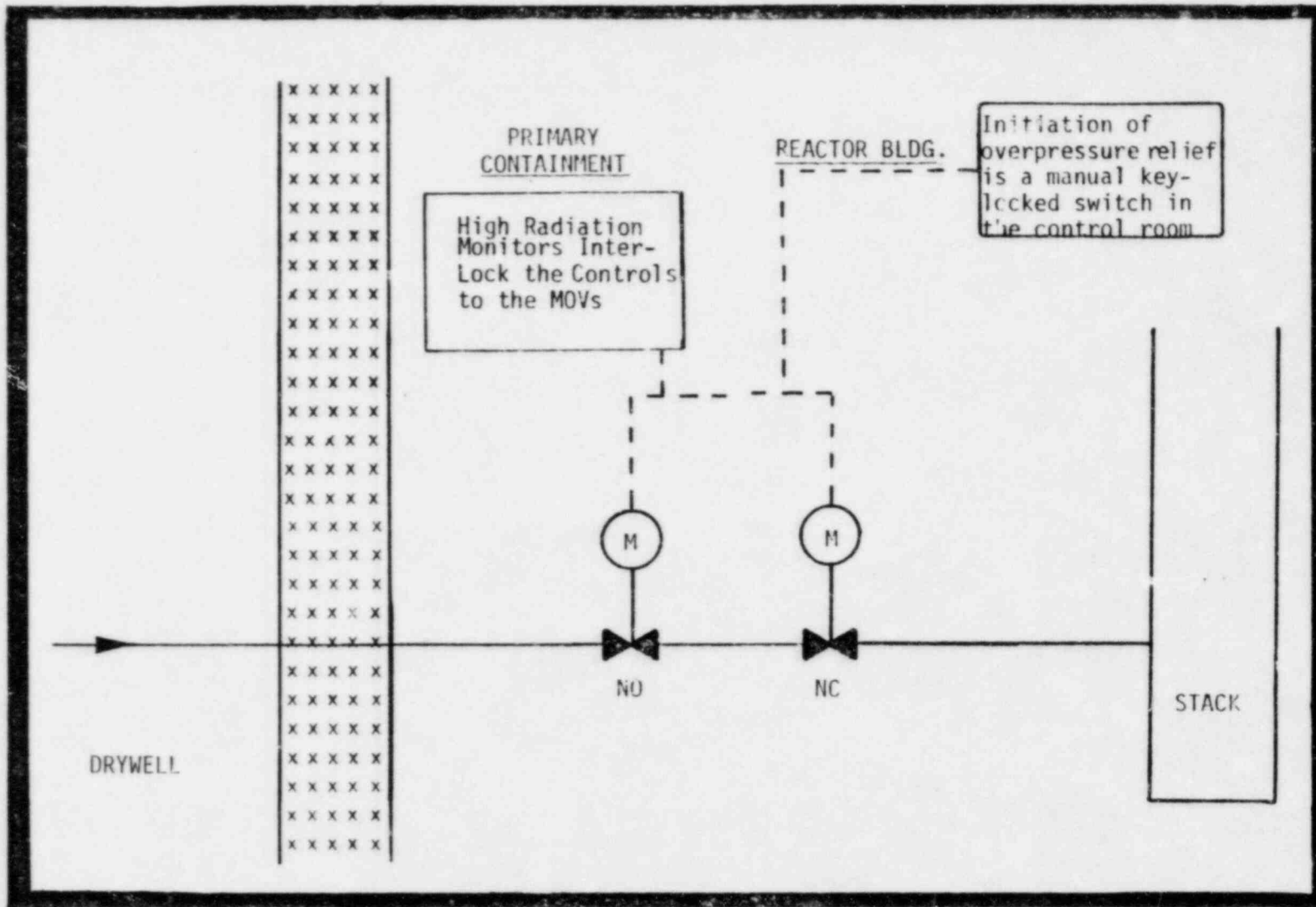
Figure B.4.1   Schematic of Containment Overpressure System

B.4.4   Containment Isolation and Containment Integrity

The maintenance of containment integrity during a demand
(e.g., a containment pressurization or a core melt) requires that:

- Leakage be low and within a specified tolerance
- Containment isolation of penetrations occur.

In WASH-1400 the plant containment leakage had a direct effect
on the ECCS system response because of the requirement for a net positive
suction head (NPSH) on the low pressure pumps. However, the LGS has im-
proved pumps with no such requirement; therefore, the principle effect of
losing containment integrity through leakage or failure to isolate is the
potential for radioactivity to escape to the environment if the leakage
occurs during a core degradation event.

The postulated leakage of containment can be qualitatively
understood from the following points:

1.   Some leakage from containment is recognized to occur at
      pressures below design pressure. The integrated leak rate
      test every five years gives some assurance that it is with-
      in a specific tolerance.

2.   The more than 600 penetrations in containment are all required
      to be isolable following a demand for containment isolation.

3.   The dome head, manways, and hatches are all required to be
      properly sealed (i.e., reassembled following entry).

4.   The main coolant system piping penetrations provide a potential
      direct path of radionuclides out of containment if they are
      not isolated.

For the LGS analysis, the containment leakage effects are incor-
porated in the containment event tree. They are included under two cate-
gories:

1. Containment leakage to the Reactor enclosure is included as a containment failure mode, and its effect is determined as a function of the effective size of the leakage (i.e., within the SGTS capability or beyond the capability).

2. Failure to isolate is included as one component of the containment leakage failure modes ($\delta\epsilon$ and $\xi\epsilon$) which include no credit for SGTS. Failure to isolate is a very small probability compared with other leakage failure modes and its precise quantification does not affect the CCDF curves.

B.4.5 Containment Spray

One of the many functions of the RHR system is the ability to provide a spray flow through nozzle headers into the containment drywell. The RHR pumps draw water from the suppression pool and spray directly to the drywell. The usefulness of the containment spray, the uncertainties involved in including it in the analysis, and the accident sequences for which it could be used are discussed in this subsection.

The Limerick Probabilistic Risk assessment assumes that all systems, regardless of safety classification, are operated as prescribed in the Operator Guidelines. Use of the containment spray when the containment temperature is high can alleviate potentially adverse environmental conditions inside containment under certain accident scenarios; however, the failure of this function does not affect the reliability of the other systems used in accident mitigation. In addition to the above specified use, the containment spray system has the following potential benefits which have not been fully quantified or included in the LGS analysis:

1. Reduction of drywell temperature

2. Scrubbing of radioactivity* from the drywell atmosphere, potentially reducing the source term which may be released during a containment failure coupled with a core melt

3. Reduction of drywell pressure which may prevent containment overpressure (scenario-dependent)

---

*At present there are no chemical additives to the suppression pool which would enhance the scrubbing capability of containment spray.

4. Slowing down or stopping the core melt interaction with concrete by cooling of the molten core which may in turn limit the production of noncondensibles and the potential for containment failure due to either overpressure or diaphragm floor failure.

Because of the uncertainties on the implementation of containment spray under postulated severely degraded core conditions, the use of containment spray as an effective mitigation system is not used in the analysis.

B.5   ELECTRIC POWER SYSTEMS AND INSTRUMENTATION

B.5.1   Electric Power Safeguard System (EPS)

Purpose

The electrical power safeguard system (EPS) of the Limerick Generating Station (LGS) is designed to provide emergency power, when required, to the plant's safety systems and components.

Hardware Description

Emergency safeguard electric power is provided by offsite and onsite power sources.

Offsite Power Sources

There are three independent offsite power sources (see Figure B.5.1) to the LGS:

- 220 - 13 kV transformer connected to the 220 kV substation

- 13 kV tertiary winding on the 500 - 220 kV bus tie auto transformer

- 33/13.2 - 4.16 kV transformer for connections to the 33kV Cromby-Moser tieline.

Onsite Safeguard Power System

The onsite Class 1E (safeguard) electric power system is divided into four <u>independent</u> divisions (see Figure B.5.1), each with its separate diesel generator. The distribution system of each division consists of a 4 kV bus, a 440 V load center, several motor control centers (MCCs), and several low-voltage distributions panels.

It should be noted that when the power system is operating from the diesel generator supply, redundant load divisions cannot be manually joined because the 4 kV circuit breakers controlling the incoming preferred and alternate power supplied to the Class 1E buses are locked open to prevent the paralleling of the diesel-generators.

In addition, LGS has four independent DC Class 1E power systems corresponding to the four standby AC power system divisions (see Figures B.5.2 and B.5.3):

- Two 125/220 V DC systems (Division I and II)
- Two 125 V DC systems (Divisions III and IV).

Each DC division is energized by its own battery and chargers. The battery chargers are supplied from separate 440 V motor control centers (MCCs). Each of the MCCs is connected to an independent Class 1E AC bus. Each Class 1E battery bank has sufficient capacity without its charger to independently supply the required loads for four hours.

The chargers are capable of carrying the normal DC system load and at the same time supplying sufficient charging current to restore the batteries from the designed minimum charge state to the fully charged state within 8 hours. Each Class 1E DC system, the battery bank, chargers, and DC switchgear are located in separate compartments. Each compartment is ventilated to prevent hydrogen accumulation.
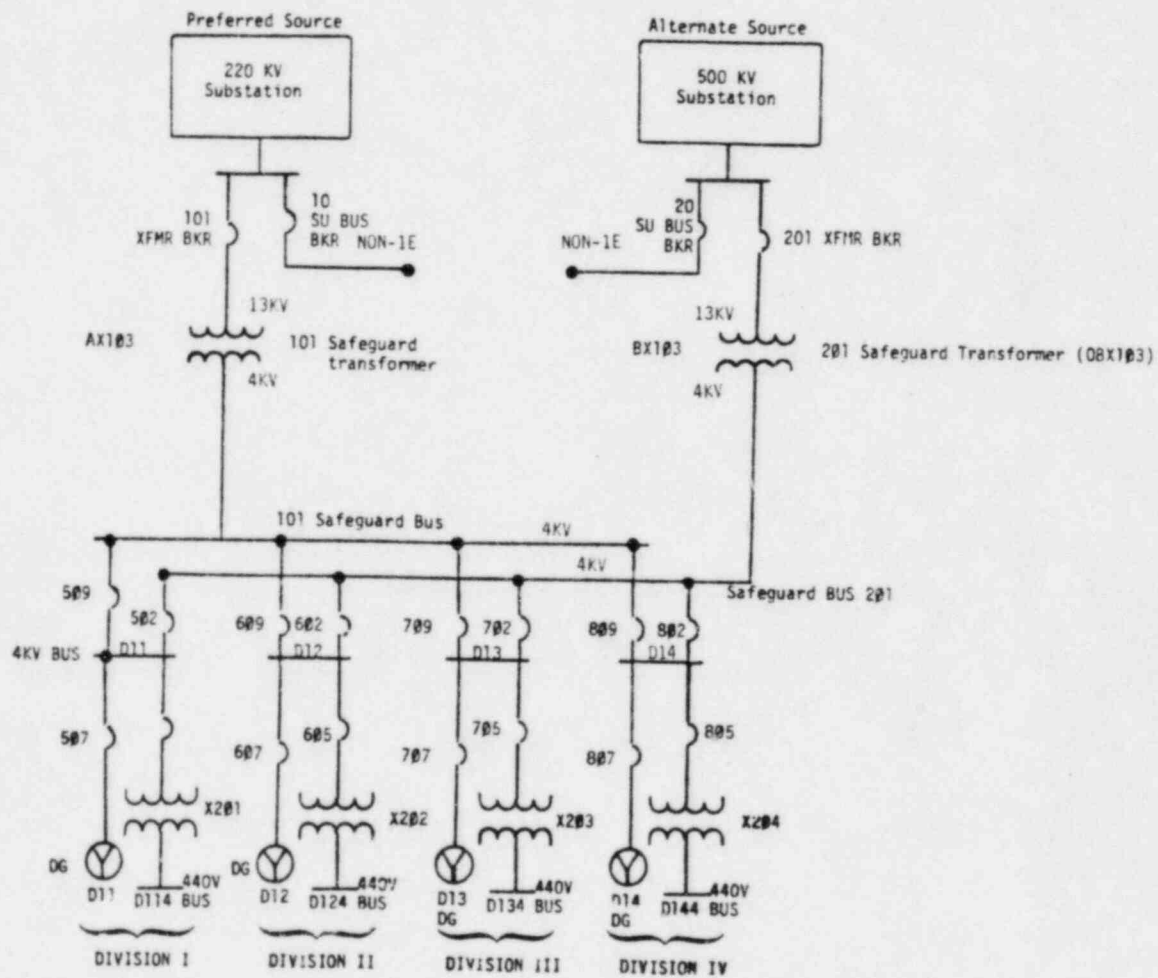
Figure B.5.1

Electrical Power System Operation

Each of the four independent Class 1E AC division buses shown in
Figure B.5.1 has connections to two independent offsite power supplies and
to a single onsite diesel generator. The power feeder breakers to each
division are interlocked so that only one of the power supplies can be
connected at any one time. In the event of the loss of the preferred
offsite power source, there will automatically be a switch to the alternate
offsite power source. If both offsite power sources are lost, an automatic
switch to the diesel generator onsite AC power source will occur. In
addition, the third possible offsite power source can be manually connected
in a 72-hour period.

The safety system loads and engineered safeguard systems load
division separation are shown in Tables B.5.1 and B.5.2. These tables
are taken from the LGS FSAR, Tables 8.1-1 and 8.1-3.

Automatic and Manual Control

Controls and indicators for the four Class 1E bus supply breakers
are provided in the control room and on the switchgear. Controls and indi-
cators for the standby AC power supplied are also provided in the control
room and on the local diesel generator control panels.

As mentioned earlier in this section, in the event of the loss of
preferred offsite source a switch is automatically made to the alternate off-
site source. If total loss of offsite power (LOSP) occurs, then the onsite
diesel generators are started automatically.

The diesel generators should start automatically when one of the
following conditions occurs: LOSP, low reactor water level, or high drywell
pressure coincident with low reactor pressure. If the diesel generators do
not start automatically, it is possible for the operator to manually start
them.

DIVISION I
CHANNEL ZA

D114-R-6
440 V MCC 10B211ZA

D114-R-6
440 V MCC 10B211ZA

125
Battery
Charger

1BCA1

125V Battery 1A2

125V Battern 1A1

1BCA2

125
Battery
Charger

125/250 VDC, 2000A BUS

Ground
Det.

1DA 250 VDC
MCC 10D201

125/250 VDC,
600A BUS

125 VDC, 2000A BUS

1PPA1 125 VDC
Distribution Panel

125 VDC, 100A BUS

1PPA2 125 VDC
Distribution Panel

DIVISION II
CHANNEL ZB

D124-R-6
440V MCC 10B212ZB

D124-R-6
440V MCC 10B212ZB

Battery
Charger

1BCB1

1B2
125V Battery

1B1
125V Battery

Battery
Charger

1BCB2

2000A

125/250 VDC BUS

10B 250 VDC
MCC 10D202ZB

125V/250 VDC,
600 BUS

Ground
Det

125 VDC, 200A BUS

1PPB1 125 VDC
Distribution Panel

DE250 VDC 10D203ZB
MCC

125/250 VDC, 600A
BUS

1PPB2 125 VDC
Distribution Panel

125 VDC, 100A
BUS

Figure B.5.2

DIVISION IV
         III

CHANNEL ZC
        ZD

D144-R-E
D134-R-E
              10B224ZD
440V MCC 10B223ZL

ID
IC Battery
1CD 101 ZC
125 VDC
1DD 101 ZD

1BCC   Battery
1BCD   Charger
        125 VDC

Ground
Det   125 VDC

1CD104 ZC
1DD104 ZD

125 VDC, 600A BUS

125 VDC, 200A BUS

1PPC1 125 VDC Power
Distribution Panel

1PPD1 125 VDC Power

125 VDC, 100A BUS

1PPC2 125 VDC
Distribution Panel

1PPD2 125 VDC

Figure B.5.3

Table B.5.1

ENGINEERED SAFEGUARD SYSTEMS LOAD
DIVISION SEPARATION*

SENSORS/SYSTEMS	DIVISIONS**			
	I	II	III	IV
Sensors	A,E,J,N,T,X	C,G,L,R,V	B,F,K,P,U,Y	D,H,M,S,W
Core Spray	A	C	B	D
RHR	A	C	B	D
RHRSW	A,C		B,D	
ESW	A	C	B	D
ADS and HPCI	ADS-A	ADS-C	HPCI-OBV[†]	HPCI-IBV
NSS Isolation Valves (Output Logic and Valve Circuits)	Inboard	--	Outboard	--
RCIC	RCIC-OBV	RCIC-IBV	--	--
Diesel Generators and Class 1E Busses				
Unit 1	D11	D13	D12	D14
Unit 2	D21	D23	D22	D24
D-G Enclosure HVAC System	A	C	B	D
SGTS	A	--	B	--
RERS HVAC System	A	--	B	--
Control Room HVAC System	--	A	--	B
Post-LOCA Recombiners	--	A	--	B
Spray Pond Pump Structure HVAC System	A	C	B	D
HVAC System Unit Coolers				
RCIC	A,B	--	--	--
HPCI	--	--	A,B	--
RHR	A,E	C,G	B,F	D,H
Core Spray	A,E	C,G	B,F	D,H
Drywell	A1,C1,E1,G1	A2,C2,E2,G2	B1,D1,F1,H1	B2,D2,F2,H2

*Sensor, logic, and actuator suffix letters and divisional allocation for ESS and RCIC and energize to operate portions of the NSSS.

**The corresponding channel identification for raceways and cables relating to divisions is as follows:

Division	I	II	III	IV
Channel	A	B	C	D

[†]OBV = Outboard isolation valve and logic
IBV = Inboard isolation valve and logic

Table B.5.2

ELECTRICAL CHANNEL SEPARATION

CHANNEL A	CHANNEL B	CHANNEL C	CHANNEL D
Standby Diesel Generator and Auxiliaries A	Standby Diesel Generator and Auxiliaries B	Standby Diesel Generator and Auxiliaries C	Standby Diesel Generator and Auxiliaries D
Class 1E 4160 V Switchgear	Class 1E 4160 V Switchgear	Class 1E 4160 V Switchgear	Class 1E 4160 V Switchgear
Class 1E 480 V Load Center	Class 1E 480 V Load Center	Class 1E 480 V Load Center	Class 1E 480 V Load Center
Class 1E 480 V MCC	Class 1E 480 V MCC	Class 1E 480 V MCC	Class 1E 480 V MCC
Class 1E 125 V DC Distribution Panel	Class 1E 125 V DC Distribution Panel	Class 1E 125 V DC Distribution Panel	Class 1E 125 V DC Distribution Panel

B.5.2   Diesel Dependency Analysis

Most of the fault tree models developed for this analysis are straightforward and require very little explanation. However, a more detailed discussion of the fault tree model developed for the diesels is presented because:

- The diesel reliability is important in the Limerick risk assessment.

- There have been wide ranging discussions concerning the reliability of diesels.

- WASH-1400 used a crude dependency model to represent the likelihood of diesel common-mode failures.

- The dependency model developed here is much more complex than most fault trees, and requires more detailed explanation.

In order to correctly model the diesel generators in the system fault trees, dependencies between diesels must be reflected. Typically, failures or unavailability of events appearing in the fault tree must be statistically independent. That is, the probability of an event occurrence is not affected by the occurrence of any other event. In the case of the diesels, both random failure and maintenance of the diesels are coupled among the diesels. The random failure dependency is determined by operating experience data while the maintenance dependency results from the plant technical specifications (no more than 1 diesel can be removed for maintenance at any one time). The following paragraphs describe the development of each of these dependency models.

A maintenance model is used to reflect the Limiting Conditions and Operations (LCOs) which allow only one diesel to be unavailable. The maintenance appearing in this model is performed due to failure of a test, or is routine preventive maintenance. When a diesel is unavailable due to maintenance, the other diesels are tested. There is a possibility that other diesels will fail and require maintenance. When this occurs, the LCOs require that the plant be shut down within approximately one day. Diesel unavailability due to this situation is treated as a common mode.

The model described below treats the combination of single diesel maintenance and all diesels being unavailable due to maintenance. Figure B.5.4 contains fault tree models reflecting the required maintenance dependencies.

The model begins by choosing a diesel and assigning a basic event representing maintenance to the maintenance tree for that diesel. The maintenance tree for the second diesel is formed by an AND gate which combines maintenance of the second diesel with the negation of the first diesel maintenance event. This results in a boolean expression which will not allow diesels 1 and 2 to be in maintenance at one time. The diesel 3 fault tree is constructed with an AND gate combining the diesel 3 maintenance event and a negated OR gate that combines diesel 1 and 2 maintenance. This results in disallowing diesel 3 maintenance while diesels 1 or 2 are being maintained. Diesel 4 maintenance is modeled in the same manner as diesel 3. When two diesel failure trees are combined in a fault tree, the resulting logic will not allow combinations of maintenance events to occur.

The random failure model for diesels is more complex than the model for maintenance, since all potential combinations of operating states for the diesel must be considered. The reflection of the data through this model requires that the probability of equipment failure intersections or the conditional probability for all combinations of events is known. Examination of the diesel data should provide these required inputs. Figure B.5.5 contains the random failure dependency fault tree, when failure events beginning with the letter A involve diesel 1 failure; failure events beginning with B involve diesel 2 failure; and so on. This model builds each diesel model from the conditional probabilities developed from the equations in Table B.5.3. These equations develop the conditional probabilities for each diesel failure as a function of all possible combinations of other diesel states. For example, diesel 2(B) can fail when diesel 1(A) is in a failed state, or when diesel 1(A) is in an operating state.
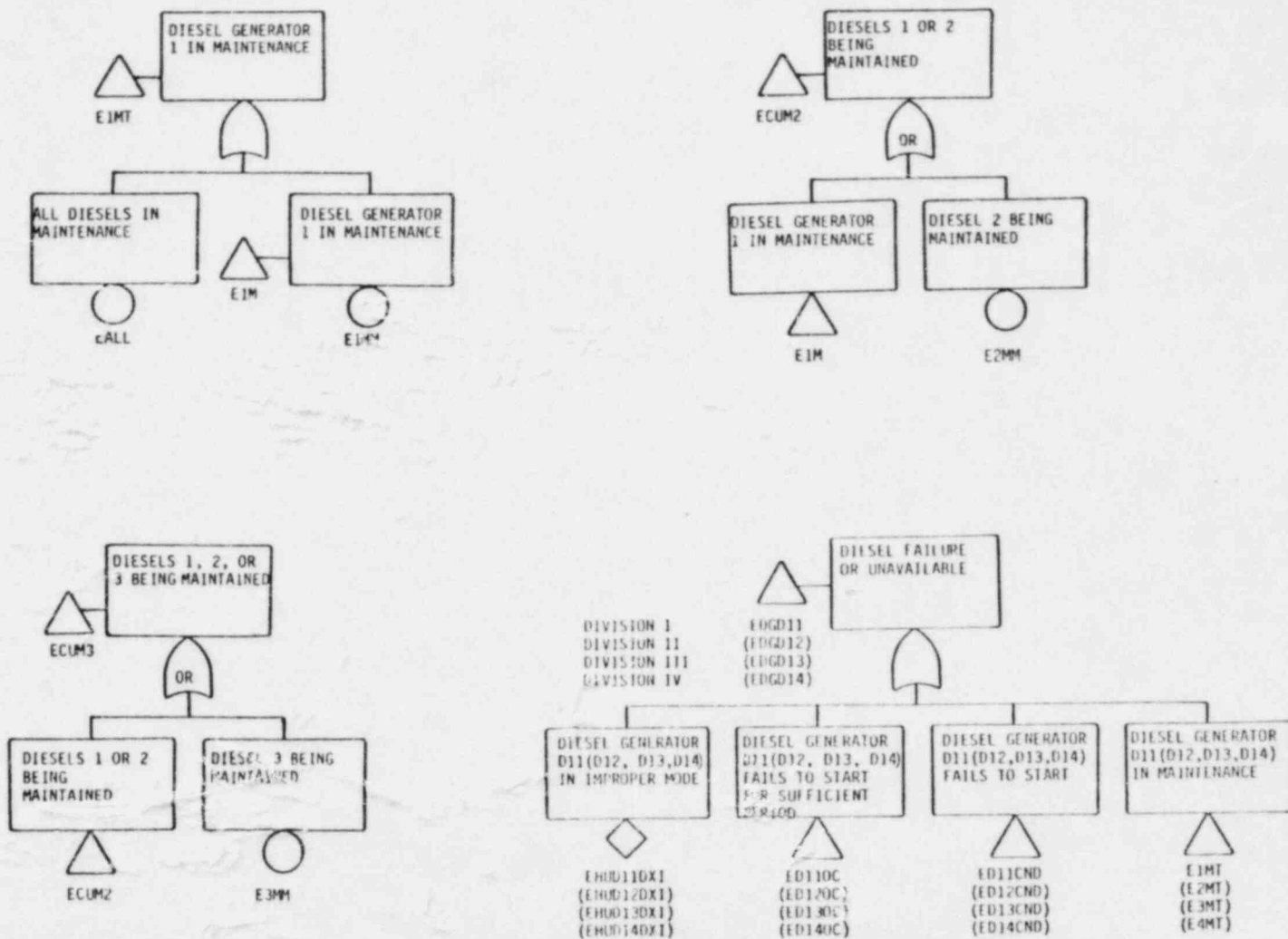
Figure B.5.4   Maintenance Representation Used for the Diesels in the Fault Tree Model
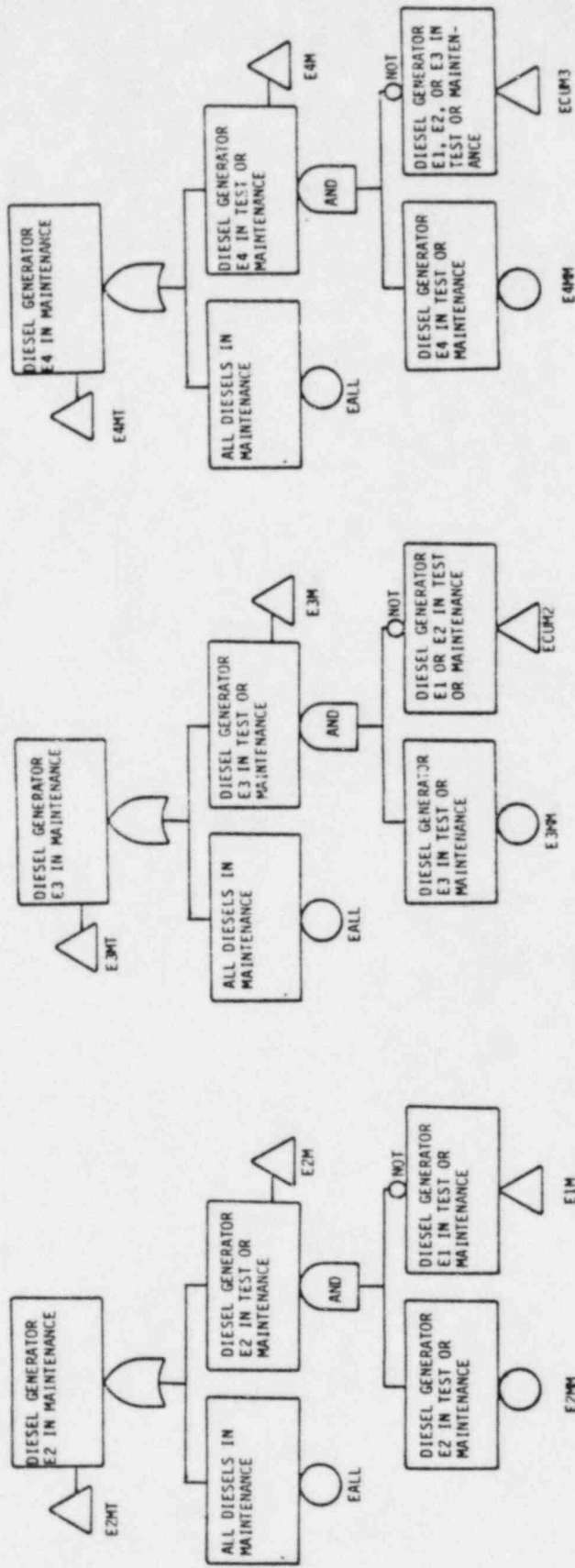
Figure B.5.4   Maintenance Representation Used for the Diesels in the Fault Tree Model (Continued).
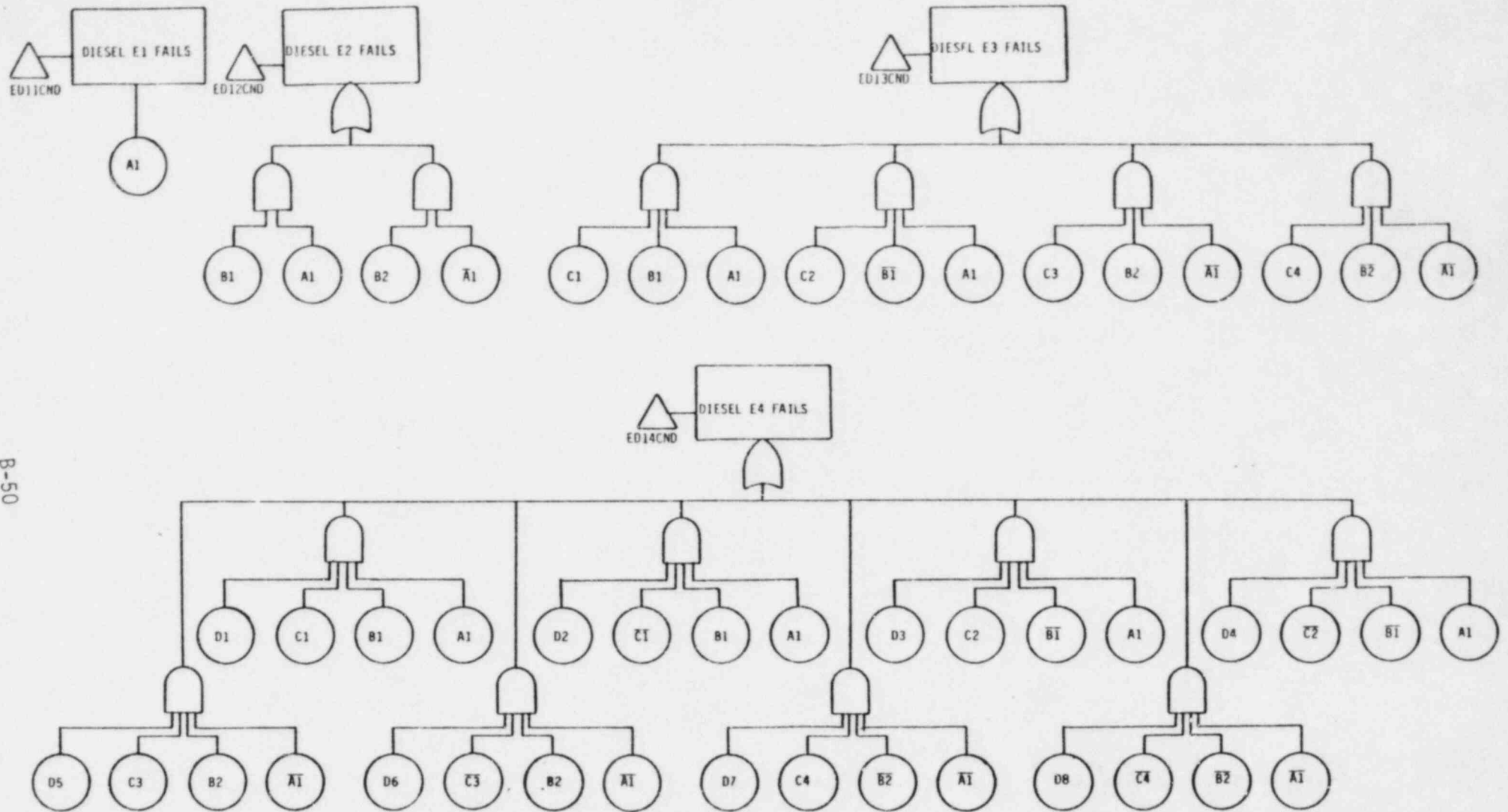
Figure B.5.5   Subtree Illustrating Dependent Event Component Models. The Fault Tree component level designators (e.g. A1, B1, etc.) are defined in Table B.5.3.

The fault tree for E2CND contains both of these combinations of events. The first AND gate combines B1, the conditional probability that diesel 2 fails given that diesel 1 is failed, with event A1, the event representing diesel 1 failure. The second AND gate combines B2, the conditional probability that diesel 2 fails given that diesel 1 is operating, with A1 which represents the event that diesel 1 is not failed. Diesels 3

Table B.5.3

FORMULAE FOR SUBTREE COMPONENT PROBABILITIES

$A \equiv$ Diesel 1 Failure

$A1 = P(A)$

$B \equiv$ Diesel 2 Failure

$B/A \equiv B1 = \dfrac{P(AB)}{(A1)}$

$B/\bar{A} \equiv B2 = \dfrac{P(B) - P(AB)}{(1 - A1)}$

$C \equiv$ Diesel 3 Failure

$C/AB \equiv C1 = \dfrac{P(ABC)}{(A1)(B1)}$

$C/A\bar{B} \equiv C2 = \dfrac{P(AC) - P(ABC)}{(A1)(1 - B1)}$

$C/\bar{A}B \equiv C3 = \dfrac{P(BC) - P(ABC)}{(1 - A1)(B2)}$

$C/\bar{A}\bar{B} \equiv C4 = \dfrac{P(C) - P(AC) - P(BC) + P(ABC)}{(1 - A1)(1 - B2)}$

$D \equiv$ Diesel 4 Failure

$D/ABC \equiv D1 = \dfrac{P(ABCD)}{(A1)(B1)(C1)}$

$D/AB\bar{C} \equiv D2 = \dfrac{P(ABD) - P(ABCD)}{(A1)(B1)(1 - C1)}$

$D/A\bar{B}C \equiv D3 = \dfrac{P(ACD) - P(ABCD)}{(A1)(1 - B1)(C2)}$

$D/\bar{A}BC \equiv D5 = \dfrac{P(BCD) - P(ABCD)}{(1 - A1)(B2)(C3)}$

$D/\bar{A}B\bar{C} \equiv D6 = \dfrac{P(BD) - P(ABD) - P(BCD) + P(ABCD)}{(1 - A1)(B2)(1 - C3)}$

$D/\bar{A}\bar{B}C \equiv D7 = \dfrac{P(CD) - P(ACD) - P(BCD) + P(ABCD)}{(1 - A1)(1 - B2)(C4)}$

$D/\bar{A}\bar{B}\bar{C} \equiv D8 = \dfrac{P(D) - P(AD) - P(BD) - P(CD) + P(ABD) + P(ACD)}{(1 - A1)(1 - B2)(1 - C4)} + \dfrac{P(BCD) - P(ABCD)}{(1 - A1)(1 - B2)(1 - C4)}$

and 4 are developed in the similar manner from the conditional probabilities. While the occurrence of diesel 1 failure is not explicitly dependent on other diesel failures, the laws of probability and boolean algebra implicitly cause diesel 1 to be dependent on the state of the other diesels, when the diesel failures are combined in the fault tree. Evaluating each diesel generator's random failure rate independently, gives:

E1CND   E2CND   E3CND   E4CND

In summary, the diesel Fault Tree is constructed in a unique manner and does not explicitly contain the failure modes or maintenance unavailabilities assigned to diesel subsystems such as the air start, fuel oil, lube oil, turbocharger, etc.; rather, actual plant operating experience is used to characterize the failure probability of the diesels and also the failure probability of multiple diesels. The data for these failure probabilities are taken from the operating experience data compiled in Appendix A.

The electric power fault tree explicitly contains the dependency of the diesels on the emergency service water system in a manner similar to other explicit system dependencies.

B.5.3   Safety System-Related Instrumentation Channels

Automatic initiation of safety systems is an important aspect of the assessment of risk at a nuclear power plant. In some cases, the same sensors, signal transmitters, reference columns, or logic units may be used in the initiation of more than one safety system. This dependency between systems must be represented to properly assess the probability of safety system operability.

Tables B.5.4 and B.5.5 summarize the reactor water level and pressure sensors used in the safety system logic at Limerick. The sensors which are used in more than one system are noted. These sensors and their logic are represented by a common name throughout the fault tree logic in order to ensure that dependencies among systems will be automatically accounted for in the analysis.

Table B.5.4

SUMMARY OF SENSORS USED IN THE SAFETY SYSTEM INITIATION

		High Pressure		ADS		RHR and CS							
		HPCI	RCIC	ADS(A)	ADS(C)	CS(A)	RHR(A)	CS(B)	RHR(B)	CS(C)	RHR(C)	CS(D)	RHR(D)
INITIATOR	**Level 2**												
	692E	X	X										
	692F	X											
	692A	X	X										
	692B	X											
	697A		X										
	697E		X										
	Level 1												
	691A (1)			X		X	X						
	691B (2)							X	X				
	691F (2)							X	X				
	691C (3)				X					X	X		
	691G (3)				X					X	X		
	691D (4)											X	X
	691H (4)											X	X
	691E (1)			X		X	X						
PERMISSIVE	**Level 3**												
	695A			X									
	695C				X								
	SHUTOFF **Level 8**												
	693A		X										
	693B	X	X										
	693E		X										
	693F	X											

Table B.5.5

PRESSURE SENSORS USED BY SAFETY SYSTEMS

	SENSOR DESIGNATOR	SYSTEMS										
		HPCI	ADS(A)	ADS(B)	RHR(A)	CS(A)	RHR(B)	CS(B)	RHR(C)	CS(C)	RHR(D)	CS(D)
INITIATION	**Drywell**											
	694A	X			X	X						
	694E	X			X	X						
	694B	X					X	X				
	694F	X					X	X				
	694C								X	X		
	694G								X	X		
	694D										X	X
	694H										X	X
LOW PRESSURE PERMISSIVE	**Reactor**											
	690A				X	X						
	690E				X	X						
	690B						X	X				
	690F						X	X				
	590C								X	X		
	690G								X	X		
	690D										X	X
	690H										X	X
	690J							X		X		
	690							X		X		
	690K						X					X
	690P						X					X

B.6   EMERGENCY SERVICE WATER (ESW) SYSTEM

Purpose

The purpose of the ESW system is to provide cooling water to the diesel generator units, RHR pumps, and room coolers required during emergency conditions to safely shutdown the plant.

Hardware Description

The ESW system consists of two independent loops (A and B), with two 50% capacity pumps per loop. The ESW system is designed to supply cooling water to the following safety-related equipment:

- RHR motor oil seal coolers
- RHR pump compartment unit coolers
- Core spray pump compartment unit cooler
- Control room chillers
- Standby diesel generator heat exchangers
- RCIC pump compartment unit coolers
- HPCI pump compartment unit coolers
- Spent fuel pools (makeup water).

During normal plant operation, all of the above equipment with the exception of the diesel generators, is provided with cooling water by the service water system. (Figure B.6.1 is a schematic of the ESW system.)

The above equipment is provided with cooling water from either ESW loop A or B. Each diesel generator can be supplied with cooling water from ESW loop A or ESW loop B. Normal system alignment, however, is such that loop A supplies cooling water to the A and C diesel generators, and loop B supplies the B and D diesel generators. ESW loop A consists of ESW pumps A and C, while loop B consists of pumps B and D.
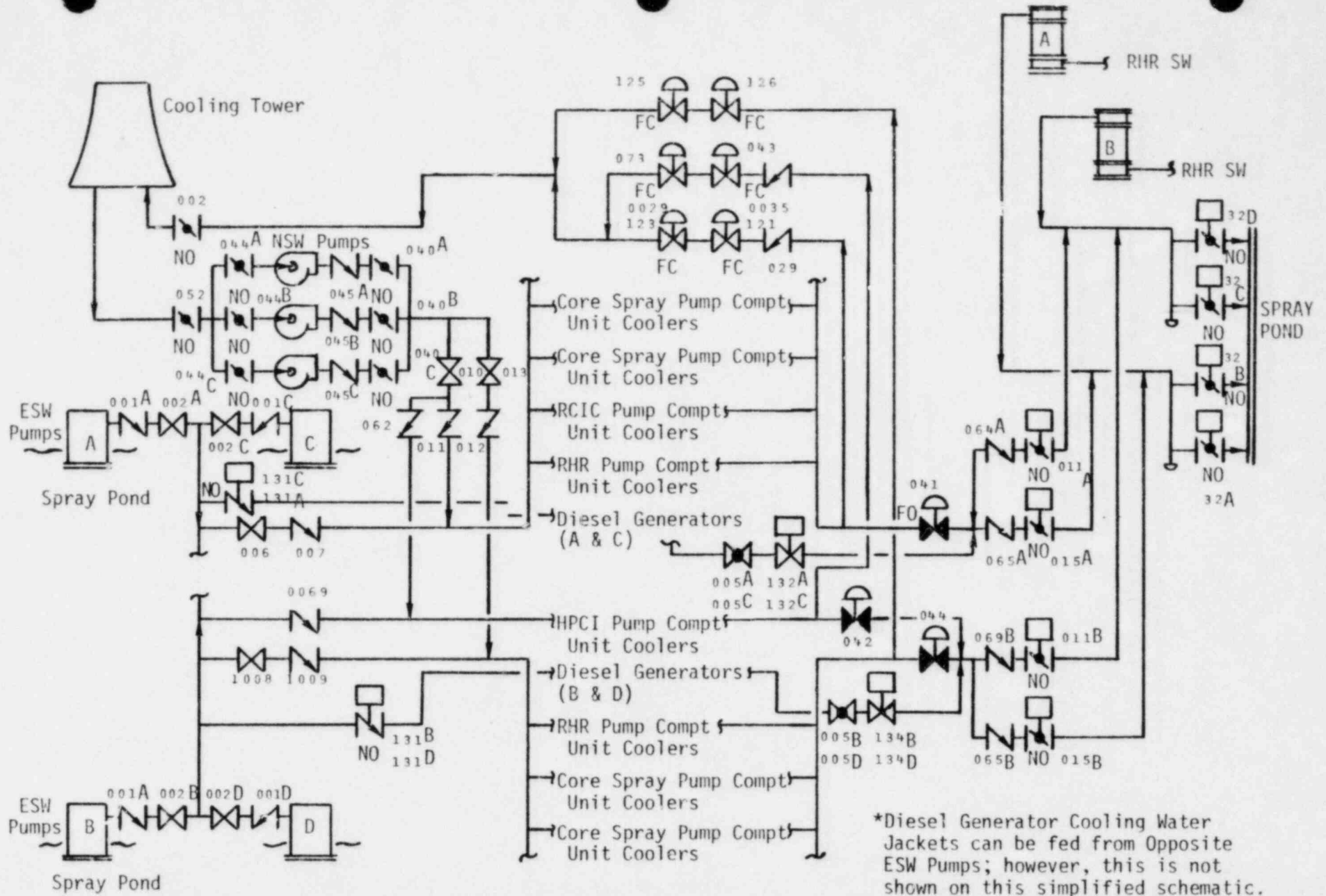
Figure B.6.1 Service Water (Normal and Emergency) System Schematic

Automatic Control

A start signal from each diesel generator initiates the automatic start of the associated ESW pump. The initiation signal is based on the diesel generator bus breaker status, bus voltage, and diesel generator speeds.

Diesel generator D11 starts ESW pump A (Division I).

Diesel generator D12 starts ESW pump B (Division III).

Diesel generator D13 starts ESW pump C (Division II).

Diesel generator D14 starts ESW pump D (Division IV).

A start signal from each ESW pump initiates the associated loop valve action. Also the start signal closes the cooling tower inlet to the associated pump wet pit and opens the sluice gate from the spray pond. The return valves from the ESW system to the cooling tower are closed and the associated return valves to the spray pond are opened.

Automatic start of each ESW pump is initiated on the following conditions:

- Forty-five seconds after the associated diesel generator bus breaker is in and closed and the bus voltage is available

- Fifty-five seconds after the associated diesel generator is operating (i.e., speed detection) and the bus voltage is available.

Once an ESW pump is started, it continues to operate until any of the following conditions occur:

- Manually stopped by the operator in the control room or, for pump A, from the remote shutdown room

- Bus lockout

- Phase over current

- Ground fault
- Bus under voltage.

Manual Control

Manual control for all four pumps and remote-operated loop configuration control valves is available in the control room. Manual control of ESW pump A and associated valves is available on the remote shutdown panel.

Electric Power Requirements

The power for the ESW pump motors and its associated loop motor-operated valves is supplied from Class 1E AC buses. Control power for the ESW pumps is supplied from Class 1E DC buses. Instrument power is supplied from Class 1E AC buses.

The controls and instrumentation (C&I) are physically and electrically separated for each of the four ESW pumps:

ESW pump A C&I are in Division I.

ESW pump B C&I are in Division III.

ESW pump C C&I are in Division II.

ESW pump D C&I are in Division IV.

The controls for the ESW valves are assigned to various divisions so that a single active failure cannot disable a complete ESW loop. In cases where two valves are in series to shut off a flow path, the valves are assigned to two different divisions. Likewise, in cases where two valves are used to provide redundant flow paths in a single loop, the valves are assigned to two different divisions.

Loop A valves are in Division I and II, and loop B valves are in Divisions II and IV. The manual control loop selection valves for each diesel generator are in the same division as the associated diesel generator.

ESW loop A normally supplies cooling water for diesels A and C, and ESW loop B feeds diesels B and D. It is physically possible to switch the ESW supply to the diesels (i.e., ESW loop A feeding diesels B and D) but no credit was taken for this feature in the analysis since it was felt that insufficient time was available to make the transfer in time to preclude diesel overheating.

The ESW system uses the ultimate heat sink (spray pond) as a source of water and discharges either to the cooling tower or back to the spray pond. The ESW and RHRSW systems discharge to the spray pond through a common header.

B.7   REACTOR PROTECTION SYSTEM

Purpose

The purpose of this section is to:

- Discuss the approach used to estimate the LGS scram reliability

- Define the range of values currently estimated for "failure to scram on demand" probabilities and to provide the value to be used in the Limerick risk assessment.

- Examine the effectiveness of ARI.

During a postulated accident sequence, an important safety function to be performed is the insertion of negative reactivity to bring the reactor subcritical. The primary method for the insertion of negative reactivity is through the insertion of the control rods. The reactor protection system and the control rod system both have a high level of redundancy which results in a highly reliable system. For complex systems with highly redundant components, fault tree analysis alone is insufficient to determine the system's reliability. Therefore, in the LGS analysis, the following approach was used to estimate the probability of bringing the reactor subcritical:

1. Examine the history of various studies to determine past evaluations of the probability of failure to scram.

2. Make use of a Bayesian analysis to arrive at a value for the LGS PRA.

3. Determine the ARI reliability using a reliability model. ARI is only effective in reducing electrical common-mode failures.

4. Use the standby liquid control (SLC) as a backup to the normal RPS. The standby liquid control system is an automatic system of two pumps and several valves. It is modeled using fault tree techniques similar to those used for other mechanical systems and quantified in a similar manner.

5. The quantification of the event sequences, see Figure B.7.1, will lead to a calculated probability for postulated unacceptable core conditions. This value can be used to compare with the following:

    •   Other accident sequence probabilities for the approximate relative contribution to risk

    •   Previous estimates of ATWS probability.

Discussion

Scram System Reliability: The calculation of scram system reliability has been an issue which has taken on both technical and philosophical aspects over the last seven (7) years. As a point of departure for this discussion, consider the past estimates of scram system reliability from various sources as shown in Table B.7.1 and Figure B.7.2.

SCRAM INITIATOR	SCRAM RELIABILITY C_E OR C_M	PREVENTION (X)	MITIGATION (U) Coolant Injection (U) Poison Injection (C_2)	DOMINANT SEQUENCE LEADING TO POSTULATED CORE MELT
T	FAILURE OF $C_{ELECTRICAL}$ — AND — FAILURE OF RPT OR ARI — AND —		FAILURE OF RPT OR SLC OR HPCI	$TC_E XU$ or $TC_E XC_2$
	FAILURE OF $C_{MECHANICAL}$ — — — AND — — —		FAILURE OF RPT OR SLC OR HPCI	$TC_M U$ or $TC_M C_2$
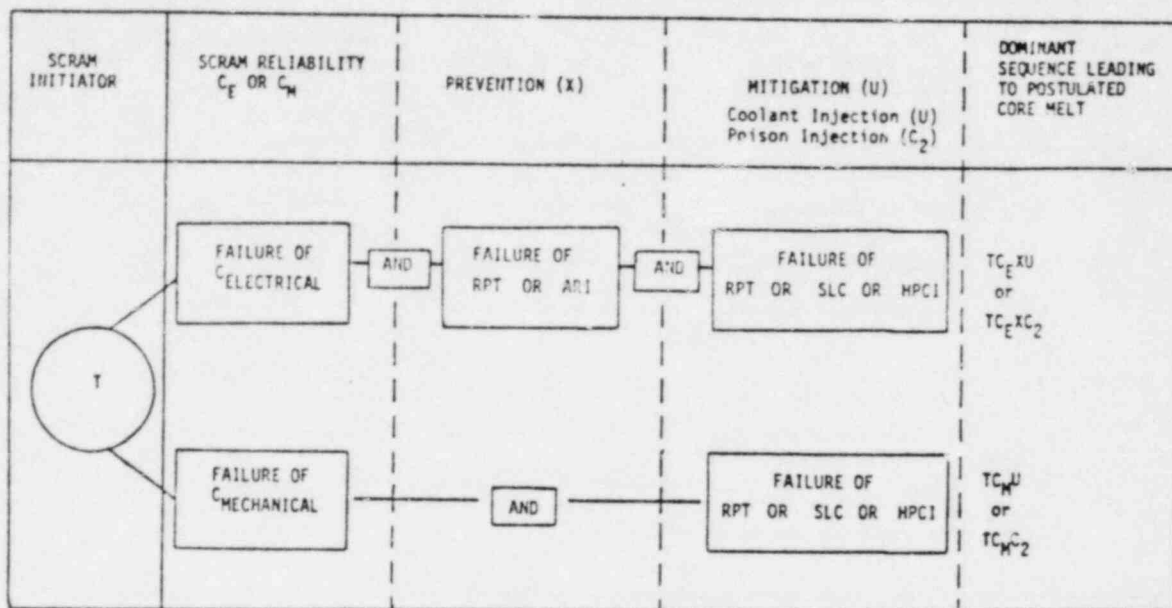
Figure B. 7. 1.   Summary of Failures Required to Result in
Unacceptable Core Conditions.

Table B.7 1

SUMMARY OF SCRAM SYSTEM UNRELIABILITY
ESTIMATES FROM VARIOUS SOURCES

MAXIMUM LIKELIHOOD SCRAM UNRELIABILITY	UNCERTAINTY BOUNDS	METHOD USED TO DERIVE SCRAM UNRELIABILITY	SOURCE
1.0×10^{-5}/Demand	± 10	Fault Tree	WASH-1400
2.0×10^{-6}	± 5	Synthesis	EPRI-265
5.0×10^{-5}	± 2	Postulated Data	WASH-1270
3.0×10^{-5}	NE*	Data/Judgment	NUREG-0460
2.8×10^{-5}	± 5	Bayesian Combination of Priors	Nuclear Safety Vol. 20, No. 6, 12/79
8.0×10^{-7}	NE*	Synthesis	GE

*NE not estimated

While there has been a significant amount of discussion as to
the correct value of the scram failure probability, the final assessed
values from a variety of published sources are remarkably close together.
In particular, WASH-1400, WASH-1270, NUREG-0460, and a recent article
from Nuclear Safety (B.7-1) all place the value in the range of 1 to 5
x 10^{-5} per demand. Even the lowest values quoted are only a factor of
5 to 10 times lower than these values. The first four sources depend
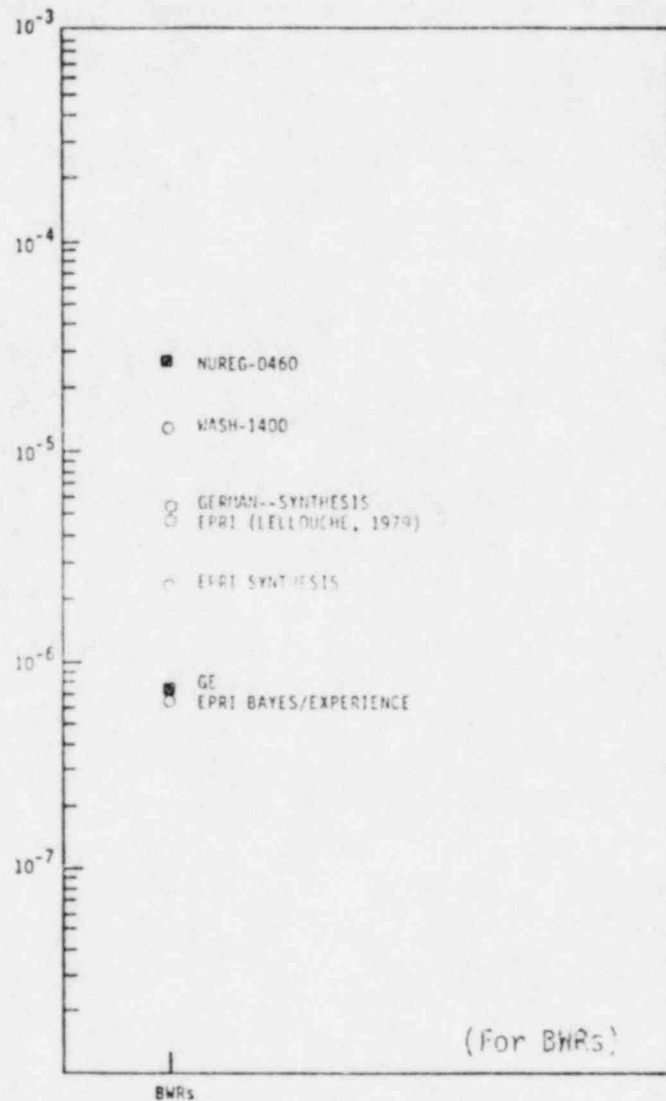
Figure B.7.2 Calculated Scram System Unreliability
(All values are point estimates.)

B-61

largely on accumulated operating experience data. Since these data are very limited (i.e., a relatively small number of operating years), the assessed failure rate is high and the level of confidence reflects the uncertainty. On the other hand, a quoted EPRI value is based upon a fault tree model* approach and can be viewed approximately as a lower bound estimate of the mean value, since common-mode or unusual failure modes are difficult to include in such a modeling assessment. Specifically, it is difficult, on a generic basis, to so thoroughly construct the fault tree of a system from a set of design drawings that all the potential common-mode effects which could be introduced into the as-built system are accounted for. Therefore, some confirmatory data is always desirable to ensure that the system evaluations are of the correct order of magnitude.

Because the available data (i.e., number of scram demands) are relatively sparse, it is difficult to support a value less 10^{-3} or 10^{-4} per demand, based strictly on available data.

It appears that prior to the Brown's Ferry incident** of June 1980, the perception of a point value representation of scram unreliability from the NRC and WASH-1400 analysis was in the range of 1×10^{-5} per demand. Industry evaluations range from 5×10^{-6} to 7×10^{-7}. In addition, these values are composed totally of electrical common-mode failures since the two cases that have resulted in scram failure were the Kahl and Monticello scram breaker failures. In contrast to this perception, the NRC staff has postulated that unidentified mechanical common-cause failures are equally as likely as the identified electrical common-cause failures.

---

*Referred to by NRC as Synthesis method.
**A partial CRD insertion at Brown's Ferry was attributed to a blockage in the scram discharge system which isolated the high level scram sensors. The Limerick design is different than Brown's Ferry in this area and thus the probability of a scram failure from this type of cause is remote.

The factor which has not yet been incorporated in the quantitative calculation of scram system probability is the following:

Improvements as the result of precursors which identify possible failure modes prior to an ATWS event requiring mitigation. In reality the failures or incidents which have occurred in U. S. BWR's to date (Monticello and Brown's Ferry 3) are precursors. There were no offsite consequences of these events.

The quantitative evaluation of rare events based upon operating experience data must account for the occurrence of precursors at a higher frequency. Therefore, plant modifications and procedural changes arising as a result of identified precursors should also be incorporated into the quantification. This type of analysis will result in an estimate of scram system reliability higher than that developed based strictly on the application of operating experience data.

However, to date there is not an effective method of incorporating rectification as a result of precursors and design changes into the assessed value of scram system failure probability.

Because of the wide disparity in evaluated scram system unreliability, it appears prudent to perform "bounding" calculations to demonstrate the effect on risk of assuming values at the high end of the probability estimates versus values at the low end. In addition, since Limerick is not completed, and there are known to be wide variations in nuclear plant reliability, a range of values is desirable, especially on such a controversial subject.

The value for scram failure probability used in the Limerick analysis is 3×10^{-5}/demand (NUREG-0460). A recent GE analysis indicates that a lower value may be appropriate.

<u>Effectiveness of ARI</u>: ARI (alternate rod insertion) is a system composed of additional sensors and logic to open additional air pilot valves on the scram headers in order to provide additional diversity and redundancy in the electrical portion of the scram system. GE has estimated the unreliability of this system to be in the range of 10^{-2} per demand.

The effectiveness of ARI is a slightly different issue and revolves around the split in scram system unreliability between electrical and mechanical common-mode failures. The NRC staff has assumed an equal distribution of relative probability between electrical and mechanical common-mode failure; however, no data are presented and no judgment is applied to justify the split chosen by the NRC staff. Since there have been no mechanical common-mode failures or precursors*, it is judged that they are much less likely than the potential electrical failures which have surfaced in the operating experience data.

If, however, one treats the Brown's Ferry event as a precursor, then one can estimate the frequency of ATWS as:

Reliability Based on Data: Events & Precursors Divided by Total Demands	X	Reliability Improvement Based Upon Operational Experience	X	Probability of a Real Event Relative to a Precursor

<u>Electrical</u>
$$10^{-4} \times (.3)^{**} \times \left(\frac{2}{3}\right) = 2 \times 10^{-5}$$

<u>Mechanical</u>
$$10^{-4**} \times (.3)^{**} \times \left(\frac{1}{3} \text{ to } \frac{1}{10}\right)^{***} = 1 \times 10^{-5} \text{ to } 3 \times 10^{-6}$$

---

*It is assumed here that the incident at Brown's Ferry, while definitely a precursor to an ATWS event, was previously identified as an area which should be modified and in fact has been modified in the Limerick design. Therefore, it is not viewed as new information on a potentially rare failure mode, but merely confirmation of the fact that there existed a single point failure which needed to be removed.

**NRC Evaluation in NUREG-0460 based upon one (electrical) and one precursor (mechanical) occurrence.

***The factor of 1/3 arises if we consider there have been two electrical common-mode problems identified (Kahl and Monticello) versus one mechanical precursor (Brown's Ferry 3). The factor of 10 is a purely subjective estimate of the relative frequency of precursors to real events.

Since no total scram system failure on a real demand has occurred in U. S. operating plants, there could be an argument that the estimated probability of scram system failure is less than that based upon data. If a plant-specific reliability model (e.g., fault tree including all common-mode failures) were constructed and properly quantified, then this information could be folded into the state of knowledge. However, without a plant-specific, as-built reliability model with potential common-mode failures clearly addressed, this result would have little impact on the calculated probability of scram system failure. The estimated split in probability between potential electrical and mechanical common-mode failures can be found from the data cited above; that is, the ratio of electrical common-mode failure to mechanical is approximately:

$$\frac{2 \times 10^{-5}/\text{demand}}{1 \times 10^{-5}/\text{demand}} = 2.$$

Therefore, it is judged that 30% (1/3) of the scram system unreliability should be considered to be mechanical and not affected by ARI. That is, ARI is effective in reducing the unreliability of the electrical portion of the scram system or approximately 70% of the estimated unreliability.

B.8   STANDBY LIQUID CONTROL SYSTEM (SLC)

Purpose

The purpose of the SLC system is to bring the reactor to a cold shutdown condition independent of the control rod drive system.

Hardware Description

The SLC system consists of an unpressurized tank for sodium pentaborate solution storage, two positive displacement pumps, two ex-plosive-actuated valves, and associated system piping, valves, controls, and instrumentation (see schematic in Figure B.8.1). Boron neutron absorber

HPCI*

LC

LC

LC

TEST
TANK

SLC
TANK

LO

MO Stop
Check
Valve
for
Outboard Isolation

SUPPRESSION

POOL

**

LO

LO

LO

Two Suction
Piping with
Heat Tracing
Devices
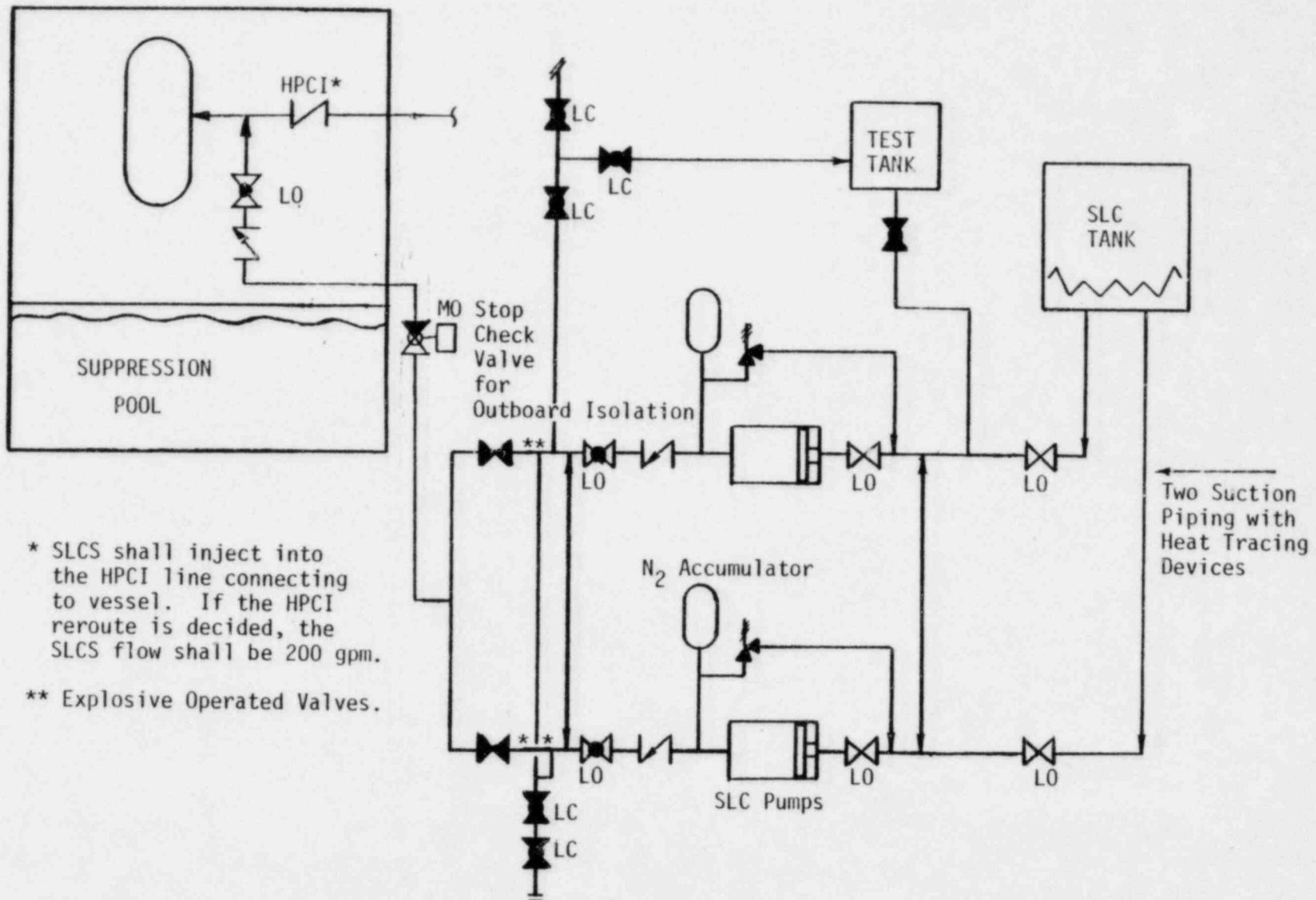
* SLCS shall inject into
the HPCI line connecting
to vessel. If the HPCI
reroute is decided, the
SLCS flow shall be 200 gpm.

** Explosive Operated Valves.

N_2 Accumulator

* **

LO

LO

LO

LC

LC

SLC Pumps

Figure B.8.1 Standby Liquid Control System Schematic

solution is pumped into the reactor vessel to achieve subcriticality. The neutron absorber solution is an aqueous solution of sodium pentaborate maintained above a specified temperature by environmental electric heaters to prevent precipitation of the sodium pentaborate. An air sparger is provided in the tank for mixing. The suction piping to the pumps penetrates the holding tank at a level sufficiently above the tank bottom to prevent any potential plugging of the system.

Automatic and Manual Control

The SLC system is automatically initiated on receipt of a reactor pressure vessel (RPV) low water level or a RPV high pressure signal coupled with time delay, downscale flux indication, and control rod position indication permissives. Once the initiation signal is processed, both explosive valves are actuated and both pumps started and the neutron absorber solution is pumped into the RPV.

The SLC pumps are stopped automatically by a low-low water level signal in the SLC tank.

In addition to the automatic operational features of the SLC system, provisions are included for remote manual startup and shutdown of each individual pump or both pumps.

Instrumentation and Alarms

Instrumentation sensors are used to monitor RPV low water level and high pressure. Additionally, instrumentation consisting of solution temperature indication and control, solution level, and heater system operation is provided locally at the tank. Indication of SLC tank level, pump discharge pressure, and valve injection status are located in the control room. There are also alarms to warn for low-low level in the tank.

Electric Power Requirements

The SLC system (pumps, heaters, valves, and controls) are powered by plant normal power supply (i.e., offsite power) and are automatically switched to the standby AC power supply in the event of loss of offsite power. Components are powered and controlled from divisionally separate buses and circuits.

Analysis of the SLC System

The SLC system has been designed to provide flow from both SLC pumps to the reactor with a high degree of reliability. However, the following failure modes could occur in the Limerick SLC system and each by itself could preclude Boron injection:

1. Single Point Failures

   • A discharge valve fails closed

     - Manual valve

     - Check valve

     - MO stop check valve

   • Tank integrity

   • Boron concentration

2. SLC system in test (i.e., 12 tests/year at 45 minutes/test).*

The probability of SLC system failure used in the evaluation of ATWS was 4×10^{-3} per demand. The LGS will be equipped with a system that meets this reliability.

---

*This assumption was used in the analysis, but a design change is presently being evaluated which would allow one SLC loop to be available during testing. The as-built Limerick SLC system may contain this feature.

B.9   GENERIC COMPONENT TREES

The following discussion is provided to describe the approximate apportioning of the assessed component failure rate among the various potential failure modes of each generic component.

The fault tree model of the available plant systems which may be useful in the event of an accident initiation have been carried down to the component level. This means that the component failure probabilities are the required input parameters for the quantification of the fault tree. In this section, the potential failure modes of concern are displayed in fault tree format for each generic component. Since very little data exists on the failure rates of components on a failure mode basis, an attempt is made to apportion the reported component failure probabilities among the various types of failure modes using the available sources.

The generic components which have their potential failure modes displayed in fault tree format are*:

1. Motor-Operated Valves

    •   Normally Open Fails Closed: NOFC

    •   Normally Closed Fails Open: NCFO

    •   Normally Open Fails Open: NOFO

    •   Normally Closed Fails Closed:NCFC

2. Manual Valves

    •   NOFC and NCFO

    •   NCFC and NOFO

3. Hydraulic- or Air-Operated Valves (NCFC and NOFO)

---

*Note that the quantification of the system level fault trees are based upon component failure rate data given in Appendix A.

4. Pumps

5. Turbine

6. Room Ventilation.

The common-mode failures (failures that occur for the same reason at the same time) explicitly included in this model are:

- Loss of electric power (AC or DC)
- Loss of actuation signals to a system
- Miscalibration of a group of sensors.

While these common-mode failures generally have a lower probability of occurrence, they also have a more far-reaching effect than single, local random failures of an individual component.

Motor-Operated Valves Disabled: Most of the critical valves in the LGS safety systems are Motor-Operated Valves (MOV). The MOV failures are classed here in two categories: those which disable the valve out of the normal position (this includes normally open valves which fail closed and normally closed valves which fail open), and those which disable the valve in the normal position (these include normally open valves which fail open and normally closed valves which fail closed).

Operating experience data indicates that of the identified causes of valve failure, personnel errors or faulty procedures are the principal causes of valve unavailability. These failures may occur during operation, maintenance, or test. A simple ranking by frequency of the failure modes observed in the operating data is included here in Table B.9.1 for information and as a guide to the relative apportionment of the valve failure rate over the observed failure modes. The corresponding generic component fault trees for MOV failures are given in Figures B.9.1 and B.9.2.

Table · B.9.1

SUMMARY OF DOMINANT FAILURE MODES WHICH AFFECT OPERABILITY OF AN MOV WHICH MUST CHANGE POSITION

Rank	Failure Mode	Approximate Apportioning of Failure Rate
1	Personnel Error or Faulty Procedure	21%
2	Mechanical Controls Failed or Out of Adjustment	16%
3	Seat/Disc Failure	12%
4	Electrical Input Fails	10%
5	Packing Failure	9%
6	Foreign Material Contamination	9%
7	Switch Failures	8%
8	Electrical Motor Fails	5%
9	Design Error	4%
10	Wear	4%
11	Lack of Lubrication	2%
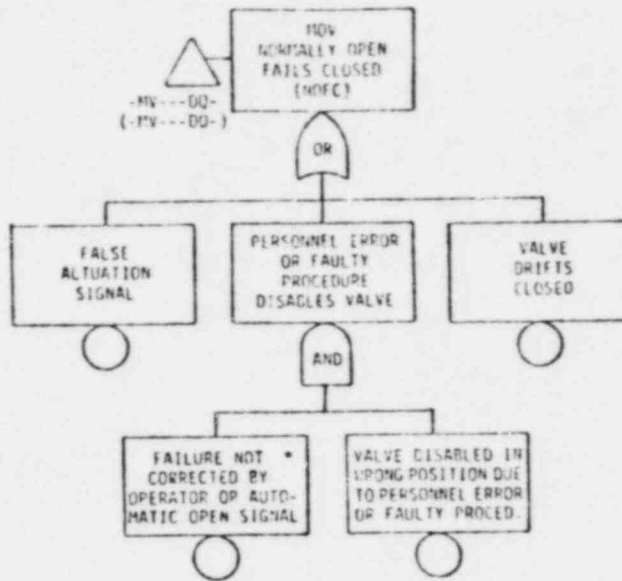
*Automatic Open (Close) Signal is given to test valves upon receipt of system initiation signal.

Figure   B.9.1   Generic Fault Tree for a Motor Operated Valve (MOV) for Cases Where the Valve is Normally Open and Fails Closed (NOFC) (These same failure modes apply to cases for Normally Closed Valves Which Fail Open (NCFO).)
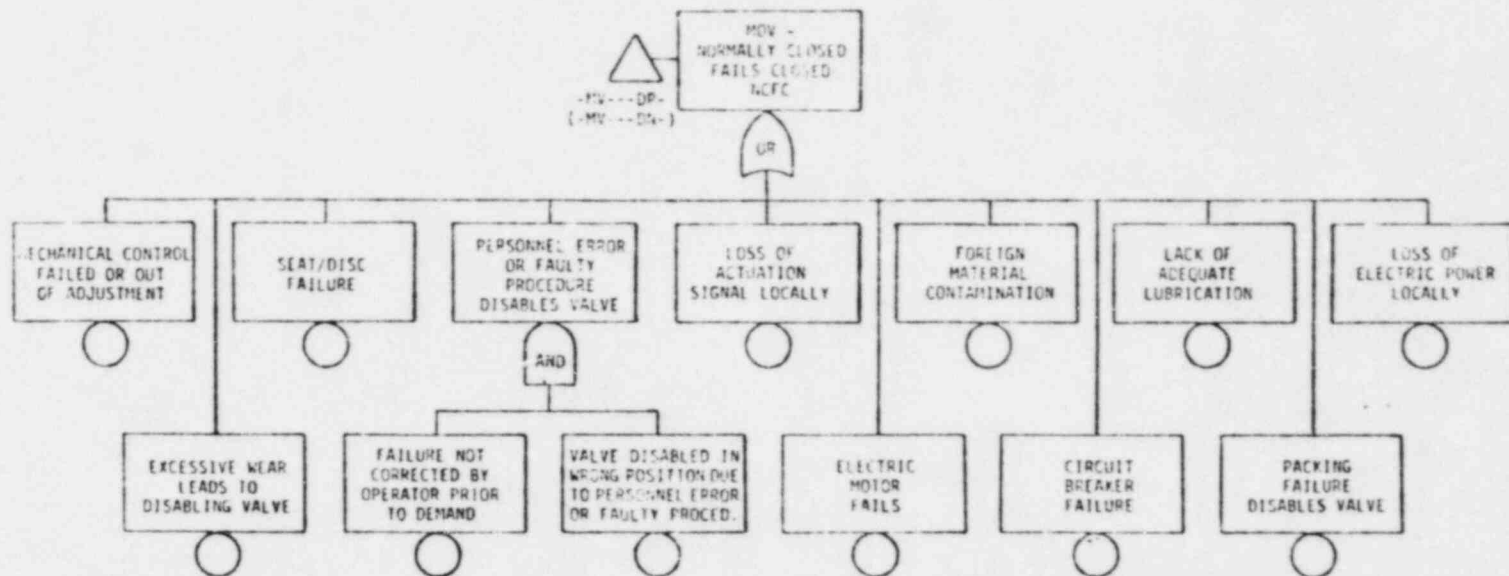
Figure B.9.2   Generic Fault Tree for a Motor Operated Valve (MOV) for Cases Where the Valve is
Normally Closed and Fails Closed (NCFC) (These same failure modes apply to cases
for Normally Open Fail Open Valves.)

<u>Manual Valves</u>: The operation of manual valves in safety systems
is relied upon only as a backup condition. The ability to open a specific
manual valve requires:

- Sufficient time for an operator to recognize the
  need for the valve operation

- Proper training and procedures to allow timely
  operation of the valve

- Adequate access for personnel to open the valve

- Proper mechanical operation of the manual valve
  and handwheel.

The generic fault tree for manual valves is given in Figure B.9.3. Note
that the failure of the operator to successfully manipulate the valve to
change state in the allowed time is treated explicitly in the system level
fault tree for each of the manual valves.

<u>Air or Hydraulically Operated Valve</u>: The generic fault tree
for the air-operated and hydraulic-operated valves is shown in Figure
B.9.4. It is similar to that developed for the motor-operated valves to
display the failure modes, except that loss of the electric motor and
electrical power is replaced by failure of the solenoid pilot valve or
loss of fluid supply. The apportioning of the failure probabilities is
also similar.

<u>Pump Fails to Start or Run</u>: A recent NRC analysis (<u>B.9-1</u>)
of reported pump failures to start or run gives an approximate breakdown
of the frequency of failure modes of emergency core cooling pumps. Figure
B.9.5 displays these failure modes. The approximate apportionment of the
overall component failure probability among the leading failure modes is
given in Table 3.9.2. It is useful to note that seal and packing failures
are the leading cause of pump failure followed by design errors and personnel
errors or faulty procedures.
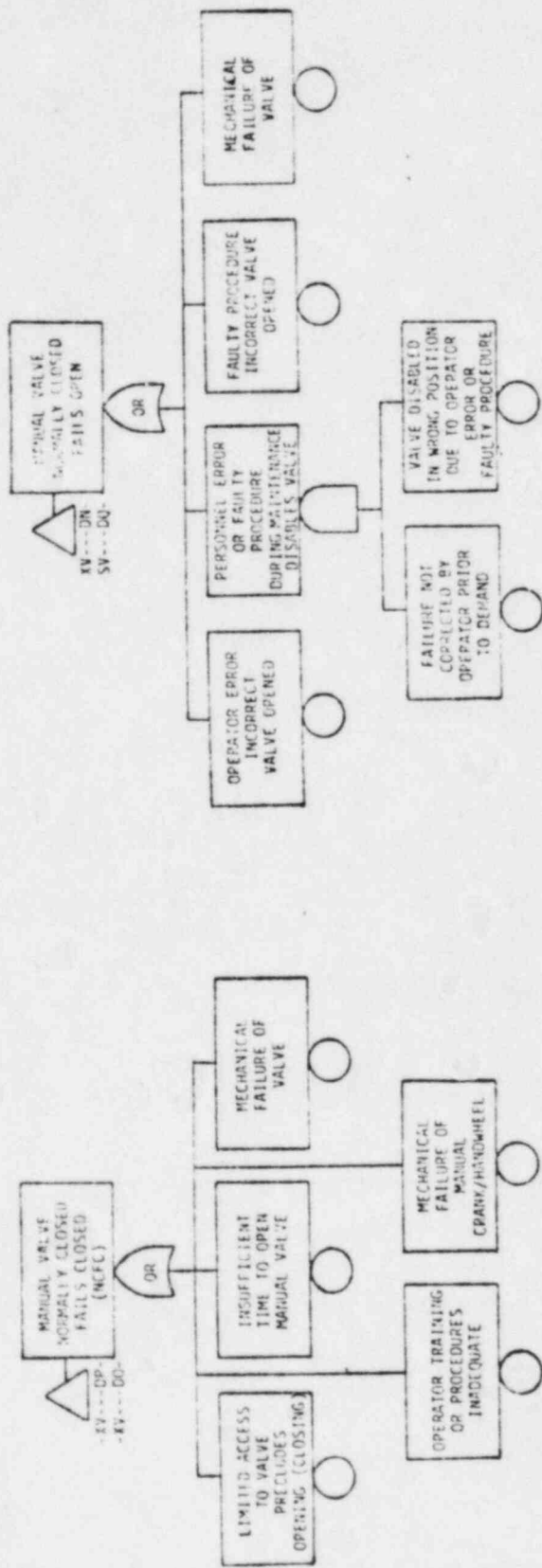
Figure B.9.3 Generic Fault Trees for Manual Valves
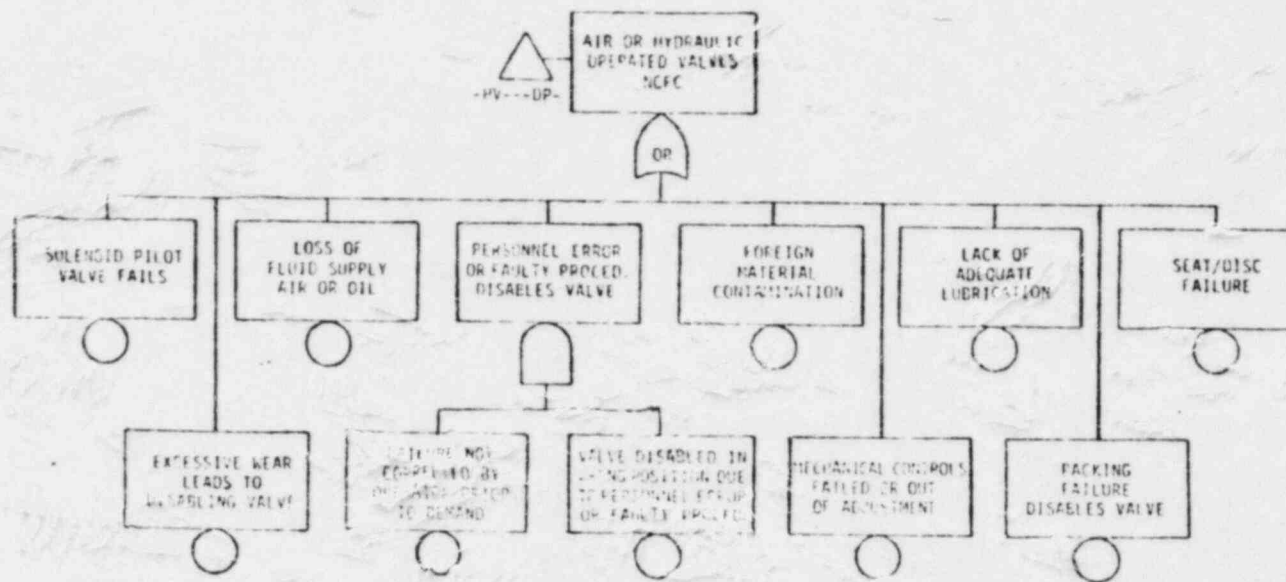
Figure B.9.4 Generic Fault Tree for an Air-Operated or Hydraulic-Operated Valve
for Cases Where the Valve is Normally Closed and it Fails Closed
(NCFC) or (NOFO)
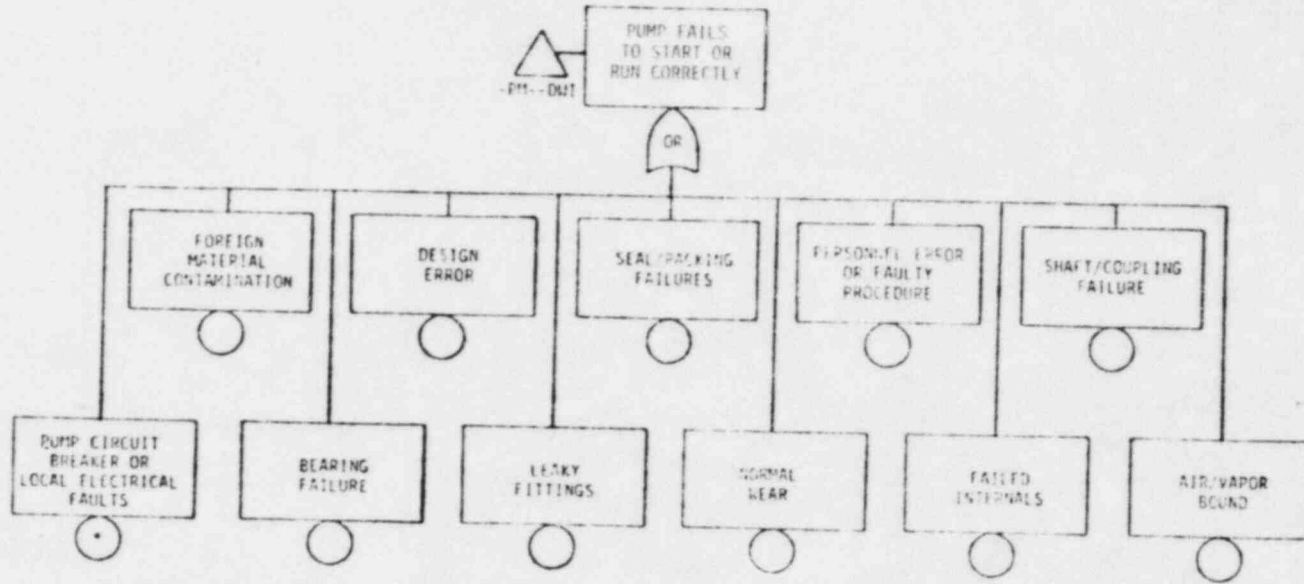
Figure B.9.5 Generic Fault Tree for Pumps, Including the Dominant Failure
Modes of Pump Failure Observed in Operation

Table B.9.2

SUMMARY OF DOMINANT PUMP FAILURE MODES

Failure Mode	Approximate Apportioning of Failure Rate
Seal/Packing Failure	20%
Design Error	16%
Personnel Error or Faulty Procedure	11%
Foreign Material Contamination	6%
Shaft/Coupling Failure	5%
Bearing Failure	4%
Leaky Fittings	4%
Air/Vapor Bound	3%
Normal Wear	3%
Failed Intervals	3%
Miscellaneous/Unknown	25%

Turbine: Both RCIC and HPCI utilize a steam turbine to supply
the motive power for the high pressure pumps. Therefore, one of the
failure mechanisms of HPCI & RCIC is the failure of the turbine. Figure
B.9.6 is the generic fault tree of the turbine and displays the potential
failure modes considered dominant in the evaluation of the turbine failure
rate.

Pump Room Cooling and Ventilation: For long-term emergency
core cooling system operation, adequate pump room cooling and ventilation
is consideration necessary. The RCIC, RHR, HPCI, and core spray pump
rooms have two sources of ventilation air:

- Reactor Building Heating and Ventilation (offsite
  power required)

- Emergency Heating and Ventilation System (emergency
  power source).

Figure B.9.7 displays some of the potential failures which could disable
the ventilation systems and preclude adequate pump room cooling. Little
data is available on the performance of pump room cooling systems; how-
ever, loss of these systems is felt to be a relatively small contributor
to pump failure compared to the other failure modes cited in the pump or
turbine generic fault tree.

Instrumentation: Instrumentation and control failures have
been recognized to be a contributor to plant or system unavailability
(B.9-2) and a major contributor to plant trips (B.9-3). The fault tree
model constructed in this analysis accounts for failures of instrumen-
tation channels in the following categories:

- Failure of Sensors (failure modes are discussed below)

- Miscalibration of Sensors (basically a human error or
  faulty procedure)

- Logic Failures
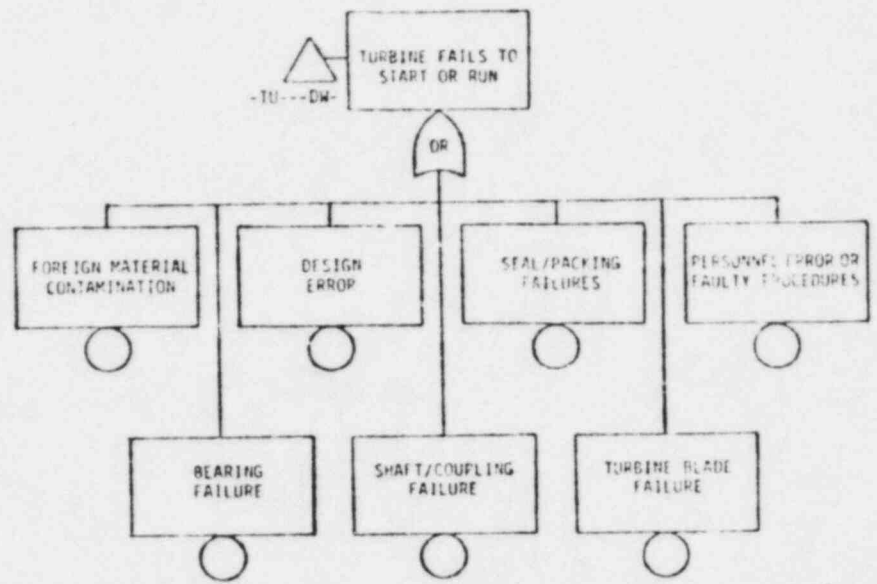
Figure B.9.6 Generic Fault Tree Model Displaying
the Potential Failure Modes of the
Turbine (RCIC or HPCI)
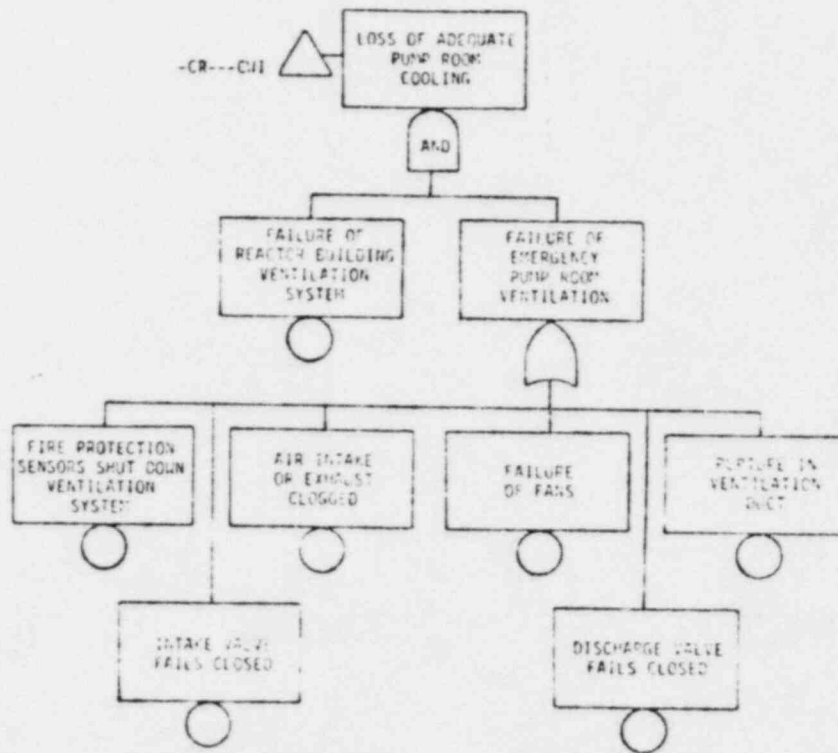
Figure B.9.7   Generic Fault Tree for the Pump Room
Cooling for the Emergency Core Cooling
Systems

• Loss of Power to Sensor (these are considered only in
those cases where failure of power prohibits an actuation
signal).

Each of the above failures is represented in the system level
fault tree where appropriate. In addition, there are a number of other
potential failure modes (B.9-2) for instrumentation/sensor failure.
These failure modes and the apportioned failure rate for each mode are
given in Table B.9.3 (see also Figure B.9.8).

In addition to component failures, calibration drift of
instrumentation outside of the range allowed in technical specifica-
tions may occur with a relatively high frequency (B.9-2, B.9-4).
It must be noted that while small calibration drift outside of allowed
technical specification limits is not good, it does not necessarily
represent a disabling failure. Specifically, the drift must be of
sufficient magnitude to preclude adequate action by the automatic
actuation signals and the associated safety systems. The precise in-
corporation in the analysis of the impact of calibration drift on system
reliability is a difficult task. The simplifying approach used in the
analysis is to include the estimated failure probability due to dali-
bration drift in the evaluated probability of instrument failure, encom-
passing those cases where the calibration drift is of sufficient magni-
tude to defeat the safety function signal.
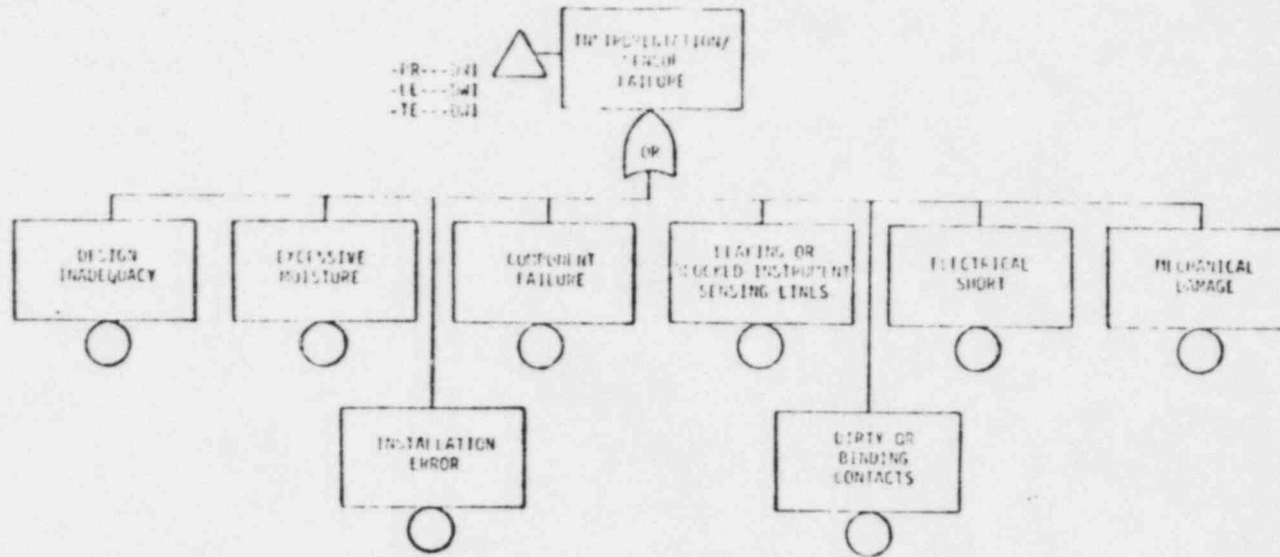
Figure B.9.8 Generic Instrumentation Fault Tree

Table B.9.3

INSTRUMENTATION/SENSOR FAILURE MODES
AND APPORTIONED FAILURE RATES FOR EACH

Rank	Failure Mode	Approximate Apportioning of Failure Rate
1	Component Failure	56%
2	Installation Error	14%
3	Dirty or Binding Contacts	13%
4	Leaking or Blocked Instrumentation Sensing Lines	6%
5	Excessive Moisture	5%
6	Design Inadequacy	3%
7	Electrical Short	2%
8	Mechanical Damage	1%
	OVERALL	100%

REFERENCES

B.9-1   W. H. Sullivan and J. P. Poloski, Data Summaries of Licensee
         Event Reports of Pumps at U. S. Commercial Nuclear Power
         Plants-January 1972 to April 1978, prepared for U. S. Nuclear
         Regulator Commission by EG&G. NUREG/CR-1205, January 1980.

B.9-2   S. L. Basin and E. T. Burns, Characteristics of Instrumentation
         and Control System Failures in Light Water Reactors, EPRI NP-443,
         August 1977.

B.9-3   E. Y. Lim, E. T. Burns, and R. J. Wilson, Component Failures
         that Lead to Reactor Scrams, prepared for Sandia Laboratories
         by Science Applications, Inc., May 1979.

B.9-4   R. A. Hartfield, Setpoint Drift in Nuclear Power Plant Safety-
         Related Instrumentation, office of Operations Evaluation, U. S.
         AEC Report OOE-ES-003, August 1974.

B.10   FUNCTIONAL LEVEL FAULT TREES

The event trees are used to tie together the key system
functions whose performance are required following the accident initia-
tors. The functions appearing in the event trees may be simple or com-
plex. This section presents the fault tree model representation for
the correct Boolean combination of these systems or functions. The
Boolean combination is necessary in those instances where there are
common dependencies among systems or functions. Some examples of such
dependencies are: (1) the requirement that maintenance on one safety
system be carried out exclusive of maintenance on certain other safety
systems and (2) that sensors used in the initiation of one safety system
are also used for another system (i.e., LPCI and ADS).

B.10.1   Transient Event Tree Functions

The first set of functional level fault trees are constructed
to define, in fault tree format, the system success criteria for each of
the functions of the transient event trees.

Initiators: These are input values determined based upon
operating experience data.

Reactor Shutdown: This is treated separately in the ATWS event
tree discussion. It is not developed as a system fault tree because of
the criticisms such evaluations have received in the past. The single
exception to this is the estimation of the failure to manually initiate
a scram during an inadvertent open relief valve (IORV) incident.

Safety/Relief Valves Fail to Open: Many of the transients which normally occur during the course of a reactor plant life never demand the safety/relief valves operate in order to protect the plant against ultimate over-pressure. However, there are a few transients which may demand that these valves operate successfully. A **fault** tree description is used in assessing the likelihood of a failure to perform this function.

Loss of Coolant Makeup to the Reactor: The functional level fault tree for the loss of coolant makeup to the reactor is a combination of four functions listed in the event tree; these are:

- Feedwater availability

- HPCI or RCIC availability

- ADS operation

- Low pressure system operation.

A functional fault tree is used to combine these functions. The principal items to note are that:

1. The quantification of the fault tree depends upon the accident sequence being evaluated. For example, CRD coolant injection alone is not considered successful for any accident sequence evaluated for LGS. Also, feedwater has a lower probability of success during an MSIV closure than during a turbine trip.

2. The depressurization function (ADSX) is defined explicitly. This function provides the only access to the low pressure system capability.

Loss of Containment Heat Removal: The final function provided
in the transient accident sequence event trees is the removal of heat from
containment. This function can be fulfilled in the following ways:

1. The power conversion system (PCS) can be used to remove decay
    heat through the main steam lines to the condenser.

2. The RHR system can be used to remove heat from the suppression
    pool, using the safety/relief valves to provide the path from
    the reactor to the suppression pool, plus the RHR service
    water to remove heat from the RHR heat exchangers.

3. The RCIC system can be used in the steam condensing mode in
    conjunction with the RHR heat exchangers and RHR service
    water system to provide methods of:

    • High pressure coolant makeup

    • Direct heat removal from the primary system

4. In addition to the above methods of containment heat removal,
    there is the containment overpressure relief function which
    will satisfy this need temporarily (i.e., for periods not in
    excess of 3 days in certain accident sequences). This function
    is logically placed in the bridge tree so that the timing and
    constraints on its use can be understood by the reader. However,
    for quantitative evaluation it is included in the functional
    fault tree for containment heat removal.

A containment heat removal functional fault tree is used with the
transient accident initiators. These systems have some interdepen-
dencies which require the fault tree evaluation of the systems. Simi-
larly, accident sequences and groups of accident sequences require the
same type of simultaneous evaluation to ensure that dependencies are
properly evaluated.

There is a dependency among accident sequences which is not explicitly incorporated in the LGS analysis, but is felt that this will not make a quantitative difference in the Limerick results. This dependency involves those accident sequences for which neither the power conversion system nor the RHR system is available to remove decay heat from containment. Under these conditions the operator is instructed to reduce the reactor system pressure before the suppression pool temperature rises above a certain limit. This action coupled with potentially high pressures inside containment could disable the turbine-driven high pressure systems (HPCI and RCIC) for the following reasons:

- The low reactor system pressure may be insufficient for turbine operation.

- The high turbine exhaust pressure may lead to HPCI/RCIC turbine trip.

- A combination of the above two conditions in a synergistic fashion.

In any event, high pressure system reliability under these conditions is appreciably degraded; therefore, reliance is placed on the low pressure coolant injection systems. Since the reason for being in the situation in the first place is the loss of RHR, it is possible that the LPCI pumps are already disabled and not available to supply coolant injection. The result of these considerations is that the net gain to be realized from the containment overpressure relief (COR) may be slightly smaller than originally estimated. This is principally due to the fact that, despite making the loss of containment heat removal a low probability occurrence, a relatively high probability exists that unacceptable core conditions may result anyway due to the inability to supply coolant injection under the postulated conditions. For the Limerick design it is found that the reliability of the emergency service water system coupled with the availability of LPCI and the condensate system should provide adequate reliability backup for coolant injection for the above postulated circumstances.

B.10.2   LOCA Event Tree Functions

The functional events used in the LOCA event trees are similar
to those explained in Section B.10.1 for the transient event trees. How-
ever, they are reviewed here for completeness.

LOCA Initiator: The LOCA initiators are divided into three
categories:

1.   Large LOCA - leads to depressurization of the reactor
      coolant system

2.   Medium LOCA - does not lead to reactor depressurization,
      but is sufficiently large to make RCIC inadequate for
      coolant inventory makeup

3.   Small LOCA - does not lead to reactor depressurization.
      RCIC is adequate for coolant.

Reactor Protection System (RPS): Section B.7 discusses the
reliability of the reactor protection system. The Limerick analysis
assumes independence between the accident initiator and the reliability
of the reactor scram system. For large LOCAs, the failure to scram is
determined based solely on the reliability of the reactor protection
system and the control rods to insert.* The Standby Liquid Control
system is not used as a backup for large LOCA shutdown requirements.
However, because of the low probability of the large LOCA, coupled
with the low probability of an RPS failure, the overall contribution
to risk from these sequences is smaller than the risk from other Class
IV ATWS sequences and has comparable consequences. Therefore, while the
consequences of a large LOCA with RPS failure has not been explicitly
calculated using INCOR (see Appendix C and Section 3.6), this highly
unlikely event is judged to be adequately incorporated in the analysis.

_____

*In the LGS analysis, as in NUREG-0460, these are treated
as independent failures from the large LOCA.

B-90

Medium and small LOCAs are incorporated in the estimated MSIV closure initiator frequency for the calculation of risk due to failure to scram. An area of large uncertainty is the method of bringing the reactor from hot shutdown to cold shutdown, but this is not addressed in the current analysis.

Coolant Injection: The event tree function associated with coolant injection is governed by a functional fault tree in which is identical to that given for transient events. The distinction to be drawn is in the evaluation of the fault tree. The differences in the quantification can be summarized as follows:

1. For Large LOCA:

System	Failure Probability	Reason
RCIC	1.0	Insufficient flow
HPCI	1.0	Insufficient flow
Feedwater	1.0	Unavailable due to MSIV closure
ADS	0.0	Not needed for large LOCA

2. For Medium LOCA:

System	Failure Probability	Reason
RCIC	1.0	Insufficient flow
FW	1.0	Isolation due to low reactor water level

3. For Small LOCA: the reliability of all systems is the same as used in the transient event trees with the exception that HPCI automatic initiation reliability is improved since high drywell pressure will occur.

Containment Heat Removal: The removal of heat from containment is a vital function in assuring the safe condition of the plant following a LOCA. The removal of heat from containment follows the same functional fault tree as developed for the transient events with the following exceptions:

1. Large LOCA:

System	Failure Probability Used in the LGS Analysis	Reason
Power Conversion System	1.0	Isolation of containment from the main condenser on low reactor water level
RCIC in the Steam Condensing Mode	1.0	Loss of steam to the RCIC turbine
Containment Overpressure Relief(COR)	1.0	Potential for radiation inside containment

2. Medium LOCA:

System	Failure Probability Used in the LGS Analysis	Reason
Power Conversion System	Reduced from transient event tree	Isolation immediately following LOCA: increased probability of failure to recover from isolation
RCIC in Steam Condensing Mode	1.0	Loss of steam to the RCIC turbine following depressurization

3. Small LOCA: the quantification of the small LOCA containment heat removal function is the same as that for the turbine trip event tree.

B.10.3   ATWS Functional Fault Trees

The functional events considered in the ATWS event tree evaluation are similar in most ways with those noted for transients. There are, however, some unique differences which require separate evaluation and these are discussed in this section. It should be carefully noted that the success criteria used in the construction of the functional level fault trees is that identified in Section 1.5 and reflects the General Electric evaluation of BWR/4 systems capability under ATWS conditions. Specifically, the system capability is based upon unpublished GE analysis and takes advantage of best estimate values for system flow and performance capability rather than the usual conservative values used in design basis analyses. In addition, containment capability beyond that usually acknowledged in design basis evaluations has been utilized.

Initiators: These input values are based upon the General Electric evaluation of operating experience data and include demands from all power levels. There is a discrimination among the types of transients in order to treat the dependent effects of the plant system on the initiating event as precisely as possible.

Reactor Shutdown: The ATWS event trees provide the vehicle in the Limerick analysis for treating the consequences associated with reactor shutdown, i.e., insertion of sufficient negative reactivity into the reactor core. Reactor shutdown for the LGS plants can be accomplished successfully through any of the following:

1. Insertion of the control rods by automatic action of the reactor protection system or by manual operator action. This is event item C_i in the ATWS event trees.

2. Insertion of the control rods by automatic action of
    the diverse and redundant backup system known as the
    Alternate Rod Insertion (ARI) system. This is referred
    to as Event V in the event trees. This backup system
    requires that the following additional features operate:

    • The control rod mechanical operation be functional

    • The recirculation pump trip (APT) be functional.

    At present, the design details of the logic, power, and
    sensors for RPS and RPT are not available for Limerick;
    therefore, possible dependencies between RPS and RPT have
    not been analyzed in detail. The possibility of a common-
    ality between the logic and sensors has not been explicitly
    evaluated. The assumptions made in the analysis are:

    • APS and APT are separate and diverse.

    • The reliability of the RPS is as specified by the
       NRC characterizations in NUREG-0460.

    • The RPT reliability is that specified by GE and
       assumed by the NRC in NUREG-0460.

3. Insertion of negative reactivity via the Standby Liquid
    Control (SLC) system which injects a sodium pentaborate
    solution into the reactor. This backup system is de-
    signed to safely shutdown the reactor in the unlikely
    event that the control rods cannot be inserted into the
    core.

Poison Injection: While poison injection was discussed briefly
above under Reactor Shutdown, it needs further discussion since its partial
operation can also be successful if other systems operate successfully.
The specific points to be gleaned from an examination of the ATWS event
trees are:

1. Loss of all SLC system capability and loss of control rod
    insertion will lead to a Class IV type event sequence.

2. Loss of one SLC system pump (i.e., half capacity) makes RCIC
    alone unacceptable to maintain adequate core coolant inventory
    and requires RHR initiation in a very short time, i.e., on
    the order of 10 minutes.

Adequate Pressure Control(N): For ATWS events the operation of the safety relief valves is required since there is a rapid pressure rise in the primary system. The number of valves required for operation under this remote postulated event is larger than that used in the typical transient event, but the dominant failure mode remains a common-mode failure of a large number of valves.

Safety Valves Reclose(P): Stuck-open safety valves are an un-desirable event at any time and during an ATWS will tend to aggravate the situation by:

- Eliminating RCIC as a successful injection mode

- Requiring both RHR heat exchanges for successful containment heat removal.

The probability of failure of the safety relief valves in the stuck-open position following an ATWS is estimated to have a higher probability than during a normal transient.

Coolant Injection: The success of coolant injection during an ATWS event requires operation of one of the high pressure injection systems: HPCI, RCIC, or Feedwater. The use of low pressure systems may result in unacceptable dilution of the boron (LPCI overfilling the vessel or ADS initiation) which may lead to an unacceptable plant condition such as high reactor or containment pressure.

The probabilities of each of the system level functions in the fault tree are dependent on the ATWS initiator. In addition, con-siderations beyond those included in the transient and LOCA event trees are included in the ATWS quantification for the following reasons:

1. For ATWS accident scenarios, HPCI system has been modified to include a failure of the HPCI to restart once it has been turned off (i.e., isolated) by the high pressure spike which accompanies ATWS. In addition, there is an increased probability of premature HPCI shutoff due to high suppression pool pressure.

2. RCIC pump seals are generally considered marginal at elevated suppression pool temperature. Therefore, the RCIC system unreliability is evaluated as higher than normal since it is available during an ATWS event where suppression pool temperature may be above $140^{o}F$. In addition, the same logic consideration noted above for HPCI applies to RCIC.

3. During ATWS events where RCIC alone is a successful coolant makeup source, RCIC could be lost due to high containment pressure (25 psig) leading to a Class III event. RCIC loss for non-ATWS transients leads to Class IV events.

4. IORV-initiated transients during which control rods cannot be inserted have some special characteristics which make the quantitative evaluation slightly different than for other transients. The normal method of recovering from an IORV is to depressurize, but ADS should not be initiated during an ATWS. Thus, the probability that the operator will fail to inhibit ADS needs to be assessed.

Containment Heat Removal: The evaluation of adequate containment heat removal following an ATWS is strongly dependent upon the ATWS initiator. For turbine trip cases where the MSIVs remain open, it is assumed that the power conversion system is more than adequate to remove the heat from containment. However, for all other cases (i.e., MSIVs closed) it is assumed that the power conversion system is unavailable due to the inability to reopen the MSIVs in time for successful PCS operation. The two paths available for adequate containment heat removal are:

1. The RHR system

2. The containment overpressure relief system.

Successful operation of these systems is dominated by the reliability associated with correct operator action.

Appendix C

INCOR

APPENDIX C

This appendix is provided to describe the computer codes used in the evaluation of containment behavior during postulated core melt scenarios for the LGS PRA. The major points discussed are as follows:

- Overview of the INCOR Code Package (C.1)

- Description of Codes (C.2)

- Discussion of the Accident Sequences Modeled (C.3)

- Results of Each Accident Sequence Modeled (C.4).

C.1   INTRODUCTION

INCOR is a computer program for predicting containment pressure-temperature response while determining the time to core uncovery, core melt, pressure vessel meltthrough, and molten core interaction with concrete.

INCOR consists of a main code (CONTEMPT-LT) and three major sub-codes (BOIL, PVMELT, and INTER). INCOR is basically a modification of CONTEMPT-LT which now allows CONTEMPT-LT to call each of the three sub-codes if an accident meltdown sequence is being modeled and determination of core uncovery, pressure vessel meltthrough, and core-concrete interaction is desired (see Figure C.1). CONTEMPT-LT, the most recent of a seris of computer programs (CONTEMPT and CONTEMPT-PS), was developed by Idaho National Engineering Laboratory to predict the thermal-hydraulic behavior of reactor containment systems subjected to postulated accident conditions. BOIL is a computer program developed in conjunction with WASH-1400 to calculate water boiloff, reactor core uncovery, and core meltdown. PVMELT is a computer program developed by Science Applications, Inc. (Palo Alto) to predict pressure vessel meltthrough. INTER is a computer program developed by Sandia Laboratories to predict molten-core and concrete interaction.

```
┌─────────────────────┐     ┌─────────────────────┐     ┌─────────────────────┐
│        BOIL         │     │       PVMELT        │     │        INTER        │
│  CORE UNCOVERY AND  │     │  PRESSURE VESSEL    │     │   CORE-CONCRETE     │
│     MELTDOWN        │     │   MELT THROUGH      │     │    INTERACTION      │
└─────────────────────┘     └─────────────────────┘     └─────────────────────┘
```

MASS   AND   ENERGY   FLOWS

```
          ┌──────────────────────────┐
          │      CONTEMPT-LT         │
          │   HEAT TRANSFER AND      │
          │  ATMOSPHERE EXCHANGE     │
          └──────────────────────────┘
```

CONTAINMENT CONDITIONS

(REACTOR VESSEL, DRYWELL, WETWELL, MISC. COMPARTMENTS)
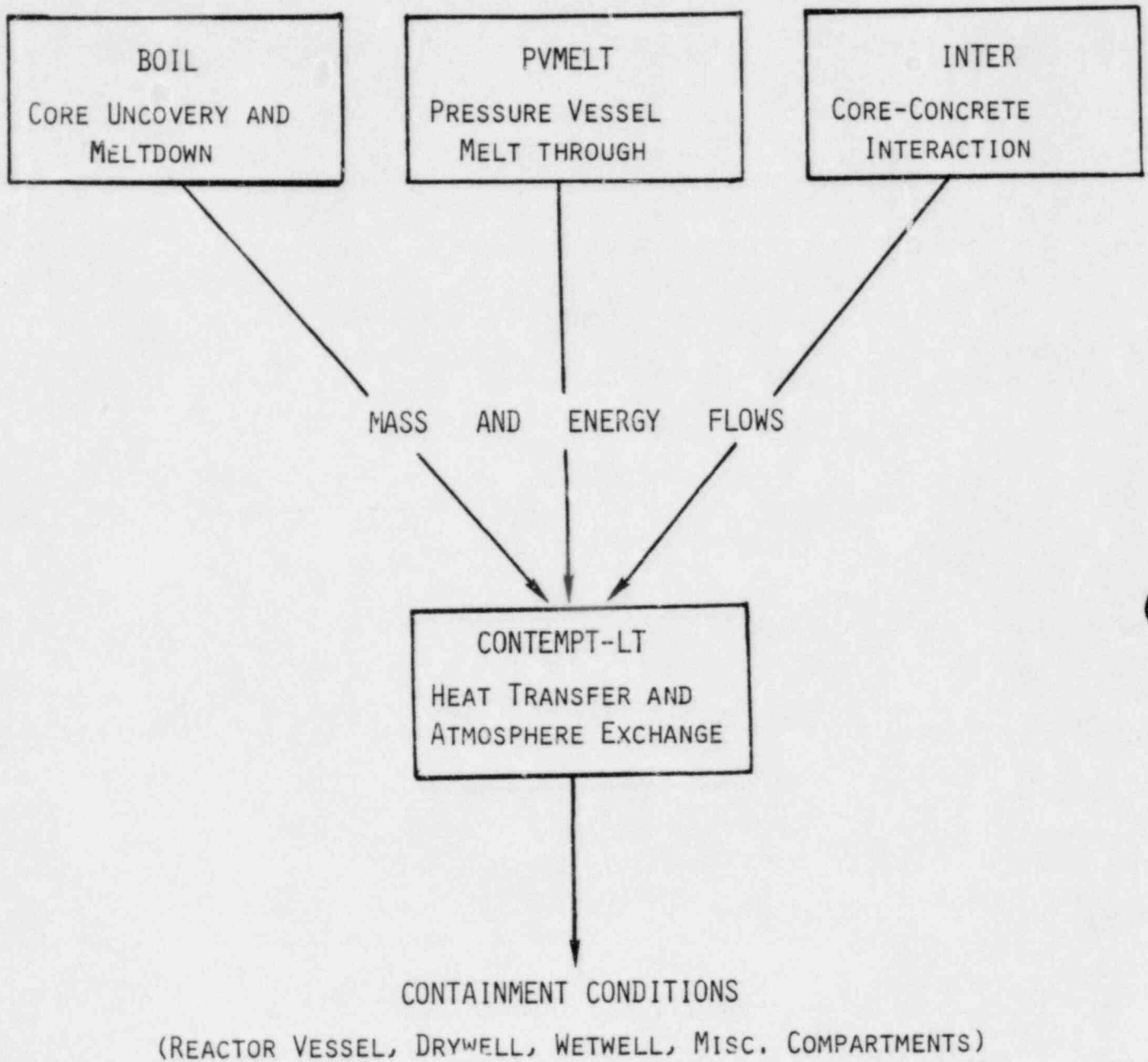
Figure C.1   Diagramatic Representation of INCOR Organization

C.2 CODE DESCRIPTION

C.2.1 CONTEMPT-LT

CONTEMPT-LT provides a numerical method for analyzing the behavior of pressurized water reactors (PWRs); boiling water reactors (BWRs) -- Mark's I, II, or III; and experimental water reactor simulators. CONTEMPT-LT predicts the interrelated effects of reactor system blowdown, heat transfer, atmosphere leakage, safeguard system operation, pressure suppression response, and miscellaneous mass and energy transfers between, and inside, various compartments. The tracking of the generation of noncondensibles (H_2, CO_2, CO, O_2, and N_2) in the various compartments is also modeled in CONTEMPT-LT.

Several generalized compartments (reactor pressure vessel -- RPV, wetwell, drywell, and an annular region) are modeled in CONTEMPT-LT. Each generalized compartment model includes a vapor region and a liquid pool region. Evaporation, condensation, and pool boiling processes are modeled. The vapor and liquid pool regions may have different temperatures and may experience heat and mass transfer. Leakage into or out of the vapor region is allowed. Heat transfer to, from, or through various structures is also provided for each region.

The drywell compartment model possesses all the features of a generalized compartment. All the mass and energy transfer processes are available to the drywell model. If a BWR pressure suppression system (PSS) is modeled, then the PSS mass and energy transfer features are also available. Also, a unique relationship exists between the RPV compartment and drywell models; an option may be selected to prevent liquid condensation fallout from the drywell vapor region during blowdown of the reactor system if a PSS is being evaluated. The condensation will be bypassed until blowdown of the reactor system has stopped and the PSS vent system flow has ceased. After these conditions are satisfied, drywell condensation proceeds normally.

The wetwell compartment model possesses all the features of a generalized compartment. Additionally, cooling sprays and associated heat exchanger models are available to the wetwell compartment. If a BWR PSS is being evaluated, then the associated mass and energy transfer processes are available to the wetwell compartment model.

The RPV (referred to as the reactor primary system compartment) possesses all the features of a generalized compartment model. Mass and energy transfer from ECCS spray operation and decay heat and metal-water reactions are modeled after blowdown of the primary system has finished. Heat transfer through wall structures between the primary system and any other compartment is allowed at any time during a problem. The exception to this is that during a blowdown no energy changes are made to the primary system until blowdown has finished. If a BWR is being modeled, a pressure setpoint for the RPV relief valves is available. This setpoint maintains the RPV at that pressure while dumping the excess steam to the liquid pool region of the wetwell.

The annular compartment model does not have all the features of a generalized compartment. Only a vapor region may exist in the compartment. The models available for mass and energy transfer with other compartments are restricted to leakage and heat structures. No engineered safeguard systems, such as fans or sprays, and no direct mass or energy additions are modeled in the annular compartment.

The output from the CONTEMPT-LT portion of the code is very extensive. The user has the option to select the printout frequency which occurs throughout the calculation (BOIL, PVMELT, and INTER). The output includes conditions in each compartment, heat structure conditions, leakages to/from each compartment, and PSS information for the drywell and wetwell compartments. Each printout reflects exclusively end-of-timestep conditions. The values are neither accumulated nor averaged between printouts. The more significant information in each category includes the following:

CONDITIONS

- Pressure (partial steam pressure in the vapor region and total pressure of compartment)

- Temperature (vapor region, liquid region)

- Energy (vapor region, liquid region, and total of compartment)

- Air mass

- Water mass (water vapor in vapor region, liquid water in vapor region, liquid water in liquid region, and total-liquid and vapor)

- Relative humidity

- Condensation rate

- Evaporation rate

- Transfer coefficients (mass and heat).

HEAT STRUCTURES

- Heat rate leaving/entering

- Heat transfer coefficients

- Thermal conductivity

- Bulk temperature

- Mesh temperatures (temperatures across heat structure).

LEAKAGES

- Leak rate

- Energy gain

- Mass losses (water vapor and air)

- Atmospheric mass losses (water vapor and air integrated over the problem time).

PRESSURE SUPPRESSION SYSTEM

- Pressure (vapor region total pressure)

- Vent clearing velocity

- Total displacement

- Mass flow rate

- Fluid exit conditions (pressure, temperature, and velocity).

C.2.2   BOIL

BOIL is the first major meltdown accident sub-code called by
the main code CONTEMPT-LT. It models core/water heat exchange by calcu-
lating water boiloff, metal/water reaction, initial core heatup, and
meltdown in the primary compartment. Level swell (water/steam mixture)
is also included. Radiation and convection heat transfer are incorporated
in BOIL. BOIL is also used to provide the mass and energy release rates
from the decay power and any metal/water reaction. The heat exchange be-
tween the reactor core and the water in the reactor system is calculated
in BOIL for the prediction of the behavior of the primary systemcompart-
ment by CONTEMPT-LT.

The approach used in the BOIL model is to divide the core into
small volumes or nodes and (1) calculate the heat produced in each node and
perform heat balances between the fuel and coolant nodes, (2) calculate the
fluid level in the core from the steam boiloff rate, and (3) perform a melt-
down calculation when the temperature of a node exceeds the melting point
of UO_2. In the process of performing these three major calculations, BOIL
does a series of calculations as follows:

HEAT TRANSFER CALCULATIONS

- Calculates the fission-product-decay heat as a function of time

- Accounts for the reduction in the heat source due to fission-
  product volatilization

- Calculates the heat produced by the zirconium-cladding/steam reaction

- Calculates convection heat transfer between the fuel rods and the steam or water coolant

- Calculates radiation heat-transfer losses from the ends of the core

- Performs heat balances on the fuel and coolant.

WATER BOILOFF CALCULATIONS

- Calculates the heat input to the water/steam region

- Calculates the steam-generation rate

- Calculates the water mass in the core

- Calculates the water level in the core

- Calculates the thermal-hydraulic response of the core to bottom-flooding (this occurs if coolant is added at a very low rate to the water at the bottom of the reactor pressure vessel).

CORE MELTDOWN CALCULATIONS

- Models core meltdown behavior

- Selects one of the following meltdown models:

  - Heat in the molten pool is transferred downward so that there is no convection to the top and sides of the pool.

  - Heat in the molten pool is transferred upward and may be transferred radially within the molten region.

  - A fuel node falls immediately to the bottom of the RPV when it melts. The fuel node is quenched in one timestep and the decay heat of the node is added to the water.

The output from BOIL is also very extensive. The printout frequency is the same as CONTEMPT-LT until fuel melting occurs, at which point BOIL output occurs every 5% of fuel melt. The more important BOIL output includes:

- Fraction of node melted in radial zone along the length of the core

- Thickness of clad reacted in radial zone along the length of the core

- Steam temperature in radial zone along the length of the core

- Fuel rods (5) temperatures in radial zone along the length of the core

- Accident time from start of calculations

- Mixture level

- Rate of decrease of mixture level

- Mass of water in core

- Total steam generation

- Steam consumed in zirconium (ZR)-water reaction

- Power produced in ZR-water reaction

- Temperature of core material in bottom head

- Fraction of fission products not lost

- Average steam temperature at top of core

- Fraction of core melted

- Core decay heat.

C.2.3   PVMELT

PVMELT, the second major sub-code called by the main code, models core/pressure vessel heat exchange. It calculates pressure vessel heatup and determines pressure vessel bottom failure by stress (creep) rupture. PVMELT initially considers that the core support plate fails

C-8

rapidly over a central section and that the molten core appears in the lower head simultaneously with completion of core melt. The model also includes a physical representation for the water displaced by the molten debris and a film boiling process occurring at the molten debris-water interface. It does not assume any fragmentation of the molten core so that there is no intimate contact of the molten debris with the water. The water in the bottom head is displaced to the top of the molten core and is boiled off. The metal/water reaction and consequent hydrogen production is not modeled in this sub-code.

The PVMELT model assumes that conduction dominates the transfer of decay to debris/water and debris/wall interfaces and that constant thermo-physical properties exist. The heat transfer calculations are performed through a one-dimensional transient analysis at the RPV center-line and as a lumped parameter analysis for the vessel insulation. The PVMELT model assumes that the molten steel is promptly transferred to the upper surface of the molten debris layer and that thermal resistance of the transferred steel is negligible.

PVMELT is called by CONTEMPT-LT when BOIL has calculated (80%) core melt. This assumption is the same as was used in WASH-1400. The molten core appears at the bottom of the RPV simultaneously with the 80% core melt. Once PVMELT has calculated RPV failure, the primary system compartment disappears with its releases being incorporated into the drywell compartment.

PVMELT printout frequency is specified by CONTEMPT-LT with output as follows:

- Normalized wall thickness of RPV head

- Water overburden thickness

- Applied stress

- Yield stress.

C-9

C.2.4   INTER

INTER, the last of the major sub-codes called by CONTEMPT-LT, models core-concrete interactions by calculating the rate of penetration of concrete by a molten LWR core, and simultaneous generation of gases.

INTER assumes convective stirring of the melt by evolved gases, admixture of concrete decomposition products to the melt, chemical reactions, radiative heat losses, and variation of heat transfer coefficients with local pressure. INTER models the molten core as a two-phase melt (metallic and oxidic). Each layer is considered to be well-mixed and isothermal in its interior as long as the layer is molten. Heat transfer from layer to layer takes place across a boundary layer or film whose thickness varies with the violence of mixing. The two main layers are assumed to be in intimate contact with each other (there can be a vapor layer at the interface with the decomposing concrete). The thickness of the boundary layer can be different for each main layer; however, in each layer, it is uniform around the periphery of the layer. Heat is radiated to the containment, conducted into the concrete, and interchanged between the layers.

INTER models the molten core as a hemispherical segment intersected by a cylinder with geometry changes as the problem advances by material interchange between the layers. Iron oxides created by reaction of the steam with iron in the metallic part of the melt are assumed to be rapidly incorporated into the oxide layer. Solid or liquid decomposition products are assumed always to go promptly to the appropriate melt layer. However, gaseous products will not pass through the melt if the interface with the concrete is vertial.

INTER also assumes gas-induced insulation cells (Figure C.2). In a normal cell, more gas passes through the outside of the melt and circulation follows as shown in Figure C.2(a). However, if the lower layer is hotter than the upper layer, more gas flows through the center and the circulation direction can be reversed. A circulation cell will be modeled if the material is molten and there is appreciable gas flow. The intensity
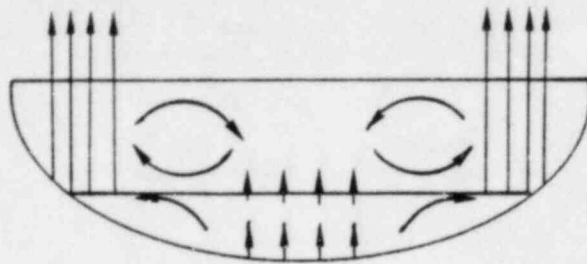
(a) Normal Cells
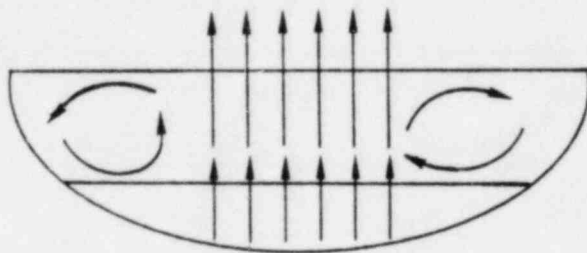
(b) Reversed Cells

(c) Bottom Layer Frozen

(d) Top Layer Frozen

Figure C.2 Gas-Induced Circulation Cells

of the circulation (hence the thickness of the boundary layer) depends on the rate of gas flows. Melt viscosity and gas flow path can also influence boundary layer thickness but are not molded in INTER.

Contact with free water is allowed either initially, when the molten core first drops onto the concrete, or whenever the radial growth exceeds a predetermined amount. INTER assumes that the initial water is instantly vaporized. The sensible heat of the melt is reduced and new temperatures are computed. Water contacting the melt later is assumed to boil off quiescently. Even though INTER was not originally written for Mark II, it can be used effectively to calculate some of the physical processes occurring following reactor vessel meltthrough and the molten core interaction with the diaphragm floor present in the Mark II containment. INTER does not treat corium drop into the suppression pool. This portion must be hand calculated.

The output from INTER is also very extensive. Its printout frequency is determined internal to the code and is a function of the timestep. INTER determines its own timestep, calculating it as large as possible without creating a mass-energy balance failure. The more significant output includes:

- Metal and oxide conditions

- Penetration depth

- Concrete decomposition rate

- Surface temperature

- Gases added to atmosphere (rate, mass, and heat).

C.3   INCOR MODELS (SEQUENCES)

INCOR was used to model four separate sequences to provide the timing, pressures, and temperatures inside containment for key accident

sequences. Since each sequence has major assumptions, the results are only used as a guideline for the calculations performed for the radio-activity release from containment (see Appendix D).

C.3.1   Loss of Coolant Makeup to the Reactor - TQUV (Core Melt--RPV Failure--Concrete Meltthrough Prior to Containment Failure)

A postulated accident sequence involving the loss of all coolant makeup capability to the reactor following a scram from 100% power (TQUV) is calculated using the INCOR code package. TQUV starts with the reactor at 100% power. Simultaneously with initiation of the transient, it is assumed that ECCS is lost, feedwater to the RPV is lost, and the MSIVs are closed. The reactor core power follows a decay power curve (C.1). The RPV is assumed to be at high pressure and maintained below a certain pressure (low setpoint of relief valves) by relieving through relief valves to the wetwell. There is an alternate scenario which would leave the reactor at low pressure prior to reactor vessel meltthrough. The containment (drywell and wetwell) is assumed to be intact and the conditions inside the various compartments to be at normal operating conditions at the start of the calculations. Normal seepage from containment to the reactor building is modeled. The molten core from the ruptured RPV is modeled to (1) drop on the diaphragm floor, interacting only with the concrete inside the pedestal or (2) drop on the diaphragm floor and flow through the doorway to interact with the concrete of the entire floor. (See Table C.1 for inputs.)

C.3.2   Containment Heat Removal Fails - TW* (Containment Failure Precedes Core Melt--RPV Failure--Concrete Meltthrough)

The second type of sequence analyzed is a transient with the loss of residual heat removal (RHR). In this sequence, the phenomen-ology begins with the containment in a failed state. This containment failure is calculated to have occurred approximately thirty hours following a scram from high power due to the inability to remove decay

---

*TW here implies an accident sequence involving containment failure due to
(continued on following page)

heat from containment. The core power at the start of the calculations is determined from the decay power curve at thirty hours and then proceeds to follow the curve. It is assumed that the MSIVs are closed and feedwater to the RPV is lost at shutdown. The RPV pressure is assumed to be brought down to a low pressure (below shutoff of LPCI) and maintained below that pressure by relieving to the wetwell (during and after containment failure). The conditions inside the drywell and wetwell are assumed to be failure conditions at the start of the calculations. The reactor building conditions are assumed to be normal operation conditions. Prior to the start of the INCOR calculations, it is assumed that the RPV coolant inventory is maintained by ECCS coolant injection from the suppression pool. At containment failure (thirty hours), the ECCS is assumed to be lost** and makeup is modeled. The code calculates the transient from containment-failed conditions until it reaches a state of equilibrium with the conditions in reactor building. The Standby Gas Treatment System (SGTS) and normal seepage from the reactor building to the outside are modeled. The molten core from the ruptured RPV is modeled to drop on the diaphragm floor, flow through the doorway, and interact with the concrete of the entire floor.

C.3.3   Failure of Coolant Inventory Makeup Following an ATWS
         (Anticipated Transient Without Scram - Case 1)

The third type of event sequence calculated using the INCOR package is an ATWS with loss of coolant injection prior to containment failure. The specific scenario chosen includes the following assumptions:

•   The ATWS sequence commences with the reactor at 100% power.

---

*(continued from previous page)
lack of heat removal from containment. The TW terminology is borrowed from WASH-1400; however, in the Limerick analysis TW does not lead directly to core melt but requires additional failures (see Sections 3-4). In any case the containment calculations here are valid for the discussed sequences which do lead to failure.
**This assumption was also made in WASH-1400. It is discussed in detail in Section 3.4.

- The MSIVs are assumed closed and feedwater to the RPV is lost.

- In addition to the failure of the control rods to insert, the liquid poison injection system is also postulated to fail for the purposes of this sequence calculation.

- HPCI is modeled to turn on at lot RPV water level and turn off permanently on high pressure turbine exhaust. This is as designed and, therefore, is a high probability occurrence.

- The RPV is assumed to be at high pressure and maintained below a certain pressure (high setpoint of the relief valves) by relieving to the wetwell.

- The containment is assumed to be intact and conditions in the various compartments to be normal operating conditions at the start of the calculations.

- Normal leakage from the containment to the reactor building is modeled.

The code has been modified in this sequence to track the water level in the RPV. The code considers that the part of the core which is covered is at 30% power while the exposed core follows the decay power curve. The core melt occurs due to loss of coolant inventory. The molten core from the ruptured RPV is modeled in two ways: (1) drop on the diaphragm floor, interacting only with concrete inside the pedestal; or, (2) drop on the diaphragm floor and flow through the doorway to interact with concrete of the entire floor. (See Table C.1 for inputs).

C.3.4   Failure of Coolant Inventory Makeup Following an ATWS with Containment Failure Prior to Core Melt (Anticipated Transient without Scram - Case 2)

The last type of sequence calculated using the INCOR package is an ATWS without adequate containment heat removal which leads to containment overpressure failure prior to core melt, referred to as a Class IV accident sequence.

The assumptions in the sequence are similar to the third sequence with the following exceptions: HPCI is allowed to stay on even after the high exhaust pressure is reached for the HPCI turbine. The pressure in containment increases until failure pressure is reached. It is assumed that at containment failure, HPCI fails. Therefore, containment failure occurs prior to Core Melt, RPV Meltthrough, and Core/Concrete Interaction for this ATWS case.

The code has also been modified in this sequence to track the water level so that the part of the core which is covered is at 30% power while the exposed portion follows the decay power curve. The core melts due to loss of coolant inventory and eventually melts the RPV to drop onto the diaphragm floor. The molten core is only modeled to drop onto the diaphragm floor and flow through the doorway to interact with the entire floor. (See Table C.1 for inputs).

C.4   INCOR RESULTS: OVERVIEW OF PRESSURES AND TEMPERATURES
        CALCULATED TO OCCUR WITHIN CONTAINMENT FOLLOWING CORE
        MELT SCENARIOS

INCOR results are only used to calculate the containment conditions, which are then used for the radionuclide release fraction calculations. In the cases where INCOR did not perform the calculations out to diaphragm floor failure, some extrapolations using simplified models were done to predict: (1) the pressure in containment by estimating the steam pressure and the pressure due to the gases produced from the melting concrete; and (2) the time of floor failure by comparing the penetration rate and decomposition rate from various INCOR runs.

C.4.1   Containment Pressure Temperature Response During Postulated
          Core Melt

The RPV pressure for each sequence oscillates as shown in Figure C.7. This pressure oscillation is around the SRV setpoint. The size of the oscillation is dependent on the timestep used in the calculation and

the number of SRVs. A larger timestep or a larger number of SRVs depletes a greater amount of steam from the RPV, resulting in a larger calculated pressure reduction. Also, as the accident progresses, the steam generation rate for each sequence decreases with time since the core power is decreasing. For some sequences, the calculated steam volume is drastically reduced in a timestep so that the steam generated in later timesteps is not enough to make up the depleted volume and the total pressure decreases. Once enough steam is generated to overcome this calculated depletion, the pressure starts to increase until the SRV setpoint is reached. This phenomena also occurs during core melting. However, the pressure in this case decreases until the molten core drops to the bottom of the reactor vessel where film boiling (steam generation) of the water occurs and the pressure then starts to increase once again.

The steam relieved from the RPV is dumped into the suppression pool. In each sequence, the pool is subcooled. The containment pressure increase is very slow until saturation is reached at which point evaporation starts to occur and drives the pressure at a faster rate. The time at which saturation is reached is dependent upon the amount of flow through the SRVs from the RPV. Those sequences which have a larger number of SRVs actuated, ATWS with HPCI unavailable and ATWS with containment failure, produce a much greater steam flow to the wetwell pool and saturation is reached very quickly (see Figures C.12 and C.15). Also, for these two ATWS sequences, makeup water (HPCI) is continually added to the RPV during a portion of the sequence. The HPCI eventually becomes unavailable in both ATWS sequences due to high exhaust turbine pressure trip or containment failure at which point the water boils off in a relatively short time and the core reaches its melting temperature. Since the core is totally uncovered, the steam generation rate is very slight and is insufficient to overcome the depletion resulting in total pressure decrease. During this time there is no SRV flow and the pressure and temperature in the wetwell remains fairly constant. However, for the TQUV sequence, core melt is initiated soon after containment isolation and the total steam generation to the wetwell pool is smaller than in the ATWS sequences and

saturation is not reached prior to the RPV rupture; therefore, the pressure rise is very slight (see Figures C.8 and C.9). In the TW sequence the pressure rises slightly until saturation is reached and then increases rapidly (see Figures C.10 and C.11).

C.4.2 Containment Pressure and Temperature Response During Reactor Pressure Vessel Failure Phase

The PVMELT module of INCOR calculates RPV failure by creep rupture failure of the bottom head of the vessel.* This type of rupture can create a large pressure spike in containment. However, it has also been postulated** that the molten core preferentially melts through the BWR control rod penetrations in the RPV bottom head creating small holes and therefore slowly reducing the pressure in the reactor system during RPV melt, so that at failure there is no large pressure spike in containment. The second assumption is used in the LGS analysis to determine the pressure rise in containment since it appears more appropriate for BWR reactor vessel designs.

C.4.3 Containment Pressure-Temperature Response During the Phase of Corium-Concrete Interaction

The next calculational phase involves the time once the molten core has failed the RPV and dropped onto the diaphragm floor in the pedestal region directly below the RPV. In this phase, which includes the corium-concrete interaction and the reaction by-products, the conditions of the core following RPV failure are fairly similar for the sequences considered in the LGS analysis. Therefore, the evaluation of the concrete-corium interaction is performed with INCOR and used for each class of accident sequence. There are two bounding cases which have been run to establish the range of potential uncertainty during this phase of the INCOR calculation.

The pedestal wall surrounding the RPV has a doorway flush with the diaphragm floor. It is uncertain whether the molten core will: (1) case 1:

---

*Applicable primarily to PWRs which have few penetrations of the bottom head.
**Appendix H discusses the more likely mode of RPV failure for BWRs.

stay inside the pedestal region; or, (2) case 2: flow through the doorway and spread across the floor outside the pedestal. Both cases are analyzed. It is assumed that the diaphragm floor will fail structurally at approximately 70 cm or two thirds of floor penetration (before the molten core melts through the floor).

The molten core interacting with the diaphragm floor inside the pedestal (Case 1) versus the entire diaphragm floor (Case 2) produces different concrete penetration, concrete decomposition, and non-condensible concrete generation rates, thus affecting the pressure-temperature conditions inside containment.

At RPV rupture, molten core conditions for Case 2 in each of these sequences are similar. It is therefore assumed that the INTER calculations for the ATWS sequence with containment failed are applicable for the TQUV and ATWS (with HPCI Failure) Case 2 sequences. Therefore, one INCOR calculation of the time to diaphragm floor failure is used to characterize the following Case 2 sequences:

- ATWS - with containment failure occurring prior to core melt initiation (Class IV)

- ATWS - with HPCI unavailable during the sequence and with containment intact (Class III)

- TQUV - with loss of coolant inventory and core melt initiation with containment in tact.

The INCOR results of the corium-concrete interaction phase are exemplified in Figures C.14 to C.16. One assumption made in these analyses which differs from that used in the REACT/CORRAL calculation for radionuclide release is that in the CORRAL calculations ten percent of the core is taken to directly interact with the suppression pool leading to an oxidation release*. However, the INCOR calculations do not include the pressure rise due to the steam generation from the ten percent steam-core interaction.

---

*The possibility of a coherent steam explosion which would lead to immediate containment failure is considered unlikely and is treated separately in the release fraction calculation discussed in Appendix D.

It should also be noted that the amount of hydrogen generated during a
postulated core melt scenario is an area of uncertainty. The INCOR hy-
drogen production model (during BOIL and INTER, see Section C.2.3) is
similar to that used in WASH-1400 and may tend to underpredict hydrogen
production during such sequences. The pressure and temperature curves
for each sequence consider neither RPV pressure relief during RPV melt
nor steam explosion after RPV rupture. The large temperature rise seen
on the graph is caused by the dumping of the mass and heat from the
reactor system into the drywell.

The drywell conditions for each sequence (Figures C.3 - C.6)
parallel those in the wetwell (for example, see Figures C.4, C.10, and
C.11). As the pressure builds up inside the wetwell, it is relieved to
the drywell through vacuum breakers once a specified pressure differential
is reached. Therefore, a pressure increase in the wetwell causes a pres-
sure (and temperature) increase in the drywell. Upon RPV rupture, dry-
well conditions are no longer determined by the wetwell. (The uncertain-
ties, assumptions and considerations mentioned previously are also appli-
cable to the drywell.) The molten core/concrete interaction now exerts
the greater influence on containment conditions. The rate of concrete
decomposition/penetration and the surface area over which the molten
core is acting mainly determines the amount of non-condensibles generated.
These gases control the pressure during this period of the analysis. As
the core penetrates the diaphragm floor, it cools and its rate of decom-
position and penetration decreases, thereby decreasing the production of
gases until the pressure inside containment becomes fairly stable (as
demonstrated in Figures C.14 - C.16).

C.4.4   Summary of Individual Sequence Results

Using the assumptions and methodology described in sections C.4.1 through
C.4.3, the results of the individual accident sequences are summarized in the
the following sections.

C-20

C.4.4.1   TQUV (Core Melt--RPV Failure--Concrete Meltthrough Prior
           to Postulated Containment Failure)

TQUV analyzed by INCOR basically denotes an accident sequence
in which there is no makeup water to the RPV causing the core to become
uncovered. The core is calculated by INCOR to begin melting approximately
1.3 hours after shutdown and reaching 80% core melt at approximately 2.5
hours after which the molten core drops to the bottom of the RPV failing
it at around 4.3 hours. By use of INCOR and appropriate extrapolation,
it was estimated that a 70 cm penetration would occur at 6 hours for
Case 1 and 6.5 hours for Case 2.

C.4.4.2   TW (Containment Failure Precedes Core Melt--RPV Failure--
           Concrete Meltthrough)

TW analyzed by INCOR basically denotes an accident sequence in
which the containment fails (approximately 30 hours after shutdown) causing
loss of makeup water to the RPV (at low pressure), thus uncovering the core.
The core is calculated by INCOR to begin melting around 36.6 hours and end-
ing around 39 hours after which the molten core drops to the bottom of the
RPV, failing it at around 40.8 hours. INCOR calculated a penetration of
70 cm at around 43.3 hours, approximately 7 hours following core melt
initiation.

C.4.4.3   ATWS (with HPCI Unavailable)

HPCI initiates automatically then trips off due to high suppression
pool pressure causing the core to become uncovered. INCOR calculates core
melting to begin approximately .85 hours from initiation of the accident and
ending around 2.5 hours, after which the molten core fails the RPV at approxi-
mately 4.3 hours. INCOR calculated diaphragm floor failure at approximately
6 hours for Case 1. It was estimated that a 70 cm penetration would occur
at approximately 6.5 hours for Case 2.

C.4.4.4   ATWS (Containment Failure)

ATWS (Containment Failure) analyzed by INCOR basically denotes an accident with failure to insert the control rods and failure of the standby liquid control system. HPCI does not trip off, thereby leading to rapid containment overpressure. At containment failure, calculated to be at approximately 40 min., HPCI is assumed to fail. INCOR calculates core melting to begin approximately 1.2 hours from initiation of the accident and to end at around 2.2 hours, after which the molten core fails the RPV at approximately 4 hours. INCOR calculated diaphragm floor failure at approximately 6.5 hours (Case 2 only).

REFERENCE

C.1   "ANS Decay Power Curve", <u>Nuclear Safety</u>, Volume 18, No. 5
        Figure 14, September - October 1977.

TABLE C.1

SIGNIFICANT INCOR INPUTS

ANALYSIS ITEM	VALUES	
Compartment Description Cards		
Total compartment volume (ft^3)		
RPV	21195.	
Wetwell	2.80E5	
Drywell	2.484E5	
Rx Building	2.0E6	
Volume of liquid pool (ft^3)		
RPV	11770.9	
Wetwell	1.186E5	(1)
Drywell	0.	
Rx Building	0.	
Temperature of vapor region (^{0}F)		
RPV	545.	(2)
Wetwell	95.	(2)
Drywell	150.	(2)
Rx Building	90.	(2)
Temperature of liquid pool region (^{0}F)		
RPV	545.	(2)
Wetwell	95.	(2)
Drywell	150.	(2)
Rx Building	90.	(2)
Total compartment absolute pressure (psia)		
RPV	1020.	(3)
Wetwell	15.45	(3)
Drywell	15.45	(3)
Rx Building	14.624	(3)
Relative humidity of vapor region (%)		
RPV	100	
Wetwell	100	
Drywell	20	(4)
Rx Building	45	
Horizontal cross-sectional area of compartment (ft^2)		
RPV	0.	
Wetwell	5.7E3	
Drywell	5266.	
Rx Building	0.	

ANALYSIS ITEM	VALUES	
Penetration Leakage Specification Cards		
Relief Valves(5)		
Identification number of compartment that leakage is into	2	
Area of throat for leakage calculation(ft^2)	.5732	(6)
Ratio of throat area to exit area	0.0	
Ratio of throat area to inlet area	1.0	
Constant multiplier for leakage calculation	1.0	
Drywell		
Identification number of compartment that leakage is into	5	
Area of throat for leakage calculation(ft^2)	.208(7)	
Ratio of throat area to exit area	0.0	
Ratio of throat area to inlet area	1.0	
Constant multiplier for leakage calculation	1.0	
Rx Building		
Identification number of compartment that leakage is into	0	
Area of throat for leakage calculation(ft^2)	.429(8) 81.0	(9)
Ratio of throat area to exit area	0.0	
Ratio of throat area to inlet area	1.0	
Constant multiplier for leakage calculation	1.0	
Vertical Vent (Mark I and Mark II) Pressure Suppression System		
System Control Card		
Number of downcomers in normal vent system	87	
Ratio of fraction of liquid water entering normal vent system to fraction of liquid water in drywell atmosphere region	.5	
Convergence criterion for vent flow	0.1	
Miscellaneous Vent Data Card		
Vent submergence (ft)	10	(10)
Absolute roughness of inside wall of vent exit pipe (ft)	1.5E-4	
Irreversible energy loss coefficient for incompressible single-phase flow	2.5	
Inside diameter of vent opening (ft)	1.9375	

TABLE C.1 (continued)

ANALYSIS ITEMS	VALUES	
Vacuum Relief System Card		
Pressure difference (lb_f/in^2) at which vacuum breakers between wetwell and drywell open	1.75	
k_{vr}, single-phase irreversible loss coefficient for vacuum relief system	5.7	(11)
A, flow area of one vacuum breaker (ft^2)	2.05	
N_{vr}, number of vacuum breakers in system	4	
Reactor Vessel and Core Description Card		
Decay Power and Time Definition Card		
Initial core power level (BTU/hr)	1.124E10	
Time from shutdown to start of calculations (sec)	0.0	(12)
Reactor Core Physical Description Card		
Active fuel height (ft)	12.5	
Fuel Rod Diameter (ft)	4.025E-2	
Pellet diameter (ft)	3.417E-2	
Core diameter (ft)	16.70	
Thickness of Zircalloy cladding (ft)	2.667E-3	
Fuel rod volumetric heat capacity ($Btu/ft^3/^0F$)	54.2	
Flow channel hydraulic diameter (ft)	3.70E-1	
Flow area in core (ft^2)	84.0	
Flow area in vessel (ft^2)	154.0	
Reactor Hardware Description Card		
Radiation interchange factor between top or core and heat sink above	.445	
Environment Parameters Card		
Initial zirconium oxide thickness (ft)	3.28E-6	
Melting temperature of fuel plus temperature equivalent of heat of fusion (^0F)	6.343E3	
Melting temperature of fuel (^0F)	5080.	
Reactor Pressure Vessel Description Card		

ANALYSIS ITEMS	VALUES	
Initial thickness of pressure vessel bottom head (ft)	.7083	
Thermal conductivity of RPV bottom head material ($Btu/hr-ft-^0F$)	18.0	
Density of bottom head material (lbm/ft^3)	460.0	
Specific heat ($Btu/lbm-^0F$)	0.15	
Latent head of fusion (Btu/lbm)	118.0	
Fuel Properties Card		
Initial thickness of molten fuel layer (ft)	4.4	
Thermal conductivity ($Btu/hr-ft-^0F$)	1.5	
Density (lbm/ft^3)	550.	
Specific heat ($Btu/lbm-^0F$)	.123	
Emissivity of molten layer	.8	
Reference Temperatures (^0F) Card		
Melting point for steel	2605.	
Failure point for insulation	3040.	
Concrete Properties Card		
Concrete thermal conductivity ($J/sec/cm/^0K$)	.0182	
Concrete specific heat ($J/gm/^0K$)	.6525	
Concrete density (gm/cm^3)	2.405	
Mass fraction of $CaCO3$	.5071	
Mass fraction of $Ca(OH)_2$	.0867	
Mass fraction of SiO_2	.3777	
Mass fraction of free H_2O in concrete	.0285	
Rebar to concrete mass ratio	.164	
Interface Heat Transfer Coefficient Card		
Metal/concrete heat transfer coefficient($j/sec/cm^2/^0K$)	.009	
Oxide/concrete heat transfer coefficient ($J/sec/cm^2/^0K$)	.050	
Materials Initial Temperature Card		
Concrete temperature (^0K)	422.	
Oxide layer temperature (^0K)	3130.	(13)
Metal layer temperature (^0K)	2560.	(13)

NOTES TO TABLE C.1

(1) TQUV and ATWS only; volume of liquid pool is 1.308E5 ft^3 for TW.

(2) TQUV and ATWS only; RPV temperature is 431.75°F, wetwell temperature is 365°F, and drywell temperature os 363°F for TW.

(3) TQUV and ATWS only; RPV pressure is 351 psia, wetwell pressure is 165 psia, and drywell pressure is 160 psia for TW.

(4) TQUV and ATWS only; drywell Ø is 100% for TW.

(5) Models flow through the SRVs.

(6) TQUV and TW only (models 4 SRVs); throat area is 2.0062 ft^2 fot ATWS (models 14 SRVs).

(7) TW only; models break in containment (drywell). For ATWS with containment failure prior to core melt, break size of 3.14 ft^2.

(8) TW only; models normal seepage from Rx Building to outside.

(9) ATWS with containment failure prior to core melt; models break in Rx building (blowout panels).

(10) TQUV and ATWS only; vent submergence is 12.25 ft for TW.

(11) ATWS and TQUV only; loss coefficient is 1.5 for TW.

(12) ATWS and TQUV only; time from shutdown to start of calculations is 1.08E5 sec (30 hours) for TW.

(13) TQUV, TW, and ATWS sequences for molten core over entire diaphragm floor; for sequences with molten core in pedestal, initial oxide layer temperature is 3630°K and initial netal layer temperature is 3060°K.
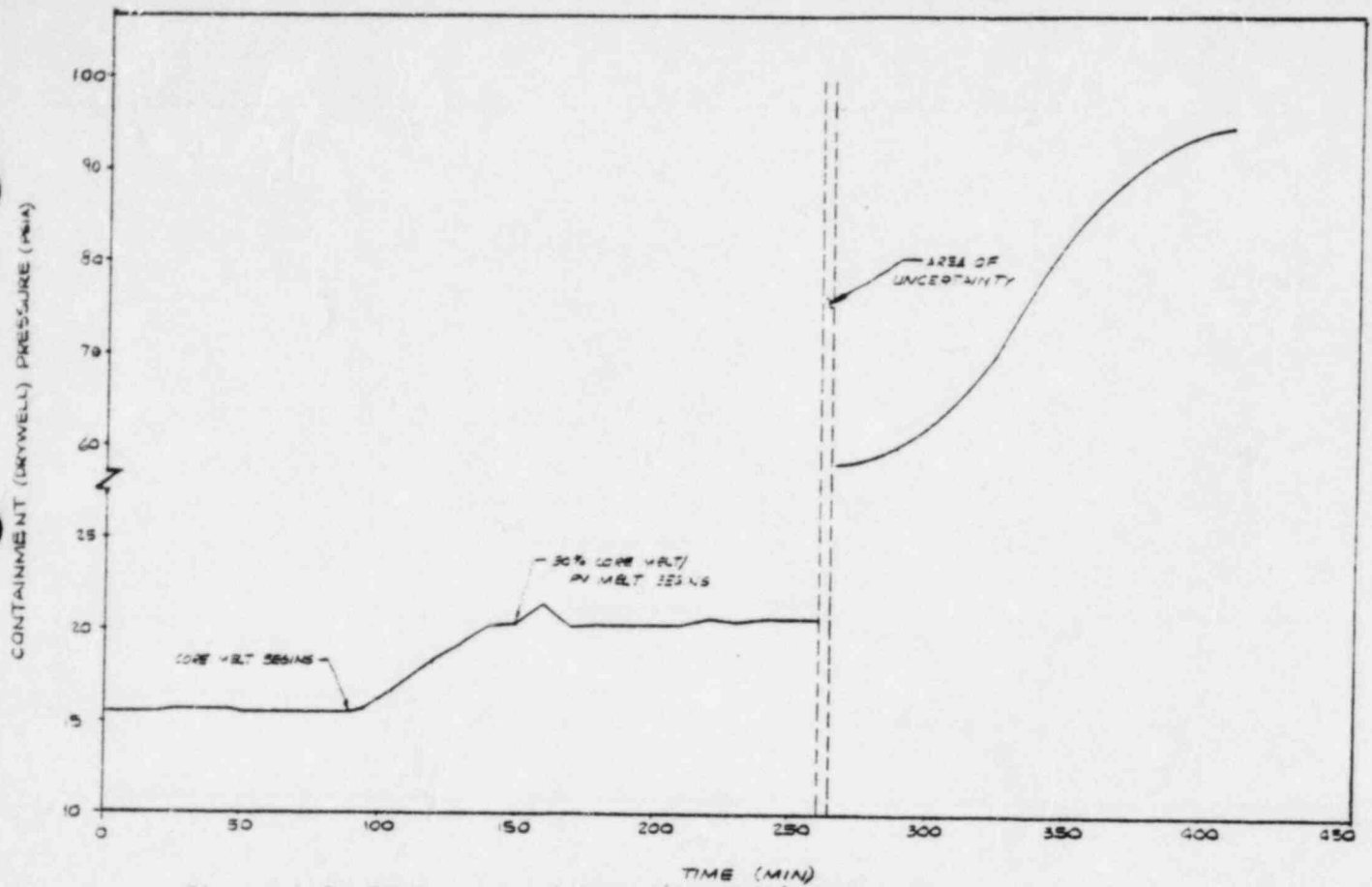
Figure C.3 TQUV - Containment (Drywell) Pressure
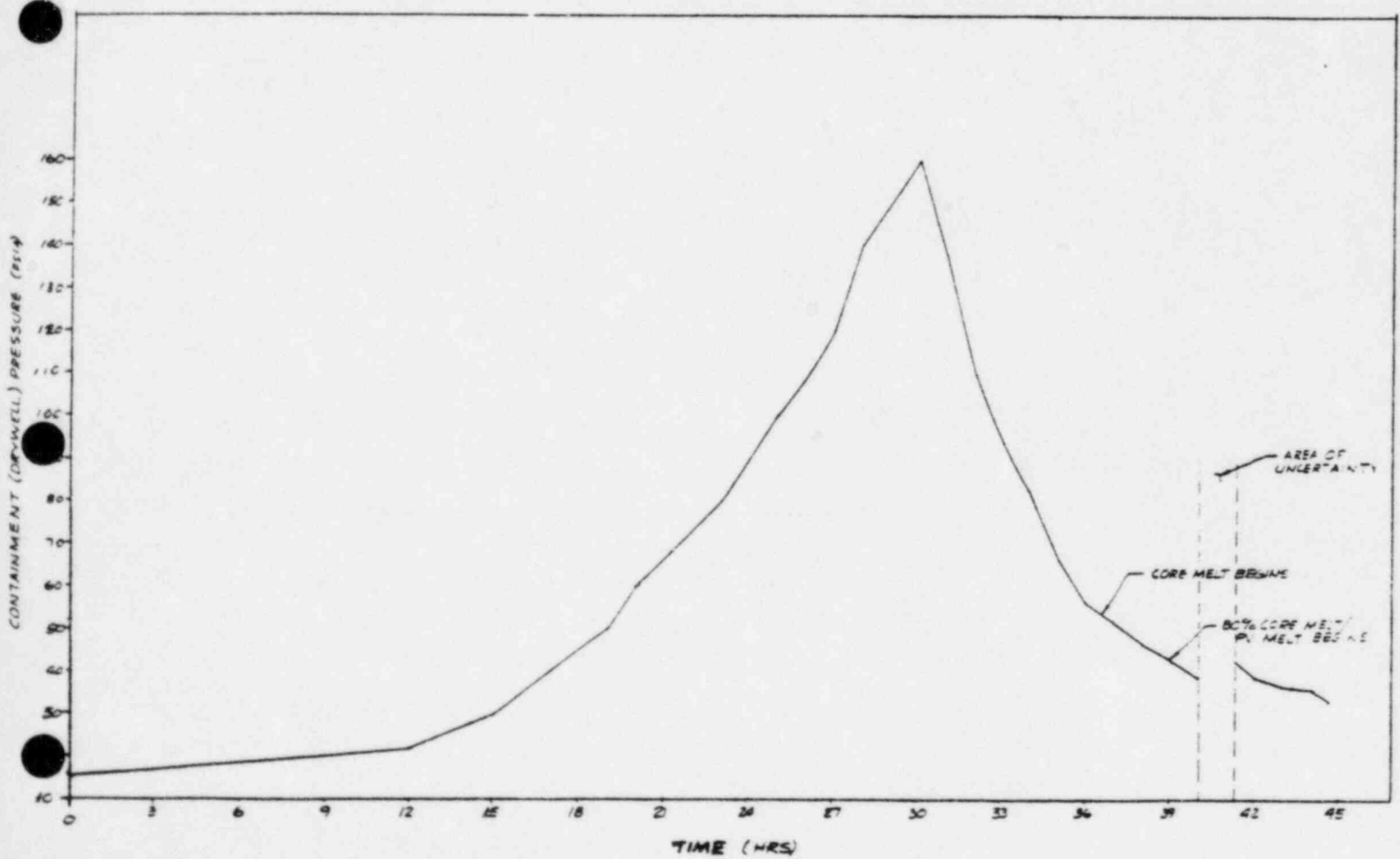
Figure C.4 - TW - Containment (Drywell) Pressure
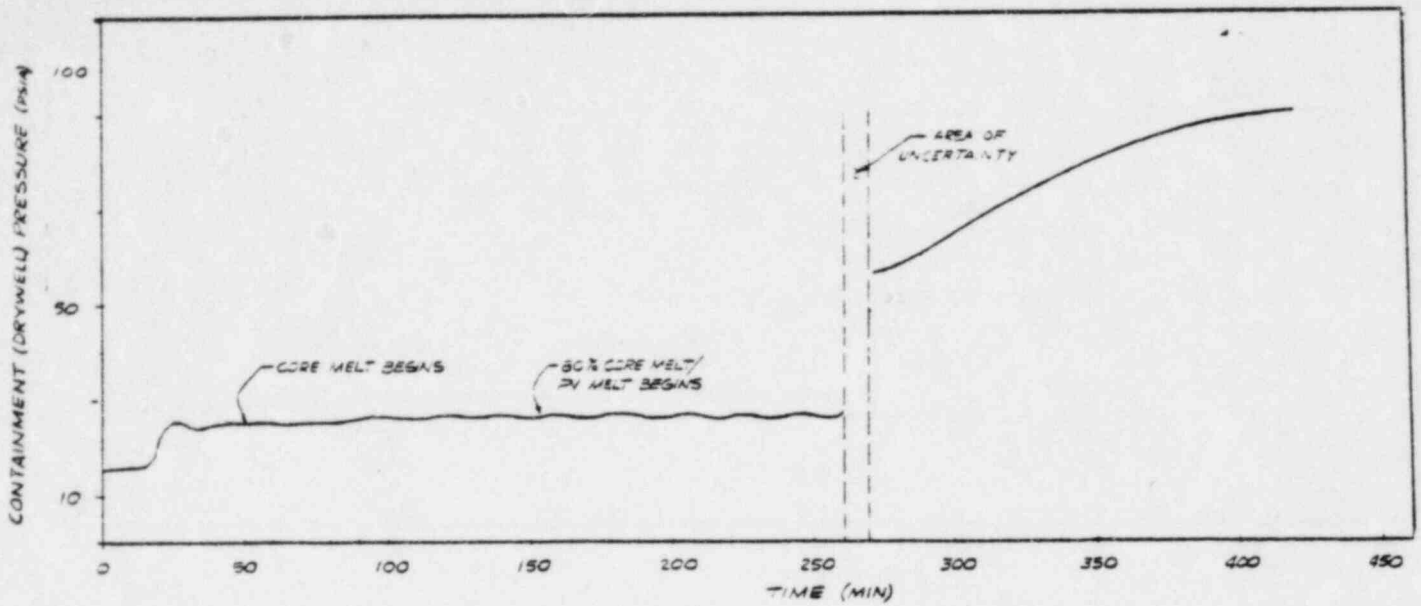
Figure C.5 ATWS (HPCI Failure) - Containment (Drywell) Pressure
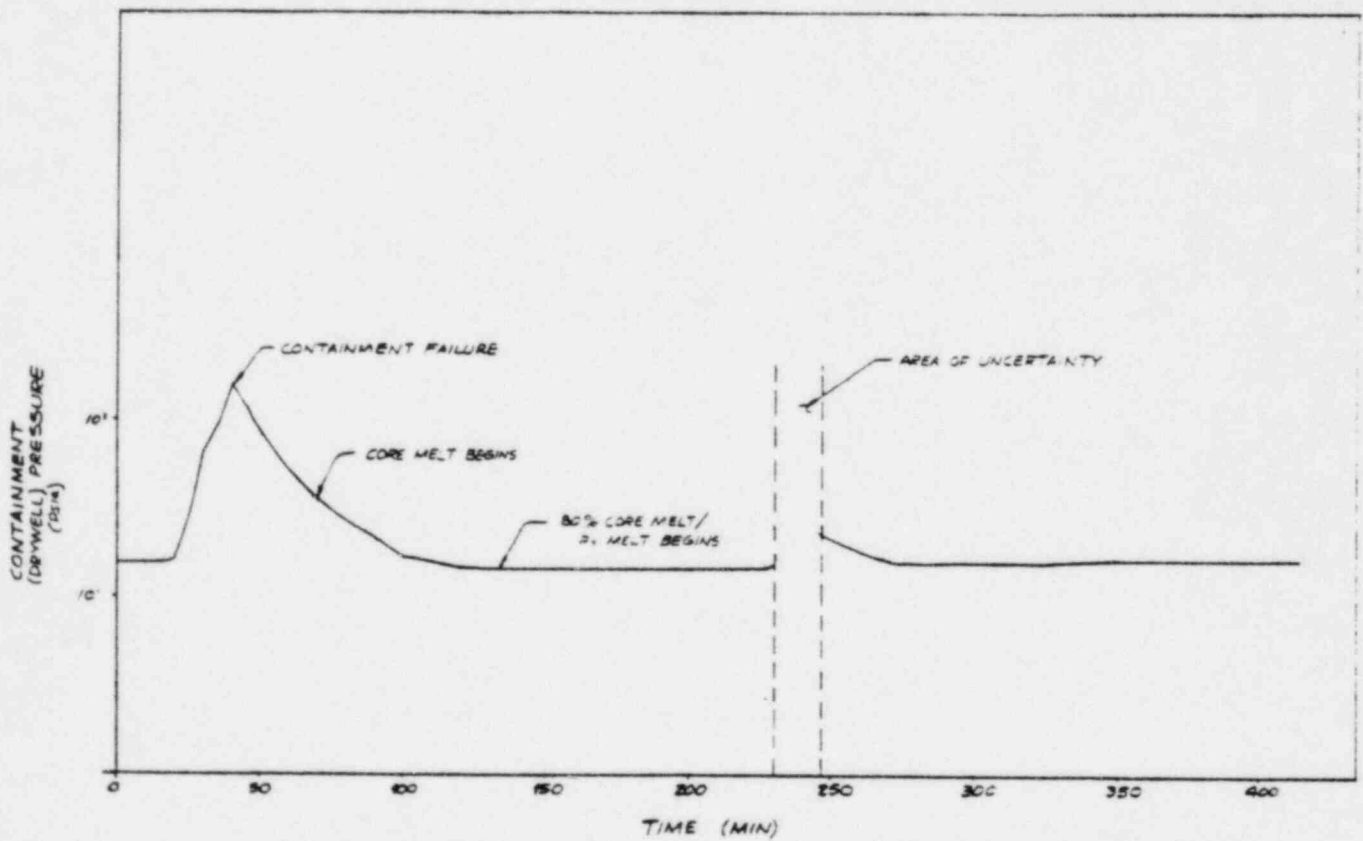
Figure C.6 ATWS (Containment Failure) - Containment (Drywell) Pressure
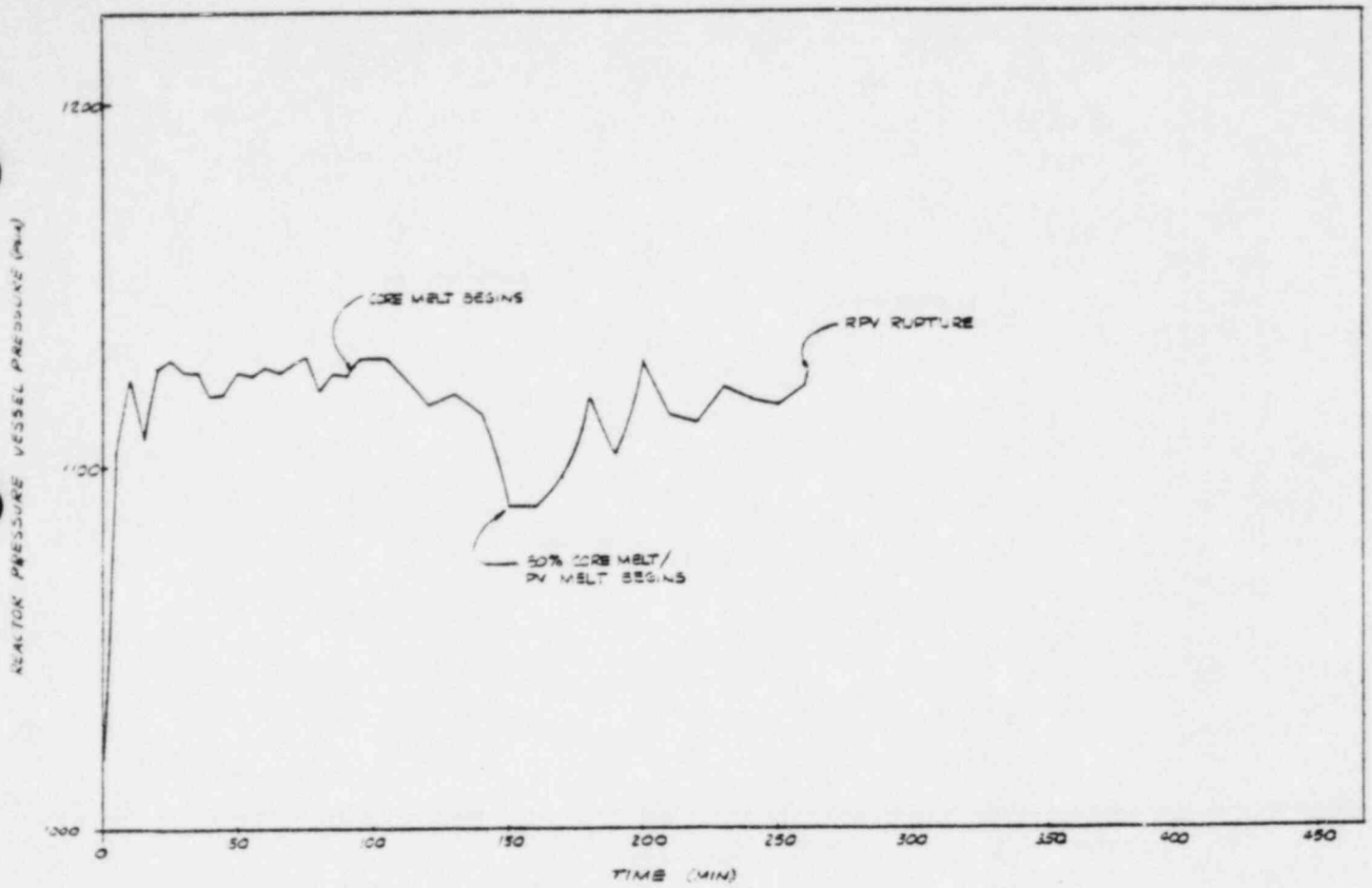
Figure C.7 TQUV - RPV Pressure
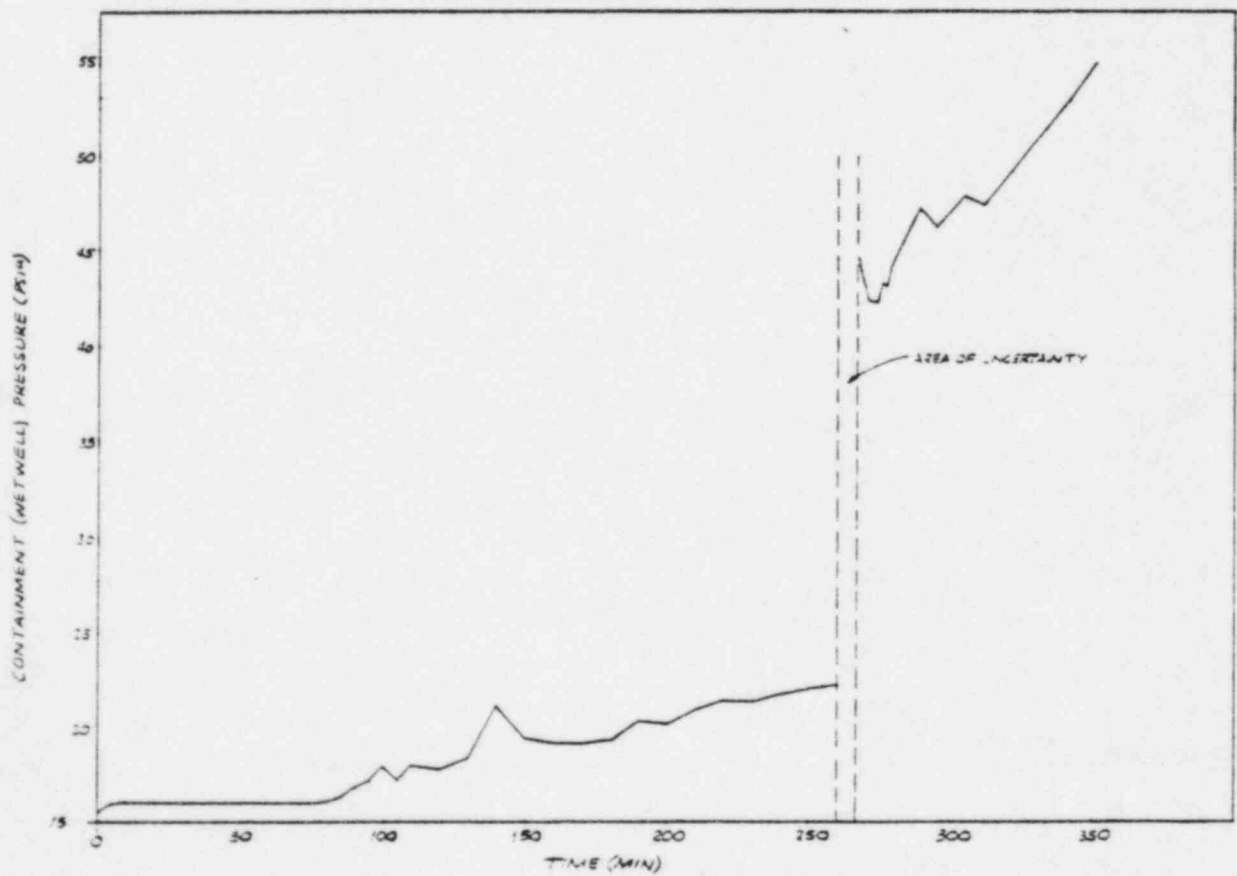
Figure C.8 - TQUV - Containment (Wetwell) Pressure
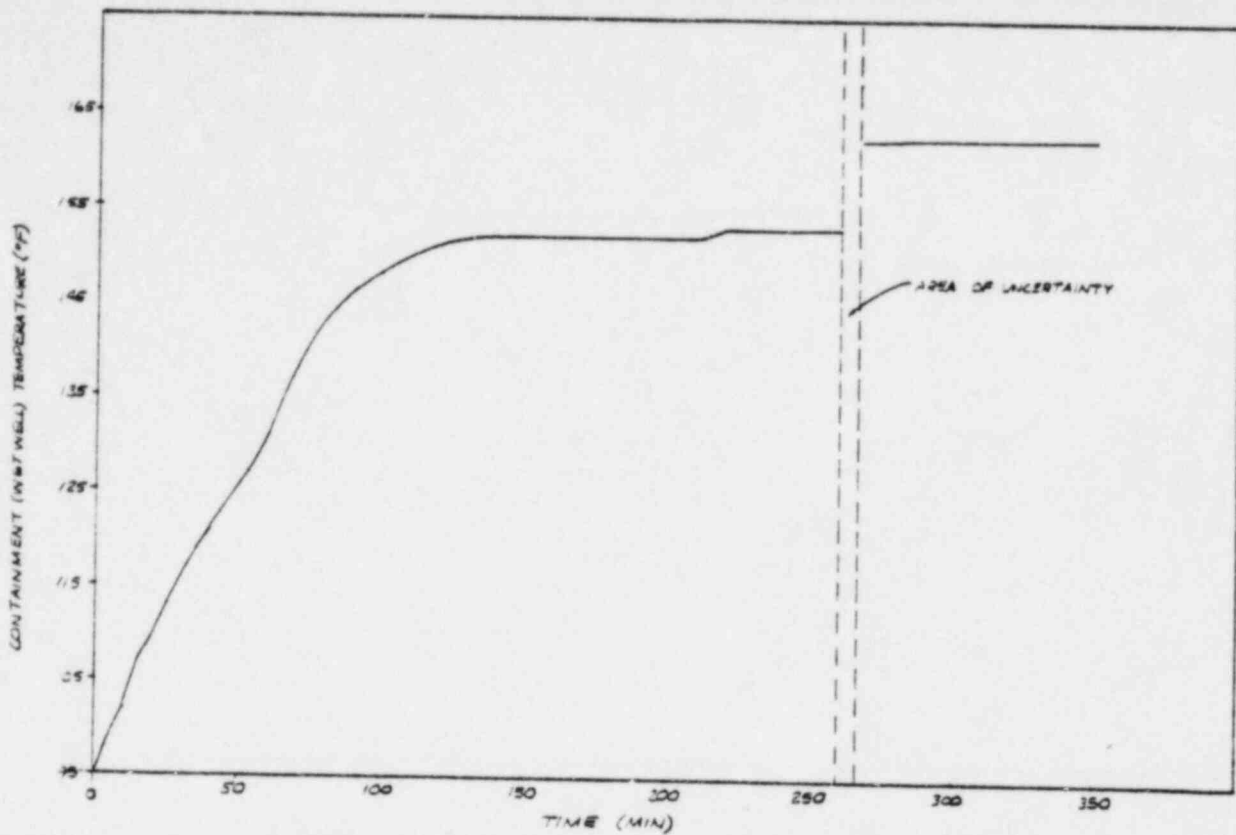
Figure C.9 TQUV - Containment (Wetwell Pool) Temperature
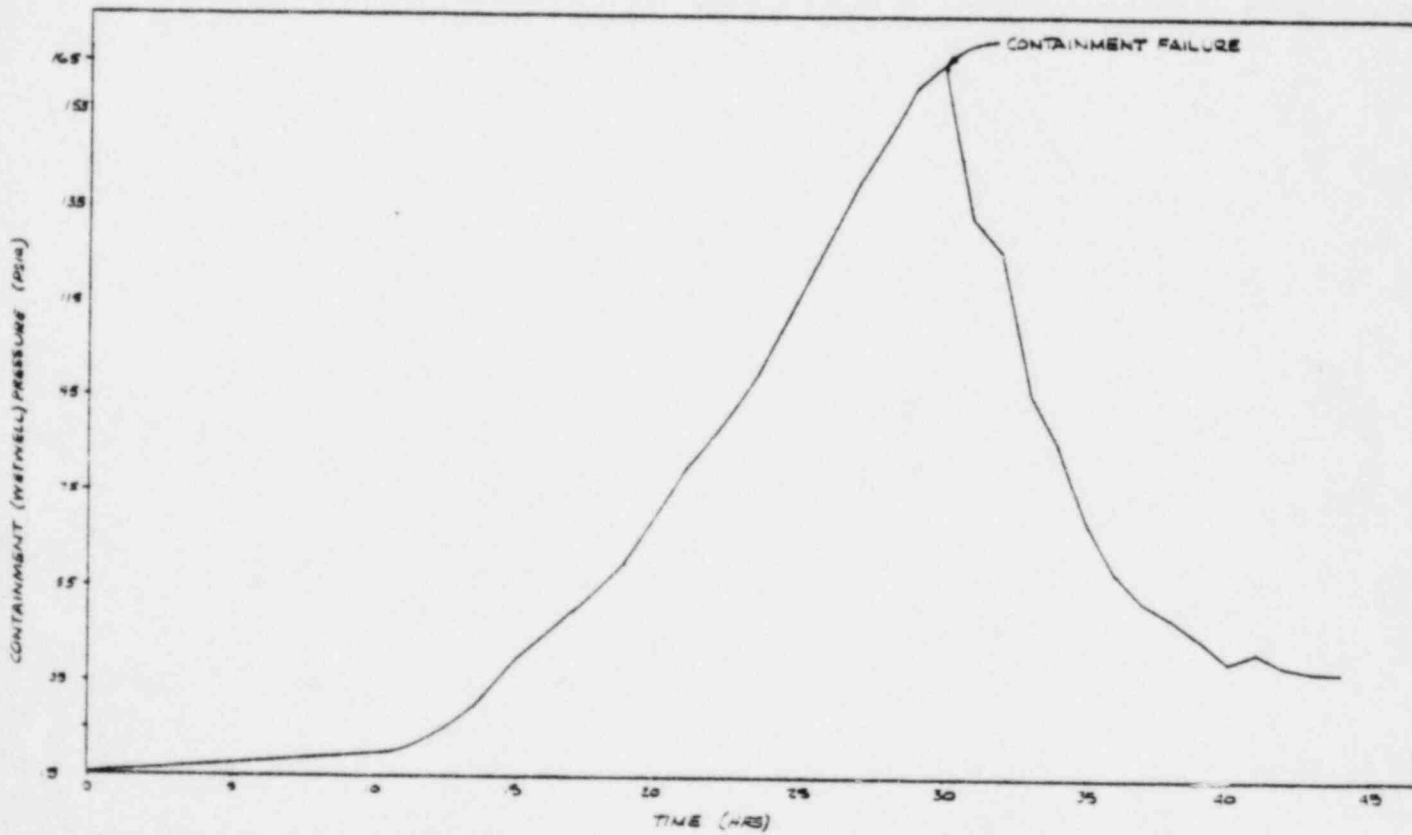
Figure C.10 TW - Containment (Wetwell) Pressure
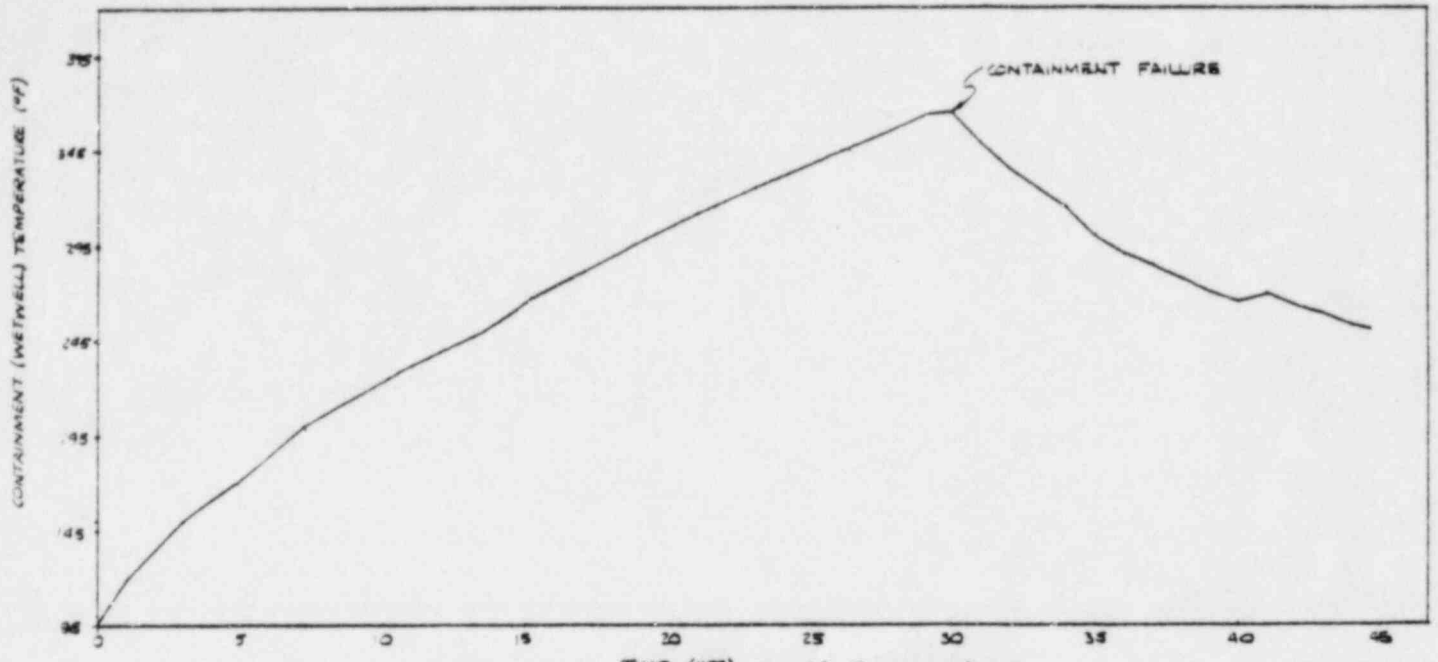
Figure C.11 TW- Containment (Wetwell Pool) Temperature
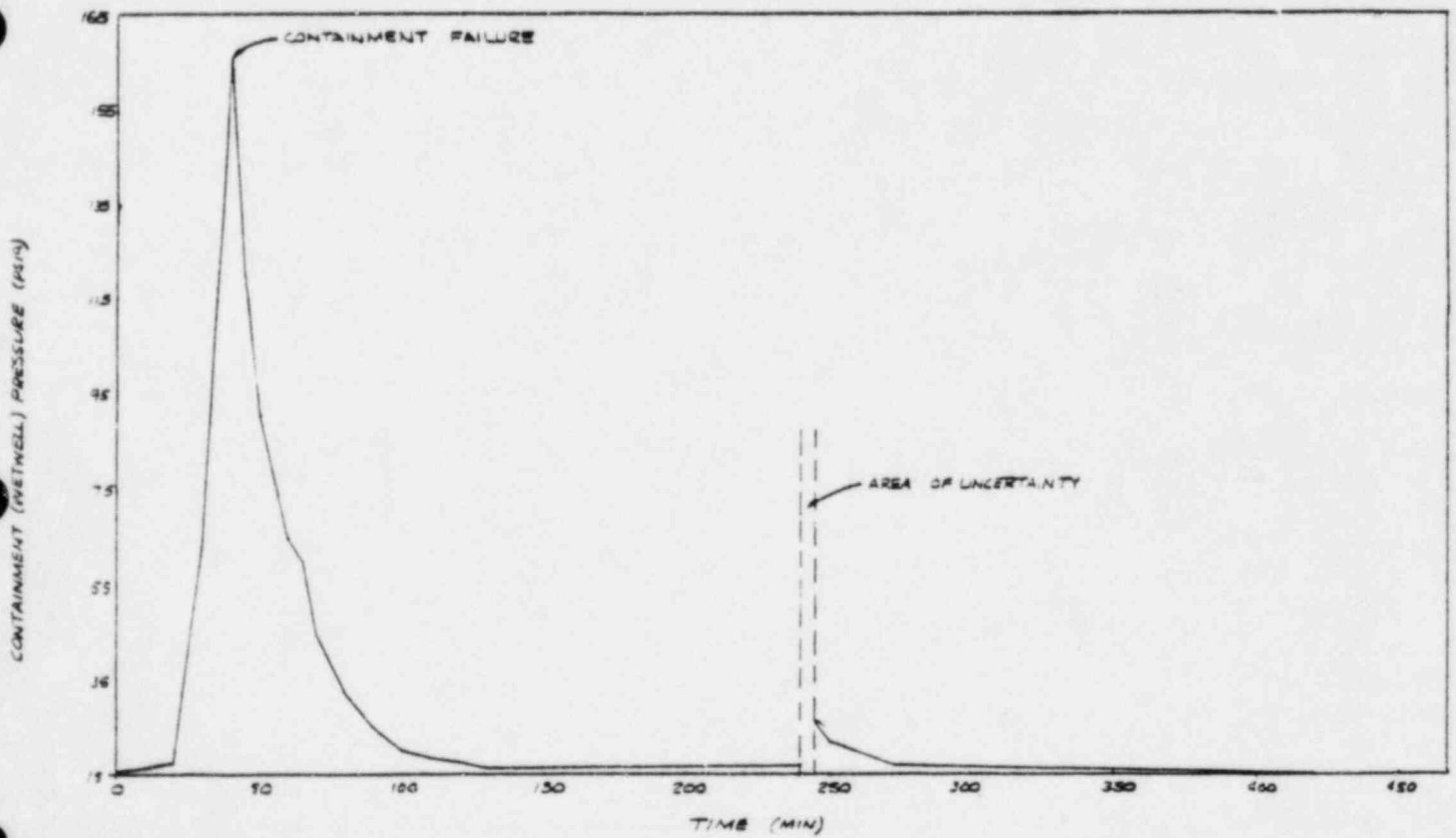
Figure C.12 ATWS -(Containment Failure) - Containment (Wetwell) Pressure

C-31
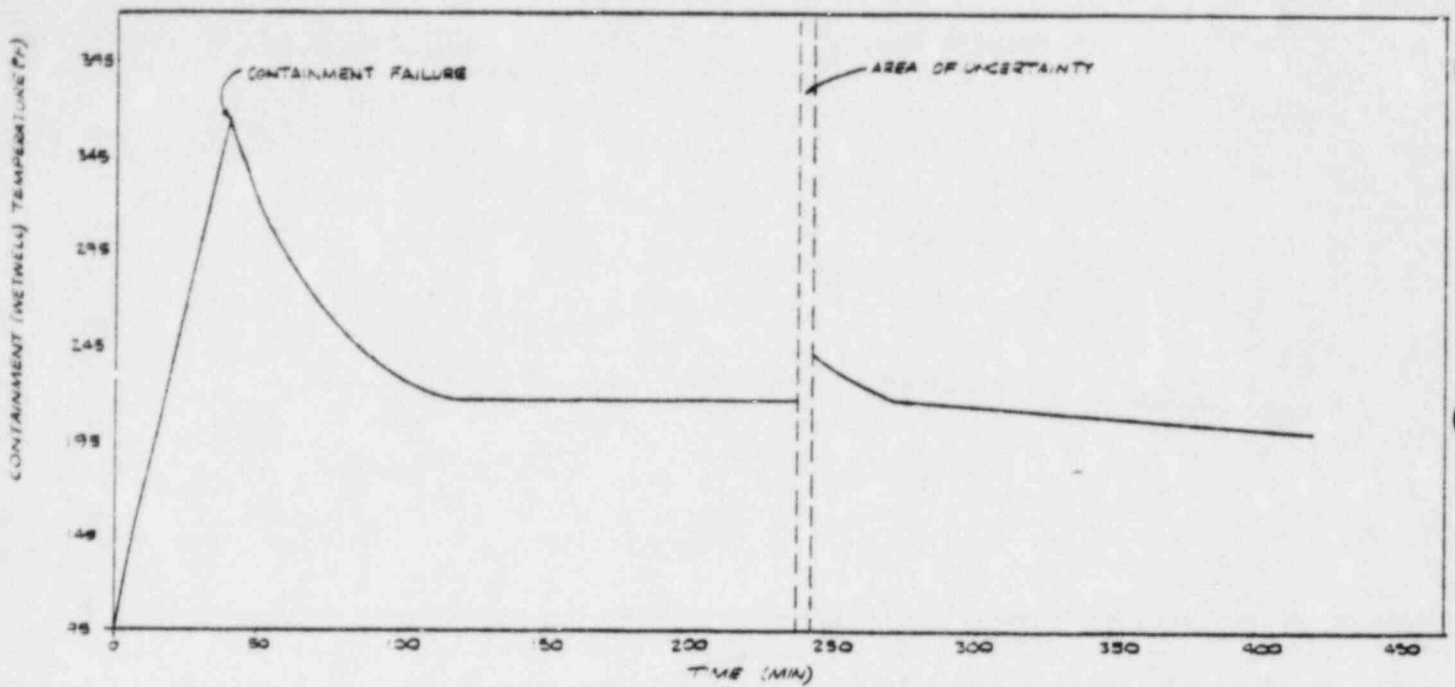
Figure C.13 ATWS (Containment Failure) - Containment (Wetwell Pool) Temperature
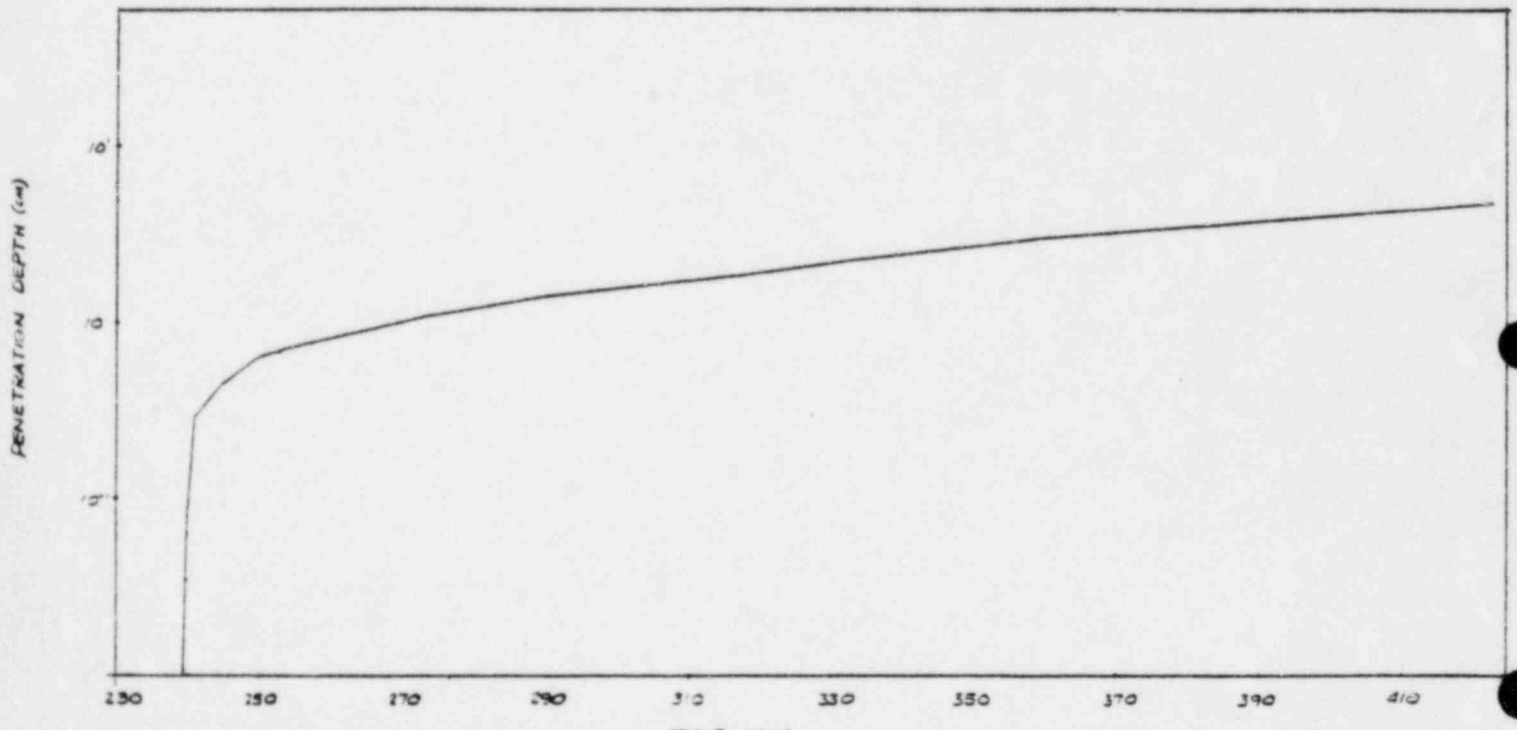
Figure C.14 ATWS (Containment Failure) - Diaphragm Floor Penetration Depth
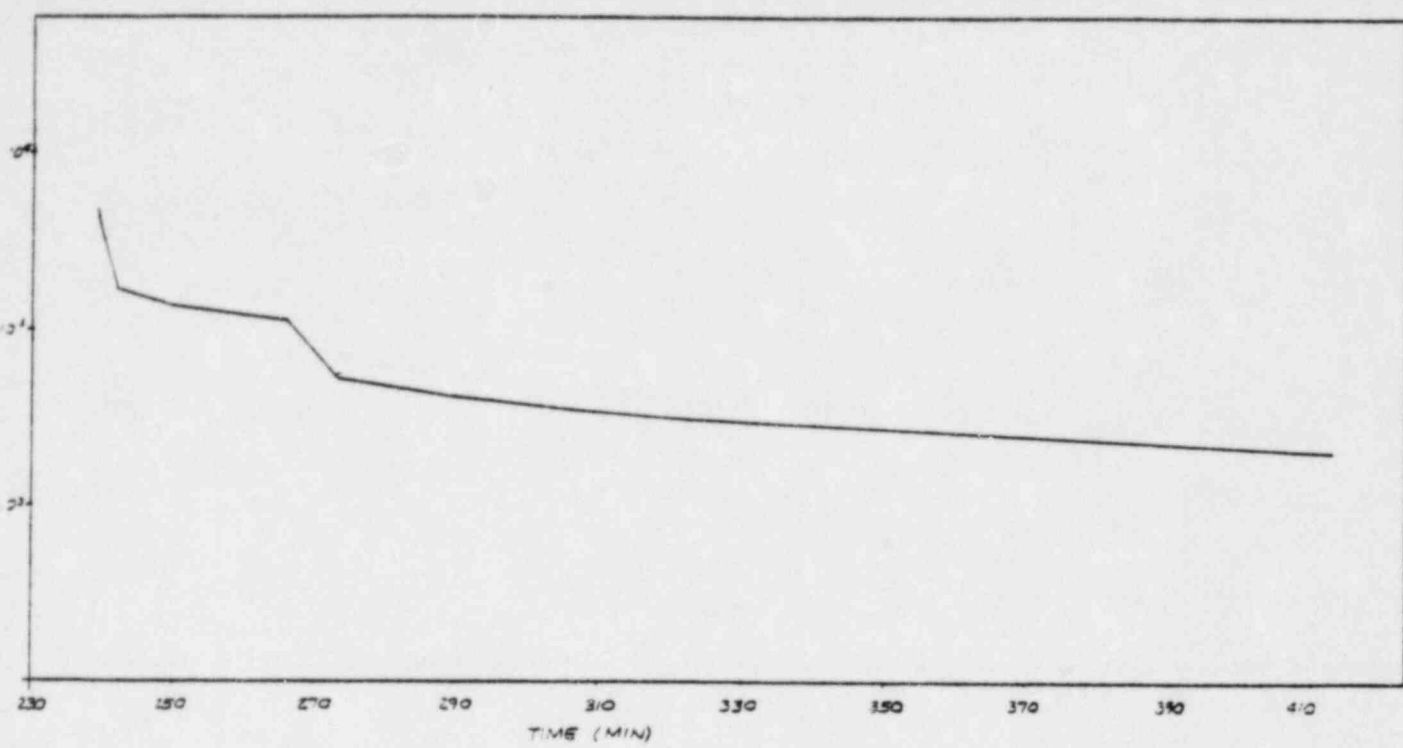
Figure C.15 ATWS (Containment Failure) - Diaphragm Floor Decomposition Rate

Figure C.16 ATWS (Containment Failure) - Gases Added to Containment Atmosphere
from Diaphragm Floor Decomposing

Appendix D

RADIONUCLIDE RELEASE FRACTIONS
FOR CORE MELT ACCIDENTS

APPENDIX D

The transport of radioactive material from the postulated core melt followed by passage through and exiting from the containment is a combination of many complex processes. The input to the release fraction calculations are the results of INCOR/CONTEMPT, which provide the pressures, temperatures, and compartment flow rates; and the radioactive source term, including the types and quantity of the isotopes.

The results of this section, in conjunction with the timing established in the INCOR/CONTEMPT runs, provides one of the inputs to the CRAC code (described in Appendix E) which calculates the external consequences to the public.

D.1   INTRODUCTION

The fraction of core fission products which could potentially be released to the environment during specific generic sequences are determined either by the SAI-REACT MARK II model or by CORRAL, which was previously used in WASH-1400. Characteristic times and physical conditions needed for the release fraction calculations are obtained from the INCOR analysis (Appendix C). The release fractions, or equivalently the amount of radioactivity released during a core melt accident, are the inputs used to determine the radioactivity dispersal and subsequently the dose and health effects using CRAC (see Appendix E).

This part of the analysis models the mechanisms of radionuclide release, its removal by natural processes and by active and passive safety systems, and the leakage paths associated with a core melt accident. These release and removal mechanisms and leakage paths are combined in a general calculational model to determine the time varying concentration of radioactivity in and between various compartments and the final cumulative amount released to the environment.

D-1

D.2   RELEASE FRACTION CALCULATIONS: SAI-REACT MARK II MODEL

SAI-REACT (Radionuclides Emitted After Core Transient) Mark
II model is one of the models used to determine the radionuclide fractions
released to the atmosphere. This model is basically of the same form
as used in CORRAL and contains similar assumptions. The primary diff-
erence occurs in the execution of the model (the differences are ex-
plained specifically for each case). REACT calculates the fraction of
fission product species (eight groups) that can be released in the event
of an accident by tracing the flow of the eight fission product groups
through each compartment and eventually to the atmosphere. In order to
estimate the release fractions, several inputs are required:

- A mathematical expression to account for the actual
  amount of radioactivity released

- The release mechanism to define the type of physical
  release

- The removal processes to account for any transportation
  filtering, settling, plateout, etc., of the radionuclides

- The containment failure modes to describe the leakage
  path, thus the rate of the release

- The specific sequences for which releases were calculated.

D.2.1   Mathematical Expression for Radionuclide Concentration

In order to determine the total amount of radioactivity released
in the event of a core melt accident, a mathematical expression or equation
is required to keep track of the flow of radionuclides through each compart-
ment until its final release to the environment. This tracking assumes a
homogeneous vapor region exists in each compartment so that convective currents
and other flows can be ignored, effectively removing spatial dependence. A
generalized mathematical expression can then be derived for the change in
radioactivity, with respect to time, in a given compartment of the form:

$$\frac{\partial C(t)}{\partial t} = S(t) - \alpha(t) * C(t) \tag{D-1}$$

The addition from sources, $S(t)$, may be modeled as any function of time, t, such as a constant rate, an impulse at time zero, or some other . nction. The removal from sinks, $\alpha(t) * C(t)$ is expressed in terms of the magnitude of the concentration at time, t, since the removal process acts within the compartment an.' treats the compartment volume as a whole. The source is independent of compartment concentration; however, it may be dependent on another compartment's concentration if leakage is occurring from one compartment to another.

An exponential solution to Equation D-1 is implied since the change in concentration with respect to time is proportional to the concentration at that time:

$$\frac{\partial C(t)}{\partial t} = S(t) - \alpha(t) * C(t); \quad S(t) = 0$$

$$\frac{\partial C(t)}{C(t)} = -\alpha(t)dt$$

$$C(t) = C_0 e^{-\int \alpha(t)dt} \quad\quad\quad (D-2)$$

Since Equation D-1 is a linear differential equation, the solution for any particular source can be found as a sum of the homogeneous solution ($S(t) = 0$) and the particular solution. This implies that concentrations as a function of time, developed from different sources or release mechanisms, can be combined by summing individual solutions to form an overall solution at any time of interest.

D.2.2   Radionuclide Release Mechanisms

In a core melt accident, there are four basic mechanisms for release of radioactivity:

- Gap Release -- occurs when the cladding ruptures and fission products are released to the reactor coolant system.

- Melt Release -- occurs when the fuel reaches its melting point, resulting in volatilization of fission products from the melting core.

- Oxidation Release -- occurs when part of the molten core drops into the suppression pool, causing a steam explosion, dispersing the hot core particles to the containment atmosphere.

- Vaporization Release -- occurs when the molten core drops onto the diaphragm floor and interacts with concrete, generating gases at the molten core/concrete interface.

These mechanisms are similar to those postulated in WASH-1400.

D.2.2.1   Gap Release

The gap release is chronologically the first release to occur in an accident sequence and the amount of radioactivity released is small compared to the other release mechanisms. Consequently, the overall release fractions of a gap release are negligible and are ignored for simplicity. The gap release is composed principally of noble gases.

D.2.2.2   Melt Release (Core and RPV Melt)

The core melt release starts after the core has uncovered and the fuel has heated to its melting point. As the fuel melts, core fission products are released. In the Limerick PRA it was assumed that the core melt release occurs linearly as 0% to 80% of the core melts. This is a simplification over WASH-1400, which assumed that fission product release occurred at the rate of core melting. The results of the BOIL indicate that this simplification is reasonable. At 80% core melt, the core grid plate is assumed to fail. At this time, the core is assumed to fall into the lower head and further radioactive release is terminated. When the core falls to the bottom of the RPV, the surface area for release is noticeably smaller. Additionally, either a crust may form due to the water on top of the molten corium or the metal in the melt could migrate to the top due to density differences. Either of these would provide a barrier inhibiting the flow of fission products. The release fractions into other containments during the core melt phase are the same as used in the Reactor Safety Study and are taken from Table VII 1-3 of WASH-1400.

D.2.2.3   Oxidation Release

At the time of RPV bottom head failure, it is assumed that
some of the molten core, approximately ten percent, also flows down
drain pipes and/or downcomers to the suppression pool causing intimate
interaction between small amounts of molten fuel and water, leading to
relatively small-scale steam explosions. This results in an oxidation
release to the wetwell atmosphere. It is not clear whether there is
sufficient oxygen or time before resettling for such a release mechanism
to actually occur; therefore, this analysis may be conservative in that
respect. An oxidation release will occur if molten core material is
finely dispersed into the wetwell atmosphere at high temperatures and
with available oxygen. The release fractions for the ten percent of the
core which enters the suppression pool were taken from WASH-1400, Appendix
VII, Section 1.

D.2.2.4   Vaporization Release

During the postulated core melt scenarios, the reactor pressure
vessel (RPV) was calculated to fail in the bottom head area due to molten
fuel interaction. Once the RPV has ruptured, and the molten core has dropped,
or is ejected onto the diaphragm floor, the corium begins interaction with
the concrete. The vaporization release process begins and is assumed to
exponentially decrease with time. The characteristic half-life of this
process is assumed to be thirty minutes based on WASH-1400, Appendix VII,
Section 1. Therefore, the source term for the general model is:

$$S(t) = e^{-kt} \text{ where } k = \frac{\ln 2}{T_{\frac{1}{2}}} = 1.39 \text{ hours for } T_{\frac{1}{2}} = .5 \text{ hrs.}$$

D.2.2.5   Summary of the SAI-REACT MARK II Model

The four release mechanisms -- gap, melt, oxidation, vapori-
zation -- form the complete set of release processes during a core melt

accident. For reasons previously mentioned, the gap release is neglected. The other release mechanisms are treated in a manner identical to that used in WASH-1400, and therefore have the same assumptions and conservatisms as that consequence analysis.

D.2.3   Radionuclide Removal Processes Used in the SAI-REACT MARK II Model

The various release mechanisms used in this analysis treat the fission product species as seven groups, each separated by their chemical properties. The seven groups considered are: (1) noble gases, (2) iodine: elemental and organic, (3) cesium-rubidium, (4) tellurium, (5) barium-strontium, (6) ruthenium, and (7) lanthanum. These groups can be divided into three major classes: gases, vapors, and particulates. In this analysis, the gases are assumed to be completely released, therefore unaffected by any removal process. The removal processes only apply to the two vapor groups and to all the particulate groups. The seven isotope groups can be divided into specific classes as follows:

- Noble gases: gases

- Iodine (elemental and organic): vapors

- All others: particulates.

At the same time that radioactivity is being released, radioactivity is also being removed. The mechanisms for removal of radioactivity from a compartment include:

- Active safety systems, such as sprays or filters

- Passive safety system (suppression pool)

- Leakage from the compartment

- Natural removal such as plateout or settling.

D.2.3.1   Active Safety System

The only active safety system considered in this analysis for
radioactive material removal is the standby gas treatment system (SGTS)
filters. The SGTS filters are utilized after containment failure and
leaks. At this point, the reactor building pressurizes up to the design
pressure of the blowout panels. If the containment break is sufficiently
small such that this does not occur, then filtering is possible. The
filtering process is commonly represented by decontamination factors (DF).
A DF is the ratio of the concentration of radionuclides into the removal
mechanism divided by the concentration output from the removal mechanism.
The ratios chosen here are taken from WASH-1400 and are:

- Noble gases: 1
- Organic iodide: 5
- Elemental Iodine: 100
- Particulates: 100.

These values are assumed independent of the accident sequence.

D.2.3.2   Passive Safety System

The suppression pool is the primary removal mechanism for radio-
activity during a melt accident. The suppression pool acts to scrub fission
products passing through it. This phenomena is extremely sequence dependent.
Some important parameters include:

- Pool conditions (saturated or subcooled)
- Flow rates through the pool
- Iodine concentration in the pool.

It should be noted that WASH-1400 took no credit for saturated pool
scrubbing. While this analysis uses WASH-1400 values for a subcooled
pool, other values are developed from experimental data for saturated
conditions. This is a departure from the WASH-1400 analysis.

The radioactive nuclides which principally affect the calculation of early effects on the public are iodine and tellurium. The remainder of the discussion on suppression pool scrubbing effectiveness will focus on the iodine release. In the Limerick PRA, non-iodine isotopes were treated the same as in WASH-1400.

The iodine concentration in any release is greatly influenced by the amount of pool scrubbing that will occur. The pool scrubbing effectiveness is included in the analysis through the use of empirical constants (decontamination factors). The decontamination factors reflect the degree to which iodine is kept in an immobile form in the suppression pool before, during, and after a postulated core melt. Generally three factors dictate the degree of suppression pool decontamination:

1. The amount of surface contact available between the water and iodine species,

2. Chemical composition of the iodine as it is released from the fuel or fuel rod gap,

3. pH balance of the pool.

For core melt scenarios in which the suppression pool is at a subcooled condition, the degree of surface interaction may be assumed to be quite high. Therefore, decontamination factors of 100 to 1000, depending on the source, can be assumed. For sequences, or portions of sequences, in which the pool is in a saturated condition, the vaporization and boiling tends to hinder surface contact between the iodine and water species, reducing the decontamination factors. Conservative estimates of saturated pool DF, range from 3 to 5, with other data evaluations giving estimates as high as 15 to 30.

The second factor in calculation of pool decontamination for iodine is the chemical form. Three forms dominate: (1) organic, (2) elemental (diatomic), and (3) inorganic (combined with cesium to form cesium iodide). The organic form, while insoluble, constitutes a very small portion of the iodine release. The elemental form was considered to be the major constituent in the WASH-1400 analysis. Later experimental evidence and date from the Three Mile Island accident indicate that the inorganic form (cesium iodide) may be a much larger constituent than previously believed. Since

D-8

cesium iodide is more soluble than elemental iodine by a factor of 10 to 100, an increased decontamination factor over pure elemental iodine was used in the Limerick PRA.

Finally, the pH or chemical makeup of the pool itself has an effect on the proposed decontamination term. Evidence indicates that the pool could be extremely basic in makeup after passage of some volume of material through it; and, the more basic the solution, the more soluble iodine is in it. Therefore, an additional credit can be taken in terms of decontamination factors.

Based on the above considerations, the set of decontamination factors chosen for use in the Limerick evaluation are:

POOL DECONTAMINATION FACTORS

Conditions	Meltdown Release	Vessel Failure and Vaporization
Containment Failure at End of Release	100	10*
Containment Failure Initiates Release	10*	10*

*Suppression pool considered saturated.

D.2.3.3   Leakage

Radionuclide removal by leakage is assumed to be a simple process. The characteristic removal rate is found by comparing the volumetric leakage rate to the compartment volume. This, in effect, gives the number of compartment volumes leaked per hour. This process is independent of whether the fission product species is a vapor or a particulate. The leakage removal, $\lambda_\ell(t)$, process from compartments is assessed from INCOR output data.

D.2.3.4   Natural Removal

The treatment of natural deposition in this analysis is
identical to that used in WASH-1400, Appendix VII.

Natural deposition, $\lambda_{NR}(t)$, affects each class of isotopes
differently. Organic iodine is not appreciable affected by natural
removal and its removal rate is set equal to zero. For elemental
iodine, the mass transfer processes deposit the iodine vapor onto the
containment surface. This deposition rate is proportional to the wall-
bulk temperature difference, as well as other containment conditions
such as density and viscosity. However, this temperature proportionally
is to the 1/3 - 1/4 power, so that large temperature changes are required
for large changes in plateout conditions of elemental iodines. The parti-
culates are removed by a settling process which is proportional to the
mean particle size, due to the fact that impact with the floor is affected
by the downward terminal velocity of the particles. As in WASH-1400, this
analysis assumes the particle size varies over time; consequently, parti-
culate settling removal rates are a function of time from the beginning
of the removal mechanism.

The general model used for the removal rate, $\alpha(t) = \lambda_{\ell}(t) +
\lambda_{NR}(t)$, for each class is both a function of time and sequence since the
conditions (pressures, temperatures) vary. The determining conditions,
however, are taken to be constant in time. This is not unreasonable since
the sequences are analyzed over a number of timesteps. Therefore, a constant
$\alpha(t)$ is used to represent each particular time period.

D.2.4   Containment Failure Modes

The leakage path for radiation released to the atmosphere is
characterized by the location and size of containment failure. The charac-
teristics of the leakage path, together with those of the release and re-
moval mechanisms for a specific sequence, completely define the total
amount of radioactivity released to the environment.

In this analysis, a number of assumptions were made relative to containment failure, these include:

1. Containment failure is assumed to occur when the pressure inside containment is in the range 120 to 160 psig (140 psig is used)

2. Containment isolation is taken to be highly reliable since:

    •   The drywell and wetwell are normally isolated and inerted

    •   Isolation of pipe line penetrations of containment are sufficiently reliable so that their potential failure mode is much smaller than other postulated failure modes.

3. The Bechtel Analysis (see Appendix J) concludes that the containment ultimate capability is above 140 psig, therefore a very low probability of containment failure is assigned to pressures below 120 psig.

4. The modes of failure for the Mark II containment are slightly different than those used in WASH-1400 (which assumed a Mark I containment).

The effective location and size of the leakage path to the atmosphere is determined by the type of containment failure and its effect on the reactor building. Containment failure types can be divided into the following generic cases:

•   Wetwell failure at the point of highest stress or penetration blowout in the wetwell (this may result in wetwell failure extending below the suppression pool water level)

•   Diaphragm floor failure

•   Penetration blowout in the drywell

•   Drywell failure at the refueling floor interface.

These failure cases, coupled with the size of the failure, determine the failure or release from the reactor building.

A failure in the wetwell pressurizes the reactor building (RB). If the size of the failure is of sufficient magnitude to pressurize the RB so that the blowout panels rupture, a direct path to the atmosphere results; otherwise, partial or complete filtering of the leaked material to the atmosphere occurs. The release with RB overpressurization occurs roughly at ground level, since the panels are not located in the exhaust stack of the SGTS; without RB overpressurization, the release will be processed through the SGTS and released at an elevated height of approximately 25 meters.

An additional effect to consider, relative to wetwell failure at the pool water line or a penetration blowout, is the leakage path of radiation contained in the drywell. The Mark II containment design is a two compartment design. Each compartment has associated with it an inventory of radioactivity. Therefore, when the containment fails there are two compartment inventories for which leakage must be defined. In the case of wetwell failures, the inventory of radioactivity in the wetwell is released to the RB directly. However, the radioactivity in the drywell passes down the vents, through the suppression pool, and then to the wetwell vapor region for leakage to the RB. This pathway has associated with it the additional removal mechanism of pool scrubbing, for which the scrubbing effectiveness is a function of the pool condition (saturated or unsaturated).

A diaphragm floor failure is assumed to result in a direct leakage path to the atmosphere for the radioactivity in both the wetwell vapor region and the drywell. This also results in a pressurization of the RB and possible actuation of the blowout panels inside the SGTS exhaust stack. Consequently, an elevated release occurs with a release height of approximately 25 meters.

A drywell containment failure has two possible failure locations. Either a leakage path to the refueling floor or elsewhere in the RB can occur with both locations assumed to be roughly equivalent. Any drywell failure

causing a secondary containment overpressurization actuates the blowout panel to the SGTS exhaust stack. Again an elevated release occurs out the top of the stack.

Since different primary containment failure locations result in leaks to different rooms in the RB, different pressurization rates could conceivably occur. For simplicity, it is assumed that the RB acts as one volume. Since there are no airlocks in the secondary containment, except between the refueling floor and RB or the RB and the atmosphere, this does not appear to be an unreasonable assumption. Given these assumptions, a series of calculations by the INTER code indicates that the secondary containment does not overpressurize even if the primary containment break size is as high as 0.2 square feet. (It should be noted that the estimated failure size for a steel-lined concrete containment from WASH-1400 is approximately equal to or less than 0.2 square feet.) However, at this break size the SGTS system must transfer to emergency mode and some leakage occurs through cracks bypassing the filters. It is estimated that 98 percent of the flow is filtered and only 2 percent leaks out by other paths. If the failure size is still smaller, then all of the containment leakage is filtered prior to release (if the SGTS is switched to emergency mode). Since the filters in the SGTS have a high removal rate, these distinctions are extremely important to the overall result.

The layout of the above mentioned leakage path identification process indicates that a large combination of leakage paths are possible. For this reason, a further simplification is made. For those cases where filtering occurs, release fractions are noticeably smaller than cases without filtering. Therefore, if it is assumed that radiation in either the wetwell vapor region or the drywell is leaked directly to the RB, three failure locations need not be considered. This assumption results in no pool scrubbing by the suppression pool when the failure location is in the wetwell. If it is also assumed that a drywell failure is equivalent to a wetwell and drywell failure, then more leakage paths are eliminated. This assumption is

not unreasonable since radioactivity in the wetwell vapor region passes
directly to the drywell through the vacuum breakers. These assumptions
result in a reduction of the leakage paths to six basic cases. They are
defined as follows:

γ^1 -- Release direct to the secondary containment and to the
atmosphere, resulting from a wetwell and drywell failure
(diaphragm floor failure). No filtering occurs due to the
large failure size. Elevated release through stack.

γ -- Release indirect to the secondary containment, resulting
from a wetwell failure. Drywell concentrations scrubbed by
the wetwell pool then leaked from wetwell vapor region to
secondary containment to the atmosphere. No filtering occurs
due to the large failure size. Ground level release through
HPCI, RCIC blowout panels.

ζ -- Release direct to the secondary containment from an assumed
drywell and wetwell failure (diaphragm floor failure). Because
of smaller leak size, a full 98 percent of the leakage is filtered
before passing to the atmosphere through the elevated SGTS exhaust
stack.

δ -- Release direct to the secondary containment from an assumed
drywell and wetwell failure (diaphragm floor failure). This leak
size is small enough such that 100 percent of the leakage is
filtered before passing to the atmosphere through the elevated
SGTS exhaust stack.

$\zeta\epsilon$ -- Release direct to the secondary containment by leakage
out of containment. Since the SGTS has failed (represented by
ϵ), only plateout on the RB surfaces mitigates this elevated
release to the atmosphere through the SGTS exhaust stack.

$\delta\epsilon$ -- Release direct to the secondary containment by leakage
out of containment. Since the SGTS has failed, only plateout
in the RB mitigates this elevated release to the atmosphere
through the SGTS exhaust stack. The leakage rate is approxi-
mately one half of $\zeta\epsilon$ holdup time, and therefore, natural de-
position is enhanced. Generally, however, $\zeta\epsilon$ and $\delta\epsilon$ are
approximately equal in release magnitude.

In summary, leakage paths are characterized by containment failure
modes. Primary containment failures are defined by pressures of around
140 psig and are coupled to secondary containment failures according to the
primary containment failure location and size.

D.2.5   Specific Sequence Calculations

Calculations for the radionuclide release fractions were done for three of the sequences modeled in the INCOR analysis -- TQUV, TW, and ATWS with HPCI failure (see ppendix C for details). These three sequences can be divided into two categories for the methodology used to calculate the release fractions: (1) Core Melt -- RPV Meltthrough -- Core/Concrete Interaction Prior to Containment Failure (TQUV and ATWS with HPCI Failure); and (2) Containment Failure Prior to Core Melt -- RPV Meltthrough -- Core/ Concrete Interaction (TW).

D.2.5.1   Core Melt -- RPV Meltthrough -- Core/Concrete Interaction Prior to Containment Failure

The basic methodology used in this type of sequence is to accumulate the radioactivity in the containment from the various releases (see Section D.2.2) and then to release the accumulated radioactivity from the containment either directly to the atmosphere or through the reactor building to the atmosphere. For each type of release, an equation is set up to define the concentration of radioactivity in the compartment being considered using general Equation D-1. This equation is then solved for two amounts: (1) the fraction of radioactivity available for release (f'_{leaked}) and (2) the fraction of available radioactivity remaining (f'_{left}) or the fraction of radioactivity available for release at a later time. The actual fractions of radioactivity released (f_{leaked}) and left (f_{left}) are equal to the product of the availab.e radioactivity remaining/left and the percentage of radioactivity that is released for that type of release.

The first release considered is the melt release which is divided into four parts: Core melt, RPV Melt, RPV failure, and Blowdown. A constant release is assumed to occur during core melt which implies a constant source of radioactivity over time; therefore, general Equation D-1 takes on the form:

$$\frac{\partial C(t)}{\partial(t)} = S_0 - \alpha C(t) \qquad\qquad (D-3)$$

D-15

Equation D-3 is then solved for the two sources: the radioactivity available for release to the wetwell pool through the SRVs (f'_{leaked}), and the available radioactivity remaining in the RPV for a later release (f'_{left}). The first solution is:

$$f'_{leaked} = \frac{\lambda_\ell}{\alpha^2 t} (\alpha t + e^{-\alpha t} - 1) \tag{D-4}$$

where $\alpha = \lambda_\ell + \lambda_{NR}$ and λ_ℓ is the leakage removal rate and λ_{NR} is the natural removal rate. It is assumed that natural deposition does not occur in the RPV; therefore, the total removal rate is only equal to the leakage removal rate ($\alpha = \lambda_\ell$). Equation D-4 then reduces to

$$f'_{leaked} = \frac{1}{\alpha t} (\alpha t + e^{-\alpha t} - 1) \tag{D-5}$$

The second solution to Equation D-3 is:

$$
\begin{aligned}
f'_{left} &= (1 - f'_{leaked}) \\
&= 1 - \frac{1}{\alpha t} (\alpha t + e^{-\alpha t} - 1) \\
&= \frac{1}{\alpha t} (1 - e^{-\alpha t}) \tag{D-6}
\end{aligned}
$$

At the time of core grid plate failure, it is assumed that no radionuclides are added to the RPV from the molten fuel (see SEction D.2.2.2). The only radioactivity available for release through the SRVs during RPV melt is that left during core melt. However, the actual radioactivity available for release during RPV melt is the product of that which is available from core melt (CM) and the solution to the equation for the concentration of radioactivity. General Equation D-3 for a no-source release takes on the form:

$$\frac{\partial C(t)}{\partial t} = -\alpha C(t)$$

and the solution is:

$$f''_{leaked} = \frac{\lambda_\ell}{\alpha} (1-e^{-\alpha t}) \quad \alpha = \lambda_\ell$$

$$= (1-e^{-\alpha t})$$

with

$$f'_{leaked} = f'_{left_{CM}} * f''_{leaked}$$

$$= f'_{left_{CM}} (1-e^{-\alpha t}) \quad\quad\quad (D-7)$$

The radioactivity available for release at a later time is then equal to:

$$f'_{left} = f'_{left_{CM}} - f'_{leaked}$$

$$= f'_{left_{CM}} - f'_{left_{CM}} (1-e^{-\alpha t})$$

$$= f'_{left_{CM}} (e^{-\alpha t})$$

At the time of RPV failure, it is assumed that the radioactivity remaining in the RPV is released to the drywell and due to the pressure increase is totally forced through the downcomers and released to the wetwell pool so that:

$$f'_{leaked} = 1 - f'_{leaked_{CM}} - f'_{leakedPVM}$$

and

$$f'_{left} = 0.$$

The next release to occur is the oxidation release. It is modeled as an impulse release, in that all the radioactivity is assumed to be released instantaneously from the fuel to the pool. This assumption implies that there is no time for removal (leakage or deposition) to occur. Therefore, general Equation D-3 takes on the form:

$$\frac{\partial C(t)}{\partial t} = S_o$$

and the solutions are:

$$f'_{leaked} = S_o$$

$$f'_{left} = 0$$

The final release mechanism is the vaporization release. It is assumed that this release is exponentially decreasing with time (Section D.2.2.4); therefore, general Equation D-3 becomes:

$$\frac{\partial C(t)}{\partial t} = e^{-kt} - \alpha C(t) \qquad (D-8)$$

It is also assumed that during vaporization release, radioactivity is available for release to the suppression pool (f'_{leaked}) and the drywell (f'_{left}), which includes the radioactivity remaining in the fuel. The solutions to Equation D-8 are then:

$$f'_{leaked} = \left[\frac{\lambda_\ell}{\alpha-k} - \frac{\lambda_\ell k}{\alpha(\alpha-k)} \left[\frac{1-e^{-\alpha t}}{1-e^{-kt}} \right] \right] (1-e^{-kt})$$

$$f'_{left} = \left[\frac{k}{\alpha-k} (e^{-kt} - e^{-\alpha t}) \right] + e^{-kt}$$

During each of these releases, the radioactivity released to the suppression pool is scrubbed and then released to the wetwell atmosphere. Natural deposition in containment is also accounted for in these calculations. At the end of each release, the radioactivity released to the wetwell atmosphere is added to the radioactivity already released to the wetwell atmosphere from the previous release(s). The next step in the calculation is to release this accumulated radioactivity in containment (drywell and wetwell atmosphere) to the atmosphere, either due to containment failure or leakage. The type of containment release will exclusively define the equation for the fraction of radioactivity released (see Section D.2.4).

The first type of containment release, containment failure, assumes a direct release from containment to the reactor building and then to the atmosphere either directly or through the standby gas treatment system filters. Containment failure releases assume that natural deposition does not have time to occur in the reactor enclosure. There are three types of containment failure due to diaphragm floor failure: large break (γ'), medium break (ζ), and small break (δ); and one type of containment failure due to wetwell failure (γ).

Filtering is assumed not to occur in the large break, and the radioactivity in containment is totally released to the atmosphere. Partial filtering is assumed to occur with the medium size break and total filtering with the small break. For the wetwell failure, the radioactivity in the wetwell atmosphere is released directly to the atmosphere (no filtering); but, the radioactivity in the drywell is released first to the wetwell pool, scrubbed, and then released directly to the atmosphere.

The second type of containment release, containment leakage, is divided into two types: large leakage ($\zeta\epsilon$) and small leakage ($\delta\epsilon$). The radioactivity in these cases is assumed to be released to the reactor building over time and partially deposited and then released to the atmosphere. Since there are sources, a no-input solution is again employed and general Equation D-3 is thus equal to:

$$\frac{\partial C(t)}{\partial t} = -\alpha C(t) \qquad\qquad (D-9)$$

In these cases, the radioactivity available for release, after deposition occurs, is assumed to be totally released and the time period for release is considered to be infinity. The solutions to Equation D-9 then become:

$$f'_{leaked} = \frac{\lambda_\ell}{\alpha}(1-e^{-\alpha t})$$

$$= \frac{\lambda_\ell}{\alpha}$$

$$f'_{left} = 0$$

D.2.5.2 Containment Failure Prior to Core Melt -- RPV Meltthrough -- Core/Concrete Interaction

The basic methodology for this type of sequence differs substantially from that outlined in Section D.2.5.1. The radioactivity in this case is not allowed to accumulate in containment during the various releases, but is constantly being released to the reactor building and then to the atmosphere. It is also assumed that natural deposition is occurring in both the containment and the reactor building. For this type of sequence, the containment failure is assumed to occur at the diaphragm floor with three different types of release: partial filtering, total filtering, and no filtering.

The first release to occur is again the core melt, which still assumes a constant release from the RPV to the suppression pool and Equation D-3 remains the same:

$$\frac{\partial C(t)}{\partial t} = S_o - \alpha C(t)$$

and with the same solutions:

$$f'_{leaked} = \frac{1}{\alpha t} (\alpha t + e^{-\alpha t} - 1)$$

$$f'_{left} = \frac{1}{\alpha t} (1 - e^{-\alpha t})$$

Natural deposition is still assumed not to occur in the RPV.

The radioactivity is constantly being released to the suppression pool, being scrubbed, and then released to the wetwell atmosphere. This release from the suppression pool acts as a constant source for the wetwell atmosphere, and, therefore, the same equations still apply. However, since natural deposition is assumed to occur, the equations for the radioactivity available for release from containment to the reactor building, and the available radioactivity left for later release are:

$$f'_{leaked} = \frac{\lambda_\ell}{\alpha^2 t} (\alpha t + e^{-\alpha t} - 1) \qquad (D\text{-}10)$$

$$f'_{left} = \frac{1}{\alpha t} (1 - e^{-\alpha t}) \qquad (D\text{-}11)$$

Again, the fission products constantly being released from the wetwell atmosphere to the reactor building act as a constant source for the reactor building. Therefore, Equation D-10 is also applicable for the radioactivity available for release to the atmosphere. However, Equation D-11 is assumed zero since the radioactivity that is not naturally deposited is assumed to be totally released to the atmosphere.

The next step is a release of the available radioactivity left in the wetwell atmosphere to the reactor building and then to the atmosphere. Since this is remaining radtioactivity, it is assumed there is no source.

D-21

It is also assumed that the remaining radioactivity which is not naturally deposited is released during a time period assumed to be infinity. The solution for a no-input source with an infinite time period then reduces to:

$$f'_{leaked} = \frac{\lambda_\ell}{\alpha} \qquad\qquad (D-12)$$

In the next release, RPV melt, the fraction of radioactivity available for release from the RPV to the wetwell pool is subjected to the same assumptions and conditions as mentioned in Section D.2.5.1. Therefore, Equation D-7 is applicable and the fraction of radioactivity available for release is equal to:

$$f'_{leaked} = f'_{left_{CM}}(1-e^{-\alpha t})$$

At RPV railure, the radioactivity remaining in the RPV available for release to the drywell is equal to:

$$f'_{leaked} = 1 - f'_{leaked_{CM}} - f'_{leaked_{PVM}}$$

Also at RPV failure, part of the radioactivity is released from the drywell to the wetwell pool due to a pressure increase. This release happens in so short a space of time that it is assumed to be an instantaneous release, and therefore, natural deposition is not assumed. Since it is also a no-source release, the radioactivity available for release to the suppression pool (where it is scrubbed) is equal to:

$$f'_{leaked} = 1-e^{-\alpha t}$$

While the radioactivity is being released to both the wetwell atmosphere and the drywell, it is also being released from these compartments to the reactor building and then to the atmosphere. These releases are

D-22

assumed to be no-source releases; therefore, the radionuclides available for release from the wetwell atmosphere and drywell to the reactor building and then to the atmosphere are estimated by Equation D-12.

The oxidation release is also assumed to be an impulse release in this sequence. Therefore, the radioactivity available for release to the suppression pool (where it is also scrubbed) is equal to:

$$f'_{leaked} = S_0$$

with subsequent releases to the reactor building and then to the atmosphere. The radionuclides available for release from these compartments are estimated by Equation D-12.

The last release, vaporization, is also assumed to be an expoenntially decreasing release in this sequence. Therefore, the radioactivity available for release from the drywell to the reactor building is equal to:

$$f'_{leaked} = \frac{\lambda_\ell}{\alpha-k} - \left[\frac{\lambda_\ell k}{\alpha(\alpha-k)} (1-e^{-\alpha t})\right] \qquad (D-13)$$

and the remaining available radioactivity released at a later time to the reactor building is equal to:

$$f'_{leaked} = \left[\frac{k}{\alpha-k} (e^{-kt} - e^{-\alpha t})\right] \frac{\lambda_\ell}{\alpha} \qquad (D-14)$$

These two fractions of radioactivity (Equations D-13 and D-14) are also released to the atmosphere. It is still assumed that the same conditions apply; therefore, the radioactivity available for immediate release to the atmosphere, and the remaining radioactivity available for later release to the atmosphere, are estimated by Equation D-12.

In each of these releases -- melt, oxidation, and vaporization -- the radioactivity releases to the atmosphere are summed to give the total amount of radioactivity released to the atmosphere for the accident sequence.

The two methodologies outlined in Sections D.2.5.1 and D.2.5.2 are only a guideline to the approach used in the calculations.

D.3   CORRAL RELEASE FRACTION MODEL

The second model used to calculate the fraction of radioactivity released to the atmosphere is the computer code CORRAL (Containment of Radionuclides Released After LOCA). CORRAL, as in the SAI-REACT MARK II model, describes fission product transport and deposition in containment. The "containment" is represented by individual compartments which are connected to each other. Radioactivity released from containment is speci- fied by four release mechanisms in CORRAL. The four release mechanisms are: gap release, fuel melting (melt) release, steam explosion (oxidation) release, and fission product (vaporization) release. These release mech- anisms are applied to each of the seven groups of fission products (see Section D.2.3). Radionuclides can be removed during the various releases by particle settling, deposition, spray removal, pool scrubbing, filters, etc.. The manner in which CORRAL utilizes these release mechanisms and removal rates is basically the same as the SAI-REACT MARK II model (see Section D.2). WASH-1400, Appendix J, contains a detailed discussion of the methodology and assumptions.

CORRAL interpolates between input data and continuously computes changing properties to determine the various leakage and fission product removal rates, each as a function of time. It keeps an inventory of the radioactivity in each compartment throughout the sequence by inputting the rates into an array of differential equations (similar to those discussed in Section D.2) and solving for the time-dependent fission product concen- trations and accumulations in each compartment. It then computes the final release to the atmosphere.
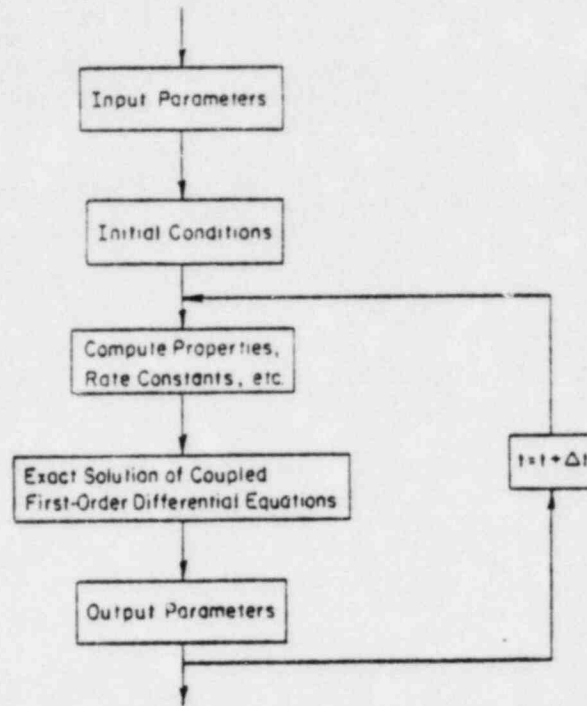
Figure D.1   Computer Code CORRAL Flow Diagram

Figure D.1 shows the basic flow chart for CORRAL. CORRAL reads
the input parameters, computes the initial conditions (all concentrations
are set equal to zero, at time zero, except for the gas release concen-
trations in the first compartment. All amounts released and dose reduction
factors are also set equal to zero). It then calculates properties and re-
moval rates as follows:

- Pressure, temperature, and water vapor content and
  $T_{Bulk} - T_{Wall}$ by parabolic interpolation

- Intercompartment flow rates and decontamination
  factors and leak rates by parabolic interpolation

- Particle sizes by linear interpolation

- Gas phase viscosities and elemental iodine diffusi-
  vities and Schmidt numbers

- Mass transfer Grashof number's and corresponding depositing rates

- Particles settling velocities and their natural deposition

- Spray lambdas for particles

- Terminal spray velocities, gas phase mass transfer coefficient, liquid phase mass transfer coefficient, and spray lambdas

- Elemental iodine equilibrium equivalent lambdas (if needed)

- Overall lambdas.

The next step is to calculate the solution of the differential equations. To properly age the various releases, they are divided into discrete impulse releases. The melt release is divided into ten equally spaced and sized releases, each independent (age wise) from the others. The vaporization release, an exponentially decreasing release, is divided into 20 impulse releases, each successive release at an exponentially lower value than the first. The sum of the first ten releases equals one half the total release, and the remaining ten equals the remaining half. The duration of the period of the first ten is one half-life. (See footnote of Table D.1.)

The last step in CORRAL is the output variables:

- Airborne contained fractions released at time, t

  - For each release: elemental and organic iodines, particulates

  - For each compartment for each release: elemental and organic iodines, particulates at time, t

D-26

- Escaped fractions released (for each release: elemental and organic iodines, particulates) at time, t

- Escape fractions of the core for any desired isotope

- Dose reduction factors for each release (elemental iodine and particulates) at time, t

- Overall dose reduction factor (elemental iodine and particulates) at time, t

- Total fraction of core iodine escaped and core particulates escaped up to time, t.

The input data for CORRAL includes two main types: constants and variables. The constant inputs are:

- Core fractions for each release -- (CFR(I,J)

- Number of compartments -- N

- Volumes -- (V(I); wall areas -- AW(I); floor areas -- AF(I); and heights -- HT(I) of each compartment

- Spray parameters (see Footnote 1, Table D.1)

- Times of events (see Footnote 8, Table D.1)

- Compartment filter decontamination rates -- FDP(I) (see Footnote 6, Table D.1)

- Fractions of compartments released due to a puff release (see Footnote 2, Table D.1)

- Option to select gas flow through the drywell on annulus from a selected compartment - MANN (see Footnote 9, Table D.1).

The variable inputs (those that change with time) are (see Footnote 3, Table D.1):

- Thermodynamic conditions of each compartment: pressure -- PI(J,I); temperature -- TMY(J,I); water vapor content -- VAPI(J,I); and temperature difference between bulk gas and walls -- DELTTI(J,I)

- Flow rates between compartments -- GI(J,K,I)

- Decontamination factors between compartments --
  EP(J,K,I) (see Footnote 4, Table D.1)

- Particle sizes -- DPE, DPL, TD

- Leak rates to atmosphere (leak decontamination factors'
  -- ELKP(J,I) (see Footnote 5, Table D.1).

Release fractions were calculated by CORRAL for each sequence analyzed by INCOR.

D.4 SAI-REACT MARK II AND CORRAL RESULTS

Tables D.2 and D.3 give several examples of REACT calculations for various release producing events in which the containment fails due to overpressure. Table D.4 gives examples of data produced with the CORRAL code. The REACT calculations served two purposes:

1) to verify the reasonableness of CORRAL-produced release fractions

2) to estimate the effect of decreasing containment overpressure failure size as well as the influence of the secondary containment.

For the first purpose, it can be seen that the REACT release fractions, as expected, do not exactly match the CORRAL data. Absolute and relative magnitudes of release fractions, especially elemental iodine and tellurium, are comparable. For the second purpose, it is evident that the $\xi\epsilon$ release size produces comparable releases to the γ' event, but that other releases do not. Therefore, a conservative ex-plant evaluation approach was used to include the probability of a $\xi\epsilon$ occurrence with that of the γ' mode and perform consequence evaluations using γ' release fractions, as defined with CORRAL.

Table D.1
FOOTNOTES TO SECTION D.3

(1) The spray parameter variables are:

HCSI	height of CSI spray above the floor
HCSR	height of CSR spray above the floor
DCSI	CSI droplet diameter
DCSR	CSR droplet diameter
CSI	flow rate
CSRI	flow rate for first set of CSR sprays
CSR2	flow rate for second set of CSR sprays
H0	equilibrium partition coefficient for I_2

$$H0 = 5000 \text{ for caustic spray}$$
$$= 200 \text{ for } HBO_3 \text{ spray}$$

CUT0V   fraction of an I_2 release below which airborne concentrations are in equilibrium with the spray liquid. CUT0V = 0.01 for the caustic and HBO_3 sprays.

TCSI	beginning time of CSI sprays
TCSIE	ending time of CSI sprays
TCSR1 TCSR1E TCSR2 TCSR2E	same for CSR sprays

The I_2 equilibrium calculations in CORRAL are carried out for the sprayed volume only (Compartment 1). A subroutine ELAM must be compiled along with CORRAL for the type of spray used. Three versions of ELAM exist:

ELAM   for HBO_3 sprays

ELAM/CAUS for caustic sprays

ELAM/NONE for sequences not having any spraying

(2) If the containment vessel is breached with rapid loss of containment atmosphere, then the variables necessary are:

TPUFF	when the puff occurs
XPUFF	the fraction of containment atmosphere still contained
DFPP	particulate decontamination factors
DFPOI	organic iodide decontamination factors
DFPI2	molecular iodine decontamination factors

(3) CORRAL divides the calculations into time nodes at which each time dependent variable is input for. The user has the option to select the number of nodes (NDATA), maximum of 20 and minimum of 1. The time input variable is TI(I).

(4) EP(J,K,I) variable representing the decontamination factors between compartments for particulates

EI2(J,K,I) variable for molecular iodine

(5) ELKP(J,I) variable representing the leakrates to the atmosphere for particulates

ELKI2(J,I) variable for molecular iodine

ELKOI(J,I) variable for organic iodide

(6) FDP(I)   variable representing the decontamination rates for particulates

FDI2(I)   variable for molecular iodine

(7) CORRAL is a multicompartment code where the various 'compart-
ments' are closed to one another. The compartment are
generalized compartments defined by the user.
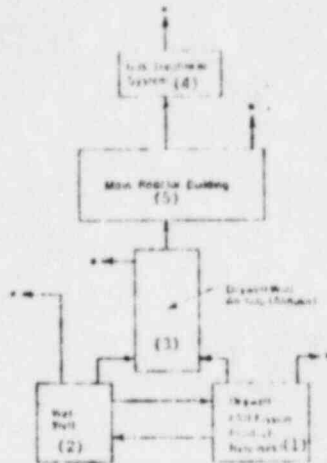
FIGURE D.2 General Flow Schematic for a
BWR - (*Possible Atmospheric
Source)

(8) DT defines the timestep used from the start of the calcula-
tions until a specified time, TJUMP1. DT2 defines the next
timestep to be used from TJUMP1 to the end of the problem,
TEND. Additional times to define the individual releases
are input to CORRAL as follows:

TMR - start of melt release

TMS - end of melt release

TEX1 - steam explosion (oxidation release), considered to
be a one step release

The vaporization release is considered to be an exponential
decay with its curve being defined in two phases: (1) rapid
increase and (2) very slow increase.

TVR1 - start of first phase of vaporization release
TVR2 - end of first phase and start of second phase
of vaporization release
TVRE - end of vaporization release

(9) If MANN is any integer other than 1, gas flow can proceed
through the drywell annulus from a selected compartment
number MCOMP (1 or 2).

Table D.2

	RADIONUCLIDE GROUPS								
FAILURE MODE	1 Noble Gases Xe,Kr	2A Elemental Iodine I,Br	2B Organic Iodide	3 Cs,Rb	4 Te[a]	5 Ba,Sr	6 Noble Metals Ru[b]	7 Rare Earths La[c]	8 Zr,Nb
γ	1	.067	.0003	.15C	.66.0	.0044	.032	.0042	.0042
γ	1	.044	.0005	.075	.115	.0044	.019	.0015	.0015
δ	1	.002	.00007	.0084	.011	.0002	.001	.00012	.0012
ε	1	.0007	.00006	.0013	.0015	.00004	.0003	.00004	.00004
εL	1	.117	.0005	.107	.290	.0055	.026	.0034	.0034
δL	1	.0036	.00052	.054	.159	.0029	.0045	.0019	.0019

(a) Includes Se, Sb
(b) Includes Rh, Pd, Mo, Tc
(c) Includes Y, Ce, Pr, Nd, Pm, Sm, Eu, Np, Pu

D-31

Table D.3

REACT RADIONUCLIDE RELEASE FRACTIONS FOR TW

FAILURE MODE	RADIONUCLIDE GROUPS								
	1 Noble Gases Xe,Kr	2A Elemental Iodine I,Br	2B Organic Iodide	3 Cs,Rb	4 Te(a)	5 Ba,Sr	6 Noble Metals Ru(b)	7 Rare Earths La(c)	8 Zr,Nb
Y'	1	.018	.0023	.117	.484	.0005	.034	.0056	.0056
Y	NC	NC	NC	NC	NC	NC	NC	NC	NC
ε	1	.0013	.0005	.0035	.014	.000016	.001	.00017	.00017
δ	1	.00018	.00006	.0012	.0048	.0000005	.000034	.00006	.00006
εc	NC	NC	NC	NC	NC	NC	NC	NC	NC
δc	NC	NC	NC	NC	NC	NC	NC	NC	NC

(a) Includes Se, Sb
(b) Includes Rh, Pd, Mo, Tc
(c) Includes Y, Ce, Pr, Nd, Pm, Sm, Eu, Nb, Pu

NC - Not Calculated

D-32

Table D.4

CORRAL RADIONUCLIDE RELEASE FRACTIONS
FOR MAJOR CONTAINMENT OVERPRESSURE EVENTS

FAILURE MODE	1 Noble Gases Xe,Kr	2A Elemental Iodine I,Br	2B Organic Iodide	RADIONUCLIDE GROUPS 3 Cs,Rb	4 Te(a)	5 Ba,Sr	6 Noble Metals Ru(b)	7 Rare Earths La(c)	8 Zr,Nb
TQUV γ'(C1)	1	.1	.007	.04	.046	.011	.0052	.00052	.00052
TW γ' (C2)	1	.057	.007	.023	.4	.0063	.04	.0047	.0047
TW εε (C2)	.75	.04	.0052	.0048	.046	.046	.0052	.00058	.00058
ATWS (C3)γ'	1	.050	.007	.024	.073	.0027	.0086	.00091	.00091
ATWS (C4)γ'	1	.25	.007	.20	.43	.029	.045	.0052	.0052

(a) Includes Se, Sb
(b) Includes Rh, Pd, Mo, Tc
(c) Includes Y, Ce, Pr, Nd, Pm, Sm, Eu, Np, Pu

APPENDIX E

OFFSITE CONSEQUENCE MODEL: CRAC

APPENDIX E

This appendix presents a brief description of the basic calculational
scheme of the CRAC code. In order to clarify the CRAC calculations, the
appendix is broken down into the following sections:

E.1   GENERAL CALCULATIONAL PROCEDURES OF CRAC

        The general procedure for calculation of risk in this study
follows the same assessment methodology of CRAC (Calculation of Reactor
Accident Consequences) as performed for the Reactor Safety Study (RSS).
The calculation of accident consequences using CRAC involves:

- The probability of radioactive release
- The amount and type of radioactive and nuclides released to the atmosphere
- The behavior of the radiation after it is released
- The number of people exposed to the radiation.

The methodology in CRAC may be summarized by the schematic outline of data and models of consequence calculations shown in Figure E.1. Input data include the accident release data, weather data, and population data. Calculation of the human consequences of a reactor accident can be mathematically expressed in a chain of factors as shown in Figure E.2.

The calculation of reactor accident consequences starts with the postulated breach of containment and release of radioactivity. Following the postulated release, the dispersion of radioactivity, cloud depletion, and ground contamination are calculated from atmospheric dispersion models. Using the resulting air and ground contamination, the dosimetric models determine the dose to individuals. Early and latent doses to individuals are determined from a number of exposure pathways as shown in Figure E.3.
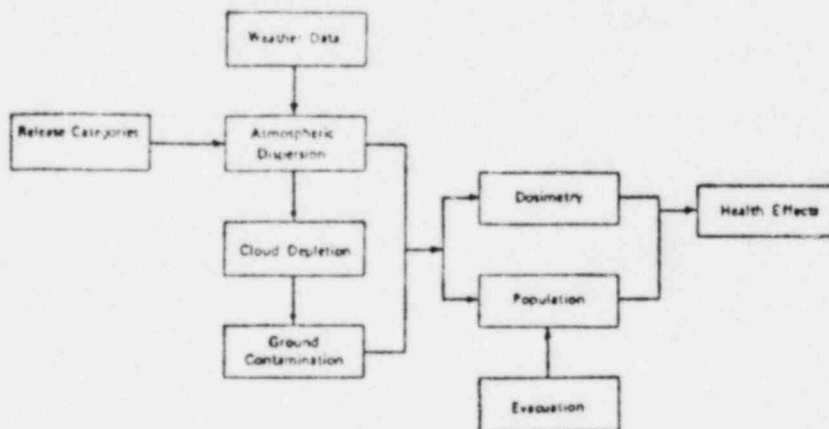
Figure E.1 Schematic Outline of Consequence Model (CRAC)

Early doses accrue from exposure to the passing cloud (direct radiation and inhalation) and early exposure to ground contamination. Chronic doses accrue from exposure accumulated at later times including doses from ingestion of contaminated food products, inhalation of resuspended ground contamination, and long term direct exposure to ground contamination (greater than 7 days).

The health effects are then determined from the calculated doses and the population around the plant. Several mitigating measures including population evacuation and relocation, and food and land interdiction are considered in the determination of the population doses and health effects.

CONSEQUENCE = RADIOACTIVE INVENTORY (Curies)

X

RELEASE FRACTION (Dimensionless)

X

ATMOSPHERIC DISPERSION (Seconds/Meter^3)

X

POPULATION EXPOSURE (Number of persons
times breathing rate
per person in M^3/sec.)
X

DOSE-CONVERSION (Rem/Curie of intake)

X

DOSE-RESPONSE (Deaths or injuries/person-rem)*
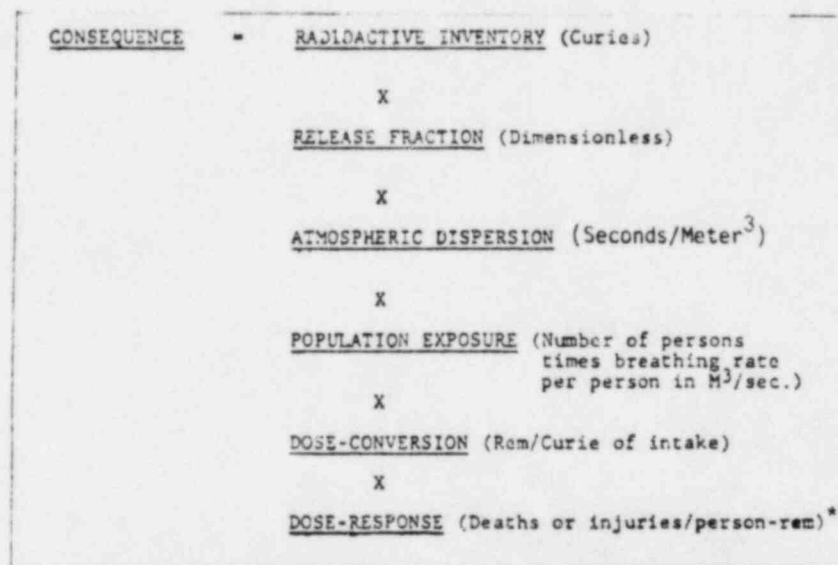
* Must incorporate dose threshold for early fatalities

Figure E.2. Accident Consequence Factors
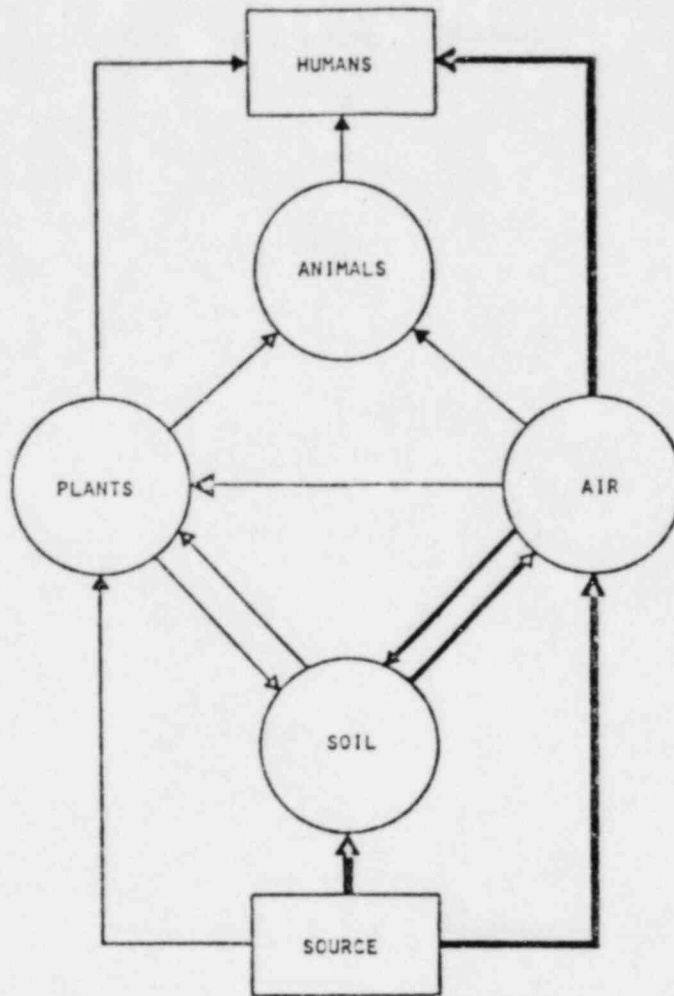
Figure E. 3 Principal Exposure Pathways

The health effects in CRAC may be divided into three categories: Early, latent, and genetic effects. Early health effects refer to injuries and fatalities occurring within a year of the accident. The latent effects refer to the somatic effects which later are manifested in the form of cancer during a plateau period assumed to be about thirty years. Genetic effects refer to effects seen in subsequent generations.

The results of the CRAC consequences model are displayed as a set of complementary cummulative distribution functions (CCDF) for specific consequences. These distributions are determined from the calculated magitude of each consequence for each combination of postulated accident release, weather, and population as well as the probability of each such combination.

The consequence Code (CRAC) used in WASH-1400 is summarized in Table E.1. The basis CRAC methodology, the dosimetric model, and the health effect models, were adopted for this analysis. Some modifications were made to adapt CRAC to the Limerick site-specific requirements. These site-specific effects include:

- The probabilities and release fraction input data (see 3.5 and 3.6)

- The Limerick site meteorology

- The population for the Limerick area.

The remaining subsections of this Appendix discuss the various models used in the limerick CRAC calculation and how they were inplemented.

E.2   BEHAVIOR OF RADIONUCLIDES IN THE ATMOSPHERE

In the event of radioactive release, radionuclides are released into the air and dispersed. Figure E.4 shows a side view of this process. The population in the area under the plume receive radiation in three ways:

1.   From external radiation received directly from the radio-isotopes in the cloud (cloudshine)

2.   From radiation received following inhalation

3.   From radiation received from material deposited on the ground (groundshine).

Table E.1
Consequence Code Model Details
as Applied in WASH-1400

	ITEM/MODEL	
I	Release Category	9 PWR categories* 5 BWR categories *PWR 1 was subdivided further to represent 2 distinct heat releases; PWR 1A & PWR 1B
	No. of Isotopes	54 Isotopes
	Fission Product Inventory	Initial source strength of the potential radioactive source was calculated by using ORIGEN code (Bell, 1973)

II	Weather Data	6 Stability Classifications, A-F
		8 Wind Velocity Groups per
		  classification each with rain/
		  no rain condition, and
		  associated probabilities.
		6 distinct composite sites
		
		Each site had at least one
		year of complete recorded weather
		data including hourly
		data on rain occurrence.
		
		The consequence code
		used completely
		stratified samples. In
		order to ensure complete
		coverage, every four
		days plus one hour
		starting time was
		selected and the weather
		condition for the next
		10 to 30 hours was
		updated every hour. Thus,
		90 weather samples are
		utilized.
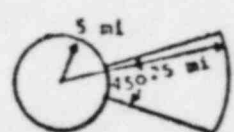
Item/Model	
III Atmospheric Dispersion Model Note: The radioactive cloud concen- tration is cor- rected for plume rise, allowance for release durations of greater than 0.5 hour , and a Spatial modifi- cation for cloud depletion by dry and wet deposition and finally for radioactive decay.	In general $$\frac{X}{Q} = \left[\pi\sigma_y\sigma_z u\right]^{-1} e^{\left[\frac{y^2}{2\sigma_y^2} - \frac{z^2}{2\sigma_z^2}\right]}$$ where the lateral concentration is assumed constant, the lateral width is taken as $$3\sigma_y = \sqrt{2\pi}\,\sigma_y\, e^{\frac{y^2}{2\sigma_y^2}} \quad \text{for } -1.5\sigma_y \le y \le 1.5\sigma_y$$ For building effects when h = 0 $$\frac{Xu}{Q} = \frac{1}{\pi\sigma_y\sigma_z + CA}$$ The standard deviation σ_y & σ_z are evaluated at each radial position as $$\sigma = A\,x^B + C$$ where A, B, C are parameters associated with each pasquill stability category, (Martin-Tikvart coefficients). The vertical diffusion, σ_z is not allowed to exceed a maximum, in this case, 0.8 L, where L is the mixing height (Holzworth 1972)
Plume Rise	The plume centerline height, h is determined by using a relationship developed by Briggs (1969) For unstable conditions $$\Delta h = 1.6F^{1/3}u^{-1}x^{2/3}$$ out to $x = 1.25Q_h^{2/5}$ For stable conditions: $$\Delta h = 2.9(F/us)^{1/3}$$ out to $X = 2.4u(S)^{-1/2}$ In these equations h is not allowed to exceed the mixing layer depth L. Δh = plume height above an initial emission height F = boyancy flux = $3.7 \times 10^{-5}Q_h$ Q_H = energy release rate (calories/sec) S = stability parameter (sec^{-2})

E.0.

Item/Model	
Expansion Factor	$$\frac{3\sigma y}{3\sigma y_o} = \left(\frac{t}{t_o}\right)^{1/3}$$ where $3\sigma y$ = new lateral width $3\sigma y_o$ = reference width t_o = reference time (0.5 hr) t = duration of release
Cloud Depletion	The dry deposition flux of the aerosols to the surface is taken to be $v_d x_o$ where v_d is the dry deposition velocity. The fraction of the cloud that is deposited is $$fr = 1 - e^{-v_d t/\bar{z}}$$ $$fr \approx v_d t/z_k \quad \text{since } \frac{t}{z_k} \text{ is small}$$ where $t = \frac{\delta x_k}{u_k}$ $$v_d = \begin{cases} 0 \text{ for Noble gases} \\ 1 \text{ cm/sec otherwise} \end{cases}$$ The wet deposition is expressed as a simple removal rate characterized by a washout coefficient $\Lambda (\sec^{-1})$. The plume concentration decreases according to $$\chi = \chi_o^{-\Lambda(t-to)}$$ where $t-t_o$ = time since onset of precipitation at time t_o Λ is assumed zero for noble gases otherwise, it is assumed 10^{-4} for stable conditions and 10^{-3} for unstable conditions.

	Item/Model	
IV	Population Data	16 Distributions Each of the 100 nuclear reactors in 68 reactor sites was assigned to one of the 6 composite sites. The actual population data around the reactors assigned to a particular site was calculated for 16 angular sectors then ranked from highest to lowest according to cumulative population within 50 miles. The highest ranked sector, for instance, assigned to sector 1, is the average of the population distributions of the highest most populous sector of the reactors assigned to the composite site. Land use fractions were also generated for each composite site.
V.	Evacuation Model [See Note.]	The population at each mesh point i is assumed to move radially away from the reactor at an effective speed until the cloud reaches them, then move in the circumferential direction. It is assumed that 30% move at 7 mph 40% move at 1.2 mph and 30% have zero effective speed The evacuation area is assumed keyhole in shape centered at the prevailing wind direction at the time of release with 5 mile and 25 mile dimensions at 45° angle.

Note: This evacuation speed distribution was not used in the final evaluation. Only the median speed of 1.2 mph was used with a multiplying factor of 1.5.

Table E.1 (continued)

	Item	
VI	Dosimetry	
1.	Internal	
a.	Inhalation Model	The dose model used for inhalation doses is the ICRP Task Group Model with some modifications to reflect more recent data. For the noble gases, the retention model of Barnard and Snyder (1975) was utilized. The dosimetry model to the GI tract is essentially due to Eve (1966). The same models are used for the inhalation of resuspended radionuclides.
b.	Ingestion Model	A modified inhalation model was utilized where the residence time of the radionuclides in the respiratory tract is assumed zero. To account for the dose received by children a correction factor is used.
2.	External Dose	All external dose conversion factors were computed with the EXREM III computer program developed by Oak Ridge National Laboratory. Only photon doses from an assumed semi-infinite cloud and an infinite smooth plane were considered. Finite cloud dose correction factors were applied to the cloud dose, and shielding factors to the ground contribution.

	Item	
VII	Health Effects	Subdivided health effects into: 1. early and continuing somatic effect; includes deaths and morbidities that are manifested within a few weeks to one year or so. 2. late somatic effects which include latent cancer fatalities and morbidities and benign thyroid nodules 3. Genetic Effects
	Fatalities	The fraction is computed as: $$\text{Early Fatalities} = f_1 + (1-f_1)f_2 + (1-f_1)(1-f_2)f_3$$ where f_i = fraction calculated for 1 = Bone marrow dose 2 = Lung 3 = GI tract Early fatalities include the deaths which occur within a few weeks to one year from the reactor accident.
	Early Morbidities	Early morbidities based on: Respiratory Impairment* GI Tract Morbidity Thyroid Morbidities Sterility Congenital malformations and Growth Retardations Cataracts, prodomal vomiting *WASH-1400 results show early morbidities due to this health effect only.

E-8

		Item	

		Late Somatic Effects	Late somatic effects include
			  Latent cancer*
			  morbidities
			  benign thyroid nodules
			
			*Calculated for individual organs:
			  leukemias for irradiated
			    children in utero
			  GI tract (subdivided into
			    stomach, pancreas and
			    the rest of the alimentary
			    tract)
			  Bone Cancer
			  Lung
			  Breast**
			
			**Dose effectiveness factor
			is not applied to this health
			effect since there is no
			evidence of reduced cancer
			rate due to fractionated
			doses received at high dose
			rates.

VIII	Dose Limits		There are essentially three
			competing risks for mortality:
			            LD 50/60
			Bone Marrow (30d)* 510 Rads
			  (Figure VI 9-1)
			Lung (1y) 1900 Rads
			  (Figure VI 9-3)
			GI tract (7 days) 3500 Rads
			  (Figure VI 9-c)
			
			*This accounts for supportive
			treatment
			
			For illness, the dose criteria
			is given as follows:
			
			             SD 50
			Respiratory Impairment 4500 Rads
			  (Figure VI 9-6)
			  Linear from 3000-6000
			  with probability of .05 to 1.0

		Item	

IX	Economic Model		The economic model estimates the direct costs of mitigating measures that are undertaken to reduce the effects of a reactor accident. The total costs incurred will depend on the specific measures undertaken for:
			1. Early exposure
			  evacuation costs
			  value of crops & milk condemned
			2. Chronic Exposure computed as
			  Interdiction costs
			  loss in value of public and
			  private property
			  loss of income during re-
			  locationand temporary unem-
			  ployment and relocation costs
			or Decontamination costs
			or both

		Dose Criteria	**Exposure** **Dose**
			
			I. External:
			  Low population 10 rem to the whole body
			  Density area in 30 years
			  Urban areas 25 rem to the whole body
			          in 30 years
			
			II. Ingestion via milk
			  Sr 3.3 rem to the bone
			          marrow in first
			          year
			  Ca 3.3 rem to the whole
			          body
			  I 10.0 rem to the
			          thyroid
			
			III Ingestion via
			  "Other pathways"
			
			  Sr 2.0 rem to the bone
			          marrow in first
			          year
			  Ca 2.0 rem to the whole
			          body.

Bases on WASH-1400 exposure dose coefficients (E.1) the "ground dose" contributes most to early fatalities and long term health effects (unless evacuation takes place within several hours).
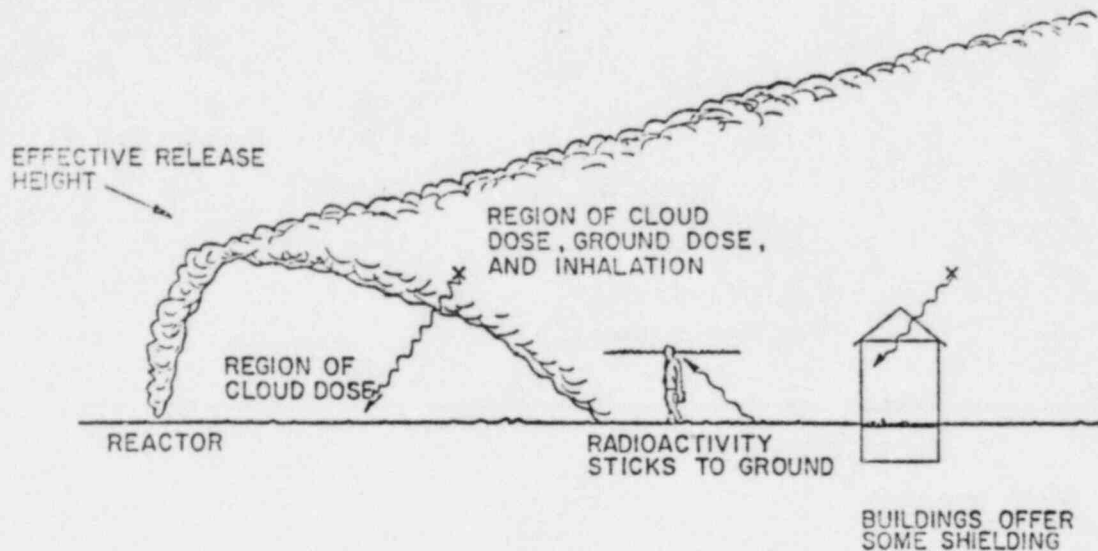

Figure E.4. Side View of Radioactive Plume

The principal contributors in the CRAC model (E-3) to the determination of the radioactive plume characteristics are:

- The dispersion of the plume due to atmospheric, terrain, and stack/building effects (E.2.1)

- The height of release of the plume which is a function of the energy of release from containment (E.2.2)

- The weather conditions at the time of release E.2.3).

E.2.1 Dispersion and duration of Release

The dispersion of the radioactive plume is affected by several factors including:

- Plant specific terrain roughness

- Radioactive decay

- Deposition on obstacles and the ground.

The specific terrain around Limerick was considered in the explant analysis by variation of plume parameters sensitive to turbulence-producing ground effects. Specifically, the z direction diffusion coefficient (σz) was altered from a flat smooth surface, to correspond to a rougher surface. This is still somewhat conservative for the region around Limerick since σz for forested regions is still larger than the value used.

Figure E.5 shows a top view of the plume path. The width of the high dose region varies depending on several conditions including meteorology. On a clear day, the plume will spread out faster than on a clear night primarily due to wind fluctuations and turbulence.
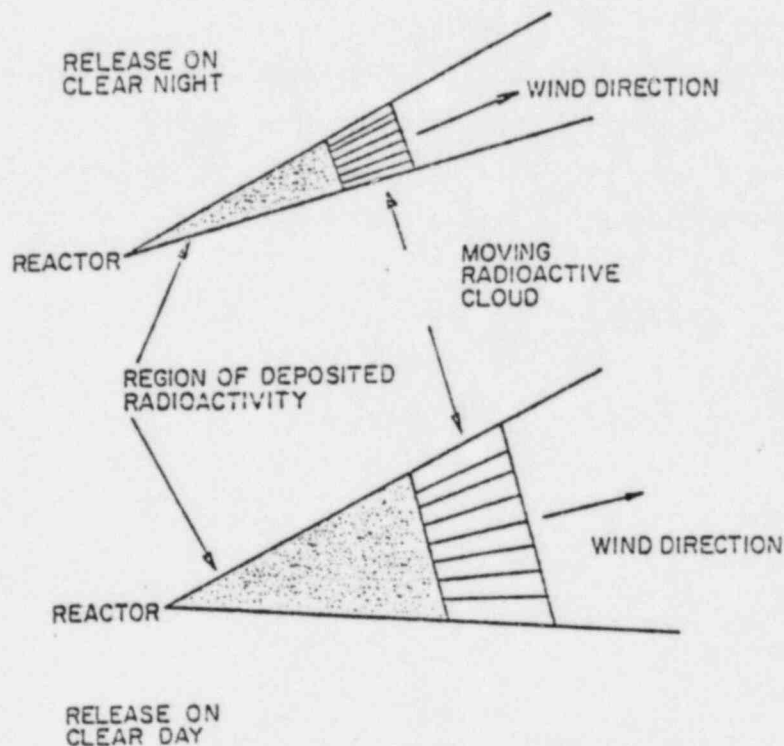
Figure E.5. Top View of the Plume

Width of the plume is also affected by the duration of release. In WASH-1400 a 3 minute release was used to model the puff release (E.2). Subsequent data indicates that a 30 minute release produces a more lateral diffusion estimate.

E.2.2   Plume Rise

WASH-1400 made use of plume rise formula developed for smoke stack plumes to predict the effective vertical size and dispersion of a release. However, there are many plume rise formula and they rarely agree outside of their specific range of applicability. In WASH-1400 the Briggs plume rise formula was used in the consequence code with a power of 0.2 to generate plume size data. In the Limerick analysis, the Briggs formula was used with a power of 0.33 vs 0.2 in order to better fit existing empirical data. The altered Briggs formula is also in keeping with NRC's site-specific review. (E-2). In calculating plume height rise for the Limerick site, two wind data measurement deviations were used depending on the release energy rate from the reactor during aerosol release.

E.2.3   Meteorology

The CRAC calculations for Limerick incorporate seasonal data on stability, wind speed, precipitation and a wind rose. These values were obtained from five years of data (1972-1976) taken at the Limerick site by PECo.

E.2.3.1 Wind

For the WASH-1400 composite site BWR analysis a wind rose was defined which assigned equal probability to wind coming from all sectors, with population variations by sector used to factor in the probability of a high population area corresponding to the wind direction during an accident. Variation of wind direction in the plume calculations, and

wind shear with altitude were not considered in WASH-1400. (It has since been shown that (E-5) wind shear variations do not significantly affect the plume dispersion calculations.) The Limerick analysis, uses seasonally varying wind roses, stability, and wind speed.

The wind measurements used in the Limerick consequence calculations are determined at the start of the radioactive release. No subsequent variations are accounted for.

E.2.3.2 Precipitation

Another consideration is the effect of precipitation on the dispersion of the plume (E-4). As rain falls through the plume, radioactive mterial falls with the rain to the ground. Thus, ground concentration of radiocativity is raised. The effects of a rainstorm on dispersion are controlled by the following variables:

- Washout coefficient - the amount of radioactivity interacting the rain

- Runoff - the amount of water not absorbed into the ground

- Rain intensity - the variation with time

- Intersection - the distance from the reactor at which the plume intersect with the rainstorm.

Occurrence of rain will tend to increase the number of early fatalities, and decrease latent fatalities since the radioactivity is dispersed in a smaller area in more concentrated amounts. The WASH-1400 precipitation model, which does not consider runoff or time-varying rainfall intensity, was used in the Limerick analysis.

E.3   PUBLIC RESPONSE MODEL

Since the consequences of a nuclear power plant accident are
dependent on public response, a response model must be included in con-
sequence calculations. The public response model used in this study is
the same as that used in WASH-1400, which considered two main facets of
the public response: evacuation and shielding.

E.3.1   Evacuation

The quickness and effectiveness of an evacuation are mainly
controlled by the following:

- Public participation in the evacuation

- Warning time for evacuation

- Speed of evacuation

- Population density of evacuated area

- Emergency preparedness.

In the WASH-1400 evacuation model, the evacuated area is in the
shape of a keyhole centered on the prevailing wind heading at the time of
release (Figure E.6).
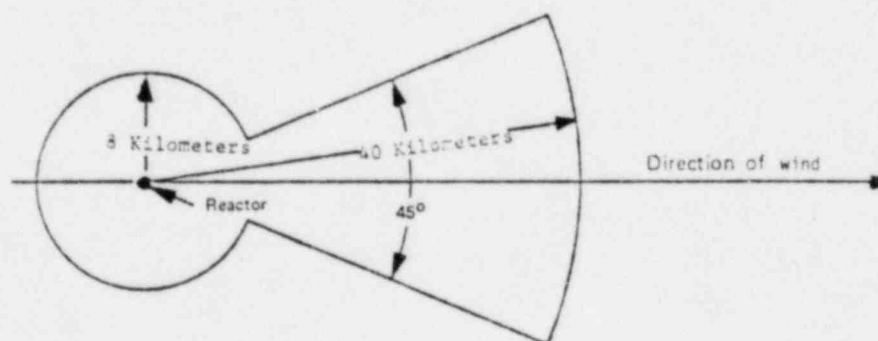
Figure E.6. Evacuation Area -- WASH-1400

In the Limerick analysis, the site-specific population distribution (Table E.7) and warning time are used to develop inputs to the CRAC code. The warning time depends upon the accident sequence. The population response is fixed, in that all persons in the evacuation portion of the effected zone head outward radially and all persons in the keyhole protion head tangentially at a constant rate of speed. In WASH-1400 the intention was to divide population into 3 groups with 3 effective evacuation speeds, in order to adequately model different levels of population participation in an evacuation. Thus 30% of the population would move with an effective speed of 0.2 mph, 40% would move with an effective speed of 1.2 mph, and 30% would move with an effective speed of 7 mph. In fact analysis of several sites showed that only the medium speed (1.2 mph) need be used if the resulting casualties were scaled by a factor of 1.5. The Limerick analysis uses the same procedure actually used in WASH-1400, i.e., a medium evacuation speed of 1.2 mph and a multiplying factor of 1.5.

E.3.2   Shielding

E.3.2.1   Cloudshine and Groundshine

People caught within or under a radioactive cloud will receive an external dose to the whole body due to gamma radiation. Buildings offer some attenuation of doses since the walls of the building will a rb and scatter gamma radiation. Recent EPRI studies (E-6) have shown that the benefit of shielding in some areas of the country may outweigh the benefits of evacuation for much of the population.

In the Limerick ex-plant consequence model, dose assessment includes consideration of cloudshine and groundshine shielding. The form of the shielding model used in Limerick is the same as that used for WASH-1400. People in structures at the time of exposure receive a lower whole body dose than those that are unprotected. A shielding factor (SF) is defined, which is the ratio of the interior dose to the dose that would have been received with no protection.

Since structures have regionally related characteristics, an assessment was made for the area around Limerick. The methodology for determining the overall shielding factor involves weighted averaging of shielding factors. These shielding factors were developed for various human situations. This model assumed that people who were outdoors or commuting would not seek shelter. Additionally, 5% of the people were assumed to take no action, even if advised to. This model also uses regional data on the percentage of brick houses. The values for ground-shine and cloudshine dose shielding factors used in the Limerick analysis are found in Table E.2a and E.2b respectively. When compared with the shielding factors of 0.33 for groundshine and 0.75 for cloudshine, as used in WASH-1400, the Limerick shielding factors are enhanced somewhat, principally because of the effect of more adequate shielding.

E.3.2.2 Inhalation

The effective inhalation rate for the peopulation affects the latent consequences of a nuclear accident. When the radioactive plume passes over a populated area, people may inhale radionuclides from the passing cloud. The breathing rate input to the CRAC code is an effective breathing rate; it is a measure of how much radiation the public receives through inhalation. The breathing rate used in WASH-1400 and the Limerick PRA was 2×10^{-4} m^3/s.

Credit was given only for the moderate reductions in inhalation dose as a result of sheltering with some subsequent effective ventilation action. The values for these sheltering factors were taken from Reference E-14. For ventilation rates consistent with closed windows, shut-down outside ventilation systems, and the reduced leakage consistent with houses equipped for energy conservation (typical of the Northeast), the indoor dose ratio, or inhalation shielding factor, is 0.53.

Table E.2a

Shielding Factors for Groundshine Given Sheltering

People at Home
(90% w/basements, 60% w/brick homes)

	Brick Basement	Brick House	Wood Basement	Wood House
Fraction of total	0.40	0.04	0.23	0.02
SF	0.05	0.20	0.10	0.40

People at Work

	Large Building	Brick Basement	Brick Building	Wood Basement	Wood Building
Fraction of total	0.065	0.076	0.008	0.042	0.005
SF	0.01	0.05	0.20	0.10	0.40

People Commuting or Outdoors

	Commuting	Outdoors
Fraction of total	0.05	0.062
SF	0.50	0.70

TOTAL SF - 0.142   WASH-1400 SF - 0.290 (Pennsylvania
                          (No sheltering   Region)
                          sought)

$$SF = 0.95* (0.142) + 0.05 (0.290) = \underline{0.150}$$

*Portion of total population participating in emergency response

Table E.2b

Shielding Factors for Cloudshine Given Sheltering

People at Home
(90% w/basements, 60% w/brick homes)

	Brick Basement	Brick House	Wood Basement	Wood House
Fraction of total	0.40	0.04	0.23	0.02
SF	0.40	0.60	0.60	0.90

People at Work

	Large Building	Brick Basement	Brick Building	Wood Basement	Wood Building
Fraction of total	0.065	0.076	0.008	0.042	0.005
SF	0.20	0.40	0.60	0.60	0.90

People Commuting or Outdoors

	Commuting	Outdoors
Fraction of total	0.05	0.062
SF	1.00	1.00

TOTAL SF - 0.531   WASH-1400 SF-0.710 (Pennsylvania
                          (No sheltering   Region)
                           sought)

$$SF - 0.95* (0.531) + 0.05 (0.710) = \underline{0.540}$$

*Portion of total population participating in emergency response

Table E.3

Shielding Factors For Inhalation Doses Given Sheltering

People at Home

	Basement	No Basement
Fraction of total	0.63	0.06
SF	0.48	0.53

People at Work

	Large Building, Brick or Wood	Basement
Fraction of total	0.078	0.118
SF	0.53	0.48

People Commuting or Outdoors

	Commuting	Outdoors
Fraction of total	0.05	0.062
SF	1.0	1.0

TOTAL SF - 0.544   WASH-1400 ÷ 1.0
                          (No Sheltering)

$$SF - 0.95* (0.544) + 0.05 (1.0) = \underline{0.57}$$

*Portion of total population participating in emergency response

Table E.3 gives the calculations for the final shielding factor. In should also be noted, from Refernce E-14, that approximately a 10% reduction is assumed for persons in their basements. Consequently, given that 95% of those inside follow directions, a total shielding factor of 0.57 is calculated.

E.4   HEALTH EFFECTS MODEL

One of the measures of consequences of a nuclear power plant accident is health effects on the public. Figure E.7 gives a summary of the isotopes which affect the consequences to the public. Health effects can be divided into two categories; short term (early) effects, which are apparent within one year from exposure, and long term (latent) effects, which can show up during the remainder of a lifetime. Cumulative Complementary Distribution Functions (CCDF) are ultimately obtained in the Limerick analysis for early and latent fatalities.
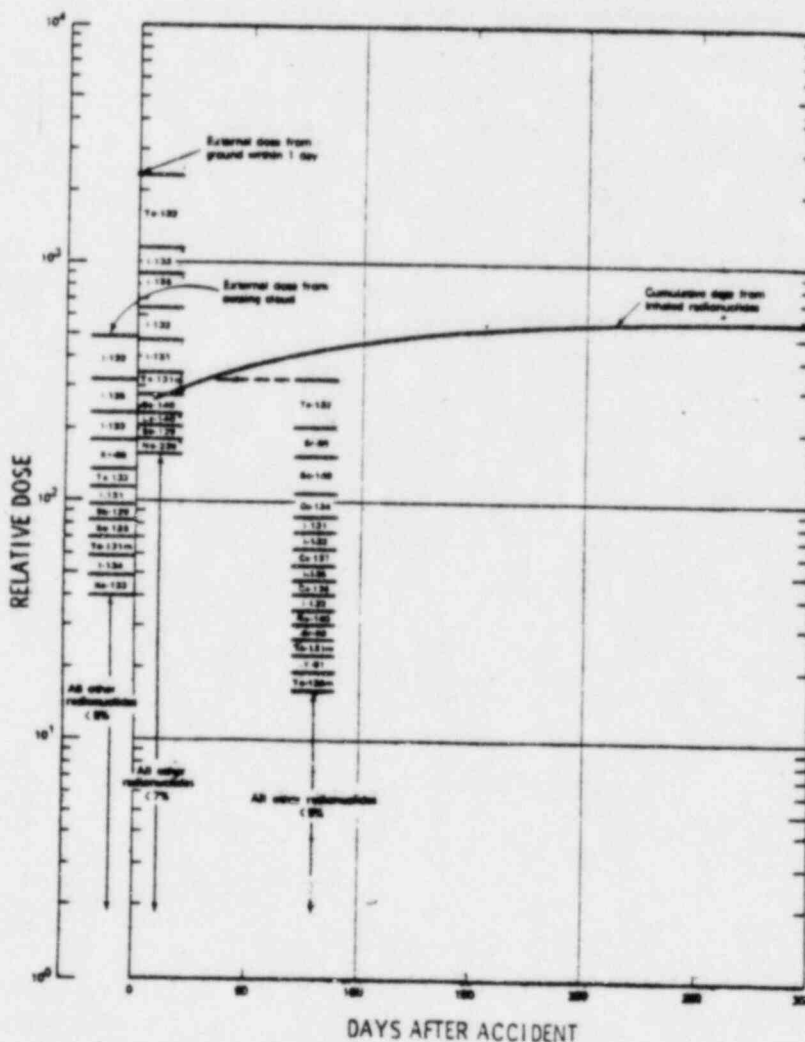
Figure E.7.   Relative Doses to Bone Marrow at 0.5 Miles from Reactor

E.4.1   Early Effects

Early fatalities, injuries, and illnesses are generally caused by exposure to large amounts of radiation during a brief time. Early fatalities due to the bone marrow damage occur above a threshold level of exposure of 150 rem. Higher thresholds are used for the lungs and gastro-intestinal tract. These early effects, are determined principally from:

- Doses to bone marrow
- Doses to the lungs
- Doses to the gastro-intestinal (GI) tract.

The early effects are reduced if it is assumed that people exposed to radiation receive medical treatment. WASH-1400 estimated that in the event of an accident involving radioactive release, 2500-5000 people could receive supportive treatment such as blood transfusions, while 50-150 people could receive heroic treatments, such as bone marrow transplants. The Limerick analysis does not include heroic treatment.

E.4.2   Latent Effects

Latent effects, are caused by exposure to small amounts of radiation over long periods of time. Such effects include:

- Sterility
- Genetic effects
- Effects on unborn
- Cancer
- Latent Fatalities (shortened life span).

E-21

The BEIR report (E-15) studied the long term effects of radiation on the Japanese atomic bomb survivors. The risk estimates in the BEIR report are based on extrapolations of these data. The extrapolations are thought to be conservative for low-level exposure, since the BEIR report did not consider a threshold dose (i.e., a dose below which there would be zero incidence probability of cancer). In the Limerick analysis, the standard CRAC methodology and input coefficients were used as defined in the user's manual (E-3).

E.5   COMPARISON WITH COMPOSITE SITE

The WASH-1400 composite site analysis assumed that the wind was equally likely to be blowing in any given direction. (A justification for this is that the wind rose did not vary directionally by any more than a factor of 3.) For a specific site there may be significant differences when the actual population and wind roses are combined. This accentuated difference is apparent when the conditional probability of the sector with the largest population being exposed is compared for the composite site and the worst season at the Limerick site (Table E.4).

Populations in the highest population sectors are similar between the WASH-1400 composite site and the Limerick site; however, the methods used to model them in CRAC, as shown in Table E.4, can lead to substantial differences as shown in Table E.5.

Table E.5 summarizes this comparison of the conditional probability of the high population sectors being exposed during a postulated release of radionuclides between the WASH-1400 composite site and the Limerick site-specific case. The composite site has a very low probability of exposing the two highest population sectors due to the way in which the WASH-1400 consequence model was constructed. For the site-specific Limerick analysis, the data suggests that there is generally a much higher probability associated

Table E.4

COMPARISON OF THE WASH-1400 COMPOSITE SITE DATA WITH THAT FOR LIMERICK

		WASH-1400 COMPOSITE SITE			LGS SITE-SPECIFIC		
RANK OF SECTOR BY POPULATION	ORIGIN OF SECTOR	CONDITIONAL PROBABILITY OF SECTOR BEING EXPOSED	WIND ROSE	TOTAL CONDITIONAL PROBABILITY OF SECTOR BEING EXPOSED	Ranking of Sectors	WINDROSE* 30 FT SUMMER 1974	170 FT WINTER 1974
1	1	.0446	1.0	.00446	(G)**	.06	.2
2	2	.00446	1.0	.00446	(F)	.12	.15
3	3, 4	.00893	1.0	.00893	(H)	.05	.05
4	5, 6	.00893	1.0	.00893	(P)	.03	.04
5	AVG. of NEXT 6	.0268	1.0	.0268	(B)	.04	.04
6	AVG. of NEXT 6	.0268	1.0	.0268	(E)	.10	.06
7	AVG. of NEXT 12	.0536	1.0	.0536	(J)	.04	.06
8	AVG. of NEXT 22	.0902	1.0	.0902	(D)	.07	.04
9	AVG. of NEXT 22	.0982	1.0	.0982	(A)	.09	.04
10	AVG. of NEXT 23	.1030	1.0	.1030	(K)	.03	.05
11	AVG. of NEXT 22	.0982	1.0	.0982	(C)	.06	.05
12	AVG. of NEXT 22	.0982	1.0	.0982	(Q)	.05	.04
13	AVG. of NEXT 20	.0893	1.0	.0893	(R)	.05	.02
14	AVG. of NEXT 20	.0893	1.0	.0893	(M)	.05	.05
15	AVG. of NEXT 21	.0948	1.0	.0948	(N)	.07	.06
16	AVG. of NEXT 22	.0982	1.0	.0982	(L)	.06	.03

*Also conditional probability of sector being exposed

**Population sector designator (Table E.12)

E-23

with the wind blowing in the direction of highest population. Table E.5 reflects the approximate increase in the conditional probability of the wind blowing in the direction of highest population.

Table E.5

TOP TWO(2) SECTORS WITH MAXIMUM POPULATION

| RANK BY POPULATION | CONDITIONAL PROBABILITY OF SECTOR BEING EXPOSED | | |
	COMPOSITE SITE FROM WASH-1400	LIMERICK SITE	FACTOR LARGER FOR LIMERICK
1	.00446	.2	~45
2	.00446	.15	~34

E.6   CRAC INPUT

The inputs to the CRAC code are summarized in Table E-6.

Wind roses for the LGS site are shown on Figures E.8 and E.9.

Table E-7 shows the sector designations and the population by sector.

Table E-8 compares the radiological core inventory used in the Limerick analysis to that used in WASH-1400. The amounts are similar for the majority of the isotopes between Limerick and WASH-1400. The major difference is seen in the particulates. The Cesium (Cs), Antimony (Sb) and Tellurium (Te) isotopes are generally greater for WASH-1400 than Limerick. However, the Rubidium (Rb), Ruthenium (Ru), and Americium (Am), isotopes are generally greater for Limerick than WASH-1400 isotopes.

TABLE E.6 INPUTS TO CRAC CODE

Data Name	Value
Maximum Distance of Evacuation (mi)	25
Evacuation Velocity (mph)	1.2
Time Lag before Evacuation (days)	0
Travel Distance while Evacuating (m)	8000
Angle of Evaluated Downwind Sectors	45^0
Criteria of Duration of Release for Evacuation	3
Cloud Shielding with Sheltering	0.54
Cloud Shielding without Sheltering	0.71
Ground Shielding with Sheltering	0.15
Ground Shielding without Sheltering	0.29
Breathing Rate m^3/s	1.1×10^{-4}
Release Height-high (m)	25
Release Height-low (m)	0
Isotopes	Limerick core inventory*
Acute Health Effects	Same as WASH-1400*
Latent Health Effects	Same as WASH-1400*
Spacial Mesh Description	Limerick site-specific*
Population Data	1970 census & PECo data (see Table E.7)
Meteorological Data	Limerick wind roses shown on Figures E.8 and E.9

*Input values on computer tape
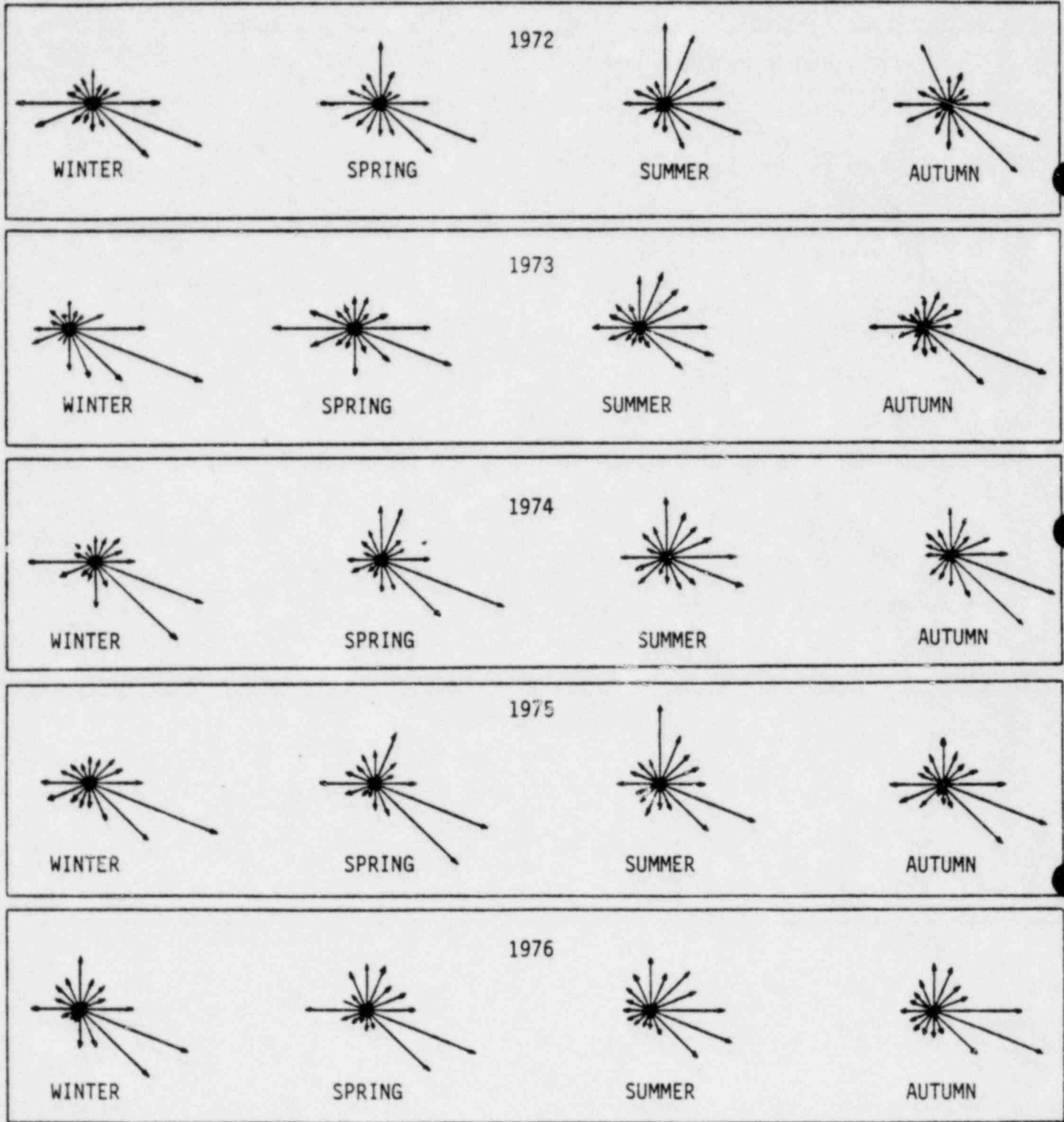
Figure E.8   Wind rose* for the Limerick Generating Station for five years of
Meteorological Data by season at a Tower Height of 30 feet

* Probability of wind bearing   during each season
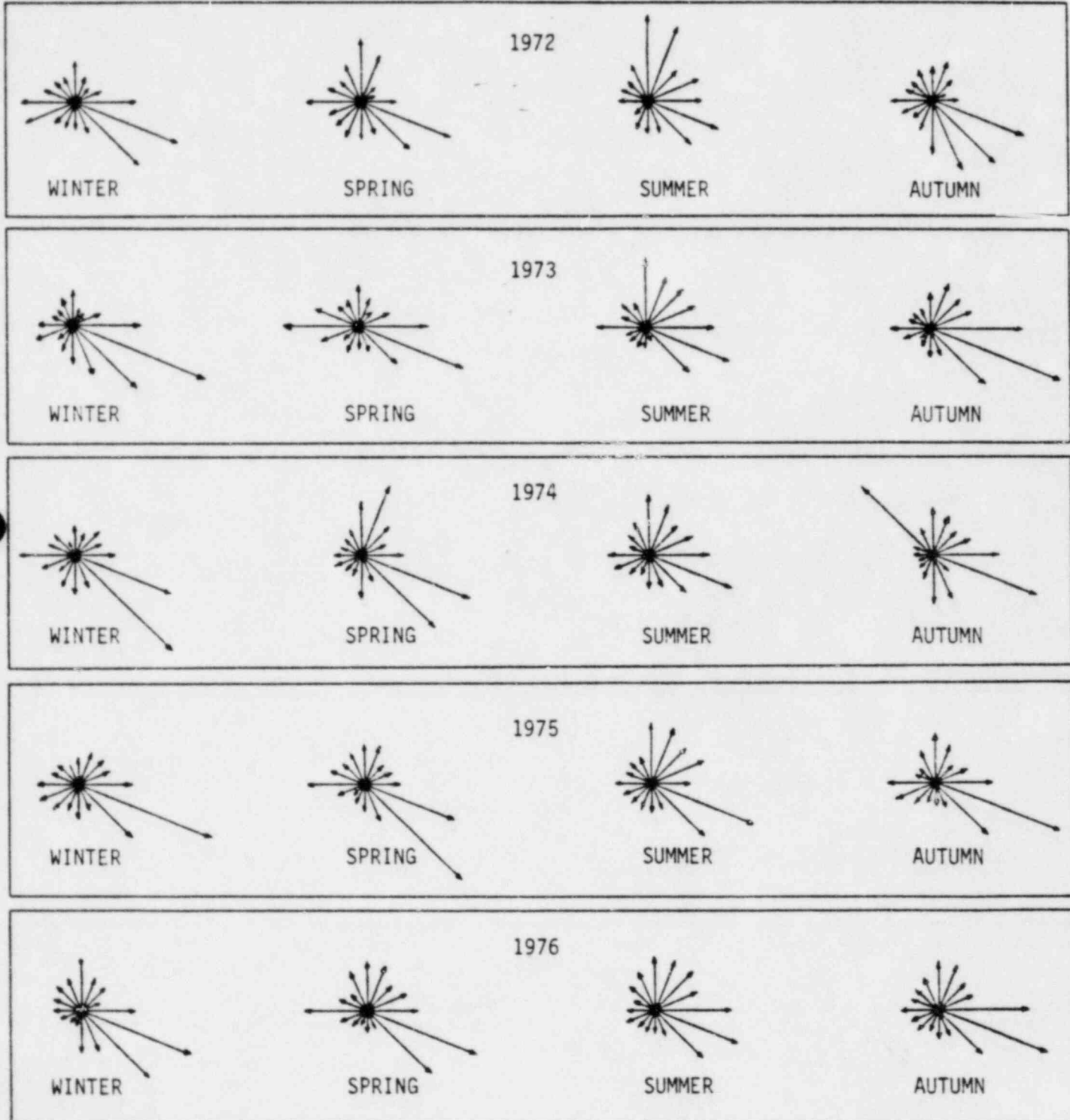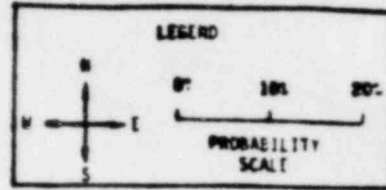
Figure E.9 Wind rose* for the Limerick Generating Station for five years of
Meteorological Data by season at a Tower Height of 175 feet

* Probability of wind bearing during each season

Table E.7a

LIMERICK PA
1970 ESTIMATED U.S. POPULATION BY SECTOR & RADIUS
RADII FROM 0 TO 100 MILES

RADIUS
(MILES)

SECTOR	CENTERLINE (DEGREES)	1 (0-10)*	2 (10-20)	3 (20-30)	4 (30-40)	5 (40-50)	6 (50-60)	7 (60-70)	8 (70-80)	9 (80-100)	TOTAL
A	0.0	9334	6253	40245	42944	27908	4549	7279	109044	200695	448251
B	22.5	4211	19178	188605	170433	35189	35493	11859	4005	34236	503209
C	45.0	3933	21396	14868	22233	38547	40211	150875	173502	445346	910911
D	67.5	2759	31121	38625	17188	28712	148947	535605	1191800	9123754	11125511
E	90.0	13294	52056	94689	164754	338592	55085	116255	253877	242603	1331205
F	112.5	15505	131917	724262	610275	73658	65533	12221	75607	19475	1728453
G	135.0	10437	90554	1255972	566597	103147	27889	16547	28815	133359	2233317
H	157.5	32092	24552	250377	25563	21282	61524	63405	11983	41854	532632
J	180.0	5084	60017	29018	332241	18248	13253	12344	53682	43991	567878
K	202.5	3310	28071	23849	36668	45361	44592	21342	15205	83859	302257
L	225.0	4142	4060	34181	9976	14319	28377	52716	237535	1409353	1794659
M	247.5	3185	7472	19717	62299	126433	53925	137186	42837	113239	566293
N	270.0	4690	3644	15006	41717	70654	65681	209098	102841	68199	581530
P	292.5	26001	123107	71310	18760	26015	19439	15473	33814	46296	380215
Q	315.0	15386	7779	16911	14553	61969	50005	51716	46750	77831	342918
R	337.5	9939	9816	14500	5792	34883	69399	75326	156339	22997	398991
TOTAL		163302	628011	2832135	2141993	1064917	783902	1489247	2537636	12107087	23748230

Note: Data for zero to 50 miles obtained from Philadelphia   Prepared by CPR.
Electric Company. Remaining data prepared by Center for Planning Research.
*Population for the 0-10 mile radius was divided into finer increments for input
to CRAC.

RADII LABELLED 1 THROUGH 18 RESPECTIVELY REPRESENT: 10, 20, 30, 40, 50, 60, 70, 80, 100,
140, 180, 220, 260, 300, 350, 400, 450, 500 MILES.
SECTORS ARE LABELLED: A,B,C,D,E,F,G,H,J,K,L,M,N,P,Q,R.
SECTOR A IS CENTERED AT TRUE NORTH (0 DEGREES).
THE SECTORS PROCEED IN A CLOCKWISE DIRECTION IN 22.5 DEGREE INCREMENTS.

Table E.7b
LIMERICK PA
1970 ESTIMATED U.S. & CANADA POPULATION BY SECTOR & RADIUS
RADII FROM 100 TO 500 MILES

RADIUS
(MILES)

SECTOR	CENTERLINE (DEGREES)	10 (100-140)	11 (140-180)	12 (180-220)	13 (220-260)	14 (260-300)	15 (300-350)	16 (350-400)	17 (400-450)	18 (450-500)	TOTAL
A	0.0	245027	162743	857026	113056	132242	284188	822000	215000	85000	2916282
B	22.5	83496	147100	911475	115588	124320	340037	2930267	235000	266005	5153288
C	45.0	869087	698718	1263367	800894	1386504	355667	395164	204469	159054	6132924
D	67.5	4241184	1159121	459590	1642904	2588880	35265	0	0	0	10126944
E	90.0	0	0	0	0	0	0	0	0	0	0
F	112.5	0	0	0	0	0	0	0	0	0	0
G	135.0	0	0	0	0	0	0	0	0	0	0
H	157.5	13989	0	0	0	0	0	0	0	0	13989
J	180.0	147034	50834	21101	730914	53143	25512	33840	0	0	1062378
K	202.5	167038	100151	595078	471638	175729	602895	811317	578080	358153	3860079
L	225.0	2791468	274475	175156	192703	254683	594368	995673	788464	1296969	7363959
M	247.5	301863	169714	122076	158092	149752	328474	799258	592059	519169	3140457
N	270.0	109654	383516	551543	2326044	630737	1268687	1630884	862729	2854524	10618318
P	292.5	170073	132213	161261	357237	967763	2171552	455883	5551462	1618808	11586252
Q	315.0	113947	80555	194499	1398628	550557	3653412	622011	50612	42326	6706547
R	337.5	126429	291179	410363	757773	51570	336000	236000	250000	120000	2579314
TOTAL		9380289	3650319	5722535	9065471	7065880	9996057	9732297	9327875	7320008	71260031

Prepared by CPR

RADII LABELLED 1 THROUGH 18 RESPECTIVELY REPRESENT: 10, 20, 30, 40, 50, 60, 70, 80, 100,
   140, 180, 220, 260, 300, 350, 400, 450, 500 MILES.
SECTORS ARE LABELLED: A,B,C,D,E,F,G,H,J,K,L,M,N,P,Q,R.
SECTOR A IS CENTERED AT TRUE NORTH (0 DEGREES).
THE SECTORS PROCEED IN A CLOCKWISE DIRECTION IN 22.5 DEGREE INCREMENTS.

Table E.8

COMPARISON OF RADIOLOGICAL SOURCE TERMS*

	WASH-1400	LIMERICK
Co 58	2.4 +2	
Co 60	9.1 +1	
Kr 85	1.75 +2	1.73 +2
Kr 85m	7.6 +3	8.41 +3
Kr 87	1.5 +4	1.66 +4
Kr 88	2.1 +4	2.34 +4
Rb 86	8.1	18.5
Sr 89	2.9 +4	3.10 +4
Sr 90	1.2 +3	1.46 +3
Sr 91	3.4 +4	3.96 +4
Y 90	1.2 +3	1.53 +3
Y 91	3.8 +4	3.86 +4
Zr 95	4.7 +4	4.62 +4
Zr 97	4.7 +4	4.74 +4
Nb 95	4.7 +4	4.40 +4
Mo 99	5.0 +4	5.04 +4
Tc 99m	4.4 +4	4.34 +4
Ru 103	3.4 +4	3.46 +4
Ru 105	2.3 +4	2.04 +4
Ru 106	7.3 +3	1.26 +4
Rh 105	1.5 +4	1.67 +4
Te 127	1.8 +3	1.76 +3
Te 127m	3.4 +2	2.40 +2
Te 129	9.7 +3	6.62 +3
Te 129m	1.7 +3	1.77 +3
Te 131m	4.1 +3	3.46 +3
Te 132	3.8 +4	3.70 +4
Sb 127	1.8 +3	1.81 +3
Sb 129	1.0 +4	7.05 +3
I 131	2.7 +4	2.53 +4
I 132	3.8 +4	3.74 +4
I 133	5.3 +4	5.56 +4
I 134	5.9 +4	6.13 +4
I 135	4.7 +4	5.22 +4
XE 133	5.4 +4	5.59 +4
XE 135	1.1 +4	1.02 +4
Cs 134	2.3 +4	1.72 +3
Cs 136	9.4 +4	5.86 +2
Cs 137	1.5 +4	1.71 +3
Ba 140	5.0 +4	4.95 +4
La 140	5.0 +4	5.04 +4
Ce 141	4.7 +4	4.59 +4
Ce 143	4.1 +4	4.49 +4
Ce 144	2.7 +4	2.73 +4
Pr 143	4.1 +4	4.46 +4
Nd 147	1.9 +4	1.84 +4
Nn 239	5.1 +5	5.08 +5
Pu 238	18.0	11.0
Pu 239	6.6	5.95
Pu 240	6.6	7.23
Pu 241	1.06 +3	1.66 +3
Am 241	0.5	1.03
Cm 242	1.6 +2	3.34 +2
Cm 244	7.2	3.95

* Values are given in Curies/MWt. Limerick, at
  100% Power, is rated at 3293 MWt. The Limerick
  isotopes, converted to curies, will yield the
  initial values of Table E.7.

REFERENCES

E-1   Reactor Safety Study, WASH-1400, U. S. Nuclear Regulatory
          Commission (NUREG-751014), October 1975.

E-2   D. Aldrich, "Dispersion Parameters: Impact on Calculated Reactor
          Accident Consequences" presented at 1979 Winter ANS meeting.

E-3   Users' Manual for CRAC Code.

E-4   Effects of Rainstorms and Runoff on Consequences of Nuclear
          Reactor Accidents, Sandia Laboratories, October 1976.

E-5   Effects of Wind Shear on the Consequence Model of the Reactor
          Safety Study, Sandia Laboratories, January 1977.

E-6   EPRI Probabilistic Safety Analysis III, April 1978.

E-7   Conditional Probability of Intense Rainfall Producing High Ground
          Concentrations from Radioactive Plumes, Sandia Laboratories,
          March 1977.

E-8   Influence of Plume Rise on the Consequences of Radioactive
          Material Releases, Sandia Laboratories, January 1977.

E-9   Evacuation Risks -- An Evaluation, U. S. EPA, June 1974.

E-10   Investigations of the Adequacy of the Meteorological Transport
          Model developed for the Reactor Safety Study, Sandia Laboratories.

E-11   Plume Rise Predictions, Environmental Research Laboratories,
          June 1975.

E-12   A Model of Public Evacuation for Atmospheric Radiological
          Releases, Sandia Laboratories, June 1978.

E-13   Correlations between Wind Flow and Population Location at 67
          Light Water Nuclear Power Plants, Sandia Laboratories, October 1978.

E-14   D. C. Aldrich and D. M. Erickson, Jr., "Public Protection Strategies
          in the Event of a Nuclear Reactor Accident: Multicompartment Venti-
          lation Model for Shelters".

E-15   The Effects on Populations of Exposure to Low Levels of Ionizing
          Radiation, report of the Advisory Committee on the Biological Effects
          of Ionizing Radiations (BEIR), National Academy of Sciences,
          November 1972.

Appendix F

SUMMARY OF DISCUSSION ON THE TYPES OF DISTRIBUTIONS
USED TO CHARACTERIZE FAILURE PROBABILITY
IN THE LIMERICK RISK ANALYSIS

APPENDIX F

A review of the uncertainty distribution representation of
component failure rates has led to the following recommendations for the
Limerick PRA:

- Use a log-normal distribution to represent the uncertainty
  in the failure rate, λ, for each component considered,
  except;

- For cases where a prior distribution can be constructed,
  and later information is available to update the prior,
  then use a discrete distribution in order to quantify
  the uncertainty.

There are several topics included in this analysis to justify
the above recommendations. They are the following:

- The methods of characterizing the uncertainty in the
  failure rate parameter, λ

- The combining of data from different sources and different
  populations

- The choice of prior distributions for λ, including the
  applicability of log-normal distributions

- The use of discrete failure rate probability distributions.

F.1   DEFINITIONS AND TERMINOLOGY

The use of various distributions, in particular log-normal,
to describe variations in the failure rate, λ, remains a very confusing
issue, with opposing views as to what is desired and what can be obtained.
Much of this confusion is caused by misunderstanding and lack of precision
in the usage of probabilistic definitions.

F-1

There are at least two major definitions of probability (F-1). In the classical or frequency sense, probability is defined in terms of a repeatable experiment, such as flipping a coin. If an experiment is repeated an "infinite" number of times, then the probability of an event (E) is the expected percentage of times that event occurs. This may be stated as:

$$P(E) = \lim_{N \to \infty} \frac{\text{Number of times E occurs}}{N}$$

This is the more common mathematical definition of probability (F-1), so this usage will be referred to as "probability". A second definition involves the concept of subjective probability. This expresses one's state of confidence or degree of belief in an event, and is often used in the form of odds, such as in horse racing, or predicting winners in elections. This form of probability will be referred to as "uncertainty". "Uncertainty distributions" will have the same properties as probability distributions, except uncertainty distributions may change in the future, as more information is gathered; probability distributions will not. For example, a coin has a fixed probability of landing "heads" and this probability will not change, even if one obtains several "tails" in a row. On the other hand, after a horse race is half over, one may be willing to adjust the odds (or the bet) since more information is now available.

Another area of misunderstanding is in the use of the terms "variability", "uncertainty", and "randomness". WASH-1400 (F-2) often uses these terms equivalently, and sometimes simultaneously. It must be remembered, however, that "just because something is unknown or uncertain does not make it random" (F-3).

The lifetimes (time to failure, TTF) of two identical components are usually different. This variability is due to randomness in the population, and can be represented by a probability distribution (an often-

used model is the exponential). The TTF is a random variable. On the other hand, the mean time to failure, MTTF (in the exponential model, the inverse of the failure rate, λ), is a single fixed number for the ntire population. The MTTF is a constant. However, due to variables s . as manufacturers, operating environments, and sampling error, the ie of this constant may not be known. The uncertainty in the value of the MTTF (or in the value of λ) might be expressed in the form of an uncertainty distribution. It might be assumed, for example, that λ has a log-normal distribution. It is important to distinguish between the probability distribution of a random variable and an uncertainty distribution of a fixed number. The flips of a coin form a population that produces variable results and leads to a probability distribution. However, a horse race only occurs once, so the result is a constant that we are uncertain of until the end of the race.

F.2   POPULATIONS AND DATA

Bayesian methods may be used to estimate the failure rate parameter. It must be noted that these methods estimate a single, constant parameter, and the population that the data is taken from must be specified. As more and more data is taken, representative of the single population, the posterior distribution should become more sharply peaked at the actual value of the mean failure rate. However, in general, data is taken from a nonhomogeneous population, as discussed above (different manufacturers, operating environments), so the posterior might not peak.

In referring to a set of data as having a certain distribution, the underlying population must be clearly understood. A failure rate cannot be determined as representative of an entire population based on data from a single component; components must be grouped by type of power plant, manufacturer, or some other means. WASH-1400 groups by published report, so the data is obtained from the population

of "published report valve failure rate" instead of "valve failures". The curve that is constructed from the data describes the group-to-group, not component-to-component, uncertainty. The shape of the curve can conceivably change, depending on how the grouping is made; therefore, it cannot be stated, in general, that all curves obtained from failure rate data are of the same distributional type.

One area that is not generally discussed in Bayesian combination of data is the discarding (censoring) of data which is not applicable. It is vitally important in the characterization of a component's failure rate that sources of data which are clearly not applicable be censored out of the data base. An example of this would be the elimination of data from cryogenic valve applications for use in the characterization of nuclear power plant feedwater regulator valves. Therefore, before the prior distribution is constructed, all the data must be filtered so that inappropriate data is not included and does not bias the results. In fact, some data may be altogether inappropriate for inclusion in prior assessment of failure rate. A specific example from the Limerick analysis would be the loss-of-off-site-power rate. It appears that this value is extremely dependent upon the reliability of the utility grid on which the plant is operating. There are wide variations in the assessed value. It is not clear that data representative of all utility grids is useful in describing the reliability of the Limerick grid. The Limerick power plant has not yet been constructed and has no plant-specific data for any form of updating. But it does have site-specific data, such as the utility grid. In this case, Bayesian updating may be performed.

F.3   CHOICE OF DISTRIBUTIONS

A prior distribution (the uncertainty distribution) is a statement of knowledge about a parameter -- whether it is known very

accurately, or there is absolutely no knowledge of its value. The
question then becomes: "What prior should be used?" Since the prior
is a statement concerning knowledge, any distribution that is believed
can be used. It could be argued that one is better than another, but
both could actually be "correct". It is better if the uncertainty dis-
tribution's mean is close to the correct value of λ, for "if the prior
probabilities...are capriciously and arbitrarily adopted for use in
Bayes' Theorem, then the end results of Bayesian manipulation may be
inaccurate and misleading" (F-4). Just how accurate the prior must
be for acceptable results remains unclear.

The only obvious requirement for the distribution of the
failure rate parameter (λ) in the exponential model is that it be de-
fined $(0, \infty)$. There is also a general concensus that the distribution
should be positively skewed. Two obvious choices for a distribution
are gamma and log-normal; both have advantages and disadvantages, but
there is no inherent reason to choose one over the other. Both are
equally "correct". Table F.1 discusses some of the advantages of
log-normal distributions.

WASH-1400 (F-2) chose log-normal and supplied a list of reasons,
most of which may also be applicable to gamma and other distributions (see
Table F.2). The best reason was "where significant data did exist", the
log-normal satisfied "statistical considerations" (WASH-1400, Appendix II,
p. 42); yet it also says that "the [log-normal] distributions [that are
used] will not necessarily 'best fit' the experience data" (Appendix III,
p. 78). It must be remembered that the data that fit a log-normal were
component failure data from the population of "reported [published] failure
rates", and not from that of "failure rates" (Appendix XI, p. 14-4). WASH-
1400 states that the reported failure rate for a certain component will be

Table F.1

SUMMARY OF REASONS FOR USING CERTAIN DISTRIBUTIONS

Reason for Using Log-Normal: WASH-1400 used it
Reason for Using Gamma: Ease of Bayesian Methods
(Conjugate Prior)

SINCE:

- There is no reason to select one over the other; they are equally "corect" and equally "incorrect" (see discussion)

- The fitted distribution will depend upon the grouping used

- WASH-1400 tested robustness and sensitivity using other similar distributions resulting in "insignificant differences." (Can we believe them?)

- The gamma and log-normal distributions have a similar shape

Gamma   Log-Normal

- In most cases we do not have any plant-specific data, so the generic data cannot be updated.

- Log-normal is convenient to use with our existing methods, so we can save a large increase in time and cost

- Many other nuclear reactor studies used the log-normal distribution

- The greatest value in the analyses is in comparison to other reactors and other studies. Therefore, it is desirable to be consistent.

WE CONCLUDE:

The log-normal distribution will be used when Bayesian updating is not performed, at the same time recognizing that there is no fundamental necessity for choosing this distribution. When plant-specific data is available and updating is performed, discrete distributions are preferred over continuous distributions because of ease of handling.

---

a random variable that follows a log-normal distribution. Despite lack
of conclusive reasons, WASH-1400 has led many to believe the log-normal
is the best distribution to use (for example see F-5). WASH-1400 is
correct in using "assessment ranges", since these accurately specify
the state of knowledge or uncertainty.
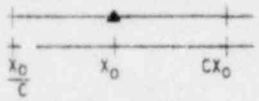
There is no theoretical foundation for or against either the
gamma or log-normal distributions, and there is little data for either
choice, particularly if the shape is dependent on the grouping. The
log-normal distribution has the advantage that it is easy to obtain
the distribution parameters from the 5% and 95% values, whereas this
is difficult for the gamma. On the other hand, the gamma distribution
forms a conjugate prior when using the exponential model (i.e., a gamma
prior leads to a gamma posterior), and this simplifies Bayesian calcu-
lations, whereas, the log-normal is difficult to work with analytically.
The choice between log-normal and gamma therefore becomes: "Do we just
desire a distribution?" (the log-normal has easily obtained parameters);
or "Will we perform Bayesian updating?" (the gamma is easier to work
with analytically).

Note: In addition, a possible, but not necessarily correct, justification
of log-normal can be the following:

> If we took a "sufficiently large group of "relatively knowledgeable"
> people and asked them to estimate a number (for example, the length
> of a room in feet), the results of each estimate might be approximately
> normally distributed around some (maybe event correct) mean. Now, if
> we asked a similar group to estimate a very small or very large number
> in power of 10 (for example, the length of a pencil in miles), the
> exponents of 10 might be normally distributed, and therefore the esti-
> mates would be log-normal (F-6). Therefore, some might be inclined
> to consider the log-normal as a reasonable distribution for uncertainty
> in our collective knowledge. Experiments might be conducted to see if
> groups of people really estimate in this fashion.

Table F.2

WASH-1400* REASONS FOR USING LOG-NORMAL

Reason	Relation to Gamma
1. "Where sufficient data did exist," the data fit a log-normal.	Rarely, if ever, was there sufficient data.
2a. Using error factors, the range can transform to $\ln x_0 \pm \ln c$ -- like using normal error spreads. 2b. Data is expressed as 10^{-c}, so if data is log-normal, then "c" is normal.	Somewhat circular logic. There is no reason to expect this.
3. Log-normal has two parameters.	Gamma has two parameters.
4a. Log-normal is positively skewed. 4b. Mean > Median > Most Probable (mode) is propagated "thus providing a protective, positive type bias".	Gamma has the identical properties.
5. "If the probabilities are decomposed into products of probabilities representing requisites for failure, then [if] when the central-limit theorem is applicable, the log-normal is the resulting distribution."	A big IF.
6. "The log-normal can become near normal or near exponential in certain situations.	The Gamma can become near normal, and the Gamma has exponential and chi-squared as special cases.
7. "Its application as a general distribution for...reliability processes is established and has often been validated."	Gamma is often applied to reliabilty processes also.

*Appendix II, p.42

F.4   DISCRETE FORMS

In performing Bayesian analysis, conjugate distributions (in one case, gamma) are often used. Evans (F-7) complains that "by some stroke of fate, the priors are usually the conjugate distributions, so that the mathematics are tractable". It must be remembered though, that "in our work we cannot, in general, restrict ourselves to conjugate families of distributions" (F-5). The discrete formulation offers an alternative. "It shares (if indeed it does not actually surpass) the mathematical simplicity of the continuous conjugate, it offers almost infinite choice of distributional shape, and it avoids many of the dilemmas and difficulties associated with the continuous approach"(F-4).

The main advantages to discrete formulations are (see F-4 for more detail):

- Mathematically tractable

- Flexible -- the use of discrete values allows almost any distributional shape

- Not constrained to unimodality -- subsidiary peaks may arise earlier giving more rapid indication of an inappropriate prior

- Highly visible -- the posterior can easily be drawn and is visible at all times.

The method of defining a discrete prior is subject to much debate. This is often performed by first selecting the size and location of cells (discrete intervals on the parameter to be estimated). A panel of "experts" ("design engineers who are well versed in the equipment, familiar with its developmental history and performance, and familiar with the reliability characteristics of similar or related equipments in similar or related applications") (F-4), then estimate the relative "odds" of the parameter occurring in each cell. These estimates are then averaged between the judges and normalized.

There are many aspects of discrete Bayesian analysis that must be carefully considered. First of all, each cell that has any possibility of occurring must have a prior probability greater than zero. If a cell has zero prior probability, direct substitution into Bayes' Equation reveals that the cell has zero posterior probability even if the parameter being estimated actually lies in that cell. The cell width must also be considered. Smaller widths lead to greater accuracy, but as more and more cells are obtained, mathematics (as well as the estimation) becomes difficult. The usual procedure is to use small widths in areas where greater accuracy is desired, such as near the more probable values, and larger widths in areas that require less accuracy, such as extreme values.

The legitimacy of Bayesian methods is often comprised due to "the tendency of some researchers to develop (or change) their prior information (e.g., the prior distribution) after observing the experimental results" (for example, F-5). This, of course, is not allowed. If the prior is changed to obtain an "acceptable" posterior, then an "acceptable" posterior might as well be chosen and eliminate the purposeless mathematics. Instead priors should be used that "have been preanalyzed and found to fairly represent a concensus of posterior subjective probability no matter what the test results were" (F-8). This is a way to decrease "the lack of ability to specify a prior distribution whose influence relative to the data is effectively controlled" (F-9). In other words, it is desireable to find a middle ground between a "strong" prior, where the prior dominates the posterior, and a "weak" prior, where the data dominates the posterior (see F-4 for an example).

In terms of measure of central tendency for discrete Bayesian formulations, the mode is the most preferred, and the mean is least preferred. However, if the posterior is unimodal with no subsidiary peaks, the mean may be usable with caution. The confidence limits are easy to obtain from discrete distributions by simply removing the necessary probability from the two tails.

Finally, it must be remembered that the prior is being used to express uncertainty in a parameter, and therefore sharply peaked priors should be avoided. (F-7).

REFERENCES

F-1   G. J. Hahn, S. S. Shapiro, Statistical Models in Engineering,
        Wiley, New York.

F-2   Reactor Safety Study, Nuclear Regulatory Commission, WASH-1400,
        (NUREG-75/014), October 1975.

F-3   Union of Concerned Scientists/Sierra Club, Preliminary Review
        of the AEC Reactor Safety Study, November 1974.

F-4   W. J. McFarland, "Bayes Equation, Reliability, and Multiple
        Hypothesis Testing", IEEE Trans. Reliability, August 1972.

F-5   Kaplan, Apostolakis, et al., "Data Specialization for Plant-
        Specific Risk Studies", Nuclear Engineer and Design, 56, 1980.

F-6   A. E. Green, "Reliability Assessment of Nuclear Systems with
        Reference to Safety and Availability", in Fussel and Burdick,
        Nuclear Systems Reliability Engineering and Risk Assessment,
        Society for Industrial and Applied Mathematics, 1977.

F-7   Ralph A. Evans, Editorial, "Bayesian Trivia", IEEE Trans.
        Reliability, Vol. R-26, No. 5, December 1977.

F-8   Ralph A. Evans, Editorial, "Bayes vs. Whim"; IEEE Trans.
        Reliability, Vol. R-27, No. 5, December 1978.

F-9   Ronald V. Canfield, John C. Teed, "Selecting the Prior Distri-
        bution in Bayesian Estimation", IEEE Trans. Reliability, Vol.
        R-26, No. 4, October 1977.

Appendix G

DISCUSSION OF MEAN VALUES

APPENDIX G

The question arises as to whether the mean or median should be used to characterize or display the point estimate results of the accident sequence probability calculations. The following points are important in this discussion:

1. The fault tree quantification is performed using mean values for all input parameters in the point value calculation. The mean values propagate through the fault tree to accurately represent the top event for independent input events (see Section G.2). However, in addition, in order to present a consistent set of values with those presented in WASH-1400, an estimate of the median (along with the appropriate error range) is provided for display purposes.

2. The question of which measure of central tendency to display (mean or median) is more philosophical than mathematical. In the case of a normal (Gaussian) distribution, either one would suffice since the mean = median. This is not true for asymmetric distributions (see Figure G.1).

3. This appendix discusses the applicability of using the mean or median valve of a probability distribution as the point estimate in accident sequence probability calculations for the Limerick PRA. The following points are important in this discussion:

Mode Median Mean

Log-Normal Distribution

Mean, Median
Mode

Normal Distribution

Mean Median Mode
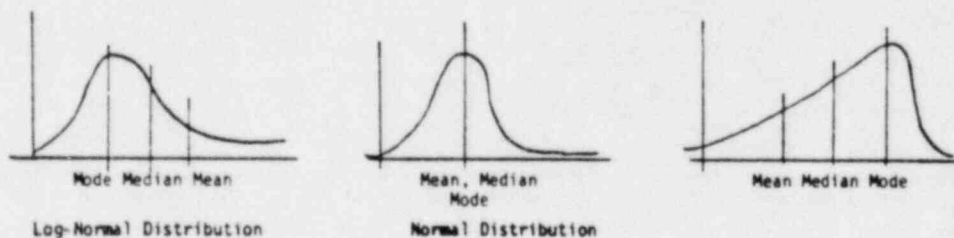
Figure G.1 Schematic Comparison of Three Possible Distributions Which Would Alter the Relationship Between the Mean and Median.

G.1   COMPARISON OF MEAN AND MEDIAN VALUES

Mean

There are a number of advantages associated with using mean values as opposed to median values. The mean value has several properties which make it suitable for use in the calculational phase of a problem. For example, means will propagate through the Boolean algebra calculation required to combine "a group of sequences" to determine the final probability (see Section G.2). Medians cannot, in general, be used in this calculational phase. They can be multiplied (AND gates) if the distribution is known to be log-normal, but they cannot be added (OR gates).

Also, mean values provide more information than do median values about the effect of extreme values which may be present in a skewed distribution &such as hypothesized nuclear power plant risk curves).

The ultimate use of the failure rate, however, may be in a value-impact analysis. In such an analysis, where consequences associated with failures are combined with the probabilities, the distribution may be skewed. In such cases (where a value-impact analysis is involved), it appears to make more sense to use a mean value as the parameter representing central tendency.

Median

The median value has properties which also make it desirable, as noted in the matched quotations below:

the median ofcen is an appropriate measure of central tendency for random variables that are not symmetrically distributed (G-1).

...particularly if it is desired to eliminate the effect of extreme values (G-2).

Summary

An example of the difference between the mean and median for
typical results from WASH-1400 (G-3) is shown in Figure G.2. Figure
G.2 summarizes a comparison of the mean and median values associated
with BWR Category 3 from WASH-1400. As can be seen, the median is in-
deed smaller than the mean. The difference in this case is a factor
of 1.43. The error factor on the sum of accident sequences is approxi-
mately 4 in this category. The difference for the example shown in
Figure G.2 is quite small relative to the stated error bounds.

The use of either the mean or median should always be identi-
fied; otherwise the results may become misleading. See Reference G-4
for a complete treatment of the use of mean and median values.

In the case in which the distribution is known (or is believed
or assumed known), and only one parameter is unknown, the mean and median
are equally useful; one is obtainable from the other. As the Lewis Com-
mittee stated:

> [The question of mean versus median] should not have been a
> major issue.... In our opinion, this is more an issue of
> scrutability than of statistics (G-5).

If the log-normal assumption is used, the ratio of $\frac{median}{mean}$ is given by
$e^{-\frac{1}{2}\sigma^2}$, where:

$$\sigma = \frac{\ln \text{ (Error Factor)}}{1.64} \; ; \; EF = \frac{X_u}{\sqrt{X_u X_1}} \quad \text{where } X_u = X_{0.95}, \; X_1 = X_{0.05}$$

which is about 0.37 for EF=10, and 0.80 for EF=3.
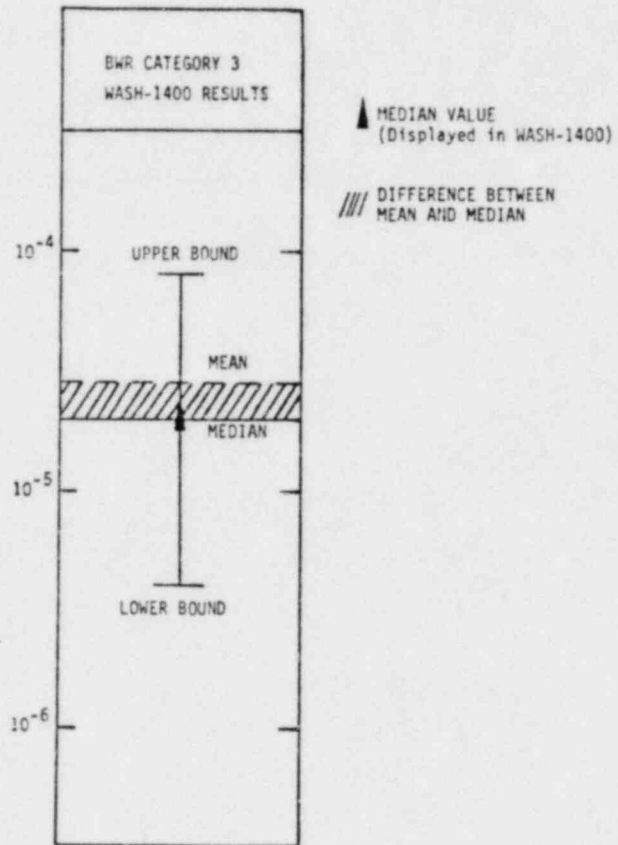
Figure G.2   Example Comparison of the Effect of Using the Mean
Versus Median on the Calculated Sequence Probabilites.

Despite the equal usefulness of both the mean and median when the distribution is known, criticisms are still made against one or the other. It is argued by Kendall (G-6) that if only the median is used (dropping the context of the log-normal distribution and the 90% and 10% points), nuclear reactors would have the appearance of being safer than they really are. This is true, since the "best estimate" sequence probability estimates for each category are calculated as a median; if the mean is used to represent the sequence probabilities, the point estimate will appear higher (see Figure G.2). However, this discussion ignores a point that is repeated several times in WASH-1400: "One cannot generally use point values and treat them as being exact, since there will always be variation and uncertainties" (Ref. 6-7). The method of analysis used requires that some form of distribution or spread be stated. Any statement of the result is incomplete if the associated uncertainty is not specified, i.e., as a variance.

It is believed that the use of either a mean or median for display purposes is technically correct and can be justified. An estimate of the medians is provided to display the results for consistency with WASH-1400. (Since the results will be compared with WASH-1400, it is felt that the Limerick results should be available in the same form as those in WASH-1400.) However, the median values are only estimated, based upon calculations using the mean values, and assuming a distribution for the final calculations using the mean values, and assuming a distribution for the final sequence values. It cannot be overemphasized that the real importance of any comparison of sequence probabilities lies in the comparison of the total uncertainty range established in WASH-1400 versus the range established in the Limerick study, and not in a comparison of the central tendency or best estimate values.

G.2   PROPAGATION OF MEAN VALUES THROUGH A BOOLEAN ALGEBRAIC
       EXPRESSION (i.e., Fault Tree)

The following section describes the mathematical basis for the propagation of mean values through a fault tree, assuming that all basic

input components are independent. Many computer codes, such as WAMBAM, will propagate any set of pointwise input values to generate a point estimate of the top gate. Here it is shown that if these input values are means, then the output for the top event will be a mean value.

In the following discussion it will be useful to adopt the following notation (G-8):

1. P(A) = the probability of event A occurring. This has a value between zero and one. P(A) will be considered as an "uncertainty variable" (see Appendix F) which has the same properties as a random variable.

2. For convenience let $X = P(A)$ and $Y = P(B)$. X and Y will be treated as though they are random variables with $0 \leq x, y \leq 1$.

3. X and Y have probability density functions $g(x)$ and $h(y)$ respectively with the following properties:

    a) $g(x) \geq 0, 0 \leq x \leq 1$ a') $h(y) \geq 0, 0 \leq y \leq 1$

    b) $\int_0^1 g(x)dx = 1$ b') $\int_0^1 h(y)dy = 1$

    c) $P(a<X<b) = \int_a^b g(x)dx$ c') $P(a<Y<b) = \int_a^b h(y)dy.$

4. X and Y have a joint probability density function $f(x,y)$ such that:

    a) $f(x,y) \geq 0, \quad 0 \leq x,y \leq 1$

    b) $\int_0^1 f(x,y)dxdy = 1$

    c) $P(X,Y) \in S) = \int_S \int f(x,y)dxdy.$

5. Two events are independent if, and only if, P(A and B) = P(A) · (P(B). Two random variables are independent if, and only if, $f(x,y) = g(x)h(y)$ where:

    $g(x) = \int_0^1 f(x,y)dy$ marginal distribution of X

    $h(y) = \int_0^1 f(x,y)dx$ marginal distribution of Y.

6. The mean of a random variable X is defined as $\int_0^1$
    The mean of a function of two random variables A(X,Y) is defined as $\int_0^1 \int_0^1 A(x,y)f(x,y)dxdy.$

The propagation of mean values through fault trees will now be considered for several simple examples with independent or mutually exclusive inputs. Only AND, OR, and NOT gates need to be considered since all Boolean statements (i.e., fault trees) can be formed using only these gates (G-9).

AND

AND
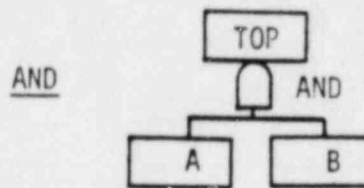
By the definition of independent events, it is known that the Boolean representation of an AND gate is $P(A \text{ AND } B) = P(A)P(B)$. $P(A)$ and $P(B)$ are treated as though they are random variables, so $P)A \text{ AND } B)$ is also a random variable, which can be written as $P(A \text{ AND } B) = X \cdot Y$. This equality implies that the mean value of the random variable $P(A \text{ AND } B)$ is equal to the mean value of the random variable $(X \cdot Y)$.

The mean of $(X \cdot Y)$ is, by definition, equal to $\int_0^1 \int_0^1 xyf(x,y)dxdy$. Since A and B are independent events, $P(A)$ and $P(B)$ are independent random variables. Therefore, $X(=P(A))$ and $Y(=P(B))$ are independent random variables, and it can be seen that:

$$\text{mean of } X \cdot Y = \int_0^1 \int_0^1 xyf(x,y)dxdy = \int_0^1 \int_0^1 xyg(x)h(y)dxdy$$

$$= \left(\int_0^1 xg(x)dx \right) \left(\int_0^1 yh(y)dy \right) = (\text{mean } X(\text{mean } Y).$$

In other words, if the mean value of $P(A)$ and the mean value of $P(B)$ are input to a simple AND gate (A and B independent), the use of the Boolean formula $P(A \text{ AND } B) = P(A)P(B)$ gives the mean value of $P(A \text{ AND } B)$.

OR
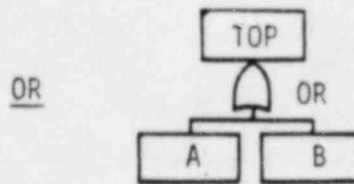
The Boolean algebra calculation for a simple OR gate makes use of the well-known (G-8) formula that P(A OR B) = P(A) + P(B) - P(A AND B). A and B are assumed to be independent events, so this can be written as P(A OR B) = P(A) + P(B) - P(A)P(B). In addition, P(A) and P(B) are treated as though they are random variables. Therefore, P(A OR B) is also treated as a random variable and can be written P(A OR B) = X + Y - X·Y. This equality implies that the mean of the random variable P(A OR B) is equal to the mean value of the random variable (X + Y - X·Y).

The mean value of (X + Y - X·Y) is, be definition, equal to:

$$\int_0^1\int_0^1 (x + y - xy)f(x,y)dxdy = \int_0^1\int_0^1 xf(x,y)dxdy + \int_0^1\int_0^1 yf(x,y)dxdy$$
$$- \int_0^1\int_0^1 xyf(x,y)dxdy;$$

by the definition of independence:

$$= \int_0^1 x(\int_0^1 f(x,y)dy)dx + \int_0^1 y(\int_0^1 f(x,y)dx)dy - \int_0^1\int_0^1 xyg(x)h(y)dxdy$$

by the definition of marginal distributions:

$$= \int_0^1 xg(x)dx + \int_0^1 yh(y)dy - (\int_0^1 xg(x)dx)(\int_0^1 yh(y)dy)$$

$$= (mean\ X) + (mean\ Y) - (mean\ X)(mean\ Y).$$

In other words, if the mean value of P(A) and the mean value of P(B) are input to a simple OR gate (A and B independent), the use of the formula P(A OR B) = P(A) + P(B) - P(A)P(B) yields the mean value of P(A OR B).

Now consider the case when A and B are mutually exclusive, and
thus dependent. Then P (A AND B)=0, and P (A OR B) = P(A) + P(B) -
P(A AND B) = P(A) + P(B). This equality would then imply that the mean
value of the random variable P(A OR B) is equal to the mean value of
the random variable P(A) + P(B), i.e., X + Y. Therefore, for a simple
OR gate, the propagation of mean values would hold with the formula
P(A OR B) = P(A)+P(B), where A and B are dependent and mutually exclusive.

NOT
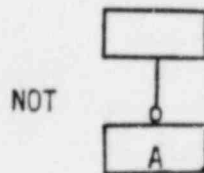
It is also known that P(NOT A) = 1 - P(A). Again P(A) is
treated as a random variable, so P(NOT A) is treated as a random variable
that can be written as P(NOT A) = 1 - X.

Therefore, the mean of P(NOT A) is equal to the mean of $(1-X)$,
which is by definition:

mean $(1-X) = \int_0^1 (1-x)g(x)dx = \int_0^1 g(x)dx - \int_0^1 xg(x)dx$, since
the area under a probability distribution sums to 1:

$= 1 - (mean\ X)$.

In other words, if the mean value of P(A) is input into a NOT
gate, the use of the formula P(NOT A) = 1 - P(A) results in the mean value
of P(NOT A).

Therefore, it has been shown that if the inputs to a gate are
assumed independent, then when the data is input as means of the distribu-
tions, the propagated value will be the mean value of the gate.

However, it is not necessarily true that all inputs to
higher level gates of a fault tree are independent, even if the com-
ponents are independent. Take, for example, the following tree with
independent components A, B, and C:
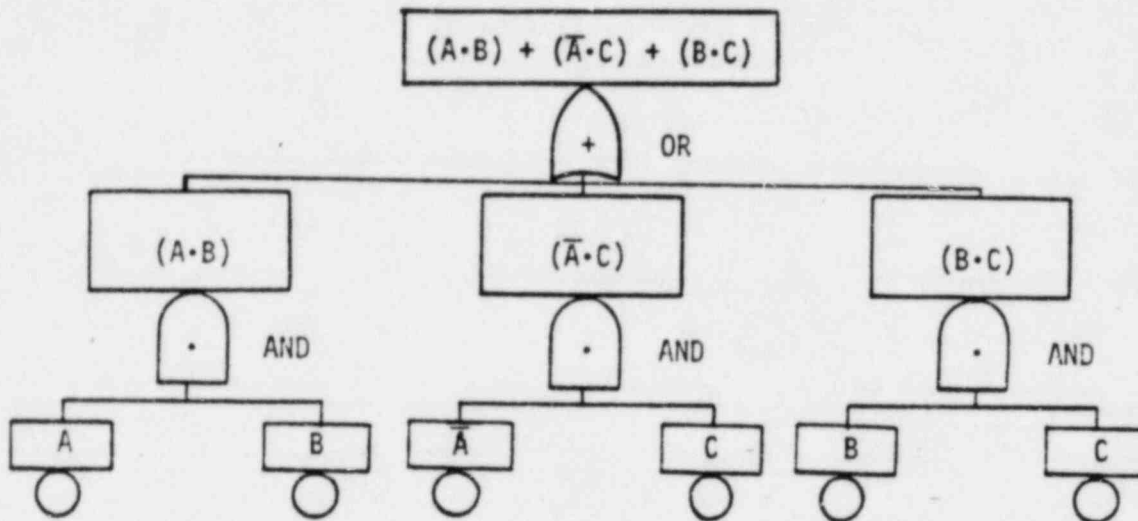
Figure G.3 Example Fault Tree

In this case, the gates immediately above the component level have inde-
pendent inputs (since the components are assumed to be independent), but
the top gate does not have independent inputs. For example, (A·B) and
(B·C) are not independent since component B appears in both inputs, There-
fore, the previous discussion about simple gates must be extended to apply
to this tree.

All Boolean expressions (i.e., fault trees) can be transformed
into equivalent and unique (principal disjunctive normal) form also known
as the "sum of products canonical form" (see G-9). In this form the pro-
pagation of means is valid. A simple method of creating this form is by
using a truth table.

For example, the following truth table may be formed from the
fault tree in Figure G.3, showing all possible success or failures of
the component, A, B, and C.

---

* + = OR
  · = AND
  $\overline{A}$ = NOT A

Table G.1   TRUTH TABLE OF EXAMPLE FAULT TREE
(See Figure G.3)

A	B	C	A·B	$\overline{A}$·C	B·C	(A·B) + ($\overline{A}$·C) + (B·C)
1*	1	1	1	0	1	1
1	1	0	1	0	0	1
1	0	1	0	0	0	0
1	0	0	0	0	0	0
0*	1	1	0	1	1	1
0	1	0	0	0	0	0
0	0	1	0	1	0	1
0	0	0	0	0	0	0

Hence, it can be seen that the top event, (A·B) + ($\overline{A}$·C) + (B·C), occurs only when A AND B AND C occurs, or when A AND B AND NOT C occurs, or when NOT A AND B AND C occurs, or when NOT A AND NOT B AND C occurs. Another way of writing this is:

$$(A \cdot B) + (\overline{A} \cdot C) + (B \cdot C) <=> (A \cdot B \cdot C) + A \cdot B \cdot \overline{C} + (\overline{A} \cdot B \cdot C) + (\overline{A} \cdot \overline{B} \cdot C)$$

(principal disjunctive normal form)

Notice that a principal normal form contains a series of unique terms, each term contains every component exactly once.

If we assume that each component is independent from the others, then all components in each term are independent, since each component occurs only once. Furthermore, all the terms in the principal disjunctive normal form are mutually exclusive. The discussion above of a simple OR gate, with two mutually exclusive input events, can be easily extended to a case with more than two mutually exclusive input events.

---

*1 = the component fails
 0 = the component does not fail

In this manner, a fault tree may be changed to a Boolean logic form, i.e., principal disjunctive normal form of a series of unique terms. Therefore, when distinct component inputs are independent, the previous discussion applies, and mean value inputs to a fault tree lead to the mean value of the top event.

REFERENCES

G-1   G. J. Hahn and S. S. Shapiro, Statistical Models in
       Engineering, John Wiley, New York, p.37.

G-2   Irwin Miller and John E. Freund, Probabilities and
       Statistics for Engineers, Prentice Hall, N.J., 1977,
       p. 150.

G-3   Reactor Safety Study, WASH-1400, U. S. Nuclear
       Regulatory Commission (NUREG-75/014), 1975.

G-4   Darrell Huff, How to Lie with Statistics, W. W. Norton,
       New York, 1954, Chapter 2.

G-5   Lewis Committee, "Risk Assessment Review Group Report
       to the USNRC", September 1978, p.12.

G-6   Kendall, N. W., et al., "The Risks of Nuclear Power
       Reactors, A Review of the NRC Reactor Safety Study
       WASH-1400", Union of Concerned Scientists, Cambridge,
       MA., August 1977.

G-7   Op-cit. WASH-1400, Appendix XI, p. 3-60, 1975.

G-8   Ronald E. Walpole, Raymond H. Myers, Probabilities and
       Statistics for Engineers and Scientists, MacMillan,
       NY, 1972.

G-9   J. P. Tremblay, B. Manohar, Discrete Mathematical
       Structures with Applications to Computer Science,
       McGraw-Hill, 1975, pp. 53-58.

Appendix H

REVIEW OF SELECTED CONTAINMENT PHENOMENA

Fauske and Associates, Inc.

627 Executive Drive

Willowbrook, Illinois 60521

PHENOMENOLOGICAL ASSESSMENT OF

HYPOTHETICAL SEVERE ACCIDENT

CONDITIONS OF THE LIMERICK GENERATING STATION

Prepared By:

Robert E. Henry

Table of Contents

List of Tables

List of Figures

EVALUATION OF PHENOMENOLOGICAL AREAS ASSOCIATED WITH

THE PROBABILISTIC RISK ASSESSMENT AT THE LIMERICK STATION

In evaluating the public risk associated with various postulated ac-
cident sequences at the Limerick Station, several key phenomenological
areas must be addressed in a realistic manner. These include 1) the po-
tential for occurrence of and the possible damage resulting from in-vessel
steam explosions, 2) the potential for additional hydrogen generation
within the primary system, 3) the nature of reactor vessel failure for
definite sequences which progress to that state, 4) the disposition of
core material following postulated reactor vessel failure, 5) the nature
and implications of any ex-vessel steam explosions, and 6) the available
mechanisms for achieving permanent coolability of the core material with-
in the primary containment. This list is chronologically oriented for
the sequences in general and the areas will be addressed in this order
since the results of one may have a significant influence on those which
follow.

I.   Steam Explosions (In-Vessel)

Stea. explosions were considered in the Reactor Safety Study (RSS),
WASH-1400 [1], as a possible containment failure mechanism for hypotheti-
cal core melt accidents. With the parametric model used as the analytical
tool in the RSS, postulated steam explosions within the reactor vessel
were calculated to cause a failure of the reactor vessel and propelled
the conceptual missile against the containment wall with sufficient ener-
gy to fail this boundary as well. To establish a basis for comparison,
the following subsections will discuss the issue as follows. First, the
event as envisioned in WASH-1400 will be reviewed along with the experi-
ence in small test reactors. With this background, the specific reactor
structural configurations for boiling water reactors will be compared to
that considered in the RSS. Then pertinent literature on steam explosions
is reviewed and a comparison of the available results are made to the as-
sumed and calculated behavior described in WASH-1400. Finally, the pos-
sibility and magnitude of steam explosions within the containment build-
ing, assuming a hypothetical release of core material from the reactor
vessel is evaluated.

A.   Steam Explosions as Modeled in the Reactor Safety Study (WASH-1400)

In the study a degraded core state was assumed in which the core was
uniformly molten and totally separated by the grid plate from the water
contained in the lower plenum. It was considered unlikely that a par-
tially molten core would drain into the lower plenum. Consequently, the
core was assumed to collect on the grid plate which failed in a catastro-
phic manner releasing all the molten debris into the water. This failure
causes the debris to be instantaneously fragmented to some pre-specified

fragment size as well as instantaneously and uniformly dispersed through-
out the coolant. These conditions were assumed and not the result of mech-
anistic calculations describing the grid plate failure, the fragmentation
process, and the mixing of the water and core material; all of which are
rate dependent phenomena not represented in the WASH-1400 analyses.

Once this intimate dispersal is assumed, the thermal energy transfer
is calculated by considering convection, conduction, and radiation between
the degraded core debris and water. Energy transfer results in a rapid
($\sim$ 10 msec) pressure rise in interaction zone and this accelerates an as-
sumed continuous, overlying liquid slug, made up of half water and half
core debris, vertically upward through an open vessel in a piston-like
manner as shown in Fig. 1-1. The various processes modeled are summarized
in Table 1-I and illustrated in Fig. 1-2. Calculations are carried out
for various levels of fragmentation and melt-drop times (melt addition
interval). Acceleration and displacement of the postulated slug (inertial
layer) continues until it impacts upon the vessel head and for some pos-
tulated cases this is calculated to occur with sufficient energy to cause
the head to fail and propel it against the containment wall with the energy
necessary to fail the containment. One such set of calculated results for
an instantaneous melt addition and a particle size of 400 μm is shown in
Fig. 1-3.

The analytical description used in WASH-1400 is a simplistic represen-
tation of both the specific configurations in question and the explosive
phenomenon itself. Without doubt, these calculations misrepresent the
explosive behavior in that (1) they assume that all liquid-liquid systems
with a substantial temperature difference can explode, (2) there is no
consideration given to the rate at which the materials are brought into
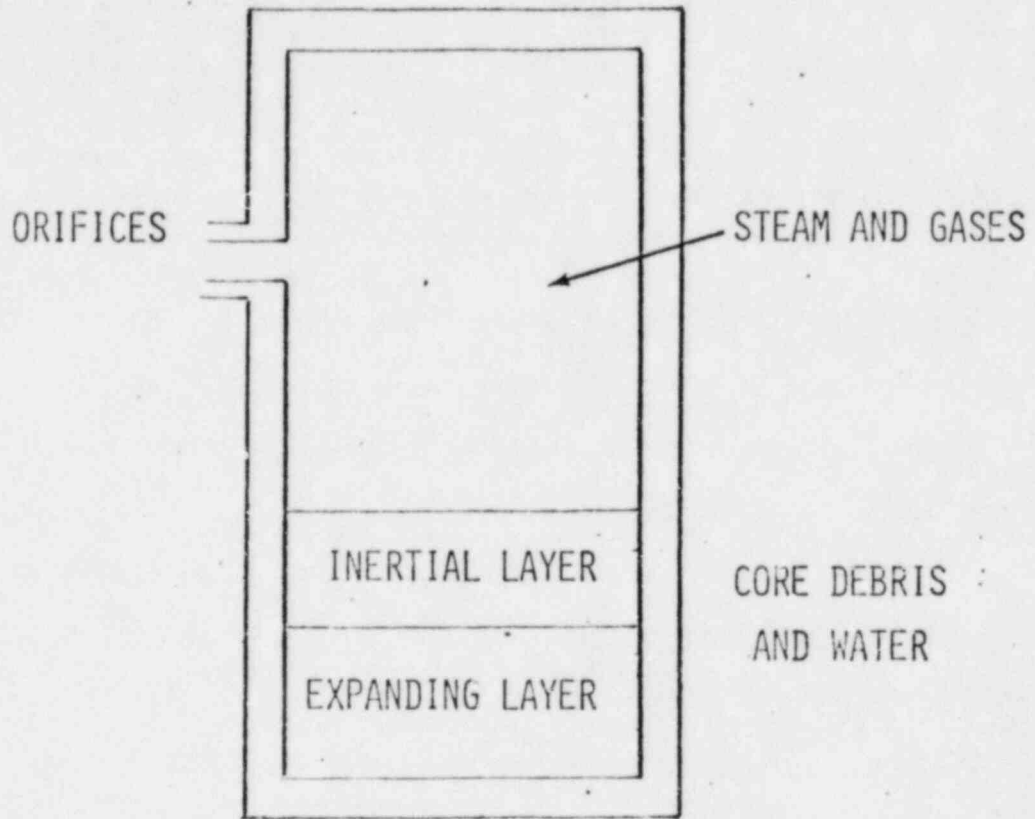
FIG. 1-1 MODEL GEOMETRY USED IN WASH-1400
STEAM EXPLOSION ANALYSES.

Table 1-I

In-Vessel Steam Explosion Sequence - WASH-1400

1. Uniformly molten core, totally separated from the water in the lower plenum.

2. Catastrophic collapse of the core support such that the molten core material falls into the water.

3. Rapid (instantaneous) intimate mixing of the water and core material.

4. Coherent interaction between the molten core debris and water.

5. Slug formation and acceleration upward through the vessel in a piston-like manner.

6. Coherent slug impact on the vessel head.
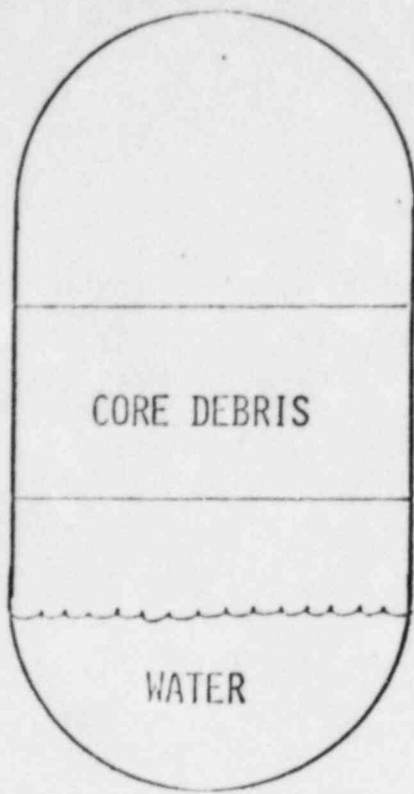
A) INITIAL SEPARATED
CONFIGURATION
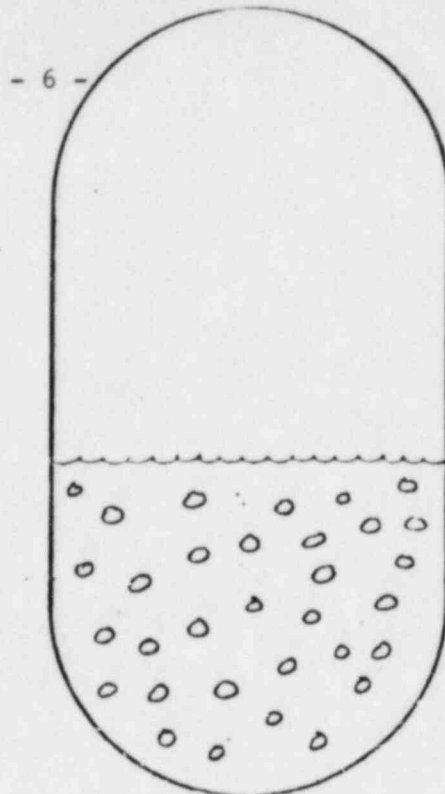
B) CATASTROPHIC FAILURE
AND INSTANTANEOUS MIXING
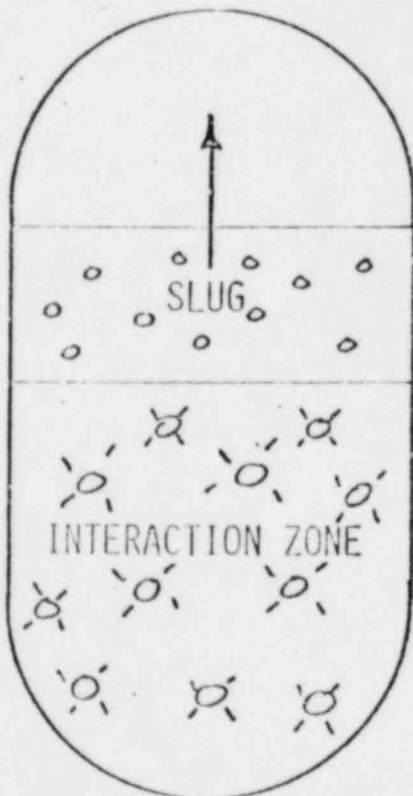
C) SUSTAINED ENERGY TRANS-
FER AND SLUG ACCELERATION

D) SLUG IMPACT

FIG. 1-2 BEHAVIOR MODELED IN WASH-1400.

FIG. 1-3 COMPARISON OF PREDICTED PRESSURE-TIME BEHAVIOR FROM
WASH-1400 (400 µM PARTICLE SIZE) AND AVAILABLE EX-
PERIMENTAL RESULTS FOR STEAM EXPLOSIONS.

contact, (3) intermixing is assumed to be instantaneous, uniform, and require only negligible energy and (4) they grossly overestimate the rate of mechanical energy released by a steam explosion. Clearly, such overly simplistic analytical representations are of use in safety evaluations only if they show that even with these overwhelming conservatisms, there is still no co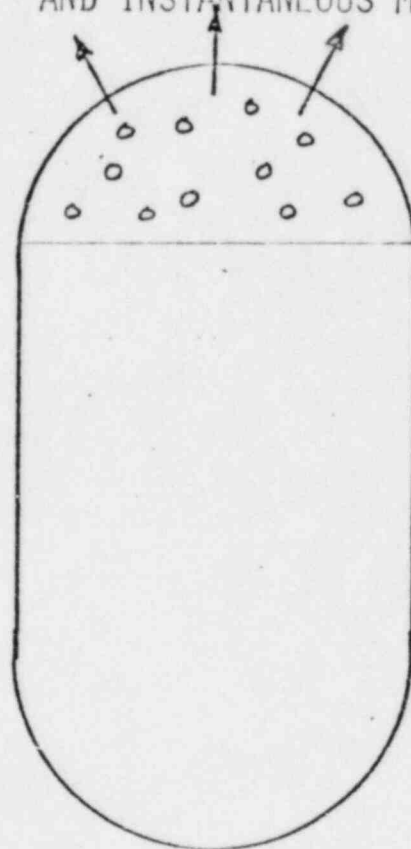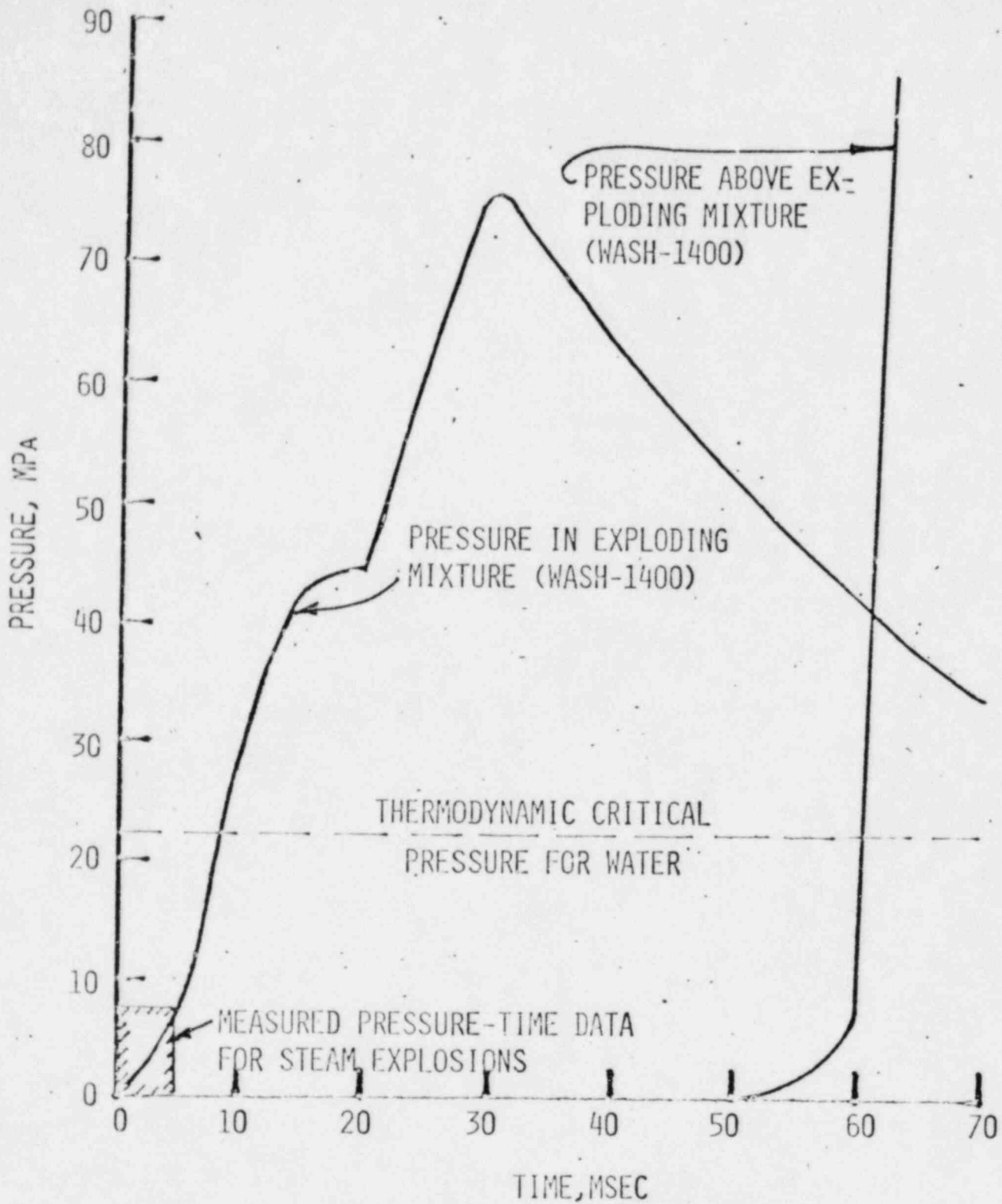ncern for public health and safety. On the other hand, if the conclusion of such calculations is that the phenomenon does provide a considerable risk, then the basic assumptions used in the calculational model must be scrutinized to discern if such a conclusion, derived from an overly simplistic model, is indeed valid. This will first be addressed in terms of the experiences with small test reactors and then with regards to the in-vessel structural components, both above and below the core, which were discussed in the RSS but essentially ignored.

B.   Relationship to Previous Reactor Experience

The explosion model used in WASH-1400 resulted principally from concerns generated by the low pressure BORAX [2] and SPERT [3] destructive experiments and the SL-1 accident [4]. Reactor conditions leading to this accident and the destructive transients in BORAX and SPERT produced a fundamentally different system than that representative of a postulated severe accident in a boiling water reactor. It is not only important to realize these differences, but it is essential to understand the resulting implications on the phenomenon as well.

1.   All these events, including the SL-1 accident, were produced by power excursions in which the core was driven to molten conditions in 30 msec or less. Such reactivity transients are not possible in power reactors and were neither addressed in WASH-1400 nor are they considered here.

2. For these three reactors which were fueled with uranium-aluminum alloy fuel plates clad with aluminum, the fuel and water were uniformly premixed and finely divided in a cold condition prior to the excursion.

3. The reactor was essentially at atmospheric pressure and the water was at room temperature. Hence, the pressure was much less than the normal operating pressures for BWRs and net vaporization was not required in the fragmentation stage.

4. With the specific core design, the SL-1 reactor could be brought to criticality by the withdrawal of one control rod. In the accident this rod was rapidly withdrawn which caused a nuclear excursion with sufficient energy deposition to melt the high thermal response fuel-clad plates while in an extensively premixed state. This was also true for the BORAX and SPERT test reactors.

5. Since the reactors were essentially at room temperature prior to the excursion, the vessels were filled with water except for a small free-board volume at the top, i.e. a coherent overlying liquid slug was already in place.

6. The internal geometries of the vessels were very simple and open, which provided little attenuation or dispersion of any slug movement.

With these pre-transient conditions, the configuration established was essentially that assumed in the RSS. The essential feature of the strong reactivity transient is that it brought the fuel and clad to melting before this configuration could substantially change. Given these particular characteristics, a slug impact following a steam explosion

within the core would indeed be the expected chain of events. *However, this is fundamentally different than an initially separated system of high temperature molten core material and saturated water existing at an elevated pressure with substantial internal structure to prevent catastrophic collapse, intimate mixing, and slug formation.*

C.   BWR Structural Considerations

Boiling water reactors are substantially different in their designs than pressurized water reactors. The obvious differences are that the core inventory is larger for the same thermal power, the vessel is larger and there are additional components within the vessel including the steam separators and the steam dryers. Another major difference is the manner in which the core is supported, i.e. for BWRs the foundation is made up of many tubes (4 assembly per support tube (control rod guide tubes)) which extends upward from the bottom of the vessel with the control rod spindles within the tubes.

Given this core support configuration, which is illustrated in Fig. 1-4, it is virtually impossible to conceive of a sequence whereby a degraded core would catastrophically collapse into water. In addition, it is equally difficult to envision any process whereby rapid and intimate mixing could occur. The specific details of this reasoning process are given below.

1.   Under normal operating conditions, the structure is designed to support the entire core. The major change in the material properties occurs when substantial overheating takes place, but this can only occur in the absence of water. If water is absent then an in-vessel steam explosion cannot occur.
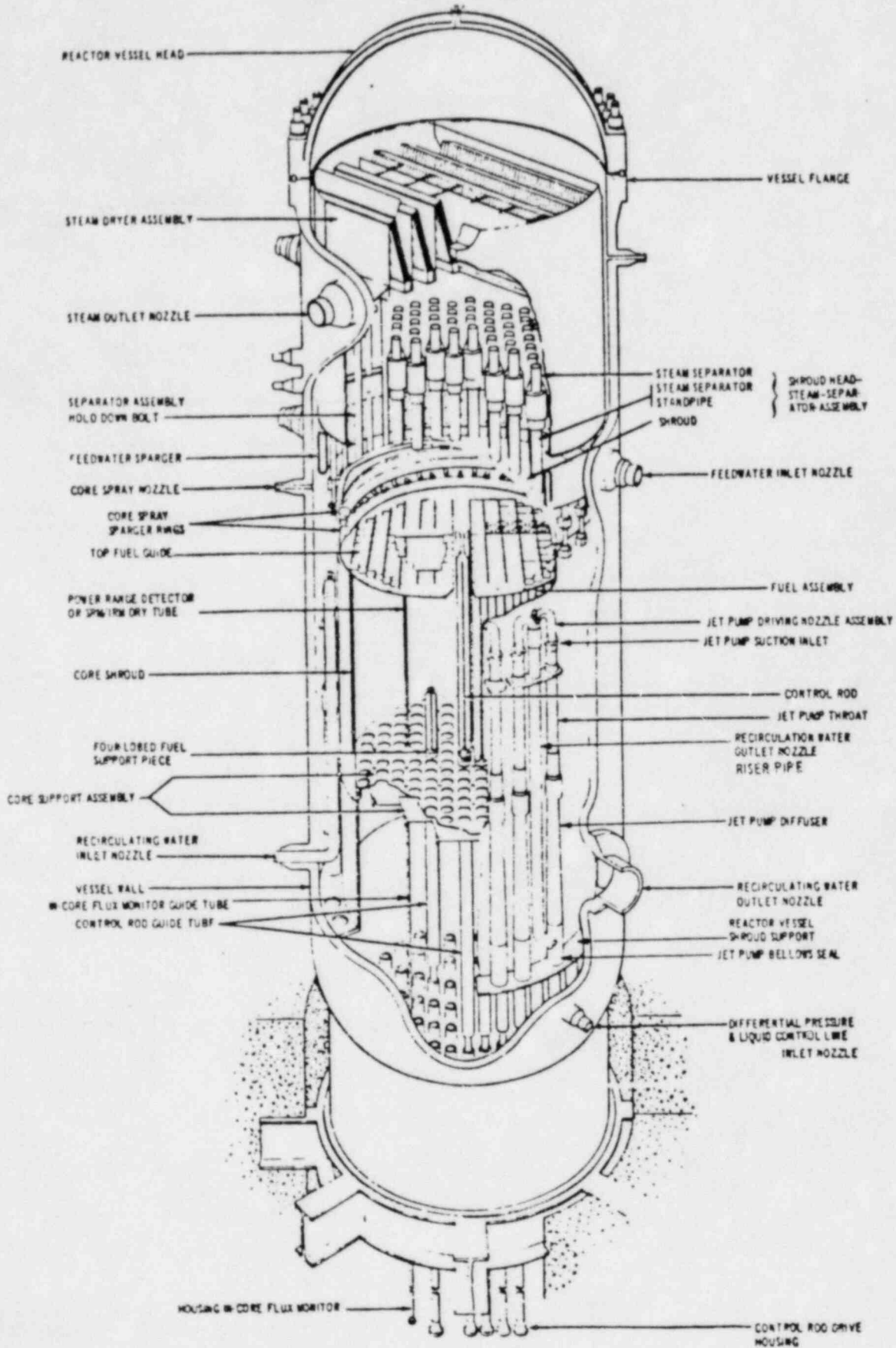
FIG. 1-4

REACTOR VESSEL.

2. In addition, each assembly is, in effect, individually supported and
    if a degraded core condition is assumed, the most likely way in which
    molten core material would eventually travel to the lower plenum is
    through the fuel assembly orifice located on the support tube. This
    would undoubtedly be a very incoherent process and the molten core
    material would freeze within the tube, thus thermal attack of the
    tube itself would not begin until the water had been boiled away
    outside of the tube. Consequently, not only would the melt progres-
    sion be incoherent, but the core material could not participate in
    a global interaction until the water was vaporized, i.e. the poten-
    tial for a steam explosion becomes a moot point.

3. If all these substantial physical restraints are completely disre-
    garded and one assumes that coherent core collapse occurs in any event,
    then one must consider the forest of support tubes, control rod thim-
    bles, and instrument tubes which exist below the core. This massive,
    cold structure, which could freeze the core debris on contact, would
    prevent any large scale, intimate mixing of the molten debris and
    coolant.

These three points, all dealing with the below core structure, show that
catastrophic collapse in the presence of water cannot occur, the downward
progression of any postulated scenario would be incoherent and occur with-
in the support tubes (and only in the absence of water), and large scale,
intimate mixing could not be achieved. Therefore, large scale steam ex-
plosions involving substantial masses of core material can be ruled out
on geometric considerations alone. In addition, these can be considered
in light of the massive, coherent interaction required in WASH-1400 before

vessel failure was calculated. These below core structures were ignored for the WASH-1400 BWR analyses.

One can be equally critical of the slug formation, displacement, and impact model from WASH-1400 as it relates to the actual design.

1. With the below core structure segmenting the water with the core support tubes, the formation of a continuous, overlying liquid slug can also be discarded.

2. If such a slug is postulated the core grid at the top of the fuel assemblies would destroy the coherence as the material travels upward through the vessel.

3. Steam separators, located above the core as shown in Fig. 1-4 are large structural components which do not provide straight-through flow paths. Hence, this would also interfere with the upward transmission of a coherent liquid slug.

4. Steam dryers are postitioned above the steam separators. These components, like the steam separators, also have a tortuous flow path, and thus, provide another barrier to the postulated coherent behavior.

These arguments have been formulated on the basis of specific components available in the reactor vessel but ignored in the Reactor Safety Study. As discussed, these differences are indeed extensive and the discussion of each shows that their neglect in WASH-1400 grossly overestimated (1) the likelihood of an event, (2) the amounts of material involved, and (3) the damage potential represented by an event. Considerations of the structural components allows one to individually rule out (a) catastrophic collapse, (b) rapid and intimate mixing, (c) coherent slug forma-

tion, (d) coherent slug transmission and (e) coherent slug impact. As summarized in Table 1-1, all of these are required in order for the WASH-1400 analysis to be applicable. However, there is even a more fundamental misrepresentation in the RSS and that is the characterization of steam explosion themselves. This is addressed in the next section.

D.   Steam Explosion Phenomena

The assessment of the relevant phenomenology for in-vessel steam explosions must be considered in light of the specific sequences of interest. These generally can be divided into three different areas characteristic of accident evaluations: (1) a large break LOCA, (2) a small break LOCA, and (3) a transient condition in which the core degradation occurs at a pressure close to the nominal operating pressure. More specifically the sequences can be characterized in terms of the system pressure at potential core melting by: (a) a low system pressure such as $0.4 - 1.0$ MPa, (b) an intermediate pressure in the range of 1.0 to 5.0 MPa and (c) high pressures ranging up to 7.0 MPa for BWRs. In the evaluation of in-vessel steam explosions, the phenomena was considered in terms of these sequences and their characteristic pressure regimes.

1.   High Pressure Systems

Two models have been published [5,6] which predict that explosive interactions can be suppressed by elevated system pressures. Both of these models predict essentially the same pressure level for termination of explosive events and the reason for this behavior is the strong decrease of "energetic boiling" with increasing pressure. Because this predicted characteristic clearly sets these models apart from other models proposed in the literature, such as the parametric approach utilized in WASH-1400,

specific experiments were performed to test this behavior. Table 1-II summarizes the vapor explosion (vapor explosion is the general category of which a steam explosion is one specific type) data where various pressure levels were tested [5,7-11]. As illustrated, this data includes both large and small scale systems, simulant and real reactor materials, and both "free contacting" mode and "externally triggered" events. A comparison of these latter two methods for initiating an explosive event show a slight sensitivity to the "trigger" magnitude, [7] i.e. the cutoff pressure is slightly higher for a system with a strong external trigger. A comparison between Figs. 1-5 and 1-6 illustrates such an effect for the interaction between Freon-22 and mineral oil. For an ambient pressure of 0.1 MPa energetic explosions can be generated with either an external trigger, Fig. 1-5 or in the free contacting mode, Fig. 1-6, and the shock waves generated by these events may be in excess of 2.0 MPa. When the ambient pressure is increased to 0.23 MPa, the free contacting mode experiments demonstrate no explosive interactions while the externally triggered tests experience explosive interactions with peak shock wave pressures again approaching 2.0 MPa. With a small additional increase in the ambient pressure to 0.3 MPa, the externally triggered systems record only very weak explosions and a further pressure increase to 0.5 MPa is sufficient to suppress explosive interactions, even in the presence of a 25 J exploding wire.

Both of these analytical models were used to provide pre-test predicti as for the large scale molten sodium chloride-water tests carried out at :he Euratom Ispra Laboratory. These pre-test predictions are documented in the test plan for these experiments [12], and the results are summarized in Table 1-III. As illustrated the Buchanan model has a predic-

Table 1-II

Experiments Demonstrating a High Pressure Cutoff

Laboratory	Materials Used	Explosive Pressures Measured (MPa)	System Pressure Required to Eliminate Explosion (MPa)	Reduced Pressure
Argonne [5]	Freon-22 and Mineral Oil	2.5	0.2	0.04
*Argonne [7]	Freon-22 and Mineral Oil	2.0	0.5	0.10
Argonne [8]	Sodium and Water	2.0	1.0	0.05
Ispra [9]	Sodium Chloride and Water	6.0	1.0	0.05
*Sandia [10]	Corium and Water	1.5	0.75	0.04
*Winfrith [11]	Uranium Dioxide and Water	3.0	0.9	0.05

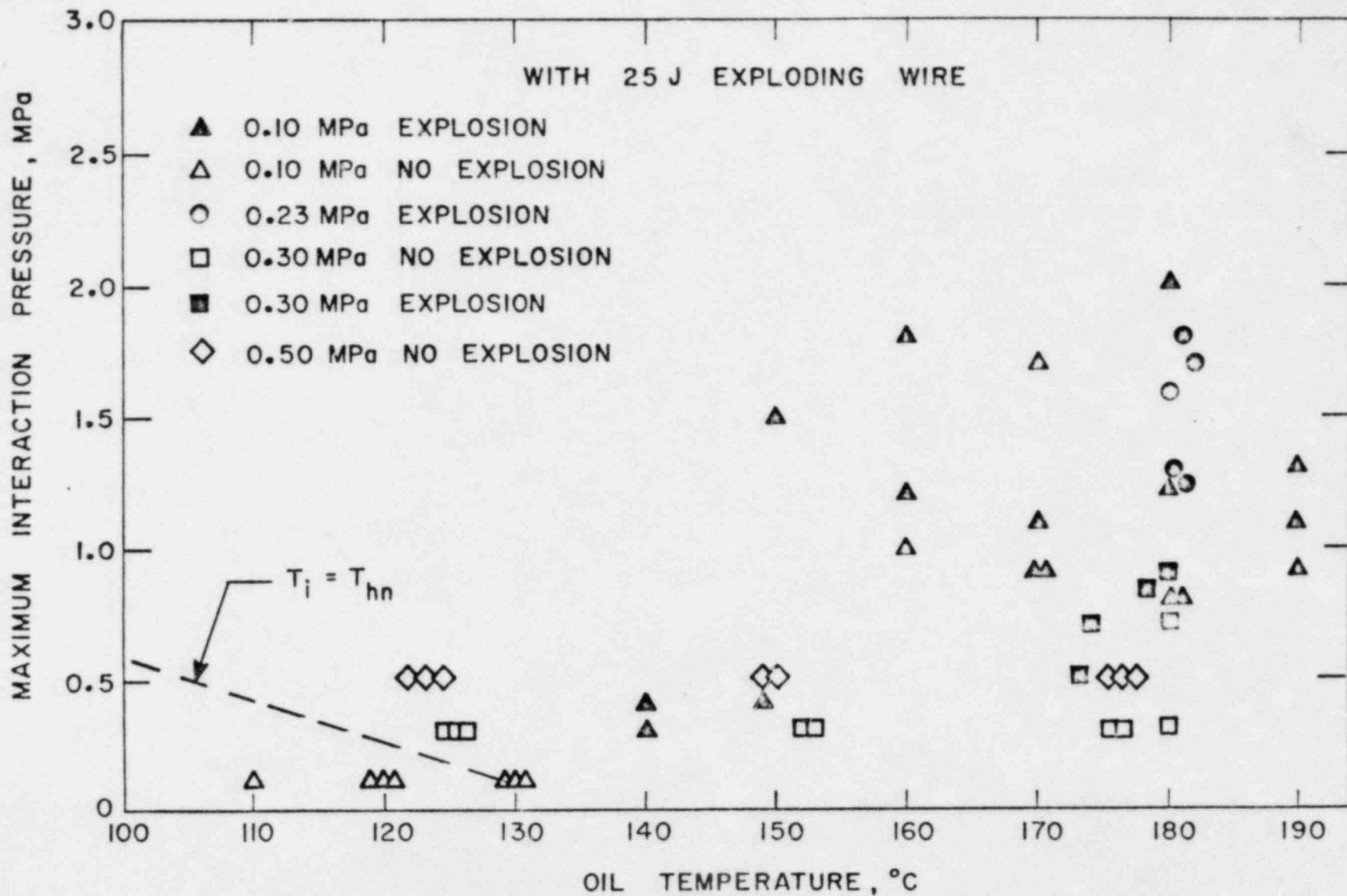*Externally triggered systems.

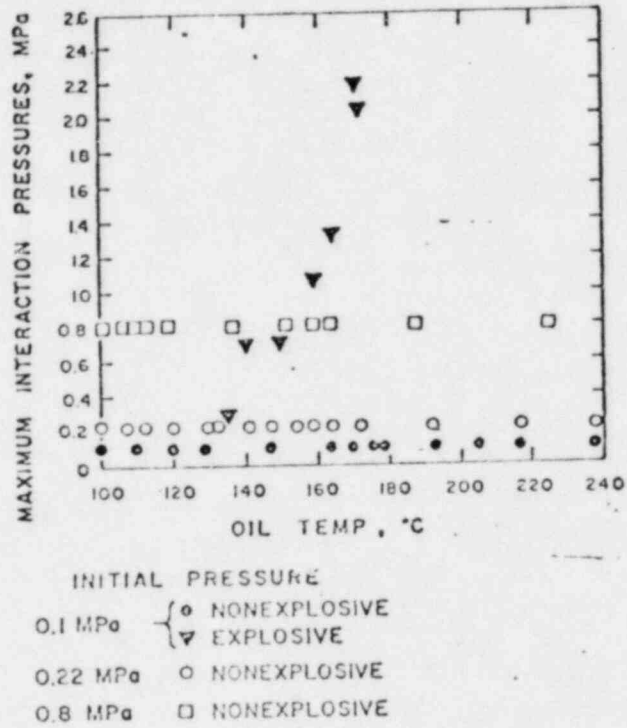FIG. 1-5 ILLUSTRATION OF PRESSURE EFFECT IN THE PRESENCE OF TRIGGER.

- 18 -

FIG. 1-6 ILLUSTRATION OF PRESSURE EFFECT
IN THE ABSENCE OF TRIGGER.

TABLE 1-III

CUTOFF PRESSURE PREDICTIONS

		Buchanan (6)	
System	Henry-Fauske (5) MPa	Homogeneous Nucleation MPa	Preferred Site Nucleation MPa
Freon-22	~ 0.15	0.21	0.66
Water	1.0	1.3	6.7

tion for both homogeneous and preferred site nucleation characteristics, whereas the Henry-Fauske model which is based upon spontaneous nucleation, (homogeneous nucleation is assumed in this case) predicts a single value for a given fluid. Pressure level predictions for the homogeneous nucleation mechanism in the Buchanan model are in good agreement with those of the Henry-Fauske model, although somewhat higher, and both are in agreement with the experimental data. Those predictions based upon preferred site nu leation in Ref. [6] are considerably greater than the experimental observations. It should also be noted that both of these models represent a "free contacting" mode configuration, but since the sensitivity to an external trigger has been experimentally demonstrated to be small, they provide a good representation of these events as well.

Since there is some variation in the predicted cutoff levels and since data is available for a large scale water system as well as small scale experiments with reactor materials, a designation of the actual cutoff level for water is best guided by the experimental results. The Ispra tests [9] were free contacting mode experiments and these provided vigorous explosions at 1 atm. For a pressure of 0.5 MPa, the results could perhaps contain some very weak explosive interactions, but at the pressure level of 1.0 MPa all explosive activity was suppressed. These are in agreement with the small scale, externally triggered tests carried out at Sandia with reactor materials [10], in which explosive interactions could be triggered for pressures as high as 0.5 MPa, but not at a level of 0.75 MPa. In the Winfrith UO_2-water experiments [11], which can be considered to be lightly triggered, the explosive interactions were suppressed by a system pressure of 0.9 MPa. Therefore, a cutoff value of 1.0 MPa bounds the available experimental steam explosion results for water,

and this is a valid basis upon which to evaluate the potential for such phenomena in LWR reactor systems, although as will be illustrated in the discussions on mixing and formation of a continuous slug, the same conclusions would be reached even if the cutoff pressure were considerably greater.

When the pressures predicted by both models and the experimental data are compared to the conditions typical of the various accident categories, only the large break sequences result in such reduced pressure levels.

Consequently, for these sequences in which the lowest primary system pressure is greater than this cutoff level, the probability of a steam explosion itself is insignificant and it follows that the probability of containment failure is also negligible.

2. Low System Pressures (Large Break Sequence)

For low pressures within the reactor coolant system (less than 1.0 MPa) the potential of a steam explosion, given direct contact between molton core material and water, must be considered. This is based on the experimental evidence at these pressures as well as the numerous events which have occurred in the foundary and paper industries. As discussed in WASH-1400 steam explosions have done extensive damage to light industrial structures and are a hazard to operating personnel. However, the information compiled with regards to these foundary explosions shows that the injuries to personnel resulted from hot molten metal dispersed by the explosive event, as opposed to the shock waves generated by the explosion. This suggests that steam explosions are a mild event compared to those associated with chemical detonations, i.e. the concussion from a chemical detonation shock wave can be lethal. This is in agreement with the measured wave propagation velocities which can be several thousand meters

per second for chemical detonations, but have been measured to be of the order of 100 m/sec for steam explosions [13].

Since the central issue of this evaluation is the damage potential represented by in-vessel steam explosions, one must evaluate the amounts of material which can come into contact and mix on an intimate scale prior to the onset of an explosive interaction. The calculations performed in WASH-1400 assumed that all the material within the core was instantaneously and intimately mixed with all the water in the lower plenum. Obviously this would not be the case, given such a hypothetical accident, and as will be discussed below, only very small fractions of this material can be mixed to provide an explosive interaction. Also the liquid-liquid film boiling mixing process itself makes the formation of a coherent overlying slug essentially impossible. These effects will be discussed individually, beginning with the ability to trigger such an interaction within a reactor pressure vessel.

Both large and small scale experiments with high temperature molten metals and reactor materials have demonstrated that explosive interactions with water require an external trigger. It should be noted that the requirement for an external trigger with very high temperature materials (specifically when the interface contact temperature exceeds the thermodynamic critical point) was one conclusion of the nucleation formulation for the Henry-Fauske model. This effect was also demonstrated experimentally in Ref. [5]. In many molten metal experiments, [14,15], this trigger has been produced by the contact between the melt and the bottom of the vessel. Such a "trigger" provides a mechanism whereby the amount of material and the level of mixing can both be identified for a given system.

The mechanical energy available for mixing prior to the explosive interaction is that energy available in the gravity drop, or pour, of the material from the lower portion of the core to the bottom of the reactor vessel. It should be noted that this energy is directed such that the result is to continue and sustain the mixing process. However, as discussed earlier in this section, a BWR has a large number of support tubes below the core region. Consequently, any attempt to accumulate molten core material and have it pour into a water pool would only result in a pour into a very confined configuration, i.e. the support tubes. For these conditions, only a very limited amount of material could interpenetrate the water pool before it would contact a solid wall, thus promoting an interaction. Such behavior would be very incoherent and would be of negligible consequence to the reactor vessel or any of its internal structure.

Anticipated events for these low pressure conditions are discussed with respect to (1) the trigger, (2) intimate mixing, (3) pool boilup (slug formation, and (4) rapid liquid-liquid intimate mixing.

a. Trigger

The time for pouring the material into the core support structure and the lower plenum becomes significant when considering how much material can be available before the explosion is initiated. The large scale aluminum-water experiments conducted by Long [14], and Hess and Brondyke [15] have shown that large scale explosions are initiated when the melt contacts the bottom of the vessel. As discussed above, for a gravity pour, assuming all available flow area in the lower core support structure, this would correspond to a very short time interval between initiation of the pour and the onset of the explosion as initiated by trap-

ping water against a solid wall. Consequently, the amount of material involved in the interaction would be a negligible fraction of the total core.

b. Mixing

The next subject to be addressed is the rate at which material can be intimately mixed before an explosion is initiated. The core support structure itself is a major barrier to any mixing between the core material and water. In this subsection the immense energy requirements necessary to mix these materials on a very short time scale as assumed in WASH-1400 will be evaluated.

The mixing energy required for an intimate dispersion has been evaluated by Cho, Fauske and Grolmes [16], and the details of such an evaluation are included here as Appendix A. These calculations reflect two different types of mixing processes, one in which the intimate dispersion is accomplished in a one-step process, and another in which it is postulated to occur with the minimum mixing energy, entitled progressive mixing. If it is postulated for the sake of this argument, that the total core (about 200,000 kg) is instantaneously dropped into a lower plenum, filled with water, the mixing energy would be that available from a gravity drop, i.e. the change in potential energy, or about 6 MJ. If the end state of the mixing process is assumed to be particle sizes of approximately 1 cm in diameter, as required for vessel failure in the WASH-1400 calculations, this mixing energy would require a time of 1.2 s for progressive mixing and 2.3 s for the one-step process for mixing the entire core. These mixing intervals alone are long compared to the maximum melt-drop times used in WASH-1400 for conditions in which the vessel was predicted to fail. In addition, one must add the time interval required for

total time is longer than that associated with potential containment fail-
ure in the RSS even incorporating all the other conservative assumptions.
As will be seen, these times are also much longer than the characteristic
times for vapor generation due to film boiling alone and the resultant
"boilup" of any postulated overlying liquid pool. Therefore, there is
insufficient energy associated with an assumed gravity drop of the entire
core (in the absence of internal structures) to affect a rapid and inti-
mate mixing on the size scale modeled in the RSS, which ignored the neces-
sity of such requirements.

c.   Pool Boilup (Slug Dispersal)

As postulated the mixing and inner dispersion progresses in the hy-
pothetical open configuration, the hot and cold liquids, are in liquid-
liquid film boiling. Since the hot liquid is at a temperature of approxi-
mately 2500°K, the principle mode of energy transfer would be via radia-
tion from the hot debris to the water. This energy transfer (q) can be
approximated as

$$q = 4\pi r^2 \sigma (T_F^4 - T_f^4) \qquad (1-1)$$

where r is the radius of the hot particles, σ is the Stefan-Boltzmann con-
stant, T_F is the emperature of the degraded core debris, and T_f is the
saturation temperature of the water. The resulting energy transfer is
calculated by the product of this radiation heat transfer and the number
of particles involved. The particle number (N) is determined by a con-
sidera ion of the total mass involved (m_T) in the interaction

$$N = m_T / [\rho_F \, 4/3\pi \, r^3] \qquad (1-2)$$

where ρ_F is the density of the molten core debris. For these low pressure
sequences, the thermal energy in the below core structure as well as the

radiant energy from the degraded core will ensure that the water in the lower plenum is essentially saturated. Consequently, any boiling (or vaporization) during the mixing phase will result in net vapor formation. This vapor will either cause any overlying pool to "boilup" until the average void fraction is sufficiently large to allow the vapor to be transmitted through the pool at a rate equal to its generation. The vapor production rate ($\dot{m}_v$) is given by

$$\dot{m}_v = Nq/h_{fg} \qquad (1-3)$$

where h_{fg} is the latent heat of vaporization for the water. Since the mass flow rate is a product of the vapor density (ρ_g), the area of the vessel (A_v), and the superficial vapor velocity (U) (this reflects the stability of the overlying pool), this latter term can then be evaluated from the expression

$$U = \frac{3 m_T \sigma (T_F^4 - T_f^4)}{\rho_g A_v \rho_F r h_{fg}} \qquad (1-4)$$

If this superficial vapor velocity is tabulated for various particle sizes and system pressures, the results are shown in Tables 1-IV and 1-V for pressures of 0.1 and 1.0 MPa respectively. These tables show the particle size, the number of particles, and superficial vapor velocity. In order to prevent pressurization of the pool, this amount of vapor must "slip" through any overlying slug. In order to allow this "slippage", the overlying pool must "boilup" to a given void fraction. The relationship between the superficial velocity and the void fraction has been represented by Zuber [17] as

$$U = 1.53 \sqrt[4]{\frac{g\sigma}{\rho_f}} \left[\frac{\alpha}{1 - \alpha} \right] \qquad (1-5)$$

In this expression σ is the liquid-vapor surface tension, ρ_f is the density

Table 1-IV

Pool Boil Up (Slug Dispersal)
Pressure = 0.1 MPa, Core Debris - 10^5 kg

Particle Radius (m)	Number of Particles	Superficial Velocity m/sec	Pool Void Fraction	Temperature Rise Rate °C/sec	Pressure Rise Rates MPa/sec Min	Max
1	3.4	5.5	0.99	1.6	0.007	4.4
0.1	3,400	55	0.99	16	0.07	44
0.01	3,400,00	550	0.99	164	0.7	440
0.005	27,300,000	1100	0.99	329	1.4	880

Table 1-V

Pool Boil Up (Slug Dispersal)
Pressure = 1.0 MPa, Core Debris - 10^5 kg

Particle Radius (m)	Number of Particles	Superficial Velocity m/sec	Pool Void Fraction	Temperature Rise Rate °C/sec	Pressure Rise Rates MPa/sec	
					Min	Max
1	3.4	0.71	0.75	1.6	0.04	6.2
0.1	3,400	7.1	0.97	16	0.4	62
0.01	3,400,00	71	0.99	164	4.0	620
0.005	27,300,000	710	0.99	329	8.0	1240

of saturated water, g is the acceleration of gravity, and α is the pool average void fraction. The resultant pool void fractions are listed in Tables 1-IV and 1-V and it is obvious that a continuous overlying liquid slug could not exist in the presence of this vapor flow, as demonstrated by the high void fractions required to transmit the imposed vapor flow. In fact, for the superficial velocities characteristic of the amount of material and particle sizes discussed in WASH-1400, the core debris itself would be levitated. This is in agreement with Long's [14] experiments in which explosions were not observed for water temperatures exceeding $60^{\circ}C$, i.e. the net vapor formation could have been sufficient to disperse either the water or the aluminum or both. In addition, Long also observed that breaking up the molten aluminum stream before it entered the water prevented explosions; probably the result of a larger film boiling heat transfer due to increased surface area.

If vapor "slippage" is assumed not to occur, then the pool must pressurize. A lower bound of the pressurization rate can be calculated by assuming all the energy transferred is uniformly mixed in the water and the pressure is the saturation value corresponding to the average pool temperature. The temperature rise rate of the liquid resulting from the film boiling energy transfer and the corresponding rise in the saturation pressure of the water are also shown as a function of the particle size in Tables 1-IV and 1-V. These calculations were carried out for an equal volume mixture of core debris and water and the salient conclusion is that fine particle sizes would rapidly generate sufficient pressure to quickly separate the high temperature degraded core material and the water if the vapor is not allowed to escape. Thus, large quantities of high temperature core material cannot penetrate the water and intermix in a film boil-

ing mode. If the vapor is not dispersed, then the pool would begin to pressurize from within which would disperse the pool, terminate the energy transfer, and destroy any coherent slug. As mentioned, a lower bound on the pressurization rate (dP/dt) is given by assuming all the energy transferred uniformly increases the sensible heat of the water. An upper bound on such a rate can be calculated by assuming the energy transferred equals the vaporization rate and the vapor volume remains constant, which is a rate given by

$$\frac{dP}{dt} = \frac{3 P m_T \sigma (T_F^4 - T_f^4)}{r \rho_F m_g h_{fg}} \tag{1-6}$$

These rates were calculated for a 10% void fraction and are also given in Tables 1-IV and 1-V. The differences between the minimum and maximum pressurization rates are large and these are only meant as general bounds for the assumed behavior. The conclusion from both rates is that pressurization of the mixture due to film boiling alone would disperse the constituents and stop the mixing if the vapor were not allowed to "slip" through the pool.

It should be noted in evaluating the minimum and maximum pressurization rates that since water has a relatively low thermal conductivity, the energy cannot be readily distributed throughout the water. The amount which can be conducted away from the available steam-water interfaces can be estimated by the error function solution where the constant surface temperature (T_i) is assumed to be $300^\circ C$ (saturation pressure of 8.6 MPa) which overestimates the energy transfer into the water. The energy transferred into the water (Q) at any given time (θ) is

$$Q = 2 k_f A (T_i - T_o) \sqrt{\frac{\theta}{\pi \alpha_f}} \tag{1-7}$$

where k_f is the thermal conductivity of the water, α_f is the thermal diffusivity of the water, T_o is the initial water temperature, and the surface area is given by

$$A = N(4\pi r_F^2) \tag{1-8}$$

Using a 1 cm radius particle as a reference size the energy transferred into the water in a time interval of one second is about 1600 MJ as compared to 8800 MJ transferred from the hot particles via thermal radiation. Thus, the actual pressurization rate would be much closer to the maximum pressure rise rate than the minimum value.

Therefore, in a slowly developing dispersion (time scale of 1 sec or longer) the vapor throughput would be substantial and preclude the formation of a continuous overlying liquid slug. If the vapor is assumed to be retained in the pool, the pressurization would disperse the pool, hence no slug formation would occur. Without the continuous slug formation, the only pressure imposed on the vessel is that due to the explosion itself, which experiments have shown to be a few MPa typically [18], and could conceivably be as high as 10 MPa. However, such pressure levels do not threaten the integrity of the vessel.

d. Rapid Liquid-Liquid Intimate Mixing

The only mechanism which could be postulated __ overcoming these large vapor fluxes is a very rapid intimate mixing of these materials under very high sustained pressures. In this hypothetical configuration, the mixing would be forced into a liquid-liquid configuration, which is the specific configuration addressed by the authors in Ref. [16]. To achieve such mixing requires enormous amounts of energy and this is clearly illustrated by the tabulated results in Table 1-VI. In this calculation,

Table 1-VI

Mixing Requirements

Time Scale (sec)	Penetration Depth (μm)	Percent Energy Release (%)	Particle Radius (μm)	Mixing Energy		Mechanical Work J	Mixing Energy / Mechanical Work	
				One-Step J	Progressive J		One-Step	Progressive
0.001	22	100	66	7.2×10^{14}	1.0×10^{12}	1.2×10^9	6×10^5	8×10^3
		10	660	7.2×10^{13}	8.1×10^{11}	1.2×10^9	6×10^4	675
		1	6600	7.2×10^{12}	5.8×10^{11}	1.2×10^9	6×10^3	483
0.010	69	100	210	2.3×10^{12}	9.2×10^9	1.2×10^9	2×10^3	7.67
		10	2100	2.3×10^{11}	6.9×10^9	1.2×10^9	192	5.75
		1	21000	2.3×10^{10}	4.6×10^9	1.2×10^9	19.2	3.83

the core debris was assumed to mix on a very short time scale. These cal-
culations were carried out for both the one-step process and progressive
mixing. The mechanical work was taken to be 1% of the thermal energy
within the melt, which is the upper bound efficiency in the large scale
experiments reported in Ref. [18]. In this tabulation, the mixing energy
is compared to the mechanical work released in this postulated event, and
as illustrated, the mechanical work is itself much less than the mixing
energy required to intimately disperse one material throughout the other,
i.e. the mixing necessary for the event would require a "trigger" larger
than the explosive interaction itself. (This calculation assumes that
such large systems could be intermixed and interacted which as illustrated
by the pool dispersal calculations is essentially impossible. Such a con-
servatism is used for illustration only and this must be continually kept
in mind when viewing the comparisons). This represents an unachieveable
state for a self-sustaining propagating interaction. However, even this
calculation overlooks one very essential physical feature of an intermix-
ing process in which materials at greatly different temperatures are as-
sumed to be rapidly interdispersed within each other; the heat transfer
is assumed to not impede the mixing process.

e.   Impedance of Mixing by Energy Transfer

As a material at very high temperature is forced into water at high
speed (rapid intimate mixing), the energy transfer occurs first on that
face of the particle which initially contacts the water. This initial
energy transfer rate is extremely high, and in the normal case, promotes
the rapid formation of a stable vapor film. However, to achieve the sin-
gle-phase state discussed above, which is required to prevent the pool
from dispersing, this stable vapor film must be suppressed. If this is

- 34 -

suppressed, then the surface will experience rapid, subcooled nucleate boiling, and the heat flux resulting from such a state would be enormous. The energy transferred to the coolant is stored in the liquid as an increase in the sensible heat. However, the temperature rise at the interface is also accompanied by a corresponding rise in the saturation pressure, which is also the pressure acting on the surface of the particle as it attempts to move through the water. This local pressurization is directed to impede the mixing process by slowing down the hot fragments. This type of transient behavior was observed by both Walford [19] and Stevens and Witte [20] in their convective film boiling experiments in which the sphere was rapidly driven through subcooled water. In these experiments, explosive vaporization off the leading surface of the particle was observed for specific conditions. This vaporization occurred as the particle penetrated the vapor film ahead of the leading surface. In this regime, Walford estimated that the local heat fluxes could achieve values approaching 170 megawatts per square meter, and when the experiment was conducted in a darkened room, the leading surface of the sphere was clearly much cooler than the trailing surface. The local pressure generated upon contact can be estimated by the saturation pressure corresponding to the interface contact temperature (T_i) given by

$$
T_i = \frac{T_F + T_f\sqrt{\frac{k_f \rho_f c_f}{k_F \rho_F c_F}}}{1 + \sqrt{\frac{k_f \rho_f c_f}{k_F \rho_F c_F}}}
\tag{1-9}
$$

Where T_F and T_f are the initial temperatures of the degraded core material and water and k_f, ρ_f, c_f, k_F, ρ_F and c_F are the thermal conductivities, densities and specific heats of the water and core material respectively. For the high temperature melts considered in these postulated events, the

resulting pressures would be supercritical. As a result of these experiments and others relating to rapid nucleate boiling, it is evident that a hot particle attempting to rapidly penetrate through a cold medium would achieve a self-limiting condition, i.e. if rapid relative velocity is initiated, the pressure at the interface upon contact acts to slow down the particle and perhaps even reverse its movement. Therefore, rapid energy exchange itself, which is vectored opposite to the intermixing, limits the rate of penetration of the two media. This particular aspect of the intermixing process has been neglected by the various models proposed in the literature in which a fine interdispersion is assumed to pre-exist and further fragmentation and intermixing is not opposed by any forces resulting from energy transfer between the hot and cold liquids. This is a major shortcoming of such models in their attempt to represent the physics of the explosion process itself. The criticism is particularly valid for the steam explosion formulation in WASH-1400, since both intimate dispersion and fine scale fragmentation were assumed to exist, and were achieveable instantaneously in the calculational model.

As a result of the above discussions, a picture of an actual process for a steam explosion in a low pressure system is one in which slow intermixing, via liquid-liquid film boiling, is developed over an extended time period with limited quantities of materials involved. Therefore, while an explosive interaction could potentially occur for such sequences, the amounts of materials involved are severely limited and the resulting explosive energy is far less than that represented in WASH-1400. In addition, no continuous overlying slug could develop and the pressures experienced within the reactor pressure vessel would be less than the nominal operating pressure.

E. Conclusions with Respect to In-Vessel Steam Explosions

Given the total evaluation of the steam explosion phenomenology as applied to in-vessel events for boiling water reactors, the following conclusions can be made.

1. The formulation provided in WASH-1400 is an overly simplistic and highly conservative representation of the state-of-knowledge for steam explosions.

2. Prior experiences in small test reactors have related solely to configuration of a pre-existing intimate dispersion of fuel and water in a cold condition, as well as a pre-existing continuous, overlying liquid slug. These reactions were then initiated by a strong reactivity ramp induced by the rapid withdrawal of a single control rod. This is a fundamentally different condition than a totally separated system at greatly different temperatures which is assumed to mix and interact in this state. Consequently, these previous systems are irrelevant for the particular conditions being addressed.

3. Previous analyses have ignored the above and below core structures in their formulations. As discussed, these structures have a major role in determining where, when, and how much material is distributed throughout the core region as well as the lower plenum. In addition, these structures would play a major role in the movement of any assumed continuous, overlying liquid slug through the vessel itself. In essence, these structures would not allow catastrophic collapse, intimate mixing, formation of a continuous overlying slug, and the transmission of this slug upward through the vessel in a piston-like fashion.

4. An evaluation of the experimental data available for systems at elevated pressures shows that explosive interactions can indeed be suppressed by elevated system pressures in many of the accident sequences of interest for BWR accident analyses. In these high pressure sequences, the potential for a steam explosion itself is insignificant, thus there is no threat to the containment integrity.

5. Evaluations of the available trigger, mixing, and intimate dispersion, show that the available models which assume a pre-existing intimate dispersion and resulting fragmentation with mixing on a rapid scale have either assumed away or grossly misrepresented the physical processes involved in attempts to rapidly interdisperse one liquid into another in the presence of strong temperature differences.

6. The failure mechanism in WASH-1400 was the formation and transmission of a liquid-like slug, but an evaluation of the potential for such a slug formation shows that it could not be formed because of (1) the available structures in the lower plenum region and (2) the necessary intimate dispersion for an explosive interaction would preclude the formation of a continuous slug. Hence, even for low pressure systems where steam explosions are possible, the slug impact failure mechanism is incredible.

7. Steam explosions outside the reactor vessel are possible for the conditions postulated, but they provide no threat to the containment integrity.

The above conclusions added together show that a steam explosion within the vessel does not provide a threat to the integrity of the reac-

- 38 -

tor vessel or any of its components. Table 1-VII compares the sequence of events envisioned in the WASH-1400 model and the actual conditions in BWRs. This comparison shows that each and every element of the model represents a physically unachieveable state. Consequently, such a mechanism does not provide a threat to the integrity of the reactor vessel and thus no threat to the primary containment building.

Table 1-VII

Comparison of the WASH-1400 Model and Actual Conditions for BWRs

WASH-1400	BWRs
1. All core melt sequences can produce steam explosions.	1. High pressure sequences prohibit steam explosions, only low pressure sequences can have steam explosions.
2. Coherent core melt involving all the core.	2. Axial and radial power profiles dictate a three-dimensional incoherent core melt taking tens of minutes.
3. Hold up and catastrophic collapse of core debris into water.	3. Core supported from below - no catastrophic collapse.
4. Instantaneous and intimate dispersal throughout the coolant.	4. Support tubes preclude any rapid and intimate mixing.
5. Coherent interaction between core debris and water.	5.1 Support tubes contain the fuel until the water is vaporized, i.e. no coherent interaction.
	5.2 Support tubes and control rod spindles would prevent and coherent intermixing.
6. Slug formation and acceleration through the vessel in a piston-like manner.	6.1 Slow intermixing in liquid-liquid film boiling would disperse the mixture before substantial amounts are involved.
	6.2 Support tubes and control rod spindles would prevent any slug formation.
7. Coherent slug impact on the vessel head.	7.1 Since only low pressure systems can explode, calculations for film boiling during intermixing show any continuous overlying liquid layer would be broken up, i.e. slug could not be formed.
	7.2 Steam separators do not provide a straight-through flow path for any slug movement.

II. Additional Hydrogen Generation

In many of the LWR accident analyses performed to date, chemical re-
actions between the zircaloy cladding and steam has not only been assumed
to occur during the initial overheating process when the core geometry is
still intact, but also when the material has "slumped" to the lower plenum
of the reactor vessel. In many such calculations, this has been a major
fraction of the total hydrogen produced in the calculated degradation pro-
cess for the specified accident sequence. In modeling such behavior for
postulated accident sequences in the Limerick system, it is necessary to
adequately represent the effect that these specific configurations would
have on such processes. In particular, the extensive below core struc-
ture would have a major influence on the ability to continue the oxidation
process between unreacted zircaloy and steam.

Core degradation is calculated when an accident sequence is specified
which either eliminates or limits the amount of water supplied to the core.
In general, this involves a failure of the major safety injection systems
including the core spray. In such cases, the degradation process would
progress within the fuel assembly cans and the amount of oxidation would
be minimal since the only water supplied to the core is that from the con-
trol rod drive system and this flows between the fuel assembly cans, and
thus does not provide a continuing source of steam for the oxidation pro-
cess. As continued heating of the core material occurs and the geometry
integrity is lost, the molten material would progress downward through the
fuel assembly cans, but further oxidation would only be minimal since the
available water supply is outside of the cans themselves. If sufficient
water is still denied by the specified accident scenario, the degraded

core material would begin progressing downward through and outside of the control rod guide tubes which support the fuel can assemblies. Since the CRD flow, if available, would be flowing upward through the guide tubes, the preferential path for downward progression would be outside of the control rod guide tubes where water would be essentially unavailable. Consequently, the downward progression would occur in the absence of a significant water source for continued oxidation of the zircaloy material. In addition, for those sequences where the CRD flow is available, the core degradation may be slowed to the point where melting of the material would not even occur. If melting were to occur, and severe distortion of the core, that portion which progressed into the lower plenum region would be the portion which received the greatest amount of cooling since that is the injection point of the CRD flows.

In summary, the amount of continued hydrogen generation for specified accident sequences where the core degradation results in "slumping" into the lower plenum region, the amount of continued zircaloy oxidation would be a very limited, slow process, and considering the cold structural members present as well as the water which could be available within the control rod guide tubes, this process could be determined by oxygen diffusion through a solid mixture of uranium-dioxide, zirconium-dioxide, and the zircaloy metal until the water is completely boiled off. In this case, the amount of hydrogen generated during the total core degradation process until the reactor vessel failure is postulated, would be essentially that formed while the core geometric configuration remained intact. The assumption of rapid fragmentation and continued oxidation as the core material progresses into the lower plenum region represents a very conservative formulation of the actual physical processes.

- 42 -

III.   Vessel Failure Mechanism

If in a defined accident sequence water cannot be supplied to the re-
actor vessel to establish in-vessel removal of the decay power from the
damaged core, then eventually the core will melt along with the fuel as-
sembly cans, the core support plate, and the core support tubes. This
mass of molten material will accumulate in the lower head of the vessel
and will thermally attack the vessel wall and vessel penetrations. Boil-
ing Water Reactors have a forest of penetrations in the lower head because
the control rods are driven from the bottom and the in-core instrumenta-
tion also enters the vessel from the bottom. For the Limerick reactors,
there are 175 control rods, each with its own penetration, several addi-
tional penetrations for in-core neutron flux monitors, and a reactor ves-
sel drain. Figure 3-1 illustrates the general configurations utilized
for both control rod penetrations and in-core instrument tube penetrations.
In both cases the weld area would be subject to a three-dimensional ther-
mal attack in the presence of any significant accumulation of degraded
core material. Because of the large number of penetrations and the three-
dimensional type of melting attack that these would experience, as opposed
to the essentially one-dimensional melting at the vessel wall, these pene-
trations would be the first element of the primary system pressure bound-
ary to fail, particularly for meltdown scenarios in which there is con-
siderable pressure within the reactor vessel.

In the event that a control rod drive support is melted through and
the mechanism is ejected, the resulting vessel breach would be approxi-
mately 10 cm in diameter. Figure 3-2 schematically illustrates a con-
figuration in which the molten core material flows through the penetration

IN-CORE
PENETRATION.
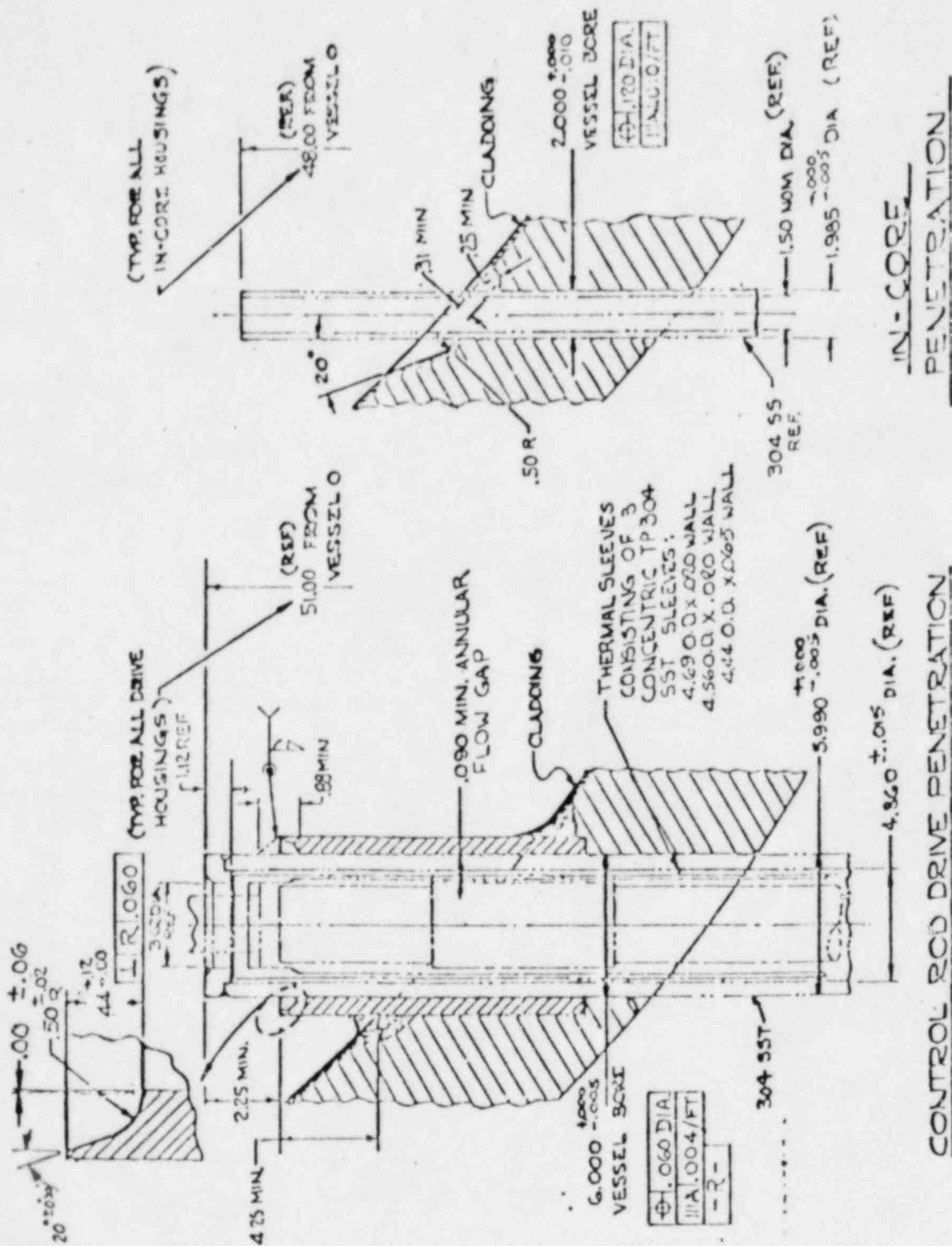
CONTROL ROD DRIVE PENETRATION
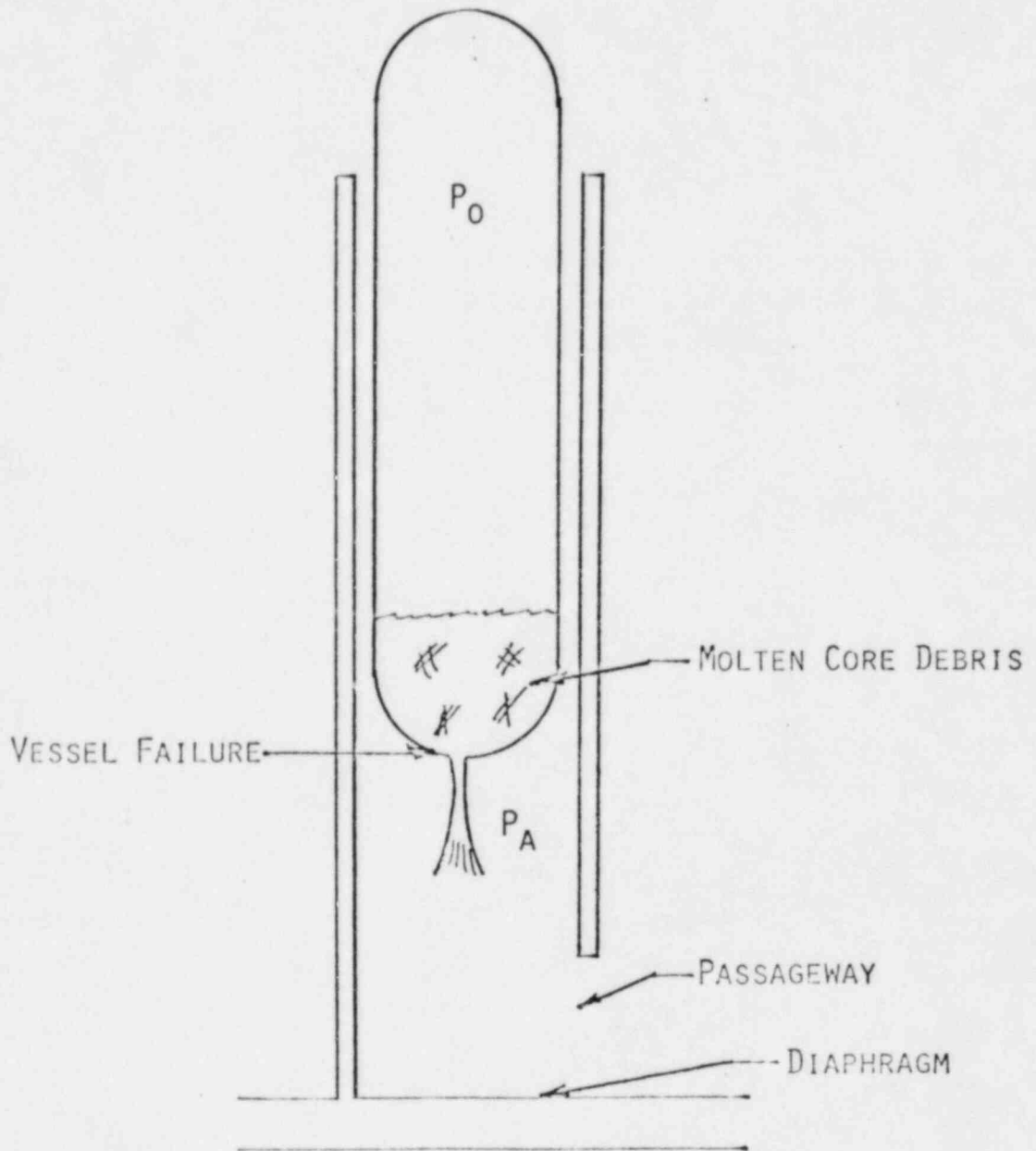
FIG. 3-1 REACTOR VESSEL PENETRATION.

FIG. 3-2 MATERIAL DISCHARGE FOLLOWING
VESSEL FAILURE.

breach under the driving pressure of the overlying steam/gas mixture. The velocity of this discharge (U) can be estimated by Bernoulli's equation where the core material is assumed to be all liquid.

$$U = \sqrt{\frac{2(P_o - P_a)}{\rho_F}} \tag{3-1}$$

The pressures P_o and P_a represent the vessel and primary containment conditions respectively and ρ_F is the density of the molten core material.

As the high temperature liquid flows through the breach, it will contact the comparatively cold steel of the reactor vessel wall in the process. The interface temperatures developed upon contact are expressed

$$T_i = \frac{T_F + T_s \sqrt{\frac{k_s \rho_s c_s}{k_F \rho_F c_F}}}{1 + \sqrt{\frac{k_s \rho_s c_s}{k_F \rho_F c_F}}} \tag{3-2}$$

where T_F and T_s are the initial temperatures of the degraded core material and vessel steel and k_F, ρ_F, c_F, h_s, ρ_s and c_s are the thermal conductivity, density and specific heat of the core material and steel respectively. For the conditions of interest ($T_F \sim 2200^o C$ and $T_s \sim 250^o C$) this interface temperature ($\sim 650^o C$) is well below the melting points of both the steel ($\sim 1500^o C$) and the fuel-zirconium oxide mixture ($\sim 2000^o C$ for the mixture). Consequently, the molten material would freeze upon contact forming a thin crust of material as shown in Fig. 3-3 which tends to insulate the steel from the molten stream. The solid crust receives energy (q) from the convective stream at a rate given by the expression

$$q = hA (T_F - T_{m,F}) \tag{3-3}$$

where h is the convective heat transfer coefficient, A is the surface area of the crust, and $T_{m,F}$ is the melting point of the uranium dioxide-

BUFFER ZONE

UO_2 FLOW

SOLID UO_2 CRUST

LAMINAR SUBLAYER
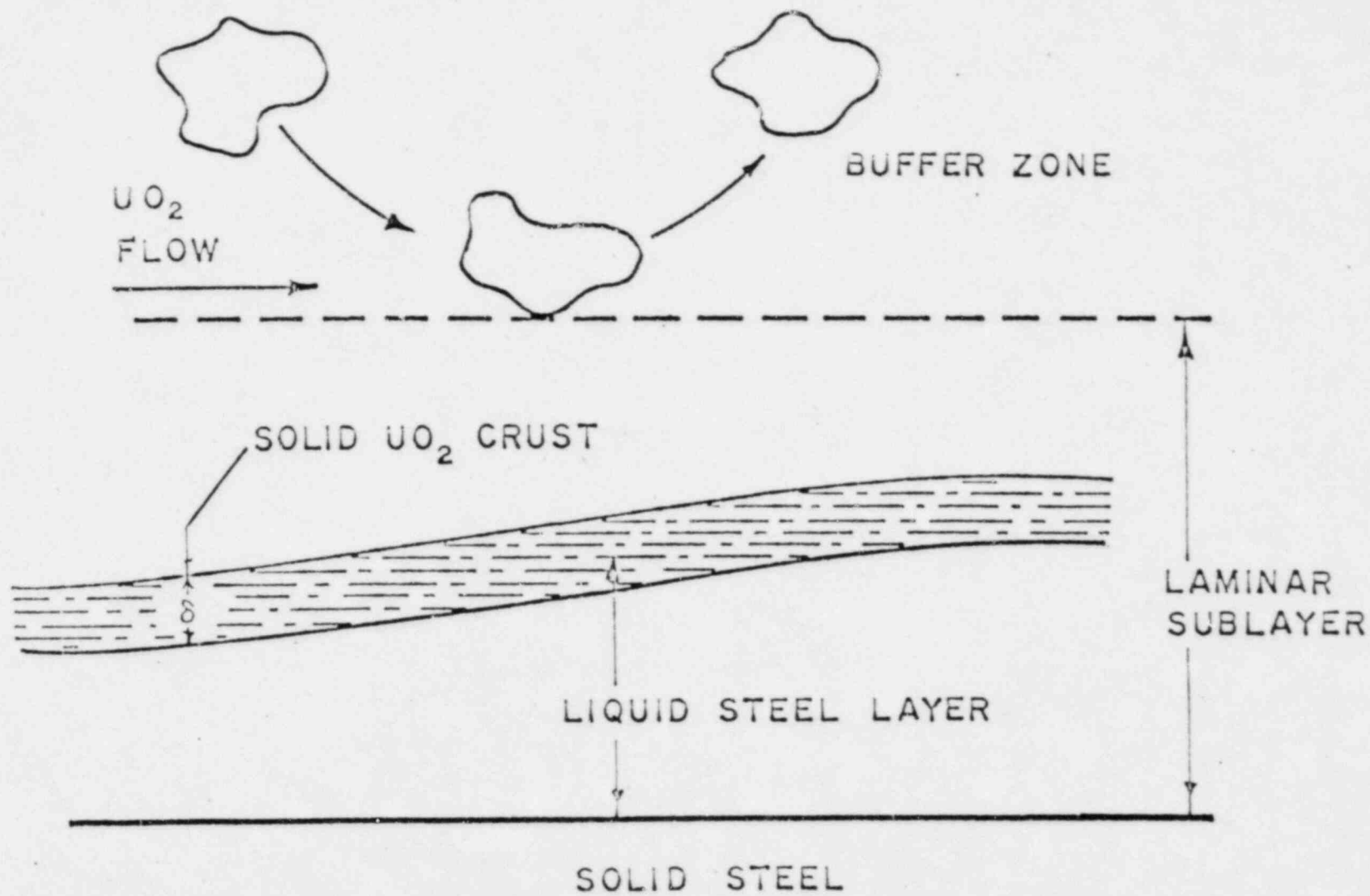
LIQUID STEEL LAYER

SOLID STEEL

FIG. 3-3 FUEL CRUST FORMATION BETWEEN STEEL AND MOLTEN FUEL.

zirconium dioxide mixture. Assuming that Reynold's analogy applies the heat transfer coefficient can be related to the discharge velocity by

$$h = f \frac{\rho_F C_F U}{2} \tag{3-4}$$

where f is the dimensionless friction factor (f $\sim$ 0.005). If the vessel pressure is assumed to be 7.0 MPa and the drywell pressure is 0.3 MPa, the discharge velocity would be about 43 m/sec, and the corresponding heat transfer coefficient would be approximately 450 kw/m^2°C. The imposed heat flux must be transferred through the crust and into the steel. If the crust is too thick to transmit the required energy, it will remelt until it is sufficiently thin and if the steel cannot absorb the imposed heat flux it will also melt. The time required for thermal boundary layer development within the steel to the point where it can no longer remain solid can be estimated from the error function equation where the interface temperature is assumed to be the steel melting point $(T_{s,m})$.

$$h(T_F - T_{F,m}) = k_s(T_{s,m} - T_s)/\sqrt{\pi \alpha_s \theta} \tag{3-5}$$

The steel thermal diffusivity is designated by α_s, T_s is the initial steel temperature, and the time interval by θ. Thus, the expression for the time interval before steel melting begins is obtained by rearranging the above equation to:

$$\theta = [k_s(T_{s,m} - T_\infty)]^2/\pi \alpha_s [h(T_F - T_{F,m})]^2 \tag{3-6}$$

For the conditions outlined above, this time for the onset of steel melting is 0.04 sec which is very short compared to the discharge time for the core debris. Consequently, even with the presence of an insulating crust, the steel substrate would be quickly driven to melting as a result of the high heat flux imposed by the high temperature convective stream. Melting of the steel substrate below the fuel crust would jeopardize the

stability of this crust. This thickness of this solid layer (δ) can be estimated from:

$$\delta = k_F(T_{F,m} - T_{s,m})/h(T_F - T_{F,m}) \tag{3-7}$$

For the temperatures and flow conditions listed above, the crust of core debris would only be approximately 66 μm thick which would have negligible strength, and this is in agreement with the stability arguments presented by Epstein, et.al. [21]. Therefore, once steel melting begins, the thin crust of core material would be continually formed, destroyed, and re-formed, with the only significant implication of the crust being the limitation that it provides in the energy transfer process, i.e. it determines the driving temperature difference for the convective heat transfer from the molten stream.

As a result of the behavior described above, the steel would be melted very shortly after the penetration fails and flow is established and the high temperature convective stream would continually attack the vessel steel wall. This ablation process will enlarge the original failure size at a rate which can be obtained by equating the convective energy transfer to the energy required to melt the steel.

$$hA_s(T_F - T_{F,m}) = \rho_s A_s(c_s(T_{s,m} - T_s) + \gamma_s) \frac{dr}{dt} \tag{3-8}$$

The derivative dr/dt is the growth rate of the breach radius, A_s is the exposed cylindrical surface area of the steel, and γ_s is the heat of fusion of the steel. From this expression, in which the discharge velocity remains constant, the growth rate of the breach is a constant and is given by

$$\frac{dr}{dt} = \frac{h(T_F - T_{F,m})}{\rho_s(c_s(T_{s,m} - T_s) + \gamma_s)} = B \tag{3-9}$$

which for the condition used in the above examples gives a value of approximately 0.9 cm/sec. As a result, the available flow area through which the molten material could be expelled from the vessel would increase substantially during the core ejection stage.

With the configuration illustrated in Fig. 3-2, the incompressible molten material would be forced out of the vessel by the high pressure, compressible gas/steam mixture above the core debris. Si' ce the volume occupied by the molten core would be small compared to the initial volume of the gas/steam mixture, the vessel pressure and, therefore, the discharge velocity (U), would remain essentially constant during the expulsion process. Thus the discharge flow ($\dot{m}$) can be described by

$$\dot{m} = \rho_F A_c U \tag{3-10}$$

where

$$A_c = \pi r^2 = \pi (r_o + Bt)^2 \tag{3-11}$$

The quantity r_o is the radius of the initial vessel failure, i.e. the radius of a control rod drive penetration. To express the total mass discharged (Δm) at any point in time (t), one only has to integrate Eq. (3-10) with respect to time

$$\Delta_m = \rho_F U \pi \int_0^t (r_o + Bt)^2 dt = \rho_F U \pi \left[r_o^2 t + r_o Bt^2 + \frac{B^2 t^3}{3} \right] \tag{3-12}$$

and this mass discharged as a function of time is graphically illustrated in Fig. 3-4. It is apparent from the function form that the flow rate would continually increasing because of the linear growth of the radius with time. But the breach diameter required to exhaust the mass of molten material would be less than one-tenth of the vessel diameter. This, and the comparatively short time scale for complete discharge, are the prin-
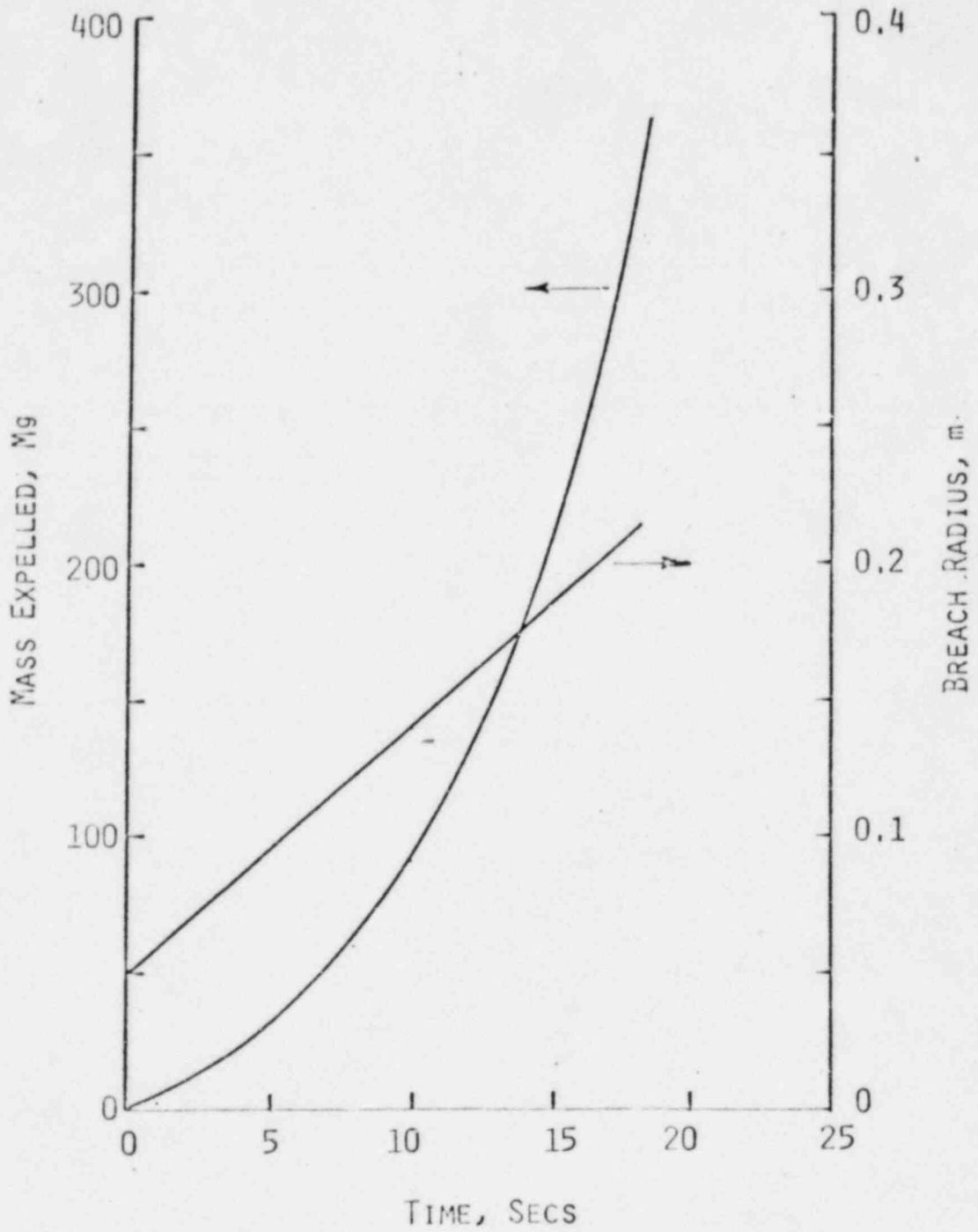
FIG. 3-4 MASS DISCHARGED AND BREACH RADIUS
VERSE TIME.

ciple results illustrated by this analysis. Subsequent discharge of th
follow-on gas/steam mixture should be calculated based upon this available
vessel breach.

With the final radius of 0.2 m, the breach size ablated by the high
temperature material would essentially encompass nine control rod penetra-
tions. Since the accumulation of core debris would attack more than one
penetration, but generally in the same locale as the initial failure point,
the evaluation of a single penetration as the incipient failure is a good
approximation of the behavior for these conditions; particularly in light
of the time required for complete discharge of the material. However, the
sensitivity to multiple simultaneous and independent failures can be easi-
ly calculated since the available area for discharge is

$$A_c = n\pi r^2 = n\pi(r_o + Bt)^2 \tag{3-13}$$

where n is the number of simultaneous failures. This sensitivity can be
obtained by comparing Figs. 3-5 and 3-6 which represent assumed failures
of one and five CRD penetrations respectively. While there is some re-
duction in the discharge interval, the difference is only a factor of two
for five times the number of assumed failure locations. The key point ob-
tained from these calculations is that the discharge would occur over a
time frame of at least 10 secs. and the resulting breach in the reactor
vessel wall for these hypothetical conditions would have a diameter of ap-
proximately 0.4 m. This calculated breach can then be used in subsequent
evaluations of the pressure response in the drywell as the follow-on steam/
hydrogen mixture is discharged through this breach in the reactor vessel
wall.

For some hypothetical core melt sequences, large break LOCAs with
postulated safety system failures where the primary system is essentially
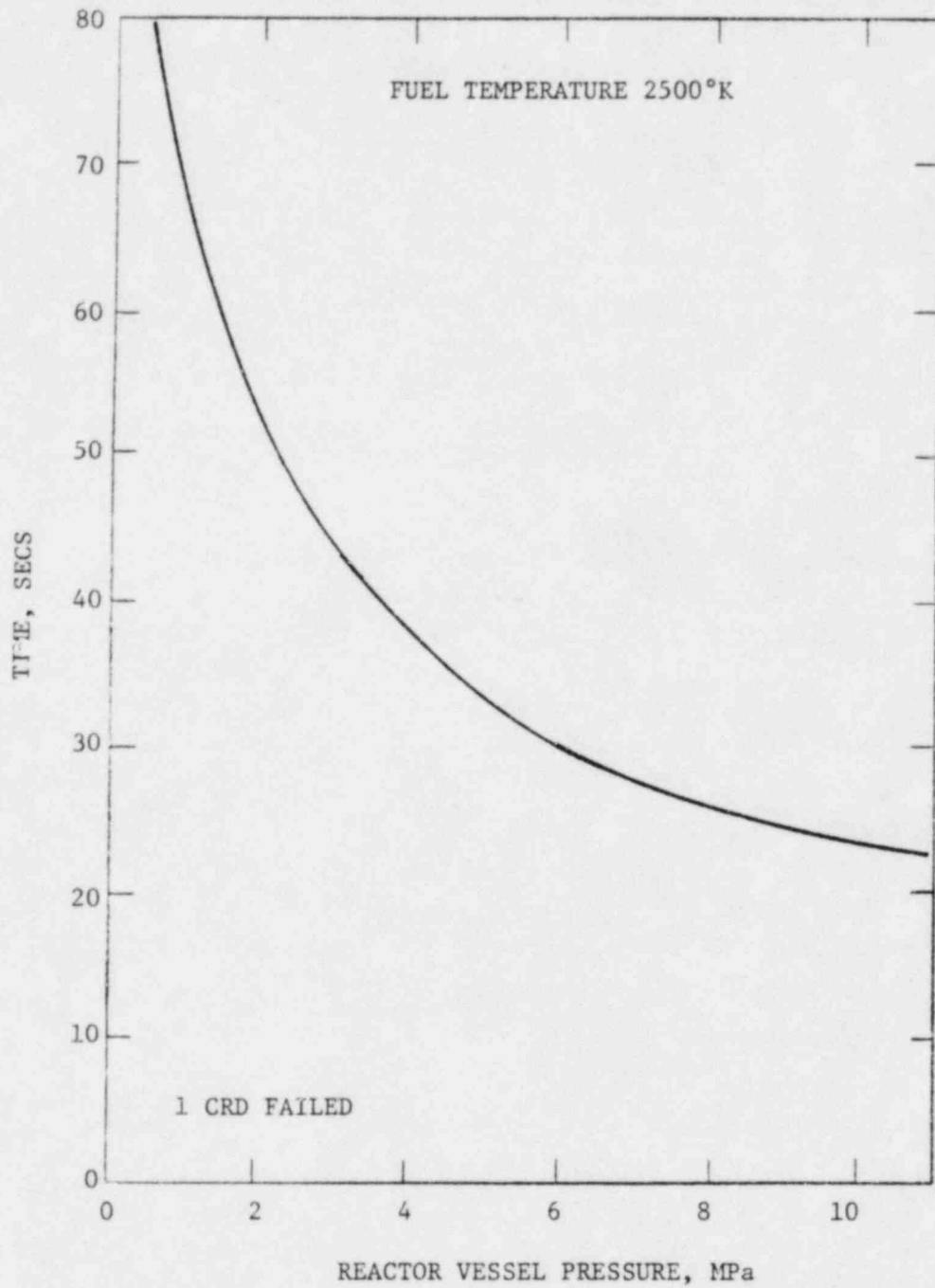
Fig. 3-5 Discharge Interval as a Function
of Reactor Vessel Pressure.
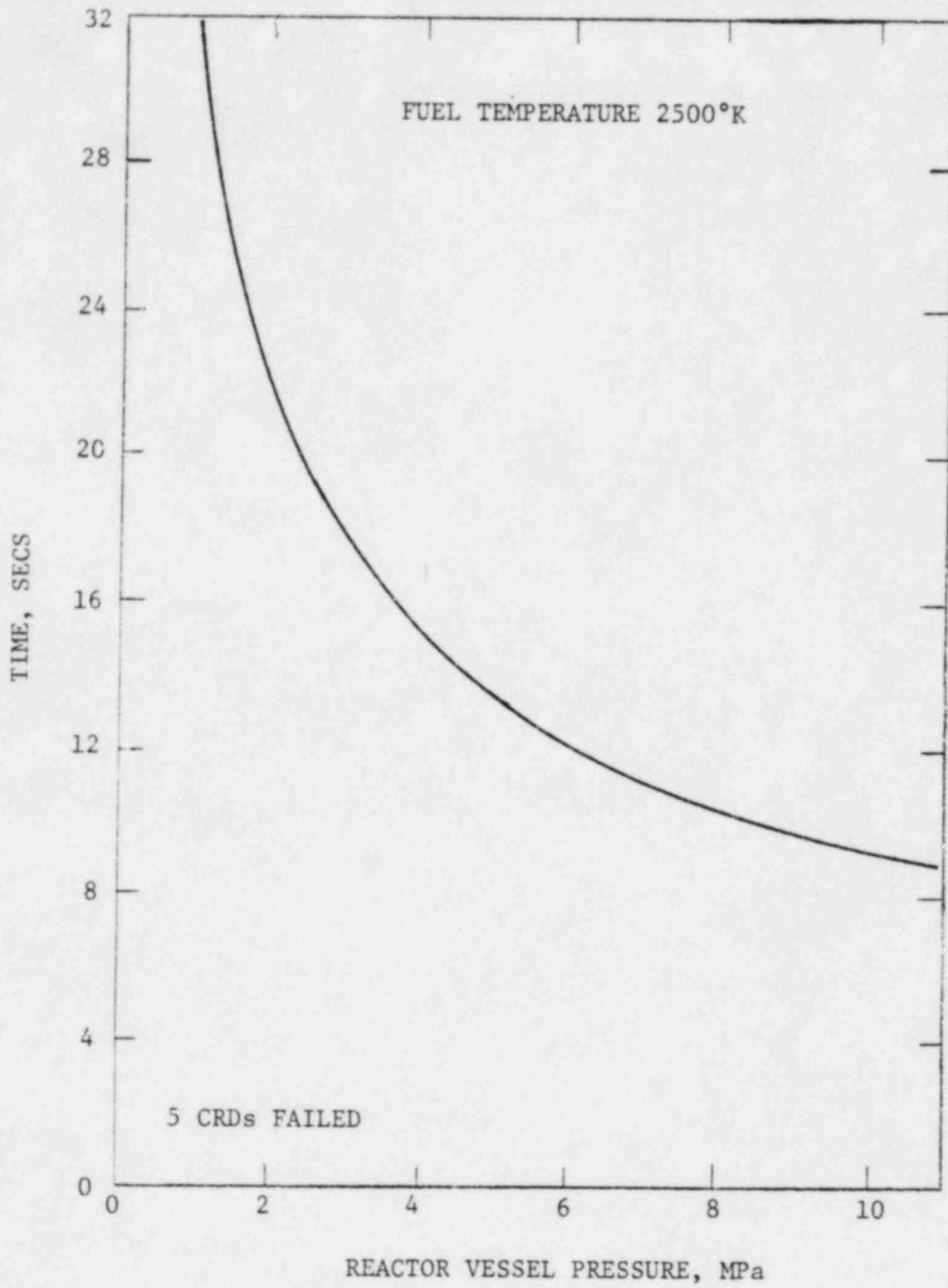
Fig. 3-6 Discharge Interval as a Function
of Reactor Vessel Pressure.

depressurized to the drywell pressure, the driving force for discharge of degraded core material through the reactor vessel breach would be the gravitational head of the degraded core material.

If the molten core material were to accumulate in the bottom of the vessel and one or more control rod drive penetrations is assumed as the failure location, the fuel would flow out of the reactor vessel by its own gravity head. The height of the liquid level above the vessel breach would determine the discharge rate of the degraded core material.

The total volume of the molten core material (V_F) would generally be less than that of the hemispherical reactor vessel bottom, the maximum liquid level to the lowest point in the vessel, H, can be calculated as shown in Fig. 3-7.

$$V_F = \frac{M_F}{\rho_F} = \int_0^H \pi r^2 dh \tag{3-14}$$

where M_F is the mass of accumulated degraded core material. The vessel radius (r) at any height h is given by

$$r = \sqrt{R^2 - (R - h)^2} \tag{3-15}$$

and h is the instantaneous liquid level. Substitute Eq. (3-15) into Eq. (3-14) and integrating yields and expression for the liquid height as a function of the mass inventory.

$$\frac{M_F}{\rho_F} = \pi \int_0^H (2Rh - h^2) dh = \pi (RH^2 - \frac{H^3}{3}) \tag{3-16}$$

The liquid velocity at the breach is determined by the static head:

$$U_F = \sqrt{2gH} \tag{3-17}$$

As in the cases with an elevated pressure within the reactor vessel, the ablation rate at the failure location is given by Eq. (3-9). However, B
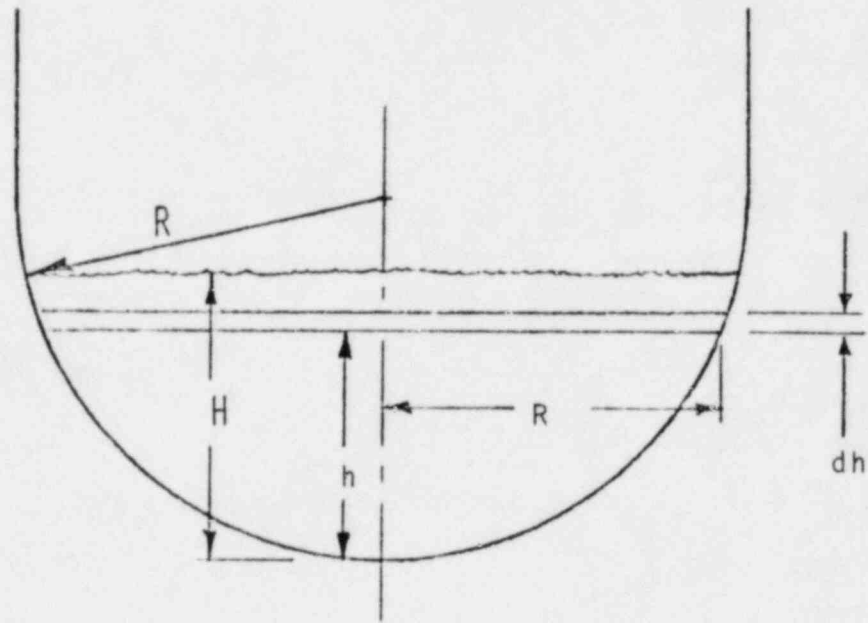
Fig. 3-7 Configuration for Calculating Core
Debris Accumulation in the Lower Plenum.

is a function of H, hence a function of time t. The discharge rate of the molten material is represented by

$$\dot{m} = \rho_F U_F A_b = \rho_F U_F \pi r_b^2 \tag{3-18}$$

where A_b and r_b are the area and radius of the breach respectively. The breach radius can be calculated from

$$r_b = r_o + \int_0^t B(t)dt \tag{3-19}$$

The liquid level decreases when the inventory of degraded core material decreases.

$$\frac{dV_F}{dt} = \frac{1}{\rho_F} \frac{dM_V}{dt} = \rho_F \pi H(2R - H) \frac{dH}{dt} \tag{3-20}$$

Combine Eqs. (3-18) and (3-20) yields

$$\frac{dH}{dt} = \frac{-U_F r_b^2}{H(2R - H)} \tag{3-21}$$

These equations can be solved by a simple forward marching numerical technique.

Figure 3-8 illustrates the discharge velocity and the breach radius as a function of time for a gravity driven case. The amount of material remaining in the vessel (M_F) is shown in Fig. 3-9, and the calculation demonstrates that the discharge is essentially complete within a two minute interval.
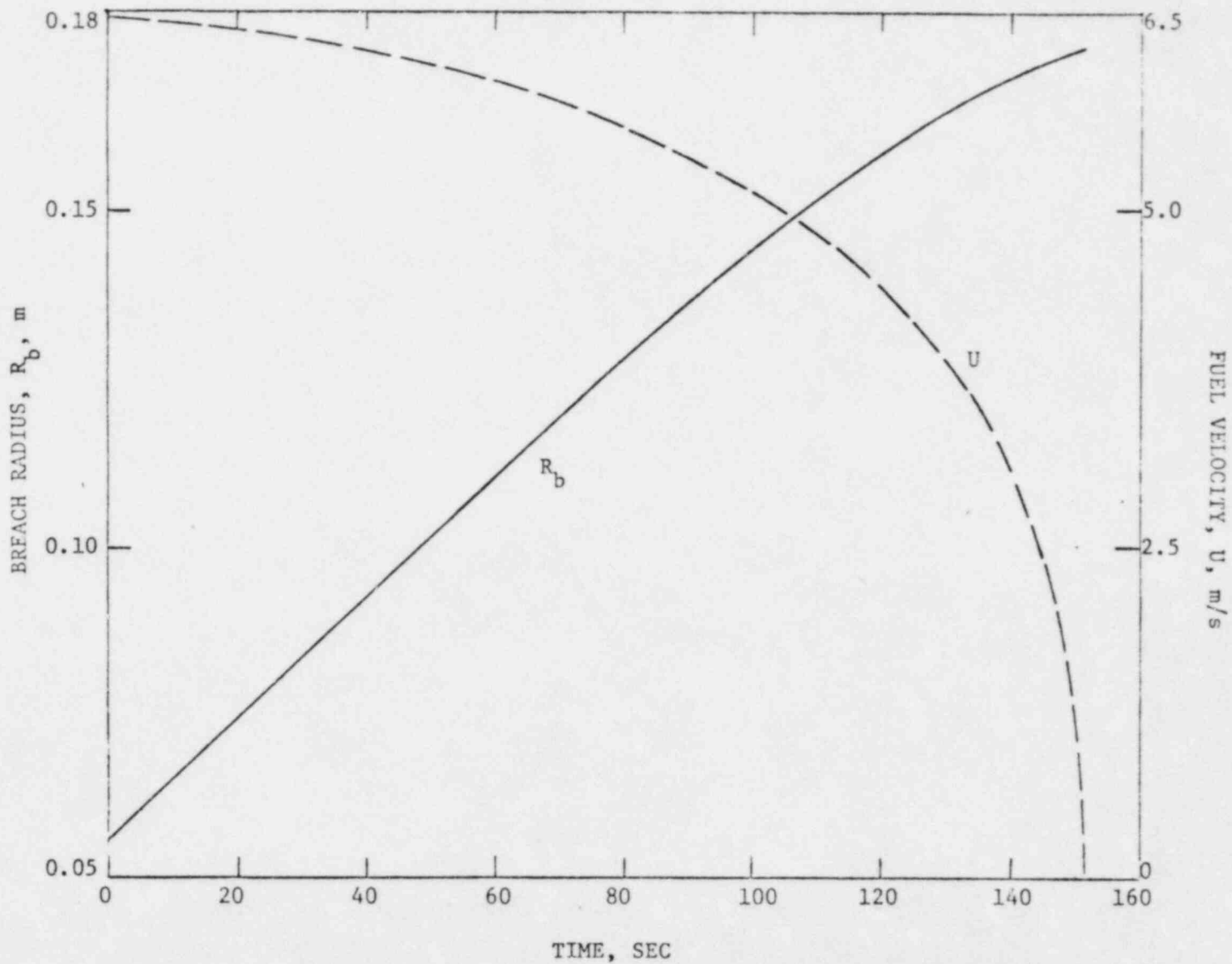
Fig. 3-8 Discharge Velocity and Reactor Vessel
Breach Radius for Gravity Driven Flow.
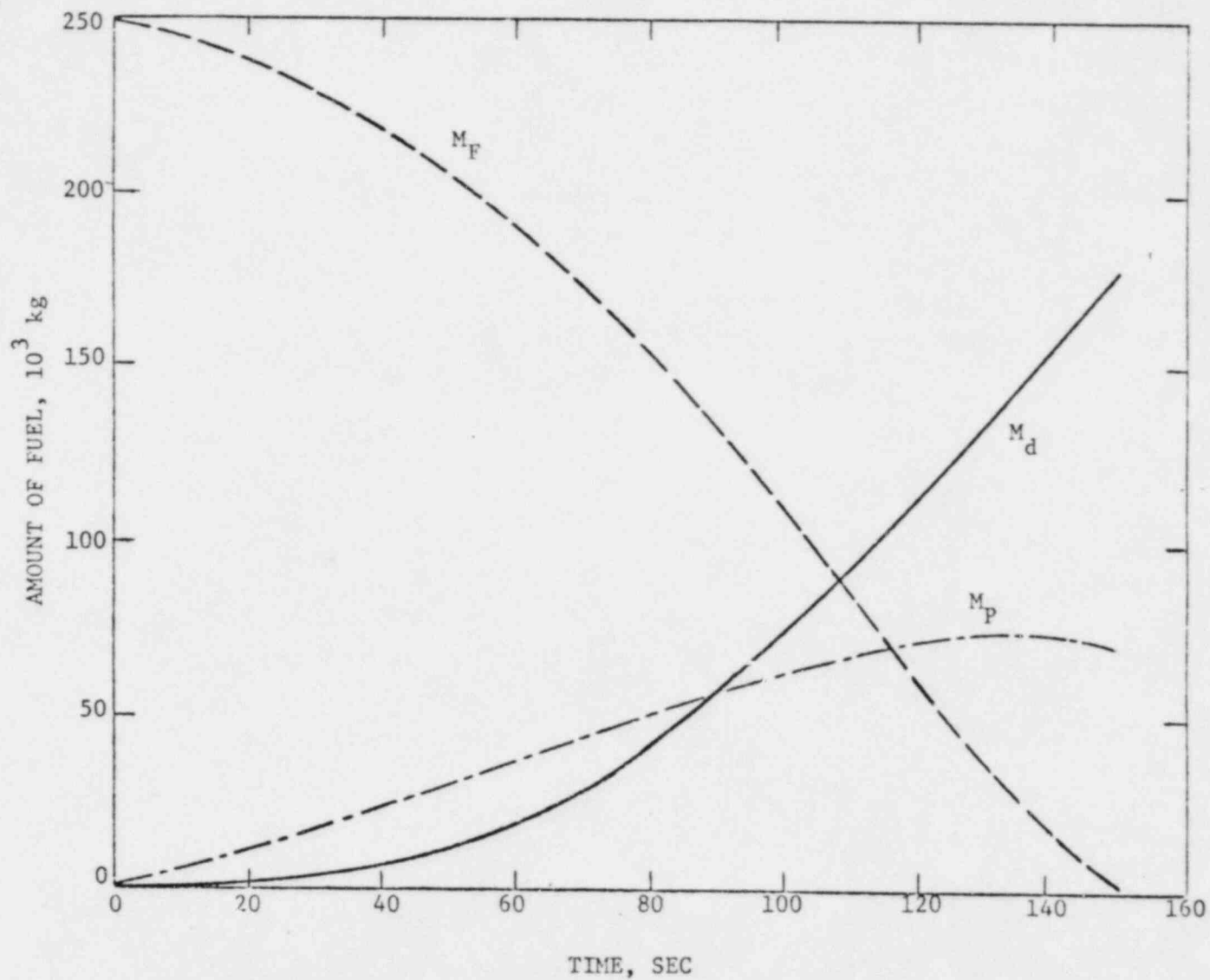
Fig. 3-9 Mass Inventory History for the Reactor Vessel,
Drywell, and Pedestal for Gravity Driven Flow.

IV.   Disposition of Core Material

As the material is discharged from the reactor vessel, it would accumulate in the CRD room and would flow onto the diaphragm floor. A general description of this behavior is required to provide the specific conditions necessary to evaluate the potential for, as well as the implications of, both ex-vessel steam explosions and thermal attack of the concrete. To make such assessments, it is necessary to evaluate the accumulation of fuel in the control rod drive room, the dispersive capacity of an ex-vessel steam explosion for those sequences where water is available on the diaphragm floor, the flow of the material onto the diaphragm floor, the dispersion of the molten core material and the melting attack of the liner and downcomer pipes, by the follow-on gas/steam mixture. These processes will be considered separately and will be quantified in terms of the calculational examples delineated above.

A.   Ex-Vessel Steam Explosions

For some accident sequences such as a large break LOCA, the diaphragm floor may be covered with up to 45 cm of water. (This depth represents the height of the downcomer pipes above the diaphragm floor.) In this case, as the degraded material would be released from the reactor vessel it would encounter water at a comparatively low pressure, and the potential would exist for a steam explosion. The experimental observations reported in Refs. [14,15 and 18] showed that a steam explosion could be triggered in water when the molten material contacts a wetted, solid wall. In this hypothetical reactor condition, the contact with a solid wall would first occur when the high temperature material penetrated through the 45 cm layer and contacted the upper surface of the diaphragm. The degraded

core material which could be involved in this explosive interaction would be that material already submerged in the water. For an assumed failure of one CRD penetration, this would essentially be the penetration cross-sectional area times the water depth, i.e. about 0.0035 m^3 ($\sim$ 24.5 kg) of material. If this is at a temperature of 2200°C and the water is at 100°C, the thermal energy contained within this mass of melt would be approximately 31 MJ. Using the experimental data reported in Ref. [18], the upper bound on the efficiency of such interactions, which were conducted with an iron-aluminum oxide thermite and melt quantities of this magnitude, was 1% of the thermal energy of the melt. This would yield 310 kJ of mechanical work which is negligible level compared to that required for failure of the primary containment boundary and its major effect would be to displace the water from the CRD room and cause portions thereof to flow into the downcomer pipes.

The immediate reaction of an ex-vessel steam explosion would be to disperse the water and degraded core material through the CRD room. This would enhance the contact between the two media and would result in an augmented steam production. The remainder of the material released from the vessel at this point in time, while not participating in the explosion, could be rapidly quenching as a result of this dispersion process. As a result of this accelerated vaporization, the drywell pressure would increase causing the level in the downcomer pipes to be decreased.

In summary, ex-vessel steam explosions could occur for those defined sequences where water is available on the diaphragm floor, but the amount of material involved would be very limited. In fact the major effect would be a rapid quenching of that material which had been released from the vessel at the time of the explosive event was initiated.

B. Accumulation in the CRD Room

The control rod drive room is formed by the cylindrical concrete walls of the reactor vessel pedestal and the diaphragm floor. There is a 7' x 3.5' passageway through the pedestal wall for personnel access, which would allow material discharged from the vessel to flow out onto the diaphragm floor. Thus, the accumulation with the CRD room is determined by the competitive processes of discharge from the reactor vessel and flow onto the diaphragm floor through the personnel passageway.

Molten material discharged from the vessel will first encounter thermal insulation which will not provide any significant resistance to continued penetration of the high temperature jet. Below the insulation are several steel beams, the remaining control rod drives, and a densely packed array of hydraulic lines for the control rod drives. This structure would temporarily break up and disperse the high velocity jet causing some material to be discharged through the pedestal windows which contain the hydraulic lines, and in addition it would distribute the material in a fairly uniform manner on the floor. It should be noted that this dispersal by the available structures would cause any ex-vessel steam explosion to be less coherent, but the rapid quenching process and the water displacement would be approximately the same. After a few seconds, that structure directly below the initial failure location would be melted and the jet would be essentially discharging directly onto the floor of the CRD room.

It should be noted that the hydraulic lines below the reactor vessel which would be melted during this postulated sequence of events are the water lines supplying the CRD flow. These would provide a means whereby water could be directly discharged into the CRD room for post-accident

cooling which will be discussed subsequently.

As material begins to accumulate in the CRD room, the flow through the personnel passageway is driven by the static head of the molten material. The velocity at any depth (u) can be estimated with Bernoulli's equation for frictionless flow,

$$u = \sqrt{2gy} \tag{4-1}$$

where y is the distance below the melt surface as shown in Fig. 4-1. Using this expression, the mass flow rate ($\dot{m}_F$) through the passageway is given by

$$\dot{m}_F = \rho_F W_P \int_0^{y_1} \sqrt{2gy} \; dy = 2/3 \; \rho_F W_P \; \sqrt{2gy_1}^{3/2} \tag{4-2}$$

where y_1 is the depth of molten core material at any instant and W_P is the width of the passageway. The rate of change of molten pool depth within the room is determined by the difference between the vessel discharge and the flow out of the room.

$$\rho_T U \pi \; [r_o^2 + 2r_o Bt + B^2 t^2] - 2/3 \; \rho_F W_P \; \sqrt{2gy_1}^{3/2} = \rho_F A_c \frac{dy_1}{dt} \tag{4-3}$$

where A_c is the cross-sectional area of the CRD room. This can be rearranged as

$$\frac{dy_1}{dt} = \frac{U\pi}{A_c} \; [r_o^2 + 2r_o Bt + B^2 t^2] - 2/3 \; \sqrt{2g} \; \frac{W_P}{A_c} \; y_1^{3/2} \tag{4-4}$$

which can be solved numerically by a forward marching technique. Using the calculational examples discussed above and the additional values of 29 m^2 for the CRD room floor area, a 1 m wide passageway, and a total discharge of 250,000 kg, the pool depth history is calculated to be as shown in Fig. 4-2. At the time that the vessel discharge is completed, (about 17 secs), the depth in the CRD room would be approximately one meter.
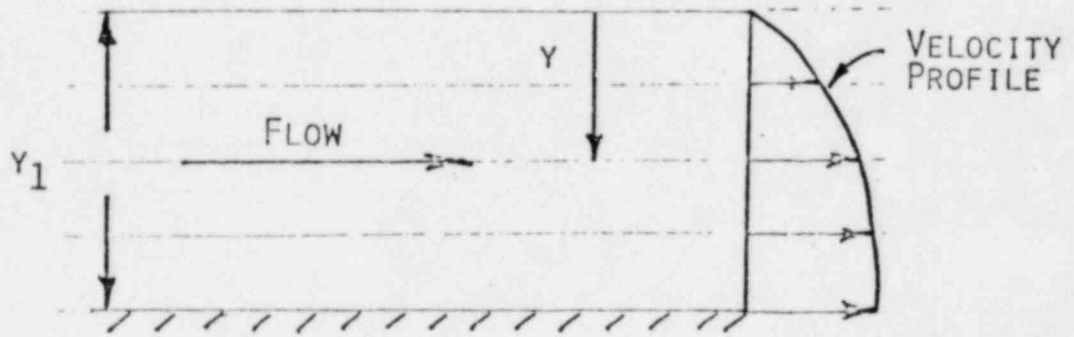
FIG. 4-1 GRAVITY INDUCED FLOW.
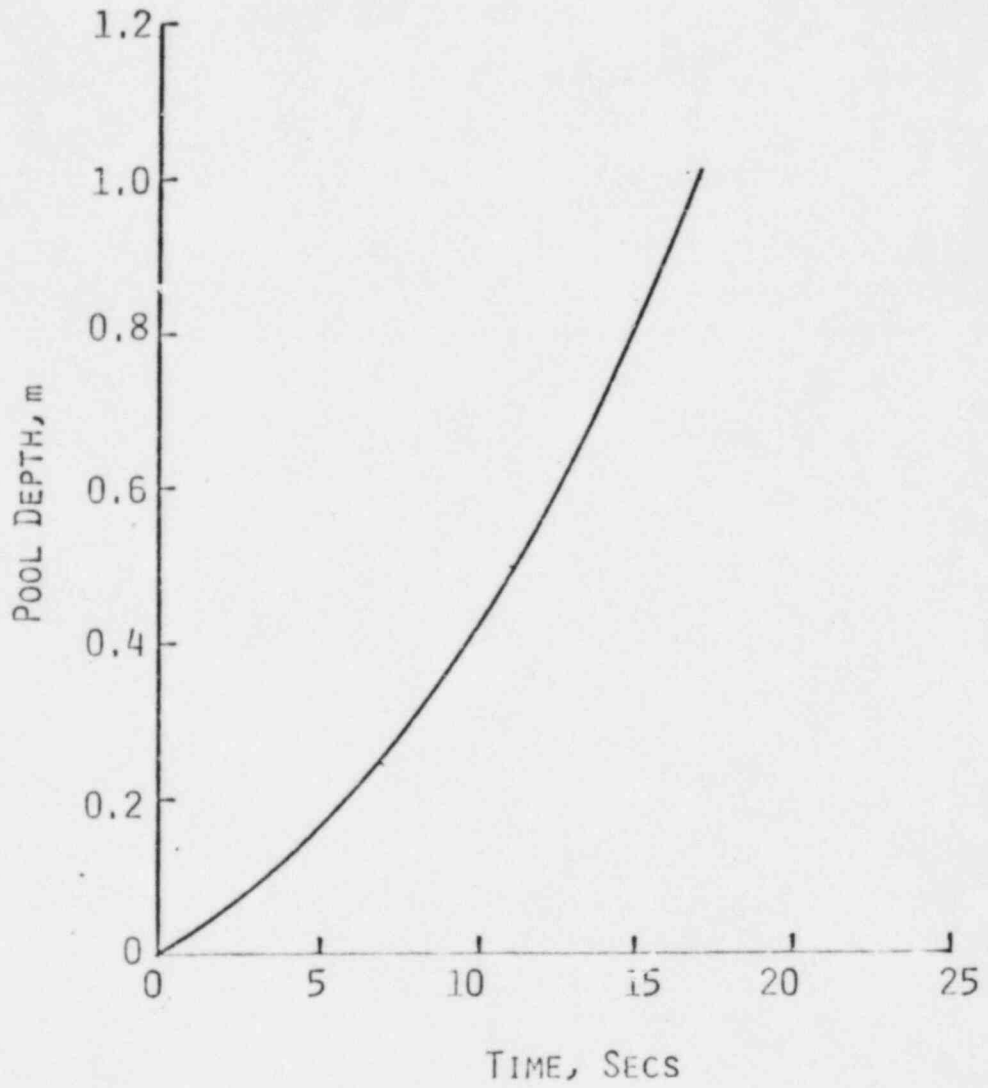
Fig. 4-2   Pool Depth Verse Time During
Discharge Stage.

C.   Flow of Material onto the Diaphragm Floor

After discharge from the reactor vessel is complete, the molten debris continues to flow out of the CRD room, and if no other phenomena influences the process, the rate of decrease in the pool level would be given by

$$\frac{dy_1}{dt} = - \; 2/3 \; \sqrt{2g} \; \frac{W_P}{A_c} \; y_1^{3/2} \tag{4-5}$$

which can be integrated to

$$t = 3 \; \frac{A_c}{\sqrt{2g} \; W_P} \left[\frac{1}{\sqrt{y_2}} - \frac{1}{\sqrt{y_1}} \right] \tag{4-6}$$

If the above calculational examples are again employed, the depth of the pool would decrease to a depth of 0.1 m in about 43 secs. Therefore, the total time to discharge and distribute the molten core material would be approximately one minute. Figure 3-9 illustrates the accumulation of material within the pedestal region and flow of material onto the rest of the diaphragm floor (drywell) as a function of time for the gravity driven flow case. As illustrated, within two minutes the material is essentially uniformly distributed on the drywell floor for the postulated accident conditions.

D.   Dispersion of the Molten Core

For the cases calculated above in which the pressure within the primary system is at an elevated level, the completion of the molten liquid discharge will initiate the discharge of the high pressure steam/gas mixture. Since this mixture is at an elevated pressure, the mass flow rate from the vessel will be limited by critical flow.

During the gas blowdown stage, the steam/gas mixture will cool as it depressurizes, and this will establish a potential for conductive, con-

vective, and radiative heat transfer from the hot vessel and its remaining internals to the expanding gases. Depending upon the specific configurations and quantities involved, this could be a substantial amount of energy during the blowdown. In order to approximate this energy transfer, yet retain a simple formulation for the overall behavior, an isothermal expansion is assumed for the steam/gas mixture and the properties of the mixture are assumed to be identical to saturated steam.

The reactor vessel and the steam lines up to the main steam isolation valves can be considered as a fixed volume which is discharging high pressure gas through the reactor vessel breach,

$$V_v = m_g v_g = \text{Constant} \tag{4-7}$$

where V_v is the vessel volume, m_g is the mass of gas in the vessel at any instant, and v_g is the specific volume of the gas. Differentiating Eq. (4-7) with respect to time gives

$$v_g \frac{dm_g}{dt} = -m_g \frac{dv_g}{dt} = -m_g \frac{dv_g}{dP} \frac{dP}{dt} \tag{4-8}$$

and if the gas mixture is assumed to behave as a perfect gas so that

$$v_g = \frac{RT}{P} \tag{4-9}$$

for an isothermal process the change in specific volume with respect to pressure is

$$\frac{dv_g}{dP} = -\frac{v_g}{P} \tag{4-10}$$

and Eq. (4-8) can be expressed as

$$\frac{dm_g}{dt} = \frac{m_g}{P} \frac{dP}{dt} \tag{4-11}$$

The mass discharge rate from the vessel is the product of the critical flow rate per unit area and the vessel breach area A_b

$$\frac{dm_g}{dt} = -GA_b \tag{4-12}$$

where the critical flow rate is given by

$$G = \eta P_o / \sqrt{RT} \tag{4-13}$$

(η is the isothermal critical pressure ratio of 0.6). With these expressions, Eq. (4-11) can be rewritten as

$$\frac{A_b \eta \sqrt{RT}}{V_v} = - \frac{1}{P} \frac{dP}{dt} = C_1 \tag{4-14}$$

where the left hand side is a collection of constants. Integration of the above equation results in

$$P = P_o e - \left[\frac{A_b \eta \sqrt{RT}}{V_v} \right] t \tag{4-15}$$

which describes the vessel pressure as a function of time, and this is graphically represented for a specific set of conditions in Fig. 4-3.

As the gases exhaust from the vessel into the CRD room, the room will pressurize to a level at which the flow into the room (from the vessel) equals that discharged through the passageway and the ports through which the control rod drive hydraulic lines pass. If the gas is again assumed to behave in an isothermal manner and the outflow is approximated as incompressible, the mass discharge rate from the CRD room can be represented by

$$\left. \frac{dm_g}{dt} \right)_{CRD} = A_p \sqrt{2\rho_g (P_g - P_d)} \tag{4-16}$$

where A_p is the available flow area in the pedestal, ρ_g is the density and P_g the pressure of the gas in the CRD chamber, and P_d is the pressure in the drywell. Using the ideal gas equation,

$$\left. \frac{dm_g}{dt} \right)_{CRD} = A_p \sqrt{\frac{2 P_g (P_g - P_d)}{RT}} \tag{4-17}$$
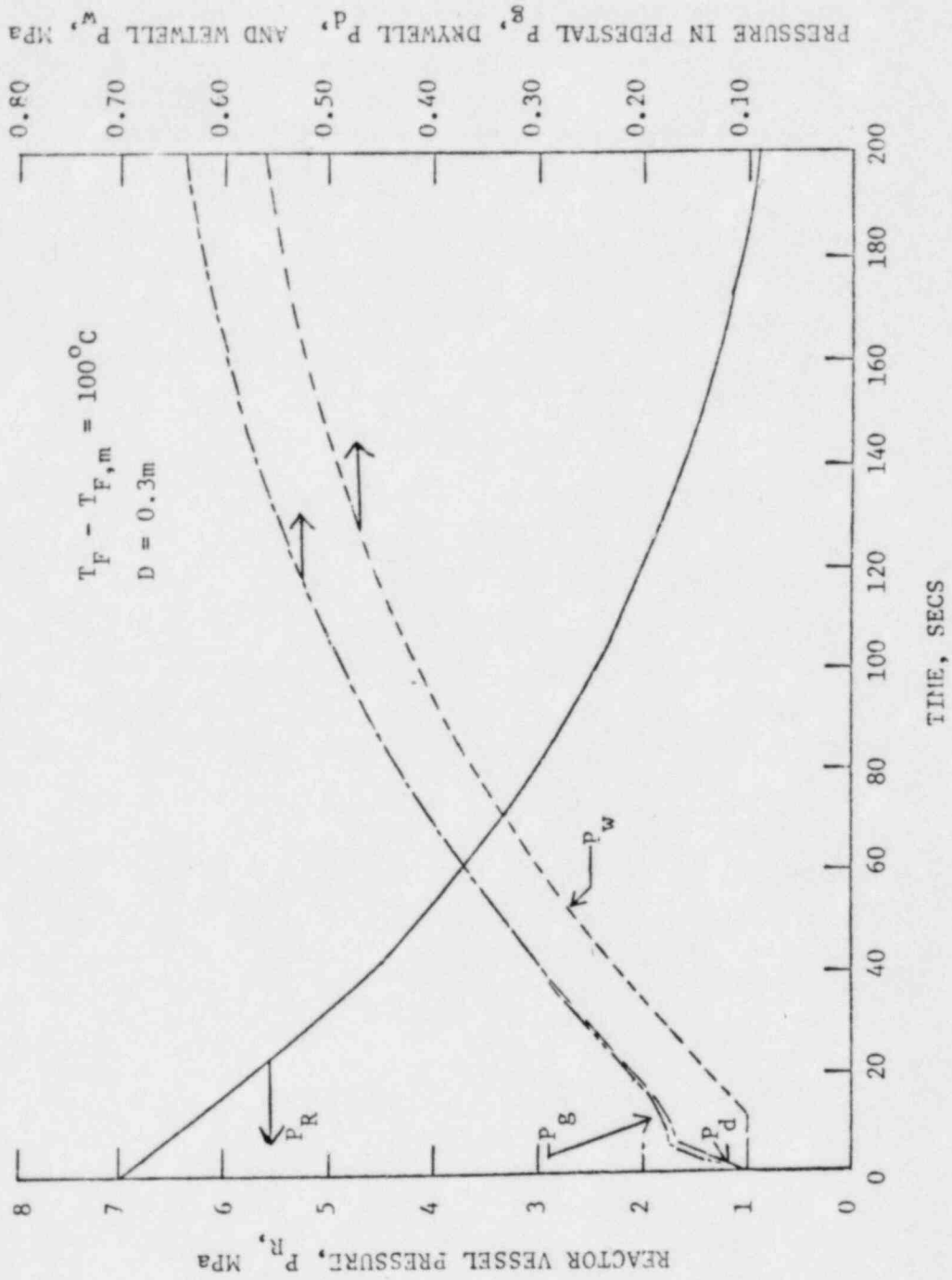
Fig. 4-3 Calculated Pressure Histories for the Pressure Vessel, Pedestal, Drywell and Wetwell.

From continuity

$$A_b \eta P_o / \sqrt{RT} = A_p \sqrt{\frac{2 \, P_g (P_g - P_d)}{RT}} \tag{4-18}$$

or

$$\frac{1}{2} \left[\frac{A_b \eta P_o}{A_p} \right]^2 = P_g^2 - P_g P_d \tag{4-19}$$

and this quadratic equation can be solved for P_g when specific accident conditions are given. For example if the vessel pressure is 7.0 MPa, the breach diameter is 0.4 m, the vent area in the pedestal is 5.0 m^2, and the drywell pressure is 0.3 MPa, then the pressure within the CRD room would be 0.32 MPa which corresponds to an 0.3 m static head of core debris material. Consequently, the pressure rise within this room would not be excessive, but the resultant velocity of the gases through the passageway, about 150 m/sec, could have an effect on the ultimate distribution of the molten core material accumulated on the CRD room floor. This entrainment and dispersion phenomenon will be considered next.

Pressurization in the CRD chamber has two effects which have to be considered in describing the movement and relocation of the core material. First it increases the effective driving force for moving the material onto the diaphragm floor, and secondly, the high velocity gas flow can entrain and disperse the material. With respect to initial point, the additional overpressures typified by the above example are small compared to the static head of the accumulated molten material at the beginning of the gas discharge stage. This would be a minor effect which is not included here, and in fact, that flow of material which is not entrained should be adequately represented by the gravity driven calculation given above.

On the other hand, the entrainment behavior could potentially have a substantial influence on the ultimate distribution of the degraded core material; principally on the timing and extent of material which is deposited within the wetwell. As the gas discharge phase begins, both the impingement of the high velocity jet on the central region of the accumulated pool and the high velocity flow of gases over the surface of the pool and out of the passageway will cause waves on the surface of the molten material. These surface disturbances, which could be sizable, would increase in amplitude and concentrate the local drag forces until they would be torn away from the surface. If the resultant particles could be broken down to sizes that would be levitated by the gas stream, then these could be distributed through the primary containment. It should also be noted that sizes larger than a levitation size could be generated and distributed without being levitated, but a levitation criterion defines that size and amount of material which could be dispersed throughout the containment volume, including the wetwell.

A force balance on a droplet equates the particle weight and the drag force.

$$(\rho_F - \rho_g) \frac{4}{3} \pi r^3 g = C_D \pi r^2 \frac{\rho_g U_g^2}{2} \qquad (4\text{-}20)$$

In this expression C_D is the drag coefficient and can be assumed to a value of 0.5 for this analysis, r is the particle radius, and U_g the gas velocity. This can be rewritten as

$$U_g^2 = \frac{8}{3} \frac{(\rho_F - \rho_g) r g}{C_D \rho_g} \qquad (4\text{-}21)$$

As a result of the dynamic forces, droplets could breakup in a flowing gas stream, and this disintegration would continue until a balance existed be-

tween the dynamic forces, tending to breakup the drops, and the stabilizing surface tension forces. A dimensionless ratio of these forces is called the Weber number,

$$We = \frac{\rho_g U_g^2 d}{\sigma} \qquad (4-22)$$

where d is the droplet diameter and σ is the surface tension of the melt. Experiments have shown that a critical value where break will occur is about 12, [22]. Combining Eqs. (4-21) and (4-22) and using a Weber number of 12 yields

$$U_g^4 = 32 \left[\frac{g\sigma(\rho_F - \rho_g)}{\rho_g^2} \right] \qquad (4-23)$$

or

$$U_g = 2.4 \sqrt[4]{\frac{g\sigma(\rho_F - \rho_g)}{\rho_g^2}} \qquad (4-24)$$

for the velocity required to initiate entrainment. As discussed in Ref. [23], experiments addressing the onset of liquid film flooding and entrainment have found that the constant in Eq. (4-24) is between 3.0 and 3.7, which is close to the approximate value from this simple formulation.

With the parameters used in the sample calculations outlined above, the velocity required for entrainment (with a constant of 3.0) is about 36 m/sec, and this is much less than the velocity of the gas steam during the blowdown. Under such conditions, one would expect extensive entrainment. In fact, for a gas velocity of 200 m/sec, a Weber number of 12 results in a fuel particle of about 88 μm, and such fine particulate, should it occur, would be thoroughly dispersed throughout the primary containment. While such extensive particulation is certainly important, the most rele-

vant question for the overall containment response is the extent of entrainment and the rate at which this would occur.

One means by which this entrainment could be effected is through the impact of the gaseous jet on the upper pool surface. As the jet exhausts from the vessel, it will expand to the asymptotic, one-dimensional velocity (u_1) given by [24]

$$u_1 = \frac{P_g - P_t}{G_t} + u_t \qquad (4\text{-}25)$$

where P_t is the static pressure in the vessel breach (throat), u_t is the velocity in this locale, and G_t is the flow rate per unit area in the throat. For the conditions given above, this velocity is about 760 m/sec and the diameter of the gas jet would be approximately 1.1 m. Stagnating this high velocity jet would result in stagnation pressures (P_2) on the central region of the pool surface equal to:

$$-\int_{P_g}^{P_2} v_g \, dP = \int_{u_1}^{0} \frac{d(u^2)}{2} \qquad (4\text{-}26)$$

If an isothermal process is again assumed, this expression can be integrated to

$$\ln P_2/P_g = \frac{\rho_g u_1^2}{2P_g} \qquad (4\text{-}27)$$

which gives a stagnation pressure of about 1.5 MPa. This pressure is far greater than the static head of the accumulated material and would distort the surface in the form of a large wave and force more material through the passageway as well as provide for substantial entrainment of molten core material in the process.

Given this large impact pressure of the gas jet, the surface of the pool will be depressed in the center; probably down to the floor of the

diaphragm as illustrated in Fig. 4-4. The area of this central cavity must be sufficient to stagnate the downward flow and allow it to reverse and flow upward. This would require an area of about 1.9 m^2 or a diameter of approximately 1.5 m. A displacement of this magnitude would cause the pool level to increase by 6 cm; a comparatively minor change for a quasi-steady condition, but the dynamic processes, such as wave formation, resulting from the impact forces could be considerably different. In general, the "swell" of the pool would not be sufficient to close off the doorway, the steam/gas mixture would exhaust through the passage at a velocity several times that required for entrainment.

The region where most of the liquid entrainment would occur is in the passageway itself and the "line of sight" path between the doorway and the outer wall of the primary containment. Since the gas flow issuing from the CRD room is essentially incompressible, it would spread by entraining the surrounding ambient gases, principally nitrogen, which would cause the jet to decelerate. Spreading of incompressible jets occurs with a 10° half angle, and given the specific geometry of the containment (1 m wide doorway and a primary containment diameter of about 23 m) the jet velocity would be decreased by about a factor of 2.7 when it reached the primary containment wall. Thus, the one-dimensional velocity at all points along the path would be sufficient for entrainment.

The pedestal configuration in the Limerick design allows the extent of entrainment to be estimated in a very simple manner. This design has four large ports available in the pedestal wall for the CRD hydraulic lines, and these are located above the passageway. Each port has an area of about 0.92 m^2 while the available gas flow area through the passageway (assuming a pool depth of 1 m) would be about 1 m^2; thus the four ports
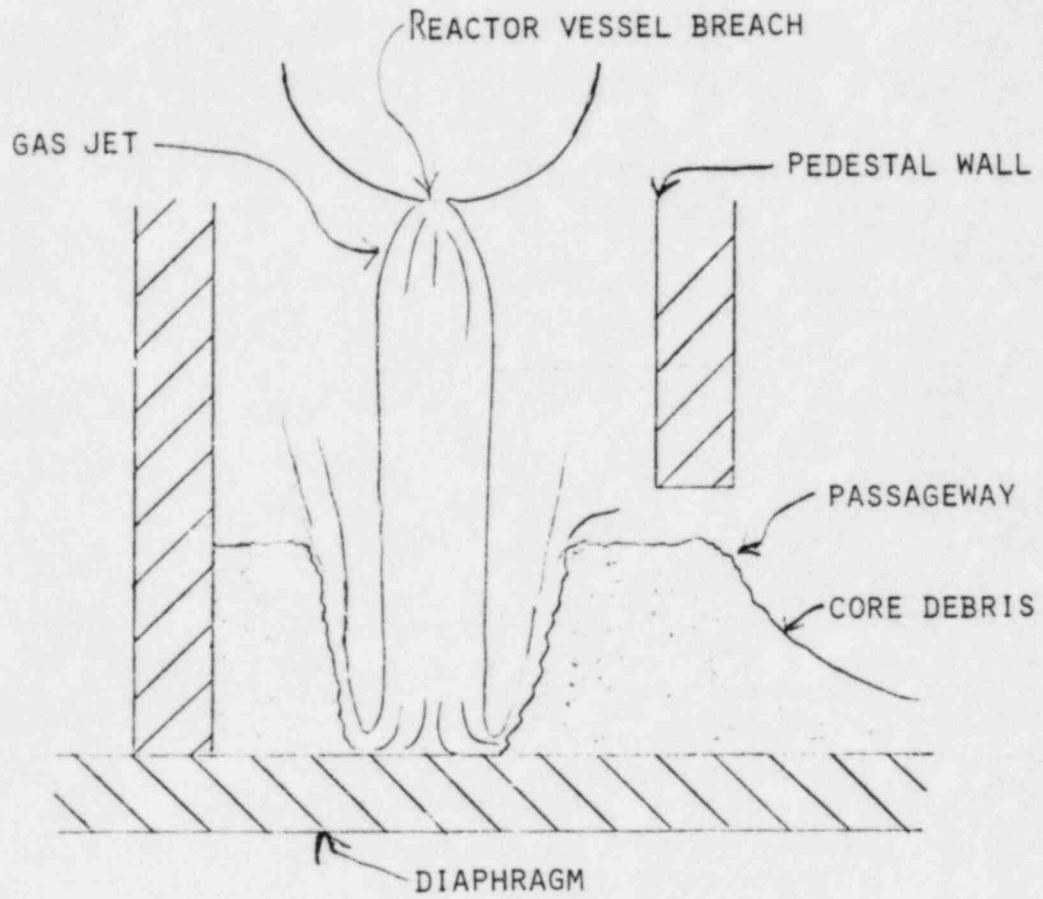
FIG. 4-4 DEPRESSION OF THE MOLTEN POOL BY
THE EXPANDING GAS JET.

represent approximately three-fourths of the available area for gas discharge. With this large "by-pass" flow, the pressure difference between inside and outside of the pedestal is not significantly affected by the mass discharge through the doorway. Therefore, entrainment can only continue as long as the imposed pressure differential can maintain the gas velocity above the entrainment level. In the calculation discussed above, the entrained sizes would represent a very fine structure which would be quickly accelerated by the gas phase at the expense of some kinetic energy in the continuous gas stream. In the limit, this combination of a fine particulate flow and a high velocity gas stream would approach a homogeneous condition. However, the velocity of this flow would be greatly reduced because the kinetic of the gas would be expended in accelerating the dense entrained material. The velocity of this two-phase stream must remain above the minimum entrainment level, so

$$P_g - P_a = \frac{\bar{\rho} u_e^2}{2} \tag{4-28}$$

where $\bar{\rho}$ is the homogeneous density

$$\bar{\rho} = \alpha \rho g + (1 - \alpha)\rho_F \tag{4-29}$$

and u_e is the entrainment velocity given by Eq. (4-24) with a constant of 3. If no entrainment occurs, the imposed pressure difference would result in an incompressible acceleration given by

$$P_g - P_a = \frac{\rho_g u_g^2}{2} \tag{4-30}$$

and this can be used to non-dimensionalize Eq. (4-28) to

$$\frac{u_g^2}{u_e^2} = (1 - \alpha) \frac{\rho_F}{\rho_g} + \alpha \tag{4-31}$$

where α is the flow area occupied by the gas phase and can be approximated

in magnitude by unity.

$$\left(\frac{u_g^2}{u_e^2} - 1\right) \frac{\rho_g}{\rho_F} = (1 - \alpha) \tag{4-32}$$

From continuity considerations for the dispersed phase,

$$W_F = \rho_F A_F u_e = \rho_F (1 - \alpha) A u_e \tag{4-33}$$

a substitution of Eq. (4-31) into Eq. (4-32) yields

$$W_F = \rho_g \left(\frac{u_g^2}{u_e^2} - 1\right) A u_e \tag{4-34}$$

Since it is the driving pressure which is known, this can be restructured
to

$$W_F = \left(\frac{2(P_g - P_a)}{u_e} - \rho_g u_e\right) A \tag{4-35}$$

to obtain the mass flow rate of the entrained phase, and this can be in-
tegrated over the blowdown time to determine the total amount of entrained
material.

While this homogeneous analysis provides an overestimate of the en-
trainment fraction, the values used in the above calculational examples
would predict an entrainment fraction somewhat less than 15% over the en-
tire gas blowdown stage. Thus, the entrainment is a necessary part of the
basic understanding and is important in evaluating the core cooling char-
acteristics of the core debris, but it only represents a small fraction
of the material released from the vessel. Also, the pressure drop limit-
ation would mean that some fuel material would precipitate out of suspen-
sion as the gas stream slows down in the primary containment. As a result
of this calculation, it appears that most of the molten core debris would
distribute itself on the diaphragm floor and the principle mechanism for
the distribution would be spreading due to the gravitational head.

E.   Spreading on the Diaphragm Floor

At the elevated temperatures necessary for reactor vessel melt-
through, the molten degraded core material would wet the steel liner on
the diaphragm floor. As a result of this wetting, material would spread
rapidly, but as the molten material contacts the diaphragm floor, the in-
terface temperature upon contact will be less than the freezing point of
the molten debris as well as that of the steel liner. Therefore, a thin
crust of debris will form at the interface and temporarily insulate the
steel and the rest of the molten material. In addition, the growth of
this crust will be limited by the fuel thermal diffusivity, which is small,
and the resulting crust will be thin compared to the depth of material.
This last point suggests at the crust formation will not significantly
inhibit the flow.

The mass flow rate of molten core material entering the drywell is
then:

$$\frac{dM_d}{dt} = \frac{2}{3} \rho_F W_p \sqrt{2g(h_p - h_d)^3} \qquad (4-36)$$

where h_p is the pool height within the pedestal and h_d is the height in
the drywell. The propagation velocity (U_2) of the molten material on the
drywell diaphragm can be approximated as:

$$U_2 = \frac{2}{3} \sqrt{2gh_d} \qquad (4-37)$$

with the assumption that the molten material forms an uniform layer in-
stantly. Let M_p and M_d be fuel in the pedestal and the drywell at any
time and A_p and A_d be the areas covered by these fuel masses respective-
ly, then the thickness of fuel at each chamber is

$$h_p = \frac{M_p}{A_p \rho_F} \qquad (4-38)$$

$$u_d = \frac{N}{A_d \, \rho \, r} \qquad (4\text{-}39)$$

Then by assuming that the molten fuel flows out of the pedestal in a semi-circle pattern, A_d can be expressed as

$$A_d = \frac{\pi}{2} \ell^2 \qquad (4\text{-}40)$$

with

$$\ell = \int_0^\tau U_2(\tau) dt \qquad (4\text{-}41)$$

After the ridge of molten pool reaches the wall of the containment build-ing, the fuel is then assumed to travel along the annulus between the pede-stal and the building walls. This two-prong movement is simplified for the calculation so that the fuel is moving in a straight path with a width twice of R_d, the distance between the pedestal and building walls. The area covered by the molten pool is then

$$A_d = \frac{\pi}{2} R_d^2 + 2R_d(\ell - R_d) \qquad (4\text{-}42)$$

until A_d equals to the floor area of the drywell.

F. Pressure History in the Containment Building

To determine the pressure difference between pedestal and drywell, one must evaluate the gas discharge rate from the reactor vessel. As discussed above, hot gas in the vessel and the pedestal is treated as expansion of the isothermal process.

To evaluate the transient pressure history in the drywell, it is assumed that no steam condensation will occur in the drywell since the components and building structure would have been heated by the thermal radiation from the core material as it spread on the floor. Also we as-

sume for simplicity that gas only received sufficient energy from molten fuel to maintain the isothermal state. Let M_a and M_v be the nitrogen and steam masses in the drywell, $C_{p,a}$ and $C_{p,v}$ their heat capacity, respectively, the gas temperature in the drywell is

$$T_a = \frac{M_a C_{p,a} T_a + M_v C_{p,v} T_v}{M_a C_{p,a} + M_v C_{p,v}} \tag{4-43}$$

The partial pressures of nitrogen, P_{aa} and steam, P_{va} are expressed as

$$P_{aa} = \frac{M_a R_a T_a}{V_a} \tag{4-44}$$

$$P_{va} = \frac{M_v R_v T_a}{V_a} \tag{4-45}$$

with V_a the drywell volume. The total drywell pressure is

$$P_a = P_{aa} + P_{va} \tag{4-46}$$

The value of M_v is evaluated through the change of vessel pressure, ΔP_v, as

$$M_v = \frac{\Delta P_v V_v}{R_v T_v} \tag{4-47}$$

If the pressure difference between the drywell and the wetwell exceeds the static head of water column in the downcomer pipes, the drywell gas will vent into the wetwell through these pipes. (The dynamic response of the water within the downcomer pipes was found to be of negligible concern for the calculated pressurization rates within the drywell). The steam will condense as it passes through the suppression pool. This static head of the displaced water column is

$$\Delta P_{aw} = \rho_{H_2O} gH \tag{4-48}$$

where H is the length of the section that the downcomer pipes are submerged in the water. The gas will redistribute itself in these two cham-

bers so that a balance of pressure can be achieved, i.e.

$$P_a' = P_w' + \Delta P_{aw} \tag{4-49}$$

Suppose ΔP is the excessive pressure in the drywell, i.e.,

$$\Delta P = P_a - P_w - \Delta P_{aw} \tag{4-50}$$

the partial pressure contributed by nitrogen in ΔP is

$$\Delta P_{aa} = \Delta P \left(\frac{P_{aa}}{P_a} \right) \tag{4-51}$$

The amount of nitrogen available for pressure balance is

$$\Delta M_{aa} = \frac{\Delta P_{aa} V_a}{R_a T_a} \tag{4-52}$$

If ΔP_{ww} is defined as the pressure increase caused by ΔM_{aa} entering the wetwell,

$$\Delta P_{ww} = \frac{\Delta M_{aa} V_w}{R_w T_w} \tag{4-53}$$

Let A_{aw} be the portion of ΔM_{aa} staying in the drywell, then the increase of pressure in the wetwell is

$$(1 - A_{aw}) \frac{\Delta M_{aa} V_w}{R_w T_w} = (1 - A_{aw}) P_{ww} \tag{4-54}$$

The balance of pressure between the wetwell and the drywell results in

$$P_a - (1 - A_{aw}) \Delta P = P_w + \Delta P_{aw} + \Delta P_{ww} (1 - A_{aw})$$

or

$$P_a - P_w - \Delta P_{aw} = (\Delta P + \Delta P_{ww})(1 - A_{aw}) \tag{4-55}$$

From Eq. (4-50) we have

$$1 - A_{aw} = \frac{\Delta P}{\Delta P + \Delta P_{ww}}$$

or

$$A_{aw} = \frac{\Delta P_{ww}}{\Delta P + \Delta P_{ww}} \qquad (4-56)$$

The newly establishe˜ wetwell pressure, P'_w, is

$$P'_w = P_w + (1 - A_{aw})\Delta P_{ww} \qquad (4-57)$$

and drywell pressure, P'_a, can be found by Eq. (4-49).

G. Integrated Calculational Model

Using the formulations discussed above for the individual phenomena involved following a postulated failure of the reactor vessel, an integrated calculational model was formulated to determine the detailed interrelationship of the various phenomena, with the particular goal of obtaining the drywell pressure history as a function of time. This process begins with discharge of the molten core debris from the reactor vessel and continues the calculation until the pressure between the reactor vessel and the drywell have equilibrated.

Figure 4-5 illustrates the formulation used in the calculational model, wherein the the discharge of fuel from the reactor vessel is determined by the vessel pressure and this is used to calculate the fuel distribution within the reactor vessel pedestal region and the drywell itself. As the material is exhausted from the vessel, and the discharge of the high pressure steam/gas mixture ensues, the isothermal blowdown from the reactor vessel is calculated in terms of the pressure response with˜ the drywell and wetwell respectively. In addition, the fuel distribution affected by the high velocity gaseous discharge is also evaluated, but as was discussed above, this is an small quantity compared to a total amount of mass release from the reactor vessel. Figure 4-6 then illustrates the method of solution for the various individual phenomena and their interrelationship in the overall program. Calculational

SUMMARY OF FLOW CHART FOR LIMERICK STATION

Discharge of molten fuel from reactor vessel breach driven by vessel pressure.

Pressure field calculation in the containment building.

Fuel dispersion due to entrainment in the jet.

Fuel distribution in the containment building due to gravity head.

Temperature profile in the concrete wall and floor of containment building.
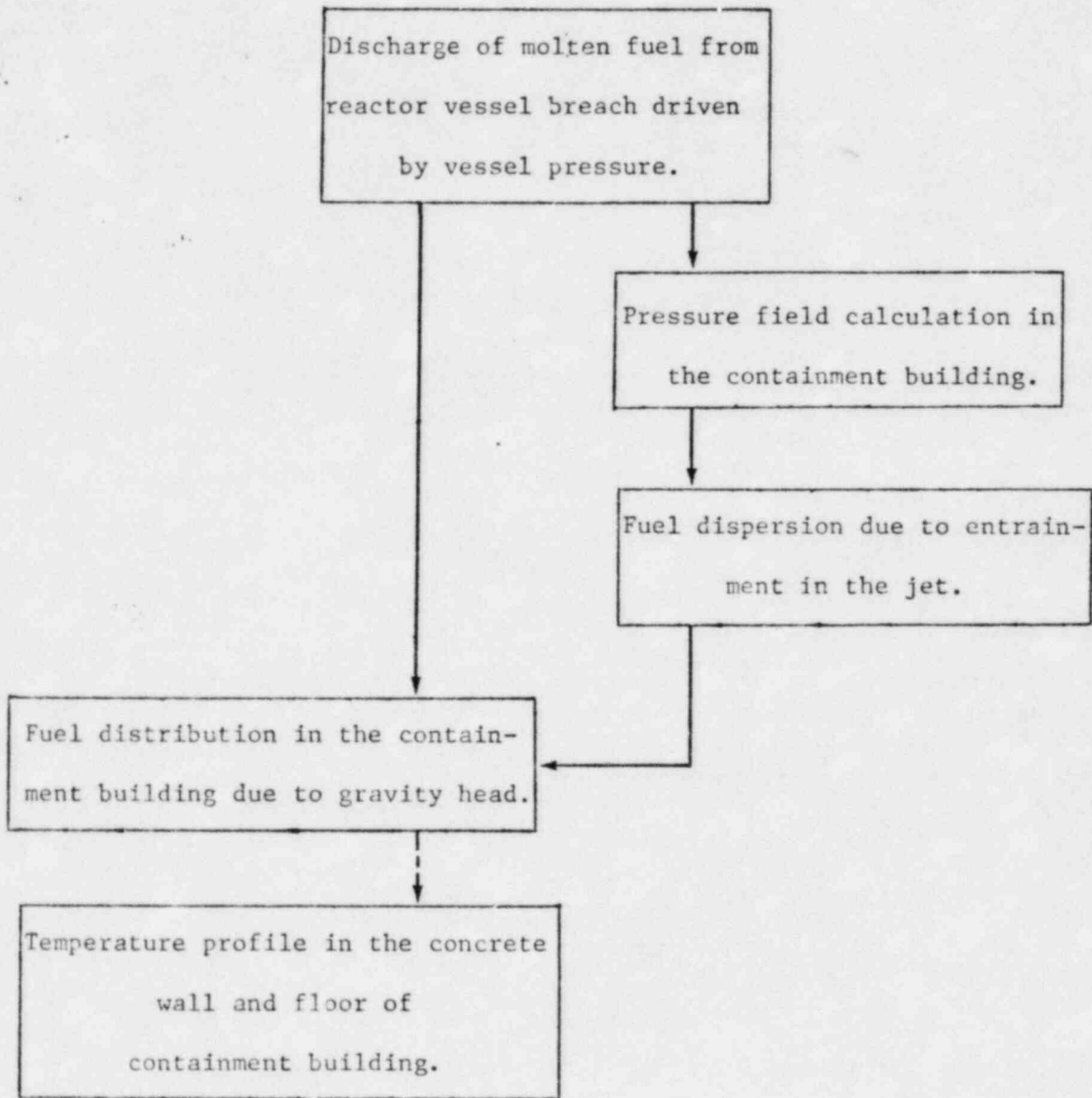
Fig. 4-5

PROGRAM FLOW CHART OF LIMERICK STATION

Read: P_v, M_v, N, r_o, T_F, T_{ao}, T_v, $\Delta\tau$

$M_p = Md = 0$; $\tau = 0$,
$\rho = 0$, $hd = 0$

$$U_F = \sqrt{\frac{2(P_v - P_{atm})}{\rho_F}}$$

$$B = \frac{fC_{p,F}\rho_F(T_F - T_{F,m})U_F}{2\rho_s[C_{P,s}(T_{sm} - T_s) + \gamma_s]}$$

$\tau = \tau + \Delta\tau$

$$\frac{dMv}{d\tau} = -\rho_F U_F \pi (r_o + B\tau)^2 \cdot N$$

$$Mv = Mv + \frac{dMv}{d\tau} \cdot \Delta\tau, \quad h_p = \frac{M_p}{P_F A}$$

$$\frac{dM_p}{d\tau} = -\frac{dMv}{d\tau} - \frac{2}{3}\rho_F W_P \sqrt{(h_p - h_d)^3} \cdot 2g$$

$$M_p = M_p + \frac{dM_p}{d\tau}\Delta\tau$$

$$\frac{dM_d}{d\tau} = \frac{2}{3}\rho_F W_P \sqrt{2g \cdot (h_p - h_d)^3}$$

$$M_d = M_d + \frac{dM_d}{d\tau}\Delta\tau$$

$1 < 29.5$ m — No

Yes

$$h_d = \frac{M_d}{A_d \rho_F}$$

$$\bar{U} = \frac{2}{3}\sqrt{2gh_d}$$

$$1 = 1 + \bar{U}\Delta\tau$$

$$h_d = \frac{M_d}{A_2 \rho_F}$$

Yes — $1 \leq Rd$

No

Fig. 4-6

$$A_d = A_{do} + \frac{\pi}{2} \, 1^2$$

No

$$Ad = A_{do} + \frac{\pi}{2} \, R_d^2$$

No

$$Mv \leq 0$$

Yes, $\tau = \tau_1$

$$r_f = r_o + B\tau_1, \quad A_b = \pi r_f^2 \cdot N$$
$$M_{de} = 0, \quad M_{dh} = M_d, \quad h_{dh} = h_d$$

$$\tau = \tau + \Delta\tau$$

Containment Pressure
Fields Calculation

$$A_1' = A_1 - A_j$$

$$h_p = \frac{M_p}{\rho_F A_1'}$$

$$A_j, \; P_a, \; P_g, \; \rho_g, \; U_e$$

No

$$2(P_g - P_a) \geq \rho_g U_e^2$$

Yes

No

$$\frac{dM_P}{d\tau} = -\frac{2}{3} \rho_F W_P \sqrt{2g(h_p - hd)^3}$$

$$\frac{dM_{dh}}{d\tau} = -\frac{dM_P}{d\tau}$$

$$M_{dh} = M_{dh} + \frac{dM_{dh}}{d\tau} \Delta\tau$$

$$M_p = M_p + \frac{dM_p}{d\tau} \Delta\tau$$

Yes

$$\frac{dM_{ph}}{d\tau} = -\frac{2}{3} \rho_F W_P \sqrt{2g(h_P - h_d)^3}$$

$$\frac{dM_{pe}}{d\tau} = -[2(P_g - P_a) - P_g U_e^2] \times \frac{(A_p - h_p \times W_p)}{U_e}$$

$$\frac{dM_{dh}}{d\tau} = -\frac{dM_{ph}}{d\tau}, \quad \frac{dM_{de}}{d\tau} = -\frac{dM_{pe}}{d\tau}$$

$$\frac{dM_p}{d\tau} = \frac{dM_{ph}}{d\tau} + \frac{dM_{pe}}{d\tau}$$

$$M_p = M_p + \frac{dM_p}{d\tau} \Delta\tau$$

$$M_{dh} = M_{dh} + \frac{dM_{dh}}{d\tau} \Delta\tau$$

$$M_{de} = M_{de} + \frac{dM_{de}}{d\tau} \Delta\tau$$

No

$$1 < 29.5 \text{ m}$$

Yes

Fig. 4-6 (Continued)

$$h_d = \frac{Mdh + Mde}{\rho_F A_2}$$

$$h_{de} = \frac{Mde}{A_2 \rho_F} \, , \quad h_{dh} = \frac{Mdh}{A_d \rho_F}$$

$$h_d = h_{de} + h_{dh}$$

$$\bar{U} = \frac{2}{3} \sqrt{2gh_{dh}}$$

$$1 = 1 + \bar{U} \, \Delta\tau$$

$$1 \leq Rd$$

$$Ad = A_{do} + \frac{\pi}{2} R_d^2 + R_d(\rho - R_d)$$

$$Ad = A_{do} + \frac{\pi}{2} \rho^2$$

Yes

$$h_p \geq 2h_d$$

STOP

Fig. 4-6 (Continued)

PRESSURE FIELD CALCULATION (Subroutine PRESS)

$$\tau = \tau + \Delta\tau$$

$$C_1 = \frac{\eta A_b}{V_R} \sqrt{R_V T_V}, \quad M_V = 0$$

$$\eta P_V \geq P_g$$

$$\Delta P_V = P_V (1 - e^{-C_1 \Delta\tau})$$

$$P_V = P_V e^{-C_1 \Delta\tau}$$

$$\Delta M_V = \frac{V_R \Delta P_V}{R_V T_V}$$

$$\Delta M_V = A_b \sqrt{\frac{2 P_g (P_V - P_g)}{R_V T_V}}$$

$$\Delta P_V = \frac{\Delta M_V R_V T_V}{V_R}$$

$$P_V = P_V - \Delta P_V$$

Calculation of Ta, Pa, Ma, Pw

$$P_g = \frac{P_a}{2} + \frac{1}{2} \sqrt{P_a^2 + \frac{2\eta^2 A_b^2}{A_p^2} P_V^2}$$

$$A_j = A_b \frac{\eta P_V}{P_g}$$

$$P_g = \frac{P_a + \frac{A_b^2}{A_p^2} P_V}{1 + \frac{A_b^2}{A_p^2}}$$

$$A_j = 0$$

$$P_V > 1.2 P_g$$
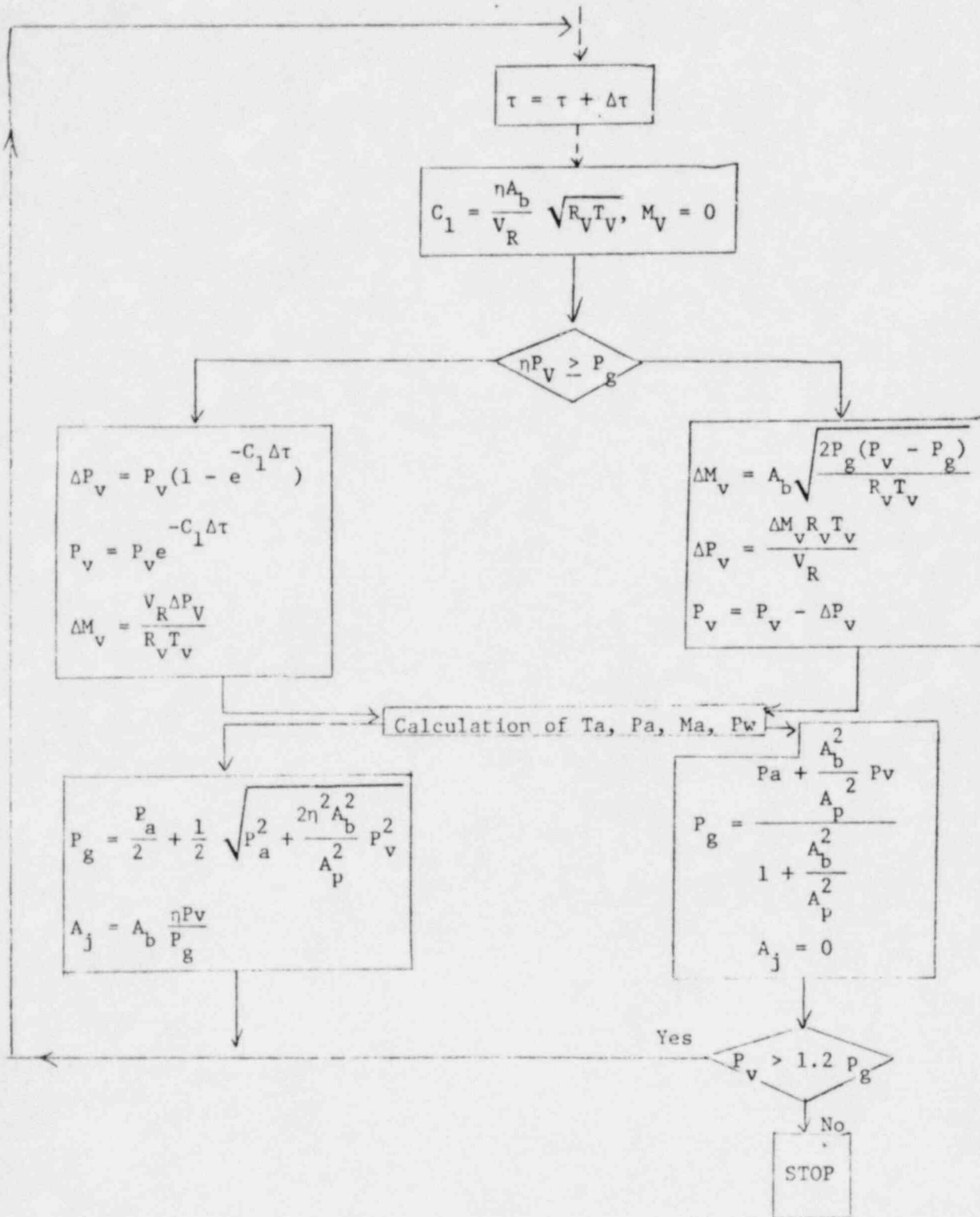
Yes

No

STOP

Fig. 4-6 (Continued)

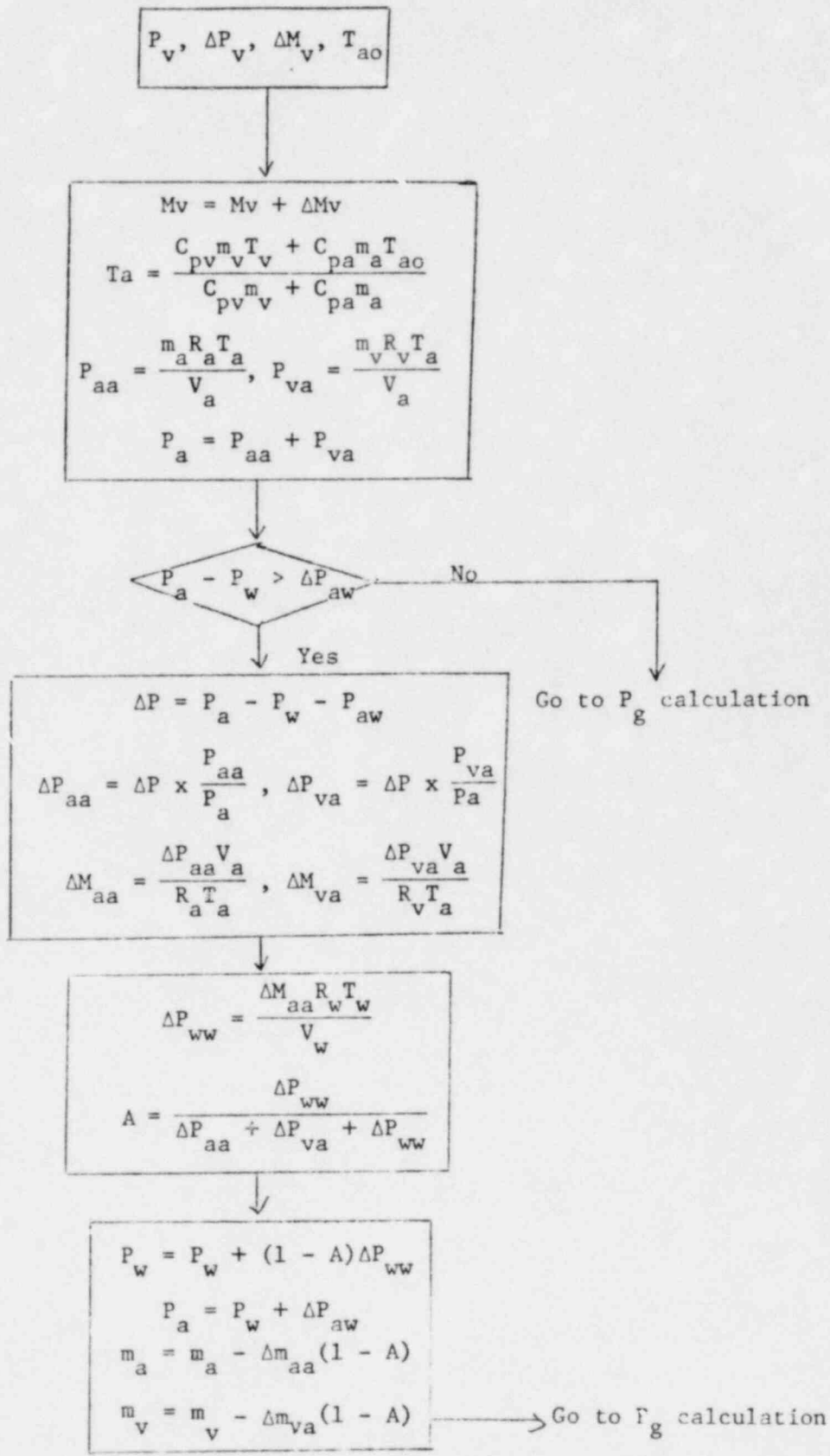CALCULATION OF Ta, Pa, Ma, Pw, (Portion of Subroutine PRESS)

Fig. 4-6 (Continued)

- 88 -

results are illustrated in Fig. 4-3 for the combined relationship between the reactor vessel pressure, pedestal pressure, drywell pressure and wetwell pressure as a function of time. These calculations were carried out for a superheat in the melt (temperature above melting temperature) of $100^{o}C$ and a final vessel breach diameter of 0.3 meters, which resulted from the ablation calculation for the flow of degraded core material through the initial breach of a control rod drive penetration. As illustrated, the maximum pressure within the drywell at the time of equilibration between the reactor vessel and the drywell itself is approximately 0.36 MPa with the wetwell pressure being approximately 0.33 MPa. This pressurization of the drywell occurs over a time frame of approximately 200 seconds which is longer than the time required for spreading of the molten degraded core material on the diaphragm floor. Thus, while the flow of the high pressure gas may act to accelerate the distribution of the molten material within the drywell, the distribution of the material would have occurred in essentially the same time frame, to approximately the same locations, even in the absence of the high velocity gas.

Given this distribution of the material on the drywell floor, the next features to be addressed are the time frame for developing a path for material discharged from the drywell directly into the wetwell, and the corresponding cooling behavior of the material retained on the diaphragm floor.

H.   Summary

In considering the sequence of events following the postulated vessel failure for these hypothetical accident conditions, the following conclusions can be made:

1.   While ex-vessel steam explosions could occur, the amount of material involved would be quite limited and the major influence of such events would be in the distribution of the material throughout the drywell and wetwell regions.

2.   The accumulation of material within the control rod drive room would occur over a time interval of 20 to 30 seconds and could accumulate to a depth of approximately 1 meter.

3.   As the material accumulated within the control rod drive room, the potential for flow onto the diaphragm floor would be determined by the height of the accumulated pool and the calculations for the flow of this material out of the CRD room and around the floor of the diaphragm show that this occurs in an interval of approximately 2 minutes.

4.   Estimates of the amount of material which could be entrained by the blowdown of a high pressure steam/hydrogen mixture show that an upper bound on this material would be approximately 15% of that accumulated within the CRD room. This material would be dispersed throughout the drywell and some of it could potentially be deposited in the wetwell.

5.   Calculations of the integrated behavior show that the pressure within the drywell immediately following the postulated vessel failure reaches a maximum of approximately 0.36 MPa when the drywell and reactor vessel pressures have equilibrated. This is for a transient in which the pressure at the postulated vessel failure was 7 MPa (nominal operating pressure of the boiling water reactor), which pro-

vides an upper bound on this containment pressurization as a result of the vessel failure.

6. The onset of vessel failure does not provide an overpressurization of the primary containment and the time response for pressurization of the wetwell is slow compared to the pressure rise rate within the drywell.

V.   Long-Term Containment Interactions

Following the transient behavior imposed upon the primary containment following a postulated reactor vessel failure, the fuel material is distributed on the diaphragm floor with some portions perhaps being transmitted through the downcomer pipes into the wetwell. Such a material distribution would result in thermal attack of the diaphragm as a result of energy conducted from the fuel into the metal liner and concrete slab, the upper structures in the drywell as a result of radiation from the distributed core debris, and also attack of the steel downcomer pipes and the steel covers for other penetrations through the diaphragm such as equipment and floor drains. Time scale for these thermal attacks on the various system features can be determined and compared to the time scales for distribution of core material over the surface of the diaphragm.

A.   Thermal Attack of the Diaphragm Covers

Penetrations through the diaphragm, such as equipment and floor drains, are designed as 4 in. pipes penetrating through a 1 ft. diameter hole in the concrete diaphragm slab. The diaphragm integrity is then maintained by a 1 in. annular steel ring which spans the gap between the concrete hole and the floor drain as illustrated in Fig. 5-1. Figure 5-2 shows the similar configuration for the 4 in. equipment drains and the material coupling the concrete hole and the 4 in. drain pipe is equal to or thicker than that used for the 4 in. floor drains.

Since there are two floor drains available at the outer regions of the control rod drive room and also along the innerradius of the drywell floor, these will be thermally attacked by an accumulation of core debris on the diaphragm floor. The time required for this attack to result in
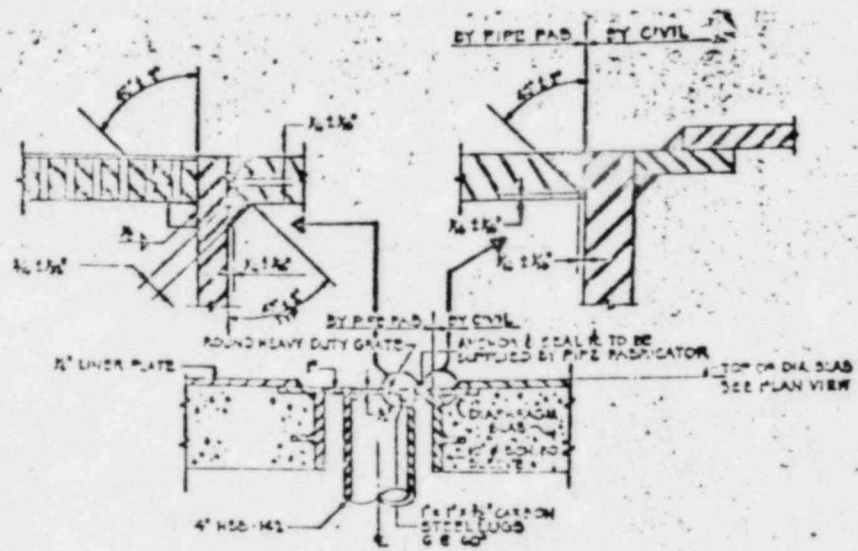
4" FLOOR DRAIN CONNECTION DETAIL

NO SCALE

FIG. 5-1

4" EQUIPMENT DRAIN CONNECTION DETAIL

NO SCALE

Fig. 5-2

failure of the annular gap by melt-through can be estim ted from the air function solution as it describes the thermal conduction within the layer of molten core debris. The energy transferred per unit area from the accumulated debris (Q/A) as a function of time (θ) is expressed by

$$Q/A = 2k_F(T_F - T_i)\sqrt{\frac{\theta}{\pi\alpha_F}} \tag{5-1}$$

where the interface temperature (T_i) is assumed to be that value determined upon contact between the molten debris and the cold steel, k_F and α_F are the thermal conductivity and thermal diffusivity of the core material respectively, and T_F is the initial temperature of the core debris. This will provide an overestimate of the energy transferred from the degraded core material as a function of time, but it will adequately characterize the time available to melt through the annular plate. The energy transferred from the core material is then equated to that required to increase the temperature in the steel plate from its initial value (T_o), assumed to be $100^{o}C$, until its melting temperature ($T_{s,m}$) of $1500^{o}C$.

$$Q/A = \rho_s z c_s(T_{s,m} - T_o) \tag{5-2}$$

In this expression ρ_s is the steel density, z is the thickness of the plate, and c_s is the specific heat of the steel. Equating these two expressions results in an expression for the time required to achieve this melt-through. This is approximately 179 seconds (3 minutes) for the assumed condition in which the interface temperature remains constant. In actuality, as the steel increases in temperature, the temperature at the interface also increases and reduces the heat flux from the degraded core material. A more realistic assessment of the actual time required for melt-through would be given by an expression in which the interface temperature is assumed to be the average steel temperature over the transient (approximately $800^{o}C$), and if this value is used for the interface

temperature, the resulting time required for melt-through is 340 seconds
(almost 6 minutes). These time intervals are meaningful in the respect
that they show that melt-through of the annular plate forming the diaphragm
seal is a time longer than that required for discharge of the core material
and distribution of this material around the drywell floor. Consequently,
since the material is distributed in this time frame, and has begun to
solidify as a result of conduction into the concrete and radiation to the
upper structure in the drywell, the amount of material available for flow-
ing through these melt-through locations is quite limited and thus the
amount of material being transported into the wetwell region is itself
quite limited. In fact, the major effect of this melt-through is simply
to disrupt the diaphragm and establish pressure equilibration between the
drywell and wetwell gas volumes.

Another potential path for transmitting the degraded core material
into the wetwell is through the downcomer pipes, which are 24 in. diameter
pipes with a 3/8 in. wall thickness. Carrying out the above calculations
for this thickness of pipe gives time intervals of 25 and 48 seconds for
the interface temperatures of $270^{\circ}C$ and $800^{\circ}C$ respectively. Since this
attack would not begin until the material began to spread on to the dia-
phragm floor, these time intervals are then compared to the time required
for the spreading itself. As discussed earlier, this is a time interval
of approximately 1 minute, which suggests that the failure of downcomer
pipes by melt-through would be on a comparable time scale with the spread-
ing of the material. Consequently, while the pipe walls would fail as a
result of this hypothetical accident sequence, the amount of material
available for transportation directly into the wetwell would again be
limited. In addition, for this specific case in which the downcomer pipe

would be the transmission duct for the entry of degraded core material in-
to the wetwell, the initial quenching which would occur as this material
progressed down into the water contained within the pipe or the wetwell
itself, would produce a steaming rate which would tend to impede the con-
tinued discharge of core material, under the gravity head of the local
thickness, into the downcomer pipe. In any case, it is demonstrated that
this melt-through before complete spreading of the material occurs on the
drywell floor would be a localized behavior attributable to those down-
comer pipes directly outside of the pedestal passageway, as opposed to an
early effect in which large quantities of the degraded core material would
be directly introduced into the wetwell. As a result, the quenching rate
and the resulting steaming rate would not pose any direct threat to the
primary conta   boundary.

B.   Permanent Coolability

Given the distribution of the degraded core material after it is re-
leased from the vessel, the principle location of which is on the diaphragm
floor, the debris would transmit its stored energy into the concrete via
conduction and upward to the structural members in the drywell including
the pipes, the concrete structural material, the steel liner, etc. In the
Limerick containment design, two sprays are provided within the drywell
itself, as well as the core spray within the reactor vessel and the hy-
draulic lines for the control rod drive mechanisms. For those sequences
where water can be introduced into the drywell through any of these sys-
tems, permanent cooling of the degraded core material can be affected by
vaporization off of the material surface with subsequent condensation in
the wetwell and removal of this heat from the wetwell by the Reactor Heat
Removal System. The establishment of this cooling cycle would provide

for a permanently coolable configuration in the drywell-wetwell system and the energy extraction from the accumulated material on the diaphragm floor could be accomplished via conduction alone. As has been illustrated by many different experiments with uranium-dioxide fuel, it cracks rather easily and would most likely be available in the form of large particles, typically several centimeters in diameter. Given such a size, the cooling of the core debris in the presence of water would be easily established.

Therefore, for those sequences in which water could be added to the drywell, the integrity of the primary containment would not be challenged and any fission products released into the drywell would remain there.

VI. Summary of Relevant Phenomenology

In assessing the phenomenological behavior associated with these po-
tentially severe accident sequences, several aspects of the BWR system
and the MARK-II containment have been specifically addressed. The evalua-
tion of such features is a necessary part of any evaluation in which the
total risk involved with such specific systems is being evaluated and com-
pared to other societal risks. An evaluation of these specific features
and the generic aspects associated with all BWRs and in some cases all
LWRs, lead to the following conclusions.

A. In-Vessel Steam Explosions

The assessment of in-vessel steam explosions as a potential contain-
ment failure mechanism was addressed for a variety of accident sequences
encompassing the anticipated reactor conditions for these postulated se-
vere accidents and the conclusion derived was that there is no potential
for containment failure as a result of an in-vessel steam explosion. This
evaluation was based upon the available experimental and analytical litera-
ture on the subject of steam explosions as well as a detailed evaluation
of the structural components within a boiling water reactor and the influ-
ence that they would have upon the specific rate dependent processes in-
volved in such an explosive interaction.

B. Additional Hydrogen Generation

The relevant phenomenology associated with additional zircaloy oxi-
dation during the movement of material from the original core region in-
to the lower plenum illustrates the fact that, in the absence of water,
which is required for progression of the meltdown, additional oxidation

is quite limited. As a result, the metal-water reaction and the result-
ing hydrogen generation will essentially take place during the degradation
which occurs within the original core boundaries, i.e. before the core has
lost its geometric integrity.

C.   Vessel Failure Mechanism

Evaluation of the geometric configuration in the lower head of the
boiling water reactor reveals that the likely spot for reactor vessel
failure in these postulated sequences would be around one or more of the
control rod drive penetrations or the penetrations for the in-vessel flux
monitors. Given this initial failure, the transmission of degraded ma-
terial through the reactor vessel breach would ablate a larger hole in
the vessel; the size of which could approach about 30 cm in diameter.
The size of this breach effects the blowdown processes and fuel disposi-
tion within the drywell and wetwell, and such calculations should be
based on a diameter evaluated from this analysis.

D.   Disposition of Core Material

Following reactor vessel failure, the events determining the fuel re-
lease from the reactor vessel and the resulting disposition within the
primary containment occur in a time interval of 1 to 2 minutes. An evalua-
tion of the governing processes which determine this discharge and disposi-
tion of the material show that the fuel material would originally accumu-
late within the control rod drive room, except for those sequences in
which water is available on the diaphragm floor, such as a large break
LOCA, and the distribution throughout the diaphragm would then be deter-
mined by the gravity driven flow of this accumulated pool. The flow onto
and around the diaphragm floor would be essentially complete at a time
frame of 2 minutes.

E.   Diaphragm Integrity

The evaluation of the means whereby diaphragm integrity could be lost and material could be directly discharged from the drywell into the wetwell shows that this requires time intervals between 30 seconds and 6 minutes depending upon the method of attack. The implication of this time interval is that the distribution of core material would occur prior to the loss of diaphragm integrity. Given this distributed configuration, the amount of material which can be released directly into the wetwell is severely limited.

F.   Permanent Coolability

For those sequences in which water can be added directly to the drywell, the material can be cooled in place with the energy extraction being through a vaporization-condensation heat transport cycle between the drywell-wetwell, even in the presence of a loss of diaphragm integrity, and the ultimate heat sink being the reactor heat removal system which extracts the energy from the wetwell.

References

1. Reactor Safety Study, WASH-1400, NUREG/75-0114, 1975.

2. J. R. Deitrich, "Experimental Investigation of the Self-Limitation of Power During Reactivity Transients in a Subcooled Water-Moderator Reactor - BORAX-1 Experiments, 1954," AECD-3668, 1965.

3. R. W. Miller, A. Sola and R. K. McCardell, "Report of the SPERT-I Destructive Test Program on an Aluminum, Plate-Type, Water Moderator Reactor," IDO-16883, 1964.

4. SL-1 Project, "Final Report of the SL-1 Recovery Operations," IDO-19311, 1962.

5. R. E. Henry and H. K. Fauske, "Nucleation Processes in Large Scale Vapor Explosions," Trans. ASME, J. of Heat Transfer, Vol. 101, pp. 280-287, May 1979.

6. D. J. Buchanan, J. of Physics D; Applied Physics, Vol. 7, pp. 1441-1457, 1974.

7. R. E. Henry and L. M. McUmber, "Vapor Explosion Experiments with an External Trigger," 2nd CSNI Experts Mtg. on the Science of Vapor Explosions, Grenoble, France, September 1978.

8. R. E. Henry and J. Santori, "Steam Explosion Experiments with Molten Sodium and Water," to be published as ANL report.

9. H. Hohmann, R. E. Henry and H. M. Kottowski, "The Effect of Pressure on NaCl-H_2O Explosions," 4th CSNI Specialist Mtg. on Fuel-Coolant Interaction in Nuclear Reactor Safety, Bournemouth, United Kingdom, CSNI Report #37, pp. 308-232, April 1979.

10. L. S. Nelson and L. D. Buxton, "Effects of Pressure on Steam Explosion Triggering in Corium-E Simulants," Trans. of the ANS, Vol. 28, p. 448, June 1978.

11. M. J. Bird and R. A. Millington, "Fuel-Coolant Interaction Studies with Water and Thermite Generated Molten Uranium Dioxide," 4th CSNI Specialist Mtg. on Fuel-Coolant Interaction in Nuclear Reactor Safety, Bournemouth, United Kingdom, CSNI Report #37, pp. 420-448, April 1979.

12. R. E. Henry, "Test Plan; Large Scale Molten Salt-Water Vapor Explosion Studies to be Conducted at Ispra, Italy," ANL-79-20, NUREG/CR-0728, February 1978.

13. A. J. Briggs, "Experimental Studies of Thermal Interactions at AEE Winfrith," Proc. 3rd Specialist Mtg. on Sodium/Fuel Interaction in Fast Reactors, PNC N251 76-12, Vol. 1, Tokyo, Japan, March 1976, pp. 76-93.

14. G. Long, "Explosions of Molten Aluminum and Water - Cause and Prevention," Metal Progress, May 1957.

15. P. D. Hess and K. J. Brondyke, "Cause of Molten Aluminum-Water Explosions and Their Prevention," Metal Progress, April 1969.

16. D. H. Cho, H. K. Fauske and M. A. Grolmes, "Some Aspects of Mixing in Large-Mass, Energetic Fuel-Coolant Interactions," Proc. of Int. Mtg. on Fast Reactor Safety and Related Physics, CONF-761001, Vol. 4, Chicago, Illinois, pp. 1852-1861, October 1976.

17. N. Zuber and J. Hench, Report #62GL100, General Electric Company, Schenectady, New York, 1962.

18. D. Buxton and W. B. Benedick, "Steam Explosion Efficiency Studies," NUREG/CR-0947, SAND 79-1399, November 1979.

19. F. J. Walford, "Transient Heat Transfer from a Hot Nickel Sphere Moving to Water," Int. J. of Heat Transfer, Vol. 12, 1969, pp. 1621-1625.

20. J. W. Stevens and L. C. Witte, "Destabilization of Vapor Film Boiling Around Spheres," Int. J. of Heat and Mass Transfer, Vol. 16, 1973, pp. 669-678.

21. M. Epstein, M. A. Grolmes, R. E. Henry and H. K. Fauske, "Transient Freezing of a Flowing Ceramic Fuel in a Steel Channel," Nuc. Sci. Eng., 61, 1976, pp. 310-323.

22. G. B. Wallis, One-Dimensional Two-Phase Flow, McGraw-Hill Book Co., 1969.

23. H. K. Fauske, "Boiling Flow Regime Maps in LMFBR HCDA Analysis," Trans. ANS, Vol. 22, 1975, pp. 385-386.

24. H. L. Dryden, F. P. Murnaghan and H. Bateman, Hydrodynamics, Dover Publications, Inc., 1956, pp. 540-542.

Appendix

Mixing Considerations

When considering the intermixing of hot and cold materials which are initially in a totally separate state, one must consider the energy requirements for the fine scale intimate mixing of these two materials, particularly if this is assumed to occur on a rapid time scale. Such an evaluation was presented by Cho, Fauske and Grolmes [16] at the 1976 International Meeting on Fast Reactor Safety and Related Physics. In this assessment, the energy requirements to overcome the frictional dissipation were found to be substantial for rapid intermixing.

The assessment of frictional dissipation was based upon two different types of intermixing processes. The first of which assumed that the total intermixing occurred in a "one-step" manner as illustrated in Fig. A-1, and the other formulation assumed a progressive mixing pattern as graphically illustrated in Fig. A-2. The frictional dissipation for both mixing processes is expressed by

$$\text{frictional dissipation} = N C_D \pi R^2 (\frac{1}{2} \rho_f U_m^2) L_m \tag{A-1}$$

where N equals the number of fuel particles, R is the radius of the fuel particle being mixed, U_m equals the mixing velocity, L_m is the mixing distance, ρ_f equals the water density, and C_D is the drag coefficient, which in these order of magnitude analyses is usually taken to be unity. The mixing energy is generally dominated by the frictional dissipation term, especially if rapid intermixing is postulated as was done in the WASH-1400 analyses. While this term is designated as frictional dissipation, it is principally characterizing the form drag and is not representative of a truly viscous characteristic. If the mixing velocity is assumed to be
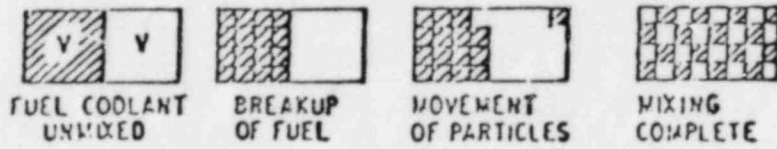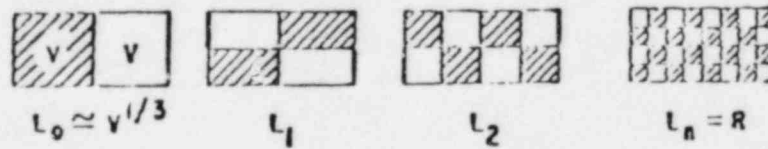
Fig. A-1 Illustration of One-Step Mixing.

Fig. A-2 Illustration of Progressive Mixing.

equal to the mixing length divided by the mixing time (t_m) and the mixing length is approximated by the cube root of the volume to be mixed, $(L_m = V^{1/3})$ the one-step mixing energy is then given by

$$(E_m) \text{ one-step} = 3/8 \frac{\rho_f V^2}{t_m^2 R} \tag{A-2}$$

As discussed by the above authors in their paper, the mixing energy depends upon the mode of breakup in intermixing of the hot and cold materials. The "one-step" mechanism requires the maximum energy and the actual energy requirements could be considerably less if the intermixing process occurs in a progressive fashion involving a number of steps. If this is assumed to occur in a finite number of steps, the expression for the energy required in progressive mixing is given by

$$E_n = V \ 3/8 \ \rho_f \frac{L_o^2}{t_m^2} \left(\frac{1 - \gamma^n}{1 - \gamma} \right) \frac{n}{\gamma} \tag{A-3}$$

where n is the number of steps in the mixing process and γ is the reduction factor of fuel particle size in each step. This energy expression exhibits a minimum energy level when

$$n = \frac{1}{1.74} \ln (L_o/R) \tag{A-4}$$

and if this minimum number of steps is considered, the progressive mixing formulation is then expressed as

$$(E_m)_{min} = 1.81 \ \rho_f V \left(\frac{V^{2/3}}{t_m^2} \right) \left(1 - \frac{R^2}{V^{2/3}} \right) \ln \left(\frac{V^{1/3}}{R} \right) \tag{A-5}$$

where the mixing length has again been assumed to be equal to the cube root of the mixing volume.

For analyses such as those conducted in WASH-1400, the rapid inter-mixing of hot and cold materials results in thermal energy transferred from the hot material and this is then realized as rapid vaporization of the water, which expands and performs mechanical work. The mechanical work estimated from large scale steam explosion experiments is a small fraction of the thermal energy in the melt, typically less than 1%, [18]. However, the amount of thermal energy extracted from the melt is a useful reference to compare against the energy required simply for mixing these materials on a very rapid time scale. This energy cannot be transferred faster than the thermal energy can be conducted to the surface of the core material and, the rate of thermal penetration into the core material can be estimated by using linear approximation of the error function solution as given by

$$x = 2 \sqrt{\alpha_F t} \qquad\qquad (A-6)$$

where x is the thermal penetration distance, t is the mixing time, and α_F is the thermal diffusivity of the molten core material. For a time scale of 1 millisecond, the thermal penetration given by this linear approximation is 22 microns. Consequently, if one assumes that all the thermal energy is transferred in this time scale, a particle radius of 66 microns would be necessary since the equivalent thermal length for spherical particle is approximately 1/3 of its radius. This is illustrated in Table 1-VI for the cases of 100%, 10% and 1% thermal energy release. A similar calculation is also provided for the mixing time of 10 milli-seconds, and these two time scales bracket the mixing times of interest for rapid intermixing. (In this context, rapid intermixing infers that the mixing process takes place on the time scale of the explosive event).

Table 1-VI lists the mixing energies required for the various particle sizes determined from the percent energy released. The salient feature depicted in the table is the immense amount of energy required to rapidly mix such particle sizes; particularly when large volumes are considered. This energy is compared to a value of 1% of the thermal energy contained in the melt, which represents the mechanical work done by the explosion. (The volume considered in this analysis is approximately 14 m^3, which represents 100,000 kg of core material). The table also shows a ratio of the mixing energy requirement to the mechanical work (1% of melt thermal energy) and it is seen that this is always much greater than unity. Since a vapor explosion is a self-sustaining process the thermal energy transferred must be far greater than mechanical work delivered by the explosion. Such a comparison shows that both the one-step and progressive mixing processes require far more energy to mix the two materials than is typical of the available large scale experimental results. These simplistic energy considerations for the rapid intimate mixing of the core materials and water from initially separated state show that the mechanical energy requirements for mixing alone necessitates a trigger which is far larger than the explosion itself.

As a result of the above considerations for mechanical energy requirements in rapid intermixing, one arrives at the substantial conclusion that such rapid interdispersion of hot and cold materials cannot be achieved. Consequently, the only means of achieving such a state is by a slowly developing, progressive mixing state.

Appendix I

RISK ASSESSMENT UNCERTAINTY EVALUATION

APPENDIX I

Probabilistic Risk Assessment (PRA) is a systematic methodology applied in an attempt to develop a measure of safety, but like most measures, it is not perfect. It provides a range of the average risk per power plant when assuming a very large amount of reactor operating experience. It cannot predict when a potentially serious problem may arise in a plant; conversely, a serious problem at one plant does not disprove the analyses because they are based on a large population of plants operating with a large cumulative base of operating experience.

This appendix summarizes the reasons for utilizing a risk analysis approach and identifies the uncertainties which can arise from this type of analysis.

Included in this appendix are discussions of the following items:

• Overview of Risk Analysis

• Completeness of Accident Sequences

• Other Accident Types

• Data Input

  - Failure Rates

  - Meterology

  - Population

• Health Effects.

I.1   OVERVIEW: RISK ANALYSIS

Risk evaluation through system analysis efforts are applicable
in at least three principle areas:

- A measurement of societal risk
- The setting of standards (occupational, public health, etc.)
- The allocation of resources for safety expenditures.

While risk analysts cannot devise means to eliminate all risk, they can
advise on how to best allocate resources to minimize societal risk. People
must invariably assume or endure risks and hazards of some amount, and
thus it is important that information be made available so that intelligent
choices can be made on the risks we will tolerate.

Risk analysis generally involves several interwoven steps as
shown in the block diagram in Figure I.1.

I.2   COMPLETENESS OF POSTULATED ACCIDENT SEQUENCES

Since risk analysis of a complex engineering system, such as
a nuclear power plant, involves the evaluation of many man-machine inter-
faces over a variety of plant conditions, it is not possible to include
all of the potential accident sequences. Rather, the number and types of
accident sequences are limited to a level which assures the incorporation
of the important sequences in the consequence analysis. Since this set of
sequences represents an approximation to the spectrum of conceivable acci-
dent sequences, sequences are chosen for analysis which conservatively
incorporate the events and consequences which may develop from the grouped
events. For example, all turbine trips are treated in a similar manner
regardless of the initial core power level. It is assessed that the course
of the accident is determined for sequences initiated from 100% core power.

I-2

```
        ↓               ↓               ↓

┌─────────────────────────────────────────────────┐
│  RISK FORMULATION:  DELPHI TECHNIQUES OR IDEA-    │
│     WRITING FOR THE IDENTIFICATION OF RISK        │
│     ELEMENTS.  THIS YIELDS NEEDS, CONSTRAINTS,    │
│     OBJECTIVES, POTENTIAL MEASURES.               │
│                                                   │
│                                                   │
└─────────────────────────────────────────────────┘
                          │
                          ↓
┌─────────────────────────────────────────────────┐
│  RISK ANALYSIS:  ESTIMATION OF PROBABILITIES OF   │
│     OCCURRENCE AND CONSEQUENCE MAGNITUDES         │
│     USING INTERPRETIVE MODELING, COST-BENEFIT     │
│     ANALYSIS, OPTIMIZATION OF SYSTEMS CONTROL.    │
│                                                   │
│                                                   │
└─────────────────────────────────────────────────┘
                          │
                          ↓
┌─────────────────────────────────────────────────┐
│  SOCIETAL INTERPRETATION:  EXPLANATION OF RESULTS │
│     IN AN UNDERSTANDABLE FASHION TO BOTH THE      │
│     PUBLIC, REGULATORS, AND OTHER COMPANY         │
│     DECISION MAKERS.                              │
│                                                   │
│                                                   │
└─────────────────────────────────────────────────┘
                          │
                          ↓
┌─────────────────────────────────────────────────┐
│  CHOICEMAKING & PLANS FOR ACTION:  DECISION PROCESS│
│     WITH RISK ANALYSIS AS ONE PIECE OF            │
│     INFORMATION INPUT.                            │
│  →                                              ← │
│                                                   │
│                                                   │
└─────────────────────────────────────────────────┘
```
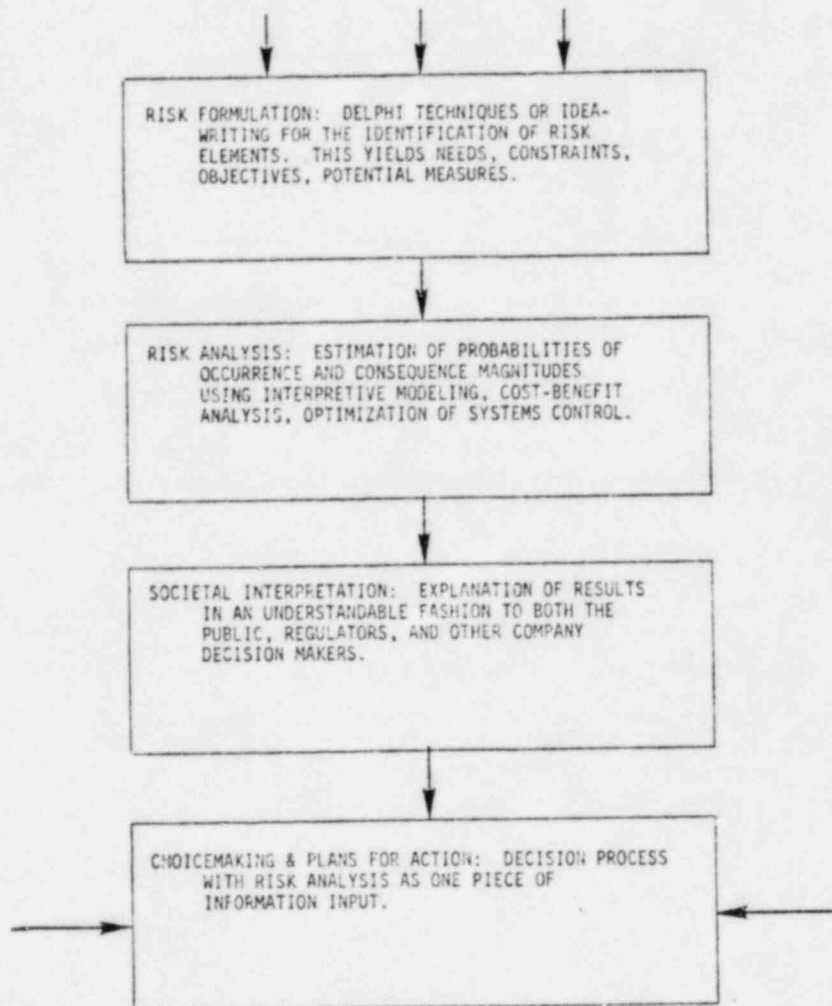
Figure I.1

The ground rules of a risk-analysis are important since they limit a problem's magnitude to a manageable level. The LGS analysis is performed consistent with the ground rules identified in Section 1.5. This limits the evaluation on a generic basis to a study similar to WASH-1400.

The plant risk (R), under the provision of the ground rules, is the summation of the risk (r_i) of N accidents that have been identified:

$$R(\text{plant}) = \sum_{i=1}^{N} r_i = \sum_{i=1}^{N} p_i C_i$$

where p_i is the accident probability and C_i is the accident consequence(s). Completeness could be achieved if there were no more than N accidents that could occur in the plant. It is not possible to prove rigorously that all potential accidents have been considered, but as will be shown, techniques exist which give assurance that the major contributors to risk have been identified.

Suppose there are additional accidents, N+1 to N+R; the error associated with not including these accidents is:

$$\text{Error} = \frac{\displaystyle\sum_{i=N+1}^{N+R} p_i C_i}{\displaystyle\sum_{i=1}^{N} p_i C_i + \sum_{i=N+1}^{N+R} p_i C_i}$$

This error is small if

$$\sum_{i=N+1}^{N+R} p_i C_i << \sum_{i=1}^{N} p_i C_i \;.$$

This is not as difficult to achieve as it might seem. Certain systematic procedures assist in identifying the major risk contributors, such as tables in which plausible and implausible accidents are listed. From these, major risk contributors are selected using approximate values for p_i and C_i. Other approaches to assuring completeness are: expert and peer review, review of previous related analyses, and analysis of barrier penetration (leak path analysis). While the preceding are effective procedures, the fact that the product of p_i and C_i must be about the same magnitude as those already identified facilitates the identification of major risk contributors. The larger the value of p_i, the more readily it is identifiable; thus, the likelihood of not detecting a risk contributor within the guidelines defined in Section 1.5 is small.

Events which might be postulated to have consequences even higher than thus far envisioned may be possible. However, no mechanism for such a release has yet been postulated. Currently included in the Limerick analysis are events with very high consequences; however, these events are found to have extremely small probabilities of occurrence. Therefore, the risk due to these events is small. Since the consequences used for these events involve a large fraction of the core inventory, the probability of higher consequences occurring than those currently considered is felt to be small.

I.3 OTHER ACCIDENT TYPES

Some of the probabilities which are calculated in this analysis are extremely small. These low values indicate that the design of the system in question is such as to render the postulated accidents extremely improbable. However, these low probability accident scenarios may have relatively large consequences and, therefore, it is prudent to consider them in the analysis. In addition, as stated in the ground rules, the following failure modes were not considered in the analysis:

- As-built interactions, such as cable routing, pipe routing, electrical supply reliability. (i.e., isolation protection)

- System inadequately designed to perform required function

- Sabotage

- Fires or initiation of fire protection

- External effects: floods, hurricanes, tornadoes, airplane crashes, seismic effects.

Each of the above items is treated as a separate design require-
ment in the layout and construction of the plant. Specifically, compliance
with the NRC Regulatory Guides outlined below provides a high degree of
assurance that these concerns do not present an undue risk.

Environmental Qualification (Regulatory Guide 1.89)

The requirements delineated include principles, procedures,
and methods of qualification which, when satisfied, will confirm the
adequacy of the equipment design for the performance of Class 1E functions
under normal, abnormal, design-basis-event, post-design-basis-event,
and containment-test conditions.

Control Room Habitability (Regulatory Guide 1.78, 1.95)

Several hazardous chemicals are identified as possibly resulting
in control room uninhabitability if sufficient quantities are released
accidentally. The general design considerations in assessing the habita-
bility of the control room during and after a postulated external release
of hazardous chemicals are presented. In particular, the detailed design
provisions to protect control room operators from an onsite chlorine
release are described.

Security Requirements (Regulator Guide 1.17)

It is important to protect nuclear power plants against surreptitous acts of industrial sabotage, which could lead to a threat to the health and safety of the public. Both procedural measures and physical security criteria for this purpose are described.

Fire Protection (Regulatory Guide 1.120)

A fire protection program for safety-related systems and equipment and for other plant areas containing fire hazards is developed to implement the general design criteria for fire protection. This program is to ensure the capability to shut down the reactor and maintain it in a safe shutdown condition and to minimize radioactive releases to the environment in the event of a fire.

External Effects (Regulatory Guides 1.12, 1.29, 1.48, 1.59, 1.60, 1.61, 1.76, 1.100, 1.102, 1.117, 1.122, 1.132)

Several external effects, such as earthquate, flood, and tornado are considered in relation to the safety of the nuclear power plant. Subjects that are addressed include: instrumentation, design limits and loading combinations, design response, qualification of electric equipment, and site investigations. Compliance with these guides is taken to provide adequate assurance that the reactor can be safely shut down in the event of adverse external effects.

1.4   DATA INPUT

The quantification process necessarily requires input data of a wide variety in order to characterize the probability and consequences of postulated accident sequences. Despite extensive operating experience with nuclear and fossil plants, the availability of accurate component or

system failure rates is still lacking. In addition, meterological data is characterized by general, recent weather patterns at the site and information on weather 20 to 50 miles from the site is insufficient. This section discusses the limitations of the following:

- Component failure rates (I.4.1)
- Meterological data (I.4.2)
- Population data (I.4.3)
- Accident consequences (I.4.4).

1.4.1   Component Failure Rates

The potential problems associated with component failure rate data arise from the fact that the specific plant being analyzed may have little or no direct operating experience with components failing in service. Even with plants of considerable experience, the number of failures of a component of a specific type employed in a specific environment are few.

Suppose there have been m failures in n components during T years of plant experience. The point value failure probability can be approximated as

$$f = \frac{m}{nT} \ .$$

Of the numbers composing this ratio, n, the number at risk, may be known by simply counting components; similarly, the operating experience, T, may be known, but the accuracy associated with m is approximately $1/\sqrt{m}$. This may be uncertain if m is a small number. To improve the statistical accuracy, it is common practice to use data for similar components in similar environments. Obviously, this introduces a new error because similar components may be only superficially similar, and manufacturing processes, procedures, and tolerances may result in a considerably different

component reliability. Similarly, component reliability is very much affected by the environment in which it operates. For example, valve reliability is strongly affected by the moisture in the environment, the operating temperature, and the fluid with which it operates.

The major limitations in the component failure rate characterization are:

- Assumption of similar environment for all components of the same type

- No modeling of the age dependence of failure rates

- Treatment of all components of similar types as part of the identically same population

- Only a portion of all failures have been reported, processed, and finally appear in one of the available data sources, such as:

  - NRC LER file

  - WASH-1400

  - CE component information retrieval (CIR) system

  - (NPRDS (nuclear plant reliability data system).

In addition to the above items, there is a potential concern arising from the implementation of component failure rate data. The data reported is generally taken and treated as random independent failures. The inclusion of dependent failures, known as common-cause or common-mode failures, plays a very important role in the evaluation of risk.

The term common-mode refers to two or more items failing as a result of the same cause or failure mode. Concern for this type of problem arises since there is a limit to the attainable reliability with a sinle component or subsystem; but, if components fail independently of each other, it is possible to use several so that the failure of one or more is circumvented by one or more operational units.

It is apparent that common-mode failures are primarily significant for redundant systems. For example, suppose a subsystem has two redundant components each with a probability of failure of 0.01; the probability that both have failed is 0.01 x 0.01 = 0.0001. But if the components fail at the same time due to a common cause, the probability of the redundant system failure is that of a single component: 0.01. The change between coupled and uncoupled failures is even larger for more redundant systems. Common-mode or common-cause failures are very important, **but** there are aspects that assist in their identification and elimination. These are noted as follows:

1. Common-mode effects have safety significance only in redundant systems, thus all systems need not be examined for these effects. This selection must be done with care, however, because some backup arrangements are not always obvious.

2. Common-mode effects are minimized by design, manufacture, and procedural diversity.

3. Isolation barriers are used to minimize such common-mode effects as pipe whip, fire, and missiles.

WASH-1400 used a mathematical artifice when common-mode effects could not be identified. This was severely criticized by the Lewis Committee and has been mentioned previously. WASH-1400 employed the rationale that the true failure rate of a redundant system is bounded at the low end by assuming completely independent subsystems and at the high end by assuming completely dependent subsystems keyed to the failure of the highest failure rate subsystem. Having established these bounds, the RSS chose the expected value as being the geometric mean of these extremes. It is obvious that there is no hardware basis for this selection and it is avoided in the "realistic" analyses presented in the LGS risk assessment.

There is another type of common-mode coupling that has received less attention than the type discussed in Section I.4.5. This is the fact that the consequences from one type of failure can modify the operating

environment of other components and result in both accelerated failure as well as possibly immediate failure. This type of common-mode is primarily addressed through the Code of Federal Regulations and through the Regulatory Guides by requiring equipment certification as to operability in a degraded environment. In the LGS analysis, the environmental changes that result as an accident progresses through its sequences is continually examined. When the environment exceeds operability requirements for a component, it is assumed to fail. This is a conservative assumption, but more realistic treatment cannot be justified in the absence of test data extending beyond design specifications (see also Section I.3).

I.4.2   Meterological Data

The consequence analysis carried out using the CRAC computer code makes use of several simplifying assumptions to model the transport of fission products from the site and release to the environment. The principal components of the modeling are:

- Wind direction at various elevations
- Wind speed at various elevations
- Atmospheric/plume dispersion
- Rainfall.

The wind direction and speed could be modeled continuously at all heights and distances from the site. However, the available data limits the model. The site meterological data is collected from one tower with some backup data available from satellite towers. However, the existing meterological data does not provide a continuous plot of wind direction and speed in all directions at all distances. The CRAC model used in the consequence analysis employs wind direction and speed during the course of the accident.

I-11

The CRAC model also incorporates some dispersion of the plume arising from the turbulence of the air and roughness of the terrain. The plume dispersion can have an effect on the prediction of early fatalities at large distances from the plant, since early fatalities are a threshold effect.

In a review paper, van der Hoven ($\underline{I-1}$) summarizes data on atmospheric dispersion experiments performed on various terrains in Washington, Idaho, Pennsylvania, and Tennessee. The Washington experiment used an ^{85}Kr tracer and the other measurements were made with an SF_6 (non-radioactive) tracer. These measurements were performed for Pasquill stability classes E, F, and G, in windspeeds less than 2 m/sec. The terrains were classified into the following types:

Type I   - Smooth desert-like (Washington and Idaho)

Type II - Wooded flat terrain (Louisiana and Pennsylvania)

Type III - Wooded hilly terrain (Tennessee).

The author concludes that for flat forested surfaces, the diffusion model (CRAC code) will overpredict the peak concentration by 20 to 40, whereas for hilly forested terrain, the overprediction is 50 to 500.

I.4.3   Population Data

The population at various distances and directions from the plant can be determined with sufficient accuracy to characterize the health effects resulting from the postulated accidents. Since population is grouped by sector, small uncertainty is introduced into the analysis. However, the modeling of the evacuation, sheltering, and breathing rates of the population during an accident sequence plays more important roles in determining consequences to the population in an accident.

- Rapid evacuation could result in very few or no fatalities even under the most adverse accident conditions.

- Adequate sheltering could minimize the population dose.

- Accurate modeling of the breathing rates can also drastically change the early fatality estimate.

I.4.4   Accident Consequences

There are very few benchmarks which can be used to establish the accuracy of the consequence models used in the nuclear power plant analysis. Data on the behavior of reactor systems are being gathered by many large-scale (e.g., LOFT and Semiscale) as well as laboratory-scale controlled experiments on core release functions, plate-out factors, and other factors that attenuate the release of radioactivity. Since it is impractical to perform full scale replications of accident sequences, the fragmentary data from accidents such as TMI-2, Windscale, and SL-1 must be used in system models.

There are many barriers that are designed to confine or disperse the radioactivity in the event of an accident. In general terms, these barriers are: fuel matrix, coolant, reactor system cooling boundary, primary containment, secondary containment, and the atmospheric dispersion of material before it reaches the public. Each barrier has varying abilities to confine or dissipate the materials depending on the barrier structure, geometry, and environmental chemistry and physics. The amount of material retained by or on the various barriers may be calculated using simplifying assumptions, but many inaccuracies are involved in using laboratory data for modeling the amount of release in a damaged nuclear power plant. The reason for these uncertainties are problems in applying small sample laboratory data to a model of a complex power plant and extrapolating the data to accident conditons. Because of the uncertainties, the WASH-1400 analysis tended to be conservative, i.e., predict higher than expected releases so that the consequences would not be underestimated.

I-13

Comparisons can be made of these predictions and the amount of material released in severe reactor accidents. Recently, there has been an attempt (I-2) to calculate the SL-1 accident using updated versions of the CORRAL and CRAC codes used in WASH-1400. Even though the models were more detailed than those of WASH-1400, and the SL-1 geometry is simpler, the results overestimated the release by four times the amount actually observed.

The recent accident at TMI-2 provides useful data on actual releases from damaged cores (I-3) as shown in Table I-1.

Table I.1

CORE RELEASE FRACTIONS OF TOTAL INVENTORY FROM TMI-2

Material		Release to			
	RCS	Reactor Building		Auxiliary	
		Gaseous	Liquid	Building	Environment
Noble Gas	0.6	0.6		0.05	0.05
Iodine	0.3	0.006	0.2	0.03	2×10^{-7}
Ce	0.5	<0.01	0.4	0.03	
Be, Sr	0.02		0.01		

For comparison, the Reactor Safety Study (RSS) BWR Category 4 release, which is the closest BWR release category to the TMI-2 accident, is presented in Table I.2. This shows a factor of 7,500 overprediction of the iodine release (iodine is the isotope that provides the largest contribution to the plant risk). This comparison is provided to illustrate areas of conservatism in the models used. These results were not used in the Limerick Analysis.

Table I.2

COMPARISON OF TMI-2 AND RSS BWR-4
(Release Fractions of Total Inventory)

Material	RSS BWR-4	TMI
Noble Gas	0.6	0.05
Iodine	1.5×10^{-3}	2×10^{-7}
Os - Rb	5.0×10^{-3}	N.R.*
Te - Sb	4.0×10^{-3}	N.R.
Ba - Sr	6.0×10^{-4}	N.R.
Ru	6.0×10^{-4}	N.R.
La	1.0×10^{-4}	N.R.

*Not reported, presumably not detected

The last barrier is the atmospheric dispersion of the radioactive material to the population. This is calculated with the CRAC code and uses the generalized Gaussian plume diffusion model. It is also the model recommended by Regulatory Guides 1.3 and 1.4 for the analysis of loss of cooling accidents.

1.5   HEALTH EFFECTS

Radiation affects humans in three ways:

- Early and continuing somatic effects
- Late somatic effects (cancers)
- Genetic effects.

Early and continuing somatic effects manifest themselves within a year of exposure. In contrast, latent cancers would be observed two to forty years after exposure and genetic effects would be evident in succeeding generations. Late somatic and genetic effects stemming from a major release of radioactive material would manifest themselves as an increase in the spontaneous incidence of cancer or genetic effects in the exposed population. Since early and continuing somatic effects are usually observed after large, acute doses of radiation (e.g., whole-body doses of 100 rads), they would be limited to persons within approximately fifty miles of the reactor even for the largest conceivable release. Conversely, late somatic and genetic effects may result from very low doses albeit with low incidence. Consequently, these effects may occur at long distances from the reactor.

Mortality criteria for early effects are often stated in terms of the dose that would be lethal to fifty percent of the exposed population within sixty days (designated as $LD_{50/60}$). This value varies from 350 rads if there is little treatment, to 520 rads with supportive treatment, and up to 1050 rads for heroic treatment.

The starting point for the health effects model used by WASH-1400 and contained in CRAC is the report issued by the National Academy of Sciences on the Biological Effects of Ionizing Radiation (the BEIR report) (I-4). The BEIR report estimates risks on both an absolute and relative basis by using thirty-year and lifetime plateaus. For the reasons given in Appendix VI of WASH-1400 (I-5), the LGS study used the absolute basis and a thirty-year plateau for the evaluation of reactor risks.

The BEIR report relied heavily on the ongoing study of the Japanese atomic bomb survivors, who received a very high dose rate exposure

of gamma, beta and neutron (high linear energy transfer (LET)) radiation. Furthermore, the dose magnitudes were estimated to range from 10 to over 300 rem. Those survivors receiving less than 10 rem were used as a control population group for the BEIR estimates. The doses from a reactor accident would be almost exclusively due to low-LET radiation (i.e., no neutrons and less than 1% due to alpha radiation). Except for a few individuals who might be irradiated by the passing cloud very close to the reactor, the dose rates to the whole body would be less than 1 rem per day which, with respect to latent cancer induction, is a low dose rate. For the above reasons, the exposures resulting from a reactor accident would be different from the exposures on which the BEIR report based its estimates with respect to quality of radiation, dose rate, and dose magnitude. The risk estimates generated in the BEIR report are based on a linear extrapolation from the aforementioned data to zero doses, without any threshold dose (i.e., a dose magnitude below which there would be zero induction of cancer). Both the BEIR and United Nations (I-6) reports caution that this linear hypothesis is likely to overestimate the risks for low doses and/or low dose rates of low-LET radiation and that, in cases of low exposure, it cannot be ruled out that the risk may actually be zero.

Clearly, there are other problems with the linear hypothesis because there is no limit on the affected population group. By simply extending the calculations to larger distance, larger amounts of population can be included as being affected by a theoretically very small but non-zero dose and hence health effect. This practice can be made more realistic by calculating the fractional dose to the affected population as compared with the dose and health effects the same population group would receive from natural background. This has the advantage of cancelling out the model assumptions contained in the linear hypothesis by treating the health effects of accident radiation the same as natural radiation.

The RSS, in the final report, used a different approach by considering data that reflect non-diversities of the dose/health effects relationship at low doses. Since the objective of the Reactor Safety Study

was to make as realistic an assessment of risks as is possible and to place bounds on the uncertainty, the study made three estimates of the number of latent cancers from a reactor accident. The upper bound is based on the BEIR estimates with some small changes reflecting recent data. For the central (most realistic) estimate, the upper bound is modified by dose-effectiveness factors which are stated in Table I-3.

Table I.3

DOSE-EFFECTIVENESS FACTORS*

Total Dose (rem)	Dose Rate (rem per day)		
	< 1	1-10	> 10
< 10	0.2	0.2	0.2
10 - 25	0.2	0.4	0.4
25 - 300	0.2	0.4	1.0

*From WASH-1400

These factors, which are based on recent experimental data for animals, reduce the expected incidence of latent cancers for small doses and/or low dose rates. In the opinion of the study, these central estimates would represent a more realistic assessment of latent cancer fatalities arising from a reactor accident; the study's medical advisors were of the unanimous opinion that these dose effectiveness factors still probably overestimate the true risk. The overall pattern of data shows no observable difference from an unirradiated control population for persons receiving either an acute dose of less than 25 rem or a chronic dose of less than 1 rem per day to the whole body. As an approximate indication of the possible nonzero lower bound, the study estimates the population dose received by individuals in excess of a threshold and applies the incidence rate used for the central estimate.

Finally, the accuracy of national and international radiation standards have been challenged. One of the more recent is the so-called "hot spot" theory (I-7) put forth by Tamplin and Cochran. The theory assumes that the health effects of alpha emitters should be based on the ionization density rather than the total energy deposited. If this were true, the 50 years of development that resulted in world standards for radiation effects on man would be seriously in error by more than a factor of one thousand. This hypothesis, its refutation, and the supporting data are well-documented in reference (I-7) which also reviews the foundations on which the dose-health effect relationships rest. The basic explanation of the error of the "hot spot" theory is that the effect has already been included in the experimental method whereby the dose-health effect relationship is measured.

References

I-1 I. Van der Hoven, "A Survey of Field Measurements of Atmospheric
     Diffusion Under Low-Wind Speed Inversion Conditions." Nuclear
     Safety 17, March-April 1976, Pp. 223-230.

I-2 C.A. Stevens and Z.T. Mendoza, "Consequences of the SL-1 Accident."
     SIA/SR-216-79-PA,1980.

I-3 A. Miller, "Radiation Source Terms and Shielding at TMI-2." Trans-
     actions of ANS, 34 (1980), Pp. 633-635.

I-4 The Effects on Populations of Exposure to Low Levels of Ionizing
     Radiation, Report of the Advisory Committee on the Biological
     Effects of Ionizing Radiations (BEIR), National Academy of Sciences,
     Washington, D.C. 20006, November 1972.

I-5 Reactor Safety Study, An Assessment of Accident Risks in the U.S.
     Commercial Nuclear Power Plants. USNRC report WASH-1400, October 1975.

I.6 United Nations Scientific Committee on Atomic Radiation, Ionizing
     Radiation: Levels and Effects, Report E72 IX:18, Volume I and II,
     United Nations, New York, 1972.

I-7 W.J. Bair, C.R. Richmond, and B.W. Wachholz, A Radiobiological Assess-
     ment of the Spatial Distribution of Radiation Dose from Inhaled
   Plutonium. WASH-1320, September 1974.
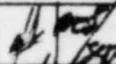
Appendix J

EVALUATION OF BWR MARK II CONTAINMENT CAPABILITY

ULTIMATE PRESSURE CAPACITY

OF

LIMERICK PRIMARY CONTAINMENT

STUDY IN SUPPORT OF RISK ASSESSMENT OF
LIMERICK GENERATING STATION

CONDUCTED BY GENERAL ELECTRIC/SCIENCE
APPLICATIONS INC.

BECHTEL POWER CORPORATION
SAN FRANCISCO, CALIFORNIA

△	2/10/81	Issued As Final Report	

ULTIMATE PRESSURE CAPACITY

OF

LIMERICK PRIMARY CONTAINMENT

ULTIMATE PRESSURE CAPACITY

OF

LIMERICK PRIMARY CONTAINMENT

1.0 GENERAL

1.1 Introduction

Bechtel Power Corporation was requested by Phil-
adelphia Electric Company to assist General Electric/
Science Applications Inc. investigating the ultimate
pressure capacity of the containment in support of the
Limerick risk study. This report contains the
results of this investigation and presents the con-
clusions reached.

1.2 Conclusions

The conclusion of this investigation is that the
containment structural integrity will be maintained
up to an ultimate internal pressure capacity of 140 psig.
The pressure capacity criterion has been defined as
that pressure at which a general yield state is reached
at critical structural sections. A lower bound of
120 psig was established on the basis of infinite
cylinder calculations using the geometry, reinforcement,
liner plate and material properties of the midheight
of the containment wetwell wall. An upper bound of
160 psig was established on the basis of a finite
element analysis of the containment as a whole including
concrete cracking and steel yielding. The ultimate
internal pressure capacity is 140 psig after consideration
of the assumptions and accuracies of the two analysis
techniques. Only a general failure mode can be defined
due to the limitations of the analysis techniques and
the schedule required to support this investigation.

The ultimate pressure capacity investigation of the
refueling head, equipment hatch, personnel airlocks,
and other pressure retaining components of the liner
system concluded that all calculated membrane stresses
were below yield at 120 psig. The investigation also
concluded that deformations at flanged faces exceeded
original criteria, but no quantitative leakage rates
could be established.

The investigation of primary boundary valves
concluded that no valves are expected to fail
below 300 psig, and that the lowest pressure where
excessive leakage might occur is in the 150 to 200
psig range.

2.0 CONTAINMENT GENERAL

2.1 General Arrangement

A typical section through the containment structure
is shown in Figure 1. Relative size and location
of the primary load and pressure resisting structural
elements are shown here.

2.2 Criteria

The containment ultimate pressure is defined as
the internal pressure which causes a general
yield state of all steel components of a structural
section. In the case of the highly indeterminate
containment shell, a general yield state is reached
when the hoop and inclined reinforcement as
well as the liner plate has yielded. In the
case of the refueling head and hatches, a general
yield state is reached when the critical steel
section has yielded through the entire thickness.

2.3 Material Properties

Some material properties used for the analyses done
in this investigation were taken from construction
test records. Table 1 gives a summary of the
properties used.

3.0 CONTAINMENT ULTIMATE PRESSURE CAPACITY

3.1 Idealized Infinite Cylinder

A study of the lower containment wall (wetwell wall)
was made idealizing it as an infinite cylinder.
This assumption neglects the restraint provided
by the base slab and diaphragm slab and stress
concentrations in the walls due to discontinui-
ties (hatches, penetrations, embeds, etc). This
study was also made due to the difficulties
caused by the inclined reinforcement in an overall
analysis. The ultimate pressure value thus
obtained is a lower bound and an indication
of the structural strength in case of partial or

complete failure of the support mechanism at the slabs, specifically at the diaphragm slab.

The infinite cylinder model for this analysis consists of meridional, hoop and inclined reinforcement, liner plate and the concrete as shown in Figure 2. The meridional direction tension force is due to the internal pressure (pr/2) and is reduced by the dead load, while the hoop tension force is due entirely to the internal pressure (pr). The Bechtel inhouse computer program CECAP was applied to establish force equilibrium and strain compatibility for this model.

A general yield condition is reached at 120 psig internal pressure. The final steel component to approach yield is the diagonally inclined reinforcement. At this internal pressure, the hoop rebar strain is 178 percent, the meridional rebar strain is 17 percent, and in the inclined rebar is 98 percent of the yield strain. The corresponding radial displacement is 2.2 inches.

3.2 Finite Element Calculations

A study of the whole containment structure was made by a finite element model. This analysis modeled the overall response of the entire structure to the increasing internal pressure. The restraining effect of the base slab and diaphragm slab on the typical wetwall wall section can therefore be determined. Stress concentration effects at local discontinuities (hatches, penetrations, embeds, etc) were not investigated by this analysis since local discontinuities cannot be modeled with axisymmetric elements. The typical wall to slab section stress concentration effects were evaluated. The failure mode and location were determined from this analysis.

The finite element analysis was performed using the model shown in Figure 4 for the FINEL computer program. This program has the capability of modeling concrete cracking in tension. The redistribution of forces and moments are calculated for the statically indeterminate structure. The model used has the same elements as were used for the design of the containment but the material properties were changed to the values found by tests during construction.

The loads applied to the finite element model study were dead load, live load and internal pressure load. The effects of temperature on the containment

were not considered in the investigation of the containment. Since 120 psig causes general yielding of an infinite cylinder, this pressure was used as an initial pressure for the finite element study. The results of the analyses at 120 psig and 150 psig are shown in Figure 4, Figure 5 and Table 2. Details of critically stressed sections are shown in Figures 6 and 7.

When the applied pressure is 120 psig, the maximum stress and strain in the hoop reinforcement is 70 percent of the yield, while in the shear reinforcement at the base-slab-cylinder intersection the stress and strain is 78 percent of the yield. The largest radial displacement is 1.0 in. approximately in the middle of the cylindrical wall. The average tensile stress across the liner plate at the diaphragm slab is calculated to be 16 KSI which is 67 percent of the yield.

When the applied pressure is 150 psig, the maximum reinforcement stress and strain in the hoop direction is 99 percent of the yield, while locally at the joint of the base slab and cylinder at the inside corner the diagonal shear reinforcement just approaches the yield point. The largest radial displacement of the cylindrical wall is 1.4 in. The average tensile stress across the liner plate at the diaphragm slab is 21 KSI, which is 88 percent of the yield.

3.3 Summary

An evaluation of the infinite cylinder analysis concluded that 120 psig is a lower bound on the ultimate strength capacity. A. evaluation of the finite element analysis concludes that the ultimate strength capacity can be increased due to the influence of the base slab and diaphragm slab on the response of the wetwell wall. However, at approximately 170 psig internal pressure, the diaphragm slab containment wall connection becomes overstressed and a general yield state occurs in the midheight of the containment wall. It was also found from a simple equilibrium equation that the reinforcement anchoring the top head of the structure starts yielding at an internal pressure of approximately 170 psig.

The ultimate internal pressure capacity is therefore determined to be 140 psig after consideration of the assumptions and accuracies of the two analysis techniques used. An internal pressure of 140 psig is the pressure up to which the structural integrity of the containment is assured. The predicted failure above 140 psig is a split along a meridional (vertical) crack at the wetwell wall midheight. The vertical crack failure is contained to the midheight of the containment by the restraint of the base slab and diaphragm slab. However, at the failure of diaphragm slab connection (across liner), the wall loses its restraint at the diaphragm slab and the vertical crack will propagate very rapidly towards the top of the wetwell wall.

4.0 REFUELING HEAD AND HATCH PRESSURE CAPACITY

This section summarizes the results of Chicago Bridge and Iron's investigation. The complete investigation is given in a final report prepared by CB&I.*

4.1 Refueling Head

No membrane stress intensities were calculated which exceeded the yield strength at the pressures specified. The location of critically stressed areas in the refueling head is shown in Figure 9. The values of these critical stresses are given in Table 3. Deflections at the flange face exceeded CBI's original criteria for a leaktight joint and the gasket could be subject to some damage. However, no quantitative figure has been established for a possible leakage rate.

4.2 Hatches

No membrane stress intensities exceeding yield were found in the analysis of the equipment and personnel hatches. Deflections at the flanged face were not in excess of the projection of the gasket. However, possible leakage is dependent on the condition of the elastomer and cannot be readily evaluated.

No membrane stresses exceeding yield at 120 psig were found in evaluating all remaining small miscellaneous pressure retaining components. The evaluation at 160 psi indicated that the Refueling Head Manway and Suppression Chamber Access Hatch blind flanges experience stresses in excess of yield.

Also, the Bulkhead stiffener attachment welds indicate a throat stress in excess of the yield at 160 psi. The Equipment Hatch and Equipment Hatch-Personnel Airlock eyebolt support welds indicate stresses above

*"Risk Assessment Report." Chicago, Bridge and Iron - August 25, 1980

yield at 160 psi. No assessment of the actual
structural capacity of these members at these
internal pressures has been attempted.

5.0 PENETRATIONS AND PRIMARY BOUNDARY VALVE PRESSURE CAPACITY

5.1 Primary Valves

The potential for primary containment isolation valves
to leak excessively or fail due to containment over-
pressurization was examined to determine if credit
can be taken for such leakage as a vent path.

5.1.1 Investigation

Valves investigated were those located in
potential vent paths, as shown in Figure 8,
which are defined as:

(1) Open to the containment atmosphere, and
(2) Open to the reactor enclosure atmosphere
     (via ducting, relief valve, etc.)

The potential vent paths were identified
and the types of valves in them were investigated
with respect to design/test pressures, tendency
to seat with pressure, and other considerations
as discussed below:

Butterfly Valves: The design pressure for
all these valves is 62 psig, and the valves
are tested for leak tightness at 75 psig at
the factory. The manufacturer advises that
their experience is that these valves may not
start to leak excessively until a pressure
range of 150-200 psig. The manufacturer also
states that these valves could begin to fail
(distortion of the disc) above 300 psi.

The butterfly valve design is such that it
would not be expected to seat with increased
pressure. However there may be unpredictable
effects on the seal, such as a flaw closing
up with higher pressure.

The Limerick butterfly valve design temperature
is 340°F, and the manufacturer estimates that
the Viton rubber seals would not be adversely
affected by temperature below 500°F.

Peach Bottom local leak rate testing (LLRT) data was studied to see if the butterfly valves typically exhibited leakage. (PBAPS valves are from a different supplier than LGS). While some butterfly valves did leak at 65-66 psig (typical rates of 60-100 cc/min), others had zero leakage at this pressure.

Gate, Globe and Check Valves

These types of valves are tested in accordance with MSS-SP-61 for Limerick, except allowable leakage limits are less (2cc/min/in vs. 10cc/min/in).

Containment isolation valves 2" and smaller are 1500# rating on LGS. For these valves, a seat leakage hydrotest of 3600 psi at no more than 2 cc/minute/inch nominal valve diameter is specified.

Valves 2" and smaller that are not classified as containment isolation valves greater than 2" are at least 150# rating valves, and a seat leakage test at 300 psi at no more than 2 cc/min/inch is specified.

MSS-SP-61 also allows an air test in lieu of a hydrotest, at 80 psi at no more than 0.1 SCFH/inch nominal diameter for all valve ratings. Limerick valves, however, are usually hydrotested.

The gate and check valves tend to seat with increased pressure. Globe valves will tend to seat when pressure is above the disc. Globe valves are typically oriented on Limerick with the direction of normal flow under the disc, and some of the identified vent paths have normal flow from the containment. The specified seat leakage tests are performed for both sides of the valves, however, and globe valves also have the feature of the stem/operator resisting seat lifting.

These valves are designed for a maximum temperature of 340°F.

Other Considerations:

Although the valves are tested for leakage across the disc, leakage can also occur through the stem packing. However, experience indicates

that leakage is less likely from the stem than
across the disc. Stem packing leakage is also
a function of periodic maintenance.

Periodic testing throughout the life of the
plant also tends to minimize leakage of certain
valves. Integrated leak rate testing (ILRT)
and LLRT serves to identify leakage of
containment isolation valves, with corrective
action being taken when limits are exceeded.
In addition, other valves in the identified
vent paths not encompassed by the ILRT or
LLRT programs may be periodically examined/
corrected for leakage to the reactor enclosure
in a new program, currently under development
for Limerick, that has been mandated by the
NRC as a result of TMI lessons learned.

Another consideration is the limiting size
and number of valves in the identified vent
paths, since all the valves in a given path
must leak, and leakage could be limited by
the smallest valve in the path. Of the 46
paths 'entified, only 4 are 18" or larger
and with only 2 valves in the path. Seventy-
five percent of the paths are limited by valve
sizes 3" and smaller, and 75% of the paths
have 3 or more (closed) valves in them.

5.2   SUMMARY

The investigation shows that no valves are expected to
fail below 300 psi, and that the lowest pressure where
excessive leakage might occur is in the 150-200 psi
range.

Most of the valves in question are subjected to periodic
testing and maintenance, and there are few "good" leakage
paths.

On this basis, and in view of the 140 psig internal pres-
sure capacity identified earlier in this report, it does
not appear that leakage or failure of any specific valve
could be credited as a reliable venting mechanism.

TABLE I

MATERIAL PROPERTIES

MATERIAL	COMPRESSIVE STRESS	YIELD STRESS	ULTIMATE STRESS	MODULUS OF ELASTICITY	POISSON RATIO	REMARK
CONCRETE	4000.0 psi	—	—	3605.0 KSI	0.17	—
REINFORCE-MENT	—	68000.0 psi	100000.0 psi	29000.0 KSI	0.30	ASTM A618 GRADE
LINER PLATE	—	24000.0 psi	—	29000.0 KSI	0.30	ASTM A-285 GRADE A FIREBOX QUALITY

TABLE 2

(A) RESULT— INFINITE CYLINDER ANALYSIS

PRESSURE	STRESS KSI			STRAIN INCH/INCH×10^{-6}		
	HOOP	MER.	DIAG.	HOOP	MER.	DIA
120 psi	68.00	11.60	69.63	4173	401	2287

(B) RESULT—FINITE ELEMENT ANALYSIS

PRESSURE	LOCATION	STRESS KSI fy = 68 KSI			STRAIN INCH/INCH × 10^{-6} εy = 2345×10^{-6} in/in		
		HOOP	MER.	DIAG/SHEAR	HOOP	MER	DIAG/SHEAR
120 psi	BASE SLAB & WALL	24.5	36.67	53.13	879	1264	1832
	MID-HEIGHT	45.64	38.64	—	1574	1332	—
	DIAPHRAGM SLAB & WALL	47.30	41.10	22.55	1631	1591	820
150 psi	BASE SLAB & WALL	36.755	52.08	64.55	1398	1796	2226
	MID-HEIGHT	67.24	58.33	—	2319	2011	—
	DIAPHRAGM SLAB & WALL	55.00	53.09	29.61	1902	1831	1020

TABLE 3

PRESSURE	SECTION	MAXIMUM STRESS INTENSITY KSI	
		TEMPERATURE 340°F	TEMPERATURE 70°F
120 psi	1	30.0	23.8
	2	5.3	7.9
	3	7.5	9.3
	4	6.3	4.7
	5	9.2	9.1
	6	18.0	18.0
160 psi	1	14.0	41.70
	2	3.7	11.2
	3	0.8	16.0
	4	6.3	6.9
	5	9.1	12.0
	6	24.0	24.0

STRESS AT CRITICAL SECTIONS SHOWN ON FIG. 9

REFERENCE : CB & I REPORT
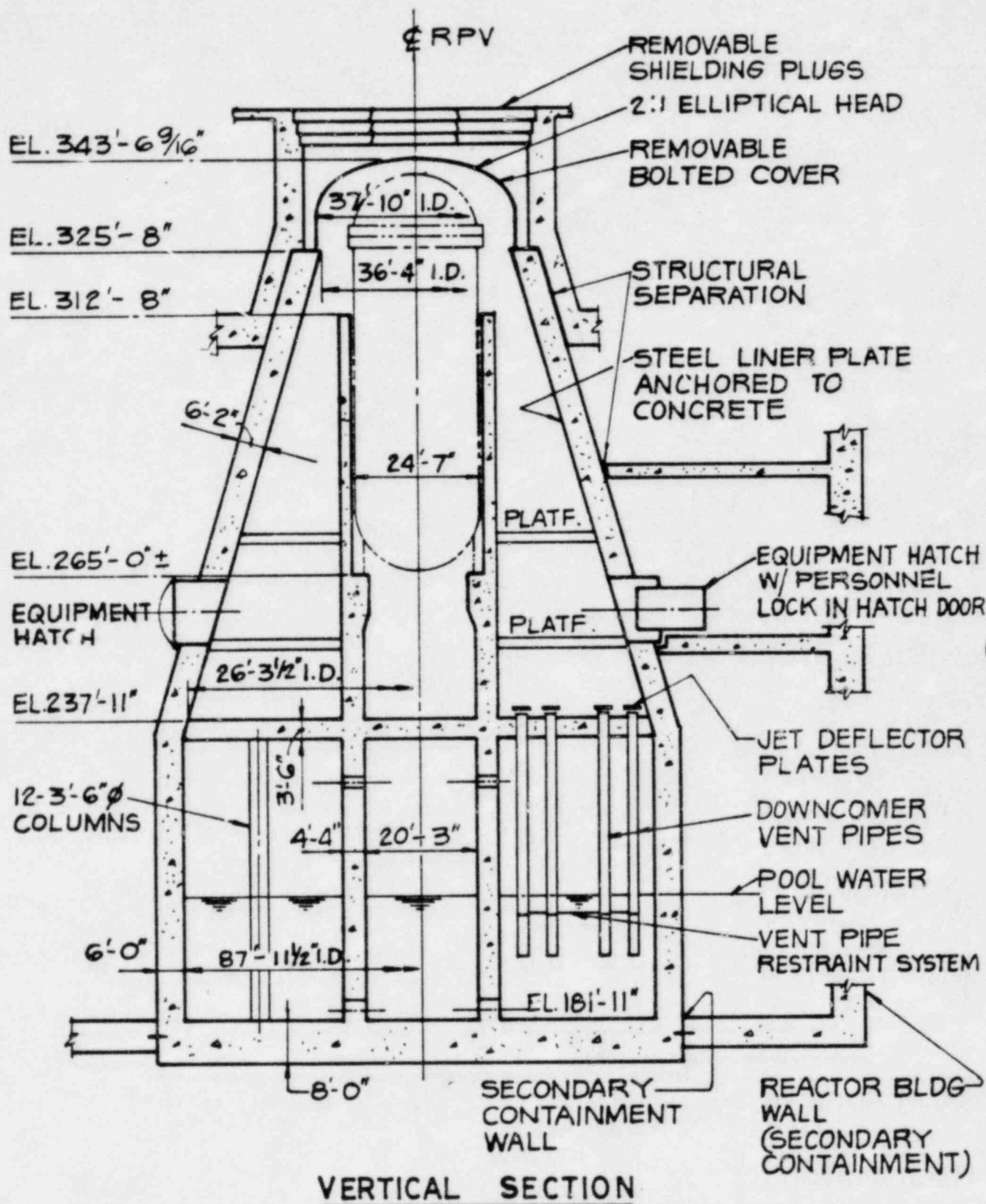
VERTICAL SECTION

FIGURE I - CONTAINMENT GENERAL ARRANGEMENT
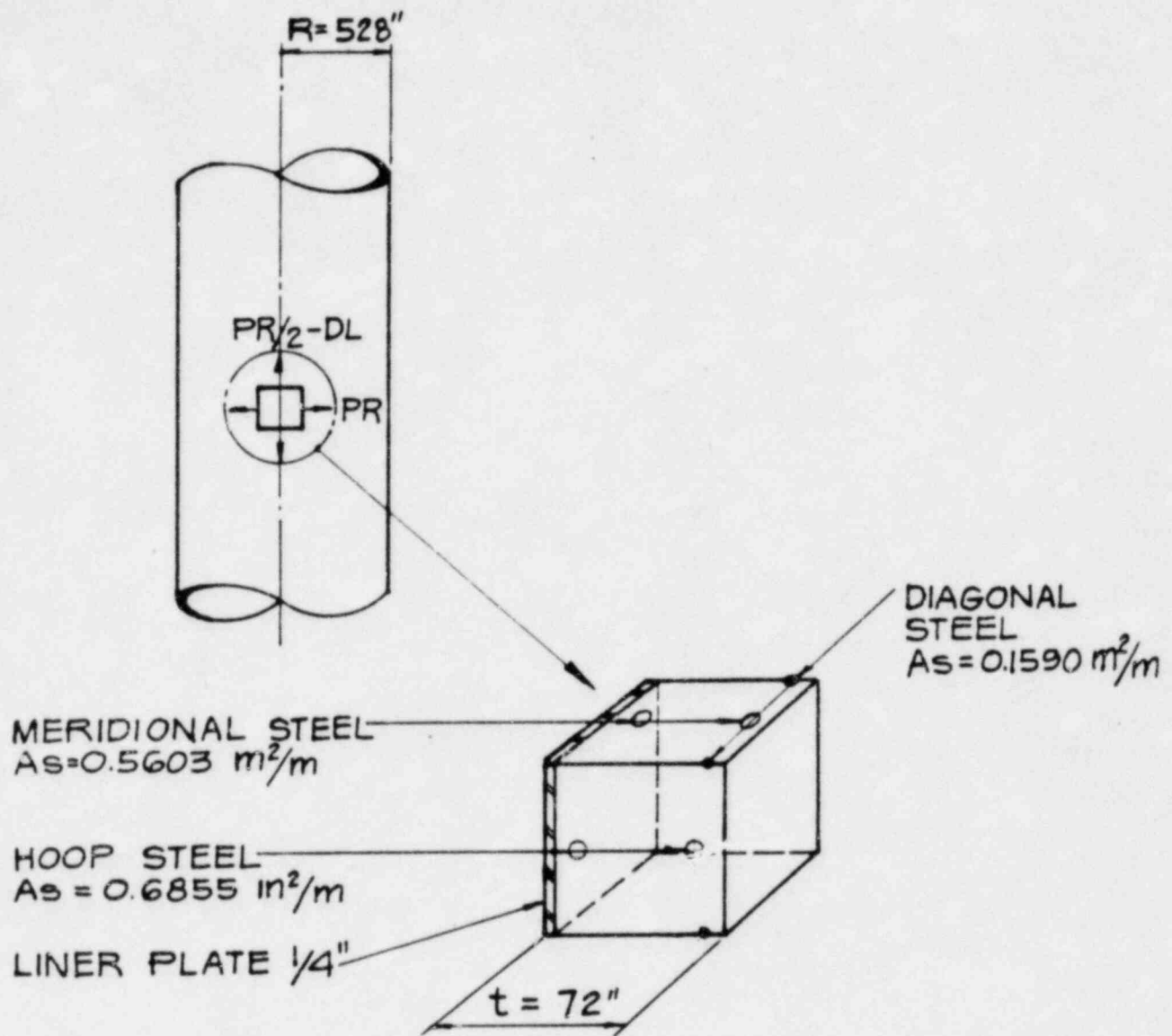
FIGURE 2 — INFINITE ANALYTICAL MODEL

Figure 3 has been deleted
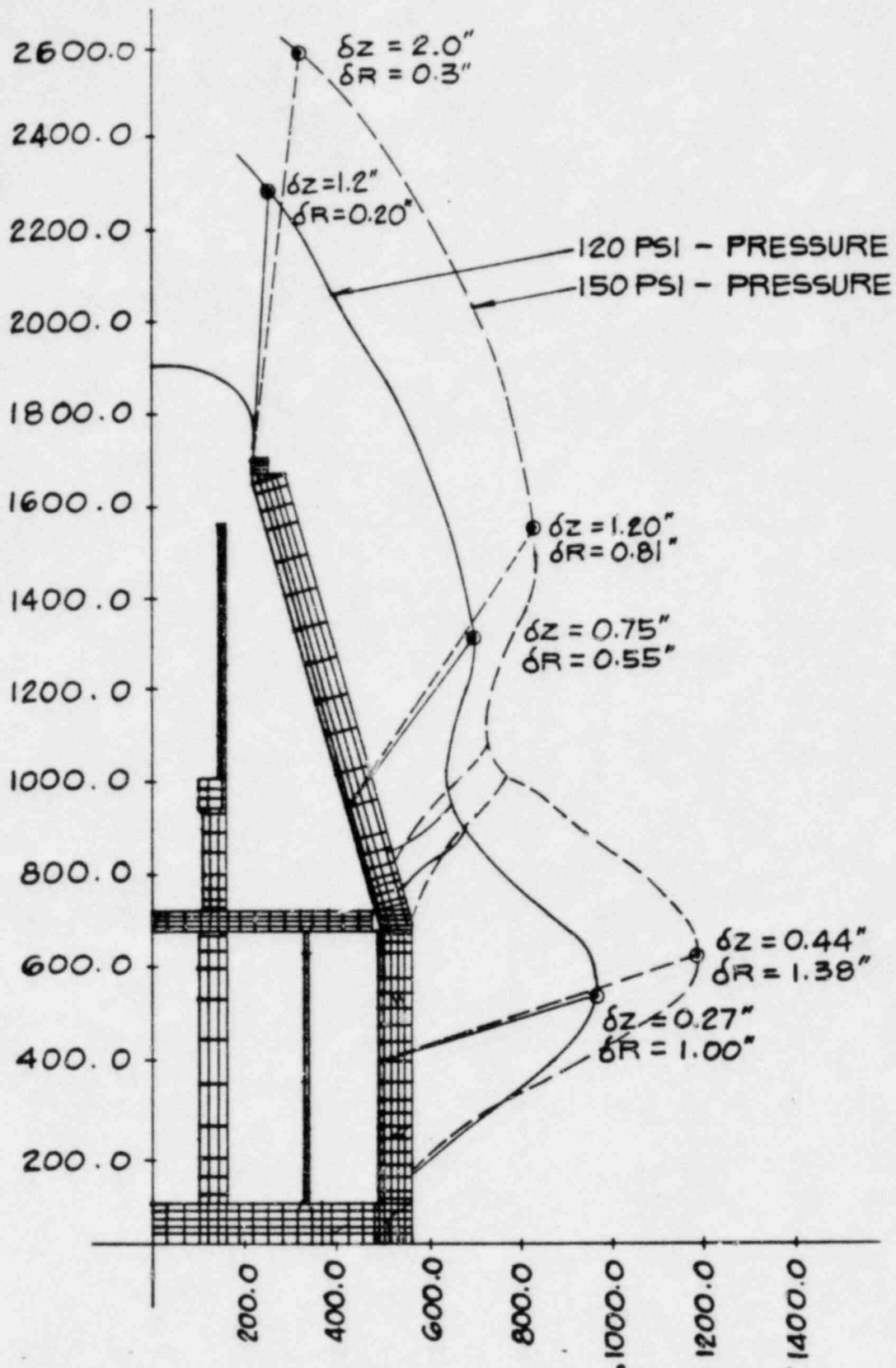
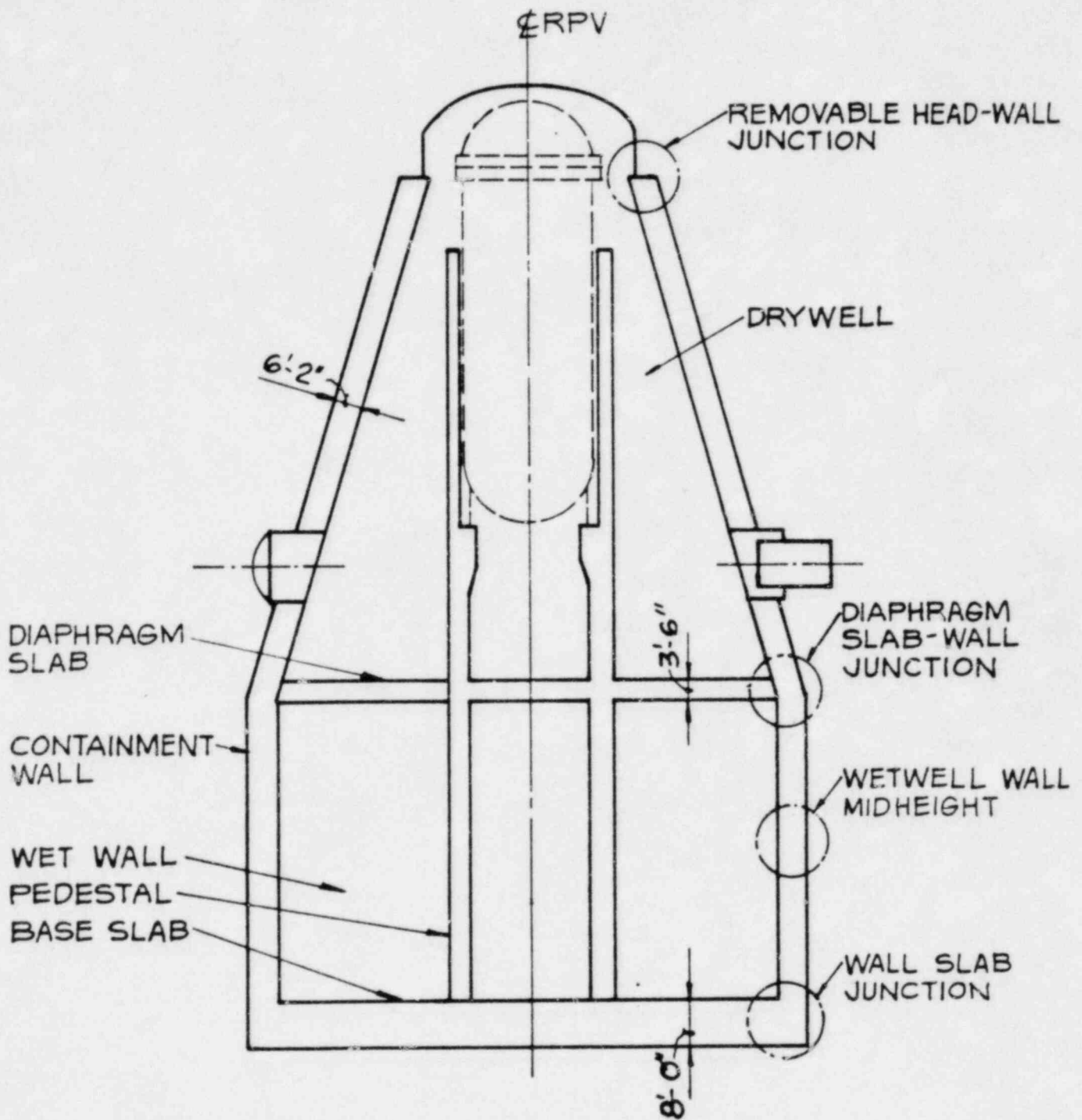FIGURE 4 - FINITE ELEMENT MODEL WITH DISPLACEMENTS AT 120 & 150 PSIG

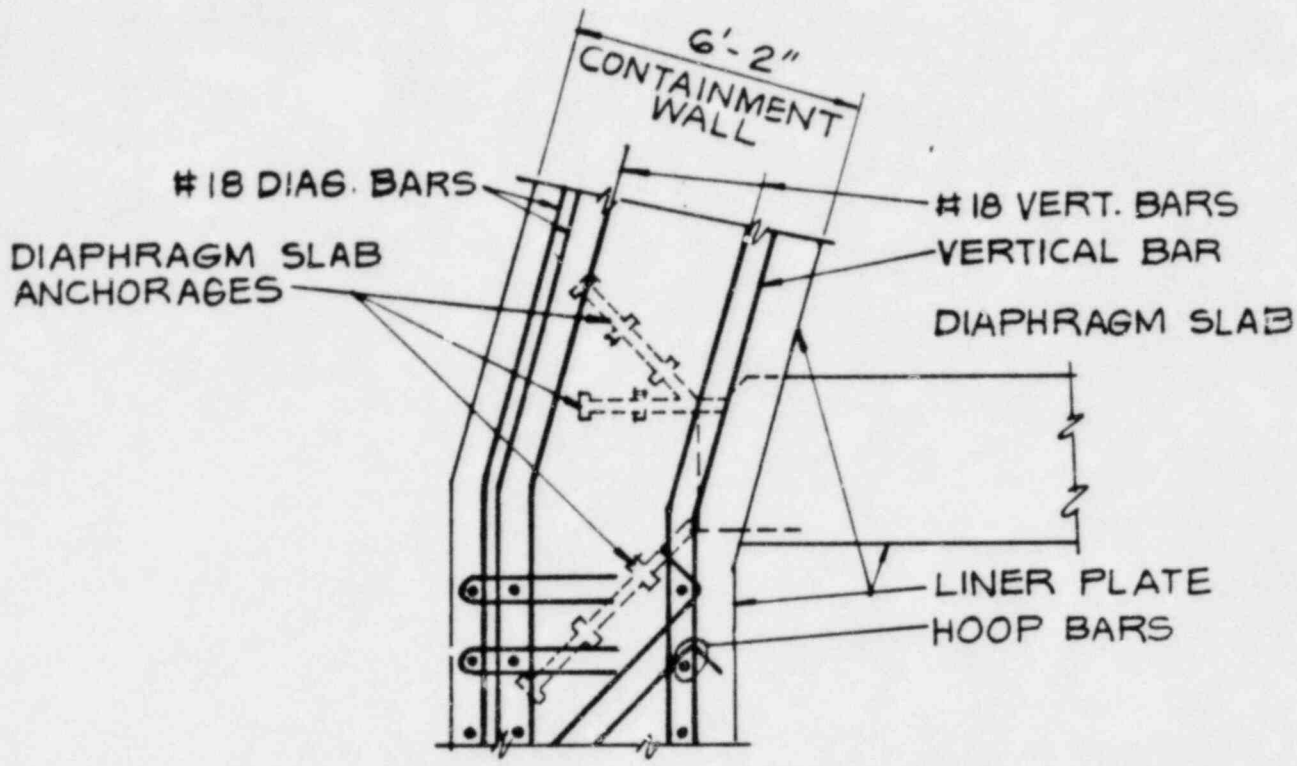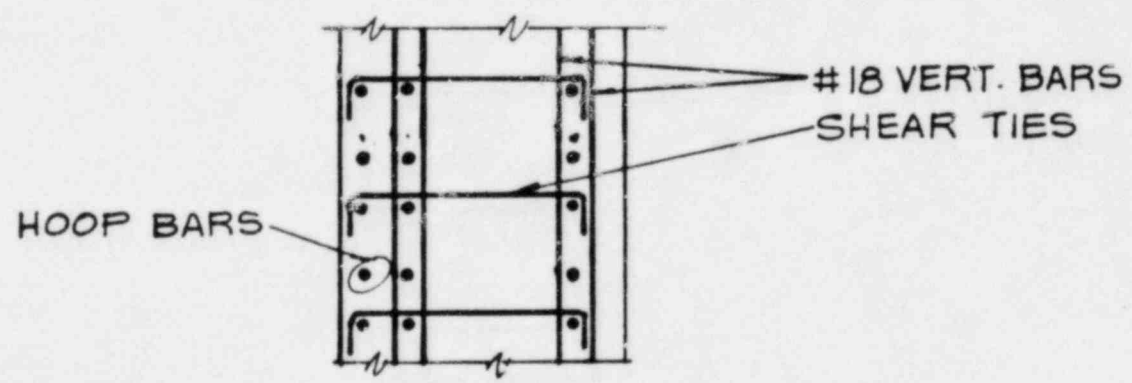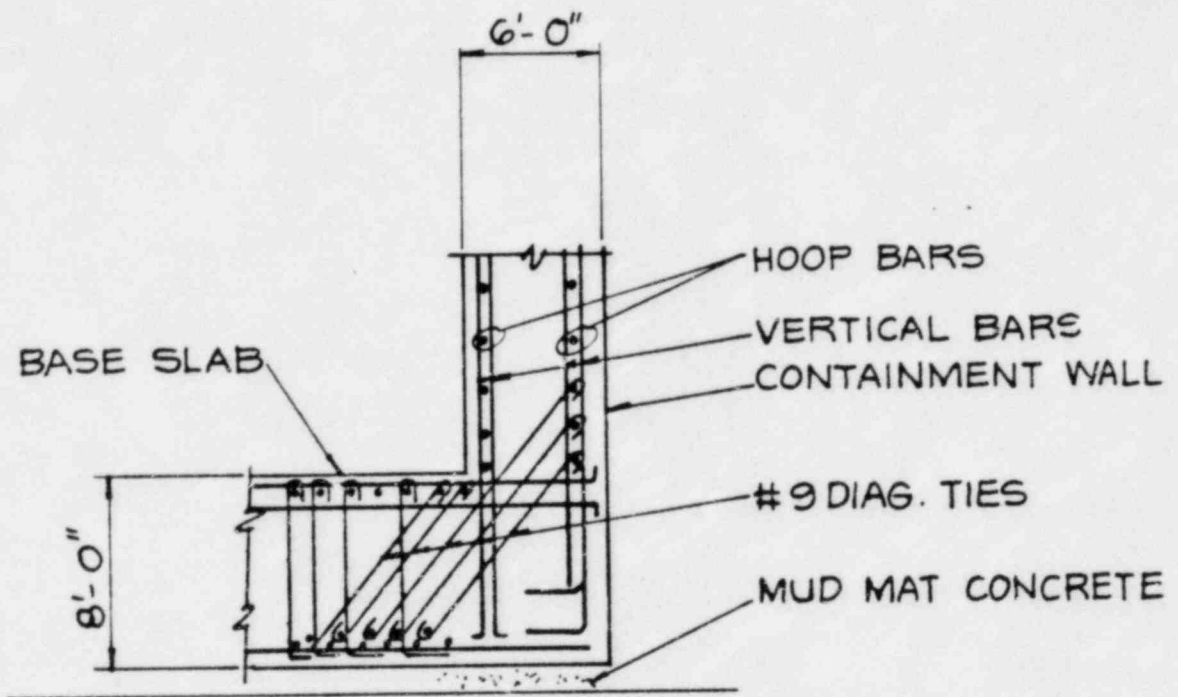FIGURE 5 – LOCATION OF CRITICAL SECTION

6'-2"
CONTAINMENT WALL

#18 DIAG. BARS

DIAPHRAGM SLAB ANCHORAGES

#18 VERT. BARS
VERTICAL BAR

DIAPHRAGM SLAB

LINER PLATE
HOOP BARS

DIAPHRAGM SLAB-WALL JUNCTION

#18 VERT. BARS
SHEAR TIES

HOOP BARS

WALL—MIDHEIGHT

FIGURE 6 — DETAIL OF CRITICAL SECTION
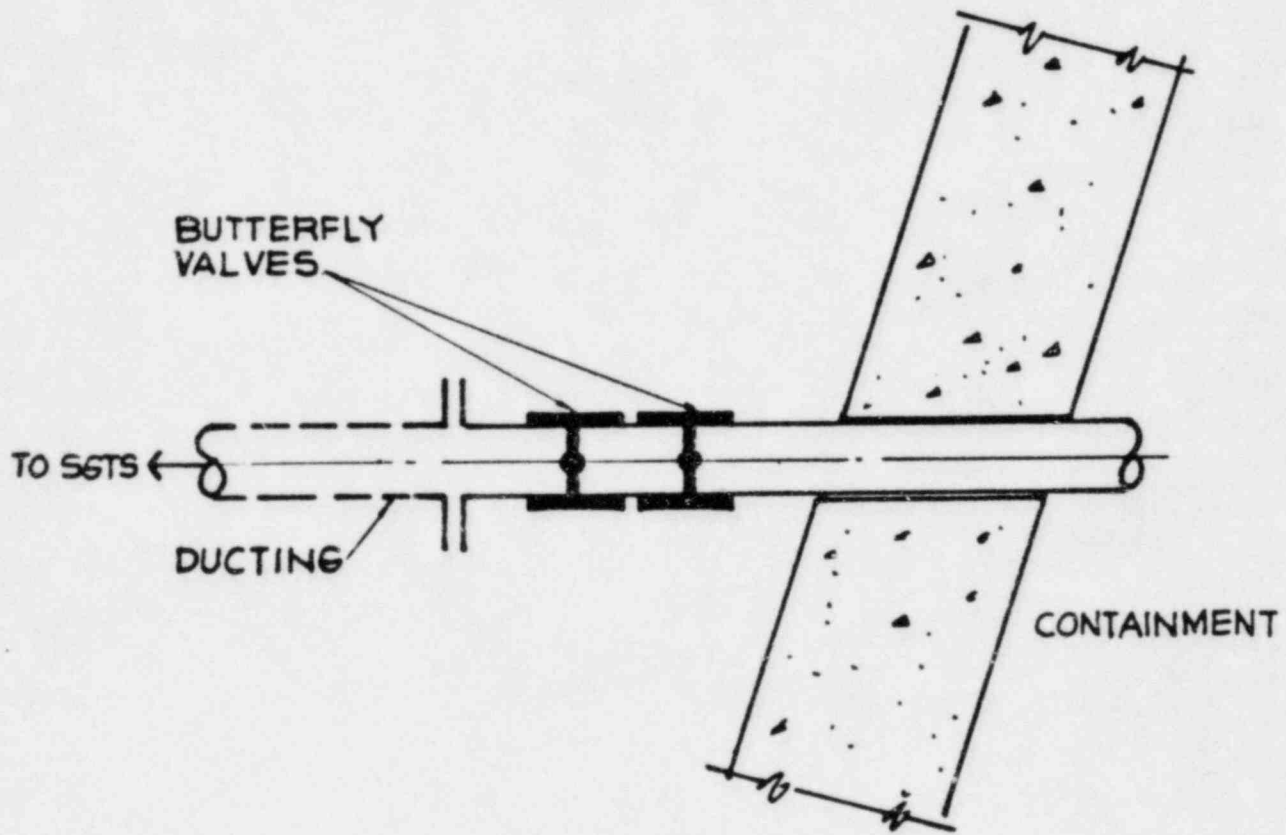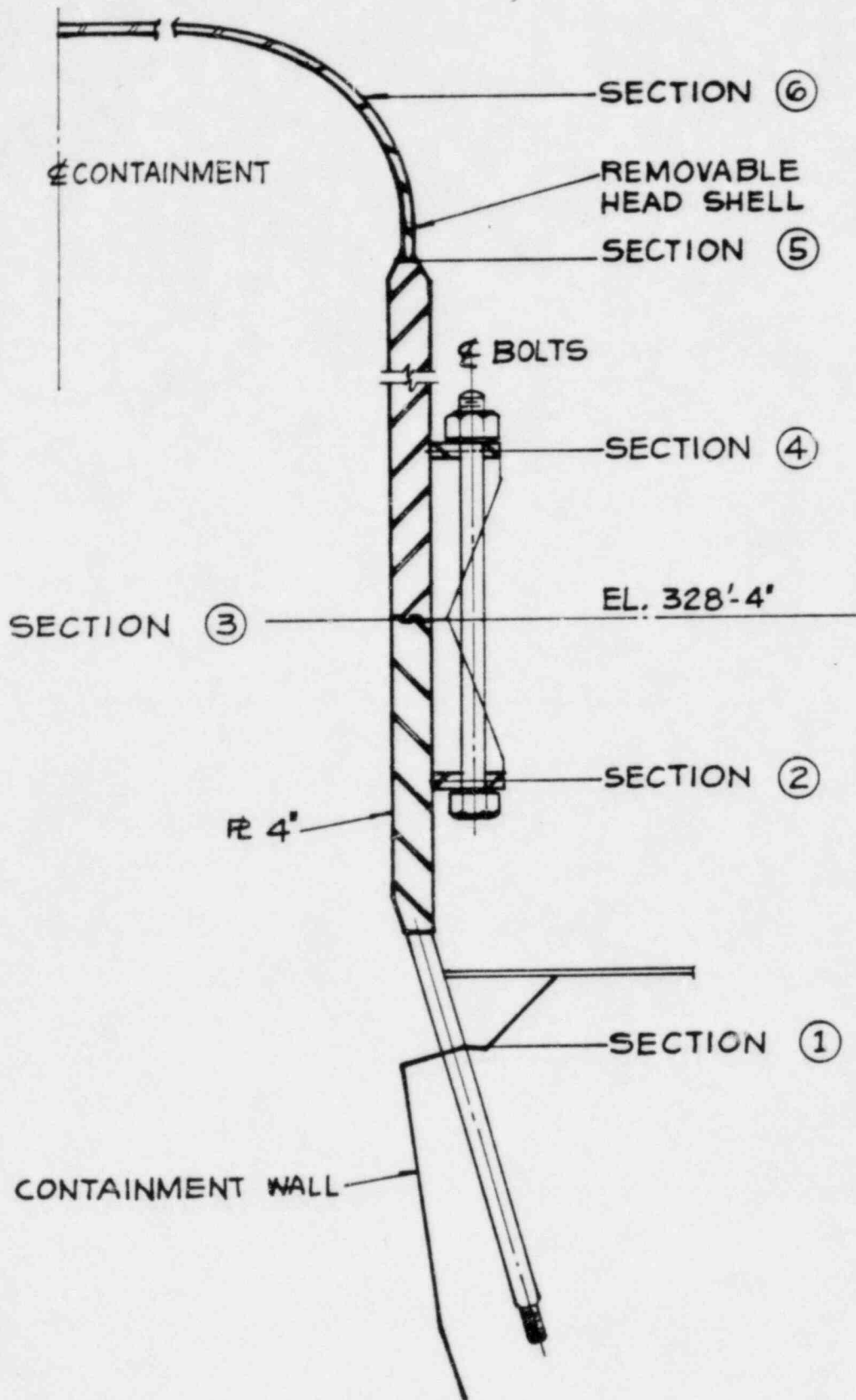
WALL SLAB JUNCTION

FIGURE 7 — DETAIL OF CRITICAL SECTION

FIGURE 8-TYPICAL POTENTIAL VALVE LEAKAGE PATH

FIGURE 9 - REMOVABLE HEAD WALL JUNCTION

Appendix K

SUMMARY OF COMPUTER CODES USED IN THE
QUALITATIVE AND QUANTITATIVE ANALYSIS OF
EVENT TREE AND FAULT TREE LOGIC DIAGRAMS

APPENDIX K

A recognition of the usefulness of computational techniques in estimating system availability (and unavailability) has encouraged Science Applications, Inc. (SAI) to examine existing codes and develop new codes to automate the procedure for numerically evaluating logical, probabilistic models of systems and event sequences. The following codes have been developed to handle the large number of calculations required in the complex fault tree models necessary to accurately model nuclear power plant safety systems:

1. WAMBAM: A code for the quantitative point-wise evaluation of system failure probability using Boolean Algebra

2. WAMCUT: A code to determine qualitatively the cutsets (failure sets) which lead to failure of the system or lead to unacceptable consequences

3. SPASM: A code which utilizes Monte Carlo calculations to determine the uncertainty of the top event based upon the distributio.. of input failure probabilities.

Development of the first code was accomplished basically in two steps: 1) evaluation of existing codes and the methodologies they employ, and 2) evolution of a new code which handles the type of problems encountered in WASH-1400 (K-1). The new code incorporates many features of existing codes. The numerical evaluation program, called BAM*, utilizes basic Boolean techniques, as in the GO computer code (K-2). The preprocessor, WAM**, is designed to ease the amount of user effort required in modeling a system. It is similar to the PREP portion of the PREP-KITT code (K-3).

---

*Boolean Arithmetic Model
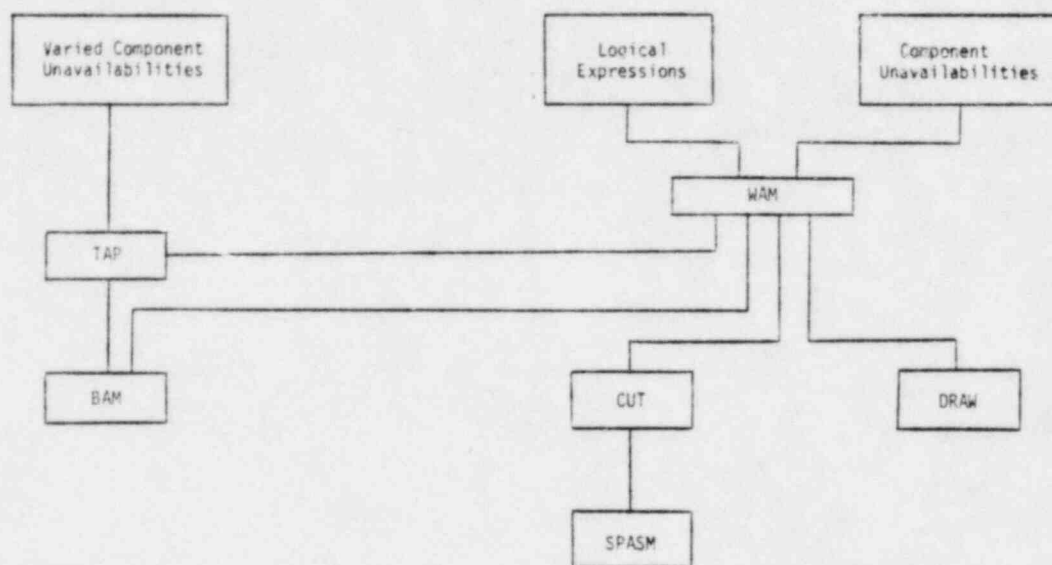
**WAM is not an acronym

The work involved in evaluation of the existing codes and development of BAM is documented in an Electric Power Research Institute (EPRI) report entitled, "Generalized Fault Tree Analysis for Reactor Safety" (K-4).

In an assessment of methods for accident sequence quantification, limitations of the procedures should be considered. One of the central difficulties involved in the description of system availability using fault trees (or any other method) concerns the inability to ensure that all possible faults are described. This includes such items as dependent and common-mode faults which may impact system availabilities. Interactions caused by all possible sources should be considered, since the process of forming accident sequences from only the most critical system faults is a focusing process. This process, of a redundant system and common fault modes such as floods or earthquakes, can be specified diagrammatically and analytically via these methods. Moreover, all failure modes are shown in the fault trees in a natural way, at their point of interaction with the system, rather than being appended to quantified equipment fault trees in a somewhat arbitrary manner.

Figure K.1 depicts the functional relationship between code modules. The preprocessor named WAM allows the system analyst to easily communicate with the BAM and CUT codes. WAM accepts the logic tree in which components and gates are input with alphanumeric names, and allows up to eight inputs per AND* and OR* gate. A multitude of checks are performed to advise the user of mistakes in his model. In addition, the input to the desired evaluation module is optimized to reduce running time and maximize accuracy.

---

*The AND, OR, NOT gates represent the intersection, union, and "not" logical operations between sets. Also see reference (K-6).

```
┌─────────────────┐              ┌──────────────┐   ┌─────────────────┐
│ Varied Component│              │   Logical    │   │   Component     │
│ Unavailabilities│              │ Expressions  │   │ Unavailabilities│
└─────────────────┘              └──────────────┘   └─────────────────┘
```

Figure K-1. Code Module Interrelationships

BAM = Boolean Arithmetic Model
SPASM = System Probabilistic Analyses by Sampling Methods
TAP, WAM, CUT, DRAW = Not anacronyms

        The inputs to WAM allow models which include all sixteen Boolean
operations between two variables. Basically, this extension is accomplished
by the incorporation of NOT* gates. This makes possible the explicit model-
ing of dependent events. WAM also allows the input of combinational failures,
i.e., when a system fails because at least N of M branches fail. The input
to WAM to describe the combinational failures is the name (M) of each branch
and how many (N) must fail to cause system failure. Up to eight branches
are allowed as inputs to the "combination" gate.

_____

*The AND, OR, NOT gates represent the intersection, union, and "not"
logical operations between sets. Also see reference (K-6).

The WAMBAM (K-5) code uses Boolean algebra minimization techniques to find the resultant logic expressions from an input tree and then calculates the associated point unavailability. WAMBAM first forms all possible combinations of events and then forms a truth table that describes each event and gate as a function of these combinations. This basic methodology is computationally optimized, based on techniques used in the GO computer code (K-2).

Fault tree construction in WASH-1400 employed AND and OR logic operations (or gates). In addition, the INHIBIT gate, which acts as a switch to turn on specific logic when a conditional input is satisfied, was also utilized. The basic events identified in these fault trees correspond to independent events for the purpose of quantification. Dependent conditions are bounded and otherwise approximated by modification of the assigned probability values.

WAMBAM allows for additional modeling capabilities, since all of the sixteen logical operations for two variables can be included. Basically, the extension to include any of these logical operations is accomplished by incorporation of the NOT operation capability with the use of AND and OR gates. The inclusion of NOT gates makes possible the explicit modeling of dependent events, including disjointed events and common-mode events.

Analysis of fault trees can proceed in either a quantitative or qualitative fashion. If one wishes a single number for the mean value of the top-of-the-tree, then the mean values for the individual event probabilities can be inserted into the tree to produce it. If, however, information on the most likely event paths or on the probability distribution (not just the mean value) of the tree top is wanted, then it is most efficient to proceed to a cutset analysis. This requires a code, WAMCUT (K-6), which can very efficiently determine the cutsets of a complex fault tree.

A cutset of a gate is defined as the set of components which, when simultaneously failed, cause the gate to fail. Hence, a cutset can be interpreted as the intersection of the components in that gate. A gate can have more than one cutset since it may be failed by more than one combination of failing components. Hence, the Boolean expression for that gate is the union of its cutsets.

The WAMCUT code is divided into two sections. The first, WAM, is the same preprocessor used in the WAMBAM code which reads the fault tree description and checks for logic and syntax errors. The second section, CUT, is the cutset finder routine which takes the restructured input fault tree from WAM and finds the cutsets of each gate, working from the bottom to the top of the tree.

In order to form the cutsets of a gate from the cutsets of its inputs, three operations need to be defined: the ANDing of the cutsets of the two inputs, the ORing of the cutsets and the NOTing of cutsets. These operations are a functionally complete set of logic operations, i.e., any of the sixteen Boolean functions of two variables can be formed from these three operations. WAMCUT can process large fault trees with up to 1500 gates and 1500 components (primary events) without large expenditures of computer time. There is no limitation on the size of the cutsets although the number of cutsets per gate is limited to 2000. The availability of the NOT logic enables the user to model any complex system with WAMCUT gate types. The significant cutsets are identified by using the first moment component unavailabilities to estimate cutset significance in the overall evaluation of the system being modeled.

All the WAM series codes have been developed, checked, and made operational by SAI for EPRI, and they are currently available through the EPRI code center.

The SPASM (System Probabilistic Analysis by Sampling Methods) is a computer code designed to complement the WAM series of codes. It makes use of Monte Carlo simulation to obtain information* about system performance

---

*Expressed as a distribution

from input data of the components (events) of the system. Based on this information, the system failure probability (unavailability) may be estimated. The inputs required are the following: (1) an "equation"* describing the system as a function of the components (events), and (2) a table defining the parameters (if necessary) of the distributions of the random variables representing the component states. In addition, the system model may be created via an option in WAMCUT.

---

*In a FORTRAN Function.

REFERENCES

K-1   Reactor Safety Study, WASH-1400, U. S. Nuclear Regulatory
       Commission (NUREG-75/014), October 1975.

K-2   William Gateley, Dan Stoddard, and R. L. Williams, GO, A
       Computer Program for the Reliability Analysis of Complex
       Systems,KN-67-704(R), Kaman Sciences Corp., April 1968.

K-3   W. E. Vesely and R. Narum, PREP and KITT: Computer Codes for
       Automatic Evaluation of a Fault Tree, Idaho Nuclear Corp.
       Report, IN-1349, August 1970.

K-4   E. T. Ruble, F. L. Leverenz, and R. C. Erdmann, "Generalized
       Fault Tree Analysis for Reactor Safety", submitted to the
       Electric Power Research Institute by Science Applications, Inc.,
       EPRI Report 217-2-2, March 1975.

K-5   F. L. Leverenz and H. Kirch, User's Guide for the WAM-BAM
       Computer Codes, EPRI 217-2-5, January 1976.

K-6   R. C. Erdmann, F. L. Leverenz, and H. Kirch, WAM-CUT, A
       Computer Code for Fault Tree Evaluation, EPRI NP-803,
       June 1978.